

QA: QA

**Civilian Radioactive Waste Management System
Management & Operating Contractor**

**Saturated Zone Flow and Transport
Process Model Report**

TDR-NBS-HS-000001 REV 00 ICN 01

August 2000

Prepared for:

U.S. Department of Energy
Yucca Mountain Site Characterization Office
P.O. Box 30307
North Las Vegas, Nevada 89036-0307

Prepared by:

TRW Environmental Safety Systems Inc.
1180 Town Center Drive
Las Vegas, Nevada 89144

Under Contract Number
DE-AC08-91RW00134

DISCLAIMER

This report was prepared as an account of work sponsored by an agency of the United States Government. Neither the United States Government nor any agency thereof, nor any of their employees, nor any of their contractors, subcontractors or their employees, makes any warranty, express or implied, or assumes any legal liability or responsibility for the accuracy, completeness, or any third party's use or the results of such use of any information, apparatus, product, or process disclosed, or represents that its use would not infringe privately owned rights. Reference herein to any specific commercial product, process, or service by trade name, trademark, manufacturer, or otherwise, does not necessarily constitute or imply its endorsement, recommendation, or favoring by the United States Government or any agency thereof or its contractors or subcontractors. The views and opinions of authors expressed herein do not necessarily state or reflect those of the United States Government or any agency thereof.

**Civilian Radioactive Waste Management System
Management & Operating Contractor**

**Saturated Zone Flow and Transport
Process Model Report**

TDR-NBS-HS-000001 REV 00 ICN 01

August 2000

Prepared by:

P. R. Dixon For
P.R. Dixon
Saturated Zone Lead

08/17/00
Date

Approved by:

M. J. Kelley for
M.J. Kelley
Checker

8/17/00
Date

P. R. Dixon For
P.R. Dixon
Responsible Manager

08/17/00
Date

CHANGE HISTORY

<u>Revision Number</u>	<u>Interim Change Number (ICN)</u>	<u>Description of Change</u>
00	00	Initial issue
00	01	ICN 01 incorporates U.S. Department of Energy comments and editorial changes. Changes are designated by a change bar in the right margin.

INTENTIONALLY LEFT BLANK

EXECUTIVE SUMMARY

The U.S. Department of Energy is evaluating Yucca Mountain, Nevada, for the potential development of a geologic repository for the disposal of spent nuclear fuel and high-level radioactive waste. If radioactive materials are to be placed in the mountain, assurances must be made that materials escaping the engineered and natural barriers and migrating to the accessible environment will remain below regulatory limits. A number of engineered and natural structures are expected to be capable of acting as barriers to release of radionuclides from the potential repository.

Under the groundwater contamination scenario, groundwater beneath Yucca Mountain is the primary medium through which most radionuclides might move away from the potential geologic repository. Although groundwater is a transport mechanism, the entire saturated zone (SZ) system is expected to act as a barrier to the movement of radionuclides. The role of the SZ, as a barrier, is to delay the transport of radionuclides to the accessible environment and reduce the concentration of radionuclides before they reach the accessible environment.

This report, the *Saturated Zone Flow and Transport Process Model Report (SZ PMR)*, describes the flow of water and movement of radionuclides through groundwater in the SZ from beneath the potential repository to the accessible environment at the proposed compliance boundary. The SZ PMR is supported by 13 analysis model reports that describe details of the various models and analyses. The primary purpose of the SZ PMR is to document development of models for use in the Total System Performance Assessment (TSPA), an analysis to evaluate the postclosure performance of the SZ. The models and analyses in the SZ PMR consider two principal factors (factors that might greatly affect the performance of a potential repository) and two other factors (factors of secondary importance). The two principal factors are retardation of radionuclide movement and dilution of radionuclide concentrations during migration. The two other factors are advective pathways and colloid-facilitated transport. The site-scale SZ flow and transport model is supported by data collected near Yucca Mountain (i.e., site data) that allow for model calibration against field observations and assist in validation using independent data sets. The model is built upon the Integrated Site Model, the Hydrogeological Framework Model (sound conceptual models of flow and transport through the SZ), and the construction of a numerical grid. Uncertainties associated with the models range from uncertainties in individual parameters and processes to uncertainties in the conceptual and numerical models.

The Yucca Mountain SZ flow system is contained within the Alkali Flat-Furnace Creek Groundwater Basin, which is part of the Death Valley Regional Groundwater Flow System. In this groundwater basin, water generally moves from recharge areas at higher elevations north of Yucca Mountain to southern areas of discharge at Alkali Flat (Franklin Lake Playa).

A large amount of information about the hydrogeology of this region is known from Yucca Mountain Site Characterization Project (YMP) activities, as well as from numerous additional hydrogeologic studies that have been conducted in the region. Specifically, sufficient information is available to describe regional stratigraphy, structure, and hydraulic properties of rocks, recharge and discharge regions, and groundwater flow paths for purposes of constraining volumetric groundwater flow rates through the site-scale SZ flow and transport model area and for constraining general conceptual models of groundwater flow in the site-scale area. Although

a large amount of data exists for the site, there is uncertainty in many parameters. There is, however, enough information available to evaluate the uncertainty by bounding the uncertain values and by incorporating variability into the TSPA.

As groundwater in the Death Valley system moves from recharge to discharge areas, flow rates and paths depend largely on the hydraulic properties of the rocks along the flow paths. Geologic studies have resulted in a sufficient understanding to identify the important rock types and their spatial distribution. The rock types that play the largest role in regional hydrogeology are Paleozoic carbonates, Quaternary-Tertiary volcanic rocks, and Quaternary-Tertiary sediments and volcanic tuffs that fill structural depressions (referred to as valley fill in portions of this report). The valley fill is dominantly alluvium. Relatively shallow flow occurs in the volcanic rocks and valley fill. Deeper, and more regionally extensive, flow occurs in the carbonate aquifer.

The permeability of volcanic rocks in the vicinity of Yucca Mountain typically is increased by the presence of fractures. An extensive suite of field observations and interpretations of borehole logs, hydrologic tests in boreholes, lab-scale tests, and field tracer tests (C-wells Complex) confirm that fractures enhance groundwater flow in the volcanic rocks. Flow in the alluvium occurs through the primary porosity of these sediments.

The potentiometric surface (water table) in the Yucca Mountain area can be divided into three general areas: (1) the area of the northern end of Yucca Mountain, where potentiometric level exceeds 1,000 m (3,300 ft) above sea level; (2) the area west of Solitario Canyon where the potentiometric levels are about 775 (2,540 ft) m above sea level; and (3) the area at Yucca Mountain and to the south and east, where potentiometric levels are about 730 m (2,395 ft) above sea level. The boundary between the first and third areas is defined by a large hydraulic gradient over which potentiometric levels change more than 260 m (850 ft) in about 2 km (1.2 mi). The boundary between the second and third areas contains a moderate hydraulic gradient over which potentiometric levels change about 45 m (148 ft) in 1 km (0.6 mi). The third area is characterized by a small hydraulic gradient; potentiometric levels change only about 2 m (6.6 ft) over about 10 km (6.2 mi). Water levels in boreholes that penetrate the Paleozoic carbonate aquifer near Yucca Mountain indicate upward flow from deeper to shallower levels because of head differences.

Along the flow path from the potential repository to the accessible environment (i.e., the proposed compliance boundary), the water table transitions from fractured volcanic tuffs to alluvium. Transport processes in the volcanic tuffs include advective transport dominated by fracture flow, matrix diffusion, sorption in the matrix, and dispersion. Transport processes in the alluvium include advective transport, sorption, and dispersion. Matrix diffusion in the volcanic tuffs, and sorption in the alluvium, are two important retardation mechanisms that contribute to the SZ performance. Several laboratory analyses and field tests have been completed to carefully measure parameter values for these processes for use in the SZ flow and transport model.

The site-scale conceptual model is a synthesis of what is known about flow and transport processes at the scale required for Total System Performance Assessment-Site Recommendation (TSPA-SR) calculations. This knowledge builds on and is consistent with knowledge that has

accumulated at the regional scale, but is more detailed because a higher density of data is available at the site-scale level.

The mathematical basis of the site-scale model, and the associated numerical approaches, are designed to assist in quantifying the uncertainty in the permeability of rocks in the geologic framework model and to accurately represent the flow and transport processes included in the site-scale conceptual model. An inverse approach was used to estimate the distribution of rock permeability that resulted in calculated values of hydraulic head that best match measured values. An inverse approach also was used to calculate rates of lateral flow across model boundaries that are compatible with results of the regional-scale flow model.

Confidence in the results of the mathematical model was obtained by comparing calculated to observed hydraulic heads, estimated to measured permeabilities, and lateral flow rates calculated by the site-scale model to those calculated by the regional-scale flow model. In addition, it was confirmed that the flow paths leaving the region of the potential repository are consistent with those inferred from gradients of measured head and those independently inferred from water chemistry data.

The key processes incorporated in the site-scale SZ flow and transport model are abstracted for use in TSPA. These key processes are incorporated into models that include the three-dimensional site-scale SZ flow and transport model, the colloid-facilitated transport model, and the one-dimensional decay chain transport model. The degree of abstraction of these models varies from direct use in TSPA to using the model to justify neglecting certain processes. In the development of the process models, the uncertainties in parameters, processes, and conceptual models are identified and qualified where possible; TSPA analyses then are used to evaluate the importance of these uncertainties on the performance of the potential repository.

The general approach of the site-scale SZ flow and transport model analysis is to calculate unit breakthrough curves for radionuclides at the interface between the SZ and the biosphere using the three-dimensional site-scale SZ flow and transport model. These breakthrough curves contain information on radionuclide transport through the SZ that is used in the TSPA calculations to determine the mass fraction of radionuclides delivered to the accessible environment.

Uncertainties are explicitly incorporated into the TSPA site-scale SZ flow and transport abstractions through key parameters and conceptual models. The probabilistic analysis of uncertainty is implemented through Monte Carlo realizations of the site-scale SZ flow and transport system, in a manner consistent with the TSPA simulations implemented with the GoldSim software code. Alternative models of groundwater flux and horizontal anisotropy are included as uncertainty among six SZ groundwater flow fields. Uncertainty in the location of the contact between volcanic units and the alluvium is represented in the site-scale SZ flow and transport model as variability in the extent of the alluvium zone. Alternative models of colloid-facilitated transport of radionuclides are considered in the uncertainty analysis through the use of two coexisting modes of colloid-facilitated transport. The nominal case of SZ flow and transport for the TSPA-SR explicitly incorporates many features, events, and processes of the SZ system and implicitly includes others.

A series of radionuclide mass breakthrough curves were generated for the expected-value realization of the site-scale SZ flow and transport model, and the distribution of transport times from beneath the potential repository to the proposed compliance boundary (a distance of 20 km [12.5 mi] from the potential repository) were examined. These breakthrough curves contain conservative information on radionuclide transport through the SZ that is used in the TSPA calculations to determine the mass fraction of radionuclides delivered to the accessible environment. The importance of the breakthrough curves cannot be assessed independent of the TSPA. For example, the breakthrough curves do not contain information on the length of time between waste emplacement, the failure of waste packages, and the time until radionuclides reach the SZ. For radionuclides not subject to sorption (e.g., carbon), simulated transport times generally were less than 1,000 years. For radionuclides subject to minor sorption in the alluvium, simulated transport times were 1,000 to 2,000 years. For radionuclides that irreversibly attach to colloids (actinides), simulated transport times in the SZ were somewhat less than 10,000 years. Delay in the migration of colloids with attached radionuclides in the SZ results from the filtration and resuspension process for the colloids. For radionuclides subject to moderate to high sorption, simulated transport times were greater than 10,000 years. These transport times are generated for use in TSPA calculations and should not be interpreted independently of the TSPA.

Assessment of the importance of the breakthrough curves requires coupling these results with other components of the TSPA-SR analyses and sensitivity analyses. For example, interpretation of the results presented here does not include the impact of radioactive decay. Considerable reduction of radionuclide mass may occur for the radionuclides with half-lives that are short relative to their potential transport in the SZ.

The site-scale SZ flow and transport model and the TSPA-SR calculations include simplifications that are conservative with regard to performance of the potential repository. Consequently, results of the TSPA calculations may be more conservative than the best estimate of expected behavior of the SZ flow and transport system. Examples of such simplifications include neglecting the sorption of radionuclides onto the surface of rock fractures, neglecting transverse dispersion, and assuming that groundwater flow instantly adjusts to a wetter climate in the future.

In addition to the treatment of the various technical issues on SZ flow and transport, the SZ PMR summarizes comments and concerns by various overseeing bodies (i.e., the U.S. Nuclear Regulatory Commission, the Nuclear Waste Technical Review Board, and the Advisory Committee on Nuclear Waste), TSPA peer review groups convened by the Yucca Mountain Site Characterization Project, and by internal Project workshops. The issues raised by the U.S. Nuclear Regulatory Commission are of particular interest and are discussed in a separate section of the SZ PMR.

CONTENTS

	Page
EXECUTIVE SUMMARY	vii
ACRONYMS AND ABBREVIATIONS	xix
1. INTRODUCTION	1-1
1.1 OBJECTIVE	1-7
1.2 SCOPE	1-8
1.2.1 Scope of the Saturated Zone Flow and Transport Process Model Report	1-8
1.2.2 Principal Factors and Other Factors Considered	1-8
1.3 FEATURES, EVENTS, AND PROCESSES	1-9
1.4 QUALITY ASSURANCE	1-13
1.4.1 Acquired and Developed Data	1-13
1.4.2 Software	1-13
1.5 RELATIONSHIP TO OTHER PROCESS MODEL REPORTS AND KEY PROJECT DOCUMENTS	1-14
1.5.1 Integrated Site Model Process Model Report	1-14
1.5.2 Unsaturated Zone Flow and Transport Process Model Report	1-15
1.5.3 Biosphere Process Model Report	1-17
1.5.4 Relationship with Other Key Yucca Mountain Project Documents	1-17
1.6 ISSUES FOR SATURATED ZONE FLOW AND TRANSPORT	1-17
1.6.1 Summary of Current Understanding of Saturated Zone Flow and Transport at Yucca Mountain	1-17
1.6.2 Issues from the Total System Performance Assessment-Viability Assessment	1-19
1.6.3 Issues from the Total System Performance Assessment-Viability Assessment Peer Review	1-21
1.6.4 Issues from the Saturated Zone Flow and Transport Expert Elicitation Project	1-21
1.6.5 Issues from the Advisory Committee on Nuclear Waste	1-22
1.6.6 Issues from the Nuclear Waste Technical Review Board	1-22
1.6.7 Issues from the U.S. Nuclear Regulatory Commission	1-22
2. EVOLUTION OF THE SATURATED ZONE PROCESS MODEL	2-1
2.1 OVERVIEW AND DEVELOPMENT APPROACH	2-1
2.2 SITE CHARACTERIZATION AND DATA COLLECTION	2-2
2.2.1 Hydraulic Testing	2-5
2.2.2 Water Level Monitoring Program	2-8
2.2.3 Data Reduction and Analysis	2-8
2.2.4 Modeling	2-9
2.3 PREVIOUS SATURATED ZONE MODELING	2-9
2.4 PREVIOUS TOTAL SYSTEM PERFORMANCE ASSESSMENT MODELING	2-17
2.4.1 Total System Performance Assessment Modeling Before the Total System Performance Assessment-Viability Assessment	2-17
2.4.2 Total System Performance Assessment-Viability Assessment Modeling	2-19

CONTENTS (Continued)

	Page
2.5 CURRENT SATURATED ZONE FLOW AND TRANSPORT MODEL.....	2-21
3. SATURATED ZONE FLOW AND TRANSPORT MODEL AND ABSTRACTIONS FOR TOTAL SYSTEM PERFORMANCE ASSESSMENT FOR SITE RECOMMENDATION	3-1
3.1 SATURATED ZONE FLOW AND TRANSPORT CHARACTERIZATION	3-1
3.1.1 Description of the Saturated Zone System.....	3-1
3.1.2 Summary of Hydrologic Data.....	3-17
3.1.3 Summary of Hydrochemical Data Pertinent to Transport	3-28
3.1.4 Summary of Laboratory Data	3-36
3.2 CONCEPTUAL MODEL OF SITE-SCALE SATURATED ZONE FLOW AND TRANSPORT	3-46
3.2.1 Hydrogeologic Framework and Hydrogeologic Units.....	3-47
3.2.2 Groundwater Occurrence and Flow	3-49
3.2.3 Boundary Conditions	3-58
3.2.4 Solute Transport Processes	3-61
3.2.5 Alternative Conceptual Models	3-74
3.2.6 Changes in the Saturated Zone Flow System	3-78
3.3 MATHEMATICAL AND NUMERICAL MODELING APPROACH.....	3-82
3.3.1 Mathematical Model of Groundwater Flow	3-82
3.3.2 Mathematical Model of Radionuclide Transport.....	3-83
3.3.3 Numerical Solution of the Groundwater Flow Equation	3-85
3.3.4 Numerical Solution of Transport Equation.....	3-86
3.3.5 Flow Model Development	3-89
3.3.6 Model Calibration	3-94
3.3.7 Calibration Results.....	3-101
3.3.8 Sensitivity Analysis	3-104
3.4 MODEL VALIDATION	3-105
3.4.1 Comparison of Permeability Data to Calibrated Permeability Values	3-106
3.4.2 Comparison of Fluxes Derived from Regional Model with the Boundary Fluxes Calculated by Calibrated Model.....	3-108
3.4.3 Comparison of Measured Upward Hydraulic Gradient with Predicted Upward Hydraulic Gradient.....	3-112
3.4.4 Comparison of Hydrochemical Data Trends with Calculated Particle Pathways	3-112
3.4.5 Natural Analogues	3-115
3.5 ASSUMPTIONS, USES, LIMITS OF THE SATURATED ZONE SITE-SCALE FLOW AND TRANSPORT MODEL.....	3-128
3.5.1 Groundwater Flow Processes.....	3-129
3.5.2 Radionuclide Transport Properties	3-131
3.5.3 Use of the Site-Scale Model in Site Characterization Activities	3-133
3.5.4 Modeling Limitations.....	3-133
3.5.5 Process Model Uncertainty	3-134

CONTENTS (Continued)

	Page
3.6 SYNTHESIS OF SATURATED ZONE MODEL AND MODEL ABSTRACTIONS	3-135
3.6.1 Introduction.....	3-135
3.6.2 Results of Synthesis	3-135
3.6.3 Analysis Approach to Saturated Zone Flow and Transport for Total Systems Performance Assessment Analyses	3-136
3.7 SATURATED ZONE SITE-SCALE FLOW AND TRANSPORT NOMINAL CASE	3-145
3.7.1 Description of the Nominal Case.....	3-145
3.7.2 Parameter Uncertainty Distributions.....	3-146
3.7.3 Probabilistic Analyses.....	3-152
3.7.4 Results.....	3-153
3.7.5 Interpretations	3-155
3.8 SUMMARY OF OTHER VIEWS AND ALTERNATIVE MODELS	3-161
3.8.1 Disruptive Events and Rises in the Water Table	3-162
3.8.2 Saturated Zone Flow at Yucca Mountain	3-169
4. RELATIONSHIP TO U.S. NUCLEAR REGULATORY COMMISSION ISSUE RESOLUTION STATUS REPORTS	4-1
4.1 SUMMARY OF THE KEY TECHNICAL ISSUES.....	4-1
4.2 RELATIONSHIP OF THE SATURATED ZONE FLOW AND TRANSPORT PROCESS MODEL REPORT TO THE KEY TECHNICAL ISSUES	4-2
4.2.1 Radionuclide Transport.....	4-2
4.2.2 Structural Deformation and Seismicity.....	4-4
4.2.3 Total System Performance Assessment and Integration.....	4-5
4.2.4 Unsaturated and Saturated Flow under Isothermal Conditions	4-6
4.3 U.S. NUCLEAR REGULATORY COMMISSION ACCEPTANCE CRITERIA	4-8
5. SUMMARY AND CONCLUSIONS	5-1
5.1 SATURATED ZONE FLOW AND TRANSPORT CHARACTERIZATION	5-1
5.2 CONCEPTUAL MODEL OF SITE SCALE FLOW AND TRANSPORT	5-3
5.3 MATHEMATICAL MODEL AND NUMERICAL APPROACH.....	5-4
5.4 SUMMARY OF SATURATED ZONE MODEL ABSTRACTION FOR TOTAL SYSTEM PERFORMANCE ASSESSMENT-SITE RECOMMENDATION	5-5
5.5 CONCLUSIONS.....	5-6
6. REFERENCES	6-1
6.1 DOCUMENTS CITED.....	6-1
6.2 CODES, STANDARDS, REGULATIONS, AND PROCEDURES.....	6-19
6.3 SOURCE DATA, LISTED BY DATA TRACKING NUMBER	6-20
APPENDIX A - ISSUES FOR SATURATED ZONE FLOW AND TRANSPORT.....	A-1
APPENDIX B - U.S. NUCLEAR REGULATORY COMMISSION ISSUE RESOLUTION STATUS REPORTS AND KEY TECHNICAL ISSUES.....	B-1

INTENTIONALLY LEFT BLANK

FIGURES

	Page
1-1. Conceptual Relationships Among the Analysis Model Reports, Process Model Reports, and Other Higher-Level Yucca Mountain Site Characterization Project Documents	1-2
1-2. Relationship Among Saturated Zone Models and Analyses.....	1-6
1-3. Domains of the Site-Scale Saturated Zone Flow and Transport Model, the Geologic Framework Model, and the Unsaturated-Zone Model	1-16
2-1. Boundaries of the Death Valley Regional Groundwater Flow System, the Regional-Scale Flow and Transport Model, the Nevada Test Site, and the Site-Scale Saturated Zone Flow and Transport Model	2-3
2-2. Prominent Geographic Features in the Death Valley Regional Groundwater Flow System.....	2-4
2-3. Nye County Early Warning Drilling Program Boreholes and the C-Wells Complex.....	2-6
3-1. Hydrogeologic Units in the Death Valley Regional Groundwater Flow System Area.....	3-4
3-2. Regional-Scale Potentiometric Surface Map	3-7
3-3. Groundwater Flow Paths Near Yucca Mountain	3-8
3-4. Structural and Tectonic Features Units within the Site-Scale Saturated Zone Model Area	3-12
3-5. Site-Scale Potentiometric Map and Structural Features	3-15
3-6. Potentiometric Surface Map Developed Using Water-Level Data from 1993	3-19
3-7. Boreholes Near Yucca Mountain.....	3-21
3-8. Physical System, Conceptual Model, and Normalized Tracer Responses from the Prox Pass Tuff Multiple Tracer Test.....	3-30
3-9. Normalized Tracer Responses in the Bullfrog Tuff Multiple Tracer Test.....	3-31
3-10. Rock Beaker Diffusion	3-41
3-11. Diffusion of Tritium, Uranium, and Plutonium through a Devitrified Tuff	3-43
3-12. Cumulative Recoveries of Tritium, Technetium-95, and Neptunium-237 in a Fractured Tuff Column	3-44
3-13. Fence Diagram of the Site-Scale Model Domain	3-50
3-14. Geological Features Represented in the Site-Scale Flow and Transport Model	3-59
3-15. Conceptual Model of Transport Processes in the Volcanic Tuffs and the Alluvium	3-62
3-16. Estimated Dispersivity as a Function of Length Scale	3-70
3-17. Conceptual Model of Colloid-Facilitated Transport of Radionuclides.....	3-71
3-18. Three-Dimensional Representation of the Computation Grid	3-91
3-19. Modeled Temperature at the Water Table for the Site-Scale Model Domain	3-95
3-20. Simulated Potentiometric Surface and Calibration Residuals	3-102
3-21. Flow Paths Predicted by Site-Scale Saturated Zone Flow and Transport Model	3-103
3-22. Estimated and Observed Permeabilities for Nine Stratigraphic Units at Yucca Mountain.....	3-107

FIGURES (Continued)

	Page
3-23. Estimated and Observed Permeabilities for Four Aquifers at the Nevada Test Site ...	3-108
3-24. Zones Used for Comparing Groundwater Fluxes between the Regional- and Site-Scale	3-110
3-25. Paths of Particle Starting at 600 Meters Elevation	3-113
3-26. Natural Analogue Sites Used for Comparison with Yucca Mountain	3-116
3-27. Decrease in Relative Concentrations of Radionuclides in the Snake River Plain Aquifer with Distance from the Idaho Chemical Processing Plant	3-124
3-28. The Convolution Integral Method Used in Saturated Zone Flow and Transport Calculations for TSPA-SR	3-144
3-29. Alluvial Uncertainty Zone	3-148
3-30. Simulated Unit Breakthrough Curves of Radionuclide Mass Flux for the Expected-Value Case	3-154
3-31. Simulated Unit Breakthrough Curves and Histogram of Median Transport Times of Mass Flux for Carbon	3-156
3-32. Simulated Unit Breakthrough Curves and Histogram of Median Transport Times of Mass Flux for Technetium	3-157
3-33. Simulated Unit Breakthrough Curves and Histogram of Median Transport Times of Mass Flux for Neptunium	3-158
3-34. Simulated Unit Breakthrough Curves of Mass Flux and Histogram of Median Transport Times for the K_c Model of Colloid-Facilitated Transport for Highly Sorbing Radionuclides	3-159

TABLES

		Page
1-1.	Thirteen AMRs Directly Support the Saturated Zone Process Model Report.....	1-3
1-2.	Roadmap for the Saturated Zone Process Model Report.....	1-7
1-3.	Screening Results for Saturated Zone Features, Events and Processes	1-11
1-4.	Summary of Hypothesis Concerning Flow and Transport Features and Processes.....	1-18
2-1.	Regional-Scale Saturated Zone Flow Models Encompassing Yucca Mountain	2-10
2-2.	Some Sub-Regional Saturated Zone Flow Models in the Yucca Mountain Area	2-11
2-3.	Site-Scale and Subsite-Scale Saturated Zone Flow Models in the Yucca Mountain Area	2-12
3-1.	Transport Parameters Deduced from Bullfrog Tuff and Prow Pass Tuff Tracer Tests	3-33
3-2.	Field- and Laboratory-Derived Sorption (K_d) Parameters for Lithium	3-34
3-3.	Sorption-Coefficient Data and Distributions for Saturated Zone Units.....	3-38
3-4.	Vertical Grid Spacing Used in the Site-Scale Saturated Zone Flow and Transport Model	3-90
3-5.	Number of Nodes Assigned to Hydrogeologic Units in the Site-Scale Saturated- Zone Flow and Transport Model	3-92
3-6.	Permeability Zones Established in Site-Scale Saturated Zone Flow and Transport Model with Upper and Lower Bounds Applied During Calibration	3-100
3-7.	Groundwater Fluxes Computed from the Regional-Scale and Site-Scale Groundwater Flow Models	3-111
3-8.	Saturated Zone Factors Important to Repository Safety and Corresponding Natural Analogues	3-115
4-1.	Issue Resolution Status Report and Key Technical Issues Related to the Saturated Zone Process Model Report.....	4-2
A-1.	Issues for Saturated Zone Flow and Transport	A-1
B-1.	Issue Resolution Status Report Technical Acceptance Criteria.....	B-1

INTENTIONALLY LEFT BLANK

ACRONYMS AND ABBREVIATIONS

AMR	analysis model report
AP	administrative procedure
CNWRA	Center for Nuclear Waste Regulatory Analyses
DIRS	Document Input Reference System
DOE	U.S. Department of Energy
EBS	engineered barrier system
ETF	Effluent Treatment Facility
FEP	feature, event, and process
GFM	geologic framework model
HFM	hydrogeologic framework model
ICPP	Idaho Chemical Processing Plant
INEEL	Idaho National Engineering and Environmental Laboratory
IRSR	Issue Resolution Status Report
ISM	integrated site model
KTI	key technical issue
LA	license application
MM	mineralogic model
NAS	National Academy of Sciences
NRC	U.S. Nuclear Regulatory Commission
NCEWDP	Nye County Early Warning Drilling Program
NTS	Nevada Test Site
NWTRB	Nuclear Waste Technical Review Board
PA	performance assessment
PFBA	pentafluorobenzoate
PMR	process model report
QA	quality assurance
REE	rare-earth element
RPM	rock properties model
RSS	repository safety strategy
SR	site recommendation
SZ	saturated zone

ACRONYMS AND ABBREVIATIONS (Continued)

TSPA	total system performance assessment
USGS	U.S. Geological Survey
UZ	unsaturated zone
VA	viability assessment
YMP	Yucca Mountain Site Characterization Project
YMSD	Yucca Mountain Site Description
1-D	one-dimensional
2-D	two-dimensional
3-D	three-dimensional

1. INTRODUCTION

The U.S. Department of Energy (DOE) is investigating the possibility of using the unsaturated zone (UZ) at Yucca Mountain, Nevada as a permanent repository for the disposal of spent nuclear fuel and high-level radioactive waste. The acceptability of the potential repository is based on the ability of the natural geologic environment and the engineered barrier system (EBS) to prevent migration of radionuclides from a repository to the accessible environment in excess of regulatory limits. The evaluation of the potential repository must consider the potential transport of radionuclides from their introduction at the water table below the repository to a hypothetical well located 20 km (12.5 mi), or at an alternative location specified in regulations, downgradient from the site. CRWMS M&O (2000c) provide details regarding the location of the hypothetical well and the characteristics of the hypothetical receptor, who is an average member of the critical group of people assumed to be most at risk in the proposed U.S. Nuclear Regulatory Commission (NRC) standard (64 FR 8640), or is the reasonably maximally exposed individual in the proposed EPA standard (64 FR 46976). The DOE will also use information about the saturated zone to demonstrate compliance with the EPA's proposed groundwater standard (64 FR 46976). Under the groundwater contamination scenario, the most likely pathway for radionuclides to reach the accessible environment is through the uppermost groundwater aquifers below the potential repository. The role of these aquifers, collectively referred to as the saturated zone (SZ), is to delay the transport of radionuclides to the accessible environment and reduce the concentration of radionuclides before they reach the accessible environment.

The DOE is progressing on an aggressive schedule to complete a Site Recommendation Report (SR) if the site is suitable. The SR will document the information considered by the Secretary of Energy in deciding whether to recommend the Yucca Mountain site to the President for development as a geologic repository for spent nuclear fuel and high-level radioactive waste. A series of documents that include the *Yucca Mountain Site Description* (YMSD) (CRWMS M&O 1998d), the Total System Performance Assessment (TSPA), and a set of nine Process Model Reports (PMRs) support the SR. The PMRs summarize the technical basis for the process models supporting the TSPA. The PMRs are supported by a series of lower-level Analysis Model Reports (AMRs). The relationships among these documents are shown schematically (Figure 1-1). The nine PMRs encompass the following areas:

- Integrated Site Model
- Unsaturated Zone Flow and Transport
- Near Field Environment
- EBS Degradation, Flow, and Transport
- Waste Package Degradation
- Waste Form Degradation
- Saturated Zone Flow and Transport
- Biosphere
- Disruptive Events.

The PMRs contain a summary and synthesis of the detailed technical information presented in the AMRs. This technical information consists of data, analyses, models, software, and

documentation that will be used to demonstrate the applicability of each process model report (PMR) for its intended purpose of evaluating the postclosure performance of the potential Yucca Mountain repository system. The PMR process will ensure the traceability of this information from its source, through the AMRs, PMRs, and eventually to how that information is used in the TSPA.

This document is the PMR for the SZ flow and transport model, and hereafter this report is referred to as the SZ PMR. The SZ PMR considers important features, events, and processes (FEPs) concerning flow and transport through the SZ. The SZ PMR is supported by 13 AMRs that cover specific aspects of SZ flow and transport (Table 1-1). Some of these AMRs are, in essence, data reports with limited in-depth analysis; others primarily discuss development and documentation of computer models; and the remainder document Performance Assessment (PA) abstraction of the models for subsequent use in the YMSD and TSPA.

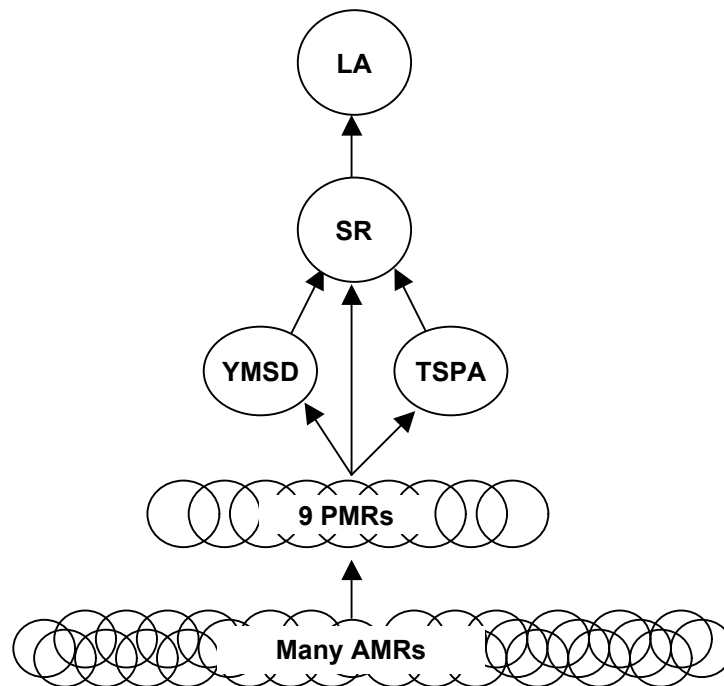


Figure 1-1. Conceptual Relationships Among the Analysis Model Reports, Process Model Reports, and Other Higher-Level Yucca Mountain Site Characterization Project Documents

Table 1-1. Thirteen AMRs Directly Support the Saturated Zone Process Model Report

AMR Title	AMR ID Number	Citation	PMR Section
<i>Hydrogeologic Framework Model for the Saturated Zone Site-Scale Flow and Transport Model</i>	S0000	USGS 2000a	3.1, 3.2
<i>Water-Level Data Analysis for the Saturated Zone Site-Scale Flow and Transport Model</i>	S0005	USGS 2000b	3.1, 3.2, 3.3, 3.4
<i>Recharge and Lateral Groundwater Flow Boundary Conditions for the Saturated Zone Site-Scale Flow and Transport Model</i>	S0010	CRWMS M&O 1999a	3.1, 3.2
<i>Modeling Sub Gridblock Scale Dispersion in Three-Dimensional Heterogeneous Fractured Media</i>	S0015	CRWMS M&O 2000i	3.6, 3.7
<i>Saturated Zone Transport Methodology and Transport Component Integration</i>	S0025	CRWMS M&O 2000j	3.3
<i>Probability Distribution for Flowing Interval Spacing</i>	S0030	CRWMS M&O 2000k	3.6, 3.7
<i>Saturated Zone Colloid-Facilitated Transport</i>	S0035	CRWMS M&O 2000l	3.6, 3.7
<i>Geochemical and Isotopic Constraints on Groundwater Flow Directions, Mixing, and Recharge at Yucca Mountain, Nevada</i>	S0040	CRWMS M&O 2000m	3.3, 3.4
<i>Calibration of the Site-Scale Saturated Zone Flow Model</i>	S0045	CRWMS M&O 2000n	3.3, 3.4
<i>Uncertainty Distributions for Stochastic Parameters</i>	S0050	CRWMS M&O 2000o	3.6, 3.7
<i>Input and Results of the Base Case Saturated Zone Flow and Transport Model for TSPA</i>	S0055	CRWMS M&O 2000p	3.6, 3.7
<i>Features, Events and Processes in SZ Flow and Transport</i>	S0075	CRWMS M&O 2000q	1.0
<i>Unsaturated Zone and Saturated Zone Transport Properties</i>	U0100	CRWMS M&O 2000r	3.1, 3.6, 3.7

Of the 13 supporting AMRs, three describe components, or sub-process models, of the site-scale SZ flow and transport model. These are the AMRs describing the hydrologic framework model (USGS 2000a), the SZ transport methodology (CRWMS M&O 2000j), and the calibrated SZ flow model (CRWMS M&O 2000n). The hydrologic framework model is a methodology to interpolate, extrapolate, and interpret geologic data. The result is a static, three-dimensional (3-D) description of the geometry of hydrostratigraphic units within the region of the site-scale SZ flow and transport model. The transport methodology is an approach, based on particle tracking, to represent advection, dispersion, diffusion, and sorption of radionuclides. Particle tracking is superior to finite element methods for this type of analysis because particle tracking does not introduce numerical dispersion or dilution of the source-term radionuclide concentration. For these reasons, particle tracking is used instead of a finite-element solution of an advection-dispersion equation. The calibrated SZ flow model is intended to provide the best estimate of SZ groundwater flow that is consistent with available measurements of hydraulic head and rock permeability. The remaining 10 PMRs are concerned mainly with data analysis, model abstractions, and parameter distributions.

The basic approach of the SZ PMR is to provide a comprehensive summary of the SZ flow and transport issues that are discussed in the supporting AMRs. The SZ PMR documents the technical basis for evaluations of potential radionuclide migration in the SZ from a potential repository at Yucca Mountain. The SZ PMR contains a summary of relevant site characterization data, a summary of the hydrological setting, the conceptual model of groundwater flow and radionuclide transport based on those data, a description of the resulting

process-level numerical model, and the TSPA analysis methods utilizing that numerical model. These five components of the SZ PMR constitute the logical progression used in the evaluation of the SZ system. This PMR also provides an overview of the models that use output from the SZ PMR. A high-level summary describes how the SZ PMR relates to technical topics presented in other PMRs and relevant Yucca Mountain Site Characterization Project (YMP) documents. In addition, references to sites around the world provide important support to views stated in the PMR.

The objective of the TSPA-SR analyses is to represent flow and transport in the SZ as realistically as possible. However, defensibility of the assumptions, modeling approach, and selection of parameter values was given high priority in developing the site-scale SZ flow and transport model for use in TSPA-SR analyses. Consequently, the use of some model assumptions or parameter distributions yield model results that show more rapid radionuclide transport relative to alternative assumptions or parameter distributions. Conservative bounding of other factors was done when there was not enough information or resolution to realistically model these factors (Section 3.3.6.4) or when inclusion of a particular process was judged to seriously jeopardize the defensibility of the analysis. The resulting potential conservatism in simulations of radionuclide transport with the site-scale SZ flow and transport model may be embedded in the underlying conceptual model, the numerical implementation of the model, or in the uncertainty distributions for parameters used in the TSPA analyses. There is, however, no intent or claim that the overall results of the TSPA-SR are more conservative than the best estimate of expected behavior of the SZ flow and transport system.

Conservative model assumptions are sometimes used to simplify models if more complex models are not defensible or are not needed. For example, sorption of radionuclides onto the surfaces of rock fractures is neglected (Section 3.7.1), transverse dispersion is neglected (Section 3.6.3.3.5), and groundwater flow is assumed to instantaneously adjust to a wetter climate in the future (Section 3.6.3.3.3).

There are two ways in which the distribution of a particular parameter is potentially conservative. First, the mean of the distribution might be biased such that it results in poorer predicted repository performance. This approach is used if an unbiased selection of a mean is not defensible. For example, the uncertainty distribution for sorption coefficient values in volcanic units was selected from among the distributions defined for vitric, devitrified, and zeolitic rock types that constitute the lowest values. Second, the range of a parameter might be unrealistically large if the uncertainty for that parameter is large. Consequently, use of values from one of the tails of the distribution could result in unrealistically poor estimates of performance. Specific discharge is, for example, one parameter with a large range. Calculations using values from the fast tail of this distribution could result in unrealistically fast transport of radionuclides.

Since 1983, under authority of the Nuclear Waste Policy Act of 1982, the DOE has been investigating a site at Yucca Mountain, Nevada, to determine whether it is suitable for development as the nation's first repository for permanent geologic disposal of spent nuclear fuel and high-level radioactive waste. If the site is found suitable, there is an additional goal of licensing, constructing, operating, and closing a high-level waste disposal facility. These suitability investigations, referred to as site characterization, have been designed to yield

information to support a determination of whether there is reasonable assurance that a monitored geologic repository constructed at Yucca Mountain would not pose an unreasonable risk to public health and the environment. The three main components of site characterization are testing, design, and PA.

In this PMR, details of the SZ modeling efforts are provided. The SZ flow and transport process model (i.e., the model rather than the report) describes the movement of contaminants and groundwater through the SZ (i.e., in the aquifers below Yucca Mountain) to simulate the potential transport and release of radionuclides from a repository. This information is used in PA models to predict the possible dose that a receptor (e.g., a hypothetical human who is a member of the critical group) might be expected to receive during the postclosure period.

The relationship among the SZ PMR and the constituent sub-process models, abstraction models, and analyses (as applicable) developed under administrative procedure (AP) AP-3.10Q, Analyses and Models, is shown schematically in Figure 1-2. As depicted, a set of models and analyses provide data and information to the site-scale SZ flow and transport model (a process level model). This model, plus additional models and analyses, provide information and data to the site-scale SZ flow and transport model for TSPA (the PA Abstraction). Finally, the results of this model, plus additional supporting information and the results of other PMRs and AMRs (not shown in Figure 1-2), provide data for the TSPA dose calculations, the results of which address dose to the accessible environment.

The SZ PMR is organized as follows (Table 1-2):

Chapter 1. Description of the objectives and scope of the PMR and the principal factors and other factors that were identified in the Repository Safety Strategy (RSS) (CRWMS M&O 2000a). The key hypotheses for the PMR are described as well as SZ flow and transport issues raised by various overseeing bodies, peer review groups, PA workshops, the NRC, and others. Chapter 1 concludes with the Quality Assurance (QA) status and issues regarding the data and software used in the supporting AMRs.

Chapter 2. Evolution of field and laboratory testing, data collection activities, process modeling, and TSPA modeling of flow and transport in the SZ at Yucca Mountain. The rationale for the evolution of the testing program and the major advances that have been made in modeling of the SZ are presented in this section.

Chapter 3. Main technical information in the SZ PMR. All of the sub-process models that are considered in the SZ PMR, and how they are abstracted for use in TSPA, are described and summarized in this section. These descriptions and summaries include the site-scale SZ flow and radionuclide transport model. In addition, the necessary framework for the models in terms of hydrogeological information, conceptual models, and numerical grids are presented in this section.

Chapter 4. Key Technical Issues (KTIs) on SZ flow and transport that have been identified by the NRC. Each KTI is identified, and pointers are provided to the relevant sections in the SZ PMR where the KTIs are discussed.

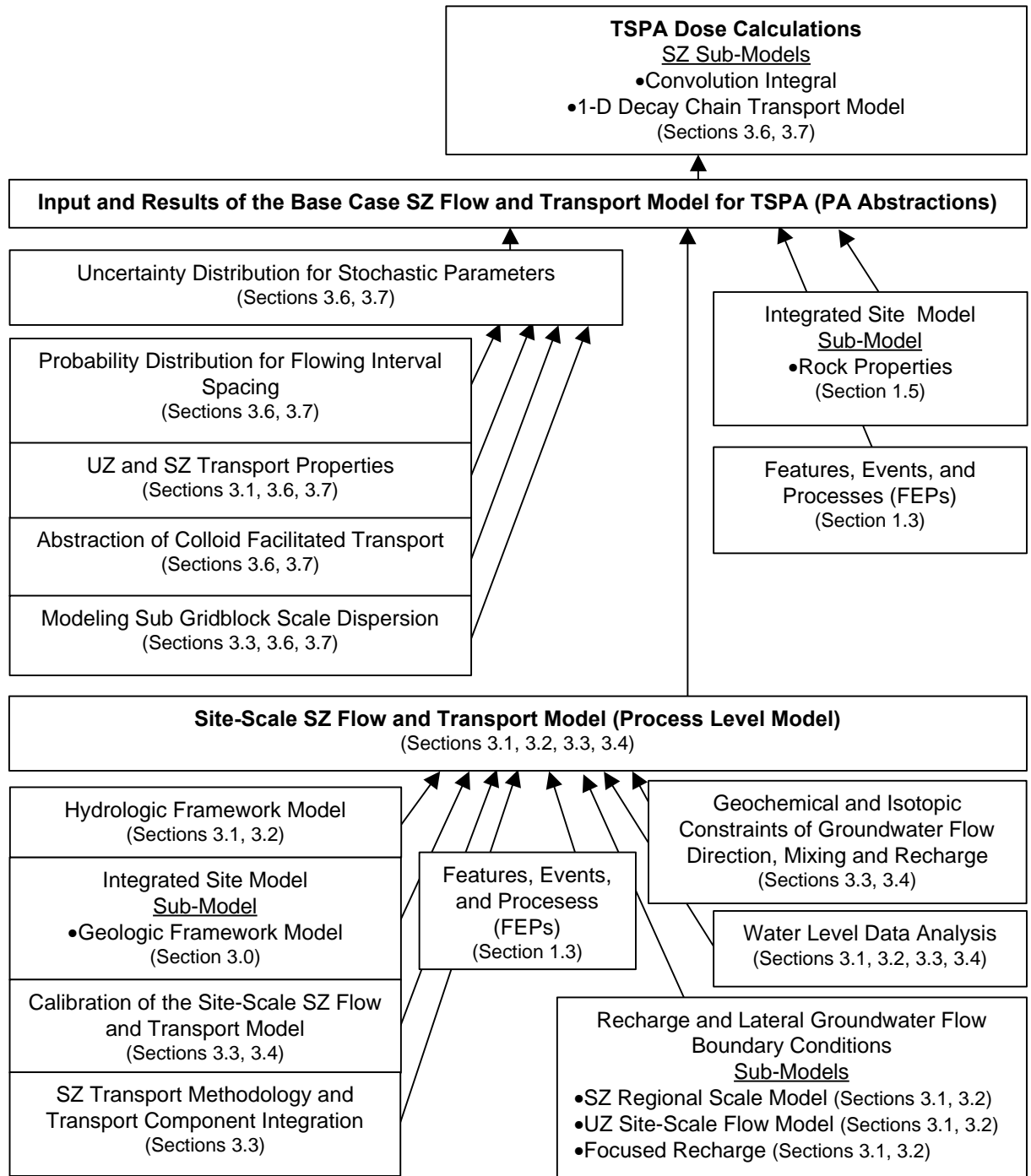


Figure 1-2. Relationship Among Saturated Zone Models and Analyses

Table 1-2. Roadmap for the Saturated Zone Process Model Report

Information	Report Section	Cross-Referencing
Objectives and Scope of the PMR	Section 1.1 and 1.2	N/A
Key Issues for the SZ PMR	Section 1.6	Pointers to sections of the PMR for detailed discussions.
Key Issues from NRC, Nuclear Waste Technical Review Board (NWTRB), Peer Review Groups, and others	Section 1.6	Pointers to sections of the PMR where each issue is discussed.
Features, Events, and Processes and their Screening	Section 1.3	N/A
Evolution of Field Testing and Model Development	Section 2	N/A
Data and Conceptual Models	Section 3.1 and 3.2	N/A
Key SZ PMR Models and Analysis	Section 3.3 through 3.7	For each model, data inputs, relationships to other models, data outputs, and intended uses in TSPA are described.
Alternate Views	Section 3.8	N/A
Key NRC Issues and Subissues	Section 4	Pointers to sections of the PMR where each issue is discussed.
Summary and Conclusions	Section 5	N/A

Chapter 5. Summary and conclusions of the SZ PMR.

Chapter 6. References.

Appendix A. Issues for SZ flow and transport, including source and PMR approach.

Appendix B. NRC issue resolution status reports (IRSRs) and KTIs, including IRSR technical acceptance criteria.

1.1 OBJECTIVE

The main objectives of the SZ PMR are:

- To synthesize all important data, analyses, model, and model abstractions of flow and transport within the SZ in a single document
- To summarize the development of the site-scale SZ flow and transport model and key sub-process models used to analyze the various data sets from the SZ
- To summarize the abstraction process and results for the site-scale SZ flow and transport model used for TSPA.

The various AMRs supporting this PMR, and the PMR itself, are key documents that the YMP will rely upon and reference in the SR.

1.2 SCOPE

This section explains the information presented in, and the content of, the SZ PMR. It uses flowcharts to show the evolution of information from data to TSPA output and the evolution of information within the SZ PMR. The section also describes where to find relevant subject matter not included in the SZ PMR. References to related discussions in Chapter 2 are provided. This PMR is written for a readership of knowledgeable persons in technical and regulatory fields.

1.2.1 Scope of the Saturated Zone Flow and Transport Process Model Report

The purpose of the site-scale SZ flow and transport model is to describe the spatial and temporal distribution of groundwater as it moves from the water table below the potential repository, through the SZ, and to the point of uptake by the receptor of interest. The SZ processes that control the movement of groundwater and the movement of dissolved radionuclides and colloidal particles that might be present, and the processes that reduce radionuclide concentrations in the SZ, are described.

Summary information from other PMRs (e.g., the UZ PMR and the Integrated Site Model [ISM] PMR), the interface between this PMR and the TSPA document, and the conclusions of this PMR are described. The discussion of model inputs and outputs, as implemented in the AMRs, is restricted to information needed for the assessment of postclosure performance of the potential repository.

1.2.2 Principal Factors and Other Factors Considered

The magnitude of the YMP, and the complexities associated with both the natural and engineered systems, dictate that the YMP prioritize its activities and focus on the factors most important to performance, hereafter named the Principal Factors. The principal factors are integral to the potential RSS that supports the postclosure repository safety case. The principal factors are those central to determining and demonstrating long-term safety of the repository system. In the RSS (CRWMS M&O 2000a), 7 principal factors, and 20 Other Factors of second-order importance, have been identified. The selection of the principal factors was based on preliminary TSPA analyses and expert judgement. The 7 principal factors, the 20 other factors, and the PMR to which each factor belongs are listed in the RSS (CRWMS M&O 2000a, Table 3-1).

The principal and other factors provided the focus of planning documents in support of the SR and license application (LA) decisions discussed in Volume 4 of the Viability Assessment (VA) (DOE 1998a). Since the VA, SR work has been underway following the planning documents.

Four important features of the SZ were identified during the RSS (CRWMS M&O 2000a) analyses. For the site-scale SZ flow and transport model, two principal factors (retardation of radionuclide and dilution of radionuclide concentrations during migration) and two other factors (advective pathways and colloid-facilitated transport) were identified.

1.2.2.1 Principal Factors

The principal factors of the post closure case are those central to determining and demonstrating long-term safety of the repository system (CRWMS M&O 2000a). The two factors given below are the only principal factors relevant to the SZ (CRWMS M&O 2000a, Table 3-1).

Retardation of Radionuclide Migration—This factor describes the effect of processes that delay the transport of dissolved or colloidal radionuclides in groundwater moving through the volcanic aquifers and alluvial valley fill of the SZ. This factor focuses on radionuclides that are important to system performance but could experience substantially retarded migration in the SZ. In the current approach to the postclosure safety case:

- The site-scale SZ flow and transport model would be used to estimate advective pathways below the water table; in particular, the pathways in the alluvium.
- Retardation in the SZ would be estimated using the site-scale SZ flow and transport model and appropriate input parameters for the radionuclides that may be of particular importance to dose but may experience considerable retardation (i.e., neptunium, plutonium, and uranium).

Dilution of Radionuclide Concentrations During Migration—This factor describes the reduction of radionuclide concentration and spreading of the contaminant plume in groundwater that occur during transport in the SZ flow system. The dominant processes are dispersion of the contaminant plume during migration through heterogeneous media, mixing of groundwater from different sources, and dilution during pumping. Dilution during pumping is expected to be the most important of these three. The dose rate is estimated assuming a pumping volume based on the water use of the hypothetical community defined in applicable regulations as defined in proposed 10 CFR 63 (64 FR 8640).

1.2.2.2 Other Factors

Advective Pathways in the Saturated Zone—This factor describes the pathways for water that might transport radionuclides in the SZ and includes the pathways through the volcanic aquifers and the valley-fill alluvium in Amargosa Valley. In general, the site-scale SZ flow and transport model is used to estimate the advective pathways below the water table.

Colloid-Facilitated Transport in the Saturated Zone—This factor describes the transport of radionuclides sorbed to colloids, in moving groundwater. Preliminary analyses for the VA (DOE 1998a) indicate that colloid-facilitated transport of plutonium provided an important contribution to annual dose, and additional work in this area is underway by the YMP. For the postclosure safety case, this evaluation is conducted using simplifications in the representation of colloid-facilitated transport of radionuclides.

1.3 FEATURES, EVENTS, AND PROCESSES

An initial set of FEPs was developed for the YMP TSPA by combining lists of FEPs identified as relevant to the YMP (CRWMS M&O 1999b). This combined list consists of 1,261 FEP entries from the Nuclear Energy Agency working group, 292 FEPs from YMP literature and site

studies, and 82 FEPs identified during YMP project staff workshops. The FEPs were identified by a variety of methods including expert judgment, informal elicitation, event tree analysis, stakeholder review, and regulatory stipulation. All potentially relevant FEPs have been included, regardless of origin. The compilation included the FEP entries and 151 layers, categories, and headings, resulting in a list of 1,786 FEPs. This approach led to considerable redundancy in the FEP list because the same FEPs frequently are identified by multiple sources, but it also ensures that a comprehensive review of narrowly defined FEPs will be performed.

Each FEP has been classified as either primary or secondary. This classification resulted in the identification of 310 primary FEPs for which detailed screening arguments are developed. The classification and description of primary FEPs strives to capture the essence of all secondary FEPs that map to the primary. Secondary FEPs are either FEPs that are completely redundant or that can be aggregated into a single primary FEP. The primary FEPs have been assigned to associated PMRs. The assignments were based on the nature of the FEPs so that the analysis and resolution for screening decisions reside with the subject-matter experts in the relevant disciplines. The resolution of other than system-level FEPs are documented in AMRs prepared by the responsible PMR groups. In this section, a summary of the screening decisions associated with the FEPs for the SZ PMR group is presented. Details of the screening processes are documented by CRWMS M&O (2000q).

The purpose of FEPs screening is to document and justify the treatment of the primary FEPs identified as potentially affecting the SZ. The FEPs that are deemed potentially important to repository performance are evaluated, either as components for the TSPA or as separate analyses in the AMR. The scope for this activity involves two tasks:

- Identify FEPs that are considered explicitly in the TSPA (called included FEPs) and describe how those FEPs are included in the TSPA.
- Identify FEPs that do not need to be included in the SZ flow and transport models and justify why these FEPs do not need to be included.

Of the original list of FEPs, 46 primary FEPs were identified as potentially affecting the SZ. The approach used for this analysis is a combination of qualitative and quantitative screening. The analyses are based on the criteria provided by the NRC in the proposed 10 CFR 63 (64 FR 8640) and by the U.S. Environmental Protection Agency in the proposed 40 CFR 197 (64 FR 46976) to determine whether or not each FEP should be included in the TSPA. For FEPs that are excluded from the TSPA based on NRC or U.S. Environmental Protection Agency criteria, the screening argument includes a summary of the basis and results that indicate either low probability or low consequence. As appropriate, screening arguments cite work performed outside this activity, such as in other AMRs.

FEPs designated as included are those directly represented in TSPA models and process-level models that support TSPA. Therefore, the treatment of these FEPs is described in other sections of this document and in the associated AMRs. Twenty-two of the primary SZ FEPs are included in the TSPA. Eighteen of the SZ FEPs do not need to be included in the SZ flow and transport model based on insignificant consequence. The six remaining FEPs are related to the thermal effects of the potential repository on the geosphere, and igneous and tectonic activity. Due to

their potential impact on the waste package and UZ flow and transport, these six FEPs are evaluated in separate PMRs. Some of these FEPs are excluded from the TSPA on the basis of low probability of occurrence or insignificant consequence. Others are included in the UZ flow and transport models or in the analysis of disruptive events (CRWMS M&O 2000d).

For example, the probability and potential effects of water table rise on the UZ are evaluated in CRWMS M&O (2000b). Because the FEPs related to water table rise are evaluated with respect to their effects on UZ flow and transport processes (e.g., shorter travel path through the UZ) it is considered appropriate that all potentially significant effects will be represented as variability in timing and rate of contaminant transport to the SZ. This would affect the input parameter values for the site-scale SZ flow and transport model but would not require alteration of the site-scale SZ flow and transport model.

The primary FEPs identified as potentially affecting SZ flow and transport are listed in Table 1-3. This table shows the FEP number, FEP description, screening decision (include, exclude, or not include in SZ PMR), and basis for exclusion and non-inclusion decisions. Details of the screening processes and arguments and disposition of individual SZ FEPs are discussed in CRWMS M&O (2000q).

Table 1-3. Screening Results for Saturated Zone Features, Events and Processes

YMP FEP Database ID Number	FEP Description	TSPA Screening Decision
1.2.02.01.00	Additional Fractures	Not included in SZ PMR – low consequence
1.2.02.02.00	Faulting	Not included in SZ PMR – low consequence
1.2.03.01.00	Seismic Activity	Not included in SZ PMR – low consequence
1.2.04.02.00	Igneous Activity Causes Changes to Rock Properties	Not included in SZ PMR - low consequence
1.2.06.00.00	Hydrothermal Activity	Not included in SZ PMR – low consequence
1.2.09.02.00	Large-Scale Dissolution	Not included in SZ PMR – low consequence
1.2.10.01.00	Hydrologic Response to Seismic Activity	Not included in SZ PMR – low consequence
1.2.10.02.00	Hydrologic Response to Igneous Activity	Not included in SZ PMR - low consequence
1.3.07.01.00	Drought/Water Table Decline	Not included in SZ PMR - low consequence
1.3.07.02.00	Water Table Rise	Included changes in flux, other effects not included in SZ PMR - assumed low consequence
1.4.07.01.00	Water Management Activities	Included
1.4.07.02.00	Wells	Included
2.1.09.21.00	Suspension of Particles Larger than Colloids	Not included in SZ PMR - low consequence
2.2.03.01.00	Stratigraphy	Included
2.2.03.02.00	Rock Properties of Host Rock and Other Units	Included
2.2.06.02.00	Changes in Stress Produce Change in Permeability of Faults	Not included in SZ PMR - low consequence
2.2.06.03.00	Changes in Stress Alter Perched Water Zones	Not included in SZ PMR - low consequence

Table 1-3. Screening Results for Saturated Zone Features, Events and Processes (Continued)

YMP FEP Database ID Number	FEP Description	TSPA Screening Decision
2.2.07.12.00	Saturated Groundwater Flow	Included
2.2.07.13.00	Water-Conducting Features in the Saturated Zone	Included
2.2.07.14.00	Density Effects on Groundwater Flow (Concentration)	Excluded - low consequence
2.2.07.15.00	Advection and Dispersion	Included
2.2.07.16.00	Dilution of Radionuclides in Groundwater	Included
2.2.07.17.00	Diffusion in the Saturated Zone	Included
2.2.08.01.00	Groundwater Chemistry/Composition in UZ and SZ	Included
2.2.08.02.00	Radionuclide Transport Occurs in a Carrier Plume in the Geosphere	Included
2.2.08.03.00	Geochemical Interactions in the Geosphere	Included
2.2.08.06.00	Complexation in the Geosphere	Included
2.2.08.07.00	Radionuclide Solubility Limits in the Geosphere	Not included in SZ PMR - low consequence
2.2.08.08.00	Matrix Diffusion in Geosphere	Included
2.2.08.09.00	Sorption in the UZ and SZ	Included
2.2.08.10.00	Colloid Transport in the Geosphere	Included
2.2.08.11.00	Distribution And Release of Nuclides from the Geosphere	Included
2.2.09.01.00	Microbial Activity in Geosphere	Included
2.2.10.01.00	Repository Induced Thermal Effects in the Geosphere	Not included in SZ PMR - assumed low consequence or probability
2.2.10.02.00	Thermal Convection Cell Develops in SZ	Not included in SZ PMR - low consequence
2.2.10.03.00	Natural Geothermal Effects	Included
2.2.10.06.00	Thermo-Chemical Alteration	Included
2.2.10.07.00	Thermo-Chemical Alteration of the Calico Hills Unit	Not included in SZ PMR - assumed low consequence or probability
2.2.10.08.00	Thermo-Chemical Alteration of the SZ	Not included in SZ PMR - assumed low consequence or probability
2.2.10.13.00	Density Driven Groundwater Flow (Thermal)	Not included in SZ PMR – assumed low consequence
2.2.11.01.00	Naturally-Occurring Gases in the Geosphere	Not included in SZ PMR - low consequence
2.2.12.00.00	Undetected Features	Included
2.3.02.02.00	Radionuclide Accumulation in Soils	Not included in SZ PMR - low consequence
2.3.11.04.00	Groundwater Discharge to Surface	Excluded - low consequence
3.1.01.01.00	Radioactive Decay and Ingrowth	Included
3.2.07.01.00	Isotopic Dilution	Excluded - low consequence

1.4 QUALITY ASSURANCE

Pursuant to evaluations (CRWMS M&O 1999d, 1999e) performed in accordance with QAP-2-0, *Conduct of Activities* (Superseded by AP-2.21Q, *Quality Determinations and Planning for Scientific, Engineering, and Regulatory Compliance Activities*), it was determined that activities supporting development of the SZ PMR and its component models and their documentation are quality-affecting activities that are subject to the QA requirements of the *Quality Assurance Requirements and Description* (DOE 2000).

The SZ PMR was prepared in accordance with AP-3.11Q, *Technical Reports*, and reviewed in accordance with AP-2.14Q, *Review of Technical Products*. The QA procedures under which the component AMRs were developed are identified in the respective AMRs and associated planning documents. The AMRs were prepared and reviewed in accordance with AP-3.10Q, *Analyses and Models*. This technical product was planned in accordance with AP-2.13Q, *Technical Product Development Planning*, under a document development plan (CRWMS M&O 2000u), and in accordance with AP-2.15Q, *Work Package Planning Summaries*, under four work package planning summaries (CRWMS M&O 1999c; 1999f; 1999g; and 1999h).

This document may be affected by technical product input information that requires confirmation. Any changes to the document that may occur as a result of completing the confirmation activities will be reflected in subsequent revisions. The status of the input information quality may be confirmed by review of the Document Input Reference System (DIRS) database.

1.4.1 Acquired and Developed Data

The status of the acquired and developed data that support this PMR is included in the supporting AMRs and in the DIRS database. The data are incorporated in the Technical Data Management System. Data verification and qualification were carried out in accordance with procedures AP-3.15Q, *Managing Technical Product Inputs*, and AP-SIII.2Q, *Qualification of Unqualified Data and the Documentation of Rationale for Accepted Data*.

This document and its conclusions may be affected by technical product input information that requires confirmation. Any changes to this document or its conclusions that may occur as a result of completing the confirmation activities will be reflected in subsequent revisions. The status of the input information quality may be confirmed by review of the DIRS database.

1.4.2 Software

No software codes or routines were used directly in the development of the PMR. However, all software codes and routines used in the analyses and models supporting this PMR, and the quality status of those codes, are listed in the appropriate AMRs. These codes were managed in accordance with AP-SI.1Q, *Software Management*, or used under Section 5.11 of AP-SI.1Q. The primary software codes used in the SZ models and analysis are:

- **FEHM** (Finite Element Heat and Mass) is used to calculate hydrologic flow and the transport of radionuclides, the latter by a particle-tracking algorithm. This software was used in CRWMS M&O (2000i; 2000j; 2000n; 2000p).

- **LaGriT** (Los Alamos Grid Toolbox) is used for generating 3-D finite element and finite volume meshes. This software was used in CRWMS M&O (2000n).
- **PEST** (parameter estimation) is used to perform the parameter optimization for the hydrogeologic and feature permeabilities optimization algorithm. PEST is used in conjunction with FEHM to produce the calibrated site-scale SZ flow and transport model. This software was used in CRWMS M&O (2000n).
- **STRATAMODEL** is used to perform 3-D geological modeling. This software was used in USGS (2000a).
- **GoldSim** is used to perform probabilistic simulations of complex systems such as simulating the entire potential repository and natural system for TSPA. Parameter definitions and distributions, used as input to the site-scale SZ flow and transport model, are simulated using GoldSim. Radionuclide mass breakthrough curves, produced by the site-scale SZ flow and transport model, are provided as input to GoldSim to estimate radionuclide mass flux at the interface of the SZ and the biosphere. This software was used in CRWMS M&O (2000l; 2000o; 2000p).

1.5 RELATIONSHIP TO OTHER PROCESS MODEL REPORTS AND KEY PROJECT DOCUMENTS

The overall relationship between this SZ PMR and other key project documents is shown in Figure 1-1. More specifically, the SZ PMR interfaces directly with three other PMRs: the *ISM PMR* (CRWMS M&O 2000e), the *UZ Flow and Transport Model PMR* (CRWMS M&O 2000b), and the *Biosphere PMR* (CRWMS M&O 2000c). The SZ PMR summarizes inputs from the ISM and UZ PMRs, and discusses outputs of the SZ PMR to the TSPA-SR calculations. In this section, a summary-level statement of purpose and a description of each of these PMRs are given. In addition, the way in which the SZ PMR interfaces and overlaps with these three PMRs is discussed.

1.5.1 Integrated Site Model Process Model Report

The ISM PMR (CRWMS M&O 2000e) describes the overall framework for discussing the geologic properties (e.g., stratigraphy, structural characteristics, rock properties, and mineralogic properties) of the Yucca Mountain site. The ISM, which incorporates three other models, merges details of the Yucca Mountain geology into a single model that can be used for subsequent simulation (e.g., hydrologic flow and radionuclide transport models) and design of the potential repository. The ISM PMR summarizes the outputs that are input to the UZ flow and transport model, the SZ flow and transport model, the tectonic hazards analysis, and the EBS design.

The three components of the ISM are the geologic framework model (GFM), the rock properties model (RPM), and the mineralogic model (MM). The GFM is a description of the distributions of rock layers and faults in the subsurface at Yucca Mountain, and it is the framework into which rock properties and mineralogic distributions are placed, and thus serves as the framework of the ISM. The GFM is a 3-D interpretation of the geology surrounding the location of the potential

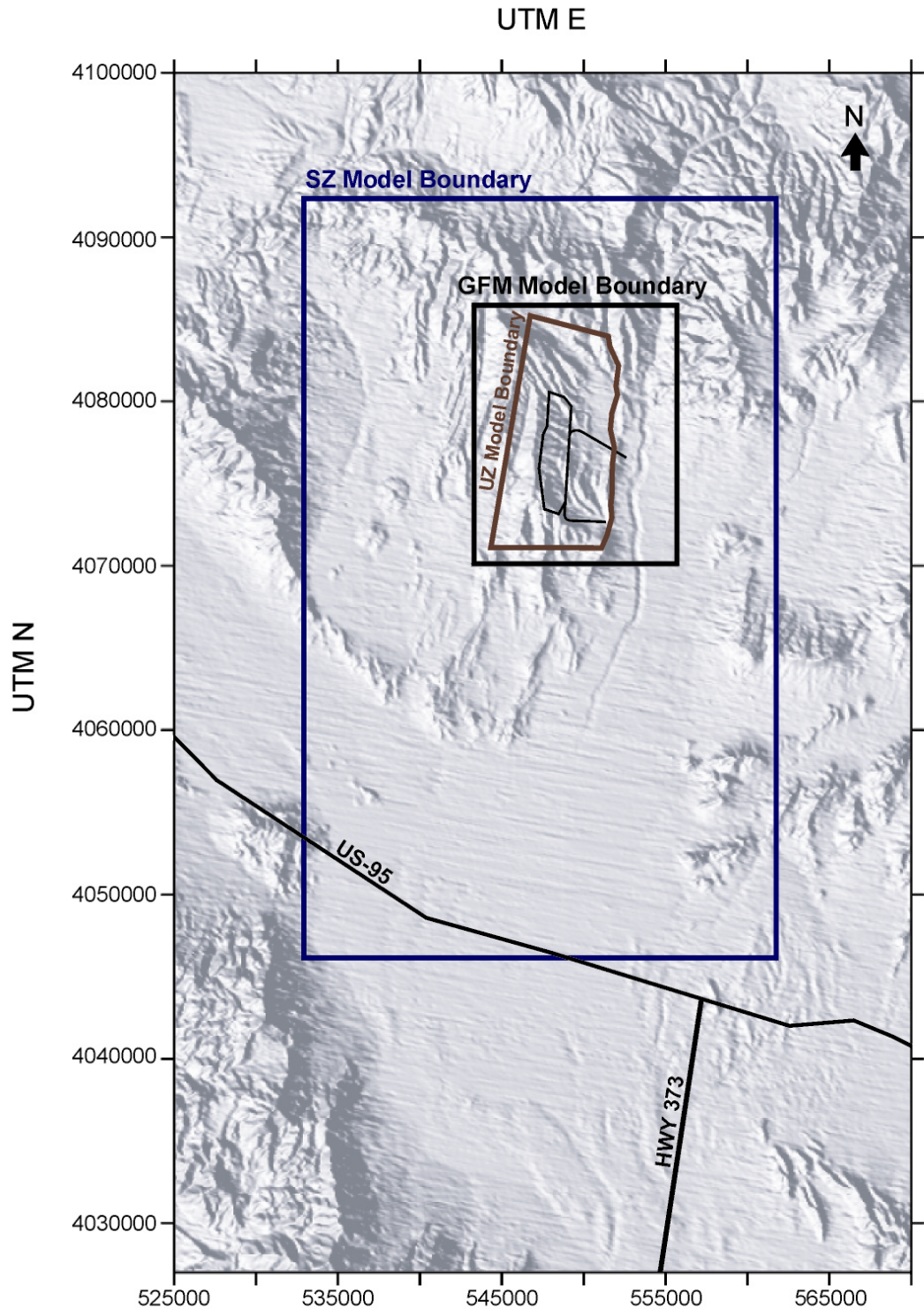
repository, an area of 170 km² (66 mi²) and a volume of 771 km³ (185 mi³) (Figure 1-3). The boundaries of the GFM were chosen to encompass a widely distributed set of exploratory boreholes and the area of interest for hydrologic flow and radionuclide transport modeling through the UZ. The depth of the model is constrained by the estimated depth of the Tertiary-Paleozoic unconformity that reaches a depth of 3,962 m (13,000 ft) in the area considered by the model. The GFM was constructed primarily from geologic map and borehole data, but information from measured stratigraphy sections, gravity profiles, and seismic profiles were incorporated where appropriate. The GFM is incorporated into the hydrogeologic framework model (HFM) for the site-scale SZ flow and transport model, which encompasses a much larger volume than the GFM. The hydrogeologic framework development is discussed in the HFM AMR (USGS 2000a). The HFM provides a representation of the spatial distribution of hydrologic properties for the 3-D site-scale SZ flow and transport model domain. This representation, in turn, is founded on the underlying geologically defined stratigraphic and structural framework.

The RPM is a description of the rock material properties including matrix porosity, whole-rock bulk density, matrix-saturated hydraulic conductivity, lithophysal porosity, and whole-rock thermal conductivity for most of the stratigraphic intervals described in the GFM. The RPM results in a spatial distribution of the rock properties based on the locations and uncertainty in measured values within the UZ at Yucca Mountain. Values of matrix porosity and bulk density from the RPM are incorporated in the site-scale SZ flow and transport model.

The MM is a 3-D weighted, inverse distance model that enables project personnel to calculate mineral abundance at any position, within any region, or within any stratigraphic unit in the model volume to support the analyses of hydrologic properties, radionuclide transport, mineral health hazards, potential repository performance, and potential repository design. The MM is referenced to the stratigraphic framework defined in the GFM and was developed from mineralogic data obtained from boreholes. The MM supports the analyses of hydrologic properties, radionuclide transport, mineral health hazards, potential repository performance, and potential repository design.

1.5.2 Unsaturated Zone Flow and Transport Process Model Report

The UZ flow and transport PMR (CRWMS M&O 2000b) describes the processes affecting the amount of water entering and flowing through the UZ above the potential repository, contacting wastes in the potential repository, and the movement of water with dissolved radionuclides or colloidal particles through the UZ below the potential repository. The purpose of the model is to describe the spatial and temporal distribution of water flow through the UZ and the spatial and temporal distribution of water seepage into the underground openings of the potential repository. The UZ flow and transport PMR also describes inputs from other PMRs and outputs from the UZ flow and transport model to the SZ flow and transport model, the EBS design, and the TSPA. The emphasis of the discussion of model inputs and outputs is on information needed for the assessment of postclosure performance. The SZ flow and transport model receives inputs of spatial and temporal distribution of recharge and radionuclide mass from the UZ flow and transport model for the purpose of TSPA calculations.



00034DC-SZ-PMR-36.cdr

Figure 1-3. Domains of the Site-Scale Saturated Zone Flow and Transport Model, the Geologic Framework Model, and the Unsaturated-Zone Model

Recharge boundary conditions for the SZ model (UZ domain) are specified based on the groundwater flux simulated at the base of the UZ model. Coupling of radionuclide transport between the UZ and the SZ is accomplished using the convolution integral method. The convolution integral method is used to combine the unit breakthrough curves calculated by the SZ flow and transport model with the time-varying radionuclide sources from the UZ.

1.5.3 Biosphere Process Model Report

The Biosphere PMR (CRWMS M&O 2000c) describes the processes affecting the movement of radionuclides after they have been released from the geosphere to the environment. The biosphere model describes the lifestyle and habits of individuals living in present-day Amargosa Valley and produces dose conversion factors that are used by TSPA to estimate the annual dose to which those persons might be exposed. The model considers three basic exposure pathways (inhalation, ingestion, and external exposure) by which radionuclides could travel from groundwater (via a well that is located 20 km [12.5 mi] from Yucca Mountain) to a receptor. Radionuclides considered are those expected to be responsible for contributing the most to human dose. The environmental pathways, radionuclide inventory, and unit concentrations (1 pCi/L) of these radionuclides are used to calculate biosphere dose conversion factors. Biological dose conversion factors based on unit concentrations permit researchers to calculate doses expected to be received from any concentration.

1.5.4 Relationship with Other Key Yucca Mountain Project Documents

Regulatory requirements and SR/LA design feed the allocation analysis and the RSS (CRWMS M&O 2000a). The RSS determines the most important factors (principal factors) that affect performance of the potential repository. The RSS provides input to the AMRs and the SZ PMR; the AMRs also feed the SZ PMR. The SZ PMR, along with eight other PMRs, provide input to the TSPA and the YMSD.

1.6 ISSUES FOR SATURATED ZONE FLOW AND TRANSPORT

1.6.1 Summary of Current Understanding of Saturated Zone Flow and Transport at Yucca Mountain

The SZ PMR considers many parameters, processes, and models that describe the flow of water and transport of materials from under Yucca Mountain to the proposed compliance boundary in the Amargosa Valley. An understanding of SZ flow and transport has been gained through the collection of site data and the modeling of relevant processes. Hypotheses that reflect the current understanding of some flow and transport features and processes are summarized in Table 1-4, and pointers are provided from each statement to the detailed discussions in relevant sections of the PMR. The statements listed in the “Current Understanding” column of Table 1-4 are a mixture of observations, hypothesis, and modeling insight and only should be considered brief summaries of complex information.

Table 1-4. Summary of Hypothesis Concerning Flow and Transport Features and Processes

Type	Current Understanding	Addressed in Section
Recharge to the SZ	Recharge to the SZ is localized and focused at higher elevations and along major surface drainage channels.	3.1.1.1.2, 3.1.1.1.3, 3.2.3.2
Flow Through the Tuff	Groundwater flow in the volcanic tuffs primarily occurs in fractures and in discrete flowing intervals.	3.2.4.1
Matrix Diffusion in the Tuffs	Matrix diffusion occurs in the volcanic tuffs in which radionuclides can diffuse from the fast flowing groundwater in fractures into the stagnant water in the matrix.	3.2.4.2, 3.3.2, 3.3.4
Dispersion in the Tuffs	Transverse dispersion in the volcanic tuffs and alluvium	3.7.2
Large Hydraulic Gradient	The large hydraulic gradient is caused by low-permeability material upgradient from Yucca Mountain. Alternative view: The large hydraulic gradient is a reflection of perched water bodies above the main groundwater system. Regardless of the cause of this hydraulic feature, it is represented in the SZ flow and transport model in such a way that it represents the measured heads.	3.2.5.1 3.2.2.3, 3.2.5.1
Role of Faults	Faults may be high permeability features that provide a fast flow path. Alternatively, faults may have low permeability due to rock alteration or formation of gouge. In addition, faults alter the permeability to flow crossing the fault by offsetting or juxtaposing hydrostratigraphic units	3.2.3.4, 3.2.2.3, 3.2.2.5
Horizontal Anisotropy	Horizontal anisotropy in permeability may be caused by the preferential orientation of faults and fracture zones.	3.2.5.3
Groundwater Flow in the Alluvium	The alluvium behaves as a porous medium. Consequently, average flow rates are slower than in the tuffs, and more matrix surface area is available for sorption.	3.7.2
Alluvium in the Flow Path	The flow path from the potential repository transitions from the volcanic tuffs into the alluvium	3.7.2
Sorption in Alluvium	Laboratory analyses of samples from the alluvium indicate that sorption of some radionuclides (neptunium and iodine) is greater in the alluvium than in tuffs.	3.1.4.1
Upward Hydraulic Gradient	Increasing hydraulic head with depth, which may result into upward flow from the Carbonate aquifer to the overlying volcanic aquifers, was documented in UE-25P#1 (the deep well) in the Yucca Mountain area. Other wells completed in the carbonate aquifer on the Nevada Test Site also have noted the increasing heads with depth. The site-scale SZ flow and transport model simulates an upward hydraulic gradient in this area. The upward flow will keep the flow paths from the potential repository confined to the shallow groundwater at or slightly below the water table.	3.2.2.3, 3.4.3, 3.1.2.3
Sorption in Volcanic Units	Sorption of radionuclides may occur in the matrix of fractured tuffs.	3.2.4.3
Climate Change	In the future, wetter, glacial climate conditions will result in faster groundwater flow in the SZ and higher water table elevations.	3.2.6

The YMP has received extensive and detailed input from internal and external peers, experts, and oversight groups concerning the credibility and defensibility of the YMP in general and the TSPA prepared for the VA (DOE 1998b). Many of the issues concern how the YMP is addressing SZ flow and transport (Appendix A). Issues were identified, and a workshop was held in February 1999 (Kuzio 1999) to identify how these issues would be addressed in future iterations of the TSPA. The YMP also must address the KTIs that have been identified by the NRC as the basis for acceptance criteria for a LA. These issues, and others raised at and since

the February 1999 workshop, are discussed and identified in the following sections and in Appendices A and B.

1.6.2 Issues from the Total System Performance Assessment-Viability Assessment

The data and analyses in the TSPA-VA (DOE 1998b) provide part of the information needed to evaluate performance of the potential repository. The analyses include an assessment of model enhancements and analyses that could improve future assessments of performance of the potential repository, including the representation of SZ flow and transport. Issues that were identified as having the potential to enhance confidence in the future assessments of SZ flow and transport, and suggestions that were made for additional work, are summarized in this section.

Issues for SZ flow and transport that were recognized in the TSPA-VA (DOE 1998b) include:

- Data are lacking for the SZ from approximately 10 km (6.2 miles) downgradient from the potential repository to 20 km (12.5 miles) downgradient.
- There is uncertainty about where flow in the shallow SZ enters alluvium along the flow path, or even if flow occurs in the alluvium within 20 km (12.5 miles) of the potential repository.
- There are few site-specific data on the hydraulic, mineralogic, or geochemical characteristics of the downgradient alluvium.
- Additional SZ geochemical and isotopic data are needed.
- Reliable age dating of groundwater is needed along the flow path downgradient from the potential repository.
- Additional oxidation/reduction potential data from the SZ are needed.
- Additional measurements of hydraulic and transport parameters are needed from locations and depths that have not yet been tested.
- Hydrochemical data are needed from existing boreholes and new Nye County Early Warning Drilling Program (NCEWDP) boreholes, and these data need to be incorporated into the conceptual and predictive models for SZ processes.
- Whether sorption onto colloids is reversible or irreversible needs to be evaluated.
- A 3-D flow model for the SZ is needed. An improved, site-scale flow model should be consistent with all available data from the site.
- Variability and uncertainty should be incorporated in aquifer properties and numerical methods for simulating solute transport with minimal numerical dispersion.
- Uncertainty in the dilution factor for the SZ should be reduced.

- SZ modeling should attempt to better reflect climate change (i.e., wetter climates) in the Yucca Mountain region.
- More realistic models of colloid-facilitated transport should be implemented in the SZ models, and these models should be tied to site-scale observations of colloidal transport.
- An improved definition and modeling of the interface between the geosphere and biosphere are needed to lend further credibility to the calculations.
- More information is needed on how pumping from a well could mix contaminated and uncontaminated waters (as might storing water from multiple sources in tanks), and how these would dilute any contamination.
- Transport model measurements are needed to support incorporating dispersion, chemical retardation, and matrix diffusion resulting from fracture-matrix interaction.

In the TSPA-VA (DOE 1998b), it was suggested that upon resolution of these issues, the refined process models will be adapted for use in the TSPA-SR. The TSPA-VA identified additional efforts needed to develop the regional-scale flow model in cooperation with the U.S. Geological Survey and DOE/Nevada Operations. Hydrochemical data suggest that the groundwater flux beneath Yucca Mountain may be smaller than assumed for present conditions, but this possibility has not yet been included. Sorption behavior and chemical precipitation along transport pathways with reducing conditions could be quite different from those included in the model, and there is some evidence that such conditions exist. The conceptualization of flow in stream tubes may not be appropriate, and there is a lack of treatment of matrix diffusion.

Additional modeling and characterization work was performed to address these issues. The site-scale model representing movement of groundwater and transport of radionuclides in the SZ has been updated to include the following:

- Revised regional hydrostratigraphic data from geologic mapping south of Yucca Mountain.
- Hydraulic and transport testing results from previous and planned testing of the Bullfrog/Upper Tram and Prow Pass units at the C-wells Complex.
- Results from hydraulic tests in borehole USW WT-24.
- Regional hydrochemistry and isotopic data, including apparent groundwater age, oxidation/reduction potential, pH, and chemical analyses.
- Results from the model are abstracted for use in the TSPA and for evaluation of model sensitivity and uncertainty.
- Information from natural and man-made analogs is used to build confidence in models of water movement through the SZ at site scale.

The regional-scale model of water movement through the SZ is being updated to incorporate the following:

- Revised regional hydrostratigraphic data from geologic mapping south of Yucca Mountain
- Hydrostratigraphy results from the NCEWDP drill holes
- Hydrostratigraphy results from boreholes at Yucca Mountain and the Nevada Test Site Environmental Restoration Program
- Stratigraphic information obtained from existing geophysical survey data.

Characterization activities include the Alluvial Test Complex established in cooperation with Nye County. Hydraulic and tracer tests are planned at this complex. These tests will be designed to evaluate aquifer and transport parameters within the alluvium. Alluvium samples recovered from the NCEWDP will be tested to evaluate transport properties and sorption coefficient (K_d) values.

Hydraulic and tracer tests are planned at a site downgradient from the C-wells Complex where the water table is within the volcanic aquifer (also downgradient from the potential repository). These tests will be designed to evaluate aquifer parameters over a wide area along a flow path and obtain effective hydrologic properties averaged over a large volume of rock. Hydraulic and tracer tests at this site will continue to experimentally determine whether the total concentration of tracers is reduced. These tests will allow a direct measurement of the reduction in concentration due to the flow through the volcanic hydrogeological units.

1.6.3 Issues from the Total System Performance Assessment-Viability Assessment Peer Review

The YMP convened a peer review panel to provide a formal, independent evaluation and critique of the TSPA-VA for the potential high-level waste repository at Yucca Mountain (DOE 1998b). The objectives of the panel were to describe the technical strengths and weaknesses of the TSPA-VA and to provide suggestions for its improvement. The panel issued three interim reports prior to the completion of the TSPA-VA and a final report (Budnitz et al. 1999) that was based on the completed TSPA-VA (DOE 1998b), its supporting Technical Basis Document (CRWMS M&O 1998e), and on documents cited as references to the TSPA-VA. Issues developed by the panel regarding SZ flow and transport are tabulated in Appendix A, and the sections of this document and other documents that provide information to address these issues are identified.

1.6.4 Issues from the Saturated Zone Flow and Transport Expert Elicitation Project

The DOE sponsored the SZ Flow and Transport Expert Elicitation Project (CRWMS M&O 1998b) and asked experts to characterize the knowledge and uncertainties associated with certain key issues related to the SZ system in the Yucca Mountain area and the downgradient region. A major goal of the project was to capture the uncertainties involved in assessing the SZ flow processes, including uncertainty in models used to represent the physical processes

controlling SZ flow and transport, and the parameter values used in the models. To capture a wide range of perspectives in the analyses, multiple individual judgments were elicited from members of an expert panel. The panel members, experts from within and outside the YMP, represented a range of experience and expertise. During the elicitation process, the experts identified a range of issues regarding the SZ. These issues are tabulated (Appendix A), and the sections of this document and other documents that provide information to address these issues are identified.

1.6.5 Issues from the Advisory Committee on Nuclear Waste

The NRC established the Advisory Committee on Nuclear Waste to provide independent reviews of, and advice on, topics that include disposal of high-level radioactive wastes in geologic repositories. Transcripts and summaries of transcripts from Advisory Committee on Nuclear Waste meetings for the period from December 1997 to December 1999 were examined to identify SZ flow and transport issues. These issues are tabulated in Appendix A, and the sections of this document and other documents that provide information to address the concerns are identified.

1.6.6 Issues from the Nuclear Waste Technical Review Board

The NWTRB was created by Congress in 1987 to review DOE scientific and technical activities pertaining to the management and disposal of commercial spent nuclear fuel. The activities reviewed include characterizing Yucca Mountain as a potential repository site as well as packaging and transporting commercial spent nuclear fuel and defense high-level wastes.

The NWTRB monitors the YMP to ensure that site characterization is technically sound and scientifically credible. The NWTRB reports to Congress on issues involved in characterizing Yucca Mountain, and points out the concerns of outside parties that are of interest to the scientific community. Transcripts, and summaries of transcripts, from NWTRB meetings, NWTRB reports to Congress, and NWTRB letters to the Office of Civilian Radioactive Waste Management for the period from December 1997 to December 1999 were examined to identify SZ flow and transport issues that were developed during the meetings and provided to the Office of Civilian Radioactive Waste Management or Congress. These issues are tabulated in Appendix A, and the sections of this document and other documents that provide information to address the concerns are identified.

1.6.7 Issues from the U.S. Nuclear Regulatory Commission

The NRC has identified KTIs that are considered most important to performance of the potential repository. The NRC has developed IRSRs that provide criteria for evaluating each of these KTIs. Evaluation of the criteria in these IRSRs indicate that the following KTIs have aspects pertaining to SZ flow and transport:

- Unsaturated and Saturated Flow under Isothermal Conditions
- Radionuclide Transport
- Total System Performance Assessment and Integration
- Structural Deformation and Seismicity.

The *Issue Resolution Status Report KTI: Unsaturated and Saturated Flow Under Isothermal Conditions* (NRC 1999a) provides direction concerning NRC expectations for many topics related to SZ flow and transport. A detailed listing of the applicable criteria, and pointers to sections of this document and other documents that provide information addressing the issues, are listed in Appendix B.

In addition to the criteria in the IRSRs (discussed in detail in Section 4), the NRC provided comments (Paperiello 1999) to the DOE on the TSPA-VA. These comments were examined to identify additional SZ flow and transport issues developed by the NRC. These issues are tabulated in Appendix A, and the sections of this document and other documents that provide information to address the concerns are identified.

INTENTIONALLY LEFT BLANK

2. EVOLUTION OF THE SATURATED ZONE PROCESS MODEL

In this chapter, the evolution of data-collection activities and the development of models for describing the characteristics, understanding the processes, assessing the viability of Yucca Mountain as a potential site for a nuclear waste repository, and key issues identified by overseeing bodies, peer review groups, and others are summarized. The Yucca Mountain Project has evaluated the Yucca Mountain site for over two decades. Data-collection activities have evolved from intensive surface-based investigations in the early 1980s to the current focus on underground drift tests, the Saturated Zone (SZ) Testing Complex (C-wells Complex), and the SZ Alluvial Test Complex. The models have evolved from early conceptual descriptions of the site to current site-scale SZ flow and transport model representations.

In Section 2.1, an overview and discussion of the approach to developing the SZ Process Model Report (PMR) are presented. In Section 2.2, specific activities associated with geologic mapping, hydrologic studies, geochemical sampling, and hydraulic and tracer testing are described. In Section 2.3, the evolution of the SZ flow and transport modeling, and previous modeling at the regional, site, and sub-site scales are discussed. In Section 2.4, previous Total System Performance Assessment (TSPA) modeling (including previous SZ TSPA abstraction), coupling with other components of TSPA, a summary of the TSPA-Viability Assessment (VA) modeling results, and improvement to the TSPA-VA model are discussed. In Section 2.5, an overview of the current site-scale SZ flow and transport model is presented.

2.1 OVERVIEW AND DEVELOPMENT APPROACH

Each PMR describes the information used to develop a process-level model. The PMRs summarize the technical bases that support the TSPA model. In this role, the PMRs identify, document, and describe the information needed to demonstrate postclosure performance. The process used to develop PMRs ensures that each PMR provides transparency and traceability of data, information, and references that relate to the process model and support the TSPA.

The Nuclear Waste Policy Act of 1982 was amended in 1987 to focus effort on the Yucca Mountain site. A site characterization plan was completed in 1988 for systematic surface-based investigations, underground testing, laboratory testing, and modeling activities (DOE 1988).

The *Yucca Mountain Site Description* (CRWMS M&O 1998d) summarizes the results of the site characterization program up to 1998. The *Viability Assessment of a Repository at Yucca Mountain* (DOE 1998a) applies the available data to, and discusses the uncertainties in, a TSPA. This SZ PMR, together with eight other PMRs and associated analysis and model reports, is being developed for updating the TSPA and for supporting the Site Recommendation and possibly the License Application (LA) with traceable and verifiable data. The VA and the Repository Safety Strategy (CRWMS M&O 2000a) identify four attributes for safe disposal: limited water contact with waste package, long waste package life time, low rate of radionuclide release from breached waste package, and reduction in radionuclide concentration during transport. Retardation of radionuclides and dilution of radionuclide concentrations during migration are two principal factors evaluated by this SZ PMR for assessment of the potential repository performance and safety. In addition, the SZ PMR includes the SZ flow and transport

processes from the water table beneath the potential repository to the accessible environment at the proposed compliance boundary.

2.2 SITE CHARACTERIZATION AND DATA COLLECTION

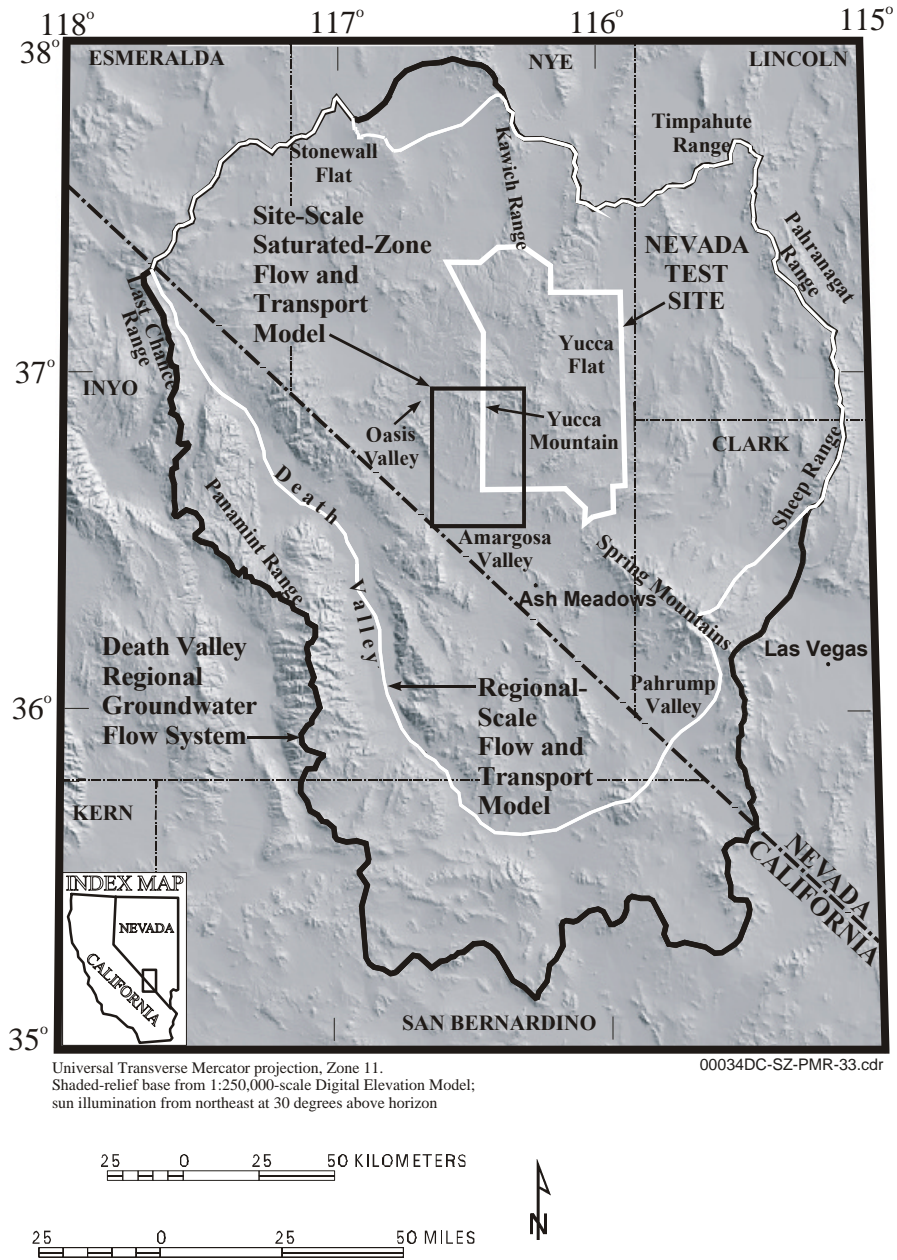
Prior to investigations of Yucca Mountain as a potential geologic repository, information on the geology and hydrology of the area was limited to surface geologic mapping and hydrologic investigations of localized groundwater development areas such as in the Amargosa Desert and Oasis Valley (Figure 2-1). The only subsurface information available was from wells J-12 and J-13, located on the Nevada Test Site (NTS) near Fortymile Wash, that were drilled in the 1960s to supply water to NTS facilities in Jackass Flats (Figure 2-2). Most of the hydrologic information about the Yucca Mountain site has been obtained from studies conducted since 1978. During the first few years of these studies, the emphasis was on describing the hydrogeology of the SZ. As additional data became available, consideration was given to locating the potential repository within the unsaturated zone (UZ), which became a new focus of site characterization activities.

Beginning in 1981, hydrologic test holes, some as deep as 1.8 km (1.1 mi), were drilled into the SZ at Yucca Mountain. The holes were logged to determine lithology and stratigraphy of the rocks that were penetrated, and tested to determine hydrologic parameters such as depth to water, total water yield, water yield as a function of stratigraphic horizon, hydraulic conductivity, transmissivity, water chemistry, and apparent carbon-14 ages of some of the waters. The upper kilometer or more of the SZ penetrated by the wells consists of extensively fractured volcanic tuffs that appear to derive most of their permeability from fractures rather than from the porosity of the matrix.

The borehole-drilling program at Yucca Mountain originally was designed to systematically characterize the subsurface geology and hydrology of the potential repository site area. Limitations were imposed by project directives on where boreholes could be drilled and by accessibility to drilling equipment. Drilling within the potential repository block was limited. Therefore, a plan was devised that would allow for the characterization of the potential repository block by constructing boreholes around the periphery of the block. Subsurface geologic and hydrologic information from these boreholes would be used to construct cross sections to interpret the subsurface geology and hydrology of the potential repository site area.

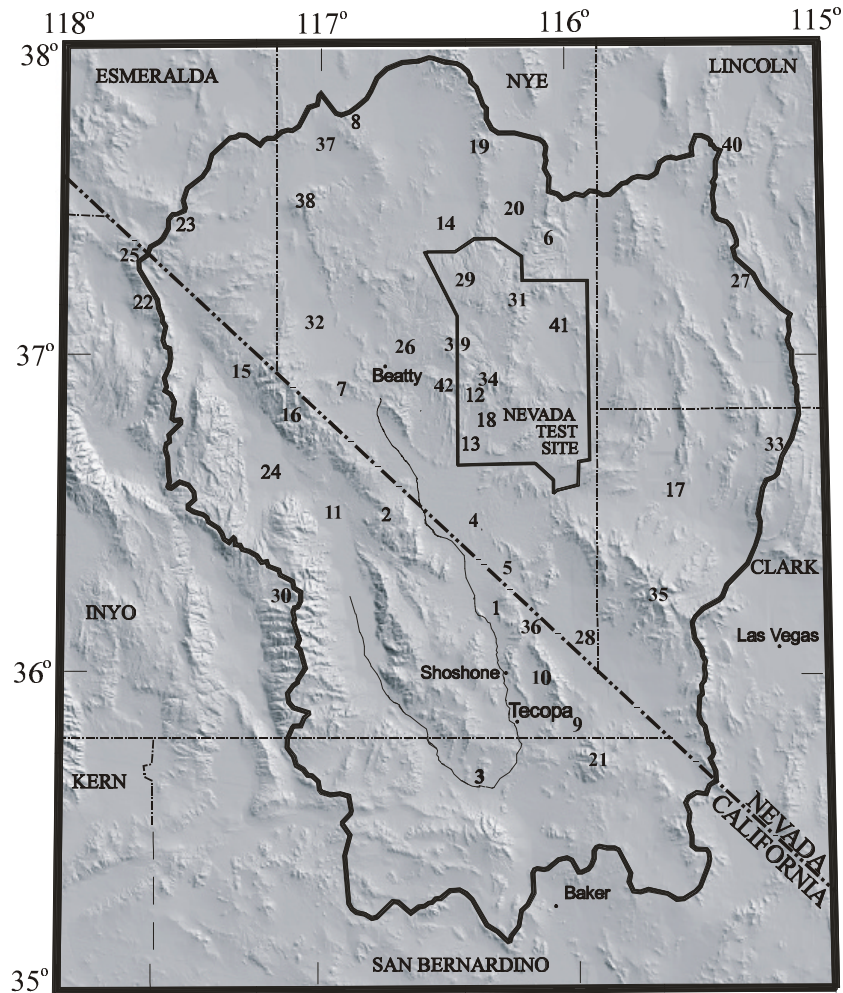
Beginning in 1978 with the drilling of borehole UE-25a#1, 33 boreholes have been drilled in the Yucca Mountain area that penetrate the SZ; numerous other boreholes terminate in the UZ. The borehole designations indicate the general area, purpose of the hole, and general sequence of drilling.

All boreholes were geologically and geophysically logged. The geophysical logs are identified in the Yucca Mountain Site Description (CRWMS M&O 1998a, Table 5.3-11). Cores were taken continuously or intermittently for laboratory analysis in 20 boreholes. Cores were analyzed for bulk density, porosity, particle density, volumetric water content, saturation, water potential, and saturated hydraulic conductivity (CRWMS M&O 1998a, Table 5.3-14). Groundwater samples were collected from all boreholes and analyzed for major-ion content and isotopic content (generally deuterium, oxygen-18, tritium, carbon-13, and carbon-14).



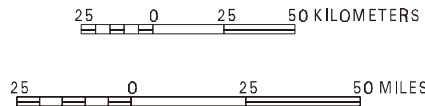
Source: Adapted from D'Agnese et al. (1997)

Figure 2-1. Boundaries of the Death Valley Regional Groundwater Flow System, the Regional-Scale Flow and Transport Model, the Nevada Test Site, and the Site-Scale Saturated Zone Flow and Transport Model



Universal Transverse Mercator projection, Zone 11.
 Shaded-relief base from 1:250,000-scale Digital Elevation Model;
 sun illumination from northeast at 30 degrees above horizon

00034DC-SZ-PMR-10.cdr



LOCATION KEY

- | | | | |
|----------------------|-------------------------|-----------------------|------------------------|
| 1. Alkali Flat | 12. Fortymile Canyon | 23. Magruder Mountain | 33. Sheep Range |
| 2. Amargosa Range | 13. Fortymile Wash | 24. Mesquite Flat | 34. Shoshone Mountain |
| 3. Amargosa River | 14. Gold Flat | 25. Montezuma Range | 35. Spring Mountains |
| 4. Amargosa Valley | 15. Grapevine Canyon | 26. Oasis Valley | 36. Stewart Valley |
| 5. Ash Meadows | 16. Grapevine Mountains | 27. Pahranaagat Range | 37. Stonewall Flat |
| 6. Belted Range | 17. Indian Springs | 28. Pahrump Valley | 38. Stonewall Mountain |
| 7. Bullfrog Hills | 18. Jackass Flats | 29. Pahute Mesa | 39. Timber Mountain |
| 8. Cactus Range | 19. Kawich Range | 30. Panamint Range | 40. Timpahute Range |
| 9. California Valley | 20. Kawich Valley | 31. Raimier Mesa | 41. Yucca Flat |
| 10. Chicago Valley | 21. Kingston Range | 32. Sarcobatus Flat | 42. Yucca Mountain |
| 11. Death Valley | 22. Last Chance Range | | |

Source: D'Agnesse et al. (1997, Figure 2)

Figure 2-2. Prominent Geographic Features in the Death Valley Regional Groundwater Flow System

Recently the county government of Nye County, Nevada carried out additional borehole drilling in cooperation with the U.S. Department of Energy (DOE). This drilling program, termed the Nye County Early Warning Drilling Program, generally is located along Highway US 95 south of Yucca Mountain (Figure 2-3). Although the program still is in progress and data continue to be analyzed, some data have been included in Civilian Radioactive Waste Management System Management and Operating Contractor reports. Borehole location coordinates and water-level measurements are presented in USGS (2000b), chemical analyses are presented in CRWMS M&O (2000m), results of hydraulic tests in three boreholes are given in CRWMS M&O (2000n), and laboratory-derived transport properties (sorption coefficients and bulk density) are given in CRWMS M&O (2000r).

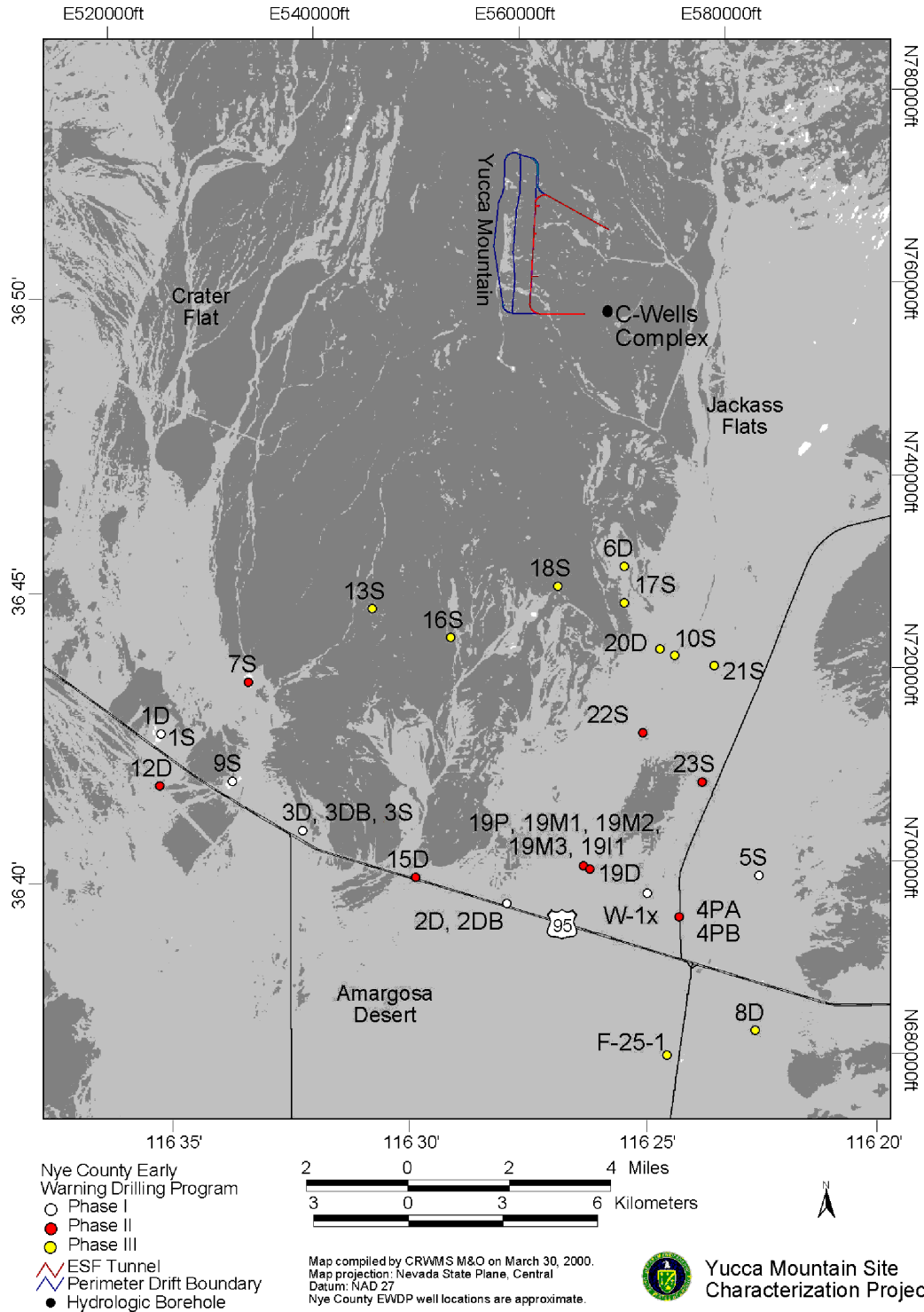
2.2.1 Hydraulic Testing

More than 150 individual hydraulic tests have been conducted on boreholes on and around Yucca Mountain. Almost all of these were single-borehole tests that were located in specific depth intervals and may have included single-well, constant-discharge pumping test; slug-injection (falling-head) tests; pressure-injection tests; temperature surveys; and tracer injection flow surveys. Multiple-well pumping tests were conducted only at the C-wells Complex (Luckey et al. 1996, p. 32).

2.2.1.1 Single-Borehole Tests

Transmissivity values were estimated from tests for the hydrogeologic units (upper volcanic aquifer, upper volcanic confining unit, lower volcanic aquifer, lower volcanic confining unit, and carbonate aquifer), and apparent hydraulic conductivity values were calculated from transmissivity. Apparent hydraulic conductivity values were based on reported single-borehole hydraulic tests and generally were calculated by dividing the reported transmissivity of the tested interval by the saturated thickness in the borehole. Hydraulic conductivity values for individual intervals in a borehole could vary by several orders of magnitude depending on whether or not water-bearing fractures were present. In intervals that contained no open fractures, hydraulic conductivity tended to be low and reflected the hydraulic conductivity of the rock matrix or of small fractures. In intervals that contained water-bearing fractures, the apparent hydraulic conductivity values may be somewhat misleading. Most, if not all, of the water produced in such an interval could have been produced by a few thin, highly conductive fractures in an otherwise thick, essentially nonproductive rock matrix (Luckey et al. 1996, p. 32).

Flow surveys were conducted in most of the deeper boreholes at Yucca Mountain. Flow surveys are useful to determine the intervals of the borehole, and possibly the fractures, that produce water. Most of the flow surveys were conducted using a tool developed for oil-field use that releases small quantities of radioactive iodine-131. As the iodine moves up or down the borehole, it is sensed by gamma-ray detectors. Most surveys were conducted while water was being pumped from, or injected into, the borehole. Static tests also were conducted occasionally. Flow surveys are useful in determining the parts of the borehole that produce (or accept) most of the flow. This information is useful when subdividing a system into aquifers and confining units and for determining the location of, and spacing between, flowing intervals.



Source: Nye County Nuclear Waste Repository Project Office (2000)

Figure 2-3. Nye County Early Warning Drilling Program Boreholes and the C-Wells Complex

2.2.1.2 Multiple-Well Tests

C-Wells Complex—In 1983 and 1984, three boreholes (UE-25c#1, UE-25c#2, and UE-25c#3; collectively called the C-wells Complex) were drilled to conduct aquifer and tracer tests. The C-wells Complex is located at the northern end of Bow Ridge on the west side of Midway Valley. This complex consists of three orthogonally spaced boreholes that are 30.4 to 76.6 m (99.7 to 251.3 ft) apart at the land surface, and each was drilled to a depth of 914 m (3,000 ft). Below the water table, which is 400 to 402 m (1,312 to 1,319 ft) deep at the site, the C-wells penetrate the Calico Hills Formation, and the Prow Pass, Bullfrog, and Tram Tuffs of the Crater Flat Group.

In 1983 and 1984, 16 falling-head slug tests and 9 pressure-injection tests were conducted in UE-25c#1. A constant-head injection test was conducted in UE-25c#2 and was later converted into a constant-flux injection test. Two unsuccessful pumping tests were attempted in UE-25c#1. One pumping test was conducted in UE-25c#2, and two pumping tests were conducted in UE-25c#3.

Testing resumed in 1995, and hydraulic tests were conducted in May 1995, June 1995, February 1996, and May 1996 to November 1997. In all of these tests, borehole UE-25c#3 was used as the pumping well, and boreholes UE-25c#1, UE-25c#2, ONC-1, USW H-4, UE-25 WT#3, and UE-25 WT#14 were used as observation wells.

Hydraulic tests conducted at the C-wells Complex from 1995 to 1997 were designed to:

- Confirm the results of the 1983 to 1984 tests
- Determine hydraulic properties on a larger scale
- Determine hydraulic properties of the six hydrogeologic intervals in the C-wells
- Determine hydraulic properties of the composite SZ section in all geological units penetrated by the C-wells
- Determine heterogeneity in the Miocene tuffaceous rocks, including the influence of faults, in the area encompassed by the observation wells.

Additionally, it was hoped that monitoring UE-25p#1 would establish whether the tuffaceous rocks are connected hydraulically to the Paleozoic carbonate rocks, a regional aquifer (Section 3.2.2.1). The Paleozoic rocks are estimated to be about 455 m (1,495 ft) below the bottom of the C-wells.

In hydraulic tests conducted from 1983 to 1997, the C-wells were either open or contained packers to isolate one or more intervals. Intervals to be packed off were determined from flow surveys, geophysical logs, and aquifer tests conducted between 1983 and 1995.

Following the hydraulic test conducted in February 1996, during which quasi-steady-state conditions were reached, sodium iodide was injected into borehole UE-25c#2 while UE-25c#3 continued to be pumped; this was the first conservative tracer test at the C-wells Complex.

During hydraulic tests from May 1996 to November 1997, additional conservative tracer tests and a multi-constituent reactive-tracer test were conducted. The conservative tracer tests began concurrently in January 1997 and concluded when pumping stopped in November 1997. While UE-25c#3 was being pumped to maintain a quasi-steady-state hydraulic gradient, a benzoic acid tracer was injected into UE-25c#2, and pyridone was injected into UE-25c#1.

Breakthrough curves from the conservative tracer tests were fitted to an analytical solution of the advection-dispersion-diffusion equation for a homogeneous, isotropic, dual-porosity medium; and values of porosity and longitudinal dispersivity were calculated. Two porosity values were calculated for each tracer test. The first, advective porosity, is attributable to a network of continuous and discontinuous fractures, connected by segments of matrix, that forms the flow pathway through which tracers move between the injection and recovery wells. The flow pathway has high hydraulic conductivity, but low storage attributes. The second porosity value, diffusive porosity (also called matrix porosity), is associated with the rock matrix surrounding the tracer flow pathway.

2.2.2 Water Level Monitoring Program

Drilling for site characterization at Yucca Mountain began in 1978, but the first hydrologic test well was completed in 1981. Although water levels were measured as each well was completed, water level monitoring, in terms of a long-term water level network, did not begin until the initiation of regularly scheduled periodic water level measurements during 1983. Periodic measuring of water levels continues through the present and generally is conducted monthly using calibrated steel tapes or electronic cable units. The continuous measurement of water levels was accomplished using pressure transducers, and water level data was collected every hour. Though referred to as continuous measuring of water level data, data loggers were programmed to receive transducer pressure hourly. This frequency of data collection is sufficient to document daily, monthly, and yearly water level changes and trends. However, to detect water level fluctuations due to seismic events, data loggers that record all transducer pressure changes were installed in several wells during 1992, and data were collected from these wells until 1996.

Since 1981, water-level data in the Yucca Mountain area have been collected and reported from 33 wells that monitor 41 depth intervals. Several wells monitor more than one depth interval. These intervals are isolated by inflatable packers or cement plugs.

2.2.3 Data Reduction and Analysis

Data resulting from the SZ field and laboratory testing program were reduced and analyzed, and the results were summarized by Luckey et al. (1996, pp. 16 to 47). These data were collected and analyzed to reduce the uncertainties in the conceptual model. The key uncertainties, in descending order, include recharge, storage properties of SZ materials, transmissive properties, discharge, and hydraulic head (Luckey et al. 1996, p. 53). Details of the data and model uncertainties are discussed in Section 3.5.

2.2.4 Modeling

Numerical models have been developed at various scales to simulate groundwater flow in the vicinity of Yucca Mountain. As data have been accumulated, and as modeling technology has advanced, the models have been refined and improved. Reviews of the principal SZ flow modeling efforts are presented in Luckey et al. (1996, pp. 6 to 7) and NRC (1999a, Section 4.5.2.14, pp. 141 to 150), and are summarized in Section 2.3. Flow and transport models are linked to other process models in a TSPA to construct a computer model for various aspects of the potential repository system and the biosphere that are important to an assessment of the overall performance of the potential repository system. A summary of previous TSPA modeling efforts is provided in Section 2.4.

2.3 PREVIOUS SATURATED ZONE MODELING

Yucca Mountain lies within the Death Valley regional flow system (Figure 2-1). Groundwater flow models that approximately encompass this entire region or that are of larger extent are here termed regional models, whereas groundwater flow models of a sub-region of this area are termed sub-regional models. Models encompassing an area of only few hundred square kilometers are called local or site models; and those for smaller scale are called sub-site models. Boundaries of the regional-scale (D'Agnese et al. 1997) and site-scale SZ flow and transport models are shown in Figure 2-1. Regional-scale SZ models use a coarser grid to describe the flow system parameters and are generally less accurate in predicting the hydraulic head than sub-regional models, but are important in describing the boundary conditions for sub-regional models and in understanding the overall hydrological conditions of the area. Local or site models are important for making transport calculations because transport depend on fine scale permeability variations.

An overview of regional (Table 2-1), sub-regional (Table 2-2), and site and sub-site (Table 2-3) scale models that were used to simulate SZ flow in the Yucca Mountain area is provided, with emphasis on the assumptions of each model. The technology of groundwater flow simulation has changed since the first flow models were applied at Yucca Mountain. Most of the models listed in the tables simulate the Yucca Mountain SZ flow system under present climatic and geologic conditions. The models are important because they improve understanding of the flow system and parameters of the area. Some of the models are used to investigate changes to the water table and hydraulic gradient due to possible climate change or disruptive geologic events. Changing climatic conditions may result in a change in the water table beneath Yucca Mountain. Possible disruptive geologic (tectonic or volcanic) conditions may result in an increase or decrease in the water table. An increase in the water level under Yucca Mountain is of concern because it will decrease the UZ barrier between the potential repository and the SZ, and it may increase the hydraulic gradient resulting in shorter radionuclide transport times through the SZ to the downgradient receptors.

Table 2-1. Regional-Scale Saturated Zone Flow Models Encompassing Yucca Mountain

Area	Dimension/Model Type/Author (year)	Assumptions	Weaknesses/Effects Not Considered	Strengths/Effects Considered
Regional NTS	2-D Finite Element Waddell (1982)	Steady-state. Confined aquifer. Isotropic transmissivity. 19 transmissivity zones. 12 fluxes.	Inaccurate heads at eastern Pahute Mesa	Calibration to minimize head residuals. Good fit to head data. Fluxes computed. Extensive sensitivity analysis on flux, transmissivity, and head.
Regional	2-D Finite Difference Rice (1984)	Steady-state. Confined aquifer. Potential evapotranspiration and actual evapotranspiration estimates.	Confined model. Not calibrated. Few transmissivity zones.	Recharge data included. Recharge sensitivity analysis.
Regional and sub-regional	2-D Finite Difference Ahola and Sagar (1992)	Initial steady-state. Free surface. Transient climatic changes. Conductivity changes due to volcanic or tectonic activity. Regional hydraulic conductivities and zones modified from Rice (1984).	Regional model not calibrated (data from previous calibrated models). Scenario recharge not based on detailed climate analysis.	First transient analysis. Unconfined aquifer (free surface).
Great-Basin Regional	Pseudo 3-D 2-layer Prudic et al. (1993)	Steady-state. Confined aquifer. 97 km ² (37.5 mi ²) grid. Carbonate aquifer only. No over-pumpage. Only large features (lakes, large rivers) modeled.	Large scale of limited use in Yucca Mountain SZ modeling.	May be used to examine boundary conditions in smaller scale models.
Regional	Pseudo-3D 2-layer with middle vertical leakage layer Finite Difference Sinton (1987)	Steady state. Confined aquifer. Recharge and discharge estimates taken from Waddell (1982) and Czarnecki and Waddell (1984).	External boundary considered no-flow. Inflow modeled as recharge at external nodes. Calibration does not consider transmissivity, or recharge residuals	Most residuals less than 15 m (49 ft).
Regional	3-D Finite Difference D'Agnese et al. (1997)	Steady state. Confined aquifer. Calibration to head and spring flow. 3 transmissivity layers.	Temporal pump test data not used in inversion. Few transmissivity and recharge zones. No spatial transmissivity geostatistics.	Use of extensive database (geology, hydrology, recharge, discharge, climate). Calibration to heads and stream flow. Compare conductivity to measured data.
Regional	3-D Finite Difference D'Agnese et al. (1999)	As above, but future (global-warming) and past (full-glacial) effects considered.	As above.	As above.

Table 2-2. Some Sub-Regional Saturated Zone Flow Models in the Yucca Mountain Area

Area	Dimension/Type/ Author (Year)	Assumptions	Weaknesses/Effects Not Considered	Strengths/Effects Considered
NTS, Pahute Mesa to Yucca Flat	Pseudo 3-D steady-state Finite Difference Oberlander (1979)	Steady state. x-z cross section with correction matrix to adjust flow perpendicular to cross section	Difficult to understand the results. No comparison to heads. Correction matrix concept non-physical.	Gives general idea of flow and connection with geology over a cross section.
Sub- regional Yucca Mountain	2-D Finite Element Czarnecki and Waddell (1984)	Steady state. Confined aquifer. X-Z cross section with correction matrix to adjust flow perpendicular to cross section. Six transmissivity zones. Used additional data not available in Waddell (1982). Calibration to head data. Some boundary conditions based on Waddell (1982).	Inaccurate heads at Franklin Lake Playa and in the area north of Yucca Mountain. Not calibrated to recharge, discharge, or transmissivity.	Finite Element model (no inactive elements). Model calibrated to heads. Points to data needs in Yucca Mountain area. Small head residuals.
Sub- regional	2-D Finite Element Czarnecki (1984); also Czarnecki (1990)	As in Czarnecki and Waddell (1984). Water table simulator.	Not calibrated to recharge, discharge, or transmissivity.	As above.
Sub- regional	2-D Finite Element unconfined aquifer Haws (1990)	X-Z cross-sectional model to understand vertical flow along a streamline.	Intentionally left blank.	Shows vertical flow up from carbonate aquifer and recharge from Fortymile wash needed to maintain heads at Yucca Mountain.
Regional and sub- regional	2-D Finite Difference saturated flow with free surface Ahola and Sagar (1992)	Initial steady-state. Transient climatic changes. Conductivity changes due to volcanic or tectonic activity. Regional Hydraulic conductivities and zones modified from Rice (1984).	Regional model not calibrated (data from previous calibrated models). Scenario recharge not based on detailed climate analysis.	First transient analysis. Unconfined aquifer (free surface).

Table 2-3. Site-Scale and Subsite-Scale Saturated Zone Flow Models in the Yucca Mountain Area

Area	Dimension/Type/Author (Year)	Assumptions	Weaknesses/Effects Not Considered	Strengths/Effects Considered
Local Yucca Mountain	2-D Finite Element Barr and Miller (1987)	Local model of site. Hand-calibration. Model used to investigate effect of “catastrophic changes” in leakage and hydraulic conductivity on flow and transport.	Difficult to accurately model effects with a 2D model. Model developed before the development of a geologic framework model.	Faults modeled using north-south high conductivity zones. Performed transport computations.
Sub-regional	Coupled 2-D Finite Element flow and strain codes Carrigan et al. (1991)	Analysis to determine effects of earthquakes and volcanism on water table.	Methodology described in a vague manner. Details on input parameters used in model not given. Model not calibrated.	Unconfined flow model coupled with induced strain and displacement.
Sub-site-scale	3-D Integrated Finite Difference Cohen et al. (1997) 2-D Cross section flow simulations	Steady flow. Transport simulated. 23 vertical layers. Fault permeability assumptions tested. Scale analysis of convective heating.	Faults have uniform permeability. Boundary conditions over-constrained.	Discretization honors dip, thickness, and orientation of strata. Fault offsets modeled. Calibrated to measured heads and long-term pumping tests. Calibrated to water table. Most well residuals < 1 m (<3 ft)
Site-scale	3-D Finite Element Czarnecki et al. (1997)	Steady state. 16 zones, 1 low conductivity zone to simulate a no-flow fault. Only minor recharge from Fortymile Wash.	Large permeability difference at C-wells Complex.	Calibrated to water table.
Site-scale	2-D integrated Finite Difference Lehman and Brown (1998)	Steady state. Fault controlled flow. Calibrated to water level data. Alternate Conceptual model. Assumes fracture “conduits” provide dominant flow paths. Large fracture volume assumed.	Coarse discretization. 2-D model. Few permeability zones. Poor agreement to observed temperatures along Solitario Canyon fault and Paintbrush fault. Data supporting wide fault zones not presented. Boundary conditions over-constrained. Permeabilities much larger than documented in some areas. Poor model documentation.	Considers fault controlled flow. Heat flow modeled.

NOTE: SZ modeling done in previous TSPA analyses not present

Oberlander (1979) performed the first numerical modeling of the Yucca Mountain area by modeling a two-dimensional (2-D) cross section between Pahute Mesa and Yucca Flat. Flow in the unmodeled third dimension was adjusted with a “correction” matrix. Oberlander (1979) estimated the flow rate through Paleozoic rocks beneath Yucca Mountain and found an upper bound to the flow from Yucca Flat to Ash Meadows.

Waddell (1982) used a 2-D steady-state finite element model to simulate the regional-scale NTS groundwater flow in the SZ. The main goals were to estimate flow fields (to be used for transport predictions of radionuclides) and to study the effects of model parameters uncertainty on these estimates. The model encompassed an area of approximately 175-km by 175-km (109 mi by 109 mi) with boundaries along topographic highs to the north and northeast and along topographic lows to the southwest. The model was calibrated by adjusting transmissivities, recharge, and discharge to minimize the weighted sum of the squared head residuals (observed head minus simulated head). Most of the absolute head residuals were less than 30 m (98 ft) in the final model. The model estimated recharge in most areas, but considered discharge in the Ash Meadows area as a known constant and modeled other areas using a constant head condition. The results from this model substantiated conclusions of some earlier conceptual models of the site. The model was not accurate in the area of Pahute Mesa, possibly due to vertical flow effects. The model was able to identify areas in which hydrologic properties were key in defining the flow direction and magnitude of adjacent regions. For example, hydrologic properties in the Eleana Formation had a major effect on the flow beneath Timber Mountain and Jackass Flats, while hydrologic properties in Fortymile Canyon and Fortymile Wash affected fluxes beneath Jackass Flats and Yucca Mountain. Groundwater barriers to the north of Yucca Mountain, recharge on Pahute Mesa, and underflow from regions north of the Pahute Mesa had a significant impact on the model. The model also identified areas in which Waddell (1982) felt that no further study was needed.

Czarnecki and Waddell (1984) developed a sub-regional model for the area near Yucca Mountain that was about one-third of the size of the Waddell (1982) regional-scale model. Some of the boundaries coincided with the Waddell (1982) model. On other boundaries, specified heads or fluxes were taken from the Waddell (1982) model. The subregional model was used to obtain a better understanding of the groundwater flow system beneath Yucca Mountain and for later use in determining the change in the hydraulic head due to increased recharge under assumed future climatic conditions. The model provided a good match to observed hydraulic head data except in areas where vertical flow components were present, such as Franklin Lake Playa (located about 8 km (5 mi) west of Ash Meadows) and where there were steep gradients such as directly north of Yucca Mountain. This model showed that groundwater tends to flow from north to south. In the region of the potential Yucca Mountain repository, groundwater flow tends to be southeasterly and then southerly.

Rice (1984) constructed a 2-D, regional-scale, steady-state model covering an area approximately the same as that of more recent model by D'Agnese et al (1997). The objectives of the model were to understand the distribution of recharge, discharge, and hydraulic head within the model area. The hydraulic head distribution obtained from this model generally is in agreement with other regional-scale 2-D models.

Czarnecki (1984) used the Czarnecki and Waddell (1984) 2-D model to assess potential effects of changes in future climatic conditions in the area of Yucca Mountain on the water table below the potential repository and the surrounding flow field. Czarnecki (1984) found that the simulated position of the water table rose by as much as 130 m (426 ft) in response to a 100 percent increase in precipitation over current conditions. A 100 percent increase in precipitation resulted in a factor of 15 increase in the model recharge rate. Czarnecki (1984) further found that changes in the flow direction at Yucca Mountain would be small and that the

magnitude of the groundwater flux would increase by a factor of 2 to 4 over that found in simulations, assuming present-day climate conditions. Czarnecki (1990) also used this model to examine water level changes due to pumping wells in Franklin Lake Playa.

Sinton (1987) modeled the same area as Waddell (1982), but with a quasi-three-dimensional (3-D), steady-state, finite-difference model. The two-layer model included a shallow upper layer of volcanic, alluvial, and carbonate rock over a deep lower layer of carbonate rock. Vertical flow was allowed between layers through a transmissive leaky unit. A sensitivity analysis was performed, and the flow system was found to be particularly sensitive to transmissivity values in the Crater Flat and Amargosa Desert areas.

Haws (1990) constructed a 2-D, vertical, steady-state, flow model along an assumed flow line extending from Timber Mountain to the north of Yucca Mountain, southward to Alkali Flat (Figure 2-2). An objective of this model was to examine vertical flow between the volcanic and carbonate aquifers. Results of the model suggest that upward leakage from the deep carbonate aquifer to the shallow volcanic aquifer must occur in order to maintain the water table at its observed elevation.

Carrigan et al. (1991) investigated the effects of earthquakes and dike intrusions on water table height below Yucca Mountain using a 2-D finite element flow model coupled with a boundary element solver used to predict volumetric strain and displacement. The possibility of high vertical-permeability anisotropy, and modeling of the UZ, were considered in the model. A number of tectonic scenarios were considered and worst-case scenarios produced excursions in the water table elevation of less than 20 m (66 ft) (Carrigan et al. 1991, p. 11). The results were of similar magnitude to observed excursions after large earthquakes. An earlier study by Barr and Miller (1987) examined the effect of increases in vertical leakage (either from the surface or from the underlying carbonate aquifer) on flow and transport in the local area surrounding Yucca Mountain.

Ahola and Sagar (1992) studied the effect of increased recharge due to climate change and volcanic and tectonic scenarios on the water table level below Yucca Mountain using regional-scale and sub-regional models. They used a regional-scale transient 2-D model in which the SZ was modeled as a free surface (unconfined aquifer) that covered the same area as that of Rice (1984). The parameters were modified to incorporate the coarser grid used by Ahola and Sagar (1992). Ahola and Sagar (1992, pp. 6-1, 6-2, and 6-5) found water table increases of about 45 m and 87 m (148 ft and 285 ft) resulted from increases in regional recharge by factors of 10 and 20, respectively. The transition time to change from the initial steady-state water level to the perturbed steady state was about 400 to 700 yrs for these simulations. This time increment does not consider the lag time for infiltration through the UZ, which will retard the onset of the climate change response and increase the transition time. An approximately linear relation between the water level rise and the factor increase in recharge was shown. This study did not consider the possibility of additional discharge (due to streams) that was produced by rises in the water table or the possibility of increased evaporation, and it was performed before the benefit of an extensive climate change analysis was available.

Ahola and Sagar (1992) also used a sub-regional model to investigate possible changes to the water table due to a reduction of hydraulic conductivity produced by an intrusion of a volcanic

dike downgradient from the potential repository or by an increase in hydraulic conductivity due to increased fracturing of the rock from tectonic activity in the postulated low conductivity region north and northeast of the potential repository. These simulations yielded water table increases from a few meters to 275 m (902 ft) (Ahola and Sagar 1992). The greatest water table rise resulted from a scenario where tectonic activity caused the hydraulic conductivity to increase by three orders of magnitude north and northeast of Yucca Mountain.

Prudic et al. (1993) developed a two-layer, pseudo 3-D, steady-state model of the carbonate rock province of the Great Basin (covering much of eastern Nevada and western Utah). This model was used to simulate regional-scale flow in the carbonate rocks that, in the vicinity of Yucca Mountain, underlie Tertiary volcanic rocks. This model suggests that flow in the carbonates is from north to south within the domain of the site-scale SZ flow and transport model.

D'Agnese et al. (1997) developed a three-layer 3-D steady-state flow model of the SZ for the Death Valley region. This model incorporated large quantities of data from the Yucca Mountain and NTS sites compiled over the past 30 yrs. Geological data, including descriptions of important faults, were considered. Ten hydrogeologic units (a hydrologic unit is an area with distinct hydrological and geological properties and considerable lateral extent) were described for the area. Well logs from over 700 wells and cross sections were used to define a 3-D framework model of the individual hydrogeologic units, and a 3-D grid was generated taking into account the shape of these units. The numerical model grid consisted of 163 rows, 153 columns, and 3 layers. The row and column grid dimension was 1,500 m (4,900 ft), and the depth to the bottom of each of the three layers was 500 m (1,640 ft), 1,250 m (4,100 ft), and 2,750 m (9,020 ft), respectively from the water table surface.

Hydraulic conductivity values were assigned to specific grid blocks in the D'Agnese et al. (1997) model using data published by Bedinger et al. (1989), and conductivity was assumed to decrease with depth. Initial recharge in the area was set using a modification of the Maxey and Eakin (1950) method. Discharge due to evapotranspiration at the Death Valley saltpan was modeled using a constant head boundary at the southwest boundary. All other boundaries were set as no-flow except for four locations in the northern part of the bottom model layer. Other sources of discharge include springs, wet playas, and irrigation pumpage. Discharge from these areas was estimated from available data. During the initial calibration process, hydraulic conductivities and recharge parameters were set to four classes for parameter estimation. Nonlinear regression was used to adjust uncertain model parameters by minimization of the squared residuals based on the difference between the observed and computed spring flows and heads. During calibration, the estimated parameter set was expanded to include layer anisotropy in hydraulic conductivity, the evapotranspiration rate factor, spring conductance, and groundwater pumpage. The initial conceptual model, permeability zone, boundaries, number of conductivity zones, boundary conditions, and recharge were changed in the calibration process.

A map of residuals and weighted head residuals (weighted residuals are the residual weighted by the expected error at a location) showed reasonable agreement between computed and measured head data in the upper model layer, except in the northwest and northeast portions where data were sparse and of poorer quality. In the region extending from the Amargosa Valley to the Pahrump Valley, the simulated hydraulic gradient was somewhat higher than the observed hydraulic gradient. Most of the computed spring flows were less than the observed flows.

However, the overall water balance was comparable to that estimated from data. A parameter sensitivity study indicated that flow was most sensitive to the highest recharge zone and the high conductivity zones prevalent in the area where wells are concentrated in the upper aquifer layer.

More recent SZ flow modeling efforts were undertaken to evaluate the impact of long-term future climate forecasts on regional flow in the Yucca Mountain area. Analysis by USGS (2000b) forecast monsoonal and glacial-transition climates during the next 10,000 years. D'Agnese et al. (1999) uses the model developed in D'Agnese et al. (1997) to evaluate the effect of full-glacial and global-warming climates on the regional flow at Death Valley, which includes Yucca Mountain. One result of this model was that under the assumption of past (full-glacial) climate, the water table rises but maintains a shape similar to that found under present climate conditions. Assuming past full-glacial conditions, D'Agnese et al. (1999, p. 2) found that simulated water levels rose between 60 m (197 ft) and 150 m (492 ft). Assuming future global-warming conditions in which atmospheric carbon dioxide doubles, the forecast recharge in the Yucca Mountain area was greater than present, but less than the full-glacial model. In this case, the simulated water level beneath Yucca Mountain was estimated to rise less than 50 m (165 ft).

A recent study by Czarnecki et al. (1997) uses the 3-D code FEHM (Zyvoloski et al. 1997a) to model flow in the SZ at the site scale. The model incorporates 16 zones and is calibrated using observed water levels at wells and approximations of the flux at the boundaries. A large gradient area at the north of the site is modeled by assuming a barrier of very low conductivity perpendicular to the high gradient area. The model boundaries were set to be coincident with model elements of D'Agnese et al. (1997). This model used a nonlinear regression to estimate subsets of parameters. Estimated permeability values differed from those measured values at the C-wells Complex, and the groundwater flux at the southern end of the boundary was twice (Czarnecki et al. 1997, p. 103) that found in the D'Agnese et al. (1997) regional-scale model.

A sub-site-scale SZ model was used to simulate 3-D steady flow in a 150-km² (58-mi²) area including Yucca Mountain (Cohen et al. 1997). These efforts simulated the detailed geologic structure and included major faults as independent elements. The effects of various vertical fault property scenarios (for faults in the Bullfrog Tuff) were tested through the transport of a tracer. Minimal transverse and vertical dispersion was observed when the faults are assumed to have high permeability, and considerable mixing occurred when the faults were assumed to have low permeability. A bifurcation of the tracer was observed when the faults were assumed to be displacement-only. A scale analysis was performed that showed that natural heat convection in high permeability units in the Bullfrog Tuff would occur on the order of 20 yrs, which implies that heat flow modeling could be important in transport. Lehman and Brown (1998) developed another sub-site-scale model. This 2-D model represents an alternate conceptual view on flow through the SZ. The model assumes a high conductivity contrast between wide fault zones and matrix rock, and it also assumes that these fault zones are long in extent. As expected under these assumptions, water moved quickly through the SZ.

A large number of viewpoints have been presented by a variety of researchers, agencies, and organizations, and many of these viewpoints are represented in the site-scale SZ flow and transport model. This diversity of input provided improved understanding of the hydrology of

the site and the expected response of the potential repository to varying climate and disruptive geologic scenarios.

2.4 PREVIOUS TOTAL SYSTEM PERFORMANCE ASSESSMENT MODELING

In this section, a summary of the manner in which the transport of radionuclides in the SZ was handled in previous TSPA analyses, and some of the results of those analyses, are presented. Implications of the present SZ methodology relative to previous approaches are discussed.

2.4.1 Total System Performance Assessment Modeling Before the Total System Performance Assessment-Viability Assessment

Initial performance assessments of a potential repository at Yucca Mountain (e.g., Sinnock et al. 1984; Sinnock et al. 1986; Barnard and Dockery 1991) either completely ignored or gave only cursory attention to the SZ by using simple 1-D approximations to the SZ. At the time, estimates of radionuclide transport through the UZ typically were more than 10,000 yrs, while the estimates of transport through the SZ were on the order of 1,000 yrs. In addition, the EPA radiation protection standard that guided post-closure PA for Yucca Mountain until 1992, 40 CFR 191 (50 FR 38066), used a metric of cumulative releases of radionuclides to the accessible environment over a period of 10,000 yrs. A cumulative release of a radionuclide is the total amount of that radionuclide that crosses a boundary over a given time period. The proposed boundary to the accessible environment was specified at a location that is 5 km (3 mi) from the potential repository, and the area within the boundary was called the controlled area. Because the transport time in the UZ appeared to be greater than the regulatory period, and because the transport time in the SZ appeared to be small compared to that in the UZ and the regulatory period, any need for detailed studies of the SZ were unnecessary.

For the first TSPA, TSPA-1991 (Barnard et al. 1992, pp. 4.51 to 4.94), it was recognized that fast paths might exist through the UZ, and two alternative conceptual models of flow in the UZ were used: a model similar to the previous models that described flow predominately in the matrix, and a new model (the weeps model) that described flow as occurring predominately in fractures. This 2-D fracture-flow model was based on modeling by Czarnecki (1984) and Czarnecki and Waddell (1984) and encompassed the controlled area around the potential repository and the 5-km (3-mi) distance between the potential repository and the accessible environment. Boundary conditions for the TSPA model were taken from the Czarnecki (1984) model. A particle-tracking method was implemented to determine radionuclide transport times and velocities from the potential repository to the accessible environment for a conservative tracer. Particles were placed in the “footprint” of the potential repository (the area in the SZ immediately below the potential repository) and transport times to the proposed 5-km (3-mi) boundary were determined. Differences in initial position and paths taken produced a distribution of transport times. In general, transport in the SZ was in a southeasterly direction with transport times varying between 900 and 1,500 yrs (velocities of 3.25 to 5.7 m/yr [10.7 to 18.7 ft/yr]), and a mean transport of about 1,200 yrs. The results of the 2-D model were abstracted for the TSPA-1991 calculations into 1-D, horizontal flow tubes in a single porous medium. For the TSPA abstraction, dispersivities were assumed to be log-uniformly distributed between 50 m and 500 m (164 ft and 1,640 ft), and porosity was set to 17.5 percent. During the

TSPA calculations, the 1-D model was used directly to solve the transport of radionuclides over the 5-km (3-mi) distance to the accessible environment.

By the time of TSPA-1993 (Wilson et al. 1994, pp. 14-4, 14-5; CRWMS M&O 1994, pp. 3-4, 3-6), it was apparent that an upcoming regulation for a potential repository at Yucca Mountain might involve a metric of radiation dose to an individual. Calculation of dose requires a method of accurately determining the concentration of radionuclides at the interface of the geosphere and biosphere where the biological environment becomes exposed to the contaminants. Cumulative releases can be estimated using only the transport times. A 3-D, confined-aquifer model was constructed for TSPA-1993 for the expressed purpose of determining whether three dimensions were necessary to properly define the SZ flow system. The analysts concluded that incorporation of 3-D geologic structures was necessary to match observed hydraulic heads (water-table heights) and that geologic structures, to a large degree, determined the direction and velocity of groundwater flow.

For TSPA-1993 (Wilson et al. 1994), as with TSPA-1991 (Barnard et al. 1992), transport and velocities were determined by calculating the transport of a conservative tracer from various locations in each of the three geologic units that intersected the potential repository footprint to a location 5 km (3 mi) downgradient from the potential repository. Porosity was set to 20 percent. Two conceptual models were investigated: one that only allowed water to leave and enter the SZ domain from the sides (the non-diversionary model), and another that incorporated a drain out of the volcanic aquifer (the diversionary model). Results showed significant variability as compared to the TSPA-1991 results. Transport times in the SZ for the various conceptual models and transport paths ranged from 230 to 1,700 yrs (velocities of 3 to 22 m/yr [10 to 72 ft/yr]), with averages ranging from 500 to 800 yrs (average velocities of 6 to 10 m/yr [20 to 33 ft/yr]).

For TSPA-1993 (Wilson et al. 1994), the detailed outflow from the UZ transport model was used as input to a 1-D, single porosity model. Longitudinal dispersivity was assumed to be uniformly distributed between 100 m and 500 m (330 ft to 1,640 ft) to match the distribution of velocities, and porosity was kept at 20 percent. Dilution, and thus final concentration, was calculated from an estimate of the cross-sectional area of the transport plume at the proposed boundary to the accessible environment; the estimate was based on assumed transverse dispersivities and mixing depths (typically 50 m [165 ft]), and ranged between 34,000 m² and 2,200,000 m² (370,000 ft² to 24,000,000 ft²). Climate change was incorporated in TSPA-1993 as a jump from one steady-state condition to another. For the SZ, future climate change was approximated by an increase in the water table; no changes were made to flow or transport parameters resulting from flow through previously unsaturated areas of the formation. A water-table rise of between 50 m and 120 m (165 ft to 395 ft) was specified using a uniform distribution. The rise in the water-table elevation caused radionuclides in the UZ, but now in the SZ, to be immediately introduced to the SZ, resulting sometime later in a pulse of higher releases and doses at the accessible environment. Cumulative releases and radiation doses (drinking-water doses only) were considered as performance metrics in TSPA-1993 (Wilson et al. 1994).

For TSPA-1995 (CRWMS M&O 1995), the emphasis was on a more accurate depiction of the EBS of the potential repository at Yucca Mountain, and no new modeling of the SZ was conducted. Velocities from the TSPA-1993 3-D model (Wilson et al. 1994) were used again in

1-D abstractions. A constant longitudinal dispersivity of 500-m (1,640-ft) was assumed. Various cross-sectional areas of the contaminant plume were estimated as in TSPA-1993. From these cross-sectional areas and the groundwater flux, dilution factors were calculated, and the radionuclide concentrations from the 1-D TSPA abstracted model were reduced by these dilution factors. In some calculations, additional dilution was assumed for mixing with other groundwater basins, and for mixing with uncontaminated water during well withdrawal. As with TSPA-1993, water-table rise was taken from a uniform distribution, however, the rise was more continuous over time.

Sensitivity studies were conducted for TSPA-1993 (Wilson et al. 1994) and TSPA-1995 (CRWMS M&O 1995) to look at how much the uncertainty and variability in parameter distributions influenced the uncertainty and variability of the results. Both TSPAs found performance of the potential repository to be sensitive to SZ parameters. For the radiation dose metric in particular, results were sensitive to parameters influencing radionuclide dilution in groundwater. In the simplified TSPA models, these parameters were the groundwater flux and the cross-sectional flow area of the contaminant plume (or the dilution factor). In the actual flow system, these parameters correspond to groundwater flux, transverse dispersion, transport path lengths, and possible well-withdrawal effects. Parameters primarily affecting radionuclide transport times (i.e., sorption coefficients and longitudinal dispersion) were found to be of lesser importance.

2.4.2 Total System Performance Assessment-Viability Assessment Modeling

The TSPA-VA, published in 1998 (DOE 1998a), focused on calculating dose 20 km (12.5 mi) downgradient from the potential repository due to changes in DOE guidance that were based upon recommendations from the National Research Council (National Research Council 1995). A series of abstraction and testing workshops were conducted to compile a prioritized list of important technical issues related to flow and transport in the SZ (DOE 1998b, p. 3-138, Table 3-19). An expert elicitation also was conducted to obtain opinions from five experts on groundwater flow and transport regarding important issues related to the SZ (CRWMS M&O 1998b). The approach for conducting the TSPA-VA analysis was based upon input from the workshops and the expert elicitation. For the TSPA-VA, numerical simulations were performed for the base case, representing the most likely future evolution of the site, and sensitivity analyses were performed to study variations of the base case.

The base case SZ flow and transport component of the TSPA-VA evaluated the migration of radionuclides from their introduction at the water table below the potential repository to the release point to the biosphere. A hierarchy of models was used to simulate the transport of radionuclides in the SZ. Explicit, 3-D modeling was not used to simulate radionuclide concentrations because it can generate numerical dispersion, which artificially lowers concentration. The TSPA 3-D SZ flow model was used only to determine flowpaths through the SZ (DOE 1998b, Section 4.1.12, p. 4-16). The TSPA 1-D SZ transport model (DOE 1998b, Section 3.7.2.1, p. 3-139) was developed based on the flowpaths from the 3-D flow modeling and used to determine concentration breakthrough curves at a distance of 20 km (12.5 mi) for unit releases of radionuclides from six streamtubes (DOE 1998b, Section 4.1.12, p. 4-16). The SZ transport component of the analysis was coupled to the transport calculations for the UZ that bring contaminants in downward percolating groundwater from the potential repository to the

water table (e.g., the spatial and temporal distributions of simulated mass flux at the water table). The coupling was accomplished by using the convolution integral method (CRWMS M&O 1998e, Section 8.3.4) to combine the unit breakthrough curves calculated by the TSPA 1-D SZ transport model with the time-varying radionuclide sources from the UZ. Changes in the SZ flow and transport system in response to climatic variations were incorporated for the three discrete climate states (dry, long-term average, and superpluvial) considered in the other components of the TSPA-VA. Specific discharge and volumetric groundwater flow-rate in the SZ streamtubes were scaled in transport simulations to reflect climate state. The SZ transport results were linked to the biosphere analysis by the simulated time history, or system response as a function of time, of radionuclide concentration in groundwater produced from a hypothetical well located at the biosphere interface. The biosphere was assumed to be located 20 km (12.5 mi) from the potential repository. Radionuclide concentrations in the hypothetical well water were then used in the biosphere component to calculate doses received by the public.

For the base case, uncertainty in the SZ system was evaluated through Monte Carlo variation in the input parameters (Wilson et al. 1994, pp. 3-19 to 3-21) that were used in the TSPA 1-D SZ transport model. Primarily, the uncertainty in radionuclide transport parameters was evaluated. The TSPA 1-D SZ transport model was used to calculate 101 unit breakthrough curves (100 Monte Carlo simulations and the expected-value case). The results of the 1-D SZ transport calculations were stored in a “library” of unit radionuclide concentration breakthrough-curves, and for each TSPA-VA realization, a SZ unit breakthrough curve was randomly drawn from the library for use in the convolution integral method.

The convolution integral method (DOE 1998b, p. 3-141) was used in the TSPA-VA calculations to determine radionuclide concentrations in the SZ, 20 km (12.5 mi) downgradient of the potential repository, as a function of the transient radionuclide mass flux at the water table beneath the potential repository. This coupling method made full use of the detailed SZ flow and transport simulations for a given realization of the system, but without requiring complete numerical simulation of the SZ for the duration of each TSPA-VA realization. The two input functions to the convolution integral method are a unit concentration breakthrough curve (in response to a step-function mass flux source as simulated by the TSPA 1-D SZ transport model) and the radionuclide mass flux history as simulated by the UZ transport model.

The TSPA-VA sensitivity studies were designed to examine five of the key issues related to assumptions about the base case SZ analysis (DOE 1998b, p. 4-2) and the importance of these issues with respect to performance of the potential repository. The effects of dilution in the SZ and vertical transverse dispersivity were investigated to address concerns from the expert elicitation panel. The impact of including heterogeneity and large-scale flow channelization in a 3-D flow and transport model was studied. A 2-D dual-porosity transport model was used to calculate radionuclide concentrations to examine the effects of the two base case assumptions: a single continuum and using effective porosity as a surrogate for the matrix diffusion process. A study to investigate the effect of calculating a population dose, compared to the dose to an individual, was performed for the base case. Finally, alternative conceptual models of colloid-facilitated plutonium transport were developed and implemented for sensitivity analysis.

Colloid-facilitated transport of plutonium in the SZ was simulated based on a conceptual model using the assumptions of equilibrium, reversible sorption of plutonium onto colloids, and the

potential for irreversible sorption of plutonium onto some colloidal particles (DOE 1998b, pp. 3-92, 3-99, and 3-104). A large fraction of the plutonium mass released was simulated to move assuming chemical equilibrium among dissolved plutonium, plutonium sorbed onto colloids, and plutonium sorbed onto the aquifer material (DOE 1998b, pp. 3-140 to 3-141). A small fraction of the plutonium mass was simulated to be irreversibly attached onto colloids and transported relatively rapidly in the SZ. The relative fraction of plutonium mass that was subject to reversible vs. irreversible sorption onto colloids was treated as uncertain and was included as a stochastic parameter in the analyses.

The three alternative climate states considered in TSPA-VA analyses (DOE 1998b, pp. 3-8 to 3-9) were dry (present-day conditions), long-term average (corresponding to oscillating pluvial and glacial conditions), and superpluvial (corresponding to severe glacial conditions). An abstraction method for three climate states, as they affect flow and transport in the SZ, was developed for use with the convolution integral method. A primary simplifying assumption was that groundwater flow in the SZ immediately changed to a new steady state following climate change. Changes in the magnitude of SZ groundwater flux were represented, based on results from the regional-scale SZ flow model (D'Agnese et al. 1997; 1999), by a scaling factor for the three climate states. Changes in the volumetric groundwater flow rate through each of the 1-D SZ streamtubes for the three climate states were based on the site-scale UZ flow model simulations for these climatic conditions.

Results of the TSPA-VA model may be expressed as dose rates in millirem per year (mrem/yr) at a point 20 km (12.5 km) down-gradient from the potential repository (the breakthrough point) for the three time periods (10^4 , 10^5 , and 10^6 yrs) studied. Breakthrough is defined as the first appearance of a radionuclide in sufficient quantity to provide a dose of 0.001 mrem/yr. During the first 10,000 yrs after emplacement, the only radionuclides expected to reach the biosphere are technetium-99, iodine-129, and carbon-14 (DOE 1998b, p. 4-25 and Figure 4-29). The breakthrough of technetium-99 is calculated to occur at about 3,500 yrs, while that of iodine-129 occurs at about 4,200 yrs. Carbon-14 provided a relatively small contribution to dose. High solubility and the assumption of no sorption account for the early breakthrough of these radionuclides compared to other radionuclides in the inventory over the first 10,000-yr period. From 10,000 yrs to 100,000 yrs after emplacement, technetium-99 and iodine-129 continue to dominate the dose to about 50,000 yrs, after which neptunium-237 begins to dominate (DOE 1998b, Figure 4-16). During this period, breakthrough of neptunium-237 occurs at about 30,000 yrs. Breakthrough of uranium-234 and plutonium-239 follow at about 50,000 and 80,000 yrs, respectively (DOE 1998b, Figure 4-16). For the time period from 100,000 to 200,000 yrs, neptunium-237 dominates the dose (DOE 1998b, Figure 4-21). From about 200,000 yrs to one million years, neptunium-237 and plutonium-242 dominate the dose rate. Notable peaks occur in the results during this last period due to assumed super-pluvial climate peaks and large numbers of cladding and no-drip package failures over large time steps in the simulations (DOE 1998b, p. 4-50).

2.5 CURRENT SATURATED ZONE FLOW AND TRANSPORT MODEL

The current site-scale SZ flow and transport model was developed in support of the upcoming TSPA-SR. The current model was built upon the model used for TSPA-VA (DOE 1998b), but includes a number of modifications to reflect the current understanding of the SZ flow and

transport, address deficiencies in the TSPA-VA SZ model that were identified by reviews, and incorporate new data collected since TSPA-VA. Changes introduced since the TSPA-VA iteration include:

- All analyses and models were developed under the quality assurance program (DOE 2000).
- Use of a 3-D numerical model to simulate the flow of groundwater and the transport of radionuclides.
- Use of particle tracking methodology (similar to that used in the UZ) to build the transport component of the model. This allowed for the elimination of numerical dispersion (inherent in finite elements and finite difference numerical method) and the solution source size dependence.
- The site-scale SZ flow and transport model is used to simulate the mass fraction of radionuclides delivered to the proposed compliance boundary for TSPA-SR calculations.
- Use of sub-grid geostatistical and heterogeneity analysis to derive values for transverse dispersion.
- Use of field and laboratory tests (hydraulic and tracer) to establish and confirm the conceptual models for radionuclide transport and colloid-facilitated transport and to derive parameter values.
- Use of the regional-scale flow and transport model, the UZ model, and the Integrated Site Model to provide the site-scale SZ flow and transport model with boundary conditions and other model parameter values.
- Use of a 500-m (1,640-ft) grid size to simulate flow and transport.
- Use of a deep bottom boundary (approximately 3,000 m [9,840 ft] deep) that coincides with that of the regional-scale model.
- Use of new hydrogeologic data including the new geologic map and cross section published by the U.S. Geological Survey.
- Use of recently collected hydraulic, geologic, geochemical, and transport data that was obtained from Nye County Early Warning Drilling Program Phase-I wells.

3. SATURATED ZONE FLOW AND TRANSPORT MODEL AND ABSTRACTIONS FOR TOTAL SYSTEM PERFORMANCE ASSESSMENT FOR SITE RECOMMENDATION

The U.S. Department of Energy (DOE) has conducted investigations to characterize and model groundwater flow and chemical transport in the vicinity of the potential Yucca Mountain repository because groundwater transport is expected to be the main means of radionuclide transport from the potential repository to the proposed compliance point. Modeling of groundwater flow in the saturated zone (SZ) has been carried out at regional and site scales. The regional-scale model (D'Agnese et al. 1997), encompassing the Death Valley regional groundwater flow system, an area of about 50,000 km² (19,300 mi²), and the potential repository, was developed to model groundwater flow. The site-scale model, encompassing an area of 1,350 km² (521 mi²), the potential repository, and the proposed 20 km (12.5 mi) compliance point (proposed 10 CFR 63.115(b)(1) [64 FR 8640]), was developed to model groundwater flow and chemical transport.

In this section, the site-scale SZ flow and transport model, abstractions, analyses, uncertainties, and limitations of the output are discussed. Discussions are provided concerning characterization of SZ flow and transport (Section 3.1); the conceptual model of site-scale flow and transport (Section 3.2); mathematical and numerical modeling approach (Section 3.3); model validation activities (Section 3.4); assumptions, uses, and limits of the site-scale SZ flow and transport model (Section 3.5); synthesis of the site-scale SZ flow and transport model and model abstractions (Section 3.6); the site-scale SZ flow and transport base case (Section 3.7); and other views and alternative models (Section 3.8).

3.1 SATURATED ZONE FLOW AND TRANSPORT CHARACTERIZATION

Discussions in Section 3.1 primarily are focused on historical data collection and characterization of groundwater flow and radionuclide transport in the SZ. Descriptions of regional and site-scale physiography, climate, soil and vegetation, geology, and groundwater flow are provided in Section 3.1.1. Also in this section is a discussion of groundwater chemistry at a scale slightly larger than that of the site-scale model domain. Hydrologic data (water levels, well testing, and recharge) are summarized in Section 3.1.2. Hydrochemical data pertinent to transport (specified patterns, results of tracer test, and oxidation potential) are summarized in Section 3.1.3. Laboratory data from sorption, diffusion, and colloidal transport experiments are summarized in Section 3.1.4.

3.1.1 Description of the Saturated Zone System

The following subsections describe the regional and site-scale geologic setting, hydrologic setting, and hydrogeochemistry. The regional description, except for the discussion of hydrochemistry, is abstracted from D'Agnese et al. (1997). The regional-scale discussion on hydrochemistry is based on CRWMS M&O (2000m).

3.1.1.1 Regional Description

Physiography—The Death Valley Region is situated within the southern Great Basin, a subprovince of the Basin and Range physiographic province. Altitudes range from 86 m (282 ft)

below sea level at Badwater in Death Valley to 3,600 m (11,800 ft) above sea level at Mount Charleston in the Spring Mountains. The relief between valleys and adjoining mountains locally exceeds 1,500 m (4,920 ft). Most of the principal mountain ranges have distinct northwest-southeast trends, although the trends of intermediate-scale topographic features are variable. The uplands occupy about 25 percent of the landscape in the region, while the remainder of the landscape is occupied by broad intermontane basins formed from tectonically down-dropped grabens. The basins are filled with alluvium and locally interbedded volcanic deposits. These deposits gently slope from the valley floors to the bordering mountain ranges, forming piedmonts.

Climate—The northern part of the region, including the Cactus, Kawich, and Timpahute Ranges (Figure 2-2), is characterized by warm, dry summers and cold, dry winters. The southern part of the region, including Death Valley and the Eastern Mojave Desert, is characterized by hot, dry summers and warm, dry winters. The central region around the Nevada Test Site (NTS) and Yucca Mountain has been called a transition desert, and represents a combination of the two climates. The upland areas receive the bulk of the annual precipitation, with mean values exceeding 700 mm/yr (28 in./yr) in the Spring Mountains, but the valleys receive much less, with a mean annual precipitation in Death Valley of only 50 mm/yr (2 in./yr). Average annual lake-evaporation values range from about 1,100 mm (43 in.) in the north to more than 2,000 mm (79 in.) in Death Valley (Grasso 1996, Table 8).

Studies of past climates indicate that in the Death Valley region, climate oscillated between glacial and interglacial episodes, although glaciers were limited to colder regions of North America. The current climate generally is typical of interglacial periods, although paleoclimate records suggest that in the Yucca Mountain region, the present interglacial period is hotter and drier than earlier interglacial episodes (D'Agnese et al. 1997). In contrast to the current climate, periods of more extensive glaciation dominated the climate of North America for most of the past 500,000 yrs. Glacial episodes (also termed pluvial episodes south of the glacier border) were characterized by wetter and colder conditions than at present, and they prevailed over approximately 80 percent of that time.

The principal effect of a cooler, wetter climate during glacial times on the SZ hydrology was increased recharge. This, in turn, resulted in larger gradients of hydraulic head, more total groundwater flow, a rise in the water table, and increased surface discharge in the form of streams, springs, and wetlands. A variety of physical evidence suggest that the water table in the Yucca Mountain region has been up to 120 m (30 ft to 394 ft) higher than the current water table (CRWMS M&O 2000w, Table 9.4-1), whether due to climate change or some other cause. Conversely, the preponderance of field data suggest that the water table has risen no more than 120 m (394 ft) above present levels for extended periods of time in the Yucca Mountain area since deposition of the volcanic units over 10 my ago (NRC 1999a, p. 30). Similarly, various hydrologic models that incorporate climate-induced changes predict that the water table was from less than 50 m to 150 m higher than the current water table (CRWMS M&O 2000w, Table 9.4-2) during the Pleistocene glacial maximum.

Soil and Vegetation—In general, soils of the mountains and hills are shallow, coarse textured, and have little moisture-holding capacity. The soils of the alluvial fans on the upper slopes of valleys are coarse in texture, but these soils are deeper, and infiltration rates are relatively high.

Infiltration rates of the alluvial basin soils are slow because the downward movement of water commonly is impeded by indurated calcium carbonate layers (pedogenic carbonate), fine-grained playa deposits, and, more commonly, by silicified hardpans that form within the soils over time. Vegetation often extracts most of the precipitation before it infiltrates deep enough to become recharge.

3.1.1.1.1 Regional Geologic Setting

Groundwater flow in the SZ is controlled largely by the distribution of rock types and their respective permeabilities and porosities. Structural features such as fractures and faults may act as avenues for preferential flow or as barriers to flow. Thus, an adequate understanding of the geologic framework is essential to effectively characterize and model groundwater flow and radionuclide transport.

Geologic History and Structure—The Death Valley region primarily consists of Precambrian igneous and metamorphic rocks, Paleozoic-Precambrian clastic rocks, Paleozoic carbonate rocks, Mesozoic sedimentary and metavolcanic rocks, Tertiary-Late Jurassic granitic rocks, Tertiary volcanic and volcanoclastic rocks, Tertiary volcanic rocks, Quaternary-Tertiary volcanic rocks, Quaternary-Tertiary valley fill, and Quaternary playa deposits.

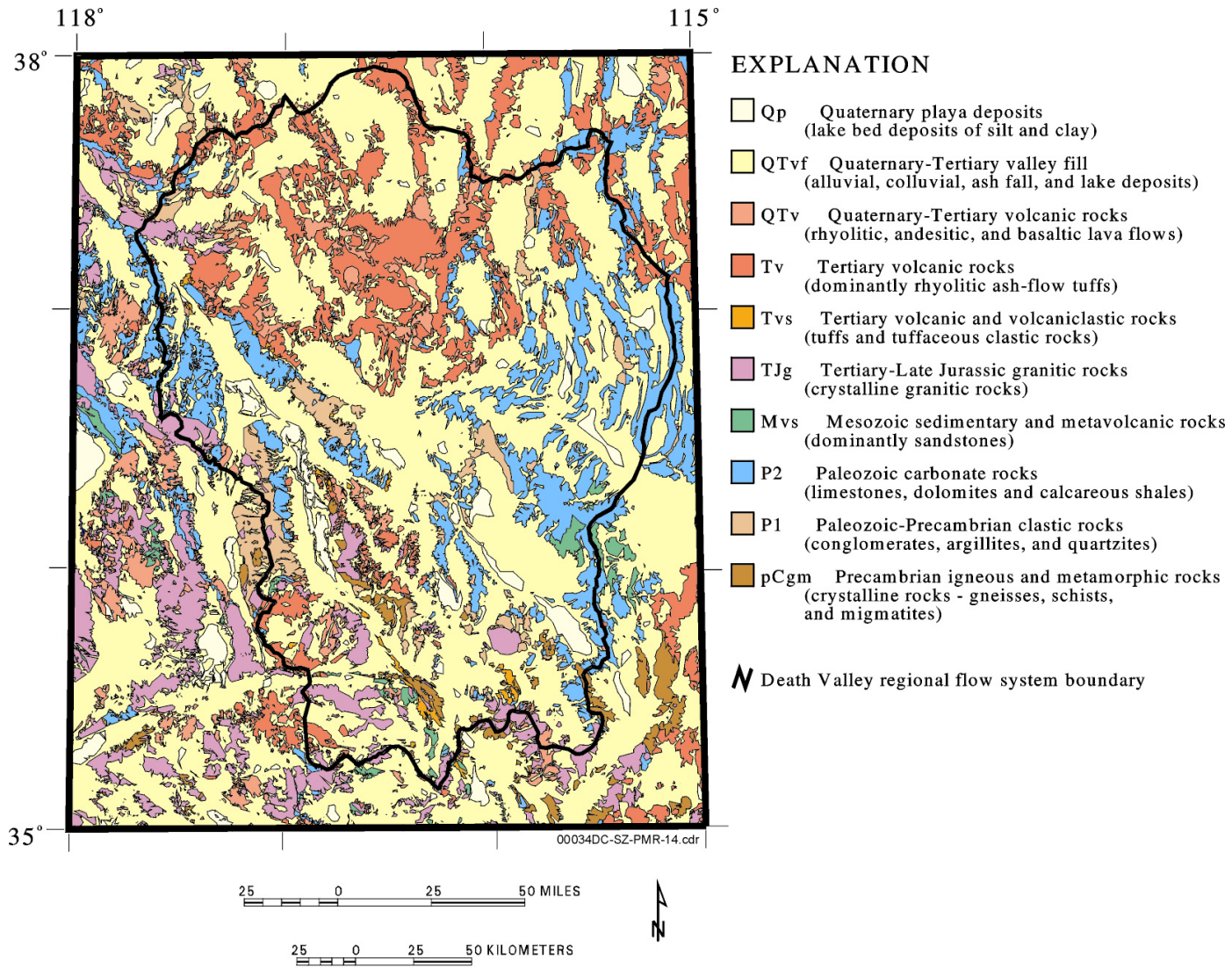
The region has been altered by several episodes of tectonic activity. Combinations of normal, reverse, and strike-slip faulting and folding episodes resulted in a complex distribution of rocks. In contrast to earlier compressional tectonism, regional uplift, erosion, volcanism, and extension occurred in the Tertiary. As a result, the Death Valley region now includes numerous north-south trending valleys containing alluvial, paludal, and colluvial materials that are interstratified with volcanic lava flows, tuffs, and tuffaceous sediments.

Hydrostratigraphy—D'Agnesse et al. (1997, pp. 17 to 20) classified the rocks and deposits of the Death Valley region into 10 hydrogeologic units (Figure 3-1). These hydrogeologic units have considerable lateral extent and reasonably distinct hydrologic properties:

Quaternary Playa Deposits—Quaternary playa deposits are relatively homogeneous deposits mainly composed of sand, silt, and clay-sized particles. In some of the valleys, these deposits are several hundred meters thick.

Quaternary-Tertiary Valley Fill—Quaternary-Tertiary valley fill is a heterogeneous mixture of fine-grained playa and lakebed deposits, fluvial deposits, heterogeneous debris flow and fan deposits, and volcanic tuffs. In many basins, the valley fill is greater than 1,300 m (4,250 ft) thick and may be as thick as 2,000 m (6,550 ft). Valley fill deposits form the major aquifer system in many valleys.

Quaternary-Tertiary Volcanic Rocks—Volcanic rocks, including lava flows and undifferentiated volcanic rocks, underlie the valleys and crop out extensively in many of the mountains. The lava flows primarily are basalts, andesites, and rhyolites. Columnar jointing and platy fractures are common in the flows, which vary from vesicular to dense. Individual flows generally are less than 30 m (98 ft) thick, and some are less than 1 m (3 ft) thick; however, in aggregate, these deposits are as much as 1,000 m (3,300 ft) thick.



Source: D'Agnese et al. (1997, Figure 8)

Figure 3-1. Hydrogeologic Units in the Death Valley Regional Groundwater Flow System Area

Tertiary Volcanic Rocks—Rhyolitic ash-flow tuffs and undifferentiated volcanic rocks underlie valleys and crop out extensively in northern and central portions of the Death Valley region, including the Yucca Mountain area where tuffs are widespread (Figure 3-1). In aggregate, these units are more than 4,000 m (13,000 ft) thick.

This hydrogeologic unit includes densely welded to nonwelded, bedded, reworked, and air-fall tuffs. The commonly moderate to high hydraulic conductivity of welded ash-flow tuffs is largely a function of secondary openings along joints, bedding planes, and partings within the flows. Where these welded tuffs are not fractured or jointed, they tend to form confining units; thus, welded tuffs can only transmit large quantities of water where they are fractured.

Nonwelded ash-flow tuffs may have a large interstitial porosity; however, they have low hydraulic conductivity and function as confining beds. Fractures and joints virtually are absent in nonwelded ash-flow tuffs. These nonwelded tuffs, however, have limited spatial extent. In the Yucca Mountain area, the Tertiary volcanic rocks include the Timber Mountain and the Paintbrush Group down to the base of the Topopah Spring Tuff.

Tertiary Volcanic and Volcaniclastic Rocks—This hydrogeologic unit is composed of tuffs and associated sedimentary rocks. These rocks include up to 1,500 m (4,900 ft) of a variety of nonwelded to welded ash-flow tuff, ash-fall tuff, tuff breccia, breccia-flow deposits, tuffaceous sandstone, siltstone, mudstone, freshwater limestone, and minor amounts of densely welded tuff. In the Yucca Mountain area, this unit includes the Calico Hills Formation, Crater Flat Group, Lithic Ridge Tuff, and older tuffs, lavas, and breccias.

Tertiary-Late Jurassic Granitic Rocks—This hydrogeologic unit is composed of crystalline granitic rocks that are widespread throughout the southern portion of the region, crop out in many mountain ranges (Figure 3-1), and underlie most of the southern portion of the region at depth. Groundwater is thought to occur in these rocks only where they are fractured, but because the fractures are poorly connected, these rocks mostly act as confining units.

Mesozoic Sedimentary and Metavolcanic Rocks—This hydrogeologic unit is composed of clastic rocks that predominantly are fluvial, lacustrine, and eolian deposits; and clastic and carbonate sedimentary rocks.

Paleozoic Carbonate Rocks—This hydrogeologic unit is composed of limestone, dolomite, and calcareous shales that underlie many valleys and crop out in some mountains (Figure 3-1). These carbonate rocks, which have aggregate thickness of about 8,000 m (26,000 ft), are generally the most permeable rocks in the area. Most of the large springs in the region are associated with the carbonate rocks. At the NTS, the Eleana Formation separates the carbonate rocks into upper and lower carbonate aquifers. The Eleana Formation, composed mostly of relatively impermeable argillites and shales, forms a locally important clastic confining unit.

Paleozoic-Precambrian Clastic Rocks—This hydrogeologic unit is composed of siltstone, quartzite, shale, sandstone, and some metamorphic rocks that form clastic confining units. Regionally, these rocks vary in aggregate thickness, with maximum thicknesses of about 3,500 m (11,500 ft).

Precambrian Igneous and Metamorphic Rocks—This hydrogeologic unit is composed of crystalline metamorphic rocks and igneous rocks that are widespread throughout the southern part of the region (Figure 3-1), cropping out in many mountain ranges and underlying most of the area at depth.

3.1.1.1.2 Regional Hydrologic Setting

A considerable amount of information concerning regional-scale hydrogeology was synthesized while conceptualizing and modeling the Death Valley regional groundwater flow system (D’Agnese et al. 1997). A general understanding of the regional-scale system is important for understanding the Yucca Mountain system because the regional-scale system sets the context for the site-scale geologic and hydrologic systems. An important aspect of the regional hydrogeologic system is that the system occurs in an enclosed basin without any surface or subsurface points of discharge to the ocean: all water that naturally leaves the region does so exclusively through the processes of evaporation or evapotranspiration.

Recharge within the Death Valley flow system occurs at high elevations where relatively larger amounts of snow and rainfall occur (D’Agnese et al. 1997, Figure 25). In the vicinity of Yucca Mountain, recharge from precipitation occurs at Timber Mountain, Pahute Mesa, Rainier Mesa, Shoshone Mountain, and Yucca Mountain itself (Figure 2-2). Closer to Yucca Mountain, infiltration of runoff in Fortymile Canyon and Fortymile Wash contributes recharge to the Death Valley flow system (CRWMS M&O 1999a). Groundwater flows through Quaternary, Tertiary, and Paleozoic aquifers to discharge areas. Discharge areas for the Death Valley flow system include Ash Meadows, Alkali Flat (Franklin Lake Playa), Oasis Valley, and Death Valley (the ultimate discharge point for the regional-scale flow system). These and other areas of discharge within the regional groundwater system are presented by D’Agnese et al. (1997, Figures 23 to 24). Gradients of hydraulic head (represented by a potentiometric surface map, Figure 3-2) determine the flow paths of groundwater as it moves from areas of recharge to areas of discharge. Flow paths within the Death Valley regional system are presented by D’Agnese et al. (1997, Figures 28 to 33).

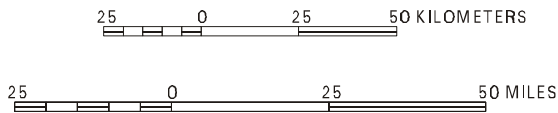
3.1.1.1.3 Regional Hydrochemistry

The application of hydrogeochemical and isotopic chemical methods make it possible to reduce some of the uncertainties concerning regional groundwater flow patterns and rates of flow. They also provide some bounds on the magnitude and timing of recharge represented by SZ waters. The discussion in this section is based on CRWMS M&O (2000m) who considered flow in a region about 2.5 times larger than the domain of the site-scale SZ flow and transport model (Figure 3-3).



Universal Transverse Mercator projection, Zone 11.
 Shaded-relief base from 1:250,000-scale Digital Elevation Model;
 sun illumination from northeast at 30 degrees above horizon

00034DC-SZ-PMR-11.cdr

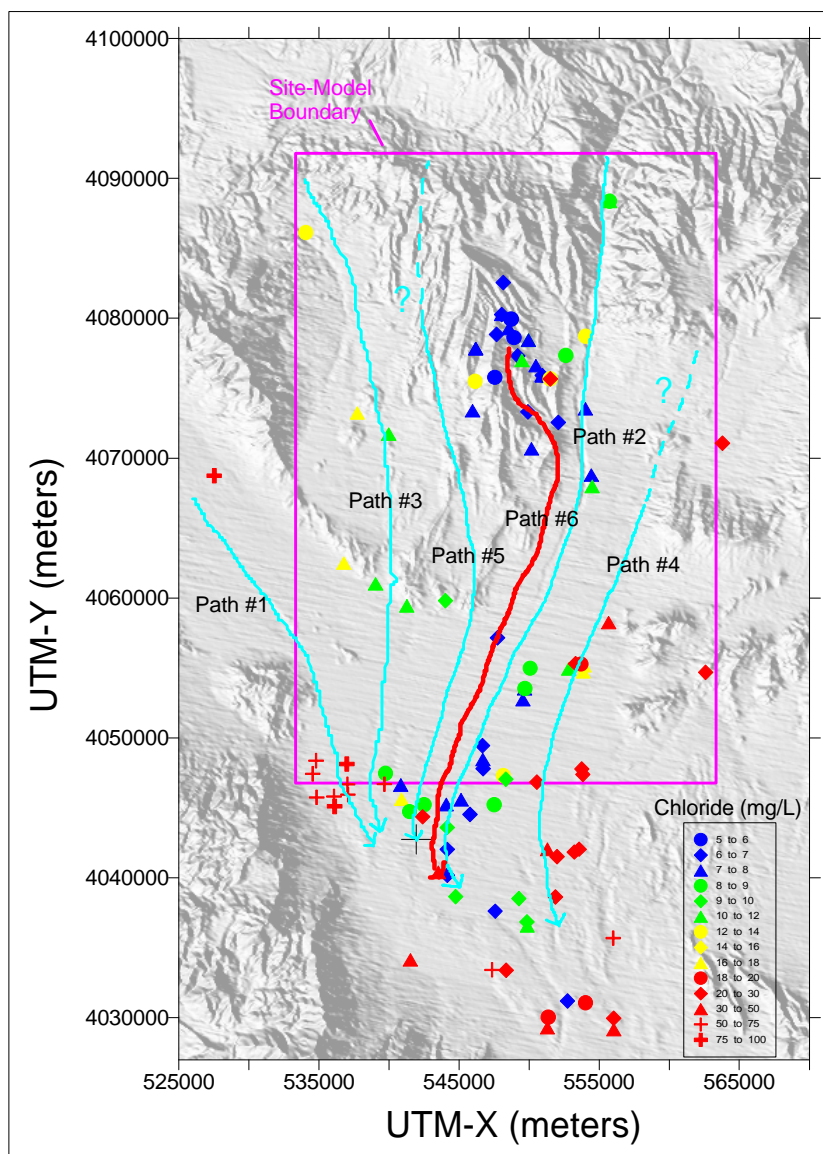


EXPLANATION

- Death Valley Regional Flow System Boundary
- 1,000— Potentiometric contour- Shows altitude of potentiometric surface. Contour interval 100 meters. Datum is sea level.

Source: D'Agness et al. (1997, Figure 27)

Figure 3-2. Regional-Scale Potentiometric Surface Map



Source: CRWMS M&O (2000m, Figure 17)

NOTE: Thickness of the flow lines does not indicate confidence interval.

Figure 3-3. Groundwater Flow Paths Near Yucca Mountain

The main process that control groundwater chemistry are:

- Precipitation (atmospheric) quantities and compositions
- Surface-water quantities and compositions in recharge areas and along stream courses
- Soil-zone processes in recharge areas and along flow paths between the soil and SZ
- Rock-water interactions in the unsaturated zone (UZ)
- Rock-water interactions in the SZ
- Temperature and pressure effects in the UZ and SZ
- Mixing of groundwaters from different flow systems.

Groundwaters that travel along different pathways can be influenced to differing degrees by these various processes. As a result, these groundwaters can attain different chemical signatures that reflect their individual histories. Chemical constituents that show the least impact from interactions with water and rocks in the UZ and SZ are called conservative constituents. These constituents are particularly important with respect to flow path delineation because their concentrations primarily reflect inputs and processes that operate in recharge areas. The main inputs and processes in recharge areas include precipitation compositions, rates of evapotranspiration, and soil zone mineral dissolution and precipitation reactions. Conservative constituents for which analytical data are available include chloride, sulfate, fluoride, delta deuterium, and delta oxygen-18. None of these species is truly conservative; for example, there are potential mineral sources of sulfate in the map area.

Groundwater Flowpaths—Spatial distributions of chemical and isotopic data were used to determine (i.e., constrain) flow paths in the region. The analysis determines flow paths by connecting upgradient areas that have distinct chemical compositions to downgradient areas that have similar chemical compositions (CRWMS M&O 2000m). The map of the potentiometric surface was used to guide, but not to determine, the selection of which downgradient areas potentially could be linked by a flow path to an upgradient area. Because the flow-path analysis assumes that groundwater can be traced in two dimensions, it does not consider the possible effects of local recharge and vertical mixing between aquifers. Neglecting the effects of recharge and aquifer mixing in this simple two-dimensional (2-D) analysis causes the estimated flowpaths to be diverted away from areas where the groundwater composition changes as a result of these processes. In reality, recharge and vertical mixing between aquifers also could divert groundwater upward or downward beneath the affected areas, as well as laterally away from these areas.

Flow paths can be traced using chemistry and isotopes only where compositional differences exist that allow some directions to be eliminated as possible flow directions. Because no single chemical or isotopic species varies sufficiently to determine flow paths everywhere in the study area, multiple chemical and isotopic species were used to infer flow paths. There are, however, anomalies in the chemical composition of waters along the inferred flowpaths. These are probably due to the wide range of sampling depths and geologic units. The flow-path analysis assumed that the delta deuterium, delta oxygen-18, chloride, sulfate, sodium, and calcium composition of groundwater along a flow path did not change because of interactions between rocks and the groundwater, local recharge of water with a different composition, or vertical mixing between aquifers.

CRWMS M&O (2000m) used the chemical composition of groundwater to infer flow paths. Groundwater in the Amargosa Desert west of Bare Mountain was inferred to flow southeast through the corner of the site-scale model domain and into the Amargosa Valley while moving roughly parallel to the Amargosa River (Figure 3-3, flow path #1). Groundwater in Fortymile Canyon flows southward parallel to Fortymile Wash and connects with downgradient areas in the Amargosa Desert (Figure 3-3, flow path #2). Groundwater in the northwest corner of the site-scale model domain flows south-southeast through central Crater Flat and then south into the Amargosa Valley (Figure 3-3, flow path #3). Groundwater in central Jackass Flats flows southwest, roughly parallel to Fortymile Wash, into the Amargosa Valley before turning south-southeast beyond the southern boundary of the site-scale model domain (Figure 3-3, flow

path #4). Groundwater in northeastern Crater Flat flows south-southeast through eastern Crater Flat, and then after reaching the southern edge of Yucca Mountain, it flows south-southwest into the Amargosa Valley (Figure 3-3, flow path #5). Groundwater beneath the potential repository flows southeast towards Fortymile Wash, but then moves south-southwest parallel to, and west of, the wash until it reaches the Amargosa Valley (Figure 3-3, flow path #6). This flow path is constrained by (i.e., flows between) flow path #2 in Fortymile Wash and flow path #5 in eastern Crater Flat. The delta deuterium and delta oxygen-18 values of groundwater reflect the composition of the recharge water and are generally not affected by interactions between the water and rocks except under special conditions (e.g. boiling temperatures, gas vents) that do not exist at Yucca Mountain. The assumption that chloride concentrations are not altered by water/rock interaction is based on the absence of chloride-bearing minerals in the volcanic aquifer. Sulfur-bearing minerals are locally important at the base of the volcanic aquifer and in the Calico Hills, but generally sparse in the volcanic aquifer. Calcium and sodium concentrations can be altered by water/rock interactions such as rock weathering, clay precipitation, and cation exchange. Calcium and sodium were used only to confirm flowpath estimates based on other chemical or isotopic indicators, or were used where other indicators did not show compositional contrasts and the spatial contrasts in calcium and sodium concentrations were sufficiently large that departures from non-conservative behavior were acceptable.

The regional flow paths constructed on the basis of the hydrochemical and isotopic data generally are consistent with flow paths that could be inferred from the potentiometric surface but have a stronger north-south component. The stronger north-south component could reflect the general north-south structural fabric of the rock, the inability of the method to account for chemical mixing due to recharge or upwelling from the carbonate aquifer, or simply the sparseness of the data in certain areas. Although it is not possible to conclusively identify the reason for the differences, the actual flowpaths probably are bounded by the two representations of the flow system, each of which relies on a different and independent set of assumptions.

Timing of Recharge—The timing of recharge for SZ groundwaters at Yucca Mountain, as determined by the uncorrected carbon-14 ages of the perched water, generally is between 11,000 and 7,000 yrs before present (CRWMS M&O 2000m). As discussed in detail by CRWMS M&O (2000m), the uncorrected carbon-14 ages of perched water are believed to represent the actual time of recharge of these waters. Corrections to the carbon-14 ages were made which consider plausible chemical reactions that may have produced the observed chemistry of the groundwater samples. The corrected carbon-14 ages were approximately one carbon-14 half-life (5,730 yrs) younger than the uncorrected carbon-14 ages (i.e., 6,000 to 13,000 yrs). Because of the assumption that all carbon contributed by carbonate dissolution had a carbon-14 activity of 0 percent modern carbon, and because the model did not consider the increase in calcium and magnesium in soil water due to evaporation in the soil zone, the corrected carbon-14 ages of groundwater are considered lower limits for the true average age. The true carbon-14 ages probably are bounded by the corrected and uncorrected carbon-14 ages.

Magnitude of Recharge—Estimates of the magnitude of recharge to the SZ in the vicinity of Yucca Mountain were obtained using the chloride mass balance method (CRWMS M&O 2000m). This method is simple and appears reliable based on comparisons with other techniques used to estimate the magnitude of recharge. Estimates of recharge range from less than 0.5 mm/yr (0.02 in./yr) beneath washes with thick alluvial cover to a maximum of 20 mm/yr

(0.8 in./yr) beneath ridge tops and side slopes. For groundwaters within the immediate vicinity of Yucca Mountain, chloride concentrations range from 5 to 9 mg/L, indicating local recharge rates of 7 to 14 mm/yr (0.3 to 0.6 in./yr). These values, based on simple methods, are consistent with UZ Process Model Report (PMR) values (CRWMS M&O 2000b, Section 3.5).

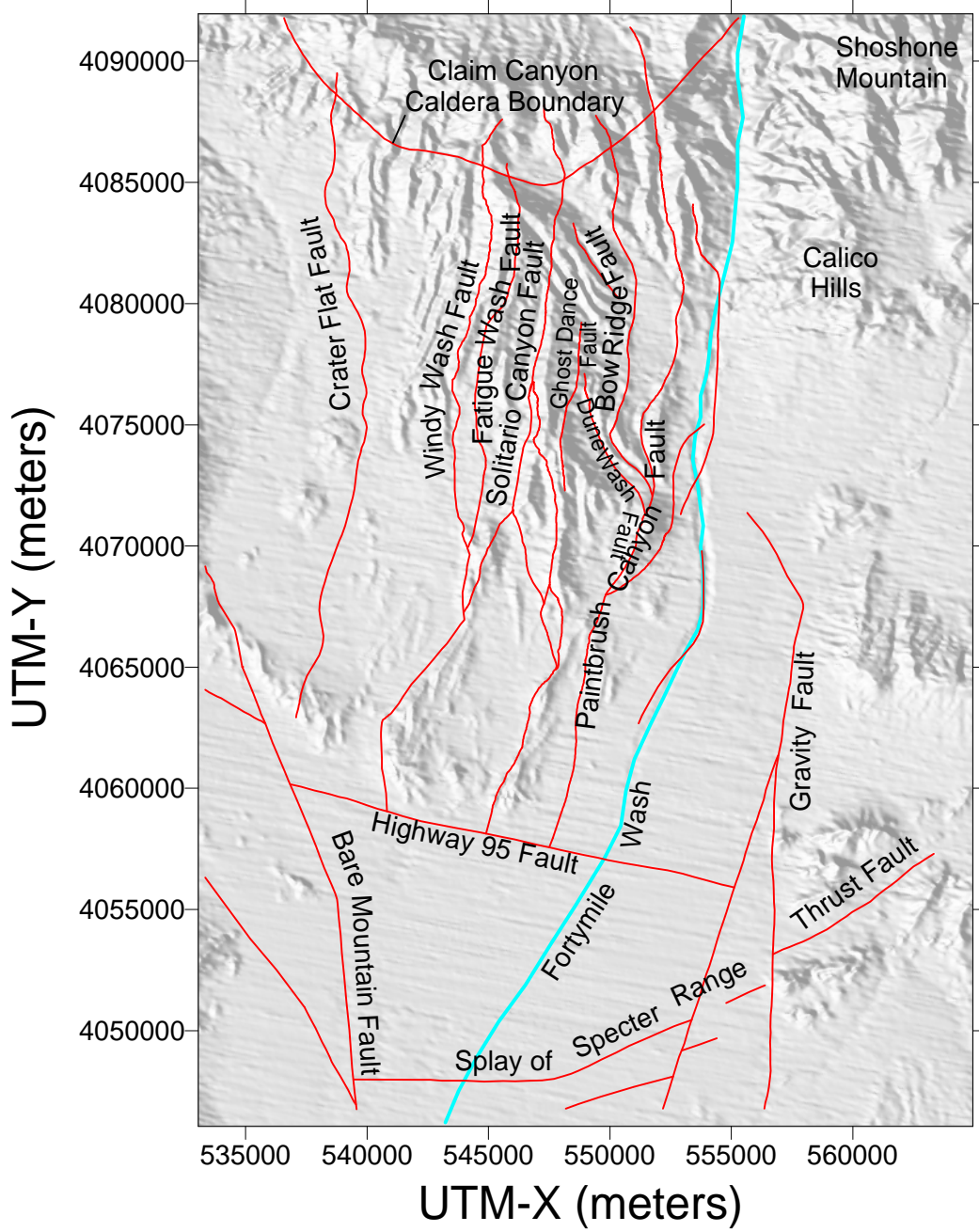
3.1.1.2 Site Description

The site-scale flow system comprises the rocks and water of the area near Yucca Mountain (Figures 2-1 and 3-4), extending from the water table down to a depth of 2,750 m (9,020 ft) below sea level. Within the site-scale model area, the physiography, climate, soils, and vegetation generally are similar to elsewhere in the region, as described in Section 3.1.1.1. However, because the altitude ranges only from about 710 m (2,330 ft) at the southern border of the model area to about 2,200 m (7,220 ft) at Shoshone Peak in the northeastern part of the model area, the climatic extremes of temperature and precipitation are less than those cited in the regional description. Descriptions of the site-scale geologic setting, hydrologic setting, and hydrochemistry are presented in Sections 3.1.1.2.1, 3.1.1.2.2, and 3.1.1.2.3, respectively.

3.1.1.2.1 Site-Scale Geologic Setting

Yucca Mountain consists of a group of north-south-trending block-faulted ridges (Figure 3-4) composed of volcanic rocks of Tertiary age that are several kilometers thick. Crater Flat, the basin west of Yucca Mountain (Figure 3-4), is composed of a thick sequence (about 2,000 m [6,500 ft]) of Tertiary volcanic rocks, Tertiary and Quaternary alluvium, and small basaltic lava flows of Quaternary age. The Solitario Canyon fault separates Crater Flat from Yucca Mountain. Fortymile Wash, a structural trough, delimits the eastern extent of Yucca Mountain. East of Yucca Mountain are the Calico Hills, an assemblage of Tertiary volcanic and Paleozoic rocks. Yucca Mountain terminates to the south in the Amargosa Desert, which consists of interbedded Quaternary and Tertiary alluvial, paludal, and tuffaceous sediments. At depths of about 1,800 m (5,900 ft) or greater at Yucca Mountain, the volcanic deposits are underlain by a thick sequence of early Paleozoic dolomites and limestones that form the lower carbonate aquifer. Subsequent to deposition, the volcanic and older rocks were faulted and tilted, resulting in a series of gently eastward-dipping fault blocks.

Aspects of the site-scale geology that pertain to groundwater flow are represented in the site-scale hydrogeologic framework model (HFM). A detailed description of the HFM, the assumptions, and the methods used to develop the model are given by (USGS 2000a). Information from geologic maps, cross sections, borehole data, fault-trace maps, and geophysical data were used to construct a 3-D interpretation of the hydrostratigraphy and geologic structure within the domain of the HFM. Stratigraphic units within the HFM are grouped into hydrogeologic units that are classified by age (e.g., older volcanics) or rock type (e.g., carbonate). Where differentiation was possible within a unit, the unit was further divided into subunits having relatively high permeabilities (aquifers) or relatively low permeabilities (confining units). The HFM specifies the position and geometry of these hydrogeologic units. In addition, the HFM identifies major faults (Figure 3-4) that affect groundwater flow.



Source: Adapted from CRWMS M&O (2000n, Figure 4)

Figure 3-4. Structural and Tectonic Features Units within the Site-Scale Saturated Zone Model Area

Ten hydrogeologic units are defined in the regional-scale flow model (Section 3.1.1.1.1); however, 18 hydrogeologic units are used in the site-scale HFM. Some of the regional-scale units are not included because they are not present in the site-scale area, and some of the regional-scale units are subdivided into additional units (USGS 2000a, Table 6-1). The 18 hydrogeologic units are represented in the site-scale flow and transport model, and all are defined in the HFM (USGS 2000a). The following description of the eight principal aquifers and confining units is based on the classification in the HFM (USGS 2000a, Table 6-1).

Basin Fill Aquifer—This aquifer underlies most of the Amargosa Desert area to the east and south of Yucca Mountain. It is composed of alluvial fan, fanglomerate, lakebed, and mudflow deposits, and has a thickness of several hundred meters. This aquifer is the main water source for domestic and irrigation use in the Amargosa Valley. In addition, the valley-fill aquifer may receive lateral flow and recharge from the volcanic tuffs.

Upper Volcanic Aquifer—The Topopah Spring unit of the Paintbrush Tuff is the uppermost water-bearing unit of the SZ and is the upper volcanic aquifer in the Yucca Mountain area. It consists of variably welded ash-flow tuffs and rhyolite lavas (nonwelded tuffs). The Topopah Spring unit is not saturated below the potential repository, but it becomes saturated to the east and south of Yucca Mountain and in Crater Flat.

Upper Volcanic Confining Unit—This confining unit consists of rhyolitic lavas, volcanic breccias, and nonwelded to welded tuffs, and commonly is argillaceous or zeolitic. It includes the lowermost part of the Topopah Spring Tuff, the Calico Hills Formation, and the uppermost part of the Crater Flat Group.

Lower Volcanic Aquifer—This aquifer consists of variably welded ash-flow tuffs and rhyolite lava. It includes most of the Prow Pass Tuff and the underlying Bullfrog and Tram tuffs of the Crater Flat Group. This aquifer underlies Yucca Mountain, but tends to produce less water than the upper volcanic aquifer.

Lower Volcanic Confining Unit—This confining unit consists of nonwelded and commonly zeolitized units of the Lithic Ridge Tuff.

Older Volcanic Aquifer—This aquifer consists of variably welded ash-flow tuffs and rhyolite lavas below the Lithic Ridge Tuff, which corresponds to the Tub Spring member and the lava flow and welded tuff aquifer. It has a moderate permeability that is comparable to the permeability of the lower volcanic aquifer.

Older Confining Unit—In areas where the upper carbonate aquifer is not present, such as in the Yucca Mountain area, the older confining unit consists of the lowermost part of the volcanic sequence and the uppermost part of the pre-Cenozoic sequence. The lowermost part of the volcanic sequence includes nonwelded and commonly zeolitized units of older volcanics at the lowermost interval of the volcanic sequence. The upper part of the pre-Cenozoic section is the Eleana Formation of Devonian or Mississippian age, which has been characterized as the upper clastic aquitard. In areas where the upper carbonate aquifer is present, such as western Yucca Flat and northern Jackass Flats, it occupies the interval between the lowermost part of the volcanic sequence and the Eleana Formation.

Carbonate Aquifer—Although upper and lower carbonate aquifers have been identified regionally, the upper carbonate aquifer (a limestone aquifer) may not be present at Yucca Mountain. It is absent from the one borehole at Yucca Mountain that penetrates the Paleozoic rocks (i.e., borehole UE-25p#1). The upper carbonate aquifer is underlain by the upper clastic confining unit (Eleana Formation) that consists of low permeability siliceous siltstone, sandstone, quartzite, conglomerate, and limestone. The lower carbonate aquifer underlies the Eleana Formation; it consists of Paleozoic dolomite and limestone, and locally is cherty and silty. The lower carbonate aquifer was penetrated in borehole UE-25p#1.

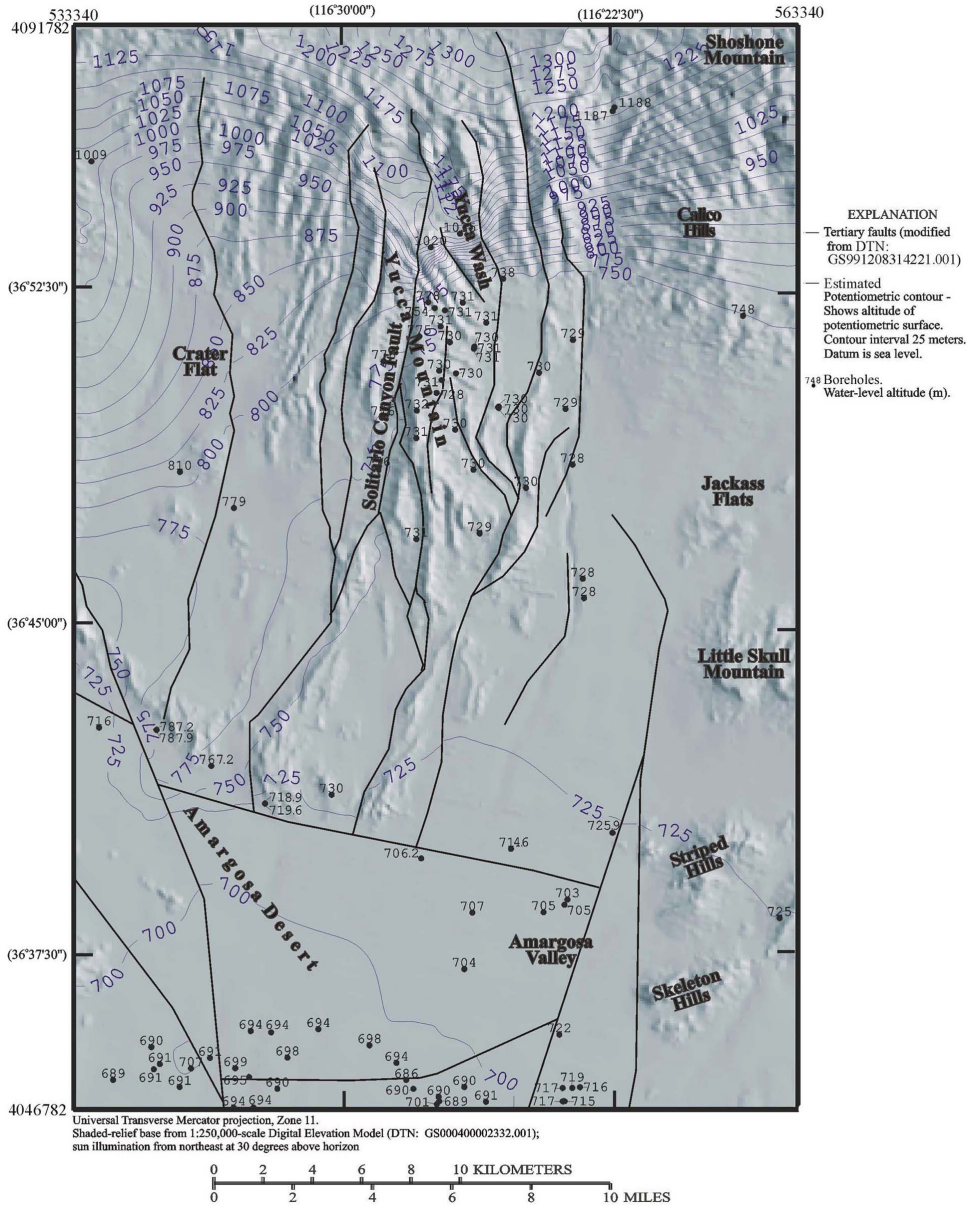
3.1.1.2.2 Site-Scale Hydrologic Setting

The site-scale SZ hydrologic setting comprises the deposits within the site-scale model domain (Figure 3-4) and extends from the water table (the top of the SZ) to a depth of 2,750 m (9,020 ft) below the water table. As described in Section 3.1.1.2.1, the surficial and shallow rocks within this volume consist mainly of alluvial valley fill to the south and pyroclastic volcanic rocks to the north of Highway U.S. 95. These rocks are underlain throughout most of the site-scale SZ model area by a thick lower carbonate aquifer consisting of fractured dolomites and limestones of early Paleozoic age.

Within the alluvial valley fill of the SZ, water occupies the intergranular pores of the granular alluvium. The matrix of the carbonate rock is dense and of low porosity, and the groundwater generally is limited to fractures, many of which have been enlarged by solution. In the volcanic rocks, intergranular porosity and fracture porosity are important. In densely welded tuffs, matrix porosity is low and groundwater is limited to fractures, but in ash-fall tuffs, matrix porosity is high and fractures are limited. A variety of rocks of intermediate porosity also occur.

Groundwater flow in the model area is southward, from regions of high hydraulic head to regions of low hydraulic head (Figure 3-5). In much of the SZ model domain, the gradient of hydraulic head is gentle. However, large differences in measured head occur over short distances north of Yucca Mountain. These large differences indicate either a locally steep hydraulic gradient in the SZ or the presence of perched water north of Yucca Mountain. In other places, heads measured at locations separated by a fault differ, indicating that the fault affects groundwater flow. For example, heads west of the Solitario Canyon fault are more than 770 m (2,525 ft), but heads east of the fault are about 730 m (2,395 ft).

Recharge to the site-scale SZ model area is limited to infiltration of precipitation and stream flow during infrequent episodes of runoff. Infiltration of precipitation largely is confined to the higher terrain in the northern part of the model area and the higher parts of Yucca Mountain (Section 3.2.3.2). Long-term recharge from stream flow in Fortymile Canyon and Fortymile Wash has been estimated by Savard (1998, Table 5). The only other sources of water to the model area are inflows along the northern, eastern, and western boundaries computed from the regional-scale site-scale flow model (D'Agnese et al. 1997). These computed inflows account for approximately 95 percent of the total flux through the site-scale SZ model area (Section 3.2.3.1).



Source: USGS (2000b, Figure 1-2)

NOTE: Potentiometric contours show elevation of the potentiometric surface. Datum is sea level. (Illegibility has no technical impact to the content of the record)

Figure 3-5. Site-Scale Potentiometric Map and Structural Features

Natural discharge (i.e., springs and evaporation of shallow groundwater) does not occur within the site-scale SZ model domain; however, substantial artificial discharge occurs from wells in the Amargosa Farms area in the southwestern part of the site-scale model domain (see the closely spaced well locations on Figure 3-5). Substantial subsurface outflow occurs across the southern boundary of the site-scale model domain (Section 3.4.2).

3.1.1.2.3 Site-Scale Hydrochemistry

Hydrochemical data provide information on several important site-scale issues including the existence and magnitude of local recharge, flow directions from the potential repository footprint to downgradient locations, and the potential for dilution of materials that could potentially be released from the potential repository.

Evidence for the Existence of Local Recharge—Hydrochemical and isotopic data from perched water at Yucca Mountain compared to similar data from the regional groundwater system suggests that local recharge is a component of the SZ waters in volcanic aquifers beneath Yucca Mountain (CRWMS M&O 2000m). The data examined included uranium isotopes (uranium-234/uranium-238) and major anions and cations. It is possible that shallow groundwater is composed entirely of local recharge (CRWMS M&O 2000m).

Likely Flow Paths from the Potential Repository Area—Likely flow paths in the Yucca Mountain area were determined by identifying areas that had similar concentrations of conservative chemical species (e.g., chloride or sulfate) and tracing paths through these chemically similar areas in a downgradient direction (CRWMS M&O 2000m). Of particular interest are paths leading from the potential repository area (Figure 3-3, flow path #6). This pathway starts with low chloride groundwater from the potential repository area just east of Yucca Mountain Crest, and passes wells along Dune Wash with similarly low chloride concentrations, before turning south-southwest near Fortymile Wash. Well WT#12, located immediately south of Dune Wash, has a higher chloride concentration, indicating that the dilute water beneath Dune Wash probably flows southeast along the Dune Wash fault towards Fortymile Wash before turning south-southwest, rather than flowing directly south under Dune Wash. From the intersection of Dune Wash and Fortymile Wash, the only downgradient borehole with a similarly low chloride concentration is borehole NCEWDP-2D (Figure 2-3). South of borehole NCEWDP-2D, the pathway is constrained by the presence of two areas of groundwater with higher chloride concentrations: (1) a western zone, composed of groundwater flowing south from Crater Flat and, possibly, southeast from Oasis Valley; and (2) an eastern zone, composed of groundwater flowing southwest from Jackass Flats and from leakage upward from the carbonate aquifer. The hypothesized flow path was extended south from NCEWDP-2D, keeping the path to the west of the axis of Fortymile Wash and east of the more highly concentrated water from Crater Flat and Oasis Valley.

Importantly, the chloride data (Figure 3-3), as well as other chemical and isotopic data, suggest that groundwater from beneath the potential repository area may not flow along the south-trending faults in the southern part of the mountain. This conclusion is consistent with the potentiometric surface map that indicates that groundwater in this area probably flows from Crater Flat.

3.1.2 Summary of Hydrologic Data

As a foundation for subsequent discussions of the site-scale SZ flow and transport model, the following sections summarize the hydrologic data. Topics include data on water levels and aquifer properties obtained from hydraulic testing of wells, and information on infiltration and recharge available within the area covered by the site-scale SZ flow and transport model.

3.1.2.1 Water-Level Data

A regional-scale potentiometric surface map (Figure 3-2) was constructed using data sets describing water levels, boundaries of perennial marshes and ponds, topographic altitudes, regional spring locations, the distribution of recharge and discharge areas, and hydrogeology (D'Agnese et al. 1997, p. 57). Supplementary data were used to help in the extrapolation of water levels in data-poor areas.

In this sparsely populated, arid, and mountainous region, most water-resource extraction and investigation has occurred in alluvial valleys. The densest concentrations of water-level data in the Death Valley regional groundwater flow system occur in the two largest agricultural communities near Yucca Mountain: the Amargosa Farms area and Pahrump Valley (D'Agnese et al. 1997, Figure 26). Additional water-level data are available from Oasis Valley, Sarcobatus Flat, and Yucca Flat. The only areas with extensive water-level data in consolidated bedrock are Yucca Mountain, Pahute Mesa, and Rainier Mesa (Figure 2-2). The remainder of the region generally is lacking in water-level data.

An automated gridding and contouring software package was used to interpolate the water-level data. Numerous intermediate gridding steps were then conducted, and adjustments were made using hand-contouring methods. Because of the limited data from water wells, additional ancillary data were used to assist the potentiometric surface map construction (D'Agnese et al. 1997). These data were used to guide interpolation of water levels in data-poor areas to produce a regional-scale potentiometric map with 100-m (330-ft) contour intervals (D'Agnese et al. 1997, pp. 56 to 59):

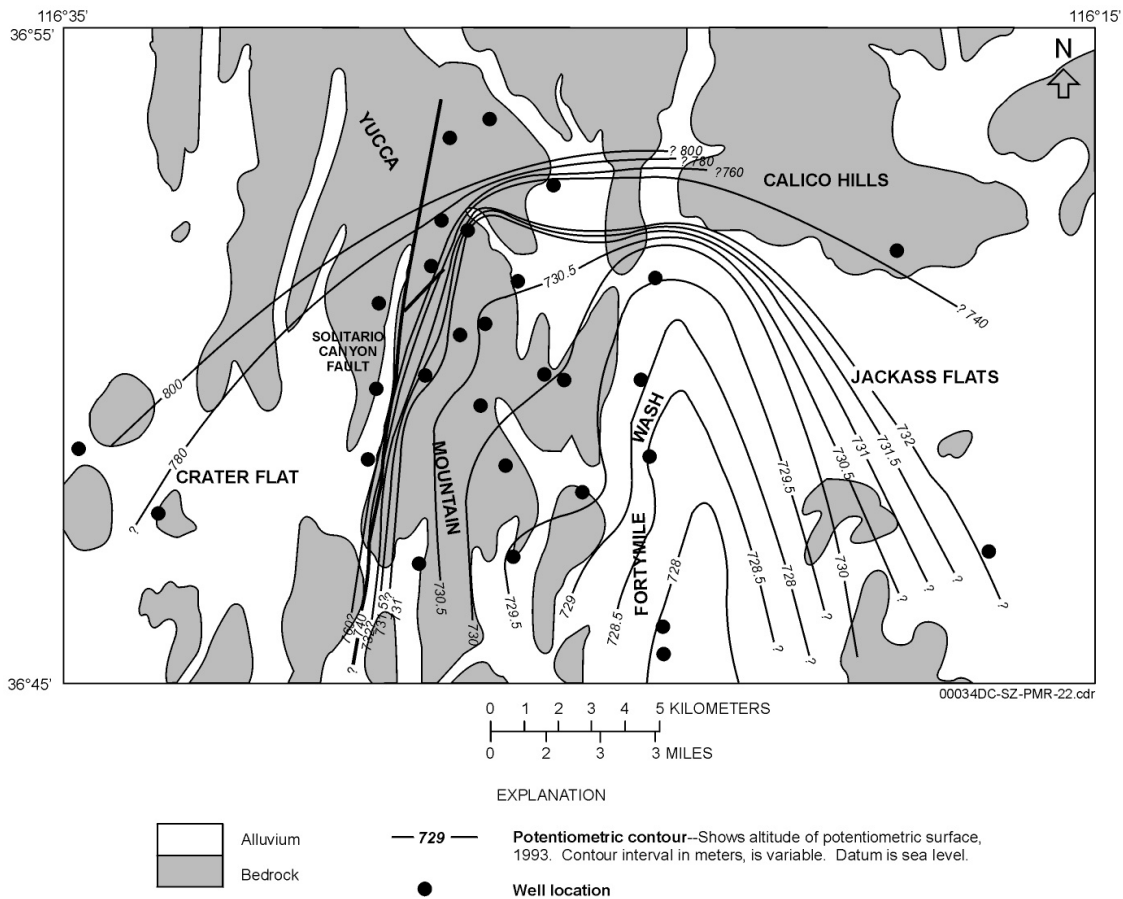
USGS (2000b) developed a potentiometric map for the site-scale SZ flow and transport model domain (Figure 3-5) that was designed to be compatible with the D'Agnese et al. (1997) regional-scale potentiometric map (Figure 3-2). The site-scale potentiometric map (Figure 3-5) implies that the SZ groundwater is a hydraulically well-connected body, although locally it may include perched water levels where perching cannot be ruled out. The site-scale potentiometric map was compiled using available water-level data within the model area, including new information from well WT-24, information from seven wells drilled near Highway US 95 as part of the Nye County Early Warning Drilling Program (NCEWDP), and information from recent Yucca Mountain Site Characterization Project (YMP) large-scale geologic mapping.

To some degree, most of the water levels used in compiling the site-scale potentiometric map (Figure 3-5) represent composite heads in more than one zone; however, it is believed that the surface represented probably is a close and reasonable representation of the water table.

Important features of the new site-scale potentiometric surface map include:

- Water-level data from newly drilled boreholes, including the NCEWDP wells, which provide control along the border between Yucca Mountain and the Amargosa Desert near Highway U.S. 95, an area of former water-level data deficiency.
- Faults are assumed to have an important effect on SZ flow.
- Contour intervals of 25 m (82 ft) represent a considerable refinement as compared to the 100-m (328-ft) contour interval of the regional-scale potentiometric map of D'Agnese et al. (1997, Figure 27), although the 25-m (82-ft) interval still is too coarse to adequately portray the small hydraulic gradient in the area between the potential repository and Fortymile Wash and between Fortymile Canyon and the Amargosa Desert. However, the large and medium hydraulic gradient area can be recognized on the 25-m (82-ft) contour interval map.
- In the fault blocks to the east and west of the Solitario Canyon fault, the new map suggests nearly level hydraulic gradients extending about 10 km (6.2 mi) southward from the vicinity of the potential repository to a fault that is parallel to Highway U.S. 95. This interpretation suggests the existence of large areas of very small hydraulic gradient that are comparable to the small gradient area between Fortymile Wash and Yucca Mountain.
- The time period represented by the new map is early 1990s for consistency with the regional-scale map of D'Agnese et al. (1997, Figure 27).
- The large hydraulic gradient is portrayed as representing the water table rather than a perched condition.

Older potentiometric maps of the immediate vicinity of Yucca Mountain based on 1983 and 1988 water-level data are described by Luckey et al. (1996, p. 21). These maps portray the areas of large, moderate, and low hydraulic gradients (Section 3.2.2.3), but do not portray the gradient near Fortymile Wash. Tucci and Burkhardt (1995) developed a potentiometric surface map based on 1993 water-level data (Figure 3-6); this map includes measurements to the east of Fortymile Wash and presents contours near Fortymile Wash. These contours indicate that groundwater flows toward Fortymile Wash from the east and the west, and then turns southward parallel to Fortymile Wash and flows toward the Amargosa Desert. The contour interval, 0.5 m (1.6 ft), is sufficient to portray details of the potentiometric surface in the area of small hydraulic gradient between Fortymile Wash and the potential repository area. While the potentiometric map of the site-scale model domain portrays the general southward direction of groundwater flow between Fortymile Canyon and the Amargosa Desert (Figure 3-5), the more detailed map provides the pattern of groundwater flow in the immediate vicinity of Fortymile Wash (Figure 3-6).



Source: Tucci and Burkhardt (1995)

Figure 3-6. Potentiometric Surface Map Developed Using Water-Level Data from 1993

3.1.2.2 Hydraulic Well Testing

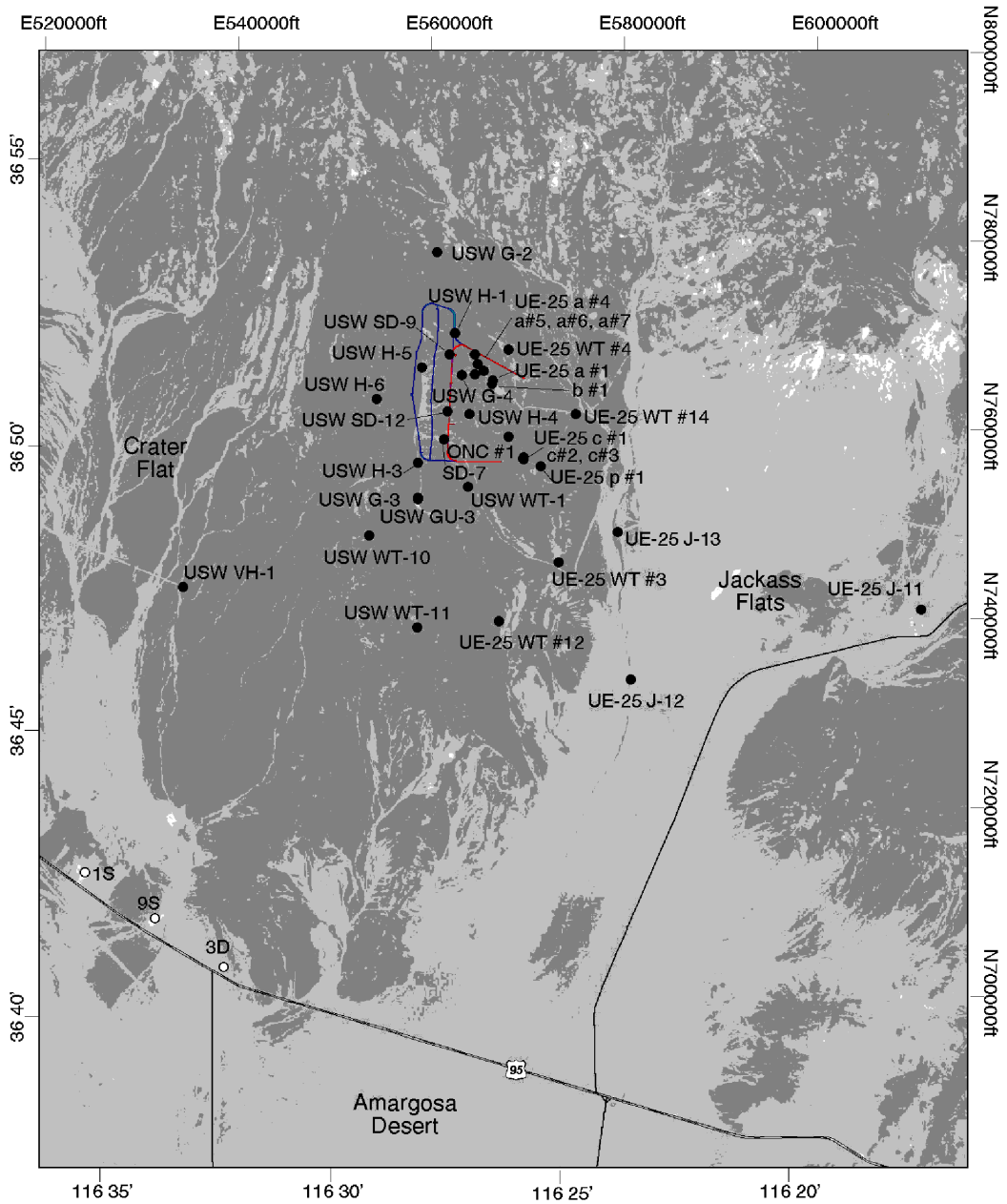
Hydraulic conductivity and effective porosity are the most important physical properties of aquifers needed for calculating the transport of groundwater and contaminants. In field practice, transmissivity (obtained from aquifer test analyses) is divided by the tested saturated thickness to obtain a first approximation of hydraulic conductivity. The degree to which this approximates hydraulic conductivity actually is representative of the transmissive properties of fractured rock. It also requires subjective evaluations of the geologic setting and the results of other tests (i.e., flow surveys) to identify water-producing zones (i.e., flowing intervals in a well within aquifers). However, the actual contributing thickness of a fractured-rock aquifer probably is less than the tested interval, and therefore this thickness generally is unknown. Therefore, for purposes of comparing hydrogeologic units and discussing the overall distribution of rock-mass transmissive characteristics, the following discussion emphasizes transmissivity.

As part of the site characterization process, more than 150 individual hydraulic tests of the SZ were conducted at 37 boreholes in and around Yucca Mountain (Figure 3-7). Other hydraulic tests have been conducted in the vicinity of Yucca Mountain for other purposes, such as the NCEWDP and the Environmental Restoration Program for the NTS. These tests are not discussed in detail in this report. Most tests at Yucca Mountain were conducted in the early 1980s, and nearly all were single-well tests over specific depth intervals. Tests included constant-discharge, fluid-injection, borehole-flowmeter, and radioactive tracer tests. Multiple-well tests have been conducted only at the C-wells Complex, but several tests were conducted at the three wells at the complex. Most test results were reported as transmissivity or hydraulic conductivity of hydraulically isolated intervals. These values can vary by several orders of magnitude, depending on the presence or absence of water-producing fractures in the tested intervals. Storativity, or specific yields, have been reported for a few of the wells. Other hydraulic tests have been conducted throughout the Death Valley region, the results of which were summarized by Bedinger et al. (1989).

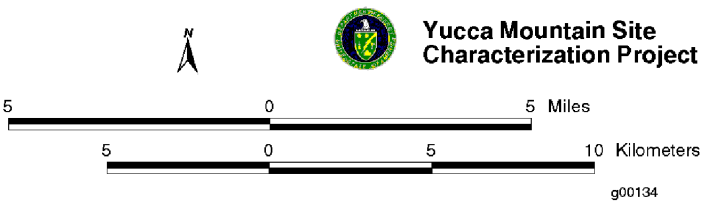
The most recent (1995-1997) aquifer tests were conducted at boreholes USW G-2, USW WT-10, UE-25 WT#12, and the C-wells Complex. Single-borehole, composite-interval, constant-discharge tests were conducted in boreholes USW G-2 in 1996 (O'Brien 1998), USW WT-10 in 1996, and UE-25 WT#12 in 1995 (O'Brien 1997). The Topopah Spring Tuff and the Calico Hills Formation were tested at borehole USW G-2. At borehole USW WT-10, the Topopah Spring Tuff was tested, and at borehole UE-25 WT#12 the Topopah Spring Tuff and the Calico Hills Formation were tested.

Permeability Data from the Yucca Mountain Area—The software used to simulate groundwater flow and transport at Yucca Mountain (Zyvoloski et al. 1997a) requires the use of permeability values rather than hydraulic conductivity or transmissivity. Permeability data from single-hole and cross-hole tests have been collected in the Yucca Mountain area since the early 1980s. A statistical analysis of data collected and published prior to 1998 is presented by CRWMS M&O (2000n, Section 6.7.7).

Single-Hole Tests—For the statistical analysis of the permeability data (CRWMS M&O 2000n, Section 6.7.7), raw data were grouped by combining permeability estimates for individual hydrogeologic units where possible, and by considering progressively more general groupings if the test interval spanned several hydrogeologic units. For instance, in cases in which the test interval was in the Prow Pass Tuff, with or without some portion of the adjacent bedded tuffs, the data were grouped with other permeability estimates for the Prow Pass Tuff. If other units within the lower volcanic aquifer also were present in the test interval with the Prow Pass Tuff, the data were considered to represent the lower volcanic aquifer. If hydrogeologic units other than those in the lower volcanic aquifer were present in the test interval along with the Prow Pass Tuff, the permeability estimate was grouped with the most general category (i.e., mixed tuffs). The mixed tuff category includes data that would not fit into a more restrictive category. All tuffs older than the Lithic Ridge Tuff are listed as Pre-Lithic Ridge Tuffs.



- Legend**
- Saturated Zone Borehole
 - Nye County SZ Borehole
 - ESF Tunnel
 - Perimeter Drift Boundary



00034DC-SZ-PMR-30.cdr
 Data Tracking Number: MO0002COV00088.001

NOTE: This map shows some of the boreholes near Yucca Mountain in which hydraulic tests were conducted.

Figure 3-7. Boreholes Near Yucca Mountain

In instances where several kinds of hydraulic tests (injection, drawdown, or recovery) were conducted in the same depth interval in the same borehole, all of the permeability data that resulted from testing of the interval were used to calculate the summary statistics. By considering multiple measurements from the same test interval, the effects of measurement uncertainty and spatial variability were considered (CRWMS M&O 2000n, Section 6.7.7).

Summary statistics were calculated using base-ten logarithms, but results were presented using the original units of measure. The analysis indicates that the deepest tuffs (the pre-Lithic Ridge Tuffs) and the mixed tuff group have the lowest permeabilities, and that the Topopah Spring Tuff and Prow Pass Tuff have the highest permeabilities. Where they could be calculated, the 95 percent confidence limits indicate that (except for the pre-Lithic Ridge Tuffs) the mean permeability values are constrained within relatively narrow limits. The results also indicate that the Calico Hills Formation, a zeolitized tuff that functions as the upper volcanic confining unit, has a higher permeability than the Bullfrog Tuff and the Carbonate Aquifer. This paradoxical result may reflect the fact that, because it is unsaturated in the western half of Yucca Mountain, the Calico Hills Formation could be hydraulically tested only in the highly faulted eastern half of Yucca Mountain, whereas the other units also were tested in less intensely faulted areas to the west.

Cross-well Tests—The C-wells Complex is a group of three boreholes (UE-25c#1, UE-25c#2, and UE-25c#3) located east of Yucca Mountain (Section 2.2.1.2; Figure 3-7). Aquifer tests have been conducted intermittently at the C-wells Complex since 1983. Preliminary pumping and injection tests that were conducted in 1983-1984, and heat-pulse flowmeter tests conducted in 1992, were re-analyzed by Geldon (1996).

Permeability data from cross-hole tests were compiled, grouped, and analyzed in a manner similar to that for the single-hole tests. Whereas permeability estimates based on single- and cross-hole tests in the Calico Hills Formation were similar, permeability estimates based on single- and cross-hole tests in the Prow Pass Tuff, Bullfrog Tuff, Tram Tuff of the Crater Flat Group, and the Middle Volcanic Aquifer (a name used in the HFM) differed by one to several orders of magnitude. These differences (higher permeability based on cross-hole data) were attributed to the larger volume of rock affected by the cross-hole tests (which allows sampling a larger number of possible flowpaths, including relatively rare, high-transmissivity flow paths). However, some of the increase may have been due to a breccia zone associated with the Midway Valley fault in the Bullfrog Tuff and Tram Member.

Permeability Data from the Nevada Test Site—Permeability data and qualitative observations from the NTS were examined and summarized (CRWMS M&O 2000n, Section 6.7.7) to help constrain permeability estimates for hydrogeologic units that were not tested or which underwent minimal testing at Yucca Mountain. In addition, the NTS data describe the hydrogeologic controls on ground-water movement and provide a regional perspective for ground-water flow at Yucca Mountain.

Lower Carbonate Aquifer—Data from hydraulic tests conducted in six boreholes that penetrated the lower carbonate aquifer were presented in CRWMS M&O (2000n, Table 10). Permeability was calculated from hydraulic conductivity, but the calculation required certain assumptions

(CRWMS M&O 2000n, Section 6.7.7.4), and the calculated permeabilities may overestimate true permeability by a factor of 2 to 3.

In addition to providing quantitative estimates of permeability for the lower carbonate aquifer, CRWMS M&O (2000n, Section 6.7.7.4) also summarize qualitative observations regarding the distribution of permeability within the aquifer. Permeability of the carbonate aquifer showed no systematic decrease with depth. No major caverns were detected. Outcrop evidence indicates that klippen, the upper plates of low angle thrust faults and gravity slump faults, have a higher intensity of fracturing and brecciation than rock below the fault planes and may have above average porosity and permeability. Zones of above average transmissivity often may not be connected to each other.

Valley-Fill Aquifer—Permeability of the valley-fill aquifer was estimated using published transmissivity estimates from four boreholes located in Emigrant Valley, Yucca Flat, and Frenchmen Flat (CRWMS M&O 2000n, Section 6.7.7.5, Table 11). Permeability was calculated from transmissivity, and the calculation required the same assumptions as those used for the lower carbonate aquifer (CRWMS M&O 2000n, Section 6.7.7.4).

In addition to the quantitative estimates of the permeability of valley fill on the NTS, CRWMS M&O (2000n, Section 6.7.7.5) also summarize observations regarding the permeability of the valley fill in the Amargosa Desert. Winograd and Thordarson (1975, pp. C84 to C85) noted that hydraulic head contours south of Lathrop Wells (now Amargosa Valley) probably reflect the effects of upward leakage from the lower carbonate aquifer into poorly permeable valley fill along the Gravity fault and associated faults, and the drainage of this water to more permeable sediments farther west. Winograd and Thordarson (1975, p. C85) argued that the discharge across the Gravity fault near Lathrop Wells probably was small because only the lowermost part of the lower carbonate aquifer is present in the area and the lower clastic aquitard, which underlies the carbonate aquifer at shallow depths, probably would not transmit much water.

Welded-Tuff Aquifer—Hydraulic tests yielding permeability estimates for the welded-tuff aquifer were conducted in two wells in Jackass Flats (CRWMS M&O 2000n, Section 6.7.7.6). Well 74-57 tested the Topopah Spring Tuff and well 74-61 tested the Topopah Spring Tuff and the Basalt of Kiwi Mesa. Permeabilities calculated from drawdown curves for these wells are provided by CRWMS M&O (2000n, Table 12).

Lava-Flow Aquifer—Rhyolitic lavas, and welded and nonwelded tuffs, fill the Silent Canyon caldera complex, which now lies buried beneath Pahute Mesa by younger tuffs erupted from the Timber Mountain caldera complex (CRWMS M&O 2000n, Section 6.7.7.7). A qualitative comparison of the water-producing attributes of these lavas and tuffs indicated that despite considerable overlap in their water-yield potential, the lavas generally were the most transmissive rocks tested, followed by the welded- and zeolitized nonwelded-tuffs (CRWMS M&O 2000n, Section 6.7.7.7). Pumping tests were conducted in boreholes at Pahute Mesa, including 14 boreholes in which the major water production came from rhyolitic lava flows (CRWMS M&O 2000n). Resistivity logs indicate that nonwelded tuffs could constitute as much as 73 percent of the upper 610 m (2,000 ft) of saturated rock at the boreholes listed in CRWMS M&O (2000n). Because most of the water pumped from the lava enters the wells from zones

that constitute only 3 to 10 percent of the total saturated thickness, permeabilities in the lava may be locally higher than the calculated mean value.

Inferences About Permeability From Regional Observations—In addition to the permeability values from the NTS summarized by CRWMS M&O (2000n), Winograd and Thordarson (1975) made numerous qualitative evaluations of the relative magnitude of permeability of different hydrogeologic units. These evaluations were based on the geologic setting, the magnitude of spring discharge in the region, the relationship between changes in hydraulic gradients and the underlying hydrogeologic unit, and the examination of core samples for fractures and mineral infilling. This section on inferences about regional permeability focuses on qualitative assessments of hydrogeologic units for which there are few actual test data and for which the qualitative evaluations become relatively more important.

Lower Clastic Aquitard—CRWMS M&O (2000n, Section 6.7.7.9) summarize published information on the lower clastic aquitard. According to Winograd and Thordarson (1975, p. C43), the large-scale transmissivity of the lower clastic aquitard probably is controlled by interstitial permeability. Although the lower clastic aquitard is highly fractured, the fractures probably do not substantially augment the interstitial permeability of the unit on a regional scale (CRWMS M&O 2000n, Section 6.7.7.9).

Upper Clastic Aquitard—The upper clastic aquitard corresponds to the Eleana Formation, which consists of argillite, quartzite, conglomerate, and limestone (Winograd and Thordarson 1975, Table 1). The upper two-thirds of the unit consists mainly of argillite and the lower one-third of the unit principally is quartzite (Winograd and Thordarson 1975, p. C118). Winograd and Thordarson (1975, p. C43) argued that fractures were unlikely to remain open in the rock at depth because of the plastic deformation behavior of the rock, evidenced by tight folds and the fact that the formation serves as a glide plane for several thrust faults at the NTS. In the hills northwest of Yucca Flat, the approximately 610 m (2,000 ft) drop in hydraulic head in the pre-Tertiary rocks over a distance of less than 16 km (10 miles) (an apparent hydraulic gradient of 38 m/km [200 ft/mi]) qualitatively demonstrates the comparatively low regional permeability of the upper clastic aquitard.

Faults—A summary of the possible effects of faults on groundwater movement in the Death Valley region is presented by CRWMS M&O (2000n, Section 6.7.7.11), and the transmissivity of faults in the Yucca Mountain region is discussed in relation to five factors:

- **Fault Orientation**—In the vicinity of Yucca Mountain, the mean orientation of the minimum horizontal stress is 306 ± 11 degrees, and faults with traces oriented north-northeast are expected to be more open and permeable than faults with traces oriented in directions which place them in a shear or compressive state.
- **Fault Fill-Material**—Fine-grained gouge or clay fill-material can cause faults to become poorly transmissive, even if their orientation relative to the stress field indicates they have the potential to be highly transmissive.
- **Juxtaposed Faults**—Differences in the permeabilities of hydrogeologic units juxtaposed by offset across a fault can affect transmissivity.

- **Behavior of Rock**—The solubility and deformation behavior of rock adjacent to faults can affect transmissivity.
- **Recent Seismic History**—Of the faults that have been mapped near the potential repository area, only the Solitario Canyon fault and short segments of the Bow Ridge fault near Exile Hill show evidence of late Quaternary (or more recent) displacement.

The role of specific faults that act as barriers to groundwater flow has been inferred from abrupt discontinuities in the potentiometric surface across faults (Figure 3-5). Lower permeability in the direction perpendicular to the Solitario Canyon and Highway 95 faults (Figure 3-4) is assumed in the site-scale SZ flow model. Direct hydraulic testing of low-permeability faults in boreholes has not been conducted at the Yucca Mountain site.

Nye County—As part of the NCEWDP, three boreholes were used for 48-hour, single-borehole, constant-discharge tests during January and February 1999 (Figure 2-3). The intervals tested in these wells include Rainier Mesa Tuff at borehole NCEWDP-01S, pre-Bullfrog bedded tuffs and Tram Tuff at borehole NCEWDP-03D, and Tiva Canyon Tuff at borehole NCEWDP-09S. The test data were analyzed by consultants for Nye County.

Borehole JF-3—Borehole JF-3 was drilled in the western part of Jackass Flats to monitor water levels in the volcanic rocks that provide water to boreholes J-12 and J-13. The saturated interval at JF-3 occurs within the Topopah Spring Tuff and the Wahmonie Formation (Plume and La Camera 1996, p. 7-9).

3.1.2.3 Infiltration and Recharge

Sources of water that enter the volcanic aquifers and confining units in the vicinity of Yucca Mountain include inflow from upgradient volcanic aquifers and confining units, local recharge from Fortymile Wash, precipitation that infiltrates the surface of Yucca Mountain (especially at higher altitudes at the northern end of Yucca Mountain), and upward flow from the underlying carbonate aquifer (Luckey et al. 1996, p. 39). The magnitudes of most of the inflows to the volcanic system have not been quantified. Potentiometric levels measured in holes that penetrate to or through the lower part of the lower volcanic confining unit indicate hydraulic connections between the deep volcanic and the underlying carbonate aquifer south of the large hydraulic gradient. Where a vertical gradient has been measured at Yucca Mountain, it generally is upward, indicating a potential for upward groundwater flow (Luckey et al. 1996, p. 28). However, no evidence of significant inflow to the volcanic rocks from the carbonates has been reported.

Potentiometric data from widely spaced boreholes upgradient from Yucca Mountain indicate that groundwater flows south from upland recharge areas in the volcanic terrain of Pahute and Rainier Mesas, beneath Timber Mountain, continuing southward beneath the Yucca Mountain area (Luckey et al. 1996, p. 39). However, the concept of inflow from upgradient regions is based on limited data, particularly between Yucca Mountain and Pahute Mesa.

Hydrochemical data (apparent, uncorrected, carbon-14 ages) indicated that water in the volcanic aquifer beneath Yucca Mountain and Crater Flat was recharged during wetter climatic conditions

approximately 12,000 yrs (well USW H-1) to 18,500 yrs (well USW H-6) before present, and 6,000 to 13,000 yrs before present based on corrected carbon-14 ages. However, these data do not preclude that some modern recharge occurs. Actual ages may be younger than apparent ages and the water probably is a mixture from recharge events that span a number of millennia. The data do not indicate whether the recharge occurred far upgradient or locally. If most of the groundwater beneath Yucca Mountain was recharged in the distant past, the flow system still may be equilibrating from an ancient recharge pulse, resulting in a gradual decline in water levels beneath Crater Flat and Yucca Mountain over time (Luckey et al. 1996, p. 39).

Fortymile Wash is a major southward-draining channel located east of Yucca Mountain, beginning in the highlands of Pahute Mesa and ending in the Amargosa Desert. During extreme runoff, Fortymile Wash would be a tributary to the Amargosa River. Average recharge along the entire 95-km (59-mi) length of Fortymile Wash is about $4.2 \times 10^6 \text{ m}^3/\text{yr}$ (3,400 acre-ft/yr) (Luckey et al. 1996, p. 40).

Savard (1998, pp 24 to 27) used data on rising water levels in three boreholes (UE-29a#1, UE-29a#2, and UE-29 UZN#91) following local precipitation and runoff to suggest that recharge occurred in 1983, 1992, 1993, and 1995 in Fortymile Wash. Savard (1998) estimated long-term (1969-1995) annual recharge to groundwater from Fortymile Wash using measured and estimated streamflow volumes and estimated streamflow infiltration losses for four reaches of Fortymile Wash between its confluence with Pah Canyon and a point in the Amargosa Valley downstream of the Highway U.S. 95 crossing. Savard (1998, Table 5) estimated average recharge of $27,000 \text{ m}^3/\text{yr}$ (21.9 acre-ft/yr) for the Fortymile Canyon reach, $1,100 \text{ m}^3/\text{yr}$ (0.9 acre-ft/yr) for the Upper Jackass Flats reach, $16,400 \text{ m}^3/\text{yr}$ (13.3 acre-ft/yr) for the Lower Jackass Flats reach, and $64,300 \text{ m}^3/\text{yr}$ (52.1 acre-ft/yr) for the Amargosa Valley reach. These estimates total to $108,800 \text{ m}^3/\text{yr}$ (88 acre-ft/yr) for the long-term average annual groundwater recharge from Fortymile Wash downstream of Pah Canyon.

As reported by Luckey et al. (1996, p. 40), tritium and carbon-14 samples were collected from boreholes UE-29a#1 (65.5 m [215 ft] deep) and UE-29a#2 (421.5 m [1,383 ft] deep), and it was found that apparently younger water was present in the shallower borehole than in the deeper borehole. Younger water at shallower depth with deeper older water indicated that recharge is occurring at or near these boreholes. In addition, the potentiometric level was about 4 m (13 ft) higher in the shallower borehole than in the deeper borehole, which also is consistent with recharge in this area.

As reported by Luckey et al. (1996, p. 40), local infiltration from precipitation probably occurs in the Yucca Mountain area, but the amount of infiltration that reaches the water table may be inconsequential in the current climate. Near-surface infiltration ranged from 0.02 to 13.4 mm/yr (0.001 to 0.53 in./yr) and averaged 1.4 mm/yr (0.06 in./yr), with the higher infiltration rates generally occurring on the northern portion of Yucca Mountain. The amount of deep infiltration would be less than the amount of shallow infiltration because airflow through the mountain would remove some moisture, and therefore, the rate of deep infiltration may be slow enough under modern climatic conditions to have no substantial effect on the SZ flow system.

In a more recent analysis, Flint et al. (1996, pp. 1 to 2) indicate that during an average-precipitation year of approximately 170 mm (6.7 in.), net infiltration ranges from zero where

alluvial thickness is 6 m (20 ft) or more, to more than 80 mm/yr (3.1 in./yr) where thin alluvium overlies highly permeable bedrock on north-facing slopes at high elevations, and that net infiltration averages 4.5 mm/yr (0.18 in./yr) over the Yucca Mountain study area. On a year-to-year basis, average net infiltration varies from zero in dry years to more than 20 mm/yr (0.8 in./yr) during years when precipitation exceeds 300 mm (11.8 in.).

For areas beyond the immediate vicinity of the potential repository, estimates of recharge to the SZ depend generally on distributed parameter approaches using mean annual precipitation data weighted by altitude and other factors. An empirical precipitation-recharge relation was developed by Maxey and Eakin (1950) from water mass-balance estimates for basins in southern and eastern Nevada. They suggest that the amount of the annual precipitation, and the percentage of precipitation that becomes groundwater, increase with increasing altitude. Maxey and Eakin (1950) assumed that no recharge occurs where mean annual precipitation is less than about 200 mm (7.9 in.), or where altitude is lower than 1,524 m (5,000 ft). Above 1,524 m (5,000 ft) in altitude, they assigned an increasing percentage of precipitation that was assumed to become recharge to a ranked series of 305-m (1,000-ft) altitude intervals.

The method developed by Maxey and Eakin (1950) was modified for use in the Death Valley regional flow model by the addition of weighting factors representing vegetation zones, slope-aspect ratio, and parent material types (D'Agnese et al. 1997, pp. 52 to 55). This approach was subsequently used in developing estimates of distributed recharge for the site-scale SZ flow and transport model.

Combined estimates of recharge from distributed recharge, focused recharge along Fortymile Wash, and recharge in the area of the UZ site-scale flow model were calculated by CRWMS M&O (1999a). The majority of the recharge entering the system in the area of the SZ site-scale flow model occurs in the northern part of the model domain. An estimated total of 1,550,000 m³/yr (1,256 acre-ft/yr) of groundwater enters the SZ system as recharge in the SZ site-scale model area. Of this total, about 212,000 m³/yr (172 acre-ft/yr) of recharge occurs in the area of the UZ site-scale flow model, and about 95,000 m³/yr (77 acre-ft/yr) recharge occurs from focused recharge along Fortymile Wash.

Recharge from Fortymile Wash is of special interest because groundwater flow along the course of the wash is expected to be the main avenue for contaminant transport from the potential repository to the compliance point near Lathrop Wells. Accordingly, CRWMS M&O (2000m, Section 6.5.7.1) estimate two-component mixing ratios based on uranium-234/uranium-238 activity in the groundwater. This method uses borehole WT-3 as the end member representing flow from Yucca Mountain, and it uses borehole UE-29a#2 as representing Fortymile Wash recharge. Calculations were made of the blends represented by samples from boreholes J-12 and JF-3. In the sample from JF-3, it was calculated that 96 percent of the water was from Fortymile Wash; in the sample from J-12, it was calculated that 50 percent of the water was from Fortymile Wash. In both examples, Fortymile Wash was a major contributor to the blend, but at JF-3, flow from Yucca Mountain appeared small (4 percent).

Summarizing the results reported by CRWMS M&O (2000m, Section 7), it was concluded that:

- Flow paths based on chemical and isotopic data are in general agreement with those based on potentiometric gradients.
- Local recharge was identified as a major component of recharge to groundwater at Yucca Mountain.
- Chemical evidence indicates the average recharge rate at the central block of Yucca Mountain during the late Pleistocene to early Holocene was less than 21 mm/yr (0.8 in./yr). Carbon-14 data suggest that the best estimate of true age of the SZ waters at Yucca Mountain are about 3,700 yrs less than the uncorrected ages.
- Hydrochemical data suggest minimal mixing between water from the lower carbonate aquifer and water in the overlying volcanic aquifers beneath Yucca Mountain.
- Hydrochemical evidence suggests that groundwater at Yucca Mountain originated largely from local infiltration via perched water zones during late Pleistocene-early Holocene. Recharge beneath Fortymile Wash is estimated to be at least as great as that estimated by Savard (1998) and perhaps several times greater, but it is orders of magnitude less than estimates based on earlier flow models.
- Hydrochemical calculations suggest that groundwater beneath Yucca Mountain makes up 4 percent to 50 percent of the blend of groundwater at two wells near Fortymile Wash. No evidence was found of modern recharge in the northern Amargosa Desert, where the age of the groundwaters appear to be similar to that of Yucca Mountain.

3.1.3 Summary of Hydrochemical Data Pertinent to Transport

Transport of radionuclides in the SZ depends on the chemistry of the groundwater, and physical and chemical properties of rocks along the flowpath. The following sections describe major-ion chemistry, results of tracer tests, and the redox state of groundwaters.

3.1.3.1 Spatial Patterns of Groundwater Chemistry

The hydrochemistry and isotopic hydrology of waters in the Death Valley regional groundwater flow system provide information on recharge and regional groundwater flow. The major-ion chemistry reflects the various processes that control water chemistry (Section 3.1.1.1.3), but provides little if any information on the timing of recharge. Isotopic chemistry provides independent information regarding the time and climatic regime under which groundwaters were recharged.

Based on regional-scale groundwater chemistry, there are two basic types of water: a relatively dilute sodium-bicarbonate water of high silica content associated with volcanic rocks and derivative sediments, and a more concentrated calcium-magnesium-bicarbonate water of low silica content associated with carbonate rocks. Where these two basic rock types are mixed (as in alluvial valley fills), a water of calcium-magnesium-sodium-bicarbonate composition commonly results. In addition, some groundwaters of the valley fills reflect concentration of the

chemical constituents due to evaporation, and these waters are distinguished by relatively higher proportions of sulfate and chloride ions.

The isotopic chemistry data consist mainly of analyses of the deuterium and oxygen-18 content of water (which are sensitive to the temperature of precipitation), the radioactive tritium and carbon-14 content (indicators of time since recharge), and the carbon-13 content (indicative of the degree to which carbon-14 has been diluted through solution of non-radioactive rock carbon).

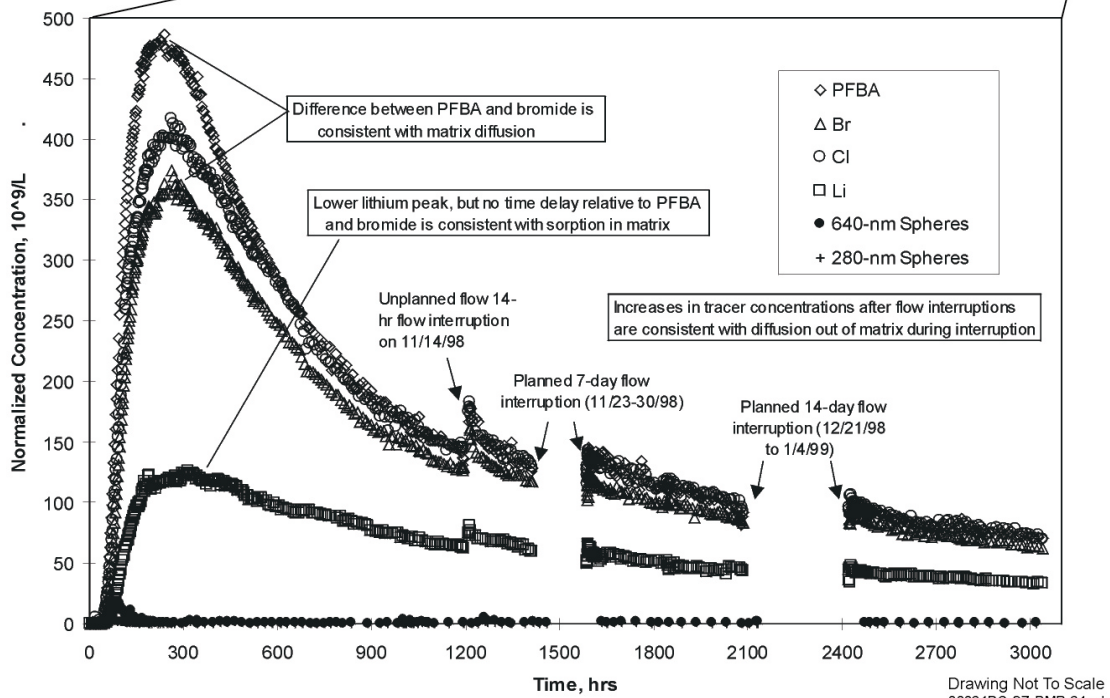
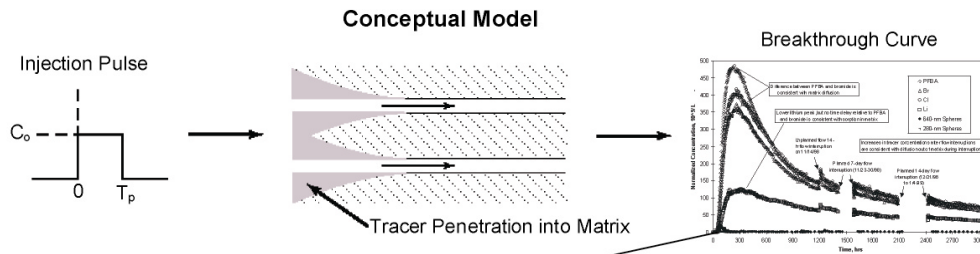
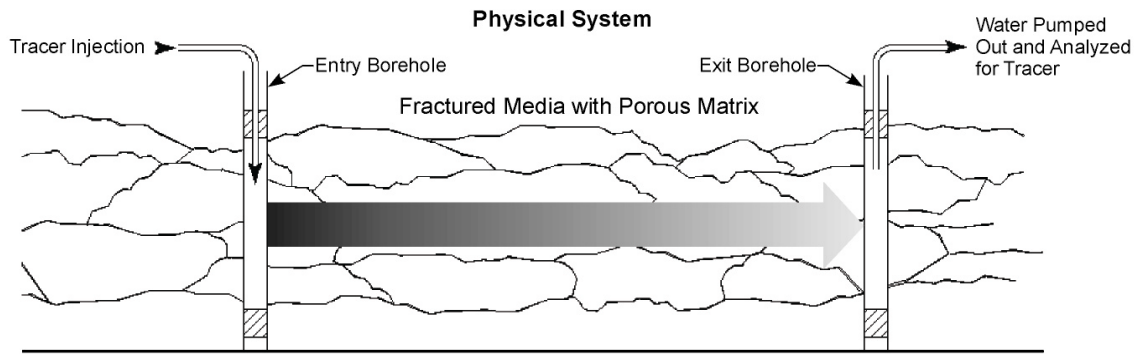
Overall, the hydrochemical and isotopic evidence is in general agreement with the hydrogeologic understanding of the groundwater flow in the vicinity of Yucca Mountain. Recharge in the vicinity of Pahute Mesa flows via Oasis Valley and Crater Flat toward the Amargosa Desert, and groundwater flow along Fortymile Wash is the main contributor to recharge in the west central Amargosa Desert. There is some evidence of modern recharge in Fortymile Canyon and Fortymile Wash, but most of the groundwater at Pahute Mesa, Oasis Valley, Yucca Mountain, and the Amargosa Desert appears to represent late Pleistocene-early Holocene recharge, suggesting that groundwater throughflow has been minimal in the present climate. The Ash Meadows flow system is distinctly different in character, representing large-scale flow through solution-enlarged openings in a thick carbonate aquifer from two major recharge areas to a single major discharge area at Ash Meadows.

3.1.3.2 Tracer Tests

3.1.3.2.1 C-Wells Tracer Tests (Saturated Zone Transport in Fractured Tuffs)

To test conceptual models of SZ transport in fractured tuffs, DOE conducted several cross-hole tracer and hydraulic tests at the C-wells Complex between 1995 and 1999 (CRWMS M&O 2000r). The discussion here focuses on two tracer tests involving the injection of multiple tracers, as these tests provided the most rigorous and convincing testing of conceptual transport models for saturated, fractured tuffs (Figure 3-8). One of these tests was conducted in the lower Bullfrog Tuff, the most transmissive interval at the C-wells, and the other was conducted in the lower Prow Pass Tuff, which had relatively low transmissivity.

Both multiple-tracer tests were conducted between wells UE-25c#2 and UE-25c#3 (a linear distance of approximately 30 m). Well UE-25c#3 was the production well in the Bullfrog Tuff test, and well UE-25c#2 was the production well in the Prow Pass Tuff test. The two tracer tests featured the simultaneous injection of several tracers having different physical and chemical characteristics: (1) nonsorbing solutes with diffusion coefficients differing by about a factor of 3 (Bromide and pentafluorobenzoate [PFBA]), a weakly-sorbing solute (lithium), and carboxylate-modified latex polystyrene microspheres that served as colloidal tracers. The simultaneous injection of multiple tracers offers important advantages over single tracer injections because it allows transport processes to be better distinguished and quantified by comparing the responses of the different tracers.



Source: Adapted from CRWMS M&O (2000r, Figure 97)

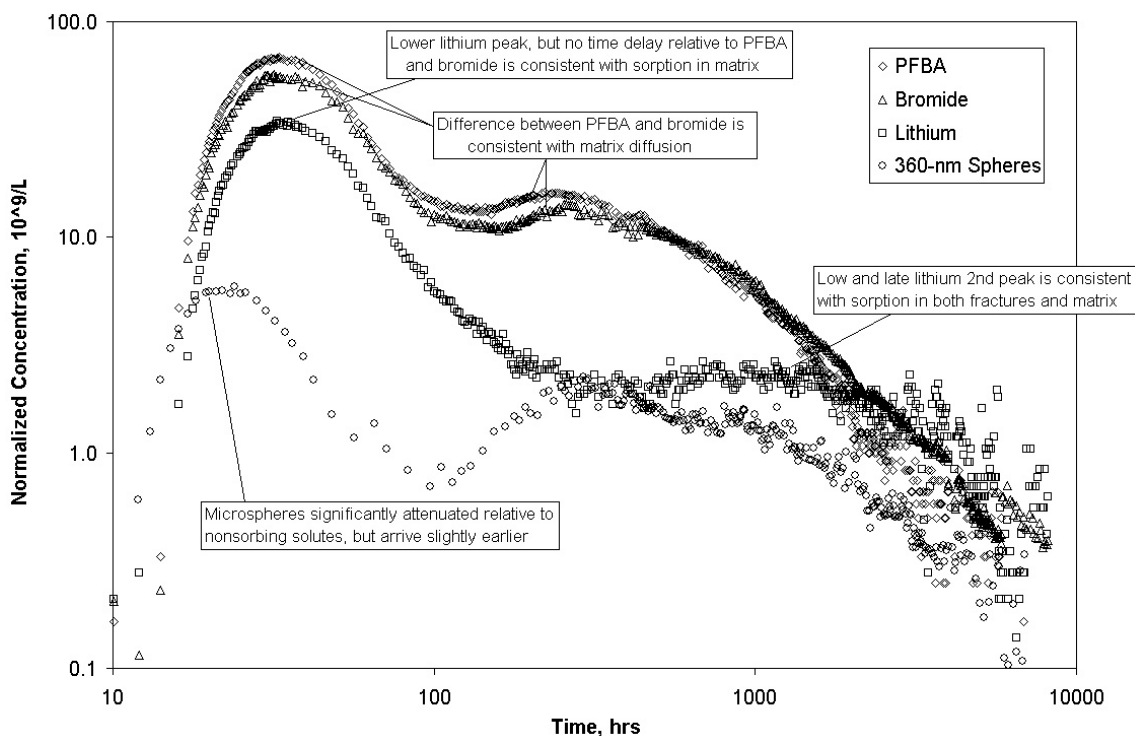
NOTE: Tracer recoveries were 52% for PFBA, 49% for chlorine (Cl), 43% for bromide (Br), 19% for lithium (Li), 0.3% for 640-nm spheres, and 0.1% for 280-nm spheres.

Figure 3-8. Physical System, Conceptual Model, and Normalized Tracer Responses from the Prow Pass Tuff Multiple Tracer Test

A series of laboratory studies were conducted in parallel with the field testing efforts to help support and constrain the interpretations of the field tests. These studies included batch sorption tests to characterize lithium sorption to C-wells tuffs, diffusion cell tests to determine matrix diffusion coefficients of tracers used in the field, and dynamic transport tests to study tracer transport in fractured and crushed tuffs under more controlled conditions than in the field. The batch sorption tests and dynamic transport tests provided estimates of lithium sorption parameters for comparison with sorption parameters derived from the field tests. Although lithium transport is not of direct concern for the YMP, such comparisons are important because they offer an indication of whether laboratory-derived radionuclide sorption parameters can be used defensibly in field-scale predictive calculations. CRWMS M&O (2000r) provide a summary discussion of the laboratory tests, and Reimus et al. (1999, Chapters 6 to 8) provide a more detailed discussion.

3.1.3.2.1.1 Summary of Multiple-Tracer Field Test Results and Interpretations

Normalized tracer responses (concentrations divided by injection masses) in the multiple-tracer tests in the Prow Pass Tuff (Figure 3-8) and Bullfrog Tuff (Figure 3-9) reveal an initial early peak concentration generally followed by a decline in concentration over time. The test conditions and tracer injection masses in the two tests are described in detail by Reimus et al. (1999, Chapter 5 [Prow Pass Tuff] and Appendix C [Bullfrog Tuff]).



Source: CRWMS M&O (2000r, Figure 96)

NOTE: Tracer recoveries were about 69% for PFBA, 69% for bromide, 39% for lithium, and 15% for microspheres. Concentrations are normalized to mass injected; both axes are log scale.

Figure 3-9. Normalized Tracer Responses in the Bullfrog Tuff Multiple Tracer Test

The most striking feature of the tracer breakthrough curves in the Bullfrog Tuff test (Figure 3-9) is their bimodal (double-peaked) behavior. This behavior is attributed to a relatively small fraction (about 13 percent) of the tracer solution exiting the injection borehole in short-residence-time pathways in the upper half of the injection interval, while the remaining tracer mass exited the borehole primarily in pathways of longer transport times deeper in the interval. These differences in travel times probably reflect differences in fracture or network permeability between the two zones, although they also could reflect differences in the length of the flow paths. Further discussion of this phenomenon is provided by CRWMS M&O (2000r) and Reimus et al. (1999, Appendix C).

The response of PFBA and bromide in the Bullfrog Tuff and Prow Pass Tuff tests show qualitative evidence of matrix diffusion. The peak normalized PFBA concentrations are higher than the peak normalized bromide concentrations in both tests, and the second bromide peak in the Bullfrog Tuff test is somewhat delayed relative to the PFBA, with a tail that appears to cross over the PFBA at long times. These features are all consistent with greater matrix diffusion of the more diffusive tracer (bromide) relative to the less diffusive tracer (PFBA). Another qualitative indication of matrix diffusion in the Prow Pass Tuff test is the increase in solute tracer concentrations after each of the three flow interruptions during the tailing portion of the test, which indicate diffusion of tracers out of the matrix and into fractures during the interruptions. Thus, the two tests support the concept of dual-porosity behavior (where flow occurs primarily in fractures, but there is a great deal of stagnant water available for tracer or contaminant storage in the rock matrix) in the saturated, fractured system at the C-wells.

The response of lithium in the two tests shows attenuation relative to the nonsorbing tracers, which is indicative of lithium sorption. The attenuation in the Prow Pass test and in the first peak of the Bullfrog Tuff test is almost exclusively a lowering of the peak concentration with little or no delay in delivery time. This behavior is consistent with lithium sorption in the matrix (after diffusion into the matrix). The attenuation in the second peak of the Bullfrog Tuff test involves a time delay along with a dramatic lowering of concentration. This behavior is consistent with sorption in the fracture flow pathways and in the matrix.

The importance of deducing that lithium sorption occurs in the matrix cannot be over-emphasized when considering the conceptual dual-porosity transport model. Although it is possible that the apparent matrix diffusion of nonsorbing tracers could be diffusion into stagnant free water in the system (rather than true matrix diffusion), such free-water diffusion is not consistent with the large attenuation of the lithium peaks. The lithium attenuation can only be explained by sorption onto a large surface area, which will be present only in the matrix. If the diffusion were only into stagnant free water with minimal surface area for sorption, the lithium response would fall between that of the bromide and PFBA (consistent with the fact that the lithium diffusion coefficient falls between that of bromide and PFBA). Thus, lithium provides strong evidence that the observed diffusion is due, at least in part, to true diffusion into the rock matrix.

The response of the latex microspheres indicates that the microspheres were attenuated relative to the solute tracers, with more attenuation in the Prow Pass Tuff test. The responses in both tests (including both sizes of spheres in the Prow Pass test) are characterized by truncated tails relative to the solutes, but with measurable concentrations that persist throughout the tests. This

behavior is consistent with filtration followed by slow detachment of the microspheres. It should be noted that while the microspheres in the Bullfrog Tuff test were injected simultaneously with the solute tracers (in a solution of approximately 0.2 M ionic strength), the microspheres in the Prow Pass Tuff test were injected in untraced groundwater two days before solutes were injected. Thus, while the response of the microspheres in the Bullfrog Tuff test may have been influenced by the destabilizing effect of the high ionic strength of the injection solution (i.e., possible coagulation), the microspheres in the Prow Pass Tuff test were not subjected to artificially high ionic strengths. Microsphere injection concentrations in both tests ranged from approximately $2.5 \times 10^{10}/L$ to $5 \times 10^{10}/L$.

In both tests, the response of the tracers was interpreted by simultaneously fitting the breakthrough curves using a semianalytical, dual-porosity transport model (Reimus et al. 1999, Appendix D). The transport parameters obtained from the model fits, with the exception of lithium sorption parameters, are listed in Table 3-1. Further discussion of how these parameters were obtained and how they compare with other studies is provided by CRWMS M&O (2000r).

Table 3-1. Transport Parameters Deduced from Bullfrog Tuff and Prow Pass Tuff Tracer Tests

Parameter	Bullfrog Tuff		Prow Pass Tuff
	Pathway 1	Pathway 2	
Mass fraction in pathway	0.12	0.59	0.75
Residence time, linear flow	37 hr	995 hr	1230 hr
Longitudinal dispersivity, linear flow	5.3 m	18.8 m	23.1 m ^c
Residence time, radial flow	31 hr	640 hr	620 hr
Longitudinal dispersivity, radial flow	3.6 m	10.7 m	6.3 m ^c
Effective flow porosity, linear (radial) ^a	0.0029 (0.0025)	0.026 (0.017)	0.0068 (0.0034)
Effective matrix diffusion mass transfer coefficient ^b	0.00158 sec ^{-1/2}	0.000458 sec ^{-1/2}	0.000968 sec ^{-1/2}

Source: Adapted from CRWMS M&O (2000r, Tables 51 and 52)

NOTES: Pathway 1 refers to pathways that resulted in the first tracer peak. Pathway 2 refers to pathways that resulted in the second peak.

^aBased on flow log information, it was assumed that 75% of the production flow contributed to the Pathway 1 responses and 25% of the flow contributed to the Pathway 2 responses.

^bThe value of the parameter for PFBA was assumed to be 0.577 times that for bromide.

^cLongitudinal dispersivities calculated after subtracting out apparent dispersion due to the recirculating flow field (Reimus et al. 1999, Chapter 5).

Lithium sorption parameters (Table 3-2) were deduced from field and laboratory tests. Lithium sorption in the field was always approximately equal to or greater than the sorption measured in the laboratory. Details of the methods used to obtain the field lithium sorption parameters, and discussions of possible alternative interpretations, are provided by Reimus et al. (1999), as are the procedures for fitting the microsphere data. The microsphere filtration and detachment rate constants deduced from the Bullfrog and Prow Pass tracer tests are provided in CRWMS M&O (2000l).

Table 3-2. Field- and Laboratory-Derived Sorption (K_d) Parameters for Lithium

Parameter	Field Sorption Coefficient	Laboratory Sorption Coefficient	
		Linear Fit to Data	Fit at Infinite Dilution ^a
Prow Pass matrix K_D assuming Central Prow Pass Tuff	0.66	0.13	0.26
Prow Pass matrix K_D assuming Lower Prow Pass Tuff	1.68	0.084	0.44
Bullfrog matrix K_D in Pathway 1 assuming Central Bullfrog Tuff ^b	0.24	0.19	0.44
Bullfrog matrix K_D in Pathway 1 assuming Lower Bullfrog Tuff ^b	0.97	0.32	1.64
Bullfrog matrix K_D in Pathway 2 assuming Central Bullfrog Tuff ^b	0.67	0.19	0.44
Bullfrog matrix K_D in Pathway 2 assuming Lower Bullfrog Tuff ^b	2.75	0.32	1.64

Source: CRWMS M&O (2000r, Table 53)

NOTES: Values based on linear sorption isotherms.

^a Values at infinite dilution obtained from slopes of Langmuir isotherm fits to the data (asymptotic slope at very low concentrations). Other values obtained from a simple linear fit to the entire range of data.

^b Pathway 1 refers to pathways that resulted in the first tracer peak in the Bullfrog reactive tracer test, and Pathway 2 refers to pathways that resulted in the second peak in this test. K_D values were calculated from the smallest matrix retardation factors obtained from alternative interpretations of the test.

Effective matrix diffusion mass transfer coefficient for lithium was assumed to be equal to that for bromide (0.816).

3.1.3.2.1.2 Conclusions from C-Wells Field and Laboratory Transport Testing

The principal conclusions from the C-wells field and laboratory tests relevant to performance assessment (PA) of the potential Yucca Mountain repository are:

- The relative responses of nonsorbing tracers in fractured tuffs are consistent with matrix diffusion. This result supports the use of a dual-porosity conceptual model to describe radionuclide transport through the saturated, fractured volcanic rocks near Yucca Mountain.
- Sorption of lithium ions in the field was greater than or equal to measured sorption in the laboratory. Although lithium does not behave identically to any radionuclide, this result suggests that the use of laboratory-derived radionuclide sorption parameters in field-scale transport predictions is defensible and may even be conservative.

Other transport parameters derived from the C-wells tracer tests include effective flow porosities, longitudinal dispersivities, matrix diffusion mass transfer coefficients, colloid filtration and detachment rate constants, and horizontal anisotropy ratios. Conclusions related to these parameters are provided by CRWMS M&O (2000r).

3.1.3.2.2 Busted Butte Tracer Tests (Unsaturated Zone Transport in Tuffs)

The Busted Butte tracer tests (CRWMS M&O 2000r, Sections 6.8.1 to 6.8.8) were conducted in unsaturated rock, so most of the results do not lend themselves directly to supporting the conceptual transport model for saturated, fractured tuffs. However, important information for understanding the SZ was produced. The most important points derived from the Busted Butte tracer tests that support the SZ conceptual transport model are that nonsorbing tracers migrated faster than sorbing tracers, fracture-matrix interactions were important to transport, and model predictions qualitatively agreed with observed results. In particular, the last point adds confidence to the SZ transport model.

3.1.3.3 Oxidation and Reduction Potential

The rate of transport of some radionuclides may be influenced by the oxidation/reduction potential (Eh) of the groundwater flow system (CRWMS M&O 2000r). These radionuclides can exist in more than one oxidation state under the conditions typical of the groundwaters in the vicinity of Yucca Mountain. For example, under oxidizing conditions, neptunium-237 in solution exists predominantly in the pentavalent oxidation state. However, under sufficiently reducing conditions, the pentavalent oxidation state is reduced to the tetravalent oxidation state. The lower oxidation state species sorb more strongly to aquifer host rocks than those of the higher oxidation state. For this reason, the Eh of groundwaters along potential flowpaths from the potential repository to the accessible environment is a parameter of considerable importance.

Eh potentials commonly are supplemented with measurements of the concentrations of redox sensitive species that may be present in groundwater samples. Such species might include dissolved oxygen and redox couples such as ferrous/ferric iron, ammonium/nitrite/nitrate, sulfide/sulfate, and other couples. Analysis of the results of such measurements, when combined with redox potential measurements, can provide constraints on the redox state of groundwater at a given location.

Measurements to define the redox state of groundwaters have been carried out on waters from a limited number of boreholes on Yucca Mountain (CRWMS M&O 2000r) and from the NCEWDP boreholes. Analyses of these data lead to the following conclusions:

- Reducing conditions (Eh less than 200 mv) were found in the deeper portions of the volcanic section (i.e., Bullfrog and Tram Formations) beneath the crest of Yucca Mountain.
- Reducing conditions were found close to the water table on the eastern flank of Yucca Mountain downgradient from the footprint of the potential repository (borehole WT-17).
- Oxidizing conditions were found in groundwater from boreholes along Fortymile Wash.
- Reducing conditions were found in some of the NCEWDP boreholes located along Highway US 95 south of Yucca Mountain.

In summary, low-Eh barriers to radionuclide transport may be present in the deeper volcanic section beneath Yucca Mountain, close to the water table in volcanic rocks downgradient of the

potential repository, and in the alluvium of the Amargosa Valley downgradient from the potential repository (CRWMS M&O 2000r). These low-Eh barriers increase the sorption affinity of redox sensitive elements such as neptunium and technetium. This affinity is quantified through sorption experiments using rock and water samples from wells located in zones of low-Eh potential.

3.1.4 Summary of Laboratory Data

This section summarizes laboratory data and interpretations that are relevant to the development and testing of conceptual and numerical transport models of the SZ at Yucca Mountain. The laboratory data obtained include sorption coefficients for various hydrologic units, diffusion coefficients, and parameters related to colloidal transport. The discussion in this section is derived from CRWMS M&O (2000r).

The radionuclides of interest include the following elements: americium, thorium, zirconium, actinium, samarium, niobium, lead, radium, strontium, cesium, lead, tin, plutonium, neptunium, uranium, selenium, nickel, protactinium, carbon, chlorine, technetium, and iodine. Sorption coefficients were obtained in several types of experiments. Most of the coefficients were obtained in batch experiments. A limited number of experiments were carried out with crushed-rock columns to check the results of the batch experiments in a flowing system. A small number of experiments were carried out with solid-rock columns to test the applicability of the results of crushed-rock experiments to transport in solid rock. Batch experiments also were carried out to evaluate the sorption of radionuclides onto colloidal-sized materials. In this set of experiments, the reversibility of the radionuclide sorption reactions was of particular interest.

Effective diffusion coefficients for radionuclides were obtained in laboratory experiments with specially designed diffusion cells and beakers made of rock samples from the site. These experiments were performed with representative water and rock compositions from the site. A limited number of experiments were performed to evaluate the sorption and diffusion of radionuclides during fracture flow.

3.1.4.1 Sorption Experiments

Because of the nature of sorption reactions, sorption coefficients for a given element are not single-valued parameters. Sorption coefficients commonly are functions of water composition, rock composition, radionuclide concentration, temperature, and other less obvious factors such as the presence or absence of microbes.

Insufficient data are available to directly obtain information on the sorption behavior of all the elements of interest as a function of all of these variables. To address this situation, an indirect approach was used based on expert elicitation. Experts who had been involved in the experimental determination of sorption coefficients for the YMP and who had read the available literature regarding the sorption behavior of the various elements of interest were asked in an expert elicitation to formulate probability distributions of sorption coefficients for the elements of interest (CRWMS M&O 2000r). These distributions were to include any information the experts were aware of regarding the influence of the factors listed above on the sorption behavior of a given element. There was an expressed intent to underestimate the limits of the distributions

(i.e., smaller values for the lower and upper limits on the distributions) as an acknowledgement of the fact that the available database was incomplete. Distributions were formulated for sorption coefficients for each of the elements of interest on devitrified tuff, vitric tuff, zeolitic tuff, and iron oxide (as a surrogate for waste package corrosion products). This expert elicitation process (CRWMS M&O 2000r) was conducted in 1993, and since then, additional laboratory data have been obtained on selected elements and used to update the distributions.

Sorption coefficients, obtained using waters and rock samples from the site, were obtained in batch experiments in which a small amount of crushed rock material is combined with water from the site; the water has been spiked with a known amount of a radionuclide. After a prescribed period of time, the water and the rock material are separated, and the concentration of the radionuclide in the water is measured. The sorption coefficient is calculated from the amount of radionuclide that was removed from solution. Although this technique is fast and straightforward, there are several questions that must be addressed regarding the application of these data in transport calculations.

One major question is whether the static nature of the batch experiments is representative of the dynamic conditions under which radionuclides would be transported at Yucca Mountain. To address this question, experiments were carried out with columns filled with crushed rock. The sorption coefficients obtained in these flow experiments were compared with the results of batch experiments.

Sorption coefficient distributions for radionuclides were derived from laboratory data obtained in experiments with waters and rock samples from the site and from data available in the literature. Laboratory experiments generally were performed with at least two water compositions (J-13 and UE-25p#1) and several pH levels to evaluate the impact of these parameters on the sorption coefficient. Waters from wells J-13 and UE-25p#1 represent end-members in the ranges of major ion concentrations found in the SZ waters at Yucca Mountain (CRWMS M&O 2000b). Other potential influences on the sorption behavior of elements of interest (e.g., radionuclide concentrations, sorption kinetics, oxidation state, and temperature) also were evaluated, as were the potential effects of organic materials on actinide sorption. Models were developed to explain the sorption coefficient data in selected combinations of water, rock, and radionuclides. These combinations included sorbing radionuclides considered to be of greatest potential risk to the accessible environment based on their combination of inventory, half-life, mobility, and dose conversion factors.

Because of the large numbers of experiments required to address the sorption behavior of every combination of water, rock, and radionuclide, some process for focusing the experimental program was required. The process developed has been called the “minimum K_d concept” (where K_d refers to the sorption coefficient). The essence of this concept is that a “minimum K_d ” exists according to which radionuclides will not reach the accessible environment through a groundwater pathway over the 10,000-yr regulatory period (NRC 1998) within some adequate margin of error. Radionuclides that can be shown to have this minimum K_d in rock and water systems similar to those at Yucca Mountain would not require as much detailed investigation as radionuclides that do not. Those radionuclides with essentially no sorption potential are eliminated from further consideration and the sorption coefficient is set to zero. This allowed the

experimental program to be focused on those radionuclides that could have the maximum impact on doses at the accessible environment over the regulatory time frame of interest.

Sorption Coefficients for Performance Assessment—Sorption coefficients for the SZ, and the distributions of these coefficients, are provided in Table 3-3. Details of the database used to derive these and other sorption coefficient distributions are presented by CRWMS M&O (2000r, Table 2).

Table 3-3. Sorption-Coefficient Data and Distributions for Saturated Zone Units

Element	Rock Type	Sorption Coefficient				Distribution Type
		Minimum (mL/g)	Maximum (mL/g)	Mean	Coefficient of Variation	
Americium (also Actinium, Niobium, Samarium, Thorium, Zirconium)	Devitrified	100	2000	—	—	Uniform
	Vitric	100	1000	400	0.20	Beta
	Zeolitic	100	1000	—	—	Uniform
	Iron oxide	1000	5000	—	—	Uniform
Plutonium	Devitrified	5	100	50	0.15	Beta
	Vitric	50	300	100	0.15	Beta
	Zeolitic	50	400	100	0.15	Beta
	Iron oxide	1000	5000	—	—	Uniform
Uranium	Devitrified	0	5.0	—	—	Uniform
	Vitric	0	4.0	—	—	Uniform
	Zeolitic	5	20.0	7.0	0.3	Beta
	Iron oxide	100	1000	—	—	Uniform
	Alluvium	0	8.0	—	—	Uniform
Neptunium	Devitrified	0	2.0	0.5	0.3	Beta
	Vitric	0	2.0	0.5	1.0	Beta (exp)
	Zeolitic	0	5.0	1.0	0.25	Beta
	Iron oxide	500	1000	—	—	Uniform
	Alluvium	0	100	18	1.0	Beta
Radium	Devitrified	100	500	—	—	Uniform
	Vitric	100	500	—	—	Uniform
	Zeolitic	1000	5000	—	—	Uniform
	Iron oxide	0	1500	30	1.0	Beta (exp)
Cesium	Devitrified	20	1000	—	—	Uniform
	Vitric	10	100	—	—	Uniform
	Zeolitic	500	5000	—	—	Uniform
	Iron oxide	0	500	30	1.0	Beta (exp)
Strontium	Devitrified	10	200	—	—	Uniform
	Vitric	20	50	—	—	Uniform
	Zeolitic	2000	5000	—	—	Log uniform
	Iron oxide	0	30	10	0.25	Beta

Table 3-3. Sorption-Coefficient Distributions for Saturated Zone Units (Continued)

Element	Rock Type	Sorption Coefficient				Distribution Type
		Minimum (mL/g)	Maximum (mL/g)	Mean	Coefficient of Variation	
Nickel	Devitrified	0	200	—	—	Uniform
	Vitric	0	50	—	—	Uniform
	Zeolitic	0	200	—	—	Uniform
	Iron oxide	0	1000	—	—	Uniform
Lead	Devitrified	100	500	—	—	Uniform
	Vitric	100	500	—	—	Uniform
	Zeolitic	100	500	—	—	Uniform
	Iron oxide	100	1000	—	—	Uniform
Tin	Devitrified	20	200	—	—	Uniform
	Vitric	20	200	—	—	Uniform
	Zeolitic	100	300	—	—	Uniform
	Iron oxide	0	5000	—	—	Uniform
Protactinium	Devitrified	0	100	—	—	Uniform
	Vitric	0	100	—	—	Uniform
	Zeolitic	0	100	—	—	Uniform
	Iron oxide	500	1000	—	—	Uniform
Selenium	Devitrified	0	1.0	0.1	1.0	Beta (exp)
	Vitric	0	1.0	0.1	1.0	Beta (exp)
	Zeolitic	0	1.0	0.2	1.0	Beta (exp)
	Iron oxide	0	500	30	1.0	Beta (exp)
Carbon	Iron oxide	10	100	—	—	Uniform
Chlorine, Technetium, Iodine	All tuffs	0	0	—	—	—
Technetium	Alluvium	0.27	0.62	—	—	Uniform
Iodine	Alluvium	0.32	0.63	—	—	Uniform

Source: CRWMS M&O (2000r, Table 2b)

NOTE: “—” means this parameter is not applicable.

Results of Batch Sorption Coefficient Experiments—For most of the elements of interest, the batch experiments show rapid sorption kinetics and reach equilibrium in hours to several days. However, data on the sorption behavior of plutonium indicate that the sorption kinetics associated with this element are slow. It could take a year or more for plutonium sorption reactions to reach equilibrium in the groundwater system at Yucca Mountain. This may reflect the fact that plutonium can occur in several oxidation states in Yucca Mountain waters. Sorption experiments using plutonium in well-defined oxidation states indicate that the sorption behavior of plutonium depends on its oxidation state. This effect was factored into the sorption coefficient distributions presented in Table 3-3. The potential impacts of microbes on the results obtained in sorption experiments have not been evaluated (CRWMS M&O 2000r). Because plutonium can simultaneously exist in several oxidation states, the sorption behavior of this element may be affected by microbes that may be present in laboratory experiments. In deriving the sorption coefficient distributions for plutonium, it was assumed that any microbial influence present in laboratory experiments would also be present in the SZ at Yucca Mountain.

Experiments with different size-fractions of crushed rock (CRWMS M&O 2000r) suggest that crushing the rock does not have an important affect on the sorption coefficients obtained for the elements tested (cesium, strontium, neptunium, and technetium). This conclusion is consistent with results of experiments using solid-rock wafers and solid-rock columns. However, this conclusion does not necessarily apply to elements not tested (e.g., plutonium).

Batch experiments with organic molecules (model organic compounds, fulvic acid, and humic acid) lead to the conclusion that the potential affect of organic complexation on the sorption behavior of plutonium and neptunium is not significant in the rock and water systems associated with Yucca Mountain. The potential impact of organic molecules on the sorption behavior of other elements was not investigated.

Results of Column Experiments—Experiments with crushed-rock columns generally corroborated the results obtained from batch experiments. However, crushed-rock column experiments with plutonium indicated that an early breakthrough fraction was present in most experiments. This fraction decreased in magnitude as the flow rate of the column was decreased. The flow-rate limit at which this fraction becomes insignificant has not been determined for most Yucca Mountain rock and water systems.

Solid-rock columns were studied only in relation to the transport of selenium under unsaturated conditions. In these studies, it was found that selenium transport rates through the columns could be modeled adequately with the results of batch experiments.

3.1.4.2 Matrix Diffusion Experiments

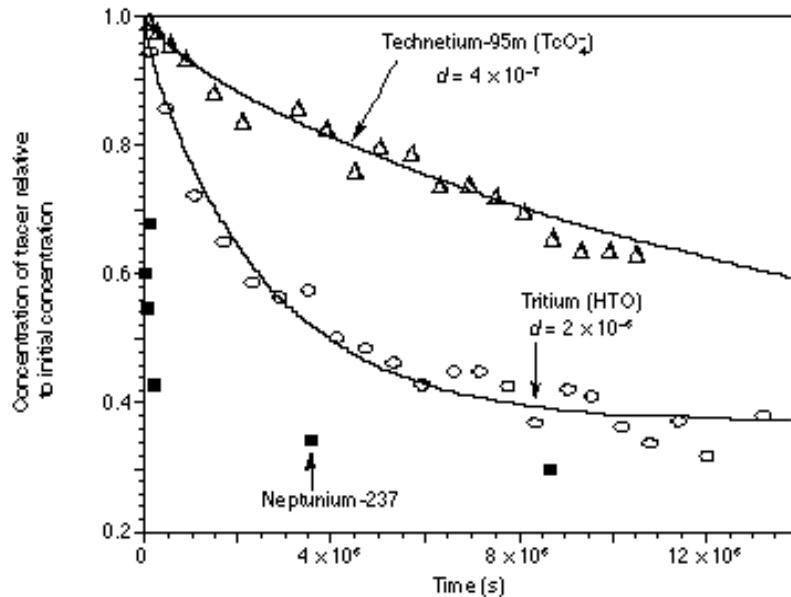
In addition to the C-wells field tracer tests, matrix diffusion under saturated conditions has been observed and quantified in the laboratory under static and dynamic (flowing) conditions. The laboratory experiments confirmed that matrix diffusion is a valid process affecting radionuclide transport, and they provided direct estimates of radionuclide and tracer diffusion coefficients in various volcanic tuff matrices. These experiments included:

- Rock beaker experiments, in which radionuclide solutions are placed into thick-walled “beakers” machined out of samples of tuff materials (saturated). Diffusion coefficients are determined from the decline in radionuclide concentration resulting from diffusion into the walls of the beaker.
- Diffusion cells, in which large concentration gradients of radionuclides or tracers are imposed across saturated tuff “slabs.” Diffusion coefficients are determined from the rise in concentrations of tracers in reservoirs on the initially tracer-free side of the slab.
- Fractured tuff column experiments, in which radionuclide solutions are passed through saturated, fractured tuff cores, and the effects of matrix diffusion are seen as lower peak concentrations and longer tails for the more diffusive tracers (analogous to the C-wells field tracer tests).

The results of these experiments are summarized in this section, and details are provided by CRWMS M&O (2000r, Sections 6.5, 6.6, 6.7, and 6.9).

3.1.4.2.1 Rock Beaker Experiments

The radionuclides tested in rock beaker experiments included tritium, technetium-95, neptunium-237, americium-241, strontium-85, cesium-137, and barium-133. Water from well J-13 was used in all experiments, and the tuff matrices studied were all devitrified. Batch-sorption experiments with J-13 water and the tuffs studied were conducted in parallel with the rock beaker experiments because radionuclide uptake by the rock matrices is dependent on the diffusion coefficient and the sorption of the radionuclide. Typical experimental results for two nonsorbing radionuclides (tritium and technetium-95, as tritiated water and pertechnetate, respectively) and a weakly-sorbing radionuclide (neptunium-237) are presented in Figure 3-10. Also shown in Figure 3-10 are the results of model simulations to match the nonsorbing radionuclide concentration histories. Technetium-95 diffuses into the matrix more slowly than tritium because of its larger size and negative charge, which repels it from the negatively-charged rock surfaces. The neptunium-237 concentration history reflects the combined effects of diffusion and sorption in the matrix. Although neptunium-237 should diffuse slowly compared to tritium, the slow diffusion is counter-balanced by sorption onto the rock surfaces, which effectively lowers the neptunium-237 concentration in the pores and keeps the diffusion gradient high to drive additional neptunium-237 into the matrix. The other radionuclides studied all had much larger sorption coefficients than neptunium-237, so they were rapidly depleted from the rock beaker solutions.



Source: CRWMS M&O (2000r, Figure 28)

NOTE: Rock beaker diffusion data for tritium, technetium-95, and neptunium-237 in a devitrified tuff.

Figure 3-10. Rock Beaker Diffusion

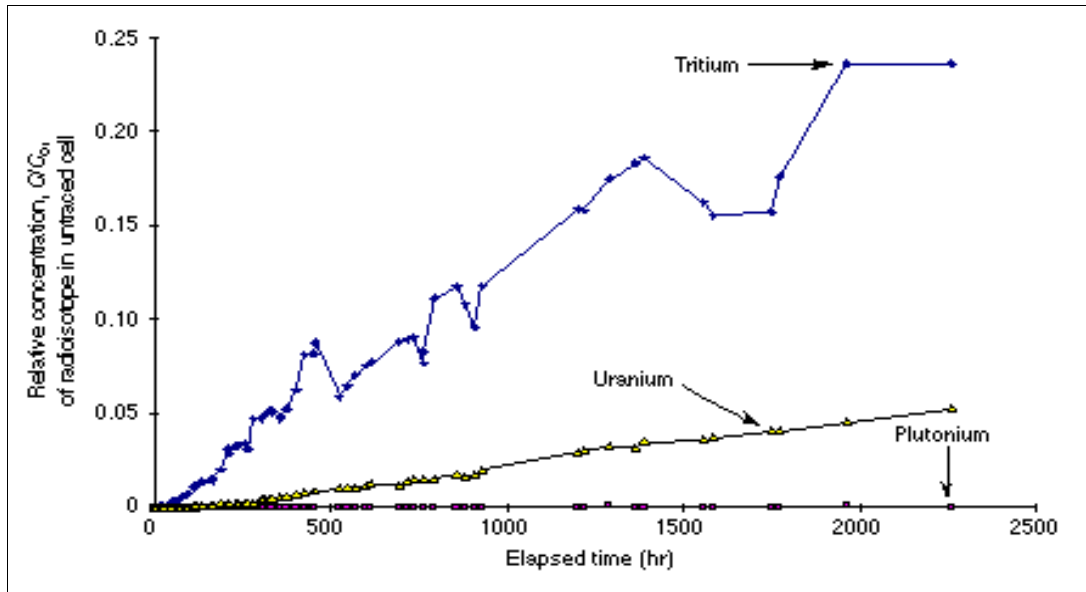
Modeling of the experimental results indicated that the uptake of radionuclides into the tuff matrices by the combined effects of matrix diffusion and sorption was underpredicted when the matrix diffusion coefficient for tritiated water was used in the models in conjunction with radionuclide sorption parameters measured in the batch experiments. It was concluded that this combination of parameters should yield conservative predictions of matrix uptake of sorbing radionuclides in PA models.

3.1.4.2.2 Diffusion Cell Experiments

Diffusion cell experiments have been conducted using radionuclides and the nonradioactive, nonsorbing tracers that were used in the C-wells field experiments. In the latter case, the experiments focused on bromide and PFBA diffusion through C-wells tuff matrices. Radionuclide experiments have examined the diffusion of tritium, technetium-95, neptunium-237, plutonium-239, and natural uranium(VI) through devitrified and zeolitic tuff matrices. Water from well J-13 and synthetic UE-25p#1 water were used in the radionuclide experiments. Water from well J-13 was considered representative of groundwater from the volcanic aquifer beneath Yucca Mountain, and the water from well UE-25p#1 was considered representative of groundwater from the underlying Paleozoic carbonate aquifer. In this way, the diffusion cell tests included a wide range of groundwater chemistries from the SZ near Yucca Mountain.

A typical set of “breakthrough curves” (i.e., concentrations as a function of time on the initially radionuclide-free side of the tuff slab) are shown in Figure 3-11 for an experiment involving tritium, uranium, and plutonium-239. Uranium concentrations are lower than tritium because of the larger size and lower diffusion coefficient of the uranium solute (probably uranyl ions) relative to tritium (as well as possibly some sorption of the uranium to the tuff). Plutonium-239 does not diffuse through the slab because of the high sorption capacity of the tuff matrix for plutonium. In general, the relative diffusion coefficients (including the effects of sorption) of the radionuclides studied were tritium > technetium-95 > uranium > neptunium-237 >> plutonium-239. Diffusion coefficients for a given radionuclide in different tuff matrices were dependent on the porosity and microstructure of the tuffs, as well as on the zeolite content of the tuffs for radionuclides that sorb strongly to zeolites (e.g., neptunium-237).

The C-wells diffusion cell experiments established a consistent 3:1 ratio of matrix diffusion coefficients for bromide and PFBA in all C-wells tuff matrices, with the smaller bromide ion having the higher diffusivity. This ratio was a critical constraint in the interpretation of the field tests. The C-wells diffusion cell experiments also established a good correlation between the log of the matrix diffusion coefficient and the log of the matrix permeability (which was measured for each diffusion cell). This correlation was better than the correlation of matrix diffusion with matrix porosity. This result suggests that matrix permeability may be a good predictor of matrix diffusion coefficients of nonsorbing radionuclides in Yucca Mountain tuffs.



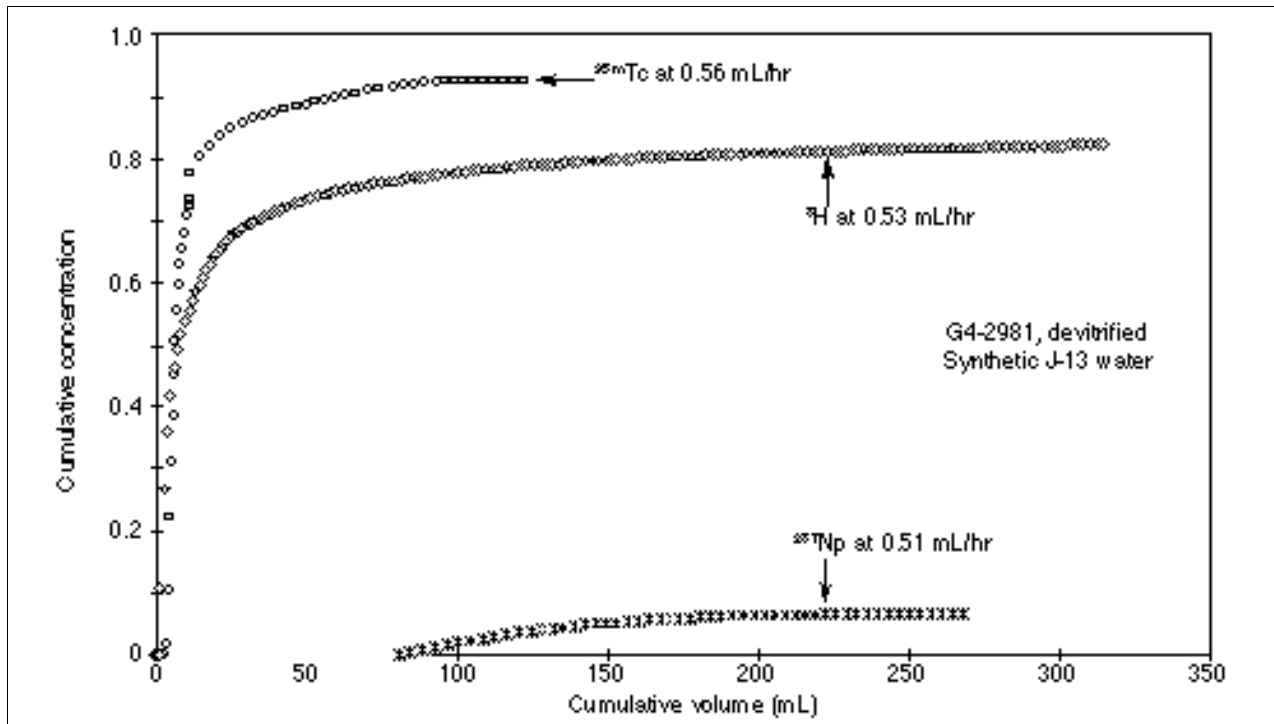
Source: CRWMS M&O (2000r, Figure 31)

Figure 3-11. Diffusion of Tritium, Uranium, and Plutonium through a Devitrified Tuff

3.1.4.2.3 Fractured Rock Column Experiments

Matrix diffusion has been observed in many saturated fractured rock column experiments. As with the diffusion cells, these experiments featured the radionuclides and nonradioactive tracers that were used in the C-wells field experiments. Fractured rock column experiments simulate field conditions more realistically than rock beaker or diffusion cell experiments because they incorporate natural fractures with realistic geometries and mineral coatings and because they include the effects of flow in the observations of transport processes. Details of the experimental methodology for fractured rock columns are provided by CRWMS M&O (2000r, Section 6.5.3).

Two types of fractured rock column experiments were conducted to demonstrate and quantify matrix diffusion. In the first type of experiment, two or more nonsorbing radionuclides or tracers of different diffusion coefficients are simultaneously passed through a fracture. As in the C-wells field experiments, the solute with the larger diffusion coefficient will have a lower peak concentration and a longer tail than will the solute with the smaller diffusion coefficient because the former loses more mass to the matrix as it passes through the fracture. For example, technetium-95 (as pertechnetate) passes through the fracture more rapidly than tritiated water because pertechnetate diffuses into the matrix more slowly than the tritiated water (Figure 3-12). Neptunium-237 is attenuated relative to both nonsorbing radionuclides because it sorbs to the fracture and matrix surfaces. Thus, these experiments also yield information on sorption processes and magnitudes under flowing conditions in fractures. The second type of fractured rock experiment yielding information on matrix diffusion actually is a series of experiments involving the same nonsorbing solute at two or more flow rates. At higher flow rates, there is less matrix diffusion of the solute because of the shorter residence time in the fracture, so the solute concentration will peak at a higher value and the tail will be shorter than at lower flow rates.



Source: CRWMS M&O (2000r, Figure 25)

NOTE: Data from borehole G4 (908.6 m [2981 ft] below surface). The earlier recovery of technetium-95 relative to tritium is the result of the smaller matrix diffusion coefficient of the pertechnetate ion relative to tritiated water.

Figure 3-12. Cumulative Recoveries of Tritium, Technetium-95, and Neptunium-237 in a Fractured Tuff Column

Both types of experiments can yield estimates of matrix diffusion mass transfer coefficients in a fracture flow system. In general, estimates of mass transfer rates in laboratory-scale fractures are greater than those deduced from the C-wells field experiments. This result may be attributable to (1) greater average fracture apertures in field experiments, which reduces mass transfer rates into the matrix, (2) an increase in matrix tortuosity (and hence a decrease in matrix diffusion coefficients) at increasingly greater distances into the matrix (field tests have longer time scales and hence larger diffusion distances into the matrix), (3) a greater diffusion resistance offered by fracture mineral coatings in the field, and (4) the tendency to have a higher percentage of diffusion into stagnant free water (with correspondingly greater effective diffusion coefficients) in the laboratory than in the field as a result of the shorter time scales in the laboratory. The mass transfer rates derived from the C-wells field experiments are more conservative, and they have the added benefit of being obtained over more relevant time and length scales. However, the laboratory experiments are useful for demonstrating the validity of matrix diffusion as an effective attenuation process in the SZ, and they are the only types of realistic flow experiments that can be conducted using radionuclides.

3.1.4.3 Colloid-Facilitated Transport Experiments

Colloids are capable of facilitating the transport of radionuclides over long distances in the SZ only if a large percentage of the colloids do not irreversibly attach to rock surfaces, and the desorption rate of radionuclides from the colloids is extremely slow (i.e., radionuclides are actually impregnated in the colloids or are very strongly sorbed to colloid surfaces), or if steady-state colloid concentrations are so high that colloid surfaces can effectively compete with immobile surfaces for radionuclides on the basis of surface area arguments. Analyses of colloid concentrations and size distributions in Yucca Mountain groundwaters have confirmed that high concentrations of colloids do not occur in the SZ around Yucca Mountain. Published correlations of colloid concentrations as a function of water chemistry, which draw upon a global database of measurements, also suggest that steady-state colloid concentrations are unlikely to ever be high enough for the latter condition to be met even under perturbed conditions (Triay et al. 1996).

The YMP has addressed the attachment and detachment of colloids by using the polystyrene microsphere data from the C-wells field tests to obtain conservative estimates of colloid attachment and detachment rates in fractured tuffs, and by using published data to obtain estimates of attachment and detachment rates in alluvial settings (Section 3.2.4.5). The published correlations of colloid concentrations as a function of water chemistry also support indirect estimates of attachment rates, as it is widely accepted that lower concentrations occur under conditions where colloids are less stable and more likely to attach to surfaces. Details of stability-based arguments for bounding colloid concentrations and attachment rates in Yucca Mountain waters are provided by CRWMS M&O (2000h).

Recent laboratory experiments addressed the magnitude and reversibility of radionuclide sorption onto colloids. Some of the earliest laboratory experiments involved the transport of cesium-137 and silica colloids in columns packed with glass beads. Cesium sorption to the silica was fast and reversible, and under these conditions, the ability of the colloids to facilitate cesium-137 transport was limited because of the large amount of competing sorptive surface area presented by the glass beads. Nevertheless, these experiments helped establish equilibrium- and kinetic-based modeling approaches for describing colloid-facilitated transport in the SZ. These experiments also showed that considerable colloid-facilitated transport would be an issue only for radionuclides that sorbed much more strongly to colloids than did cesium-137.

Recent laboratory experiments measured the magnitude and rates of sorption and desorption of strongly-sorbing, long-lived radionuclides onto several different types of colloids that may be present in the near-field (goethite, hematite) or far-field (silica, montmorillonite clay) environment at Yucca Mountain (CRWMS M&O 2000f). These studies focused on plutonium-239 and americium-243, with the plutonium being prepared in two different forms: colloidal plutonium(IV) and soluble plutonium(V). Water from well J-13 and a synthetic sodium-bicarbonate solution were used in the experiments. Colloid concentrations were varied in some of the experiments to determine the effect of colloid concentration. Details of the experiment and summaries of the plutonium-239 sorption and desorption rates are provided by CRWMS M&O (2000h). These and other results can be summarized as follows:

- The sorption of plutonium-239 onto hematite, goethite, and montmorillonite colloids was strong and rapid, but sorption onto silica colloids was slower and weaker.
- The desorption rates of plutonium-239 from hematite colloids were too small to measure even after 150 days. Desorption from goethite and montmorillonite colloids also was slow, but not as slow as for hematite. The desorption rates of plutonium-239 from silica colloids was rapid relative to the other colloids studied.
- For a given form of plutonium-239, sorption generally was stronger, faster, and less reversible in the synthetic sodium-bicarbonate water than in the natural water from well J-13. Apparently, the presence of other ions, probably calcium, in the natural water tended to slightly suppress the sorption of plutonium-239.
- There was no clear trend of colloidal plutonium(IV) or soluble plutonium(V) sorbing more strongly to the colloids. In general, plutonium(V) sorbed slightly more to hematite and silica, while plutonium(IV) was sorbed slightly more to goethite and montmorillonite.
- The sorption of plutonium-239 was greatest per unit mass of colloid at the lowest colloid concentrations (i.e., sorption was greatest when measured at low colloid concentrations). This result suggests that the colloid surface area at the lower colloid concentrations was sufficient to sorb most of the plutonium in solution, so the addition of more colloids to the solutions did not result in a corresponding linear increase in the amount of plutonium sorbed. The most conservative sorption values for PA will come from data generated at low colloid concentrations.
- The sorption of americium-243 onto hematite, montmorillonite, and silica colloids showed the same trends as plutonium-239 sorption (i.e., hematite > montmorillonite > silica), and the magnitudes of sorption for the two radionuclides were similar for the different colloids. Results of desorption measurements for americium-243 are not yet available.

There are two preliminary conclusions from this ongoing work. First, waste-form colloids such as hematite (resulting from degradation of waste package materials) pose the greatest risk for colloid-facilitated transport, although these colloids would have to travel through the UZ before reaching the SZ. Second, the transport of plutonium or americium in the SZ will be more strongly facilitated by natural clay colloids than by silica colloids.

3.2 CONCEPTUAL MODEL OF SITE-SCALE SATURATED ZONE FLOW AND TRANSPORT

The general conceptual model of SZ flow in the site-scale SZ flow and transport model area is that groundwater flows southerly from recharge areas of higher precipitation at higher elevations north of Yucca Mountain, through the Tertiary volcanic rocks of the Alkali Flat-Furnace Creek groundwater basin, toward the Amargosa Desert. Within the site-scale model area (Figure 3-4), recharge occurs from infiltration of precipitation and infiltration of flood flows from Fortymile Wash and its tributaries. In the southeastern part of the model area (within the Ash Meadows

groundwater basin), considerable flows enter and exit the area in the lower carbonate aquifer system (CRWMS M&O 1999a). This aquifer system is believed to underlie much of the Alkali Flat-Furnace Creek groundwater basin; however, the flow patterns of groundwater in this area and their relationship to flow in the Ash Meadows flow system are poorly understood due to lack of deep-well data.

Outflow from the site-scale SZ flow and transport model area mostly occurs across the southern boundary of the model and to pumpage by irrigation wells in the Amargosa Farms area. The following sections describe the HFM, boundary conditions of the site-scale SZ flow and transport flow model, and alternative conceptual models. Assumptions, uses, and limits of the site-scale SZ flow and transport model are discussed in Section 3.5.

3.2.1 Hydrogeologic Framework and Hydrogeologic Units

Building an HFM is an essential step in developing the site-scale SZ flow and transport model for the Yucca Mountain area. To this end, an HFM was constructed, incorporating data from the Death Valley Region flow model (D'Agnese et al. 1997), geologic maps and cross sections, borehole data, geophysical data, digital elevation data, and the existing geologic framework model (Figure 3-4) of the 40 km² (15 mi²) potential repository area (USGS 2000a).

The HFM represents a 3-D version of the hydrogeology surrounding Yucca Mountain (Figure 3-4) and covers an area of about 1,350 km² (521 mi²) that is 45 km long and 30 km wide (28.0 mi by 18.6 mi). Vertically, the model extends from an interpretation of the water table to the base of the regional groundwater flow model at 2,750 m (9,020 ft) below the water table (D'Agnese et al. 1997). The model domain was selected to be:

- Coincident with grid cells in the regional-scale groundwater flow model (D'Agnese et al. 1997) such that the base of the site-scale SZ flow and transport model was equivalent to the base of the regional-scale model.
- Sufficiently large to minimize the effects of boundary conditions on estimating permeability values at Yucca Mountain.
- Sufficiently large to assess groundwater flow at distances beyond the proposed 20-km (12.5-mi) compliance boundary downgradient from the potential repository area (a regulatory issue).
- Small enough to minimize the number of computation nodes used in the model.
- Thick enough to include part of the regional Paleozoic carbonate aquifer.
- Large enough to include wells in the Amargosa Desert at the southern end of the modeled area.

Assumptions used for the HFM are methodological and geological. The major assumptions are (USGS 2000a):

- The HFM is an acceptable representation of the hydrogeologic units of the SZ flow system. Underlying this assumption is the idea that it is valid to treat the hydrologic properties of a hydrogeologic unit grid cell as uniform.
- Hydrostratigraphic units influence the magnitude and direction of groundwater flow, and stratigraphic units can be simplified into hydrostratigraphic units.
- Boundaries of stratigraphic units represented on maps, wells, and cross sections are sufficiently accurate for groundwater flow modeling purposes.
- Interpolation algorithms using data on faults and stratigraphic unit tops from maps, wells, and cross sections are sufficiently accurate to characterize the top of a hydrogeologic unit.

Construction of a 3-D HFM involves the following seven steps (USGS 2000a).

- Geologic units are classified into hydrogeologic units based on hydraulic properties and lateral extent.
- Digital elevation data are combined with hydrogeologic maps to provide a series of points in 3-D space depicting the locations of outcrops of individual hydrogeologic units.
- Cross sections and lithologic logs are used to locate hydrogeologic units in the subsurface.
- Maps and cross sections are used to locate faults.
- Structure contour-maps are developed for each hydrogeologic unit by interpolating surface and subsurface positions with gridding software that incorporates unit offsets across faults.
- An HFM is developed when the structure contour maps for the individual hydrogeologic units are combined, using appropriate stratigraphic principles to control their sequence, thickness, and lateral extent.
- The potentiometric surface is used to truncate the top of the HFM.

The HFM is constructed using a grid of cells. The 30-km by 45-km (18.6 by 28.0 mi) model domain is divided into cells that measure 125 m (410 ft) on each side, and there are 240 cells in the east-west dimension and 360 cells in the north-south dimension. The vertical dimension of each cell is not fixed; rather it is determined by the thickness of each of the 18 hydrogeologic units that it penetrates. The top of the model is defined as the top of the potentiometric surface

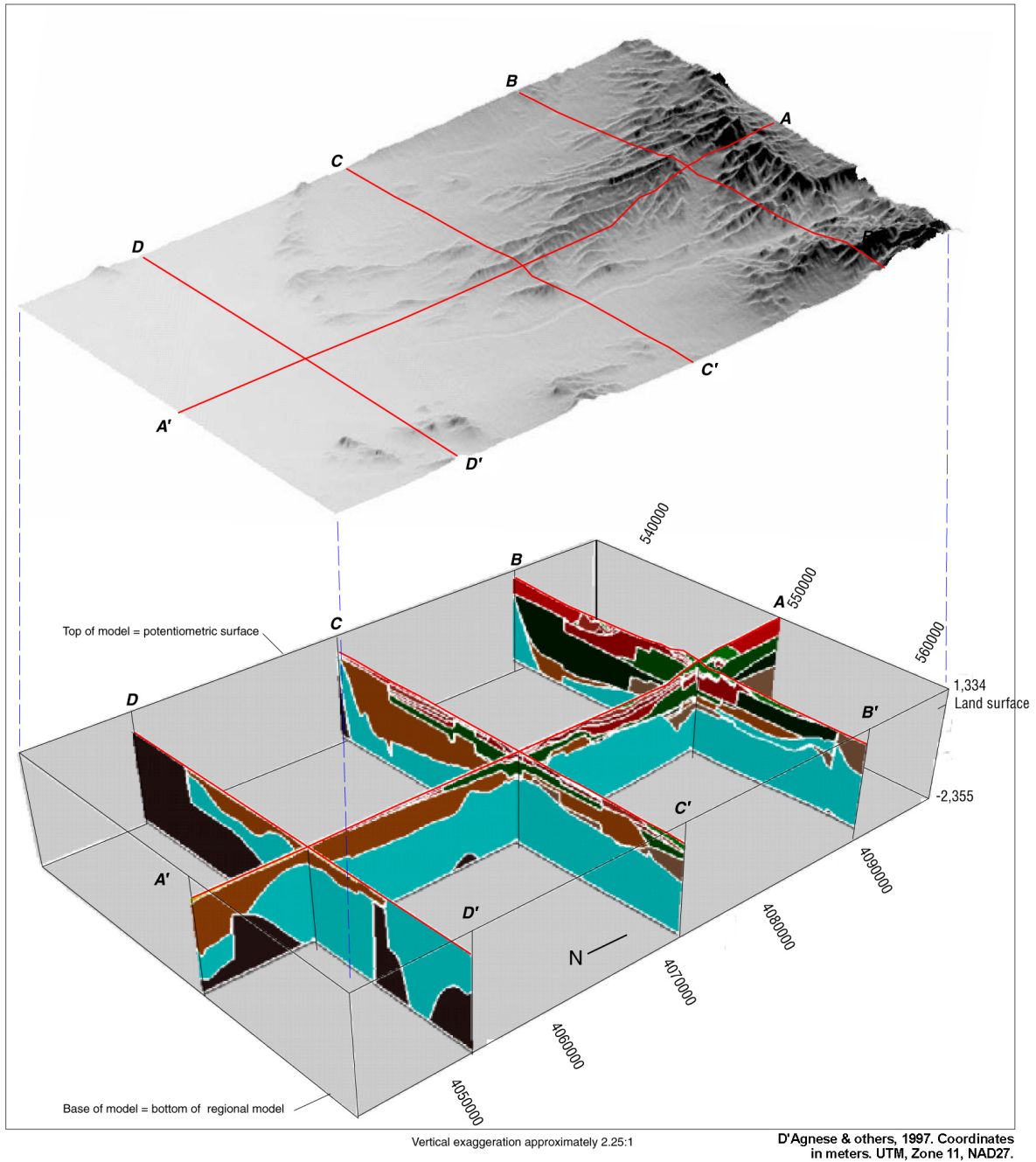
(the water table), and the bottom of the model is a smoothed surface 2,750 m (9,020 ft) below the potentiometric surface.

Hydrogeologic Units—A basic principle followed in constructing the HFM is that the hydrogeologic units at Yucca Mountain form a series of alternating volcanic aquifers and confining units overlying the regional carbonate aquifer (USGS 2000a). Many of the formations have eroded since deposition. The volcanic rocks generally thin toward the south (away from their sources north of Yucca Mountain). The volcanic aquifers and confining units interfinger with undifferentiated valley-fill and the valley-fill aquifer to the south and southeast, while structural features delimit the eastern, western, and portions of the southern edges of Yucca Mountain. The volcanic rocks and valley-fill materials generally covered the pre-existing topography, so that the top of a formation may be more planar than the base.

The geologic relationships, both actual and inferred, were simplified to accommodate computer mapping, framework modeling, and groundwater flow modeling limitations (USGS 2000a). The rocks and deposits near Yucca Mountain were classified into hydrogeologic units based on hydraulic properties. Where feasible, hydrogeologic units identified by previous investigators were retained. Many of the units are not present in the site-scale model, but are included for consistency with regional-scale models. In all, 18 hydrogeologic units are delineated in the site-scale SZ flow and transport model area. USGS (2000a, Table 6-3) summarize the hydrogeologic units and how they relate to the geologic units in the model area. Figure 3-13 illustrates, by way of a fence diagram, the complex 3-D spatial relation among these units within the site-scale model area.

3.2.2 Groundwater Occurrence and Flow

As described by Luckey et al. (1996, p. 17), the Tertiary volcanic section at Yucca Mountain consists of a series of ash-flow and bedded ash-fall tuffs that contain minor amounts of lava and flow breccia. Individual ash-flow tuffs may be several hundred meters thick, whereas bedded tuffs generally are less than a few tens of meters thick. Ash-flow tuffs range from nonwelded to densely welded, and the degree of welding varies both horizontally and vertically in a single flow unit. Nonwelded ash-flow tuffs, when unaltered, have moderate to low matrix permeability, but high porosity. Permeability is decreased by secondary alteration, and fractures are infrequent and often closed in the low-strength nonwelded tuffs. Consequently, these rocks generally constitute laterally extensive SZ confining units in the Yucca Mountain area. The properties of partly welded tuffs vary between those of fractured, welded tuffs and those of altered, nonwelded tuffs. The densely welded tuffs generally have minimal primary porosity and water-storage capacity, but they can be highly fractured. Where interconnected, fractures can easily transmit water, and highly fractured units function as aquifers. In general, the bedded tuffs have high primary porosity and can store large amounts of water. Their matrix permeability is moderate to low, depending on the degree of alteration. The bedded tuffs generally function as confining units, at least when compared to less porous but densely fractured ash-flow tuffs. Lavas, flow breccias, and other minor rock types are neither thick nor widely distributed in the Yucca Mountain area. Their hydraulic properties probably are as variable as the properties of the ash-flow tuffs, but the relatively limited spatial distribution of these minor rock types makes them generally unimportant to the hydrology of Yucca Mountain.



Source: Modified from USGS (2000a, Figure 6-1)

NOTE: This fence diagram illustrates the complex 3-D spatial relation among units within the site-scale model domain. Shading represents different hydrogeologic units.

Figure 3-13. Fence Diagram of the Site-Scale Model Domain

As described by Luckey et al. (1996, p. 17), even fractured tuffs and lavas may not easily transmit water because lithostatic loading keeps the fractures closed. In addition, where volcanic glass has been partly replaced by zeolites and clays, particularly in the originally glassy nonwelded tuffs, these secondary minerals substantially decrease permeability and slow groundwater flow through the rock. The degree of alteration can affect the water-transmitting characteristics of the volcanic sequence. Alteration, particularly in the Calico Hills Formation, increases toward the north of Yucca Mountain and probably accounts for the apparent decrease in hydraulic conductivity to the north. Alteration also tends to increase with depth and is pervasive below the Calico Hills Formation.

Fractures vary in length, orientation, connectivity, aperture width, and amounts and types of coatings, all of which may affect the flow of water. The physical parameters of fractures are characterized by outcrop mapping, borehole logging, and mapping in the Exploratory Studies Facility; however, seeps of water have not been observed in outcrop mapping or in mapping in the Exploratory Studies Facility.

Fractures at Yucca Mountain originated as a result of initial cooling of the volcanic deposits and as a result of tectonic activity. In the Tiva Canyon welded hydrologic unit, two sets of vertically orientated cooling fractures were observed dipping nearly vertically and striking towards the northwest and northeast. A third set of tectonic joints commonly abut the cooling joints, and these three sets of joints form an orthogonal, 3-D network. CRWMS M&O (1998c, Section 3.6.3) present an extensive discussion of fractures in the Yucca Mountain area.

Fracture aperture characteristics are poorly known from direct observation, and for modeling, reliance is placed on indirect effects such as changes in air and water permeability. In general, the stress due to overburden loading across high-angle fractures will be less than across low-angle fractures, resulting in higher vertical than horizontal permeability.

The volcanic rocks consist of alternating layers of welded and nonwelded ash-flow and ash-fall (bedded) tuff deposits. Each of the ash-flow units is underlain by an associated bedded-tuff layer. The ash-flow units vary in degree of welding (or recrystallization) with the maximum welding generally found near the center of the flow, where heat was retained the longest, and the degree of welding decreasing upward and downward toward the flow boundaries.

The welded units typically have low matrix porosities and high fracture densities, whereas the nonwelded and bedded tuffs have relatively higher matrix porosities and lower fracture densities. The fracture density is correlated with the degree of welding of the volcanic rocks.

Where glassy tuff has been saturated for long time periods (e.g., beneath the water table), the original glassy material generally has been altered to zeolite or clay minerals. Such alteration does not affect porosity greatly because it does not fill the pore spaces, but the permeability of the rocks is greatly reduced by alteration of the connections between the pore spaces. Alteration of silica to zeolites or clay minerals is not an important factor in densely welded zones because cooling fractures dominate permeability.

In addition to flow within the volcanic rocks, groundwater also flows in the carbonate rocks of the lower carbonate aquifer. In general, it is believed that the matrix porosity of the ancient

marine limestones and dolomites of the lower carbonate aquifer is negligible (Winograd and Thordarson 1975, p. C14) and that the large discharge from that aquifer system at Ash Meadows is due to flow through solution-enlarged fractures and along faults (Dudley and Larson 1976, pp. 5 and 9). Only one borehole, UE 25p#1, penetrates the lower carbonate aquifer near Yucca Mountain. Because of the lack of data on hydrologic conditions in the carbonate aquifer, the direction and magnitude of groundwater flow in that aquifer at Yucca Mountain is poorly understood. However, large groundwater flows have been modeled in the carbonate aquifer by D'Agnese et al. (1997, Figures 46 to 47, p. 90) in the Death Valley Regional Groundwater Flow Model within the southern part of the site-scale flow model. These are discussed in Section 3.2.2.3.

Estimates of groundwater flux in the Yucca Mountain area are based largely on indirect evidence. Although the potentiometric gradients generally are known, little definitive data exists regarding the storage properties of the rocks of the SZ, such as effective porosity and storativity (Luckey et al. 1996, p. 53).

More data are available on the transmissive properties (transmissivity and hydraulic conductivity) of the rocks of the SZ, chiefly from aquifer tests in boreholes. However, a wide margin of uncertainty exists about the quantitative validity and extrapolation of such data far from the test sites (Luckey et al. 1996, pp. 53 to 54). Groundwater flow models have been used to estimate transmissivity over large areas, but these have a large uncertainty associated with them (Luckey et al. 1996, p. 54).

3.2.2.1 Vertical Gradients

Information on vertical hydraulic gradients in the SZ is concentrated near Yucca Mountain, although Kilroy (1991) presents some information indicating the existence of vertical gradients in the Amargosa Desert. The following discussion of vertical gradients primarily is extracted from Luckey et al. (1996, pp. 27 to 29).

Luckey et al. (1996, pp. 27 to 29) report on potentiometric level measurements in multiple depth intervals in 10 boreholes at Yucca Mountain. Differences in potentiometric levels at different depth intervals in the same borehole ranged from as little as 0.15 m (0.5 ft) in borehole USW H-4 to as much as 54.83 m (180 ft) in USW H-1 (Luckey et al. 1996, Table 3). The largest differences were between the lower carbonate aquifer or the adjoining lowermost lower volcanic confining unit and the overlying lower volcanic aquifer. Within the upper part of the lower volcanic confining unit and the lower volcanic aquifer, the differences in potentiometric levels generally were 1 m (3.3 ft) or less.

Potentiometric levels generally were higher in the lower intervals of the volcanic rocks than in the upper intervals, indicating a potential for upward groundwater movement. However, at four boreholes (USW G-4, USW H-1, USW H-6, and UE-25b#1), potentiometric levels in the volcanic rocks were slightly higher in the uppermost intervals than in the next lower intervals. Overall, it appears that an upward gradient between lower and upper volcanic aquifer is maintained at these locations.

Potentiometric levels in the Paleozoic carbonate aquifer in borehole UE-25p#1 are about 752 m (2,467 ft), or about 21 m (69 ft) higher than levels in the lower volcanic aquifer. A potential for upward groundwater movement from the Paleozoic rocks to the volcanic rocks was, therefore, indicated. Because of the large difference in potentiometric levels in these two aquifers, they seem to be hydraulically separate (Luckey et al. 1996, p. 28). Testing at the C-wells Complex in 1984 suggested a hydraulic connection between the lower volcanic aquifer and the carbonate aquifer; however, testing in 1995 and 1996 using more reliable water-level measurement equipment did not confirm the hydraulic connection (Luckey et al. 1996, p. 28).

In borehole UE-25p#1, the lowermost 70 m (230 ft) of the older tuffs (lower volcanic confining unit) had potentiometric levels similar to those in the carbonate aquifer, indicating a hydraulic connection between the lowermost part of the lower volcanic confining unit and the carbonate aquifer. Such a connection could be expected in the hanging-wall rocks adjacent to a fault, and such connection is supported by calcification of the basal tuffs in the borehole. The remaining 237 m (778 ft) of the lower volcanic confining unit had a potentiometric level similar to that of the lower volcanic aquifer (Luckey et al. 1996, p. 28).

No obvious spatial patterns in the distribution of vertical hydraulic gradients around Yucca Mountain are apparent; however, some generalizations can be made as to the distribution of potentiometric levels in the lower sections of the volcanic rocks. Potentiometric levels in the lower volcanic confining unit are relatively high (altitude greater than 750 m [2,460 ft]) in the western and northern parts of Yucca Mountain and are relatively low (altitude about 730 m [2,395 ft]) in the eastern part of Yucca Mountain. Based on potentiometric levels that were measured in borehole UE-25p#1, the potentiometric levels in the lower volcanic confining unit in boreholes USW H-1, USW H-3, USW H-5 and USW H-6 may reflect the potentiometric level in the carbonate aquifer. Boreholes UE-25b#1 and USW H-4 do not seem to fit the pattern established by the other boreholes. These two boreholes penetrated only 31 m (102 ft) and 64 m (210 ft), respectively, into the lower volcanic confining unit and had potentiometric levels (about 730 m [2,395 ft]) which were similar to potentiometric levels in the lower volcanic aquifer. Penetration of the other four boreholes into the lower volcanic confining unit ranged from 123 m (403 ft) in borehole USW H-3, to 726 m (2,382 ft) in borehole USW H-1. Perhaps only in boreholes USW H-1, USW H-3, USW H-5, and USW H-6 are the potentiometric levels in the lower volcanic confining unit influenced by the potentiometric level in the carbonate aquifer (Luckey et al. 1996, p. 29).

Vertical hydraulic gradients could have an important impact on the analysis of the effectiveness of the SZ as a barrier to radionuclide transport in that they keep the flow path for the potential repository in the shallow groundwater. Based on a limited data set (five boreholes), a spatially extensive upward gradient can be inferred between the carbonate aquifer and the volcanic aquifers, which may indicate that, at least for the immediate Yucca Mountain area, radionuclide transport would be restricted to the volcanic system (Luckey et al. 1996, p. 29).

Kilroy (1991, pp. 11 to 16, Table 3) presents vertical gradient data for 21 nested piezometers, 1 well cluster, and 1 river and well pair in the Amargosa Desert area. However, none of these locations are within the area of the site-scale SZ model, so the results are not discussed in detail here. Upward gradients generally were associated with freshwater limestones, carbonate rock outcrops, and structural features (Kilroy 1991, p. 16). The association with carbonate rocks is

attributed to hydraulic connection with the carbonate aquifer regional flow system and, especially, to the Spotted Range-Mine Mountain fault zone, which is a conduit for flow from the carbonate aquifer to the basin fill.

3.2.2.2 Flow Field

Using the potentiometric surface map (Figure 3-5) and the assumption that hydraulic conductivity is isotropic, the general direction of groundwater flow within the site-scale SZ flow and transport model area can be deduced as being from north to south. Under this assumption, the direction of flow is perpendicular to the water-level contours. Under the USGS (2000a) interpretation of the water-level data (Figure 3-5), the water table exhibits a steep gradient throughout the northern part of the model area (north of the potential repository) and the contours curve southward to the west of Crater Flat.

Several faults are interpreted as barriers to groundwater flow, as indicated by offsets of contours where they cross faults (Figure 3-5). This interpretation, however, is supported only by field data at the Solitario Canyon fault, west of the potential repository, which is interpreted as causing a differential of about 45 m (148 ft) in the potentiometric surface. In Crater Flat and on the southern part of Yucca Mountain, the flow direction is nearly easterly toward Fortymile Wash. A more detailed water-level map of the immediate vicinity of Yucca Mountain (Figure 3-6) indicates that flows from the west and east converge at Fortymile Wash and turn southward toward the Amargosa Desert. The cause of the easterly gradient in Crater Flat and southern Yucca Mountain is not evident, but it suggests that a groundwater barrier exists near the northern margin of the Amargosa Desert. In any event, the potentiometric surface upgradient of the 725-m (2,379 ft) contour and the Highway 95 fault appears to have little north-south flow over an area of about 259 km² (100 mi²).

As discussed in Section 3.2.2.1, the potentiometric level in well UE-25p#1, which penetrates the lower carbonate aquifer, is about 752 m (2,467 ft), 21 m (69 ft) higher than in nearby wells tapping the lower volcanic aquifer. This indicates a potential for upward flow from the lower carbonate aquifer; however, other lines of evidence suggest that such flow is small. The direction of flow and hydraulic gradient cannot be determined from a single well; however, regional relationships suggest that the general direction of flow in the lower carbonate aquifer should be southerly in the site-scale SZ flow and transport model domain (NRC 1999a, p. 109).

Most monitoring wells in the Yucca Mountain area show little variation in water level over time (Luckey et al. 1996, p. 29). In contrast, water levels in the heavily pumped Amargosa Farms area have declined substantially since intensive irrigation development began in the 1950s. Kilroy (1991, p. 18) reported a water-level decline of as much as 9 m (30 ft) by 1987, and La Camera and Locke (1997, Figure 4) show an additional decline of about 3.4 m (11 feet) through 1996 at well AD-5, about 14 km (8.7 mi) southwest of Amargosa Valley.

3.2.2.3 Large, Moderate, and Small Hydraulic Gradients

Three distinctive hydraulic gradients of the potentiometric surface at Yucca Mountain are recognized: (1) a large hydraulic gradient of 0.13 between water-level altitudes of 1,030 m (3,380 ft) and 750 m (2,460 ft) at the north end of Yucca Mountain, (2) a moderate hydraulic

gradient of 0.05 west of the crest of Yucca Mountain, and (3) a small hydraulic gradient of 0.0001 to 0.0003 extending from Solitario Canyon to Fortymile Wash. These gradients have been portrayed on detailed potentiometric surface maps presented by Ervin et al. (1994), and Tucci and Burkhardt (1995), as well as on the maps with large contour intervals compiled by D'Agnese et al. (1997) and by USGS (2000b). The large contour-interval maps do not portray the small or moderate gradients well because of limitations imposed by contour intervals; however the large gradient is recognizable on all of these maps.

Luckey et al. (1996) present detailed descriptions of these gradient features and discuss interpretations of their causes. The large hydraulic gradient has been the subject of numerous theories. Summarized from Luckey et al (1996, pp. 21 to 25), the large gradient:

- Simply is the result of flow through the upper volcanic confining unit, which is nearly 300 m (984 ft) thick near the large gradient.
- Represents a semi-perched system in which flow in the upper and lower aquifers is predominantly horizontal, whereas flow in the upper confining unit would be predominantly vertical.
- Represents a drain down a buried fault from the volcanic aquifers to the lower carbonate aquifer.
- Represents a spillway in which a fault marks the effective northern limit of the lower volcanic aquifer.
- Results from the presence at depth of the Eleana Formation, a part of the Paleozoic upper confining unit, which overlies the lower carbonate aquifer in much of the Death Valley region. The Eleana is absent at borehole UE-25 p#1 at Yucca Mountain, which penetrated the lower carbonate aquifer directly beneath the lower volcanic confining unit.

The cause of the moderate hydraulic gradient is less controversial than that of the large gradient, and Luckey et al. (1996, p. 25) suggest that the Solitario Canyon fault and its splays function as a barrier to flow from west to east due to the presence of poorly permeable fault gouge or to the juxtaposition of more permeable units against less permeable units.

The small hydraulic gradient occupies most of the potential repository area and the downgradient area eastward to Fortymile Wash. Over a distance of 6 km (3.7 mi), the hydraulic gradient declines only about 2.5 m (8.2 ft) between the crest of Yucca Mountain and Fortymile Wash. The small gradient could indicate highly transmissive rocks, little groundwater flow in this area, or a combination of both causes (Luckey et al. 1996, p. 27).

The latest potentiometric map (USGS 2000b), which includes head data from the recently drilled NCEWDP boreholes, indicates that the small hydraulic gradient extends southward to an east-west fault approximately along Highway U.S. 95.

3.2.2.4 Heterogeneity

Physical and chemical heterogeneity of the rocks and water in the SZ can affect groundwater flow and the transport of contaminants in the SZ. The principal forms of heterogeneity in the site-scale SZ model area are physical and may be primary (i.e., related to the formation of the rocks) or secondary (i.e., related to events subsequent to their formation).

The most obvious form of primary heterogeneity is the mode of origin (i.e., volcanic rocks, clastic rocks, carbonate rocks, and alluvial deposits), which is the primary basis for subdividing the rocks into hydrogeologic units. Within each major category, further subdivisions are possible. Probably the major form of primary heterogeneity affecting groundwater flow in the site-scale SZ model area results from the origin of the volcanic rocks (i.e., ash-flow or air-fall pyroclastic deposits, lava flows, and volcanic breccias). The pyroclastic rocks (termed tuffs) primarily are nonwelded to densely welded, vitric to devitrified ash-flow deposits separated by nonwelded vitric air-fall deposits. Thus, the primary heterogeneity in physical character relates to whether the deposits resulted from massive eruptions of hot volcanic ash from volcanic centers that flowed downslope as flows of fragmental material, or whether they resulted from explosive eruptions that injected volcanic fragments into the air to fall out as bedded tuffs.

The thicker flow deposits, up to several hundred meters thick, were very hot, resulting in welding of the fragments into a dense mass. Thinner flows retained heat less effectively, resulting in partly welded to nonwelded ash-flow tuffs. Ash-fall tuffs, generally less than tens of meters thick, cooled in the atmosphere and characteristically are glassy (vitric) (Luckey et al. 1996, p. 17).

The mode of origin controls the porosity and permeability of the volcanic rocks. The densely welded tuffs generally have minimal primary porosity and water-storage capacity, but commonly are highly fractured and function as aquifers (Luckey et al. 1996, p. 17). Nonwelded ash-flow tuffs, when unaltered, have moderate to low matrix permeability but high porosity, and commonly constitute confining units. Bedded tuffs have high primary porosity and moderate to low permeability, and they generally function as confining units.

As the tuff deposits cooled, they were subjected to secondary processes, including formation of cooling fractures, recrystallization or devitrification, and alteration of the initial glassy fragments to zeolite minerals and clay minerals, all of which affect the hydrologic properties of the rocks. Beginning with deposition and throughout their subsequent history, the rocks have been subjected to tectonic forces resulting in further fracturing and faulting. They also have been subject to changes in the position of the water table, which greatly affects the degree of alteration of the initially glassy deposits.

The forms of secondary heterogeneity most affecting the SZ are fracturing, faulting, and alteration of glassy materials to zeolites and clay minerals. Fractures, where interconnected, transmit water readily, which accounts for the permeable character of the welded tuffs. Cooling fractures, which are pervasive in welded tuffs, tend to be strata-bound, that is, confined to the welded portions of flows, whereas tectonic fractures tend to cut through stratigraphic units, as do faults.

Nonwelded deposits are less subject to fracturing and more subject to alteration of the initial glassy deposits to zeolites and clay minerals, both of which reduce permeability. The presence of perched water bodies in the UZ is attributed to the ubiquitous presence of a smectite-zeolite interval at the base of the Topopah Spring Tuff, which, in the absence of through-going fractures, essentially stops the vertical movement of water (Luckey et al. 1996, p. 46).

The heterogeneity in permeability of different types of deposits led to the subdivision of the Yucca Mountain geologic section into five basic SZ hydrologic units: upper volcanic aquifer, upper volcanic confining unit, lower volcanic aquifer, lower volcanic confining unit, and lower carbonate aquifer. To accommodate the more extensive area of the site-scale flow model, (USGS 2000a) include several additional units above and below these basic five units.

In the vicinity of Yucca Mountain, volcanic deposits generally form laterally-extensive stratigraphic units; however, due to physical heterogeneity, porosity and permeability are highly variable both laterally and vertically. Within the site-scale model area, little specific information is available on the lower carbonate aquifer. However, information from nearby areas (D'Agnese et al. 1997, p. 90, Figures 46 and 47) suggests that the lower carbonate aquifer is highly and uniformly permeable, and that the high permeability is attributed to pervasive solution-enlarged fractures.

In the southern part of the site-scale SZ flow and transport model domain, the volcanic deposits thin and interfinger with valley-fill deposits. The latter are heterogeneous because of their mode of deposition (Walker and Eakin 1963, p. 14), but are not subject to the fracturing, faulting, and alteration types of heterogeneity that affect the volcanic rocks.

3.2.2.5 Hydrologic Features

As explained by USGS (2000a), the HFM represents faults and other hydrogeologic features, such as zones of hydrothermal alteration, that affect SZ flow. Information on faults includes fault trace maps showing where faults intersect land surface and faults shown on cross sections. Faults in the model area can dip at almost any angle, but most are high-angle faults. Given software constraints and the flow model resolution, faulting in the area is simplified and the faults are treated as vertical features.

Where it was thought to be hydrologically important, thrust faults were represented by repeating hydrogeologic units. When geologic structural or stratigraphic surfaces are stored as arrays, they cannot have multiple z-values at one location. This means that thrust faults and mushroom-shaped intrusions cannot be represented by an array. To deal with these problems, simplifying techniques were used. Where units were repeated by thrust faults, two different grids were created for the same hydrogeologic unit. A unit boundary map was then added to define an outline for the perimeter of the thrust sheet. Within this boundary, hydrogeologic structural altitude values were treated as defining unique additional hydrogeologic unit(s). Where units were continuous across this boundary, altitudes of surfaces are the same on each side of the boundary, making the boundary "invisible." Because of the large number of faults in the site-scale SZ model area and limitations in modeling technology, only those faults and other features of hydrologic importance are portrayed in the HFM (USGS 2000a, Figure 6-2).

As discussed by CRWMS M&O (2000n, Section 6.3), some hydrogeologic features of the HFM were accorded special treatment in constructing the site-scale SZ flow and transport model. These features include 15 from the HFM, an alluvial uncertainty zone, and a zone representing Fortymile Wash (Figure 3-14). The hydrological features included in the site-scale SZ flow and transport model primarily represent faults, fault zones, and areas of chemical alteration. The features essentially are vertical, some being linear in the horizontal extent, and some being of areal extent. These features are distinct from the subhorizontal geological formations that form zones with distinct geometry and material properties and are described in Section 3.2.1. Each of these features includes multiple geologic formations and represents zones of altered permeability within the individual formations: some features have enhanced permeability, some have reduced permeability, and others have anisotropic permeability. Each of them has an important impact on the site-scale SZ flow and transport model. The geometric definition, description, nature of permeability alteration, and impact on the model for each of these features are described by CRWMS M&O (2000n, Table 6).

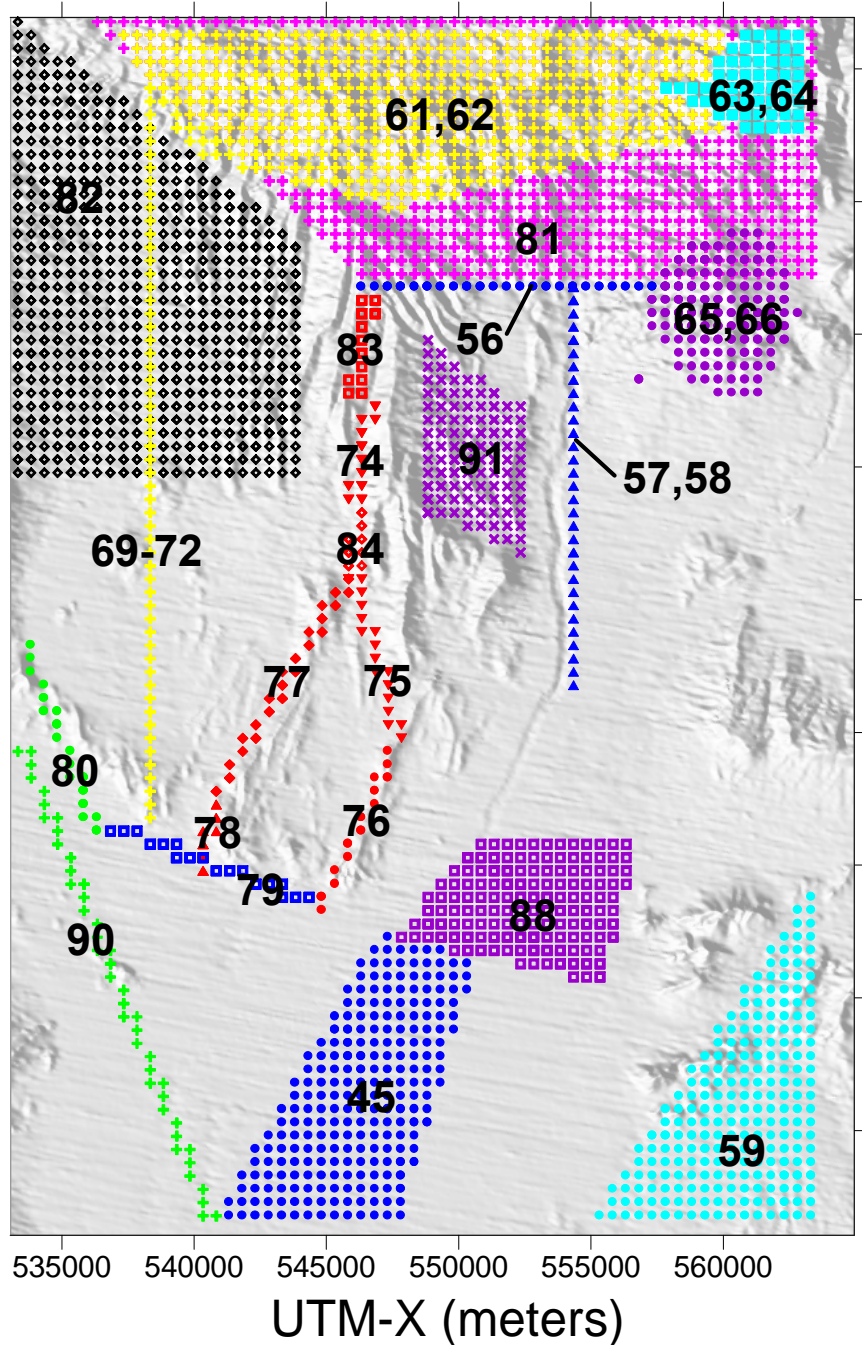
Certain hydrogeologic features of the HFM overlap (e.g., the entire Northern Zone embraces the Claim Canyon Caldera, Shoshone Mountain altered zone, and the Calico Hills altered zone). As explained by CRWMS M&O (2000n, Table 6), the rationale for segregating these smaller units within the larger northern zone is that a different permeability reduction is applied to these smaller units (CRWMS M&O 2000n, Table 12).

Where appropriate, several features are subdivided geographically (Figure 3-14). For example, Fortymile Wash, north and south; and Claim Canyon, east and west, are subdivided. As indicated by CRWMS M&O (2000n), the same parameter adjustment values were used in the model calibration process throughout each of the 17 special features.

Most of the special features were defined as extending from the top of the carbonate aquifer to the top of the model (water table). Exceptions to this generalization are the Spotted Range-Mine Mountain zone, which extends from the top of the model to the bottom; the Alluvial uncertainty zone, which extends from the top of the model down through the undifferentiated valley fill, and the Imbricate fault zone, which extends from the top of the model to the top of the undifferentiated valley fill (CRWMS M&O 2000n, Table 6).

3.2.3 Boundary Conditions

The site-scale SZ flow and transport model is designed to be compatible with the regional-scale SZ model (D'Agnesse et al. 1997), to use the HFM (USGS 2000a), and to use available data on recharge within the site-scale model area (CRWMS M&O 1999a). Recharge data for the site-scale SZ flow and transport model domain includes input from the site-scale UZ flow model, estimates of recharge along Fortymile Wash (Savard 1998), and recharge estimated from the regional-scale SZ flow model (CRWMS M&O 2000n, Figure 2).



Source: CRWMS M&O (2000n, Figure 4)

NOTE: Numbers, or ranges of numbers, identify the following regions: 45–Lower Fortymile Wash zone; 56–East-West Barrier zone; 57 and 58–Fortymile Wash zones; 59–Spotted Range-Mine Mountain zone; 61 and 62–Claim Canyon Caldera zones; 63 and 64–Shoshone Mountain altered zones; 65 and 66–Calico Hills altered zones; 69, 70, 71, and 72–Crater Flat fault zones; 74, 83, and 84–Solitario Canyon fault zones; 75 and 76–Solitario Canyon fault zones (east branch); 77 and 78–Solitario Canyon fault zones (west branch); 79–Highway 95 fault zone; 80 and 90–Bare Mountain fault zones; 81–Northern zone; 82–Northern Crater Flat zone; 88–Alluvial Uncertainty zone (expected case); 91–Imbricate fault zone.

Figure 3-14. Geological Features Represented in the Site-Scale Flow and Transport Model

3.2.3.1 Lateral Boundaries

Most of the inflows to, and outflow from, the site-scale SZ flow and transport model occurs as groundwater flows across the lateral boundaries. The best estimates of flow rates are the cell-by-cell fluxes calculated by the regional-scale model. These fluxes are compiled in four tables (CRWMS M&O 1999a, Tables 7.2-1, 7.2-2, 7.2-3, and 7.2-4) corresponding to the rectangular boundaries of the site-scale flow model. The flows are compiled by the three depth layers (0 to 500 m [0 to 1,640 ft], 500 to 1,250 m [1,640 to 4,100 ft], and 1,250 to 2,750 m [4,100 to 9,020 ft] below the water table) of the regional-scale flow model (D'Agnese et al. 1997, p. 75).

3.2.3.2 Recharge

The three recharge components (site-scale UZ model, regional-scale SZ model, and Fortymile Wash) take different forms and must be combined into a single result. Recharge from the site-scale UZ model is taken as the flow through the base of that model, the domain of which includes approximately 50 km² (19.3 mi²). The UZ flow model uses dual permeability; accordingly, the output includes fluxes for fracture and matrix flow. These data are combined into a total volumetric flow rate and an average percolation flux (CRWMS M&O 1999a, Figure 6.1.3-2).

Estimates of recharge from the infiltration of surface flows in Fortymile Wash are given by linear reaches along the wash. Recharge estimates were interpolated to a 500-m (1,640-ft) wide recharge zone for most of the wash and a broader area of distributary channels in the Amargosa Desert (CRWMS M&O 1999a, Table 6.1.3-1, Figure 6.1.3-2).

The distributed recharge, limited to the northernmost portion of the site-scale model area, was extracted from the regional-scale SZ flow model (D'Agnese et al. 1997). No recharge within the UZ model area was included. A plot of distributed recharge is provided by CRWMS M&O (1999a, Figure 6.1.1-1).

Estimated recharge from all three sources is displayed by CRWMS M&O (1999a, Figure 6.1.3-2). Total recharge was about 1,550,000 m³/yr (1,256 acre-ft/yr). Of this total, about 212,000 m³/yr (172 acre-ft/yr) was attributed to flux from the UZ model area and about 95,000 m³/yr (77 acre-ft/yr) was attributed to infiltration along Fortymile Wash, leaving a remainder of about 1,240,000 m³/yr (1,007 acre-ft/yr) from distributed recharge.

Groundwater inflows along the eastern, northern, and western boundaries of the site-scale SZ flow and transport model total 17.8 x 10⁶ m³/yr (14,430 acre-ft/yr), 6.21 x 10⁶ m³/yr (5,034 acre-ft/yr), and 3.74 x 10⁶ m³/yr (3,032 acre-ft/yr), respectively (CRWMS M&O 1999a). These inflows, totaling 27.75 x 10⁶ m³/yr (22,500 acre-ft/yr), represent nearly 18 times the estimated recharge from the surface in the model area. Of the total inflow for the eastern boundary, 17.6 x 10⁶ m³/yr (14,273 acre-ft/yr), or 99 percent, occurs in the Amargosa Desert sector (CRWMS M&O 1999a), and nearly all of that occurs in layers 2 and 3 of the regional-scale flow model (CRWMS M&O 1999a, Table 7.2-2) and represents flows in the lower carbonate aquifer (D'Agnese et al. 1997, p. 90, Figures 46 to 47).

3.2.3.3 Discharge

There is no natural discharge (i.e., springs or evapotranspiration) from the SZ within the site-scale model domain; therefore, natural discharge to the surface was not represented in the simulations.

3.2.3.4 Role of Faults

Faults, fault zones, and zones of chemical alteration are hydrogeologic features that require special treatment in the site-scale SZ flow and transport model. Faulting and fracturing are pervasive at Yucca Mountain, and they greatly affect groundwater flow patterns because they may act as preferred conduits or barriers to groundwater flow. The role that faults play in facilitating or inhibiting groundwater flow depends on the nature of the fault (i.e., whether the faults are in tension, compression, or shear) and other factors such as the juxtaposition of varying geologic units along the fault plane, the rock types involved, fault zone materials, and depth below land surface.

Faunt (1997) investigated the effect of faulting on groundwater movement in the Death Valley region and developed a map of fault traces (Faunt 1997, Figure 10) and rose diagrams (Faunt 1997, Figure 11) showing the orientation of faults within the principal structural provinces of region. Faunt (1997, p. 38) grouped the faults into three categories depending on their orientations relative to the present-day stress field (i.e., those in relative tension, compression, or shear).

Faults in relative tension are more likely to be preferential conduits for groundwater, and faults in shear or compression are more likely to deflect or block groundwater movements. Within the site-scale model area, faults assumed to have the most evident effects on groundwater movement, such as effects on potentiometric contours (Figure 3-5), include the Solitario Canyon, Stagecoach Road, Highway 95, Crater Flat, and Bare Mountain faults, all of which appear to act as barriers to groundwater flow. Faults within the site-scale model area of hydrologic importance include the Spotted Range-Mine Mountain shear zone, which Faunt (1997, p. 34) describes as a major high-permeability zone in the lower carbonate aquifer, and the following features to which CRWMS M&O (2000n) accords special treatment in the site-scale SZ flow and transport flow model: Crater Flat fault, Solitario Canyon fault, Highway 95 fault, Bare Mountain fault, Imbricate fault zone (between the Ghost Dance and Paintbrush Canyon faults at Yucca Mountain), Fortymile Wash zone (which may not be a fault), and the East-West barrier (which appears to cause the large hydraulic gradient north of Yucca Mountain). These features fall into two categories depending on their hydrologic impacts: (1) zones of permeability enhancement parallel to faults and zones of permeability reduction perpendicular to faults (Crater Flat, Solitario Canyon, and Highway 95 faults), and (2) zones of permeability enhancement (Bare Mountain fault, Imbricate fault zone, Fortymile Wash zones, Spotted Range-Mine Mountain zone).

3.2.4 Solute Transport Processes

The site-scale SZ flow and transport modeling performed by the YMP focused on the key controlling factors that influence the measured head distributions at the site. A summary of these

conceptual models and numerical implementations of these models is presented in Sections 3.2.1, 3.2.2, 3.2.3, and 3.3. The focus of this section is on the transport of radionuclides in the SZ, which in addition to flow issues, requires consideration of processes specific to the migration of solutes. The flow path from the potential repository to the proposed compliance boundary begins in the volcanic tuffs, but ends in the alluvium, and different transport processes operate in the volcanic tuffs and the alluvium (Figure 3-15). The conceptual models for transport in the volcanic tuffs and in the alluvium are different: matrix diffusion occurs only in the volcanic tuffs, and sorption in the volcanic tuffs only occurs after radionuclides diffuse into the matrix. The mathematical formulation of the conceptual model and the numerical implementation of dispersion are the same for both media, but numerical implementation for sorption is different because sorption in the volcanic tuffs is linked to matrix diffusion. A conceptual model for transport processes in the two media (i.e., fractured porous media and the alluvium) is presented. The conceptual model for the fractured porous media includes dispersion, diffusion of radionuclides into the porous rock matrix, and sorption. The conceptual model for transport in the alluvium includes dispersion and sorption.

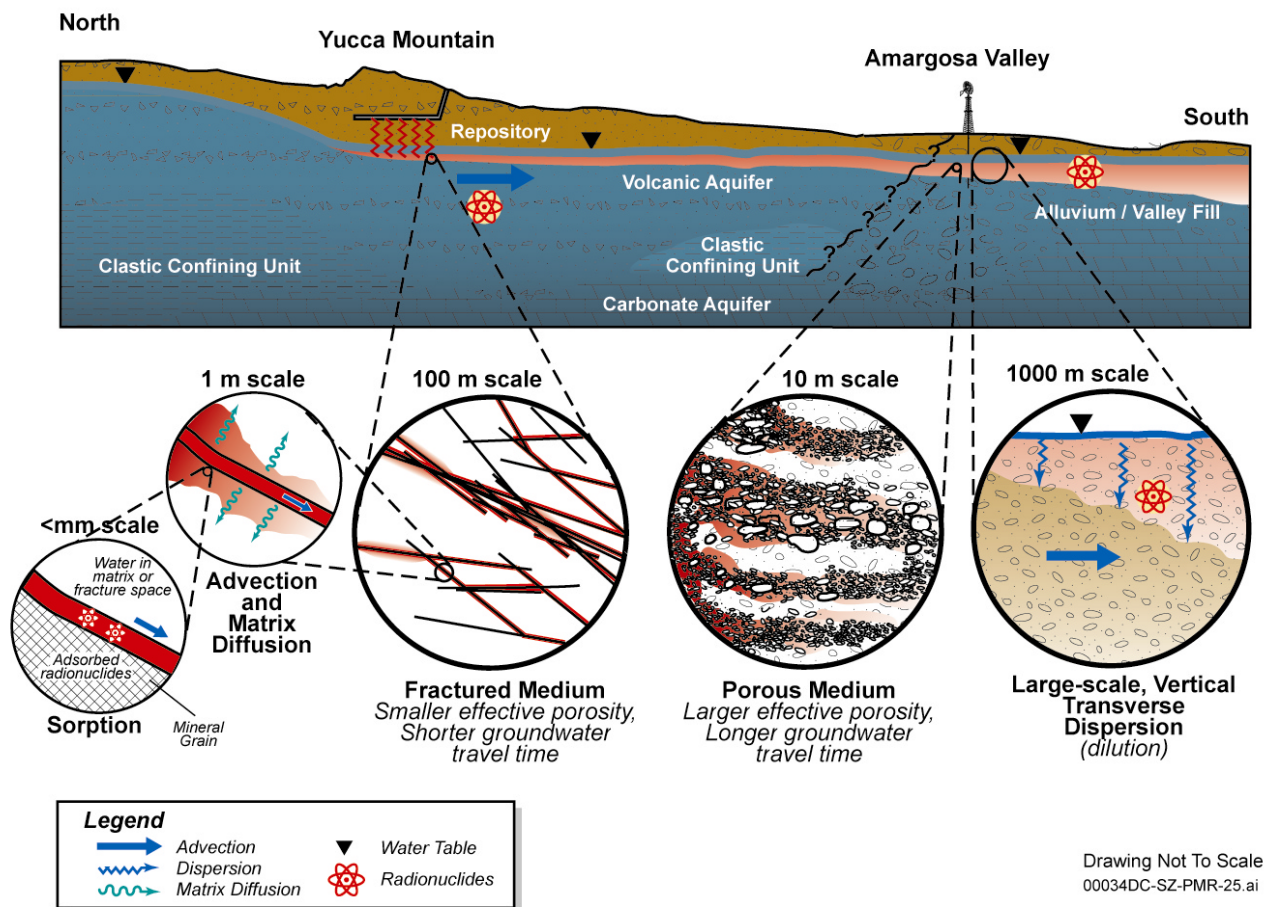


Figure 3-15. Conceptual Model of Transport Processes in the Volcanic Tuffs and the Alluvium

This description of solute transport is organized in two parts. First, the relevant small-scale flow processes that influence transport are reviewed, with focus placed on flow processes likely to influence radionuclide movement. Then a simplified matrix-diffusion model, the mathematics of the model, and simulations designed to assess the amount of matrix diffusion likely to be present in SZ transport under natural conditions are presented.

3.2.4.1 Advection

3.2.4.1.1 Advection in the Fractured Porous Media

Current hydrologic evidence supports the model of fluid flow within fractures in the moderately to densely welded tuffs of the SZ (e.g., Waddell et al. 1984). Hydraulic conductivities measured for core samples in the laboratory are orders of magnitude higher when the sample is fractured (Peters et al. 1984). Also, there generally is a positive correlation between fractures, identified using acoustic televiewer or borehole television tools, and zones of high transmissivity (Erickson and Waddell 1985, Figure 3).

Because the role of fractures is so important to the hydrology in the SZ, the permeability distribution and principal flow directions depend strongly on the spatial distribution and orientations of fractures. Erickson and Waddell's (1985) televiewer log data show that 83.1 percent of the fractures have a strike direction between N 10° W and N 55° E, with most fractures steeply dipping at angles greater than 60°. Karasaki and Galloway (1990) point out that fractures oriented perpendicular to the least principal stress direction of N 60–65° W should be more open and more permeable. Karasaki et al. (1990) tentatively conclude that the regions of high transmissivity in the C-wells correlate with fractures of this general orientation, with the steeply dipping fractures contributing most to the transmissivity.

In the natural groundwater flow state, all fractures, regardless of orientation, will have effective pressures between 71 to 163 bar. In this range, the laboratory tests of Peters et al. (1984) show a relatively minor effect of effective pressure on hydraulic aperture, at least compared with other uncertainties. Thus, it appears that the spatial distribution of fractures (densities and interconnectivities) is more important in determining the hydraulic conductivity ellipsoid than the effect of the stress field on the apertures of individual joints. However, pressure testing that greatly lowers the effective pressure in a joint will result in increased hydraulic apertures and erroneous estimates of the transmissivity. Stock et al. (1984) point out that, in some wells drilled with mud, the weight of the fluid column exceeded the minimum horizontal stress, probably resulting in induced hydraulic fracturing during drilling or the opening of favorably oriented preexisting joints. This possibility may also be true of some slug tests.

Even though the simplifying assumption is made that, from a hydrologic standpoint, all joints are under similar effective stresses, the role of in situ stress nonetheless is an important controlling factor governing the nature of fluid flow within a fracture. For transport, the result is a propensity of fluid and solute to travel preferentially along channels in which the apertures are largest. Thus, for flow within fractures in the SZ, a channel-flow model or a fracture-flow model recognizing and accounting for flow channels is necessary.

Radionuclide Transport Conceptual Model Development—Given the complex geohydrologic setting, the most appropriate approach is to construct a plausible conceptual transport model that describes the relevant processes in the SZ. This model, along with its mathematical representation, allows identification of areas of uncertainty that are necessary to explore and incorporate into the site-scale model. The radionuclide transport times could be several orders of magnitude larger than the transport times computed assuming the fluid velocity within the fractures is the effective radionuclide migration velocity. This implies that the SZ could be an important barrier to radionuclide migration. Therefore, field tests such as those at the C-wells have been designed and carried out to validate the model (Robinson 1994).

Summary of Conceptual Model—Summarizing the discussion of fluid flow behavior given above, the SZ fluid-flow model, into which transport submodels are built, is outlined below:

- Radionuclides enter the SZ via fluids percolating through the unsaturated rock above the water table. The exact nature of this transport is not expected to exert a great effect on the subsequent site-scale SZ flow and transport model, and thus, the SZ transport component of the site-scale SZ model can be developed independently from a transport model for the UZ (which acts as a source term for the site-scale SZ model).
- Flow occurs within the highly fractured portions of the tuffs near the water table. There probably is not a continuous zone of high permeability to the alluvium in Amargosa Valley. Assuming there is not, then the low-permeability regions effectively will act as large-scale heterogeneities that give rise to large-scale macroscopic dispersion due to the tortuous nature of flow over the scale of hundreds of meters to kilometers.
- Although the vertical matrix permeability is assumed to be small over the scale of several hundreds of meters, the vertical fractured-region permeabilities should be as large as the horizontal permeabilities. Thus, radionuclides will spread vertically and be present throughout the entire thickness of a fractured zone. The thicknesses of these fractured zones are difficult to estimate from the present data. However, the extent of fracturing correlates reasonably well with the degree of welding, and the degree of welding is one of the criteria used to define the submembers within a lithologic unit. Therefore, it is reasonable to assume that the heights of the fracture zones are on the order of the thicknesses of the individual lithologic members (i.e., 100 m to 200 m [328 ft to 656 ft]). This possibility is in contrast to flow zones detected in individual boreholes, where measurements reflect the intersection of specific fractures with the well. Nevertheless, these data should be useful in estimating the effective distance between flowing fractures, a parameter that may be important in quantitative assessments of radionuclide transport behavior.
- Fluid flow occurs within the fractures, while stagnant fluid resides in the rock matrix. All fractures have large contact areas due to the in situ stresses exerted on them at these depths. The conductivity of an individual fracture probably is not a strong function of its orientation because all are on the flat portion of the aperture versus effective-pressure curves. Therefore, the magnitude and direction of the components of the hydraulic conductivity tensor should be controlled by the distribution of joints of various

orientations. Fractures detected from geophysical logs generally are oriented in a north-south direction and are within 30° of vertical.

- Fluid and solute tend to travel preferentially along channels in which the apertures are largest. The fluid travels preferentially within regions of large apertures with large sections of the fracture surface containing stagnant fluid or no fluid where the faces are in contact.
- Matrix materials conduct no fluid under natural groundwater flow conditions, but are physically connected to the fracture fluid through the pore network. Fluid is stored in this pore space and is important to radionuclide migration (see below). The matrix porosities of interest are those of the rock within the fractured regions. Fractures generally are found within the moderately to densely welded tuffs, so the range of matrix porosities of these tuffs (0.06 to 0.09 for densely welded and 0.11 to 0.28 for moderately welded) more accurately reflect the fluid storage of interest rather than the generally wider ranges of values found within a specific lithologic member.

3.2.4.1.2 Advection in the Alluvium

Fluid flow in the alluvium is likely to be well represented using a porous continuum conceptual model. This is due to the more porous, less fractured nature of the alluvial material. However, this assumption does not mean that the medium is homogeneous. On the contrary, flow is likely to occur through the relatively more permeable regions within the medium, with the low-permeability regions acting as flow barriers that groundwater flows around rather than through. Data to quantify this portion of the flow path are sparse, and hydrologic parameters used in numerical models are based on regional-scale, rather than site-scale data (CRWMS M&O 2000o, Section 6.3.1), and should be considered to represent large uncertainty. Discussions of the hydraulic characteristics of the alluvium are presented by CRWMS M&O (2000n) and CRWMS M&O (2000o).

3.2.4.2 Matrix Diffusion

Instead of simply traveling at the flow rate of the fluid in the SZ, radionuclides potentially will undergo physical and chemical interactions that must be characterized to predict large-scale transport behavior. These interactions include molecular diffusion into the rock matrix, sorption on the minerals along the fractures or within the rock matrix, and transport in colloidal form.

When a dissolved species travels with the fluid within a fracture, it may migrate by molecular diffusion into the stagnant fluid in the rock matrix. When a molecule enters the matrix, its velocity effectively goes to zero until Brownian motion carries it back into a fracture. The result is a delay of the delivery of the solute to a downgradient location from what would be predicted if the solute had remained in the fracture. In hydrologic tests not involving tracers, the pore water velocity often can be estimated given assumptions about the fracture porosity. For interpreting hydrologic tests, the fracture porosity usually is the correct porosity value because pump testing is controlled by fracture flow. However, the groundwater travel time often is computed by dividing the flow path length by this velocity. This estimate potentially is a severe underestimate of the time required for a water molecule to migrate along the flow path. A more

accurate definition of travel time for predicting transport behavior takes into account matrix diffusion.

Several theoretical, laboratory, and field studies have demonstrated the validity of the matrix-diffusion model. As reviewed by CRWMS M&O (2000j), mathematical models were first used to demonstrate the likely effect of matrix diffusion and flow in fractured media. In these studies, transport was idealized as plug flow in the fracture with diffusion into the surrounding rock matrix. Experiments were performed of transport in natural fissures in granite, and it was concluded that matrix diffusion was necessary to model conservative tracer data. As reviewed by CRWMS M&O (2000j), the concept of matrix diffusion was extended to examine the coupling between matrix diffusion and channel flow usually thought to occur within natural fractures.

Transport models incorporating matrix-diffusion concepts also have been proposed to explain the often-conflicting groundwater ages obtained from carbon-14 data compared to ages predicted from flow data. Sudicky and Frind (1981) developed a model of flow in an aquifer with diffusion into a surrounding aquitard to show that the movement of carbon-14 can be much slower than predicted if only movement with the flowing water is considered. Maloszewski and Zuber (1985) reached a similar conclusion with a model for carbon-14 transport that consists of uniform flow through a network of equally spaced fractures with diffusion into the surrounding rock matrix between the joints. Their model also includes the effect of chemical exchange reactions in the matrix, which further slows the migration velocity. Maloszewski and Zuber (1985) also present analyses of several interwell tracer experiments that show that their matrix-diffusion model can be used to provide simulations of these tests that are consistent with the values of matrix porosity obtained in the laboratory and aperture values estimated from hydraulic tests. In all cases, the results are superior to previous analyses that did not include matrix diffusion effects. Finally, of greatest relevance to the SZ beneath Yucca Mountain is the C-wells reactive tracer test (Section 3.1.3.2), which demonstrated that models that incorporate matrix diffusion provide more reasonable fits to the tracer-experiment data than those that assume a single continuum. Maloszewski and Zuber (1985) demonstrated that a suite of tracers with different transport characteristics (e.g., different diffusion coefficients or sorption coefficients) produced breakthrough curves that can be explained using a diffusion model that assumes diffusion of tracers into stagnant or near-stagnant water.

Data from naturally occurring isotopes, such as carbon-14, provide valuable clues into the processes controlling transport in the SZ. However, these data sets are best used in the development of conceptual models rather than as observations used directly in formal calibration exercises. The reasons for this approach are twofold. First, there is considerable uncertainty in the conceptual model of SZ flow that gives rise to the data set. Waddell et al. (1984) observe that the hydrologic conditions that describe modern-day conditions, with recharge presumed to occur at higher elevations, probably is not correct for the climatic conditions during the Pleistocene Epoch. Yet many of the water ages in the SZ imply an origin of these fluids during the Pleistocene. Given that the chemical signature of the recharge fluid probably was different during the Pleistocene, and that more widespread recharge and discharge areas were present, the application of steady-state models to simulate the data may not be adequate.

Instead of using carbon-14 data as a calibration measurement, the ages are taken into account at the level of conceptual model development. The ages of SZ fluids are on the order of several thousand years or more. These old ages imply either that transport of carbon is slowed by matrix diffusion, or that advective porosity is much larger than is expected for a fractured media. This argument is consistent with the conceptual model of interchange of solutes between the fractures and matrix found in the matrix-diffusion model.

The fact that matrix diffusion appears to be consistent with the conceptual model does not imply that the fracture and matrix fluids must therefore be in chemical equilibrium at all locations in the SZ. The model is consistent with different chemical compositions in the fracture and matrix fluid. This situation would occur if the fracture spacing were sufficiently large that a solute traveling through fractures has insufficient time to diffuse fully within the matrix block between fractures. In reality, a spectrum of different transport regimes probably is present in the SZ, from fracture-dominated transport at some locations to complete equilibration between fracture and matrix fluids at other locations. The carbon-14 data constrain this possibly wide range of behavior by establishing that considerable communication between fractures and matrix is likely.

3.2.4.3 Sorption

Sorption reactions are chemical reactions that involve the distribution of chemical constituents between water and solid surfaces. Although these reactions can be complex in detail, they typically are represented in transport calculations by a constant called the sorption coefficient. Accurate prediction of the rate of transport of chemical constituents in a well-characterized flow system requires that three conditions are met concerning the sorption reactions: the reactions must be in equilibrium, instantaneous, and reversible.

In the case of the Yucca Mountain flow system, an important goal is the prediction of the maximum rate of transport of the mean concentrations of radionuclides. This allows the three conditions to be relaxed. For example, sorption reactions that are not fully reversible result in rates of transport that are slower than would be the case for fully reversible reactions. Therefore, for radionuclides that sorb nonreversibly, using a sorption coefficient would result in conservative predictions of transport rates.

If sorption reactions are not instantaneous for a given radionuclide, the possibility exists that the radionuclide could be transported at a faster rate than would be predicted by the use of a sorption coefficient in the transport calculations. The term instantaneous does not necessarily refer to an absolute rate but rather to a rate referenced to the flow rate. If the flow rate is slow relative to the sorption reaction rate, noninstantaneous sorption reactions need not be a problem. However, if the sorption reaction rate is slow relative to the flow rate, there could be a problem in prediction of the minimum breakthrough time. To address this possibility, the sorption coefficient distributions used in transport calculations have been biased downward for the radionuclides of interest that appear to have slow sorption kinetics (i.e., this assumes less sorption). In effect, the results of short-term experiments with these radionuclides were included in the distributions.

The issue of equilibrium in sorption reactions relates to reversibility and the rate of sorption reactions. Equilibrium can be considered in terms of the rates of the forward and backward reactions in an overall chemical reaction. At equilibrium, the forward and backward rates are

equal and the reaction is, by definition, reversible. A common occurrence in sorption reactions is the situation in which the forward reaction is relatively fast compared to the backward reaction. In this case, the reaction is not entirely reversible. Use of an equilibrium-based sorption coefficient in this case would lead to conservative predictions of transport rates. The case in which the forward reaction is slow and the backward reaction is fast also is possible. In this case, use of equilibrium-based sorption coefficients tends to predict rates of transport that are higher than expected. For the elements that show this sort of behavior, sorption coefficients based on short-term experiments, relative to the rate of flow in the aquifers, would have to be used. The database compiled by the YMP (CRWMS M&O 2000r, Table 2b) does not indicate any elements of interest with this type of behavior.

Sorption in Fractured Porous Media—Sorption of radionuclides on rock surfaces is a mechanism that will result in retardation. Radionuclide-rock interactions potentially can occur on the surfaces of fractures and within the rock matrix. This distinction is important because the surface-area to fluid-volume ratio and the mineral distributions probably are different in the fractures as compared to the matrix. Sorption on fracture surfaces is not included in total system performance assessment (TSPA) simulations of radionuclide transport. The lithium tracer in the C-wells reactive tracer experiment was modeled using a matrix-diffusion model with the sorption coefficient as an additional adjustable parameter (Section 3.1.3.2). The matrix sorption coefficient that fit the data agreed quite well with the value determined in laboratory sorption tests, thus providing an additional degree of confidence in the matrix-diffusion model. The fact that the early lithium response had the same timing as that of the nonsorbing tracers, but with a lower normalized peak concentration, is consistent with matrix diffusion coupled with sorption in the matrix.

Sorption in the Alluvium—In contrast to the fractured tuffs, there are no field-scale tracer transport tests in the alluvium south of Yucca Mountain to confirm the validity of the sorption coefficient data. However, the transport of sorbing solutes in porous media that is not controlled by fractures has been well studied (e.g., Freeze and Cherry 1979). Sorption coefficients onto alluvium from the Nye County wells have been measured for a few key radionuclides (CRWMS M&O 2000r). For the remaining radionuclides, sorption coefficients have been estimated based on the corresponding values measured for crushed tuff (CRWMS M&O 2000r).

3.2.4.4 Hydrodynamic Dispersion

Dispersion is caused by heterogeneities at all scales, from the scale of individual pore spaces to the scale of the thickness of individual strata and the length of structural features such as faults. The spreading and dilution of radionuclides that result from these heterogeneities could be important to performance of the potential repository. The largest heterogeneities are represented explicitly in the site-scale SZ flow and transport model, and other features are included in the HFM on which the model is built. For dispersion at smaller scales, it is assumed that the convective-dispersion model applies with dispersion characterized using an anisotropic dispersion coefficient tensor consisting of longitudinal, horizontal-transverse, and vertical-transverse dispersivities.

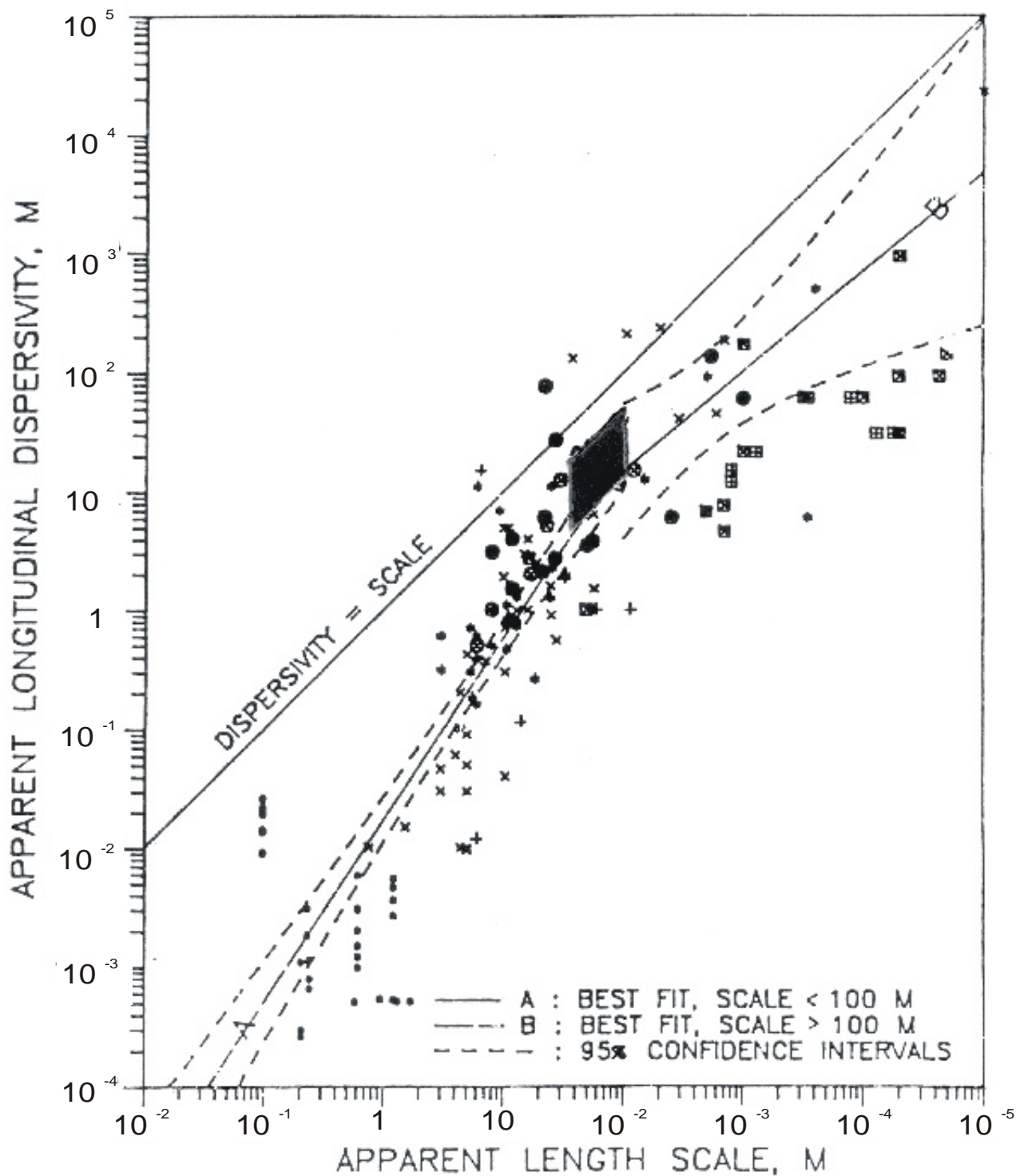
Field studies of transport and dispersion have been conducted at a variety of length scales (from meters to kilometers) to address the issue of dispersion (Figure 3-16). The results show a trend toward larger apparent dispersion coefficients for transport over longer distances. Solutes encounter larger-scale heterogeneities at larger scales, and thus, spreading is more pronounced. Also shown in Figure 3-16 is a black diamond representing the dispersivity determined for the C-wells reactive tracer experiment (Section 3.1.3.2). There is uncertainty in this estimate due to uncertainty in the exact flow paths taken by a tracer during the test. Nevertheless, the estimate falls within the range of values from other sites, suggesting that transport in the fractured tuffs exhibits similar dispersive characteristics. The values used in the simulations of radionuclide transport are somewhat higher than those estimated from the C-wells because of the larger scale that is relevant for radionuclide migration to the accessible environment. Little experimental information exists for assigning transverse dispersivity values.

An important caveat on the validity of dispersive transport models must be recognized when interpreting the results. When attempting to capture all dispersion mechanisms at scales smaller than the size of a typical grid cell with a simple dispersion model, certain features likely to be present are simulated as averages. For example, suppose the physical system has a localized, high-permeability pathway within the domain defined by a grid cell. This region may have high concentration within the pathway and lower concentrations in the rest of the domain. A continuum model averages these differences, and a single value of concentration is defined for the block. Concentration differences at scales smaller than the grid cell, if present, are not resolved.

Whether this distinction is important depends on specific performance criteria and scenarios for exposure to humans or plants. Because the site-scale SZ flow and transport model is used to predict concentrations under a well-withdrawal scenario, the potentially complex distribution of radionuclides within a grid block will be averaged in the process of extracting water from the aquifer.

3.2.4.5 Colloid Facilitated Transport

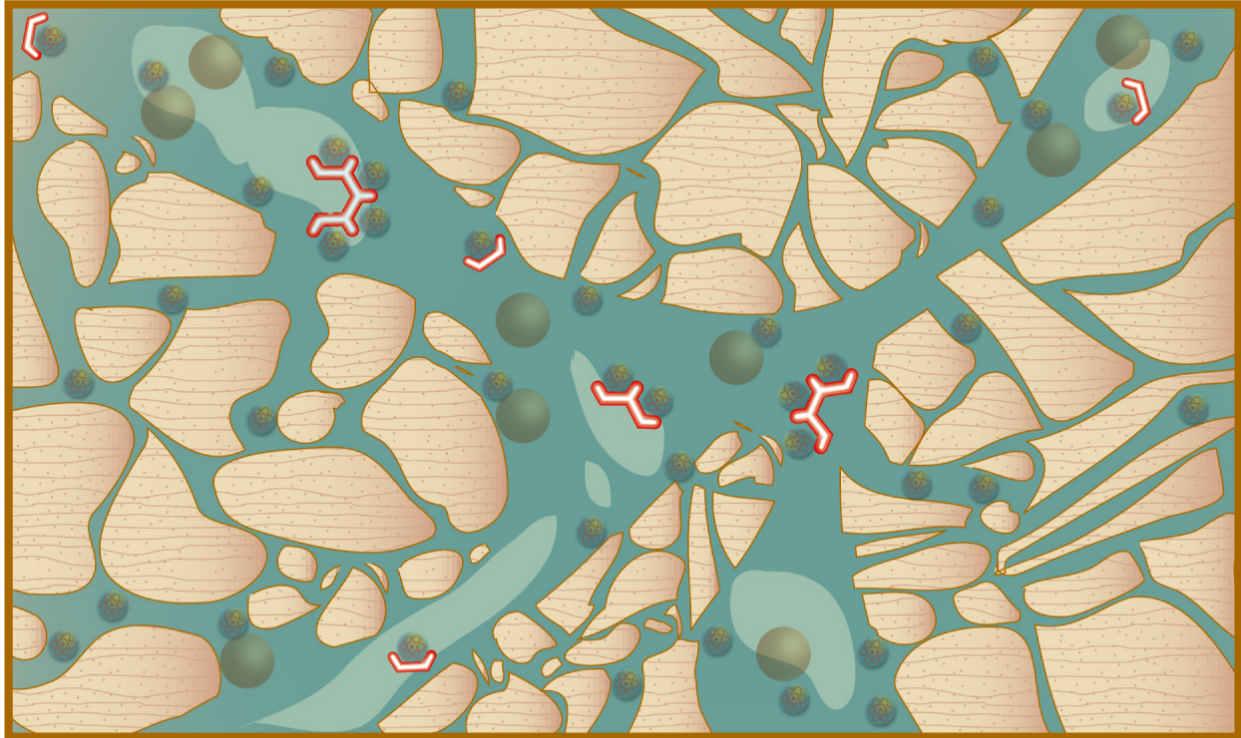
The conceptual model of colloid-facilitated transport of radionuclides in the SZ consists of two modes of transport (Figure 3-17). The first mode involves radionuclides that are irreversibly (permanently in the time frame of groundwater transport) sorbed onto or embedded in colloids. The second mode deals with radionuclides that are reversibly attached to colloids, such that at any time, radionuclides are partitioned between the aqueous and colloid phases.



Source: CRWMS M&O (2000r, Figure 100)

NOTE: The black diamond represents the dispersivity determined for the C-wells reactive tracer experiment.

Figure 3-16. Estimated Dispersivity as a Function of Length Scale



abq0063G031.ai

-  Radionuclide
-  Colloid: Reversible Sorption Type
-  Colloid: Irreversible Sorption Type
-  Radionuclide temporarily attached to colloid
-  Radionuclide permanently attached to colloid

Figure 3-17. Conceptual Model of Colloid-Facilitated Transport of Radionuclides

3.2.4.5.1 Radionuclides Reversibly Sorbed to Colloids

Radionuclides that are reversibly sorbed onto colloids reside in the aqueous phase and on the surfaces of colloids. Thus, the transport behavior of these radionuclides is governed by a combination of the transport characteristics of aqueous solutes and colloids. The conceptual model for this mode of colloid facilitated transport assumes equilibrium sorption of radionuclides on the colloids, and equilibrium sorption of the aqueous form of the radionuclide on the immobile rock surface. The colloids that form the substrate for the reversible sorption can be of any type, for example, natural colloids (typically clay or silica), waste form colloids resulting from degradation of spent fuel or glass, and iron oxyhydroxide colloids resulting from degradation of the waste container.

For TSPA-Site Recommendation (TSPA-SR), radionuclides that are reversibly sorbed onto colloids are modeled using a distribution coefficient that represents the equilibrium partitioning of radionuclides between the aqueous phase and the colloidal phase (CRWMS M&O 1997, Equation 8-10, p. 8-35). The distribution coefficient is assumed to be a function of radionuclide sorption properties, colloid substrate properties, aqueous chemistry, and colloid concentration, and not any properties of the immobile media through which transport occurs; thus, to a first approximation, the same distribution coefficient applies to transport of a radionuclide in the volcanic units and the alluvium.

In theory, a unique distribution coefficient probably exists for each radionuclide sorbing onto the colloidal material. However, except for a few radionuclides, these data are unavailable. Therefore, for TSPA-SR, the sorption coefficient for americium onto waste form colloids (CRWMS M&O 2000f) is assumed to represent a conservative bound on colloid transport for all radionuclides transported via this mechanism. Selecting a strongly sorbing radionuclide should lead to shorter transport times than if actual sorption coefficients were available. CRWMS M&O (2000o) present the cumulative probability density function used in the SZ site scale flow and transport TSPA-SR calculations.

3.2.4.5.2 Colloid Attachment and Detachment in Fractured Tuffs

As discussed in Section 3.1.4.3, it generally is accepted that colloids are capable of facilitating radionuclide transport over long distances in the SZ only if two conditions are met. First, a large percentage of the colloids must not irreversibly mechanically-filter or attach to rock surfaces; and second, the desorption rate of radionuclides from the colloids must be slow (i.e., radionuclides are actually impregnated in the colloids or are strongly sorbed to colloid surfaces). The first condition was addressed using polystyrene microspheres in the C-wells tracer tests. The second condition has been addressed by conducting laboratory sorption experiments to determine magnitudes and rates of sorption and desorption of long-lived radionuclides on different types of colloids that may be present in the near-field or the far-field environments at Yucca Mountain. These experiments have shown that plutonium-239 desorption rates from hematite colloids (near-field) are so slow that it is not possible to measure them, and desorption rates from goethite and montmorillonite colloids also are slow. Because of these observations, and the fact that there are large uncertainties due to the sparseness of the experimental data, the YMP has adopted the conservative position of assuming that a fraction of the mass of long-lived radionuclides (most notably plutonium-239 and americium) will be irreversibly sorbed to colloids. Consequently, the current conceptual model for colloid-facilitated transport in the SZ focuses on colloid attachment and detachment processes as the primary mechanisms for attenuating the transport of radionuclides irreversibly sorbed to colloids.

The conceptual model for colloid-facilitated transport of irreversibly attached radionuclides in saturated fractured tuffs includes two key elements:

- Colloids will move exclusively through fractures with negligible matrix diffusion because of their large size and low diffusivity relative to solutes.
- Colloid attachment and detachment to fracture surfaces can be described by first-order rate expressions.

Mathematically, the conceptual model is summarized by two equations (CRWMS M&O 2000I). These equations were used to fit the microsphere responses in the C-wells tracer tests, thus providing estimates of colloid attachment and detachment rate constants. In the fitting procedure, it was assumed that the spheres had the same mean residence times and dispersion coefficients as the solute tracers that were injected with them, so the rate constants were the only adjustable parameters. Details of the procedure for obtaining the rate constants are presented by CRWMS M&O (2000I).

Based on the estimated rate constants and the range of transport times being considered for transport through saturated fractured tuffs, it was shown (CRWMS M&O 2000I) that the local equilibrium assumption is valid for all but the shortest transport times, and it is conservative for the shortest transport times. Thus, transport is sufficiently long that assuming local equilibrium between mobile and attached colloids yields the same results as assuming that colloid attachment and detachment are kinetic processes.

The distribution, defined by the cumulative probability density function, will be sampled randomly to obtain retardation factors to be used in PA calculations of colloid transport in the SZ. The retardation factor will be one of many parameters that are sampled randomly for a large number of simulations that collectively will yield probability distributions for radionuclide transport through the SZ. Because radionuclides are assumed to be irreversibly sorbed to colloids, colloid-facilitated radionuclide transport in these simulations effectively will be the product of colloid transport and the mass loading of radionuclides assumed to be associated with the colloids.

3.2.4.5.3 Colloid Attachment and Detachment in the Alluvium

The conceptual model for colloid-facilitated transport in the alluvium is essentially the same as in fractured tuffs in that colloids are assumed to transport only in advective water (no diffusion into stagnant water or into grains), and colloid attachment and detachment onto alluvial surfaces are described by first-order rate expressions. Because no site-specific data for colloid transport in the alluvium are available, filtration theory and literature data are used to obtain distributions or bounds for attachment and detachment rate constants. Details of the analyses and references to the original data are presented by CRWMS M&O (2000I).

As in the case of colloid transport in fractured tuffs, it was shown (CRWMS M&O 2000I) that, for the distributions of alluvium rate constants, the local equilibrium assumption will be valid for all but the shortest transport times, and it will be conservative for the shortest transport times.

A probability density function for the retardation factor in the alluvium was constructed by randomly sampling the assumed distributions of parameters to generate a large number of potential retardation values.

3.2.5 Alternative Conceptual Models

Luckey et al. (1996, p. 52) reviewed the major conceptual uncertainties relating to the SZ flow system at Yucca Mountain. They identified the following major areas of uncertainty:

- Whether the flow system can be simulated as a porous medium or if discrete features needs to be simulated
- Uncertainty about the behavior of the flow system in the areas of the large hydraulic gradient and the moderate hydraulic gradient (Section 3.2.4.1)
- Uncertainty about recharge and the time-scale at which it comes into equilibrium with climate (Section 3.2.4.2)
- How best to translate data from field sampling and borehole testing to the scale of the flow models.

The issue of whether the flow system can be simulated as an effective continuum model is addressed in CRWMS M&O (2000n), which notes that the site-scale SZ flow and transport model uses the effective continuum representation of fracture permeability. While it is recognized that the alternative discrete fractures approach retains the discrete nature of the fractures observed in the resulting model, the present data relating to the hydrologic properties of discrete fractures are limited and are not sufficient for a viable modeling effort. Additionally, the scale of this SZ flow and transport model is discussed in Section 3.5.1.

Although the site-scale SZ flow and transport model is an effective continuum model, special hydrologic features, including selected major faults, fault zones, and zones of chemical alteration, are treated in the model as zones of enhanced or reduced permeability (CRWMS M&O 2000n, Table 6).

The issue of translation of data from field sampling scale to flow-model scale remains problematic. Extensive hydraulic testing at the C-wells Complex indicates that much higher permeabilities were obtained from multi-well testing than from earlier single-hole testing at the same wells (Luckey et al. 1996, pp. 36 to 37). This casts doubt on the quantitative importance of the single-hole test results (Luckey et al. 1996, pp. 53 to 54); however, most of the data on permeability at Yucca Mountain are from single-hole tests. Chemical tracer tests (Section 3.1.3.2) augment the data from the C-wells Complex and Busted Butte (Section 3.1.3.2.2), but additional data on the hydraulic properties of the SZ are needed, particularly in the area between Yucca Mountain and Amargosa Valley (CRWMS M&O 1998b, Table 3-2).

3.2.5.1 Large Hydraulic Gradient

Luckey et al. (1996) present detailed descriptions of the gradient features and discuss interpretations of their causes (Section 3.2.2.3). The large hydraulic gradient particularly has been the subject of numerous theories.

An expert elicitation panel on SZ flow and transport convened by DOE addressed the issue of the cause of the large hydraulic gradient and other issues (CRWMS M&O 1998b, pp. 3-5 to 3-6). The panel narrowed the theories to the two most credible hypotheses: the large hydraulic gradient is caused by flow through the upper volcanic confining unit or it is semi-perched water. The consensus of the panel slightly favored semi-perched water. The experts were in agreement that the issue was mainly one of technical credibility, that the probability of any large transient change in the configuration of the large gradient is low, and that long-term transient readjustment of gradients was of low probability (CRWMS M&O 1998b, p. 4-3).

The only important new results pertaining to the cause of the large gradient include the drilling of borehole WT-24 in the area of the large gradient and the analysis of hydrochemical data by CRWMS M&O (2000m).

Borehole WT-24 reportedly encountered a perched-water zone at 987-m (3,240-ft) elevation, then encountered unsaturated conditions to about 734-m (2,410-ft) elevation, where a water-bearing fracture was encountered. At that point, water levels in the borehole rose to an elevation of about 840 m (2,760 ft) and remained at about that level as the borehole was deepened to an elevation of 630 m (2,070 ft). The 840-m (2,760-ft) elevation, therefore, represents the potentiometric level for the fracture encountered at 734 m (2,410 ft), not another perched zone, because unsaturated conditions were present from 987 m (3,240 ft) to 734 m (2,410 ft). The borehole currently is not deep enough to test conclusively whether the small hydraulic gradient extends that far north (CRWMS M&O 2000w).

With respect to the cause of the large hydraulic gradient, the drilling of borehole WT-24 demonstrated that the previous portrayal of the large gradient (Tucci and Burkhardt 1995, Figure 4) probably included perched water; however, the question of whether perching of water is the cause of the large gradient was not fully resolved.

CRWMS M&O (2000n, Table 6) treats the large hydraulic gradient area as a linear east-west barrier or zone of reduced permeability in the site-scale SZ flow and transport model. In plots of predicted particle flow paths (CRWMS M&O 2000n, Figures 10 to 12), particles are shown detouring around the barrier to the east and west.

3.2.5.2 Perched Water

Hydrochemical information on the ratio of uranium-234 to uranium-238 presented by CRWMS M&O (2000m, Section 6.5.3) suggests that local recharge, as represented by perched water, is a major component in the groundwater at Yucca Mountain. The best estimate of the time of recharge (based on carbon-14 ages of groundwater in the SZ at Yucca Mountain) range of about 14,000 to 8,000 yrs, that is, during late Pleistocene to early Holocene time. The best estimate for the age of the perched water (based on carbon-14 data that are uncorrected for potential interaction between groundwater and carbonate minerals) suggest recharge between 7,000 and 11,000 yrs, although dates as young as 3,300 yrs were noted in a sample from borehole NRG-7a, and in one of several samples from borehole UZ-14 (CRWMS M&O 2000m, Section 6.5). Taken together, these data suggest that the SZ water at Yucca Mountain originated mainly from local recharge via perched water zones during late Pleistocene-early Holocene time, and that throughflow under the current climate is minimal. The proportion of recharge that arrives at the

water table via faults and fractures versus that which arrives via flow through the matrix beneath the perched zones has not been quantified, but the chemical resemblance of SZ water to perched water suggests that matrix flow is minimal. The weight of the hydrochemical evidence suggests that throughflows from the large hydraulic gradient to the north of Yucca Mountain, and that from the moderate hydraulic gradient to the west toward the area of the small hydraulic gradient extending from Yucca Mountain to Fortymile Wash, are minimal under the current climatic regime.

Perched water was encountered in six boreholes near the potential repository (CRWMS M&O 1998a, p. 5.3-162). The contact zone between the Topopah Spring welded and Calico Hills nonwelded hydrogeologic units is characterized by a basal vitrophyre stratum in the Topopah Spring welded hydrogeologic unit above a zone of zeolitic altered tuffs in the Calico Hills nonwelded hydrogeologic unit. For a perched zone to exist, the vertical permeability of the perching units would have to be low (less than 1 microdarcy) and fracture permeability would have to be negligible.

The perched water bodies that have been encountered were below the potential repository horizon (CRWMS M&O 1998a, p. 5.3-162). Perched water has been encountered at the base of the Topopah Spring welded hydrogeologic unit or in the top of the underlying nonwelded to partially welded tuffs of the Calico Hills nonwelded hydrogeologic unit in several dry-drilled boreholes that penetrated the contact zone between the Topopah Spring welded and the Calico Hills nonwelded hydrogeologic units. The occurrence and modeling of perched water is discussed in CRWMS M&O (2000b, Section 3.7).

The chemical character of the perched water encountered in the six boreholes is distinctly different from matrix pore waters from the same depth interval, and the isotopic character distinguishes the perched water from the deeper groundwater of the SZ. Generally, the perched waters have moderate concentrations of sodium bicarbonate, and are similar to the SZ waters. The pore waters typically have higher concentrations of sodium bicarbonate, and also are higher in chloride content than the perched waters.

The age of the perched water has been dated by carbon-14 analysis. Recharge is estimated to have occurred between about 7,000 and 11,000 yrs before present, which is younger than could be accounted for by matrix flow. The stable isotope composition (deuterium and oxygen-18) is consistent with little or no evaporation and post-Pleistocene ages. The deuterium/oxygen-18 composition of the perched water is at the heavy (i.e., less negative values) end of the range of values found in SZ waters. This suggests SZ waters in the Yucca Mountain region infiltrated under somewhat colder conditions than the perched waters within Yucca Mountain. If SZ groundwaters and perched waters infiltrated over approximately the same time interval, the difference in oxygen-18 and deuterium ratios could reflect upgradient recharge of SZ groundwaters at elevations that were higher than the surface of Yucca Mountain. Alternatively, the carbon-14 ages for SZ groundwaters may have been overcorrected and these groundwaters actually are older than the perched waters. The deuterium and oxygen-18 data could be explained if the SZ groundwaters were only a few thousand years older than the perched waters (i.e., latest Pleistocene in age).

Analysis of tritium in perched waters indicates that, if present, tritium in most groundwater samples is below the detection level of 4 tritium units, which indicates that if water affected by a nuclear bomb test has reached the perched water bodies, the amount is statistically insignificant in these samples. Only one perched-water sample contained tritium (10 TU) above the detection level (Yang et al. 1996, p. 34). This sample may have a component of post-bomb infiltration.

The importance of perched water bodies with regard to their implications for the movement of water within the UZ is discussed by CRWMS M&O (2000b). However, on the basis of chlorine-36 and oxygen-18 data, CRWMS M&O (2000m) tentatively conclude that uncorrected carbon-14 ages approximate the true carbon-14 ages, that is, they generally are between 7,000 and 11,000 yrs before present (CRWMS M&O 2000m, Section 6.5.4.2.2). In either case, these dates suggest that recharge episodes occurred several thousand years ago and that there is no evidence of a large amount of recharge under current climatic conditions.

3.2.5.3 Horizontal Anisotropy

Anisotropic conditions exist if the permeability of media varies as a function of direction. Because groundwater primarily flows in fractures within the volcanic units downgradient of Yucca Mountain, and because fractures and faults occur in preferred orientations, it is possible that anisotropic conditions of horizontal permeability exist along the pathway of potential radionuclide migration in the SZ. Performance of the potential repository could be affected by horizontal anisotropy because the flow could be diverted to the south, causing transported solutes to remain in the fractured volcanic tuff for longer distances before moving into the valley fill alluvial aquifer. A reduction in the length of the flow path in the alluvium would decrease the amount of radionuclide retardation that could occur for those radionuclides with greater sorption coefficients in alluvium than in fractured volcanic rock matrix. In addition, potentially limited matrix diffusion in the fractured volcanic units could lead to shorter transport in the volcanic units relative to the alluvium.

A conceptual model of horizontal anisotropy in the tuff aquifer is reasonable, given that flow in the tuff aquifer is believed to occur in a fracture network that exhibits a preferential north-south strike azimuth (CRWMS M&O 2000i). Major faults near Yucca Mountain that have been mapped at the surface also have a similar preferential orientation (Figure 3-4). In addition, north to north-northeast striking structural features are optimally oriented perpendicular to the direction of least principal horizontal compressive stress, suggesting a tendency toward dilation and potentially higher permeability (Ferrill et al. 1999, p. 5).

Evaluation of the long-term pumping tests at the C-wells Complex supports the conclusion that large-scale horizontal anisotropy of aquifer permeability may occur in the SZ (Ferrill et al. 1999, p. 7). Results of this hydrologic evaluation generally are consistent with the structural analysis of potential anisotropy. However, there are important uncertainties, including differences in pumping test analysis methods, the fact that only a minimum number of observation wells were used, and the additional uncertainty regarding the validity of assuming a homogenous effective continuum over the scale of the test (Winterle and La Femina 1999, p. 4-29).

Taken together, these observations and inferences support an alternative conceptual model in which large-scale horizontal anisotropy of permeability, with higher permeability in a north-

northeasterly direction, occurs in the volcanic units of the SZ to the southeast of the potential repository. Sufficient uncertainty exists in this interpretation to warrant retention of the simpler, horizontal isotropic model of permeability as the nominal conceptual model. Anisotropy is used in the TSPA calculations.

3.2.6 Changes in the Saturated Zone Flow System

In this section, factors that change the fluid flow path, flux magnitude, or water table position are considered. Changes in the SZ flow system may be brought about by climate changes, changes in the permeability field due to tectonic or volcanic events, or changes in the water table and hydraulic gradient due to increased pumpage. Changes to the SZ flow system due to climate change are likely in the next 10,000-yr period, and climate change is included in the base case model for the TSPA-VA. Large changes in the permeability field or changes in the water table and gradient due to tectonic and seismic events are considered in the features, events, and processes (FEPs) and uncertainty modeling. It is assumed that pumpage does not cause a significant change in the water table and does not change the hydraulic gradient.

Future climate is likely to change the SZ flow conditions (USGS 2000c). In particular, the amount of precipitation is important because it largely determines the amount of infiltration. Forecasting future climate (i.e., using future climate scenarios), rather than modeling future climate, was used because climate modeling, among many complications, requires knowledge of the future climate boundary conditions (e.g., wind speed, water vapor flux, and heat flux) for input to a model. These boundary conditions cannot accurately be predicted at present. Forecasts of future climates for the next 10,000 yrs are described in USGS (2000c). Some discussion is presented here on climate forecasts to about 400,000 yrs. The principle assumptions concerning future climate change are:

- Climate is cyclical, so past climates provide insight into potential future climates.
- A relationship exists between the timing of long-term past climate change (glacial and interglacial cycles) and the timing of changes in certain earth-orbital parameters. This relation establishes a millennial-scale climate-change clock that provides a way to predict the timing of future climate changes.
- A relationship exists between the characteristics of past climates and the sequence of those climates in the long earth-orbital cycle (approximately 400,000 yrs in length). The characteristics of past glacial and interglacial climates within the long earth-orbital cycle differ from each other, but they appear to differ systematically. This climate-sequence relation provides a defensible criterion for the selection of a particular past climate as an analog for a future climate.
- Long-term earth-based climate-forcing functions, primarily tectonics, that operate on the million-year time scale have remained relatively unchanged during the last long earth climate cycle and will remain relatively unchanged during the next 10,000 yrs. If changes due to the climate-forcing functions are ignored, then climate may be forecasted as cyclical with a period of approximately 400,000 yrs. The potential impact of long-

term earth-based forcing functions on climate may need to be considered for understanding climate change to one million years.

Climate proxies, or the physical remains of substances that carry the imprint of past climates, indicate that the climate in the Yucca Mountain region is not static. In the Yucca Mountain area, climate proxies are provided by the delta oxygen-18 isotopic composition of groundwater and by the Owens Lake climate record. The delta oxygen-18 isotopic composition of groundwater near Yucca Mountain is linked to the delta oxygen-18 isotopic composition and temperature at its source (i.e., the Pacific Ocean), the path taken from the source to the recharge area, precipitation losses, and the temperature at which the precipitation forms.

Climate changes may be inferred from the ancient delta oxygen-18 isotopic composition of groundwater as recorded in calcite deposits in Devils Hole, a spring located approximately 40 km (25 mi) southeast of Yucca Mountain near Ash Meadows. Devils Hole provides a record of climate change over the past 425,000 yrs. The record shows continual variation, often with rapid jumps, between cold glacial climates and warm interglacial climates that are similar to present conditions. The fluctuations average about 100,000 yrs in length. The relationship between variations in the delta oxygen-18 isotopic composition of groundwater and the precession (in degrees) of the earth is presented by USGS (2000c). A 100,000-yr component is evident in both data sets.

The Owens Lake climate record is used to describe climate conditions at Yucca Mountain based on inferences from plant and animal fossils. Sediments deposited in Owens Lake, north of Death Valley and west of Yucca Mountain, hold remains of ostracode and diatom species that now occur in Canada. The presence (cool and wet) or absence (warm and dry) of these species implies climate changes during the past 400,000 yrs. Uncertainty in the rate of sediment deposition in Owens Lake requires calibration of the time record. The reconstruction of past climate from this lake was calibrated from modern climatological data and plant macrofossils obtained from packrat middens (deposits consisting of plant macrofossils cemented by packrat urine that can be dated by radiocarbon methods).

The four assumptions above, plus the Devils Hole delta oxygen-18 isotopic record and the Owens Lake fossil deposits, establish a defensible means for assuming periodicity in climate forecasting.

The climate in the Yucca Mountain region during the last 10,000 yrs generally has been warming and drying, and presently it is warm and semiarid, with a mean annual temperature of 16°C (61°F) and mean annual precipitation of about 170 mm/yr (6.7 in./yr). Climate forecasts for the next 10,000 yrs at Yucca Mountain suggest that the modern-day climate should persist for 400 to 600 yrs, followed by a warmer and wetter monsoon climate for the next 900 to 1,400 yrs, followed by a cooler and wetter glacial-transition climate for the next 8,000 to 8,700 yrs. The range of ages represents uncertainty in the sediment accumulation rates in Owens Lake. The upper and lower bounds for each climate are described from what are believed to be meteorological stations representative of the forecasted climates. For sites potentially representing the average upper bound of the monsoonal climate, Nogales (south-central Arizona) and Hobbs (southeast New Mexico) were chosen. For the average lower bound of the monsoonal climate, Yucca Mountain was chosen. Three sites in eastern Washington were

chosen as sites potentially representing the average upper bound of the glacial climate, while the average lower bound was represented by Beowawe (north-central Nevada) and Delta (central Utah).

USGS (2000c) did not forecast climate farther than 10,000 yrs into the future, however, they did present Owens Lake data for the previous 400,000 yrs, and these data can be used to make forecasts longer than 10,000 yrs. USGS (2000c) also did not include the potential effects of anthropogenically-induced global climate change. This was because in a forecast taking into account a doubling of carbon dioxide from anthropogenic sources, D'Agnese et al. (1999) found that groundwater recharge was reduced relative to the USGS (2000c) model. Therefore, models that considered the effects of anthropogenically-induced global climate change would be less conservative than the present forecasts (USGS 2000c).

3.2.6.1 Changes in Water Table Elevation

Climate changes induce changes in the water table, groundwater flux, and recharge and discharge. An increase in the elevation of the water table under Yucca mountain is important because it decreases the UZ barrier between the potential repository and the SZ, and also because it may increase the hydraulic gradient resulting in shorter radionuclide transport in the SZ. An increase in the water table also may change the direction of the transport flow path, although change in the flow path direction is unlikely (D'Agnese et al. 1999).

A higher water table is expected to result from future climate changes (USGS 2000c). Regional-scale flow modeling, considering the full glacial climate forecast (D'Agnese et al. 1999), predicted a rise in the water table of 100 to 200 m (328 to 656 ft), depending on the assumed drain conductance of springs in the area. Geochemical studies (CRWMS M&O 1998e) provide evidence based on analysis of strontium isotopes in the UZ that the water table was about 60 m to 85 m (197 to 279 ft) higher in the past than at present. This higher water table appears associated with wetter climate conditions. Based on a mineralogic analysis of the distribution of vitric and zeolitized tuffs and the structural history of the site, CRWMS M&O (1998e) concluded that the water level has not risen more than 60 m (197 ft) above its present position. Based on the D'Agnese et al. (1999) analysis, changes in the water table elevation due to future climate changes are modeled as an increase in fluid flux along the transport path.

Other factors may cause water table changes at Yucca Mountain. Possible disruptive geologic (tectonic or volcanic) conditions may result in an increase or a decrease in the water table beneath Yucca Mountain. Transient fluctuations on the order of a few decimeters have been observed in response to barometric variations and earth tides and changes on the order of a few decimeters to a few meters have been observed following earthquakes (CRWMS M&O 1998e). Most modeling scenarios involving earthquakes or volcanic intrusions (Section 2.3) show that the maximum increase in the elevation of the water table resulting from these events is expected to be on the order of a few decimeters to perhaps 20 m (66 ft). A scenario (Ahola and Sagar 1992) involving a three-order of magnitude increase in hydraulic conductivity in the area north and northeast of Yucca Mountain (where a large hydraulic gradient exists), resulted in increases (up to 275 m [902 ft]) in the water table below Yucca Mountain. However, modeling of this scenario was not performed to show under what tectonic or volcanic conditions such an increase in conductivity could occur.

Not all investigators are in agreement concerning the hypothesis of continuous unsaturated conditions at Yucca Mountain during past epochs. Szymanski (1989) postulated and modeled possible rises in the water table due to tectonic activity. A study of fluid inclusions in calcite/opal deposits located at and near faults at Yucca Mountain by Hill et al. (1995) showed evidence of past ingress of hypogene waters of elevated temperature into the potential repository horizon. Hill et al. (1995) suggest that upwelling of waters below the potential repository as a possible source of the inclusions. Stuckless et al. (1998), however, point out a number of errors and cite other sources of evidence to arrive at the contrary conclusion that the source of waters in the inclusions was more likely infiltration through overlying soil and rock. The National Academy of Sciences also reviewed this issue and concluded that “none of the evidence cited as proof of ground-water upwelling in and around Yucca Mountain could reasonably be attributed to that process” (National Research Council 1992, p. 3). Possible scenarios in which the water table rises to saturate the potential repository have been excluded from consideration in TSPA analyses as indicated in Section 1.3, but they are discussed further in Section 3.8.1.

The 3-D site-scale SZ flow simulator assumes confined conditions within the SZ. Changes in water level are modeled by increasing the hydraulic gradient and reducing the thickness of the UZ (Section 3.3.5).

3.2.6.2 Changes in Groundwater Flux

Climate change in the TSPA-VA is modeled by increasing the groundwater flux along the transport flow path (Section 3.6.3.3.3), and an increase in solute flux is computed analytically from the increased groundwater flux. The effects of climate change on the transport of radionuclides in the SZ are incorporated in TSPA calculations by scaling the radionuclide mass breakthrough curves simulated for present climatic conditions and assumes a proportional scaling of groundwater flux in the entire SZ system in response to future wetter climatic conditions.

3.2.6.3 Changes in Recharge and Discharge

Regional discharge estimates under present and glacial-transition climate conditions have been computed by D’Agnese et al. (1997, 1999). Flow during glacial-transition climate conditions reversed at some areas such as the boundary near Pahrangat Lakes. The playa region of Death Valley becomes a lake (i.e., Lake Manly reappears) under glacial-transition climate conditions. In many low-lying areas of the central Death Valley subregion, water was shown to discharge because the simulated water table exceeded the land surface elevation. Potential discharge areas close to Yucca Mountain were examined. Drains located in the northern portion of Fortymile Wash did not discharge, however water did discharge from drains in the southern portion of Fortymile Wash where it flowed into the Amargosa River. Drains at the southern end of Crater Flat did not discharge; however, the water table was close to the land surface in this area. D’Agnese et al. (1997) assumed no well pumpage in these simulations because they were comparing future conditions to past glacial-transition climate conditions.

3.3 MATHEMATICAL AND NUMERICAL MODELING APPROACH

The mathematical and numerical modeling approach used to implement the conceptual model of flow and transport (Section 3.2) is presented below. In the first part of the section, the development of the mathematical models is presented, and this is followed by a discussion of the numerical methods used to implement these mathematical models. Then a discussion of the development of the site-scale SZ flow and transport model, the calibration of the model, and a summary of the calibration results is presented. Finally, a discussion of the sensitivity of the flow model is provided. Assumptions, uses, and limits of the site-scale SZ flow and transport model are discussed in Section 3.5.

3.3.1 Mathematical Model of Groundwater Flow

An effective continuum approach is adopted for simulating groundwater flow through the fractured rock and alluvial materials within the domain of the site-scale SZ flow and transport model (Figure 2-1). Based on this conceptualization, the equations governing groundwater flow can be derived by combining the equations describing the conservation of mass and Darcy's Law. The conservation of mass is described by

$$\frac{\partial A_{mass}}{\partial t} + \nabla \cdot \bar{f}_{mass} + q_{mass} = 0, \quad (\text{Eq. 3-1})$$

where A_{mass} is the fluid mass per unit volume given by $A_{mass} = \mathbf{f}\mathbf{r}$, \bar{f}_{mass} is the fluid mass flux given by $\bar{f}_{mass} = \mathbf{r}\bar{\mathbf{v}}$, \mathbf{f} is the porosity in the system [dimensionless], \mathbf{r} is the fluid density [M/L³], $\bar{\mathbf{v}}$ is the fluid velocity [L/T], t is the time [T], and q_{mass} is the fluid mass source.

The velocity of the fluid can be expressed by Darcy's Law:

$$\bar{\mathbf{v}} = -\frac{k}{\mu} \nabla (P - \mathbf{r}\mathbf{g}), \quad (\text{Eq. 3-2})$$

where P is pressure [MT²/L²], μ is the dynamic viscosity of the fluid [M/LT], k is the permeability [L/T], and \mathbf{g} is the acceleration resulting from gravity [L/T²].

Equations 3-1 and 3-2 can be combined to yield:

$$\frac{\partial A_{mass}}{\partial t} - \nabla \cdot \left(\frac{\mathbf{r}k}{\mu} \nabla (P - \mathbf{r}\mathbf{g}) \right) + q_{mass} = 0, \quad (\text{Eq. 3-3})$$

which is the fundamental equation describing groundwater flow. Groundwater flow is simulated in the site-scale SZ flow and transport model by obtaining a numerical solution to this equation. A more detailed discussion of the mathematical model used for describing groundwater flow is provided by CRWMS M&O (2000n, Section 6.5).

3.3.2 Mathematical Model of Radionuclide Transport

During development of the SZ conceptual model, a number of processes that affect solute transport were identified (Section 3.2.4). These processes include advection, dispersion, matrix diffusion, sorption, and colloid-facilitated transport. The mathematical models developed for describing these processes are presented below.

3.3.2.1 Advective-Dispersion Equation

As described by CRWMS M&O (2000j), the fundamental mass transport equation for transport of a nonreactive, dilute species in a saturated porous medium (with no sources or sinks) has the form

$$\frac{\partial C}{\partial t} + \nabla \cdot (\bar{v}C) - \nabla \cdot (D\nabla C) = 0 \quad (\text{Eq. 3-4})$$

where C denotes the solute concentration in units of moles per liter, \bar{v} designates the solute average pore-water velocity vector [L/T], and D denotes the dispersion tensor [L²/T].

For an isotropic medium, dispersion has the form

$$D_{ij} = \mathbf{a}_T v \mathbf{d}_{ij} + (\mathbf{a}_L - \mathbf{a}_T) \frac{v_i v_j}{v} + D_0 \mathbf{d}_{ij} \quad (\text{Eq. 3-5})$$

where \mathbf{a}_L and \mathbf{a}_T denote the longitudinal and transverse dispersivities [L], respectively, D_0 represents the molecular diffusion constant [L²/T], and \mathbf{n} is equivalent to $|\bar{v}|$, the magnitude of the velocity vector [L/T].

Using a Cartesian coordinate system, the dispersion tensor given in Equation 3-5 can be written as a nine element (3 by 3) numerical matrix. However, in an anisotropic system, the expression for the dispersion tensor is more complex, involving as many as 36 independent parameters. However, a simplified form is adopted for simulating solute transport in the site-scale SZ flow and transport model. This representation of the dispersion tensor uses three parameters: longitudinal (\mathbf{a}_L), transverse horizontal (\mathbf{a}_T^H), and transverse vertical (\mathbf{a}_T^V) dispersivities. This formulation of the dispersion tensor was chosen because of its relative simplicity and correspondence to the primary terms normally estimated in field studies.

This formulation of the dispersion tensor can be written as a nine element (3 by 3) numerical matrix. The off-diagonal terms of the dispersion tensor are important because they ensure proper treatment of dispersion parallel and perpendicular to the direction of flow when flow is not parallel to any of the coordinate axes. A detailed discussion of the mathematical formulation of the advective-dispersion equation, including the formulation of the dispersion tensor, is provided by CRWMS M&O (2000j, Section 6.1).

3.3.2.2 Matrix Diffusion

As described by CRWMS M&O (2000j), the conceptual model developed for simulating transport in the site-scale SZ flow and transport model includes the diffusion of radionuclides into the matrix of fractured rocks (Section 3.2.4.2). An analytical solution is used to incorporate the effect of matrix diffusion into the site-scale SZ flow and transport model. This analytical solution describes transient contaminant transport in equally spaced parallel fractures. The model upon which the solution is based takes into account advective transport in the fractures, molecular diffusion from the fracture to the porous matrix, adsorption on the fracture face, and adsorption within the matrix. Although the analytical solution provides for incorporating adsorption on the fracture face, this option is not used in the model due to the lack of conclusive information on this process and the anticipated small impact of this option on the radionuclide transport simulations. The model uses a no-flux condition at the mid-point of the rock matrix between fractures. The analytical solution requires the definition of a number of specific parameters, including fracture aperture, mean fracture spacing, linear groundwater velocity within the fracture, porosity of the rock matrix, retardation factors in the rock matrix and in the fracture, and the effective matrix diffusion coefficient. Based on the values specified for these parameters, this analytical solution can be used to identify the distribution of contaminants along the fracture at any point in time. A detailed discussion of the analytical solution used to incorporate matrix diffusion into the transport model is provided in CRWMS M&O (2000j, Section 6.2).

3.3.2.3 Sorption

Sorption is incorporated into the site-scale SZ flow and transport model using a linear isotherm model (Section 3.2.4.3). Based on the linear isotherm model, the distribution coefficient, K_d , is defined as the ratio of the mass of solute on the solid phase per unit mass of solid phase to the concentration of solute in solution. Using the distribution coefficient, the effect of sorption may be incorporated into the advection-dispersion equation (Equation 3-4) to obtain

$$\frac{\partial C}{\partial t} + \nabla \cdot (D \nabla C) + \frac{\mathbf{r}_b}{n} K_d \frac{\partial C}{\partial t} = 0 \quad (\text{Eq. 3-6})$$

where \mathbf{r}_b is the bulk mass density [M/L^3] and n is the matrix porosity [dimensionless].

Equation 3-6 may be rearranged into a more familiar form by defining a retardation factor, $R = 1 + (\mathbf{r}_b/n)(K_d)$, to obtain

$$R \frac{\partial C}{\partial t} + \nabla \cdot (\bar{\mathbf{n}} C) - \nabla \cdot (D \nabla C) = 0. \quad (\text{Eq. 3-7})$$

Based on Equation 3-7, the retardation coefficient may be applied to the velocity and dispersion terms to effectively account for the effects of sorption on the advective and dispersive fluxes. The application of the retardation factor within the numerical solution of the transport equation is discussed in Section 3.3.4.2. A detailed discussion of the mathematical treatment of sorption is provided by CRWMS M&O (2000r).

3.3.2.4 Colloid-Facilitated Transport

The conceptual model for colloid-facilitated transport focuses on colloid attachment and detachment processes (Section 3.2.4.5). It is assumed that in saturated fractured tuffs, colloids will move exclusively through fractures with negligible matrix diffusion and that colloid attachment and detachment to fracture surfaces can be described by first-order rate expressions. An assumption of local equilibrium has been adopted to describe these processes. Using these assumptions, and in a manner similar to the case of sorption (Section 3.3.2.3), the mathematical model for colloid-facilitated transport in fractured tuffs can be written as

$$R_c \frac{\partial C_c}{\partial t} + \nabla \cdot (\bar{v} C_c) - \nabla \cdot (D \nabla C_c) = 0, \quad (\text{Eq. 3-8})$$

where $R_c = 1 + \frac{k_{filt}}{b k_{res}}$ is the effective retardation factor for colloid transport, C_c is the colloid concentration in solution, k_{filt} is the filtration rate constant, k_{res} is the detachment rate constant, and b is the fracture half aperture.

The conceptual model for colloid-facilitated transport in the alluvium essentially is the same. Consequently, the mathematical model for colloid facilitated transport in alluvium is identical to that for fractured tuffs with the exception that R_c is defined as

$$R_c = 1 + \frac{\mathbf{r}_a k_f}{n k_r}, \quad (\text{Eq. 3-9})$$

where \mathbf{r}_a denotes the density of the alluvial material [M/L³], n is the matrix porosity [dimensionless], k_f is the attachment rate [#M-T], and k_r is the detachment rate constant [#L³-T].

A detailed discussion of the mathematical model for colloid-facilitated transport is provided by CRWMS M&O (2000).

3.3.3 Numerical Solution of the Groundwater Flow Equation

The FEHM code (Zyvoloski et al. 1997a) is used in site-scale SZ modeling to obtain a numerical solution to the mathematical equation describing groundwater flow (Equation 3-4). FEHM is a nonisothermal, multiphase flow and transport code that simulates the flow of water and air, and the transport of heat and solutes, in 2-D and 3-D saturated or partially saturated heterogeneous porous media. The code includes comprehensive reactive geochemistry and transport modules and a particle tracking capability. Fractured media can be simulated using an equivalent continuum, discrete fracture, dual porosity, or dual permeability approach.

As described by CRWMS M&O (2000n, Section 6.5), the control-volume finite element method is used in FEHM to obtain a numerical solution to the groundwater flow equation over the model domain. Finite-element methods are based on the assumption that a continuum may be modeled as a series of discrete elements. For each element, equations based on a discretized form of the groundwater flow equation are written that describe the interaction of that element with its neighbors. This discretization leads to a set of equations that must be solved to obtain the values of groundwater pressure at each node throughout the model domain.

3.3.4 Numerical Solution of Transport Equation

The numerical approach implemented in FEHM to obtain a solution for the transport equation was selected based on a number of important requirements. The transport model needs to be based on a 3-D process-level flow model. The transport model also needs to be able to handle extremes of the advective-dispersive transport that include a wide range of dispersivity values. The model must be able to handle cases of low transverse dispersivity (including no transverse dispersivity) throughout the entire travel path or higher dispersivity in the fractured volcanic rocks transitioning abruptly to low dispersivity in the alluvium. Capturing this low level of dispersion transverse to the mean trajectory of a solute plume is extremely difficult using typical finite-element or finite-volume transport models unless an extraordinarily fine grid discretization is employed.

It may be necessary for the model to simulate the transport of plumes that have smaller dimensions than the grid block size of the flow model. Finite element simulations of transport cannot capture the details of radionuclide spreading if the plumes have characteristic dimensions that are of the same order or smaller than the grid block size of the flow simulation. Numerical dispersion effects arising from such an approach can be misinterpreted as dilution. A numerical method that retains the accuracy of the local concentration for small plumes is required for the solution of the transport equation.

The numerical approach used to solve the transport equation also must include a method for introducing the radionuclide source term into the model that is flexible enough to handle small and large source regions at the water table. Spreading of radionuclide mass (computed from the UZ flow and transport model) over large areas would only be valid if the source at the potential repository is due to many waste packages leaking simultaneously and if there is sufficient transverse dispersion within the UZ to smear the source within the percolating UZ fluid. Although smearing the radionuclide mass may be a good assumption under some circumstances, releases from a small number of waste packages cannot be handled with such a model. Radionuclide mass releases from a small number of waste packages, if distributed over large areas, would introduce large and artificial dilution factors at the interface of the UZ and SZ.

The site-scale SZ flow and transport model must be able to capture the important physicochemical processes known or suspected to occur in fractured porous rock. To properly account for transport through the fractured tuff, the transport model must include a dual-porosity transport formulation. This dual-porosity transport formulation must include the effects of sorption within the rock matrix that come into play only if considerable diffusion into the matrix pores occurs as radionuclides travel through the system. The effects of sorption in the alluvial aquifer system must also be included in the transport formulation.

Finally, it must be possible to abstract the results of the process-level site-scale SZ flow and transport model for use in TSPA-SR calculations. The main purpose of the site-scale SZ flow and transport model is to predict the concentration of radionuclides in the aquifer and at a hypothetical pumping well. Because these abstractions are employed in TSPA-SR, the transport model must predict breakthrough curves at a compliance point.

To meet these requirements, a particle tracking method has been implemented in FEHM to provide a solution to the advection-dispersion transport equation. In this approach, transport is decomposed into three interrelated components: advective, dispersive, and physiochemical. For the advective component, a particle tracking method is used. A random walk algorithm was combined with the particle tracking approach to account for the dispersive component of the advection-dispersion transport equation. To incorporate the dual-porosity transport and sorption components of transport equation, special modules were incorporated into the FEHM code. These approaches to the solution of the components of the advection-dispersion transport equation are discussed below.

3.3.4.1 Particle Tracking and Random Walk Algorithm

As described by CRWMS M&O (2000j), particle-tracking methods provide an efficient numerical algorithm for modeling the large-scale transport of solutes in heterogeneous porous media. By contrast, continuum approaches involving finite difference or finite element solution methods generally suffer from numerical dispersion, primarily because of the large grid blocks required to model large-scale systems. Furthermore, when using particle tracking, plumes can be simulated at scales smaller than the grid block size, and source regions can be smaller than the grid spacing. Particle tracking methods are particularly effective for handling advection-dominated transport. Consequently, a particle tracking method is used in FEHM to solve the transport equation in the site-scale SZ flow and transport model.

The particle-tracking method incorporated into FEHM is based on placing particles at specific points in the flow field to represent a specified mass of solute. These particles can be placed throughout the model domain to represent existing solute concentrations and can be introduced as necessary over time at specific source locations to represent radionuclide migration from the UZ. The particle-tracking method assumes a Lagrangian point of view, in which these particles move with the prevailing flow velocity. Based on a velocity field derived from the flow model, the trajectories for each particle are computed one at a time. Through a series of time steps, the particles are moved according to these computed trajectories.

The dispersive component of the transport is calculated using the random-walk method CRWMS M&O (2000j). This approach is based on the analogy between the mass transport equation and the Fokker-Plank equation of statistical physics. The dispersive displacement of each particle is computed using uniform random numbers, based on the dispersivity tensor and the porous flow velocity field at the particle location. In this model, the proper terms in the random-walk algorithm are derived from an anisotropic version of the dispersion coefficient tensor (Section 3.3.2.1). During each time step, the trajectory of each particle is computed using the advective component of transport that is modified through a series of displacements due to the dispersion calculated for each particle.

The method requires the development of a flow velocity field. The velocity field is developed by computing the velocities at the finite volume cell faces surrounding each node using Darcy's Law and the hydraulic heads computed in the flow solution at each node of the computational mesh. These velocities are then interpolated within the cell using the velocity interpolation in which a semianalytical solution to the particle tracks is obtained by interpolating the flow velocities linearly within each computational cell, permitting the flow lines to be computed in an efficient manner (CRWMS M&O 2000j).

For this method to work properly, the time step must be selected such that, on average, a particle spends several time steps within each cell. In a system with large variations in pore-water velocity due to permeability and porosity differences from cell to cell, the appropriate time step can vary greatly throughout the domain. In FEHM, this factor is accounted for by dynamically determining the time step. In a given cell, the magnitude of the velocity in the cell is used to scale the time step. The time required to traverse the cell completely in each of the three coordinate directions is computed, and the minimum is determined. Then, a user-defined parameter is multiplied by this minimum time to obtain the time step for the particle within the cell. This approach ensures that several steps are taken by a particle within a cell but minimizes computational time by tailoring the time step to the characteristic velocity within each cell.

Two options have been incorporated into FEHM to report the results of the particle tracking simulations. The model options can be used to predict the delivery time and concentrations of radionuclides at a particular boundary (e.g., a compliance boundary). This can be accomplished by defining a set of finite element grid points that corresponds to the desired boundary. The code determines the first arrival of each particle at any node along this boundary and subsequently reports the cumulative arrival time distribution for all particles. This arrival time distribution is then converted to the pumping well concentration, and the resulting curves can be used as input to the convolution portion of PA analysis (Section 3.6.3.3). Alternatively, the concentrations of particles at any cell in the finite element domain can be reported as a number of particles residing in the cell divided by the fluid mass in the cell. A detailed discussion of the particle tracking and random walk algorithms used to simulate advective and dispersive transport in the site-scale SZ flow and transport model is provided in CRWMS M&O (2000j, Section 6.1).

3.3.4.2 Matrix Diffusion and Sorption

As described by CRWMS M&O (2000j), to incorporate the influence of matrix diffusion and sorption, the residence time transfer function particle-tracking method has been adapted to the particle-tracking algorithm. In this method, adjustments to the travel time of a particle are made to account for the influence of physicochemical processes such as sorption and matrix diffusion. During its path along a streamline, the particle travel time is governed by a transfer function describing the probability of the particle spending a given length of time on that portion of its path. For a cumulative probability distribution function of particle residence times, the travel time of a particle along this portion of its path is computed by generating a random number between 0 and 1 and determining the corresponding residence time. On average, if a large number of particles travel through this portion of the model domain, the cumulative residence time distribution of particles will reproduce the shape of the transfer function.

The form of the transfer function is derived from an analytical or numerical solution to capture the appropriate processes being considered. The analytical solution identified in Section 3.3.2.2, and the retardation coefficients developed in Section 3.3.2.3, are used by the model in developing the transfer function and determining the value of the delayed travel time along a pathline for each particle resulting from the effects of matrix diffusion and sorption.

As described by CRWMS M&O (2000j), the final step of the model development is to integrate the matrix diffusion model with the random-walk transport model. Specifically, the time intervals over which the time delays are applied must be set in a manner that allows for obtaining computationally efficient and accurate solutions. In this model, the time delay is applied to a particle at the time at which it exits a cell, after having determined the cumulative time the particle spent in advective transport through the cell. Within a cell, the transport properties of diffusion and sorption are, by definition, uniform, so a unique set of transport dimensionless parameters can be defined. To apply the time delay, the particle is held at that location until the time of the simulation run catches up to the time of that particle, after which the particle is allowed to resume its transport.

Finally, for sorption without matrix diffusion, the time delay is computed deterministically by computing a retardation factor based on the sorption coefficient; otherwise, the method is identical to the matrix-diffusion method. A detailed discussion of the methods (and alternative conceptual methods) used to incorporate the influence of matrix diffusion and sorption into the transport model for the site-scale SZ flow and transport model is provided by CRWMS M&O (2000j, Section 6.2).

3.3.5 Flow Model Development

As described by CRWMS M&O (2000n), development of the site-scale SZ flow and transport model requires the generation of a computational grid, the identification of the hydrogeologic unit at each node on the grid, the specification of boundary conditions, the specification of recharge values, and the assignment of nodal hydrogeologic properties. Each of these elements of model development is discussed in this section.

3.3.5.1 Grid Generation

As described by CRWMS M&O (2000n, Section 6.2), the computational grid developed for the site-scale SZ flow and transport model was formulated so that the horizontal grid is coincident with the grid cells in the regional-scale SZ flow model. The depth of the computational grid is approximately the same as depth of the regional-scale SZ flow model. The top of the computational grid begins at the water table surface and extends to a depth of 2,750 m (9,020 ft) below sea level.

Previous models of SZ flow and transport at Yucca Mountain used unstructured meshes and structured grids. However, to use the streamline particle tracking capability of FEHM, an orthogonal grid was required. Consequently, a structured grid using orthogonal hexahedral elements was developed for the site-scale SZ flow and transport model.

Although structured grids are not as flexible as unstructured meshes in fitting complex geometry, studies have shown that they provide accurate solutions as long as there is adequate resolution.

The grid must contain sufficient resolution to represent adequately the geometry of the different materials in each hydrogeologic layer. Moreover, there must be adequate resolution to adequately account for any large gradients present in the flow or transport model.

The accuracy of the flow solution and the transport solution was a principal concern during the process of formulating a grid for the site-scale SZ flow and transport model. A study was performed on ten grids to determine the appropriate resolution for representing flow and transport in the Yucca Mountain groundwater flow system (CRWMS M&O 2000n, Section 6). Although the study was based on an earlier HFM, the results show that a 500-m (1,640-ft) horizontal grid spacing is adequate for use in the site-scale SZ flow and transport model, and consequently, a 500-m (1,640-ft) horizontal grid spacing was adopted. The grid resolution in the vertical dimension also is important for adequately representing groundwater flow and transport in the SZ. Each layer in the model grid is horizontal, but the layering of the physical hydrogeologic units is subhorizontal. Therefore, a finer grid resolution was used in the vertical dimension than in the horizontal dimension, and this was sufficient to represent adequately the approximately 7 percent dip to the east of the hydrogeologic units.

The vertical grid spacing was established to provide the resolution necessary for accurately representing flow and transport along critical flow and transport pathways in the SZ. A finer grid spacing was adopted for shallower portions of the model, while a progressively coarser grid was adopted for deeper portions of the aquifer. The vertical grid spacing ranged from 10 m (33 ft) near the water table to 550 m (1,805 ft) at the bottom of the model domain. The vertical dimension of the model domain was divided into 11 zones, and constant vertical grid spacing was adopted in each of these eleven zones. The structure of the vertical layering used in the site-scale SZ flow and transport model grid is summarized in Table 3-4. In total, 38 layers were included in the vertical dimension.

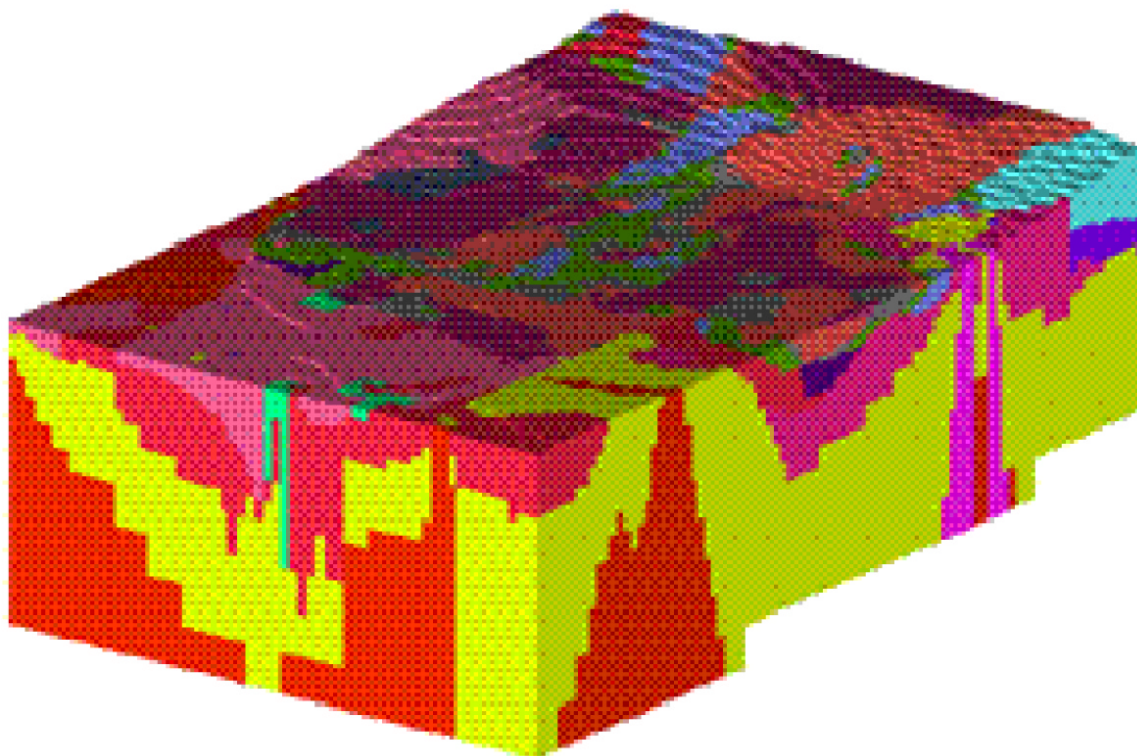
Table 3-4. Vertical Grid Spacing Used in the Site-Scale Saturated Zone Flow and Transport Model

Node Elevation Zone Boundaries (m)		Grid Spacing (m)	Zone Width (m)	Grid Lines per Zone
Upper	Lower			
1200	1000	50	200	4
1000	840	40	160	4
840	760	20	80	4
760	700	10	60	6
700	640	20	60	3
640	600	40	40	1
600	300	50	300	6
300	0	100	300	3
0	-600	200	600	3
-600	-2200	400	1600	4
-2200	-2750	550	550	1
				Total: 39

Source: CRWMS M&O (2000n, Table 4)

NOTE: Of the 39 grid lines, one defined the lower boundary of the model, and thus was not considered in the model, therefore, there were only 38 grid lines in the model.

A 3-D representation of the computational grid is provided in Figure 3-18. Not all model layers extend throughout the entire horizontal extent of the model domain. Because the model domain is truncated at the water table, and because the water table exhibits considerable variation in altitude over the model domain, those layers in the higher water table areas (i.e., to the north of the model domain) are truncated as the water table decreases in altitude toward the south. To maintain an approximately constant thickness of the model domain, several of the model layers at the bottom of the model were not extended throughout the model domain.



Source: Adapted from CRWMS M&O (2000n, Figure 3)

NOTE: This representation of the computation grid illustrates the complex 3-D spatial relation among units within the site-scale model area. Shading represents different hydrogeologic features included in the model.

Figure 3-18. Three-Dimensional Representation of the Computation Grid

3.3.5.2 Hydrogeologic Framework Model

After establishing the grid, the physical hydrogeologic unit present at each node in the site-scale SZ flow and transport model grid was identified using the HFM (Section 3.2.1; USGS 2000a). Using the 3-D geometry of the hydrogeologic units represented in the HFM, the LaGriT code (Version 2.0) was used to assign a hydrogeologic unit designation to each node of the computation grid used. This resulted in assigning 13 to 27,097 (average of 7,518) nodes per hydrogeologic unit to the valley-fill confining unit and the lower carbonate aquifer, respectively (Table 3-5). The assignment of hydrogeologic units to grid cells is shown in the 3-D representation of the grid depicted in Figure 3-18.

Table 3-5. Number of Nodes Assigned to Hydrogeologic Units in the Site-Scale Saturated-Zone Flow and Transport Model

Geologic Units	Number of Nodes
Alluvium (Valley-Fill Aquifer)	6,188
Valley-Fill Confining Unit	13
Limestones	227
Lava Flows	891
Upper Volcanic Aquifer	13,831
Upper Volcanic Confining Unit	7,845
Crater Flat - Prow Pass	5,666
Crater Flat - Bullfrog	6,472
Crater Flat - Tram	11,676
Lower Volcanic Confining Unit	9,142
Older Volcanic Aquifer	210
Older Volcanic Confining Unit	11,012
Undifferentiated Valley Fill	21,578
Upper Carbonate Aquifer	23
Lower Carbonate Aquifer Thrust	1,192
Upper Clastic Confining Unit	5,923
Lower Carbonate Aquifer	27,097
Lower Clastic Confining Unit	13,259
Granites	608
Base	0
Total Number of Nodes	142,853

Source: CRWMS M&O (2000n, Table 5)

3.3.5.3 Boundary Conditions

As described by CRWMS M&O (2000n, Section 6.1.2), data from the potentiometric map (Figure 3-5) were used to set boundary conditions for head values around the periphery of the computational grid. A uniform, constant head was applied through each layer of the model that was based on the water level at the top of the model at that location. While this boundary condition may not correspond with actual conditions and tends to limit vertical flow in the exterior portions of the model, sufficient data are not available to establish vertical gradients for boundary conditions along the boundaries of the computational grid. However, vertical gradients still are simulated internally in the model domain in response to geohydrologic conditions, and the calibrated model is capable of representing the upward vertical gradients observed between the carbonate aquifer and overlying volcanic aquifers (Section 3.4.3).

Historically, groundwater has been extracted from wells in the Amargosa Valley south of the site-scale model domain. Drawdown from the wells is represented in the potentiometric surface map that was used to establish boundary head conditions. Consequently, the affect of pumping on flow within the model domain is accounted for by the head values specified along the southern boundary. A small amount of pumping also has occurred from the southern portion of the site-scale model. This pumping was included in the regional-scale model, but not the site-scale model. Ignoring this pumping is assumed to have very little effect on the calculated flow paths and flow times to compliance boundaries.

A no-flow boundary was established for each node located along the bottom of the computational grid. While flow conditions in the deeper portions of the model domain are not well established, the depth of the bottom boundary is such that it is not likely to exert an important influence on flow in the more shallow areas where groundwater flow and transport is of greater interest to PA.

The top surface of the computational grid also is represented by no-flow boundary conditions. A no-flow boundary at the top of the model was assumed to facilitate the adoption of a confined-aquifer solution approach for the site-scale SZ flow and transport model. This approach assumes no UZ and, therefore, solves a simplified and computationally more efficient numerical model. The assumption of no-flow conditions at the top of the model does not preclude the addition of spatially varying source terms to model recharge.

3.3.5.4 Recharge

Recharge is applied to the top surface of the computational grid as a flux boundary condition. Spatial distribution of recharge developed for application to the site-scale SZ flow and transport model is discussed in Section 3.2.3.2 and is described in detail in CRWMS M&O (1999a). Using the recharge map developed in CRWMS M&O (1999a), recharge amounts were interpolated onto the computational grid for the site-scale SZ flow and transport model. Based on this interpolation, a value for mass flux of recharge is assigned to each surface node as a boundary condition. However, with the exception of the zone directly beneath the UZ model, the recharge map was developed for recharge directly to land surface. As a result, there are nodes at the top of the model (i.e., at the water table surface) where the permeability is too small to accept the recharge developed for the land surface at that location. To rectify this problem, the permeability of the top nodes at these locations was increased so that the recharge could be more easily redistributed to neighboring areas of higher permeability.

3.3.5.5 Assignment of Nodal Hydrogeologic Properties

As described by CRWMS M&O (2000n), hydrogeologic properties are specified for each node in the computational grid. For flow modeling, the hydrologic properties include permeability, porosity, and viscosity. Permeability is used as a calibration parameter, and the assignment of this value to each node is discussed in Section 3.3.6.3. Because steady-state flow is simulated in the site-scale SZ flow and transport model, the value assigned to specific storage at each node does not influence the water levels predicted by the model.

The parameter values for viscosity depend on the temperature at each node, and a uniform temperature gradient is assumed. Borehole temperature data (Sass et al. 1988) indicate that there is variability in the temperature gradient at different locations and within individual wells, presumably due to advective redistribution of heat from infiltration and vertical groundwater flow. However, these data also indicate that temperature gradients generally become more linear with increasing depth below the water table. It is important to note that the viscosity of water only changes by a factor of about 3.5 over the temperature range of 20°C to 100°C ([68°F to 212°F] Streeter and Wylie 1979) expected within the range of depths in the site-scale SZ flow and transport model domain. Thus, assuming a constant temperature gradient when calculating

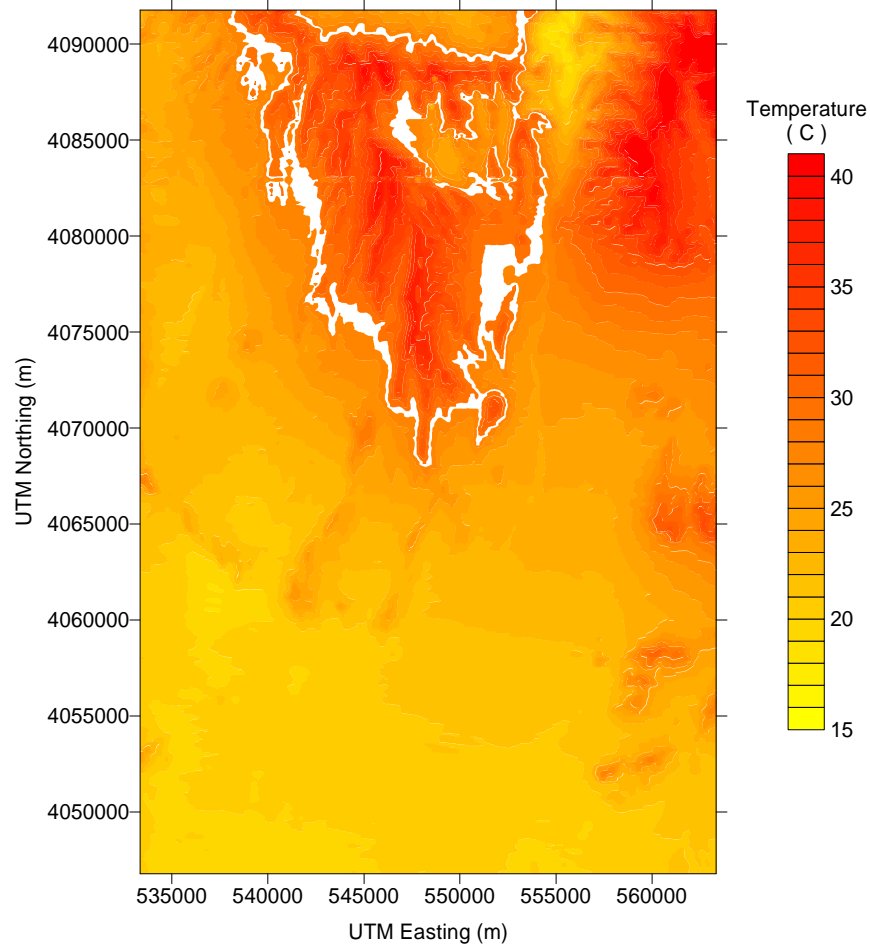
nodal viscosity values should not introduce significant error in the site-scale SZ flow and transport model.

The approach taken to incorporating groundwater temperature in the site-scale SZ flow and transport model is to evaluate the average temperature gradient (using temperature measurements in boreholes) and to use that temperature gradient to specify temperatures at grid nodes in the model. As implemented, temperatures remain fixed at the specified value, and heat-transport equations are not solved in the simulation. Thus, in the model, the specified values of temperatures are used to calculate the local groundwater viscosity, but temperature variations do not result in any variable-density flow processes because at the temperatures involved, the density of water changes by less than 1 percent.

Temperatures presented by Sass et al. (1988) were used to estimate an approximate average temperature gradient and a representative surface temperature for the site. There is considerable variability, about 15°C/km to 60°C/km (51°F/mi to 205°F/mi), in the temperature gradients observed in the wells. However, among wells, the average value of the temperature gradient is approximately 25°C/km (85°F/mi), and the average surface temperature is about 19°C (66°F). By using these values for the average temperature gradient and surface temperature, along with the water table and topographic surface evaluations, estimated temperature at the water table is calculated (Figure 3-19). Lower temperatures correspond to areas of relatively thin unsaturated thickness, and the higher temperatures correspond to a thick UZ (Figure 3-19). CRWMS M&O (2000n, Section 6.6) provide further details of the development and application of temperature profiles for establishing nodal values of viscosity.

3.3.6 Model Calibration

As described by CRWMS M&O (2000n, Section 6.4), calibration is the process by which values of important model parameters are estimated and optimized to produce the best fit between the model output and the observed data. Calibration generally is accomplished by adjusting model input parameters (e.g., permeability) to minimize the difference between observed and simulated conditions (in this case, comparing predicted and observed head values and lateral boundary fluxes). The process of selecting an optimal set of parameters (based on, for example, minimizing the difference between observed and simulated conditions) frequently is referred to as inverse modeling or model inversion. Model calibration may be performed through manual methods or through automated optimization procedures. Automated optimization procedures generally employ a carefully prescribed mathematical process that selects the optimal set of parameters based on minimizing an objective function describing the difference between observed and simulated conditions. These procedures generally provide the most structured and thorough means of calibrating a model, and frequently they provide useful additional information regarding model sensitivity to parameters and other useful statistical measures. Consequently, an automated optimization procedure has been used to calibrate the site-scale SZ flow and transport model. However, manual adjustments to the calibration also were performed to ensure an accurate model.



Source: CRWMS M&O (2000n, Figure 5)

NOTE: Data were calculated assuming a temperature gradient of 25°C/km (85°F/mi) and a surface temperature of 19°C (66°F).

Figure 3-19. Modeled Temperature at the Water Table for the Site-Scale Model Domain

The calibration process (including the parameter estimation software, the formulation of the objective function used to optimize parameters, the parameters that were optimized during model calibration, and the manual adjustments to calibration) is discussed below.

3.3.6.1 Parameter Estimation Software

Parameter estimation was achieved through the use of the model independent parameter estimation software, PEST, from Watermark Computing. PEST was selected because of the ability to couple it with FEHM without changing the FEHM code. PEST is designed to be used with virtually any model, and it previously was coupled with FEHM by Czarnecki et al. (1997) to calibrate a preliminary SZ flow model.

PEST uses nonlinear least squares regression to estimate parameters. The benefits of using nonlinear regression include an expedited determination of best-fit parameter values,

quantification of the quality of the calibration estimates, estimates of the confidence limits on parameter estimates, and identification of correlation among parameters. PEST accomplishes parameter optimization using a Levenberg–Marquardt-based algorithm, an algorithm that is well established, robust, and widely applicable.

The parameter optimization process using the coupled FEHM-PEST code is begun by specifying an initial estimate for each unknown parameter. FEHM then computes head values using the initial parameter estimates and passes the computed head values to PEST. Through a series of PEST-directed FEHM simulations with perturbations in the parameters, PEST subsequently computes the derivative of the objective function with respect to each of the parameters. Based on information derived from these derivatives, PEST determines the amount of change in the current value of parameter and uses this information to improve the fit to the data during the next iteration to further minimize the objective function. This process is repeated until the fit is within a prescribed tolerance or until no further improvement is possible.

To enable the PEST-FEHM code to search for the global minimum of the objective function, a procedure is attached to the code that carries out a simulated annealing process. This process allows the PEST-FEHM code to move from one local minimum to another, better, local minimum. This process is repeated until no further improvement occurs and it is assumed that the global minimum has been found. Thus, the PEST-FEHM code is capable of searching for the minima of a multidimensional objective function. Further details regarding the parameter estimation code and algorithm are available in CRWMS M&O (2000n, Section 6.4)

3.3.6.2 Objective Function

The objective function used during the parameter optimization was the sum of the squared differences between observed hydraulic conditions and those simulated by the site-scale SZ flow and transport model. Hydraulic conditions included water levels (hydraulic heads) at selected locations and lateral fluxes at selected model boundaries. In the calibration process, the specific water levels and boundary fluxes are referred to as calibration targets.

3.3.6.2.1 Water Levels

For calibration targets, 115 water level and head measurements were used (CRWMS M&O 2000n, Section 6.7). To correspond with hydraulic conditions simulated in the regional-scale flow model, target water level data were selected to represent hydraulic conditions in the early 1990s.

Most of the water levels are composite levels from one or more water-producing zones. For modeling purposes, it is assumed that the midpoint of the open interval, or applicable packed-off interval, is representative of the measurement location. In open holes, it is assumed that the midpoint can be calculated from the depth of the hole and the water-level altitude. When comparing simulated water levels to target water levels, the model represents water levels at the target locations by linearly interpolating the head from the eight nodes surrounding the target location.

During the calibration process, emphasis is given to minimizing the difference between observed and simulated water levels for selected calibration targets (i.e., at selected target locations). This

is accomplished by multiplying the squared differences at that location by a weighting factor. A weighting factor of 1.0 (i.e., no particular importance) normally is applied to calibration targets. However, a preferential weighting factor (20) is applied to approximately 30 calibration targets in the low-gradient region to the south and east of Yucca Mountain. These calibration targets are given high weighting because they are in the likely pathway of fluid leaving the potential repository site and because small changes in head in this area could produce a large effect on the flow direction. Calibration targets north of Yucca Mountain are given a low weighting (0.05; i.e., little importance). The five wells in this category are given low weights primarily because of the possibility of perching and the attendant uncertainty in water-level measurements in this region. The one head measurement in the carbonate aquifer is given a preferential weighting factor (20) because of the importance of this calibration target for reproducing an upward gradient in the calibrated model. The inclusion of an upward gradient within the calibrated site-scale SZ flow and transport model is considered important for generating a realistic model because an upward gradient tends to force flow along shallower pathlines as indicated by geochemical data. A complete listing of all target water level values, target locations, and the weighting applied to each target is provided by CRWMS M&O (2000n, Table 7).

3.3.6.2.2 Boundary Fluxes

The fluxes in and out of the site-scale model domain were estimated using the regional-scale and site-scale models. The differences between the two estimates were used in the objective function during parameter optimization. The computation of these fluxes is discussed in Section 3.2.3.1 and is described in detail in CRWMS M&O (1999a).

Fluxes from all of the boundary segments on the eastern and northern boundaries of the site-scale SZ flow and transport model domain were included in the objective function during parameter optimization. Fluxes from the five western boundary segments were not included in the objective function. Preliminary calibration runs indicated that it was difficult to match the fluxes along these segments predicted by the site-scale model with those predicted by the regional-scale model. This difficulty largely was a result of the different HFMs used in the site-scale and regional-scale models. It was decided that the goal of ensuring that the total flux through the site-scale model domain is similar to that predicted by the regional-scale model was best achieved by not forcing a close match along those boundary segments for which the rock types were different in the two models.

3.3.6.3 Calibration Parameters

As described by CRWMS M&O (2000n), permeability was optimized during calibration of the site-scale SZ flow and transport model. The model formulation and FEHM code allows for the specification of a permeability value at each node. However, there is not sufficient water level and permeability data to warrant identifying a specific value of permeability for each individual node during calibration. Consequently, sets of nodes were grouped into specific permeability zones based on similar permeability characteristics. A single permeability value was assigned to each zone. These zonal values of permeability served as the parameters that were optimized during model calibration.

There is a large uncertainty in recharge. Consequently, it is a candidate for use as a calibration parameter. However, the sensitivity of the calibration to recharge values is decreased by the fact that recharge applied on the upper boundary of the site-scale flow model accounts for only a small portion of the total groundwater flow through the model domain.

Permeability zones were created for hydrogeologic units identified in the HFM and for specific hydrogeologic features. With the exception of the basal unit that served as a lower boundary for the model, a permeability zone was established for each hydrogeologic unit. All of the nodes within a specific hydrogeologic unit were assigned to that permeability zone unless they were included in one of permeability zones established for specific hydrogeologic features.

For permeability, vertical anisotropy was assigned a value of 10:1 (horizontal to vertical) in the volcanic and valley-fill units in the site-scale SZ flow and transport model. Relatively lower permeability in the vertical direction may occur in stratified media, and the ratio of 10:1 is in the generally accepted range (CRWMS M&O 1998b, Table 3-2). Furthermore, the relatively high vertical gradient observed in well UE-25p#1 suggests that vertical permeability is lower than horizontal permeability.

Specific hydrogeologic features that were thought to potentially impact groundwater flow were classified as permeability zones. The permeability variable used for a specific feature was assigned to all of the nodes within that feature. The hydrogeologic features for which special permeability zones were established were primarily faults, fault zones, and areas of chemical alteration (Section 3.2.2.5). These features are distinct from the subhorizontal hydrogeologic units identified in the HFM. Each of the identified hydrogeologic features includes multiple geologic formations and represents zones of altered permeability within the individual formations. One permeability zone, the east-west barrier, is noteworthy in that it does not represent a feature of the HFM. Instead, it was added to the model specifically to reproduce the combination of the steep hydraulic gradient and the relatively flat gradient located north of the steep gradient. The necessity of using this model approach to match head observations reflects uncertainty in the geology and hydrology of this region of the model domain. These features are discussed in CRWMS M&O (2000n, Section 6.3).

As described by CRWMS M&O (2000n), 27 permeability zones were established for model calibration. In addition, permeability multipliers were assigned to four zones that contained geologic features that penetrated a number of hydrogeologic units. The permeability multipliers were used to modify the permeability values assigned to the hydrogeologic units in the area of the geologic features. While the permeability parameter or multiplier values for most zones were optimized during calibration, permeability for the upper carbonate aquifer was assigned a constant value because sensitivity analyses indicated that the model was not sensitive to this parameter value.

The parameters used in the calibration of the SZ flow and transport model were a combination of permeabilities of hydrogeologic units, permeabilities of faults and other features, and permeability multipliers of faults and features. Permeabilities of the 18 hydrogeologic units were chosen as calibration parameters because of the importance of the parameter in the flow system and the fact that each of the units was identified in the HFM. The parameters that represent these features were added because they were identified as important structural features (e.g., the

Solitario Canyon fault), they were in the regional-scale model (e.g., the Spotted Range-Mine Mountain zone), or they were necessary for some conceptual feature such as the high head gradient north of Yucca Mountain (east-west barrier). The number of parameters represent a computationally tractable set.

Upper and lower bounds were placed on each permeability variable during parameter optimization. The upper and lower bounds for the permeabilities and permeability multipliers were chosen to reflect maximum and minimum field values (permeability) or a reasonably realistic range of values (permeability multipliers). For example, when the multiplier represented flow in the plane of a fault, the multiplier was allowed to take on values between 1 and 100; when the multiplier represented geochemical alteration, the multiplier was allowed to take values between 0.00001 and 0.50000. The final calibrated values of the parameters were not sensitive to initial parameter values within the range specified.

A list of permeability zones, including the parameter type assigned to each zone, the upper and low bounds specified for the parameter, and an identification of the parameters optimized during calibration, are provided in Table 3-6 (CRWMS M&O 2000n, Table 8).

3.3.6.4 Manual Adjustments to Calibration

Proper calibration of the site-scale SZ flow and transport model requires consideration of the full range of available data. The available data include field data for water levels and hydraulic heads, permeability data from field and laboratory tests, locations of known faults and other geologic data, and hydrochemical data. Opinions expressed during the expert elicitation process (CRWMS M&O 1998b) also must be considered. The goal during development of site-scale SZ flow and transport model was to deliver to PA a model that is realistic where data exists and is conservative where data is lacking. Thus, when field data and interpretations produce conflicting trends in calibration, the data that produced a more conservative model are used.

A number of techniques were employed during parameter optimization using PEST to ensure a representative but conservative model. As previously discussed, these include the incorporation of important hydrogeologic features into the model and the placement of upper and lower bounds on the allowable permeability values. However, it was necessary to make several adjustments to the model in addition to the PEST parameter optimization. These adjustments were made to improve the model in ways that were not possible during the PEST optimization. The most important of these adjustments were made to insure that the specific discharge within 5 km (3 mi.) of the potential repository was approximately equal to the median estimate given by the SZ expert elicitation (CRWMS M&O 1998b). Because the specific discharge was calculated with the particle-tracking feature of FEHM after the flow calculations were performed, this adjustment could not easily be incorporated in the PEST optimization. The specific discharge was adjusted by changing the permeability of the Bullfrog unit. Because the Bullfrog unit is highly permeable, specific discharge could be manipulated by changing the Bullfrog unit permeability value without adversely affecting the heads in the low gradient area near Yucca Mountain. Adjustments also were made to the permeability in the lower Fortymile Wash area so that water levels in the 2-D and Washburn wells would be more consistent with those in the upper Fortymile Wash area, thus preserving the observed head gradient. Adjustments to the permeability of the alluvial uncertainty zone and the valley fill aquifer also were made to better match the fluxes estimated from the regional-scale flow model for the eastern boundary of the site scale model.

Table 3-6. Permeability Zones Established in Site-Scale Saturated Zone Flow and Transport Model with Upper and Lower Bounds Applied During Calibration

Geologic Unit	Calibrated Value ^a	Parameter Type ^b	Minimum Value ^a	Maximum Value ^a
Granites	1.96x10 ⁻¹⁶	P	1.00x10 ⁻¹⁷	1.00x10 ⁻¹⁴
Lower Clastic Confining Unit	1.00x10 ⁻¹⁶	P	1.00x10 ⁻¹⁶	1.00x10 ⁻¹⁴
Lower Carbonate Aquifer	5.00x10 ⁻¹⁴	P	5.00x10 ⁻¹⁴	1.00x10 ⁻¹²
Upper Clastic Confining Unit	1.00x10 ⁻¹⁶	P	1.00x10 ⁻¹⁶	1.00x10 ⁻¹⁴
Lower carbonate Aquifer Thrust	1.00x10 ⁻¹⁴	P	1.00x10 ⁻¹⁴	1.00x10 ⁻¹²
Upper carbonate Aquifer	4.08x10 ⁻¹⁴	P (fixed)	4.08x10 ⁻¹⁴	4.08x10 ⁻¹⁴
Undifferentiated Valley Fill	5.00x10 ⁻¹⁵	P	5.00x10 ⁻¹⁵	1.00x10 ⁻¹²
Older Volcanic Confining Unit	2.00x10 ⁻¹⁶	P	2.00x10 ⁻¹⁶	1.00x10 ⁻¹¹
Older Volcanic Aquifer	5.00x10 ⁻¹⁶	P	3.00x10 ⁻¹⁶	1.00x10 ⁻¹²
Lower Volcanic Confining Unit	2.00x10 ⁻¹⁵	P	1.00x10 ⁻¹⁵	1.00x10 ⁻¹¹
Crater Flat-Tram	2.36x10 ⁻¹³	P	1.00x10 ⁻¹³	1.00x10 ⁻¹¹
Crater Flat-Bullfrog	1.54x10 ⁻¹¹	P	1.00x10 ⁻¹³	8.00x10 ⁻¹¹
Crater Flat-Prow Pass	8.00x10 ⁻¹²	P	1.00x10 ⁻¹³	5.00x10 ⁻¹¹
Upper Volcanic Confining Unit	5.00x10 ⁻¹⁴	P	4.00x10 ⁻¹⁴	1.00x10 ⁻¹²
Upper Volcanic Aquifer	8.00x10 ⁻¹⁴	P	8.00x10 ⁻¹⁴	1.00x10 ⁻¹¹
Lava Flow Aquifer	1.00x10 ⁻¹²	P	1.00x10 ⁻¹⁶	2.00x10 ⁻¹²
Limestone Aquifer	1.00x10 ⁻¹²	P	1.00x10 ⁻¹⁵	1.00x10 ⁻¹¹
Valley Fill Aquifer	5.00x10 ⁻¹²	P	1.00x10 ⁻¹³	8.00x10 ⁻¹²
East-West Barrier	1.05x10 ⁻¹⁸	P	1.00x10 ⁻¹⁸	1.00x10 ⁻¹⁵
Solitario Canyon Fault	1.00x10 ⁻¹⁸	P	1.00x10 ⁻¹⁸	1.00x10 ⁻¹⁵
Fortymile Wash Fault	10	M	2	100
Spotted Range Thrust	11.7789	M	1	70
Northern Low Perm Zone	7.11x10 ⁻⁰²	M	1.00x10 ⁻⁰⁵	0.5
Imbricate Fault Zone	1	M	1	100
Crater Flat Fault	5.00x10 ⁻¹⁴	P	1.00x10 ⁻¹⁵	5.00x10 ⁻¹³
Alluvial Uncertainty Zone	3.20x10 ⁻¹²	P	1.00x10 ⁻¹³	1.00x10 ⁻¹¹
Lower Fortymile Wash Zone	5.00x10 ⁻¹²	P	1.00x10 ⁻¹⁴	8.00x10 ⁻¹²

Source: CRWMS M&O (2000n, Table 8)

NOTES: ^aMeasurement units for permeabilities are m²; multipliers are dimensionless.

^bP=Permeability; M=Multiplier

Values estimated for recharge and inflow to the SZ are not independent of permeability. This is because an increase in the recharge and inflow estimate causes a corresponding increase in the permeability estimate to produce the same hydraulic head field. Inflow into the site-scale model across lateral boundaries is estimated from regional-scale models (D'Agnese et al. 1997, 1999). Estimates of recharge are made by modeling infiltration through the UZ, taking into account past and future climates (USGS 2000c). Similarly, estimates from pumping tests provide a range of hydraulic conductivity for each hydrologic unit, some of which are fairly restrictive. These estimates serve to restrict the domain of possible recharge, inflow, and permeability model parameters. Uncertainty exists in these parameter estimates, and this uncertainty is addressed in the TSPA-SR.

3.3.7 Calibration Results

In this section, results of the model calibration with respect to water levels, predicted flow paths, and specific discharge at selected distances from the potential repository area are discussed. Details are presented by CRWMS M&O (2000n).

3.3.7.1 Water Levels

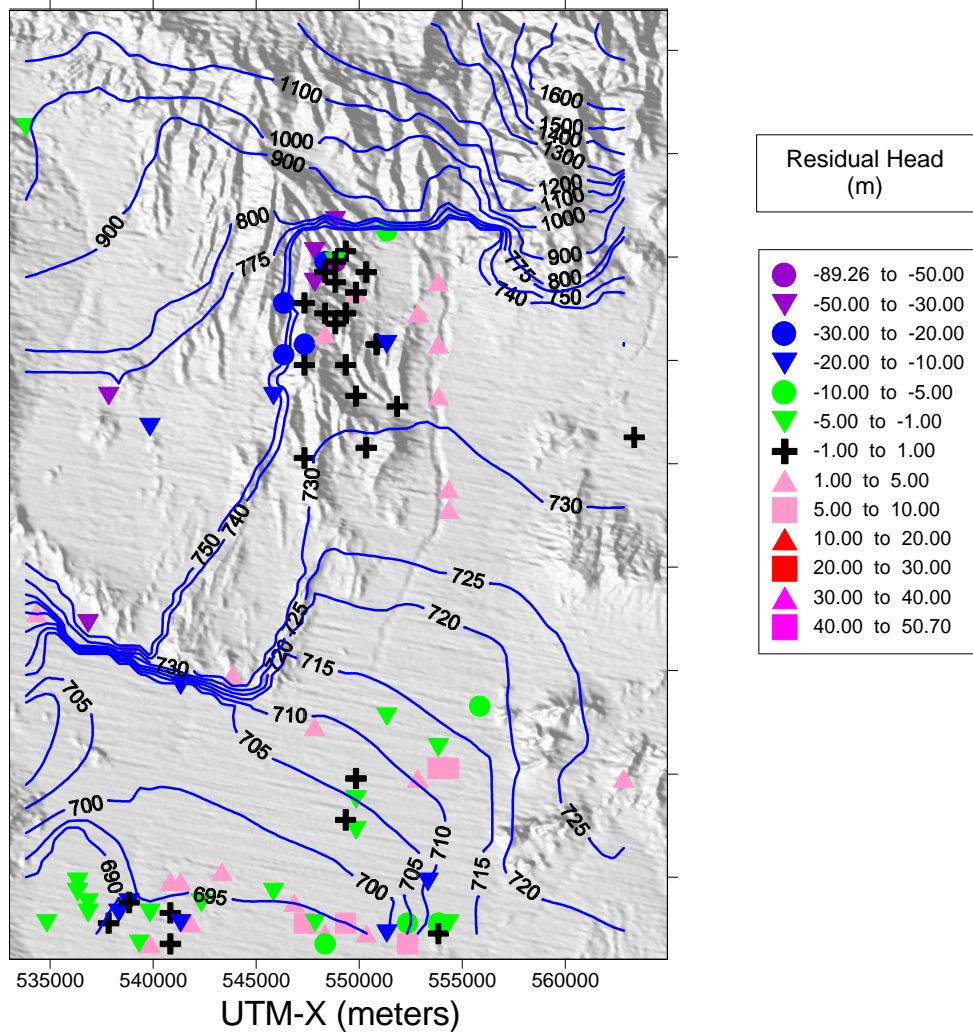
Model calibration resulted in a weighted residual sum of squares of about 27,600 m², which is equivalent to an average weighted residual of 16 m (52 ft) at each target measurement. Without weighting, the sum-squared residual was about 90,000 m², which corresponds to an approximately 30-m (98-ft) average residual for each observation. The potentiometric surface predicted by the calibrated site-scale SZ flow and transport model (Figure 3-20) is shown with residual heads at the location of each target observation. The largest head residuals (about 100-m [330-ft]) are in the northern part of the model in the high head gradient area near the east-west barrier. These head residuals are largely the result of the low weighting (0.05) assigned to these calibration targets and of the uncertainty in these measurements due to the perched conditions that may exist in this area. The next highest group of head residuals borders the east-west barrier and Solitario Canyon fault. These residuals (about 50) most likely result from a grid resolution insufficient to resolve the 780-m to 730-m (2,560-ft to 2,395-ft) drop in head that occurs over a short distance in this area.

3.3.7.2 Predicted Flow Paths

The particle tracking capability of FEHM was utilized to demonstrate flow paths predicted by the calibrated site-scale SZ flow and transport model. One hundred particles were distributed uniformly over the area of the potential repository and allowed to migrate until they reached the model boundary (Figure 3-21). The pathways generally leave the potential repository and travel in a south-southeasterly direction to the potential 20-km (12.5-mi) compliance boundary (NRC 1998). From the 20-km (12.5-mi) boundary to the end of the model, the flow paths trend to the south-southwest and generally follow Fortymile Wash. Most of the pathways pass through the designated Imbricate Zone (Zone 91 of Figure 3-14). Some of the pathways follow fault zones along Fortymile Wash (Zones 57 and 58 of Figure 3-14).

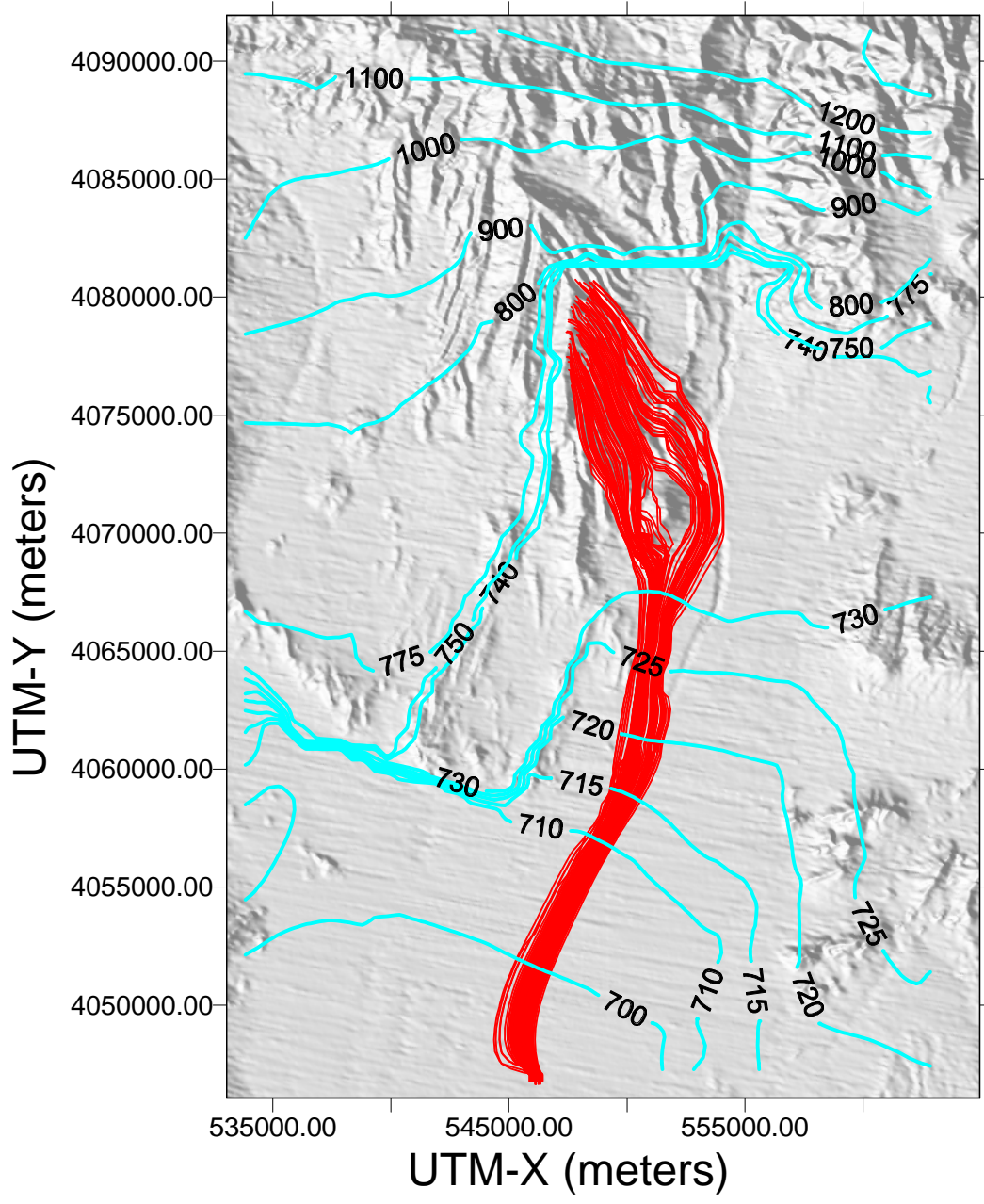
3.3.7.3 Specific Discharge

Using the calibrated flow model, specific discharge was estimated for a nominal fluid path leaving the potential repository area and traveling 0 to 5-, 5 to 20-, and 20 to 30-km (0, 3, 12.5, and 18.6 mi.). The specific discharge simulated by the flow model for each segment of the flowpath from the repository was determined using the median travel time for a group of particles released beneath the repository. Values for specific discharge of 0.67 m/yr., 2.3 m/yr., and 2.5 m/yr. (2.2, 7.5, and 8.2 ft/yr.) were obtained, respectively, for the three segments of the flowpath. The expert elicitation panel (CRWMS M&O 1998b, Figure 3-2e) estimated a specific discharge of 0.71 m/yr. (2.3 ft/yr.) for the 5-km (3-mi) distance. Thus, good agreement is found between the specific discharge predicted by the calibrated model and that estimated by the expert elicitation panel for the 5-km (3-mi) distance. The expert elicitation committee did not consider other travel distances.



Source: Adapted from CRWMS M&O (2000n, Figure 7)

Figure 3-20. Simulated Potentiometric Surface and Calibration Residuals



Source: Adapted from CRWMS M&O (2000n, Figure 8)

Figure 3-21. Flow Paths Predicted by Site-Scale Saturated Zone Flow and Transport Model

3.3.7.4 Summary of Calibration Results

The calibrated site-scale SZ flow and transport model provides a reasonable representation of the SZ groundwater flow system that matches key data from the Yucca Mountain site. The model reasonably simulates the observed water levels and hydraulic gradients, particularly in the area along the flowpath from beneath the potential repository. The flowpaths simulated by the site-scale SZ flow model generally agree with interpretations from the hydrochemical data. There is good agreement between the calibrated value of specific discharge and the value estimated by an expert panel. However, there is uncertainty in the groundwater fluxes simulated by the regional-scale SZ flow model. There is an important relationship between recharge and rock permeability in groundwater basins in which flow is at steady state. This is because the rate of groundwater flow must equal recharge at the basin scale. One implication of this relationship for flow modeling is that different combinations of permeability and recharge result in the same calculated head distribution. The domain of the site scale model, however, is only a portion of a groundwater basin. Therefore, recharge, permeability, and groundwater flow across lateral boundaries are related. Different combinations of values for these parameters result in the same calculated head distribution. The uncertainty introduced by this non-uniqueness is addressed directly in TSPA-SR calculations in that multiple flow fields are calculated by multiplying values of recharge, permeability, and boundary flux by the same factor. It is noted that recharge applied on the upper boundary of the site-scale flow model accounts for only a small portion (perhaps 5 percent) of the total groundwater flow through the model domain.

3.3.8 Sensitivity Analysis

The sensitivity of the estimated parameter values and the distribution of weighted residuals were evaluated using a sensitivity analysis (CRWMS M&O 2000n, Section 6.9). Results indicate that there is a wide range in composite scaled sensitivities, and it appears that the model is most sensitive to observations located close to Yucca Mountain. The model is most sensitive to the permeability of the Claim Canyon, Calico Hills, and Shoshone Mountain fault zones, and decreasingly sensitive to the lower-carbonate aquifer, Bullfrog unit, lower Fortymile Wash channel, and Tram unit permeabilities. The model is relatively insensitive to the remaining parameters, as reflected in their wide confidence intervals (CRWMS M&O 2000n, Table 16). The large range in parameter sensitivities indicates that the most sensitive parameters can be divided into multiple parameter zones and that the least sensitive parameters should be grouped into fewer parameters. The correlation between the permeability of the lower-carbonate aquifer and the permeability of the Spotted Range-Mine Mountain fault zone has a value of -1.0 , indicating that the two parameters cannot be estimated uniquely and that one should be set at a fixed value.

The sensitivity of recharge and boundary conditions were not considered in the analysis. However, uncertainty in these parameters is considered in the TSPA-SR. These parameters are varied over a realistic range in the TSPA.

Analysis of the distribution of weighted residuals (CRWMS M&O 2000n, Section 6.9.2) in the low hydraulic gradient region between Yucca Mountain and Fortymile Wash (Figure 3-20) reveals that most of these residuals are small negative values, indicating that the model predicts slightly more water in this area than actually is present. Because most of the residuals are

negative (rather than a sampling of positive and negative values), some aspect of the real system apparently has not been captured in the site-scale SZ flow and transport model. While predicted heads along flow paths from the potential repository area are too high (by less than 1 m [3.3 ft]), the observed gradients of head along these paths are well represented by the model.

3.4 MODEL VALIDATION

Model validation is the process of testing the validity of the conceptual, mathematical, and numeric representation of the system being modeled. For this model, validation consists of a set of confidence-building exercises. There are three components of the site-scale SZ flow and transport model: the HFM, the transport methodology, and the calibrated flow model.

Validation issues concerning the three components are described in detail in three analysis model reports (AMRs) (USGS 2000a, CRWMS M&O 2000j, 2000n; respectively). The HFM is empirical, and consequently, is not amenable for validation by comparison to independent data. It was validated instead by checking to assure that input data are consistent with a model grid representing the top of a hydrogeologic unit. Because the calibrated flow model incorporates the HFM, additional validation of the HFM was achieved as part of the validation of calibrated flow model as discussed below. The transport methodology was validated by comparing calculation results to analytical solutions to various hypothetical transport problems that include the processes of dispersion, sorption, and diffusion. The conceptualization of the transport processes also was validated through field and laboratory testing. This aspect of model validation has previously been discussed in Sections 3.1 and 3.2. The validation exercises provide sufficient confidence that the HFM and the transport methodology are adequate for use as components of the site-scale flow and transport model.

For two reasons, this section focuses mainly on validation of the calibrated flow model. First, the calibrated flow model incorporates the HFM, and therefore, validation of the flow model also adds confidence in the HFM. Second, the calibrated flow model was validated in the exact configuration that is used for TSPA-SR calculations. The transport methodology, in contrast, was validated for hypothetical problems. Validation of the transport model by comparison to field observations is not practical because such a calibration would require field tests of extremely long distance and time scales.

The ability of the calibrated site-scale SZ flow model to reproduce the potentiometric surface at Yucca Mountain is an initial indication of the validity of the flow model. The validity of the calibrated site-scale SZ flow and transport model has been further evaluated by comparing the results of the calibrated flow model to various elements of the ground-water flow system at Yucca Mountain. This further evaluation of the validity of the calibrated site-scale SZ flow model includes a comparison of the calibrated permeability values with observed permeability data (Section 3.4.1), a comparison between boundary fluxes predicted by the regional-scale flow model and the calibrated site-scale SZ flow and transport model (Section 3.4.2), a comparison between observed and predicted gradients between the carbonate aquifer and overlying volcanic aquifers (Section 3.4.3), and a comparison between hydrochemical data trends and particle pathways predicted by the model (Section 3.4.4).

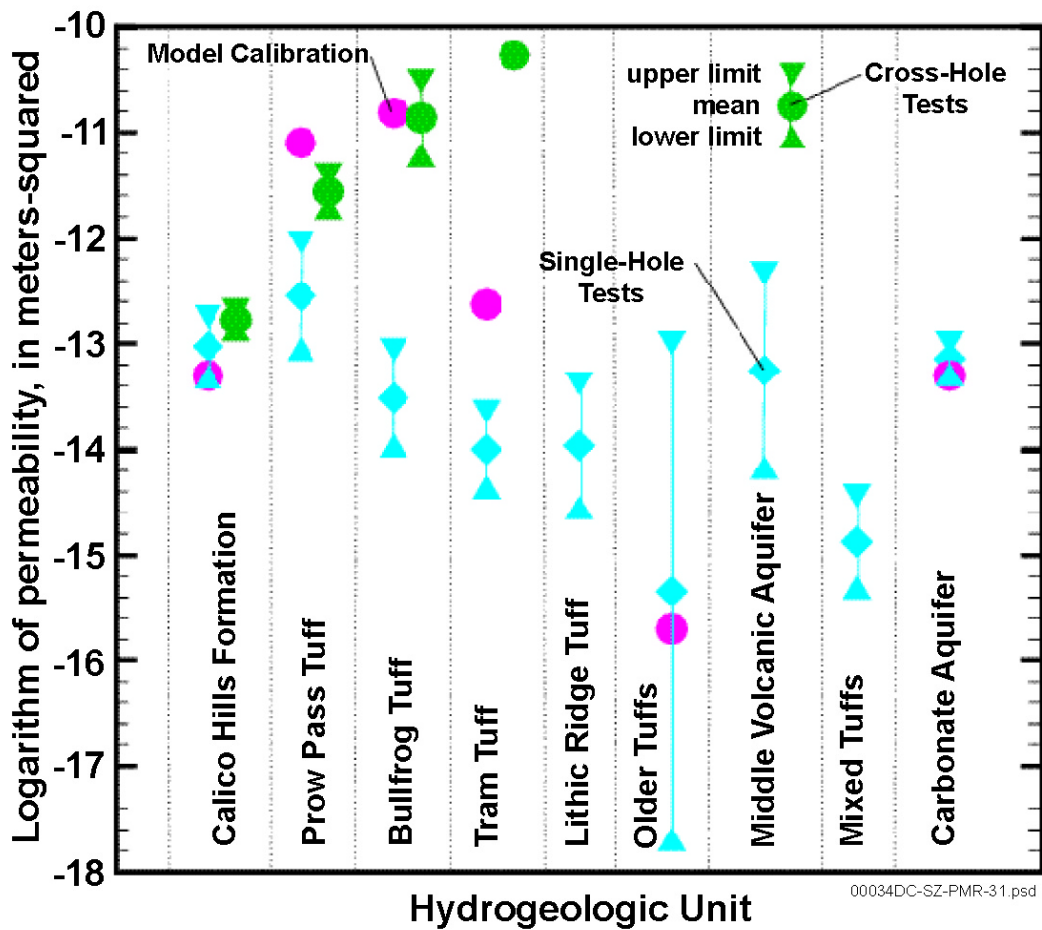
Comparisons performed for model validation indicate that flowpaths predicted by the model generally agree with those interpreted from hydrochemical data. The boundary conditions calculated by the site-scale model are close to those calculated by the regional-scale model. It is noted, however, that some of the boundary fluxes were also used as part of the model calibration target. The calculated vertical direction of flow (upward) matches the direction indicated by head measurements in the single well (UE-25p#1) that penetrates the carbonate aquifer. However, the magnitude of the calculated gradient is about half of the observed gradient. The combined results of the validation comparisons provide sufficient confidence that the calibrated site-scale flow model is adequate for use in the TSPA calculations.

3.4.1 Comparison of Permeability Data to Calibrated Permeability Values

As described by CRWMS M&O (2000n, Sections 6.7.7 and 6.7.8), permeabilities estimated during calibration of the site-scale SZ flow and transport model were compared to permeabilities determined from pump-test data from the Yucca Mountain area (Figure 3-22) and elsewhere at the NTS (Figure 3-23). Data from reports pertaining to the NTS were included in the comparison to help constrain permeability estimates for hydrogeologic units that were not tested or that underwent minimal testing at Yucca Mountain. For most of the geologic units, the calibrated permeabilities are within the 95 percent confidence limits of the mean permeabilities estimated from the data (Figures 3-22 and 3-23).

The mean-measured permeability of the carbonate aquifer is higher elsewhere at the NTS than either the mean-measured permeability at Yucca Mountain or the calibrated permeability for the carbonate aquifer (Figures 3-22 and 3-23). The calibrated permeability for the Upper Volcanic Aquifer is about two orders of magnitude less than the mean-measured permeability of this unit.

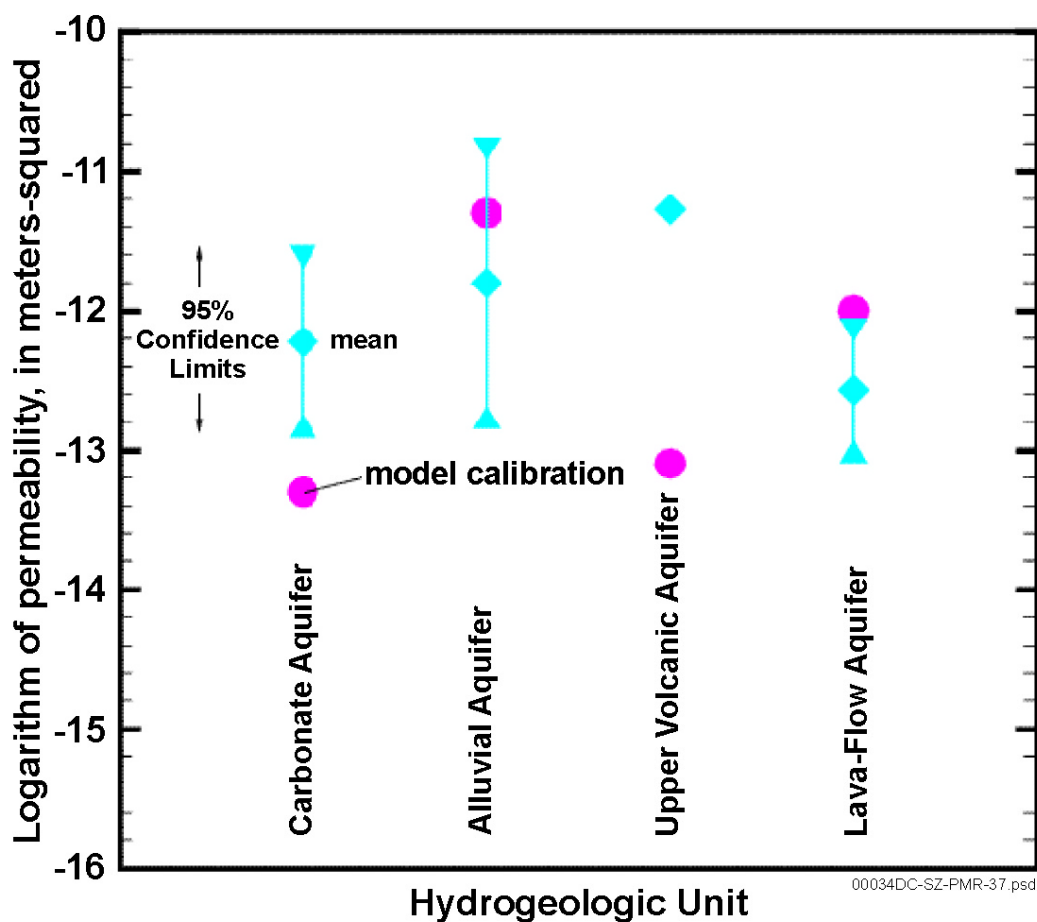
With the exception of the calibrated values for the upper volcanic aquifer, the calibrated permeabilities generally are consistent with most of the permeability data from Yucca Mountain and elsewhere at the NTS. Of particular importance are the permeabilities of the Bullfrog and Prow Pass units because they carry most of the flow in the region 5 km (3 mi.) down-gradient from the potential repository. Data from the cross-hole tests at the C-wells Complex is of high quality and has a small range (less than one order of magnitude). A good match was achieved for these units, which are important to TSPA calculations. A discrepancy exists between the calibrated permeability for the Tram Tuff and the mean permeability derived from the cross-hole tests; however, these permeabilities may have been enhanced by a breccia zone in boreholes UE-25c#2 and UE-25c#3 (Geldon et al. 1997, Figure 3).



Source: CRWMS M&O (2000n, Figure 14)

NOTE: Estimated permeabilities calculated from site-scale SZ flow and transport model. Observed permeabilities calculated from pump-test data. Bars indicate 95% confidence intervals; diamonds indicate the mean value.

Figure 3-22. Estimated and Observed Permeabilities for Nine Stratigraphic Units at Yucca Mountain



Source: CRWMS M&O (2000n, Figure 15)

NOTE: Estimated permeabilities calculated from site-scale SZ flow and transport model. Observed permeabilities calculated from pump-test data. Bars indicate 95% confidence intervals; diamonds indicate the mean value.

Figure 3-23. Estimated and Observed Permeabilities for Four Aquifers at the Nevada Test Site

3.4.2 Comparison of Fluxes Derived from Regional Model with the Boundary Fluxes Calculated by Calibrated Model

The site-scale SZ flow model domain includes only a small part of the Death Valley regional groundwater flow system and the boundaries of the site-scale model domain were not established along hydrologic boundaries. However, the domain of the regional-scale model encompasses a generally closed system and contains data from spring discharges to help fix the groundwater flux through the system (D'Agnesse et al. 1997, p. 59). Consequently, a comparison of predicted mass fluxes at the boundaries of the site-scale model domain with mass fluxes predicted by the regional-scale model should provide an indication of the validity of the calibrated site-scale SZ flow model. The expert elicitation panel (CRWMS M&O 1998b) suggested a comparison between these two fluxes as a means of validating the site-scale SZ flow model.

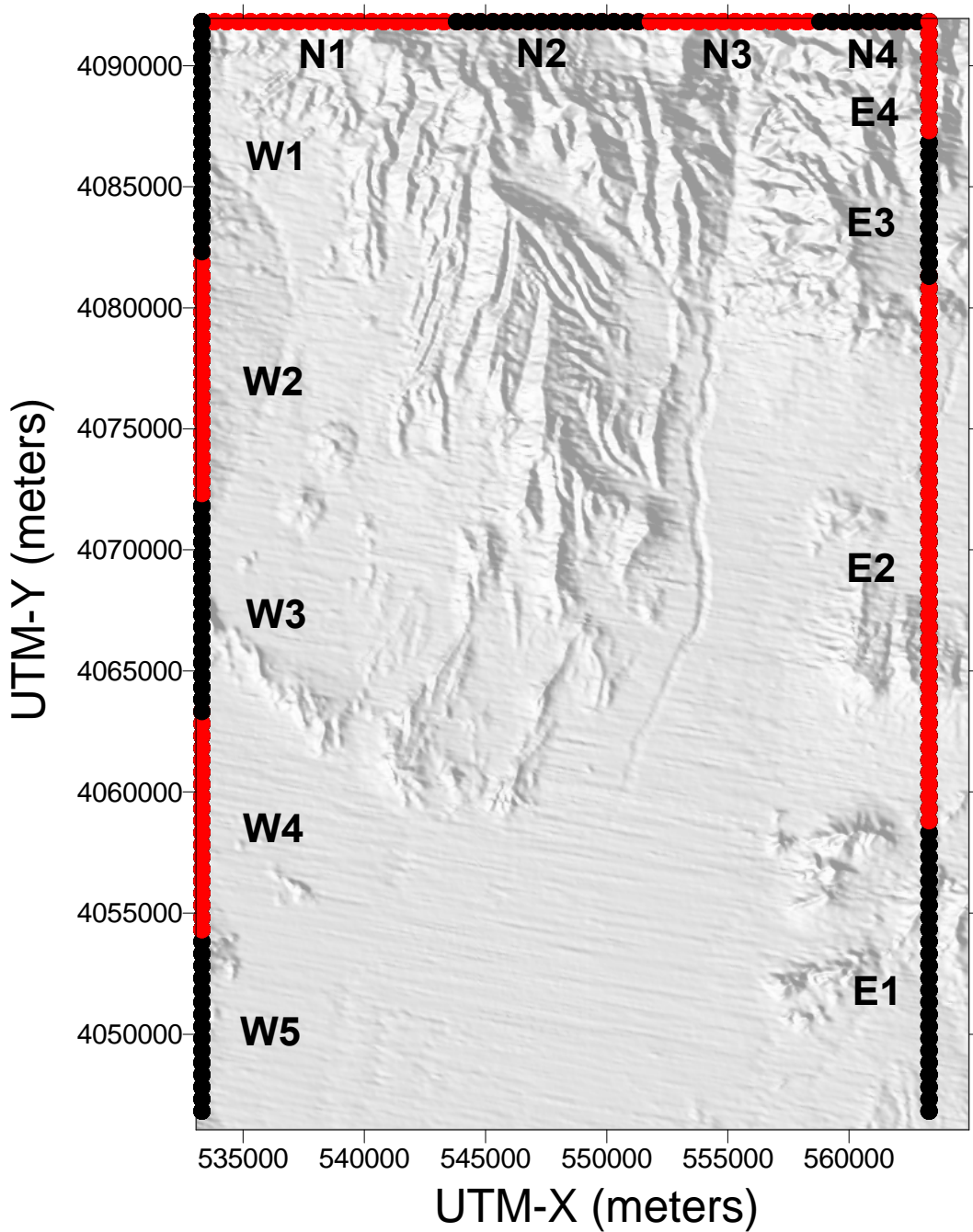
There is uncertainty associated with the groundwater fluxes simulated by the regional-scale SZ flow model. The source of this uncertainty includes limited characterization of the total groundwater budget through the regional flow system, uncertainty in the spatial distribution of recharge, and limited vertical resolution of the model (i.e., only three layers). Matching the values of simulated groundwater fluxes at the lateral boundaries of the site-scale SZ flow model implies the propagation of the uncertainties in the regional-scale flow model to the site-scale flow model. However, a relatively large degree of uncertainty in groundwater fluxes is incorporated into the stochastic realizations of radionuclide transport used in the TSPA-SR (Section 3.7.2).

As discussed in Section 3.3.6.2.2, the differences between the mass fluxes computed by the site-scale SZ flow and transport model and by the regional-scale flow model along certain segments of the site-scale SZ flow model boundary were included in the objective function used during parameter optimization. For this purpose, the north, east, and west boundary of the site-scale SZ flow model were divided into thirteen segments (Figure 3-24). The southern boundary was designated as a fourteenth boundary segment. As discussed in Section 3.3.5.3, constant head boundary conditions were established along the boundary of the site-scale SZ flow model. The mass flux computed by the site-scale model at the boundaries is determined by the head gradients and the permeability distribution along the boundaries.

A comparison of the boundary fluxes predicted by the calibrated site-scale SZ flow model and the regional-scale flow model is presented in Table 3-7. The mass fluxes of the two models match reasonably well. The total fluxes across the northern boundary computed by the regional-scale and site-scale models were $6.2 \times 10^6 \text{ m}^3/\text{yr}$ (5,040 acre-ft/yr.) and $5.4 \times 10^6 \text{ m}^3/\text{yr}$ (4,343 acre-ft/yr.), respectively, a difference of only 14 percent based on the regional-scale value. The fluxes computed for individual segments along the northern boundary by the two models are distributed somewhat differently; however, this difference is expected because the regional-scale and site-scale HFM models are different.

A comparison of the boundary fluxes computed along the east side of the site-scale SZ flow model domain indicates a good match. The match is particularly good along the lower thrust area where both models predict large fluxes across the model boundary. Both models also predicted small fluxes across the other boundary zones along the eastern boundary.

Fluxes across the western boundary computed by the regional-scale model and the site-scale SZ flow model do not match as well as those along the northern and eastern boundaries. The regional-scale model predicts a greater inflow along the western boundary than does the site-scale SZ flow model. The discrepancy in fluxes computed along the western boundary by the two models largely is the result of the different HFMs upon which the two models are based. For example, the newer HFM used as the basis for the site-scale SZ flow model includes a large amount of low permeability clastic rock along the W5 boundary segment that was not included in the regional-scale HFM. This zone of low permeability rock would not support the large flux predicted by the regional-scale model across this portion of the western boundary. As previously indicated (Section 3.3.6.2.2), the fluxes across western boundary segments were not included in the objective function used during calibration.



Source: CRWMS M&O (2000n, Figure 16)

Figure 3-24. Zones Used for Comparing Groundwater Fluxes between the Regional- and Site-Scale

Table 3-7. Groundwater Fluxes Computed from the Regional-Scale and Site-Scale Groundwater Flow Models

Boundary Zone	Regional Flux (kg/s)	Site-Scale Flux (kg/s)	Calibration Target
N1	-101.24	-60.009275	Yes
N2	-16.48	-33.442643	Yes
N3	-53.05282	-30.557419	Yes
N4	-18.41	-44.807523	Yes
W1	3.45	4.1663	No
W2	-71	-0.0071871	No
W3	-6.9	-0.0000078	No
W4	2.73	-0.0000223	No
W5	-46.99	-6.8542863	No
E1	-555.45	-553.85002	Yes
E2	-5.46	3.5334027	Yes
E3	2.65	16.4956192	Yes
E4	-3.07	16.8224586	Yes
S	918	724	No

Source: CRWMS M&O (2000n, Table 14)

NOTE: Negative values indicate flow into the site-scale model.

The southern boundary flux is the sum of the other boundary fluxes plus recharge. A comparison of the fluxes across the southern boundary computed by the regional-scale model and the site-scale SZ flow model indicates a relatively good match. The difference in the fluxes computed by the two models across the southern boundary is approximately 21 percent.

There are several differences between the regional-scale flow model and site-scale SZ flow model that influence the match between the boundary fluxes. The HFM used in the regional-scale model is older than the one used in the site-scale model. These differences appear to be responsible, at least in part, for the discrepancies in fluxes on the northern and western boundaries. The vertical resolution of the computation grid used in the site-scale SZ model is finer than that used in the regional-scale model: the site-scale SZ model uses 39 model layers, while the regional-scale model included only 3 model layers (Sections 2.3 and 3.3.5.1). As a result, the fluxes predicted by the site-scale model might depend more strongly on a few units than does the regional-scale model. This is important because many of the hydrogeologic unit permeabilities in the site-scale SZ model were constrained during calibration by field data (Section 3.3.6.3). The flux distribution predicted by the regional-scale model also is influenced by the use of permeability classes. Based on this approach, permeabilities associated with specific units were not assigned to individual nodes. Rather, the permeabilities are grouped into larger classes, which are then assigned to individual grid blocks.

3.4.3 Comparison of Measured Upward Hydraulic Gradient with Predicted Upward Hydraulic Gradient

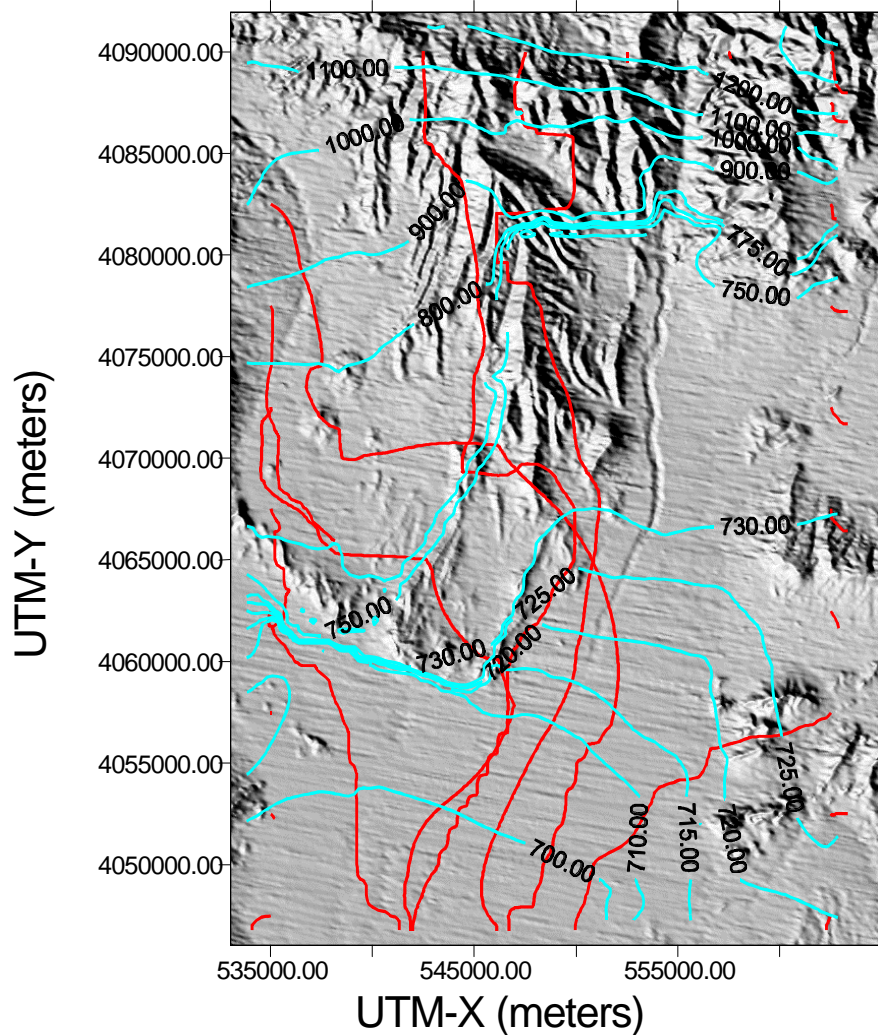
An upward gradient between the lower carbonate aquifer and overlying volcanic aquifers has been observed in the vicinity of Yucca Mountain (Section 3.1.1.2). Evidence of this upward gradient is obtained from the head measurement in well UE-25p#1, the only well that penetrates the carbonate aquifer. The measured head in the carbonate aquifer at this point is 751 m (2,467 ft). The measured heads in the overlying volcanic aquifers in the same area are approximately 730 meters. The site-scale SZ flow model predicts a head at well UE-25p#1 of 740 m (2,430 ft) (CRWMS M&O 2000n, Section 6.7.11). Thus, the upward gradient in this area is partially represented in the calibrated site-scale SZ flow and transport model.

The failure to fully represent the upward vertical gradient can be attributed, at least in part, to the constant head conditions established on boundaries of the model. As discussed previously (Section 3.3.5.3), a uniform, constant head was applied to each layer of the model at each boundary node. This specification does not allow vertical flow at the boundaries. However, vertical gradients may develop internally in the model domain in response to geohydrologic conditions. Although the upward gradient produced by the model is not as large as that indicated by field measurements, it nevertheless is sufficient to keep the simulated fluid pathlines downgradient from the potential repository in the shallow volcanic aquifers, a condition corroborated with geochemical data.

3.4.4 Comparison of Hydrochemical Data Trends with Calculated Particle Pathways

To provide further validation of the site-scale SZ flow and transport model, the flow paths predicted by the calibrated site-scale SZ flow and transport model (Section 3.3.7.2; Figure 3-21) were compared with those estimated using groundwater chemical and isotopic data (Section 3.1.1.1.3; Figure 3-3).

The particle tracking capability of the FEHM code was used to generate the flow paths predicted by the calibrated site-scale SZ flow and transport model. A detailed discussion of the development of these flow paths is presented by CRWMS M&O (2000n, Section 6.7). The flow paths were generated by placing particles along the western, northern, and eastern boundaries of the model at intervals of 5,000 m (16,400 ft) and tracing their downgradient movement. At each location along the boundaries, particles were placed at 600 m, 0 m, -600 m, and -1,200 m, (1970, 0, -1970, and -3940 ft, respectively) relative to sea level. The model was run to trace the path of these particles over one million years. The paths of particle movement for a starting elevation of 600 m (1970 ft) are shown in Figure 3-25.



Source: CRWMS M&O (2000n, Figure 10)

Figure 3-25. Paths of Particle Starting at 600 Meters Elevation

Particles follow a variety of flow paths depending on their initial location and the depths at which they originated (Figure 3-25; CRWMS M&O 2000n). Many of the particles exit the flow system at the nearest boundary, and some exit at locations not previously shown to have net outflows (Section 3.2.3). This occurs because the boundary zones included some individual cells that exhibit an outward flux at the model boundary. Some particle trajectories appear to terminate within the flow system, but these particles had not yet moved through the system within the one million years over which the particle paths were traced. The failure of these particles to exit the flow system after one million years suggests that stagnant conditions exist locally within these portions of the modeled flow system. Many particles exhibit complex trajectories in both map view and in three dimensions. These trajectories include an apparent crossing of some flow paths. A 3-D analysis of the particle paths indicates that the apparent crossing of flow paths in map view is a result of the different depths of the particle paths.

Most of the particles that originate along the boundaries in the northeastern part of the model domain exit through the eastern boundary (Figure 3-25). Only the particles that begin along the southern one-third of the eastern boundary near the Skeleton Hills exit the southern boundary. The particle trajectories also indicate that groundwater near the town of Amargosa Valley originates predominantly from flow entering from the east, rather than flow from the northeast as shown by path #4 on Figure 3-3. However, a particle originating east of Fortymile Canyon at the -1,200 m (-3940 ft) elevation also passes beneath Amargosa Valley (CRWMS M&O 2000n, Figure 13).

Particles along the northern boundary that do not immediately exit the flow system bifurcate around the east-west barrier in northern Yucca Mountain, which was used to simulate the large hydraulic gradient in that area. Particles originating immediately to the west of Fortymile Canyon flow around the western edge of the barrier and then eastward across Solitario Canyon and beneath Yucca Mountain before turning southwest in the Fortymile Wash area. Particles originating immediately to the east of Fortymile Canyon flow around the eastern edge of the barrier and, depending on the original elevation of the particle, either exit along the eastern boundary, terminate in southwestern Jackass Flats, or flow toward the southern boundary beneath Amargosa Valley (CRWMS M&O 2000n, Figures 10, 11, and 12, respectively). The particles originating toward the western end of the northern boundary flow beneath Crater Flat and southern Yucca Mountain along a somewhat more eastward trajectory than is indicated by paths #3 and #5 in Figure 3-3.

Some of the particles originating along the western boundary of the model (between coordinates 4,067,500 and 4,077,500 m) flow east-southeast beneath the southernmost portion of Yucca Mountain before turning southwest. The trajectory of these particles is more strongly eastward than the direction of flow indicated by paths #3 and #5 in Figure 3-3. The movement of the particles originating at 600 m (1,970 ft) (Figure 3-25) and 0 m (0 ft) elevation (CRWMS M&O 2000n, Figure 10) along the western boundary (at coordinate 4,062,500 m) agree with the direction of groundwater movement indicated by path #1 in Figure 3-3.

The trajectories of particles originating at the potential repository (Figure 3-25) can be compared to path #6 in Figure 3-3. Path #6 follows Dune Wash before turning southwestward near the intersection of Dune Wash and Fortymile Wash, whereas the particle trajectories shown in Figure 3-25 flow south across Dune Wash before turning southwestward. Nonetheless, the general direction of groundwater movement from the potential repository area predicted by the numerical model is in agreement with the flow direction determined from the hydrochemical and isotopic data.

In summary, some differences exist between the flow directions determined by the site-scale SZ flow and transport model and flow directions determined from an analysis of the hydrochemical and isotopic data. The most prominent difference is the stronger eastward component of flow in Crater Flat in the flow model compared to the flow directions determined in the hydrochemical analysis. The differences in the flow directions for Crater Flat could be due to the inability of the simple hydrochemical analysis to account for vertical mixing due to recharge or mixing between aquifers, the assumption in the numerical model that the rock in Crater Flat is isotropic with respect to permeability, or a combination of these factors. However, the most important flow

paths determined by the numerical model (i.e., the flow paths from the potential repository area) are similar to those estimated from the hydrochemical data.

3.4.5 Natural Analogues

The fourth of five elements comprising the postclosure safety case (YMP 1999) calls for an assessment of insights gained from the study of natural analogues. “Relevant information about the possible system performance of the site can be gleaned from analysis of natural processes that share characteristics with the potential repository system. These data may provide a degree of independent validation of the reasonableness of selected aspects of the assessments of repository performance” (YMP 1999). An understanding of the principal factors upon which the safety case is based can be strengthened through confidence-building using natural analogues.

Three factors were identified as important to the postclosure safety case for the SZ (Table 3-8) based in part on process model and TSPA sensitivity analyses. These factors serve as an organizing framework for discussing natural analogues that relate to each factor and for prioritizing the processes that need to be further bounded and quantified.

Table 3-8. Saturated Zone Factors Important to Repository Safety and Corresponding Natural Analogues

Factors Important to SZ Performance	Processes Included in the SZ Flow and Transport Model	Natural Analogues
Advective pathways Dispersion	SZ flow and transport Transverse dispersion Longitudinal dispersion	DOE sites (e.g., NTS, Hanford) Alligator Rivers
Sorption diffusion Matrix diffusion	Sorption coefficient in alluvium Sorption onto fracture coatings Matrix diffusion	NTS Palmottu Poços de Caldas Oklo
Colloid-facilitated transport	Colloidal transport in SZ	NTS Cigar Lake Poços de Caldas

3.4.5.1 Confidence-Building Using Natural Analogues

Because natural analogues can be used to test conceptual and numerical models over large distances and long time scales not possible with laboratory or field experiments, they are uniquely suited to building confidence in process-level models and are used as a means of model “validation.” Because no single analogue site is a perfect match for all of the processes at Yucca Mountain, sites with specific analogous processes are examined. An ideal analogue site for Yucca Mountain should satisfy as many of the following conditions as possible (DOE 1995): a known source term, a set of radionuclides similar to those important for safety considerations at Yucca Mountain, well-characterized site-specific data, geologic conditions similar to Yucca Mountain, identifiable boundaries of the system, and involving processes relevant to understanding performance of the potential repository at Yucca Mountain.

In addition to using natural analogues for building confidence in long-term model predictions, anthropogenic analogues may be used for testing models at shorter time scales. Anthropogenic

analogues, such as Hanford, Washington; the Idaho National Engineering and Environmental Laboratory (INEEL); and the NTS; provide possibilities for investigating physicochemical processes such as fracture and matrix interactions, sorption, and colloidal transport.

3.4.5.2 Natural Analogues to SZ Flow and Transport

Several analogue studies that have been conducted in saturated environments are reviewed in this section. These sites occur around the world (Figure 3-26), and all involve uranium ore and rare-earth (lanthanide) deposits in different types of host rock. Characteristic of these sites are the presence of redox fronts (e.g., Poços de Caldas, Oklo, and Palmottu) or weathering and periodic influx of oxidizing water (e.g., Alligator Rivers and Poços de Caldas). Although Cigar Lake involves reducing groundwater (which is not relevant to conditions at Yucca Mountain), localized oxidation may have resulted from radiolysis effects that could be useful. Anthropogenic analogues for SZ transport are discussed in Section 3.4.5.3.

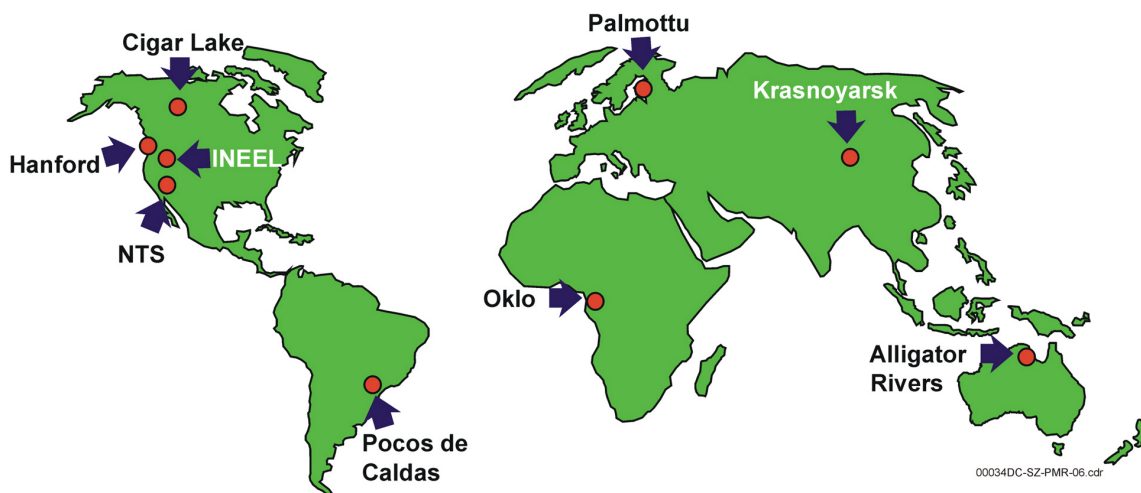


Figure 3-26. Natural Analogue Sites Used for Comparison with Yucca Mountain

3.4.5.2.1 Alligator Rivers, Australia

The Alligator Rivers Analogue Project was an investigation of radionuclide migration from the Koongarra secondary enriched-uranium deposit in the Northern Territory of Australia (Figure 3-26). The Koongarra ore body lies in two distinct parts composed of uraninite and pitchblende-bearing veins within a zone of steeply dipping, sheared quartz-chlorite schists and a fault that brings the ore body in contact with the Kombolgie sandstone. Leaching of the primary ore has resulted in the formation of four distinct zones: the unaltered primary ore consisting of uraninite and pitchblende, a uranium silicate zone formed by in situ alteration of the primary ore, a zone of secondary uranyl phosphate minerals that currently are being leached by groundwater, and a shallow dispersed uranium zone with the uranium in association with clays and iron oxyhydroxides (Isobe et al. 1992). Dissolved uranium is transported roughly from the uranium oxide zone at depth to the silicate zone, also at depth, then upward to the phosphate zone. The uranyl phosphate zone exists in the most oxidized weathered zone near the surface (Snelling 1980).

A dispersion fan has developed in the weathering zone where uranium has been mobilized. Secondary minerals are found as far as 50 m (164 ft) downstream from the ore body, with detectable concentrations of uranium-series nuclides for about 300 m (984 ft) downstream in the dispersion fan. The age of the dispersion fan is estimated to be 0.5 to 3.0 million years (Golian and Lever 1992).

The uppermost of the four mineral zones (above about 20 m [66 ft]) is the most weathered. Chlorite has been altered to kaolinite, minor smectite, hematite, and various iron oxyhydroxides. A transitional zone (20 to 25 m [66 to 82 ft] deep) of less weathered rock consists predominantly of vermiculite derived from primary chlorite (present below about 24 m [79 ft]) which is altered to kaolinite and iron oxides. Weathering of the quartz-chlorite schist produces different mineral assemblages according to degree of alteration. The migration behavior of nuclides at each depth is thought to be related to the chlorite alteration mineral assemblage (Ohnuki et al. 1990). The zone of lowest uranium concentration corresponds to the chlorite-rich zone; that of intermediate uranium concentration to the vermiculate-rich zone, and that of greatest uranium concentration to the kaolinite-rich zone. The highest uranium concentrations in the dispersion fan are associated with the lower part of the kaolinite-weathered zone (Ohnuki et al. 1990; Isobe et al. 1992).

Isobe et al. (1992) describe uranium redistribution associated with weathering. Uranium activity closely follows oxidation fronts in the slightly weathered zone and advances most readily along cracks and fissures in which percolation of oxidizing groundwater is most enhanced. Considerable flow occurs as fracture flow rather than as porous media flow. Uranium distribution in the most strongly weathered rocks depends only on the mineralogy present and is not controlled by the presence of fissures, as is the case for the more moderately weathered rocks. In the dispersion fan, processes that control the amount of radionuclides that are removed from the groundwater include equilibrium sorption; chemical incorporation into iron oxides, uranium minerals, or other crystalline phases; and recoil transfer of daughter products caused by alpha-particle decay.

Groundwaters are slightly acidic to neutral, oxidizing, relatively dilute, and the major ion chemistry is dominated by magnesium and bicarbonate. Waters from the weathered zone are not fully saturated with respect to a number of uranium-bearing minerals, consistent with the idea that the present groundwaters may be dissolving and dispersing uranium in the phosphate zone of the deposit.

Groundwater samples taken from boreholes at Koongarra were studied with respect to their colloidal contents. Boreholes closest to faults have the greatest variety of colloids. The colloids identified included particles of iron, kaolinite, chlorite, silica, lead, uranium, and titanium. All colloid samples were dominated by iron-rich particles, and uranium was only found in iron-rich species (Ivanovich et al. 1987). Low colloid concentrations (about 10^6 particles/L or less) and the absence of radionuclides in colloids outside the center of the ore body indicated that colloidal transport of radionuclides is minor at Koongarra (Payne et al. 1992).

In summary, Koongarra may represent a worst-case scenario for transport because of the near-surface exposure to oxidizing weathering conditions and monsoonal climate. The dissolution and reprecipitation of uranium in the dispersion fan is especially notable. Data

associated with the rate of migration and pattern of dispersion in the Koongarra dispersion fan could be used to test models of SZ plume dispersion at Yucca Mountain.

3.4.5.2.2 Poços de Caldas, Brazil

The Poços de Caldas caldera in Brazil (Figure 3-26) was the focus of a natural analogue study involving the Osamu Utsumi mine, which is a uranium ore body with subsidiary thorium, zirconium, and rare-earth element (REE; i.e., lanthanide) enrichment; and Morro do Ferro, which is a thorium and REE ore body with subsidiary uranium. The Osamu Utsumi uranium mine is known for its well-developed redox front within the uranium ore.

Osamu Utsumi is an open pit mine that consists of an upper weathered zone (laterite soil, top 40 m [130 ft]) that is completely argillized, depleted in silicon and potassium, and enriched in alumina. The underlying oxidized zone is approximately 150 m (500 ft) thick and consists of alternating areas of oxidized and reduced bedrock. The reduced zone consists of essentially altered phonolites (62 percent potassium-feldspar, 37 percent clay minerals with accessory pyrite, fluorite, and barite). The primary mineralogical difference between the oxidized and reduced rocks is the presence of pyrite in the reduced rocks (Smellie et al. 1989).

Primary mineralization mostly is low-grade and dispersed throughout the rock. The redox front generally is sharp, but irregular in profile as it follows the dips of faults and fractures along which oxidizing waters have penetrated. At the redox front, uranium mineralization occurs in the form of pitchblende nodules several centimeters across. The mine has been excavated to the level of the redox front.

Morro do Ferro is a hill that stands about 140 m (460 ft) above the surrounding plateau, and is 5 km north of the Osamu Utsumi mine. It has been weathered (to a greater degree than Osamu Utsumi) to a depth of at least 100 m (330 ft), and now the hill is composed of gibbsite, kaolinite, and illite, with additional veins of magnetite and manganese hydroxides that tend to form distinct layers. The thorium-REE ore occurs as elongated mineralized lenses that extend down the hill slope. Thorium and REE mineralization is very enriched, with up to 3 weight-percent thorium dioxide and up to 20 weight-percent total REE in some soils and weathered rocks (Waber 1991). No uranium mineralization is known at Morro do Ferro.

Groundwaters in the Poços de Caldas area typically have low concentrations (less than 1 mg/L) of colloids (Miekeley et al. 1989). Most of the colloids are composed of iron and organic species. Only minor amounts of uranium are associated with colloids, but thorium and REEs are transported by the colloids. The suspended particle concentration is 5 to 10 times greater at Morro do Ferro than at Osamu Utsumi, but there appears to be little thorium transport at Morro do Ferro, either by colloids or in solution. Groundwater at Morro do Ferro is lower in most major- and trace-element concentrations than groundwater at Osamu Utsumi (Miekeley et al. 1989). However, high concentrations of manganese in groundwaters are an exception and result from the presence of nodular manganese-oxides.

The groundwaters at Osamu Utsumi have high concentrations of uranium (up to 10 mg/L), whereas those from Morro do Ferro are lower (Miekeley et al. 1991). Thorium-232

concentrations are low in groundwaters from both sites (less than 0.1 µg/L) but occasionally are higher (up to 100 times) in surficial waters with abundant humic compounds or sulfate.

The groundwaters in the Poços de Caldas area have a potassium-iron-sulfate composition because of the weathering of the altered, mineralized, potassium-rich rocks (Nordstrom et al. 1990). Also, relatively high concentrations of barium and sulfate detected in the groundwater from Osamu Utsumi may be important because microcrystalline barite can act as a scavenger for radionuclides. The groundwater flow at Osamu Utsumi is upward from depth, except for the upper 10 to 15 m (33 to 50 ft) where lateral surface flow predominates.

West et al. (1989) suggest that microbial activity may encourage immobilization of uranium instead of forming mobile colloids or dissolved uranium complexes. Microbial activity is important for the oxidation of pyrite and may be responsible for the mobilization and reprecipitation of uraninite at the redox front. At Poços de Caldas, microbes were found in all samples of core and groundwater, independent of depth (West et al. 1989). West et al. (1989) reported that microbes enhance the supply of oxidants from the rock mass and thereby accelerate the rate at which the redox front advances. This could explain the observation that the redox front is moving faster than would be expected simply on the basis of dissolved oxygen concentration.

The natural plutonium concentration in a centimeter-sized nodule was measured, and the plutonium/uranium ratio was consistent with a state of secular equilibrium with the matrix phonolite. Based on the plutonium/uranium ratio in the nodule, it appears that the two elements have resided (unfractionated and in the most highly uraniferous rock in the deposit) for the last 100,000 yr. Even if alteration has occurred more recently, the processes did not significantly fractionate plutonium from uranium (Chapman et al. 1991, pp. 37, 39).

The results of the colloid study suggest that the transport of radionuclides and other trace elements by particulate material in deep groundwaters does not play an important role in the geochemical processes of weathering, dissolution, and erosion of these ore deposits. The reason for this is assumed to be filtration of particulate material, which, even in the highly fractured and porous rocks of the Poços de Caldas plateau, seems to be an efficient process (Smellie et al. 1989).

Redox front morphology provides direct evidence of flow channeling in fractures and solute transport in the rock matrix as the key controls on the shape and movement of these fronts. A consistent picture emerged of slow front movement and solute transport over the front dominated by diffusion. The front plays an important role in retarding a wide spectrum of redox-sensitive trace elements. Lichtner (1996) demonstrated that the zonation of the redox front, characterized by a narrow gap (or leached zone) separating precipitation of iron oxide on the oxidized side of the front and uraninite nodules in the reduced zone, could be explained by oxidation of pyrite and diffusive transport across the front.

3.4.5.2.3 Oklo, Gabon

The Oklo uranium mine, located in southeastern Gabon (Figure 3-26), contains the only known examples of natural fission reactors. Fourteen reactor zones have been identified among three

uranium deposits in the Franceville Basin (Gauthier-Lafaye et al. 1989). The uranium deposits containing the natural fission reactors are located at the top of the basal sandstone-conglomerate unit (Gauthier-Lafaye et al. 1989).

Two grades of ore, associated with two different occurrences of uranium as pitchblende with rare coffinite, can be distinguished in the Franceville Basin. Low-grade ore contains 0.1 to 1.0 percent uranium oxide, and high-grade ore (greater than 1.0 percent) contains up to 10 percent uranium oxide (Gauthier-Lafaye et al. 1989). Low-grade ore is primary and more common. High-grade ore is secondary and occurs within the secondary porosity of fractured sandstones (Gauthier-Lafaye et al. 1989). The formation of the high grade ore is attributed to the remobilization of low-grade ore by oxidizing hydrothermal fluids, which transported the uranium along the faults, followed by precipitation within the fracture zones under reducing conditions. In places, the uranium ore in the secondary deposit is extremely enriched (up to 70 percent uranium oxide), and at the time of formation, a critical mass of uranium-235 formed and initiated natural fission reactions. Because of the high uranium-235/uranium-238 ratio (3.5 percent) that was present 2 billion years ago (a concentration similar to uranium-235 enrichment for modern nuclear fuel), and the presence of an appropriate moderator (probably groundwater), a self-sustaining nuclear reaction was possible (Cowan 1976). Criticality was reached about $1,968 \pm 50$ million years ago and lasted intermittently for 0.1 to 0.8 million years, with reactions lasting for thousands of years (Holliger 1993).

Some of the fission products are the same radionuclides that might be emplaced in the potential radioactive waste repository (e.g., technetium, neptunium, plutonium, and americium). The fission products originally collected in the crystalline uraninite of the reactor zones as the nuclear reaction proceeded. Although little alteration of uraninite occurred subsequent to its formation, some of the fission products have escaped from the uraninite, probably by solid-state diffusion (Curtis et al. 1981), and some transport of radionuclides has occurred subsequent to their release from the uraninite.

Curtis (1986) postulated that increased temperatures and greater oxidizing conditions in the reactors led to the dissolution of technetium in hydrothermal fluids and to the migration of technetium to the surrounding rocks where it precipitated in response to declining temperature and more reducing conditions. Curtis et al. (1989) suggested that a portion of the fission-produced tellurium, ruthenium, palladium, technetium, cadmium, and molybdenum was retained essentially at the site of production and that the portion that escaped the uraninite crystals was completely removed from the reactor zone. Curtis et al. (1989) present evidence that neodymium and tin were removed from the site of production, but that they were retained within the reactor zone.

Because the reactions ended nearly two billion years ago, the short-lived radionuclides have decayed to more stable daughter radionuclides. According to Brookins (1978), plutonium, neptunium, and americium likely were retained within the reactor. Most geochemical observations at Oklo support these predictions to varying degrees. Curtis et al. (1989) conclude that the retention of fission products is related to their partitioning into uraninite or secondary mineral assemblages. Those fission products that partitioned into the secondary mineral assemblages were largely lost over time, pointing to the importance of small uraninite grains in controlling the chemical microenvironment.

3.4.5.2.4 Palmottu, Finland

The Palmottu natural analogue study is based on a small uranium-thorium deposit located in southwestern Finland (Figure 3-26). The deposit at Palmottu is hosted by Precambrian gneisses and migmatites whose protoliths were arkoses and graywackes. The deposit is up to 15 m (50 ft) thick, 400 m (1,300 ft) long, and extends to depths of 300 m (1,000 ft), but it is discontinuous in the form of uraniferous pegmatites and veins. The principal ore mineral is disseminated grains of uraninite, thinly coated with coffinite. The uranium is thought to have been derived during the latest stages of metamorphism, 1,700 to 1,800 million years ago, from late-stage granitic fluids of the nearby Perniö granite.

The ongoing natural analogue study has concentrated on processes, such as colloids and matrix diffusion, which may affect radionuclide migration and retardation in fractured crystalline rocks under groundwater-saturated conditions. A major focus has been on understanding the redox control of the system and propagation of redox fronts. The groundwaters, measured in open boreholes, show a distinct layered zonation: the upper waters are oxidizing and the lower waters are slightly saline and reducing. The change in water composition and the redox front both occur at a depth of about 125 m (410 ft). The pH increases from 7.4 close to the surface, to approximately 9.0 at the bottom (195 m [640 ft]) of the borehole (Jaakkola et al. 1989). Tritium values also decreased with depth to below detectable limits, indicating a lack of meteoric water infiltration at depth. Uranium is contained in primary uraninite, coffinite, and monazite (thorium-bearing), and is associated with iron oxides and clay minerals in the more altered areas and as fracture coatings. Coffinite precipitated along fractures short distances (less than 1 m [3.3 ft]) from uraninite grains. Considerable dissolution of uraninite has occurred at all depths, regardless of the modern, measured oxidation potential. Jaakkola et al. (1989) suggest that the oxidation potential at depth was higher in the past, perhaps because of infiltration of meteoric waters to greater depths.

The concentration of uranium is higher in the oxidizing upper waters than in the lower, more reducing waters, even though the uranium concentration in the rock is greatest at depth (Valkiainen 1989). The opposite trend is observed with uranium in particulate matter. Most particulate matter in the upper 100 m (330 ft) contains little or no uranium, whereas uranium at depth is associated predominantly with particulate matter.

Sorption onto fracture coatings, particularly calcite, efficiently retards uranium transport in fractures, and high concentrations of uranium have been measured in calcite. Long retention time of uranium in calcite, determined by uranium-series disequilibrium measurements, has been recognized. The uranium-234/uranium-238 ratio in the dissolved fraction increases with depth from a value of nearly 1.0, whereas uranium-234/uranium-238 in the particulate fraction shows a slight (though less significant) decrease with depth. The uranium-234/uranium-238 ratios of extracted phases suggest limited mixing of groundwaters in the study area (Blomqvist et al. 1995).

3.4.5.2.5 Cigar Lake

The Cigar Lake uranium deposit in northern Canada (Figure 3-26) was studied as an analogue for a potential radioactive waste disposal repository under water-saturated, reducing conditions

located deep beneath the water table. However, radiolysis effects may have produced localized oxidizing conditions that would apply to oxidation of spent fuel at Yucca Mountain. This analogue also may be useful for understanding colloidal transport of uranium. The broad aims of this natural analogue project were to investigate the stability of uraninite as a natural analogue for spent fuel and to investigate the mechanisms that caused the retention of the radionuclides in the ore body, particularly the effect of colloids. The primary mineralization occurred 1,300 million years ago (Cramer and Smellie 1994).

Several major fractures cut the ore body and the clay envelope that surrounds the ore. These originally were features of the basement rocks but were reactivated after deposition of sandstone and formation of the ore. The uranium apparently was transported upward to the base of the unconformity along the fracture zone by hydrothermal solutions and deposited as uraninite at the unconformity when these solutions came into contact with groundwater in the sandstone. These hydrothermal solutions are responsible for the alteration of the sandstone surrounding the ore body.

According to Curtis et al. (1999), naturally produced plutonium and technetium migrated short distances, but they remained within the deposit. Only one event seems to have disturbed the system since its formation (Cramer 1995). Small, isolated pockets of remobilized uranium have been found in some of the steeply dipping fractures above and in the shield rocks directly beneath the main ore body. The age of this younger event has been estimated at between 320 and 293 million years, and most likely represents the temporary opening of fractures and faults in association with tectonic movement of the North American plate that allowed groundwaters to mobilize some of the uranium (Cramer 1995).

Migration of radionuclides from the deposit into the surrounding rocks has been limited by a combination of hydrogeological, mineralogical, and geochemical factors (Cramer 1986). First, the deposit is in a basal sandstone unit, which is the main local aquifer, and this unit has a much higher groundwater flux than the deposit itself. Second, the present fluids are reducing; Eh is estimated at -0.2 to $+0.2$ volts (Sunder et al. 1988). Consequently, there is little dissolution of the uraninite or of the daughter radionuclides. Third, the clay-rich zones surrounding the ore have relatively low hydraulic conductivities compared with the sandstone of the overlying aquifer (Cramer and Sargent 1994). This effectively seals the ore zone from bulk groundwater flow and filters out colloids during mass transport from the ore zone. In addition, the clay-rich rocks and hydrothermally altered sandstones are enriched in pyrite and marcasite, providing effective redox buffering in the undisturbed system (Sunder et al. 1988). Fourth, any radionuclides that dissolve and migrate away from the ore zone encounter a naturally sorptive mineralogical barrier in the form of the clay alteration zone (Cramer 1986).

Vilks et al. (1988) studied particulate and colloid matter in groundwater and showed that half or more of the uranium in the water is carried in suspension associated with particulate matter. Radiolysis of the groundwater within the ore zone may be the cause of locally oxidizing conditions causing formation of the iron-oxyhydroxides (e.g., goethite) at the top of the ore body, as well as the uranyl minerals reported by Fayek et al. (1997). Perhaps because of absorption onto amorphous iron-silicon-hydroxides at the interface of the ore and clay, uranium concentrations in the surrounding sandstone are depleted with respect to the ore body water.

Also, the filtration of particulate matter by clay minerals probably plays a role in reducing groundwater uranium concentration (Vilks et al. 1988).

3.4.5.3 Anthropogenic Analogues of Saturated Zone Flow and Transport

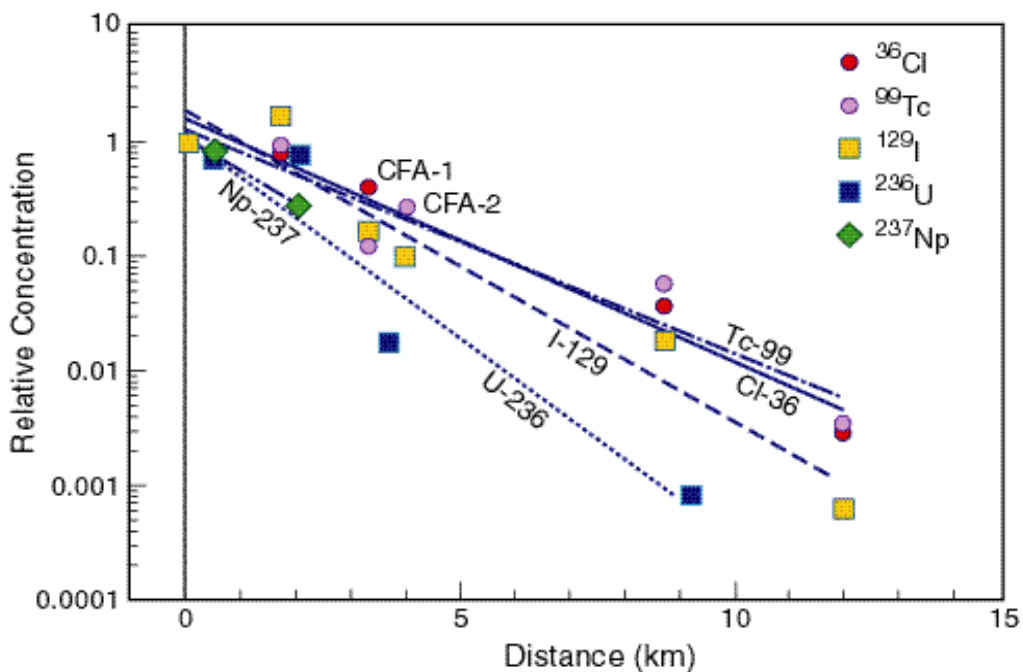
The purpose of investigating anthropogenic analogues is to obtain a better understanding of migration over shorter time scales than is amenable to study by natural analogues. In this section, radionuclide transport at INEEL, Hanford, and the NTS is discussed, as is the potential applicability of future investigations of selected radionuclide plumes in Russia as anthropogenic analogues.

3.4.5.3.1 Idaho National Engineering and Environmental Laboratory

One of the facilities at the INEEL that can provide a potential anthropogenic analogue site is the Idaho Chemical Processing Plant (ICPP). The ICPP was designed principally to recover highly enriched uranium (≥ 93 percent uranium-235) from different fuel types used in naval propulsion, research, and test reactors. From 1952 until 1984, low-level radioactive waste was discharged from the ICPP directly to the Snake River Plain by means of an injection well and seepage ponds. Over time, a suite of radionuclides has been measured in the aquifer, including hydrogen-3, chlorine-36, strontium-90, cesium-137, iodine-129 and isotopes of plutonium. Beasley et al. (1998) reported the first measurement of long-lived radionuclides (technetium-99, uranium-236, and neptunium-237) in the aquifer and downgradient changes in concentration during water transport through fractured basalt. Their study showed that chlorine-36 and technetium-99 behave conservatively during transport, while iodine-129, uranium-236, and neptunium-237 were retarded. The mobility of technetium-99 is sensitive to the redox state of groundwater.

The ICPP is located east of the Big Lost River, in the south-central part of the INEEL. Beasley et al. (1998, p. 3875) reported that water in the Snake River Plain aquifer is unconfined, with the highly fractured tops of basalt flows leading to high hydraulic conductivities. Beasley et al. (1998, p. 3876) further state that the calculated residence time of water in the Snake River Plain is 55 to 82 yr., although water travel times within different parts of the aquifer, from recharge to discharge points, are estimated between 12 and 350 yr.. Groundwater flow is from the northeast to the southwest, and depth to groundwater varies from about 60 m (200 ft) at the northern site boundary to about 275 m (900 ft) at the southern site boundary. Beasley et al. (1998, p. 3876) report that the average hydraulic gradient across the INEEL is about 2 m/km (11 ft/mi.), and water travel times between the ICPP and the southern site boundary have been estimated at 2 m/day (6.6 ft/day).

Radionuclides were sampled from 8 to 23 groundwater monitoring wells at INEEL, located 0 km (0 mi.) to 12 km (7 mi.) from the ICPP, in 1991, 1992, and 1994. Activity concentrations were measured for chlorine-36, technetium-99, uranium-236, iodine-129, and neptunium-237. To determine the relative mobility of these radionuclides, individual radionuclide activities in wells near the ICPP were normalized to those at a distance (Figure 3-27). The similarity between chlorine-36 and technetium-99 suggests that these radionuclides behave conservatively in the fractured basalt and that the decrease in concentration occurs as a result of dilution or dispersion (Beasley et al. 1998, p. 3880). Iodine-129 is attenuated, and neptunium-237 and uranium-236 are even more attenuated. Because none of these radionuclides were routinely monitored in low-level waste streams discharged from the ICPP, the possibility cannot be excluded that the relationships (Figure 3-27) could have arisen from variable discharge rates over time. However, Beasley et al. (1998) point out that even though the absolute amounts of radioactivity probably varied over time, the ratios of radionuclides in the discharges probably were consistent in order not to affect the composition of radioactivity in the waste streams.



Source: Adapted from Beasley et al. (1998, p. 3879)

NOTE: For chlorine-36, technetium-99, and iodine-129, the values are normalized to their concentrations in well-57, whereas uranium-236 and neptunium-237 concentrations are normalized to well-123.

Figure 3-27. Decrease in Relative Concentrations of Radionuclides in the Snake River Plain Aquifer with Distance from the Idaho Chemical Processing Plant

The INEEL site provides an anthropogenic analogue for testing models describing flow and reactive transport through fractured rock, as well as the interaction between fractured and nonfractured stratigraphic layers. Both of these features are important for modeling the potential Yucca Mountain repository. Characteristic features such as fracture flow and ponding on stratigraphic layers of low permeability are present at INEEL and Yucca Mountain. However, the fractured basalt at INEEL has distinctly different properties compared to fractured tuff at Yucca Mountain. For example, the basaltic flows at INEEL are interbedded with sedimentary deposits several meters thick. As such, characteristics of transport through fractured basalt at INEEL may be different than those at Yucca Mountain. However, the INEEL site provides a useful test area for predictive models such as those needed to evaluate the potential repository at Yucca Mountain.

3.4.5.3.2 Hanford Effluent Treatment Facility

The Hanford Effluent Treatment Facility (ETF) was selected as an anthropogenic analogue for modeling studies of radionuclide migration in the SZ at Yucca Mountain. The ETF is a combined treatment plant and disposal facility where waste streams resulting from various cleanup activities are treated and discharged into the UZ. The treated effluent migrates through the soil to the water table. The first detection of tritium in groundwater monitoring wells occurred in July 1996, roughly one year after operations commenced at the site. The plume emanating from the ETF site is well characterized and provides an opportunity for studying the transport of nonreactive and reactive groundwater constituents (Barnett et al. 1997). Migration of the tritium plume has been modeled using the CFEST computer code (Barnett et al. 1997), enabling a comparison between this model and the FEHM code (Zyvoloski et al. 1997a) that was used for modeling flow and transport in the SZ at Yucca Mountain.

3.4.5.3.3 Nevada Test Site

The 0.75-kiloton Cambric underground nuclear test was conducted in 1965 in tuffaceous alluvium 73 m (220 ft) below the water table (Hoffman and Daniels 1981). Data from a field experiment initiated in 1974 at the Cambric site provide information on the inferred radionuclide transport rates through alluvium. Tests began after the cavity and chimney were predicted to be filled with groundwater to the predetonation static water level. It was assumed that tritium, plutonium, and uranium fission products would be present in the cavity and in the groundwater within the cavity, and that these could be used to study possible migration from the cavity (Hoffman and Daniels 1981).

The field study began with the completion of a well (RNM-2S) that was 91 m (300 ft) from the Cambric cavity, followed by drilling of a well (RNM-1) into the cavity itself. Solid and liquid samples were taken from well RNM-1 to determine the distribution of radionuclides between the solid material and the groundwater. Water was then pumped from the satellite well to induce an artificial gradient sufficient to draw water from the Cambric cavity through the surrounding rocks.

Approximately two years after pumping began, large amounts of tritiated water were found in water from well RNM-2S, signaling the arrival of water from the Cambric cavity region. After almost six years of pumping, the tritium concentration in the pumped water reached a maximum

(Hoffman et al. 1977). By the end of September 1984, about 60 percent of the initial tritium inventory had been pumped out through well RNM-2S.

Other radionuclides also have been measured in water from well RNM-2S, including chlorine-36, krypton-85, ruthenium-106, and iodine-129. Strontium-90 and cesium-137 were not detected in water from well RNM-2S during the 10-yr experiment (Thompson 1986). A chlorine-36 pulse preceded the tritium pulse in well RNM-2S. Krypton was shown to be correlated with tritium but more strongly sorbed onto alluvium than tritium (Thompson 1986). Ruthenium-106 was detected in well RNM-2S water and is unretarded in the alluvium. Iodine-129 arrived at well RNM-2S sooner than tritium.

The Cheshire event took place in 1976. Detonation occurred at a depth of 1,167 m (3,829 ft), approximately 544 m (1,785 ft) below the water table in fractured rhyolitic lavas of Pahute Mesa. Water was obtained from two wells, one inside the Cheshire experimental site and the other 300-m (985-ft) away. Tritium, krypton, strontium, cesium, antimony, cobalt, cerium, and europium were detected in the pumped water, and all of the cobalt, cerium, and europium were associated with colloids in samples from both locations. Buddemeier and Hunt (1988) maintained that the presence of colloidal radionuclides outside the cavity indicates radionuclide transport on colloids.

The Benham test was detonated in 1968 at a depth of 1,402 m (4,600 ft) below the water table. In a recent field test, plutonium was measured in groundwater at the NTS ER-20-5 wells at a maximum activity concentration of 0.63 pCi/L (Kersting et al. 1999). The ratio of plutonium-240 to plutonium-239 indicates that the plutonium originated at the site of the Benham test, a distance of 1.3 km (0.81 mi.) from the wells. Therefore, the inferred minimum rate for plutonium migration at the NTS is 1.3 km (0.81 mi.) in 28 yr. (46 m/yr. [151 ft/yr.]). The plutonium was associated with colloidal material consisting mainly of clays, zeolites, and silica (Kersting et al. 1999). It is not likely that the plutonium was transported by prompt injection or that the soluble fraction migrated along fast flow paths. Colloidal transport is a possible mechanism for plutonium migration because colloidal transport of radionuclides was observed at the Cheshire site. However, stability arguments limit the amount of colloids in suspension. The association of plutonium in colloidal form at the NTS indicates the need to incorporate the colloidal transport mechanisms into transport process models and PA calculations for radionuclide releases at Yucca Mountain.

3.4.5.3.4 Russian Sites

Deep injection of liquid radioactive waste into confined geologic units was a frequent disposal methodology in Russia. Leakage from the confining unit has taken place at the deep injection site of Krasnoyarsk-26. The disposal setting at Krasnoyarsk provides an opportunity to investigate plume dispersion in fractured biotite gneiss. It also provides an opportunity to observe the effects of short-term (decades) of radioactivity-caused thermal effects on mineralogy in the injected medium.

3.4.5.4 Relationship of Analogue Studies to the Yucca Mountain Conceptual Model

The natural and anthropogenic analogue studies reviewed here have been confined to qualitative or semi-qualitative analysis, rather than detailed numerical studies. They may be used to place bounding conditions on the importance of various processes under different environmental conditions. A number of the analogue studies, either directly or indirectly, support confidence in modeling these processes over the long time spans required for the TSPA for the potential Yucca Mountain repository. The conceptual model for transport of radionuclides at Yucca Mountain involves processes such as advection through fractured tuff and alluvium, dispersion, colloid transport, and sorption, all of which have been studied in analogous sites.

Overall, these sites contribute to understanding migration processes at a detailed scale, in a variety of settings, and over long periods of time. They also allow placement of broad bounds on processes such as colloid transport and confirm the importance of fracture flow and sorption onto fracture-coating minerals such as calcite and hematite.

Underground nuclear tests have provided anthropogenic analogues for transport of radionuclides through fractures and alluvium, and by colloids. The INEEL analogue involves transport of radionuclides through fractured basalt and can aid in testing fracture models. The Hanford ETF analogue site provides the opportunity to test the YMP FEHM code (Zyvoloski et al. 1997a) against other codes.

3.4.5.5 Summary and Conclusions

The following conclusions can be drawn from the natural and anthropogenic analogue studies:

- At Oklo, under criticality conditions far more extreme than those anticipated at Yucca Mountain, only several percent of the uranium was estimated to have been mobilized. Technetium migrated short distances, whereas plutonium, neptunium, and americium were retained in the natural reactors. At Oklo, subsequent transport has been controlled by reducing conditions, sequestration within small uranium grains, and by hydrologic barriers.
- At Poços de Caldas, Chapman et al. (1991) showed that plutonium and uranium have reached secular equilibrium in a pitchblende nodule and that the two elements have resided, unfractionated, in a system closed to them, but not closed to groundwater circulation, for the last 100,000 yr. within the phonolite matrix. The implication from this observation (i.e. that plutonium and uranium may remain unfractionated in spent fuel of a repository) needs to be examined more completely.
- Colloidal transport of uranium was shown to be minimal at Koongarra, Cigar Lake, and Poços de Caldas, where filtration of colloids appears to be effective. The observation of rapid transport of colloids at the NTS must be tempered by knowledge that the natural system at the NTS has been disturbed by nuclear testing and by pumping.

- Fractures act as transport pathways and places of retardation at a number of the analogue sites. At Poços de Caldas, uranium has been transported small distances along fractures, and is sorbed onto iron oxide and calcite. Even at Palmottu, where migration of uranium has been extensive, sorption onto fracture coatings in the SZ has been identified as an important retardation mechanism. Advective transport along fractures has been identified as a more important transport mechanism than matrix diffusion in all of the SZ analogue sites, although matrix diffusion is a mechanism attributed to lead-loss in uraninites at Oklo and Cigar Lake (Janeczek and Ewing 1992), and plays a role in retarding uranium migration. In the YMP TSPA, transport models are not sensitive to fracture sorption, but the natural analogues suggest that fracture sorption enhances radionuclide retardation.
- Although the initial conditions and geologic medium are different at INEEL compared to Yucca Mountain, Beasley et al. (1998) provide a degree of confirmation of the conservative or retarding nature of a number of the same radionuclides as would be present in a Yucca Mountain repository (e.g., chlorine-36, technetium-99, uranium-236, iodine-129, and neptunium-237).

Taken in total, information from the analogue systems provides a qualitative validation of the conceptual model of radionuclide transport in the site-scale SZ flow and transport model. Differences in geochemical and hydrologic conditions between analogue sites and the Yucca Mountain system, as well as uncertainties in radionuclide source terms for analogue systems, generally preclude quantitative validation of the conceptual model of transport that has been developed for the SZ at Yucca Mountain. Differential migration of radionuclides resulting from sorption process at analogue sites provides an important confirmation that this aspect of the conceptual model operates at the field scale. Observations of colloid-facilitated transport of actinides in analogue systems validates the conceptual model for the site-scale SZ model that some small fraction of strongly sorbing radionuclides may be subject to transport by this mechanism. Evidence of dispersive and diffusive processes at analogue sites also provide general confirmation that the conceptual model of transport in the SZ at Yucca Mountain correctly incorporates these processes.

3.5 ASSUMPTIONS, USES, LIMITS OF THE SATURATED ZONE SITE-SCALE FLOW AND TRANSPORT MODEL

In any numerical simulation of a physical process using a mathematical model, assumptions are made and limitations apply. In the following sections, some of the assumptions and limitations of the site-scale SZ flow and transport model, as well as the parameters that are used as input in this model, are discussed. The list of assumptions presented here is not exhaustive. Many of the parameters used in the site-scale SZ flow and transport model are estimated using simple mathematical models. Other parameters may be estimated from data using methods that are biased and require extrapolation or corrections that carry assumptions. Assumptions used in estimating individual parameter values are not included in this section, but may be obtained from the AMRs. For example, stochastic parameters and their associated uncertainty distribution are presented by CRWMS M&O (2000o).

Taken in total, these data provide an appropriate and adequate basis for the conceptual model and numerical model of the site-scale SZ flow and transport system. The site-characterization information, along with inferences based on that information, support a conceptual model in which groundwater flow is controlled by the spatial distribution of geologic units and structural features. Site-specific data, together with regional-scale studies, suggest that a large fraction of groundwater flowing in the SZ enters the Yucca Mountain site area as lateral flow from the north with a small fraction contributed by recharge near Yucca Mountain. The conceptual model of radionuclide transport in fractured rocks includes the processes of advection, dispersion, matrix diffusion, sorption, and colloid-facilitated transport, as supported by site data. These components of the conceptual model are implemented numerically in the site-scale SZ flow and transport model, which represents the processes relevant to radionuclide migration from Yucca Mountain to the biosphere.

3.5.1 Groundwater Flow Processes

Assumptions used in modeling the groundwater flow process include those of the regional-scale models and the site-scale SZ flow and transport model, and those made in estimating parameters that are used as input to these models. For the following reasons, the effective continuum representation of fracture permeability is used:

- On the scale represented by the site-scale SZ flow and transport model, the site is well-represented by a continuum flow model. Pumping tests show evidence of fracture flow near Yucca Mountain (Geldon et al. 1997). Numerical modeling of fracture properties is done in one of two ways: discrete fracture models or effective continuum models. Discrete fracture models represent each fracture as a distinct object within the modeling domain. While a discrete fracture model might reproduce the flow system more accurately, flow modeling is conducted using a continuum model for the following reasons:
 - The exact characterization of hydraulic and geometric properties of fractures necessary to construct an accurate discrete fracture model does not exist for Yucca Mountain. A methodology for obtaining accurate fracture porosity in situ has not been developed, although some information may be obtained from well flow-meter surveys.
 - At Yucca Mountain, studies of the density and spacing of flowing intervals generally indicate that flow occurs through fracture zones (CRWMS M&O 2000k, Figure 15). The fractures or fracture zones are located in various geological units, and in most cases, no single zone dominates the flow through a well. Geochemical studies (CRWMS M&O 2000m) independently confirm a south-southeasterly trace of the particle flow path. For the limited set of wells (Luckey et al. 1996, Figure 11), flow appears to be carried through fracture zones separated by a few tens of meters rather than by a few individual fractures.
 - Part of the flow system is an alluvium unit for which flow and transport is appropriately modeled using a continuum model.

- The drawdown response to pumping at wells surrounding the C-wells Complex in multi-well pump tests indicates a well-connected fracture network in the Miocene tuffaceous rocks in this area (Geldon et al. 1998, p. 31).
- While the discrete fracture approach retains the discrete nature of the observed fractures within the model, the computational burden of calculating a flow solution using a discrete fracture model becomes extremely large even for relatively simple fracture models.

The following assumptions also apply to the TSPA-SR continuum modeling approach (CRWMS M&O 2000p):

- Estimates of discharge from the volcanic aquifer, elicited from the SZ expert elicitation panel, are applicable to the entire flowpath from the potential repository to the accessible environment. The estimates of specific discharge from the SZ expert elicitation primarily were based on data from hydraulic testing in wells in volcanic units and the hydraulic gradient inferred from water level measurements (CRWMS M&O 1998b, p. 3-8). The relative values of groundwater flux in the volcanic aquifer and along the flowpath farther to the south are constrained by the calibration of the site-scale SZ model. It is reasonable to extrapolate the degree of uncertainty in the absolute value of groundwater flux from the volcanic aquifer to the flowpath farther to the south.
- Horizontal anisotropy in permeability is adequately represented by a permeability tensor that is oriented in the north-south and east-west directions. For the purposes of the TSPA nominal case, horizontal isotropy and anisotropy are considered for radionuclide transport. The numerical grid of the site-scale SZ flow and transport model is aligned north-south and east-west, and values of permeability may be specified only in directions parallel to the grid. Analysis of the probable direction of horizontal anisotropy shows that the direction of maximum transmissivity is N 33° E (Winterle and La Femina 1999, p. iii), indicating that the anisotropy applied on the site-scale SZ model grid is within approximately 30° of the inferred anisotropy. Horizontal isotropy was assumed in the calibrated flow model. Inclusion of a 5:1 (north-south to east-west) horizontal anisotropy in the calibrated flow model resulted in head residuals that were less than the calibrated isotropic model along the transport path (CRWMS M&O 2000p, Figures 7 to 8).
- Horizontal anisotropy in permeability applies to the fractured and faulted volcanic units of the SZ system along the groundwater flowpaths that run from the potential repository to points south and east of Yucca Mountain. The inferred flowpath from beneath the potential repository extends to the south and east. This is the area in which potential anisotropy could have an important impact on radionuclide transport in the SZ. Given the conceptual basis for the anisotropy model, it is appropriate to apply anisotropy only to those hydrogeologic units that are dominated by groundwater flow in fractures.

- Anisotropy in permeability represents an alternative conceptual model of groundwater flow at the Yucca Mountain site. Sufficient uncertainty in the analysis of horizontal anisotropy exists to warrant consideration of two possible conceptual models: one with anisotropy and one without anisotropy (i.e., isotropic permeability).
- Current groundwater flow conditions in the SZ system are at steady state. A steady-state model of the flow conditions is used to reflect the assumption that a steady-state representation of the SZ system is accurate. Studies by Luckey et al. (1996, pp. 29 to 32) indicate that there are no long-term consistent trends in the data from wells at Yucca Mountain. Some individual wells show a positive trend in potentiometric level, but the nature of the hydrographs for these wells indicate that the rise in potentiometric levels is likely due to recovery from the drilling process which pumped the wells dry (Luckey et al. 1996, pp. 20 to 32). These conclusions are based on data collected over a period of a few years. There exists the possibility of slowly increasing potentiometric levels, not noticeable over a time period of a few decades, but large over hundreds or thousands of years. Such a trend would require a “forcing” physical effect such as an increase in precipitation or a geophysical mechanism. No such mechanisms have been identified (USGS 2000c). The convolution integral method has been extended to incorporate multiple steady-state flow conditions for alternative climate states (CRWMS M&O 2000p, Section 6.4.1).
- Changes in the water table elevation (due to future climate changes) will have negligible effect on the direction of the groundwater flow near Yucca Mountain. This assumption has been studied in regional-scale (D’Agnese et al. 1999) and subregional-scale (Czarnecki 1984) flow models. These studies found that the flow direction did not change significantly under increased recharge scenarios. The studies were based on 2-D confined aquifer models that did not take into account the free surface boundary at the water table or the saturation of geological units that currently are in the UZ overlying the present-day SZ. These UZ tuffs generally have a lower permeability than those in the SZ, and as such, UZ units are not likely to introduce faster flow paths.
- Future water supply wells that might be drilled near Yucca Mountain (including outside the proposed regulatory boundary) will have a negligible effect on the hydraulic gradient. This assumption, however, is not appropriate for water levels at the southern boundary of the site-scale SZ flow and transport model (in the Amargosa valley) that currently show the effect of well pumpage (Luckey et al. 1996, p. 41). It is assumed that future pumpage will not cause further alteration of the water table.
- Possible effects due to temperature gradients and heat transport are assumed to be negligible. Heat transport can affect flow modeling through the temperature dependence of fluid viscosity and density.

3.5.2 Radionuclide Transport Properties

Radionuclide transport is modeled using a particle tracking methodology (CRWMS M&O 2000j). The 3-D particle tracking model assumes transport along streamlines and takes into account advection, dispersion, sorption, and matrix diffusion. The particle tracking model is

semianalytical in nature and has been developed to include anisotropic structures. Modeling transport using particle tracking has some advantages over numerical solutions of an advection-dispersion equation. Two of these advantages include less numerical dispersion and the ability to model plumes on a sub-grid block scale. Disadvantages are that computations of concentration may require a large number of particles and that particles may diffuse into zones of low advection requiring a very long time to exit. Assumptions of the transport model are:

- On the scale represented by the site-scale SZ flow and transport model, the site is well-represented by a continuous flow and transport model. In particular, the specific discharge field computed by the FEHM flow model (Zyvoloski et al. 1997a) represents the specific discharge averaged over grid cells that are 500 m (1,640 ft) long. The specific discharge field is determined by the grid discretization and the scale of spatial heterogeneity of the underlying permeability field. Possible long (more than 500 m [1,640 ft]) high-permeability conduits would not be represented accurately by the present transport model because the computed discharge in the present model is based on blocks of 500 m (1,640 ft). The possible existence of relatively long, high-permeability structural features with a north-south orientation is explicitly incorporated in the site-scale SZ flow and transport model through the inclusion of horizontal anisotropy. Within the Yucca Mountain flow system, it is recognized that most groundwater flow occurs in fracture zones. This fact is recognized in transport modeling by assuming that all flow occurs through “flowing intervals” that occupy a small sub-volume of each grid block. Spatially varying transport velocities, used in the particle tracking model, are computed using the flowing interval porosity in fractured units. In the valley-fill alluvial aquifer, transport velocities were computed using the effective porosity, consistent with a porous media conceptualization for this area.
- The convolution integral method is appropriate for scaling transport to account for increasing mass flux in response to changes in the future climate. An assumption inherent to the convolution integral method is that the system being simulated exhibits a linear response to the input function. In the case of solute transport in the SZ system, this assumption implies, for example, that a doubling of the input mass flux results in a doubling of the output mass flux. This assumption is valid for the site-scale SZ flow and transport model because the underlying transport processes (e.g., advection and sorption) are linear with respect to solute mass. The method of scaling solute mass breakthrough curves for climate change is not an exact representation of the matrix diffusion process, but it does provide a reasonable approximation within the context of the ranges of uncertainty for underlying stochastic parameters.
- Fractures are equally spaced, smooth, and have constant aperture. The numerical representation of matrix diffusion assumes equally spaced, smooth, constant aperture fractures. An important question is whether matrix diffusion is modeled adequately by a parallel fracture model. Radionuclide transport depends on the fracture (flowing interval) porosity, the flowing interval spacing, and the effective diffusion coefficient, and values of these parameters were estimated from flow-meter data taken from wells near Yucca Mountain (CRWMS M&O 2000k) and laboratory data. Fluid velocity in a single fracture may be computed from fracture porosity measurements and the specific discharge found in the site-scale SZ flow model, under the assumption that a flowing

interval is represented by a single fracture and that no flow occurs in the matrix. The assumption that the fracture aperture width is equal to that of a flowing interval tends to underestimate fluid velocity, while the assumption that no flow occurs in the matrix tends to overestimate the fluid velocity in the fracture.

- Fluid in the matrix of volcanic rocks is stagnant. This assumption is conservative from the perspective of the performance of the potential repository because if mass flows in the matrix, then the mass available for faster transport and flow velocities in the flowing intervals (fractures) is reduced. The assumption will not greatly affect concentration and integrated discharge computations when the matrix permeability is an order of magnitude or more below that of the fractures because radionuclide transport to the site boundary through the fracture network (flowing intervals) occurs much earlier than transport through the matrix. A difference of an order of magnitude or more in the permeability of volcanic rocks is supported by CRWMS M&O (1998a, Section 5.2).
- Linear sorption at equilibrium. The mathematical representation assumes linear sorption due to the large temporal and spatial scales involved in radionuclide transport. Furthermore, the low relative concentrations of radionuclides support this assumption (CRWMS M&O 2000r).

3.5.3 Use of the Site-Scale Model in Site Characterization Activities

Important processes that affect radionuclide transport in the SZ are advection, dispersion, matrix diffusion, and sorption. In addition to its use for TSPA, the site-scale SZ flow and transport model is used to integrate all available data and to guide additional site characterization. The model was used to estimate a band-width for potential travel paths from the potential repository to the proposed compliance boundary. The travel path estimate was used together with other data to locate the Alluvial Test Complex and other NCEWDP wells to characterize the alluvium along the flow path from the potential repository to the proposed compliance boundary, confirm the conceptual model for flow and transport in the alluvium, and to obtain flow and transport parameter values.

3.5.4 Modeling Limitations

The site-scale SZ flow and transport model is adequate for its intended purpose, which is to model groundwater flow and radionuclide transport from the potential Yucca Mountain repository to the site-scale model boundary under present day and potential future climate conditions. Here, adequate means that the transport model is an internally consistent representation of the SZ that is subject to considerable uncertainty due to assumptions and simplification inherent in groundwater flow and transport modeling. The important processes, and the sub-process models that address them, have been identified. Many processes are inherently uncertain and this uncertainty is handled through the use of stochastic realizations. The site-scale SZ flow and transport model is not appropriate for:

- Computing transport over short distances. Over short distances (less than 1 km [0.6 mi.]), transport likely is dominated by discrete fractures or fracture zones.

- Computing scenarios involving heavy well pumpage near Yucca Mountain. These scenarios violate the assumption of a steady state groundwater system and they might involve large changes to the water table.
- Computing short-term transient hydrologic conditions. The site-scale SZ flow and transport model is not appropriate for computing short-term transient hydrologic conditions because it has not been calibrated using transient pumping tests.
- Performing analyses of disruptive events. Disruptive events may have several effects on the hydrogeologic environment at Yucca Mountain, including altering the permeability field or causing transient changes to the water table. The analysis of disruptive events may require modifying the HFM, regridding, or modifying other sub-process models and parameters to account for transient changes to the water table.

3.5.5 Process Model Uncertainty

The site-scale SZ flow and transport model and its components are comprehensive and complex. The model was used by TSPA-SR to characterize flow and transport processes that operate in the SZ below Yucca Mountain (from the potential repository to the proposed compliance boundary). Limitations and uncertainties associated with the model and its components should be recognized. The accuracy and reliability of predictions from the site-scale SZ flow and transport model are critically dependent on the accuracy of estimated model properties to which the model is sensitive, other types of input data, and conceptual models of the hydrology and geology. These models are limited mainly by the current characterization of the SZ system (including the geological and conceptual models), the continuum modeling approach, steady state flow, and the available field and laboratory data.

Investigations have indicated that a large amount of variability exists in the flow and transport parameters over the spatial scale of the SZ flow and transport model domain. Even though considerable progress has been made in this area, the major remaining uncertainties in model parameters are:

- Transport properties including effective porosity in the alluvium
- Sorption coefficients for different elements in the alluvial and volcanic units
- Matrix molecular diffusion in different hydrogeological units for different radionuclides
- Dispersivities in volcanic and alluvial units
- Location of the transition zone where the flow path from the potential repository to the proposed compliance boundary transitions from volcanic to alluvial hydrogeological units.

All of these uncertainties have been addressed in this report. The stochastic parameter uncertainty distributions are developed from limited field and laboratory data, expert elicitation,

and literature surveys. These uncertainties are addressed in Section 3.7.1, Section 3.7.2, and CRWMS M&O (2000o).

3.6 SYNTHESIS OF SATURATED ZONE MODEL AND MODEL ABSTRACTIONS

In this section, the synthesis of SZ flow and transport data and process models for abstraction in TSPA analyses is described. The incorporation of additional information relevant to radionuclide migration into the site-scale SZ flow and transport model for TSPA simulations is discussed. This section also is used to document modifications to the site-scale SZ flow and transport model for the purpose of incorporating uncertainty in SZ groundwater flux and horizontal anisotropy in permeability. Abstraction methods for conducting TSPA simulations, including the convolution integral method, alternative climate states, dilution in the water supply of the critical group, and radionuclide decay chains are described.

3.6.1 Introduction

The site-scale SZ flow and transport model represents a synthesis of available data on the groundwater flow system at the Yucca Mountain site, as well as information from regional-scale studies of the SZ. Key information utilized in the construction of the site-scale SZ flow model includes a 3-D representation of the geology of the system (USGS 2000a), water level measurements in wells (USGS 2000b), pumping tests of the volcanic units (CRWMS M&O 2000n), hydrochemical data (CRWMS M&O 2000m), and simulations of groundwater flux from the SZ regional-scale flow model (CRWMS M&O 1999a). The calibration process for the site-scale SZ flow model provides an internally consistent representation of the SZ flow system that reproduces the key observations about the system.

Additional information on the characteristics of the SZ system relevant to contaminant transport is incorporated into the site-scale SZ flow and transport model for simulating radionuclide migration. Key information incorporated into the transport model includes sorption coefficients for sorbing radionuclides, flowing interval spacing and porosity, and matrix porosity in fractured volcanic units, effective porosity in alluvial units, dispersivity, and effective diffusion coefficient (CRWMS M&O 2000o). Additional data and inferences regarding colloid-facilitated transport of radionuclides are used in the site-scale SZ flow and transport model to simulate this process (CRWMS M&O 2000l, 2000o).

3.6.2 Results of Synthesis

The primary result of this synthesis is the site-scale SZ flow and transport model used for simulations of radionuclide transport in TSPA analyses. This model includes modification of the final calibrated flow model to accommodate variable parameter values for stochastic radionuclide transport parameters and consists of six alternative groundwater flow fields that incorporate uncertainty in groundwater flux and horizontal anisotropy. The site-scale SZ flow and transport model for TSPA also produces simulation results in the appropriate format for coupling the radionuclide transport results with other components of the TSPA analyses.

3.6.3 Analysis Approach to Saturated Zone Flow and Transport for Total Systems Performance Assessment Analyses

It is desirable to integrate detailed process-level modeling into TSPA analyses to incorporate site-specific information about the system represented by the process-level model. This may be accomplished by explicitly coupling the process-level computational model into the TSPA simulator or by abstracting the process-level model results for incorporation into the TSPA analyses. An abstraction approach is chosen for the implementation of SZ flow and transport in the TSPA-SR analyses, primarily because of the size and complexity of the site-scale SZ flow and transport model. In addition, an abstraction approach that largely captures the information that is provided by the site-scale SZ flow and transport model about system behavior is possible.

The site-scale SZ flow and transport model results are abstracted by performing radionuclide transport simulations that assume a constant, unitary radionuclide mass flux at the “upstream” end of the SZ. The resulting radionuclide mass breakthrough curves at the “downstream” end of the SZ basically contain all of the information about the model behavior for those source and receptor locations, assuming steady groundwater flow. These results are obtained by running the site-scale SZ flow and transport model for each stochastic realization and saving the results for later use by the TSPA simulator.

3.6.3.1 General Approach

The TSPA site-scale SZ flow and transport model is used to simulate unit breakthrough curves for radionuclides at the interface between the SZ and the biosphere. Radionuclide concentration is then calculated as the average concentration in the water supply that is defined for the hypothetical farming community in the biosphere.

Using the streamline particle tracking algorithm of the FEHM software code (Zyvoloski et al. 1997a), radionuclide transport is simulated directly for those radionuclides that are not the product of radioactive decay and ingrowth. The convolution integral method is used to simulate the time-varying radionuclide flux to the biosphere, based on these model runs and the UZ flow and transport model results. Transport of radionuclides that occur as the daughter products of radioactive ingrowth is directly simulated with the 1-D SZ transport model implemented in the TSPA simulator. Radioactive ingrowth is the generation of radionuclide mass from the decay of a parent radionuclide.

The approach used for SZ radionuclide transport in the TSPA-SR differs from the approach used in the TSPA-VA (DOE 1998b) in several ways. For the TSPA-SR, the SZ flow and transport model is used to simulate the unit breakthrough curves for radionuclide mass at the interface between the SZ and the biosphere. Radionuclide concentration is calculated as the average concentration in the water supply for the hypothetical farming community in the biosphere. For TSPA-SR, the 3-D site-scale SZ flow and transport model is used to simulate radionuclide transport directly for those radionuclides that are not the product of radioactive decay and ingrowth using the FEHM streamline particle tracking algorithm. In contrast, for TSPA-VA (DOE 1998b), the breakthrough curves of radionuclide concentration in the SZ were simulated directly with the SZ flow and transport model. For TSPA-VA, an abstracted 1-D SZ flow and transport model was used to simulate transport of all radionuclides to generate breakthrough

curves at the accessible environment. Use of the convolution integral method to simulate the time-varying radionuclide flux to the biosphere remains the same in the approach for TSPA-SR.

3.6.3.2 Total System Performance Assessment Three-Dimensional Flow and Transport Model

The calibrated site-scale SZ flow and transport model (CRWMS M&O 2000n) lays the foundation for the site-scale SZ flow and transport model for TSPA. As described in Section 3.4, the base case SZ model is a single calibrated steady-state flow model that assumes horizontally isotropic permeability within units and present-day climatic conditions. Other than particle tracking for the purpose of flowpath delineation, the base case model does not consider relevant transport parameters or phenomena.

As described by CRWMS M&O (2000p), the calibrated site-scale SZ flow model input files are modified for use in radionuclide transport simulations to include relevant radionuclide transport parameters and to perform simulations of radionuclide transport. Input files for radionuclide transport include incorporation of values for stochastic parameters that have been generated for 100 random realizations of the SZ system. The simulated water table and particle tracking pathways for the TSPA site-scale SZ flow and transport model with isotropic horizontal permeability are shown in Figure 3-21.

In addition to the relatively high degree of uncertainty in the radionuclide transport characteristics of the SZ system, there is uncertainty in the groundwater flow in the system. Uncertainties exist in the SZ groundwater flux and in the direction of groundwater flow downgradient from the potential repository. To evaluate the uncertainty in groundwater flux, three discrete cases were examined. These consist of the mean case (corresponding to the mean flux of the calibrated site-scale SZ flow model), the low case (mean flux times 0.1), and the high case (mean flux times 10). The flux multipliers and the corresponding probabilities for these cases are quantified based on the uncertainty distribution for specific discharge in the volcanic aquifer from the SZ expert elicitation (CRWMS M&O 1998b, Section 3.7.2). The analysis is provided in CRWMS M&O (2000p, Section 6.2.5). Uncertainty in the direction of groundwater flow along the flowpath from the potential repository is incorporated as alternative groundwater flow fields, with and without horizontal anisotropy in permeability (CRWMS M&O 2000o). The result of considering both types of uncertainty is six alternative groundwater flow fields (three flux-cases times two anisotropy-cases).

Implementation of the alternative groundwater flow fields is accomplished by establishing a steady-state solution of groundwater flow in the site-scale SZ model for each of the six cases. Small variations in the simulated heads exist among the six steady-state flow solutions (generally variations of less than 1 m [3.3 ft]). All six flow fields represent acceptable matches to measured water levels. The steady-state conditions for each of these cases are imposed as the initial conditions for the appropriate TSPA realizations of radionuclide transport. In addition, a separate set of input files for the site-scale SZ flow and transport model that incorporate modifications to the boundary conditions and values of permeability for each case are constructed. Each realization is assigned to the appropriate flow field based on the values of the stochastic parameters that represent uncertainty in groundwater flux and horizontal anisotropy (CRWMS M&O 2000p).

3.6.3.3 Abstraction of Radionuclide Transport

Several types of abstraction for TSPA analyses are discussed in this section. The convolution integral method is described with regard to incorporating results of the site-scale SZ flow and transport model in TSPA calculations (Section 3.6.3.3.1). An abstraction method for including the effects of climate change is described (Section 3.6.3.3.2). Assumptions used in the abstraction of radionuclide transport are discussed in Section 3.6.3.3.3. The approach for calculating the average radionuclide concentrations in the water supply of the hypothetical farming community containing the critical group (NRC 1998) is discussed in Section 3.6.3.3.4. A simplified 1-D abstraction of radionuclide transport for decay chains is described in Section 3.6.3.3.5.

3.6.3.3.1 Convolution Integral Method

As discussed in CRWMS M&O (2000p, Section 6.4.1), the convolution integral method is used in the TSPA-SR calculations to determine the radionuclide mass flux at the assumed interface of the SZ and the biosphere, 20 km (12.5 mi.) downgradient from the potential repository. This computationally efficient method combines information about the response of the system, as simulated by the site-scale SZ flow and transport modeling, with the radionuclide source history from the UZ to calculate transient system behavior. The most important assumptions of the convolution method are linear system behavior and steady-state flow conditions in the SZ.

The convolution integral method provides an approximation of the transient radionuclide mass flux at a particular distance downgradient in the SZ. This response is a function of the transient radionuclide mass flux from the UZ. This coupling method makes full use of detailed SZ flow and transport simulations for a given realization of the system, without requiring complete numerical simulation of the SZ for the duration of each TSPA realization. The two input functions to the convolution integral method are a unit radionuclide mass breakthrough curve in response to a step-function mass flux source as simulated by the SZ flow and transport model, and the radionuclide mass flux history as simulated by the UZ transport model. The output function is the radionuclide mass flux history downgradient in the SZ.

Radioactive decay is applied to radionuclide mass flux calculated with the convolution integral software code. The convolution integral method consists of numerical integration that accounts for the contributions to the outlet radionuclide mass flux from a series of time intervals. Because the travel time for each contribution to radionuclide mass flux is known, the loss of radionuclide mass (and consequent decrease in mass flux) during transport is calculated by first-order decay for that time interval.

3.6.3.3.2 Alternative Climate States

The effects of climate change on the transport of radionuclides in the SZ is incorporated in TSPA calculations by scaling the radionuclide mass breakthrough curves simulated for present climatic conditions (CRWMS M&O 2000p, Section 6.4.2). The scaling procedure is performed as part of the convolution integral method and assumes a proportional scaling of groundwater flux in the entire SZ system in response to wetter climatic conditions. This method treats the shift in climatic conditions as an instantaneous change from one steady-state groundwater flow condition

in the SZ to another steady-state, in a manner consistent with other components of the TSPA simulations.

Estimates of the scaling factors for groundwater flux in the SZ under alternative climatic conditions are based on simulations using the regional-scale SZ flow model (D'Agnese et al. 1999) and on results from the site-scale UZ flow model (CRWMS M&O (2000b)). Simulations using the regional-scale SZ flow model were conducted for the past-climate state that likely existed about 21,000 yr. ago. This climatic state approximately corresponds to the glacial-transition state, as defined for TSPA-SR calculations. An evaluation of the change in groundwater flux in the SZ near Yucca Mountain under past-climate conditions using the regional-scale SZ model indicates an increase in flux of approximately 3.9 relative to present-day climate condition simulations. The ratio of glacial-transition infiltration in the UZ model to the present-day infiltration is the same value as the estimate of increased SZ groundwater flux from the regional-scale SZ flow model (i.e., 3.9). This correspondence suggests that the UZ infiltration ratio provides a reasonable estimate of the flux ratio for the SZ. For monsoonal climatic conditions, the ratio of UZ infiltration to the infiltration for present-day conditions is 2.7. This value is applied to the SZ flux as well (CRWMS M&O (2000p, Section 6.4.2)). The effect of changes in groundwater flux is incorporated into the convolution method by scaling the timing of radionuclide mass breakthrough curves proportionally to the change in SZ specific discharge.

3.6.3.3.3 Assumptions of the Abstraction of Radionuclide Transport

There are several important assumptions in the use of the convolution integral method (CRWMS M&O 2000p, Section 5). Groundwater flow in the SZ is assumed to be in steady state. The site-scale SZ flow model is a steady-state model of the flow conditions (CRWMS M&O 2000n), reflecting the conclusion that a steady-state representation of the SZ system is accurate. This conclusion is supported by the lack of consistent, large-magnitude variations in water levels observed in wells near Yucca Mountain (Luckey et al. 1996, pp. 29 to 32). The transport processes in the SZ are assumed to be linear with respect to the solute source term (i.e., a doubling of the solute mass source results in a doubling of mass flux). This assumption is valid for the site-scale SZ flow and transport model because the underlying transport processes (i.e., advection, dispersion, diffusion, and sorption) are linear with respect to solute mass. In addition, the flow and transport processes in the UZ and the SZ are assumed to be independent.

It is assumed that the change in groundwater flow in the SZ from one climatic state to another occurs rapidly and is approximated by an instantaneous shift from one steady-state flow condition to another steady-state flow condition. In reality, even an extremely rapid shift in climatic conditions would result in a transient response of the SZ flow system because of changes in groundwater storage associated with water table rise or fall and because of the response time in the UZ flow system. The assumption of instantaneous shifts to new steady-state conditions would tend to be conservative with regard to radionuclide transport in the TSPA calculations. The progression of climate states in the 10,000 yr. following closure of the potential repository is from drier to wetter climatic conditions, and thus, from slower to more rapid groundwater flow in the SZ. By assuming an instantaneous shift to higher groundwater flux in the SZ, the simulations tend to overestimate the radionuclide transport flow rates during the period of transition from drier conditions to wetter conditions.

Groundwater flow pathways in the SZ from beneath the potential repository to the accessible environment are assumed not to be altered appreciably for wetter climatic states. Scaling of present-day groundwater flux and radionuclide mass breakthrough curves by a proportionality factor implies that only the groundwater flow rates are changed in the SZ system in response to climate change. This assumption is supported by the observation that the shape of the simulated potentiometric surface downgradient from Yucca Mountain remains basically the same under glacial climatic conditions in simulations using the SZ regional-scale flow model (D'Agnese et al. 1999, p. 30). Wetter climatic conditions and a rise in the water table directly beneath the potential repository would tend to place volcanic units that presently are higher in the stratigraphic sequence, at or just below the water table. These higher volcanic units (Prow Pass Tuff and Calico Hills Formation) have lower values of permeability than the underlying Bullfrog Tuff. Disregarding changes in groundwater pathways, which would be redirected into these lower-permeability units with a rise in the water table, generally is conservative from the perspective of radionuclide transport.

It is assumed that the entire mass of radionuclides crossing the 20-km (12.5-mi) fence in the SZ is captured by wells of the hypothetical farming community. This assumption implies that the total volumetric groundwater usage by the hypothetical community is large relative to the volumetric flow in the plume of contaminated groundwater in the SZ and that the flow path of the contaminant plume is close to the pumping wells. This assumption is justified on the basis of conservatism with respect to the analysis of performance of the potential repository. The total mass of radionuclides released to the biosphere for a given time period cannot be larger than the amount of radionuclide mass delivered by groundwater flow (for the nominal case).

3.6.3.3.4 Dilution in Water Supply

The hypothetical release of radionuclides from the SZ to the biosphere occurs by pumping of groundwater as the water supply for a future farming community in the nominal case of the TSPA-SR (CRWMS M&O 2000p, Section 6.2.4). Based on the proposed rule 10 CFR Part 63 (64 FR 8640), this hypothetical community is located along the groundwater flowpath in Amargosa Valley at a distance of 20 km (12.5 mi.) from the potential repository. Radionuclide concentrations in the water supply of the hypothetical farming community are calculated by assuming that all radionuclide mass is captured by pumping wells and that this mass is uniformly distributed in the total volume of groundwater used by the community. Complete capture of the radionuclide plume by groundwater pumping is a reasonable assumption, given the relatively large volumetric groundwater use of the hypothetical community. The assumption of complete capture also is a bounding, conservative approach. Although it reasonably may be expected that variations in radionuclide concentration would exist among the pumping wells in the community, redistribution of radionuclides by multiple pathways of radionuclide migration in the biosphere would tend to homogenize the dose among the critical group.

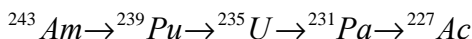
A detailed analysis of the groundwater use by the hypothetical farming community is presented by CRWMS M&O (2000c). The analysis is based on present-day groundwater use and agricultural practices of the residents in Amargosa Valley. The analysis does, however, consider potential differences between the characteristics of the present population of Amargosa Valley and the characteristics of the hypothetical future farming community. The assessment of groundwater use includes uncertainty in this parameter and presents an uncertainty distribution

for use in the stochastic realizations of the system for TSPA. The results of the analysis indicate a range of 1.79 to $2.99 \times 10^6 \text{ m}^3/\text{yr}$ (1,454 to 2,423 acre-ft/yr.) (CRWMS M&O 2000c, p. 5-5) for the expected value of total estimated annual groundwater use by the hypothetical farming community. Comparison with the total simulated groundwater flow across the southern boundary of the site-scale SZ flow model (approximately $23.5 \times 10^6 \text{ m}^3/\text{yr}$ [19,000 acre-ft/yr.] [CRWMS M&O 2000n]) indicates that the quantity of groundwater assumed to be used by the hypothetical community would be available in the SZ flow system.

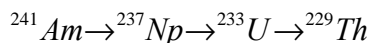
3.6.3.3.5 One-Dimensional Transport Model

The 1-D radionuclide transport model for TSPA-SR is used for simulating radioactive decay and ingrowth for four decay chains (CRWMS M&O 2000p, Section 6.5). This simplified model is required because the radionuclide transport methodology used in the 3-D site-scale SZ flow and transport model is not capable of simulating ingrowth by radioactive decay. Although it is not anticipated that the decay products from these radioactive decay chains are large contributors to the total radiological dose, regulations concerning groundwater protection may require explicit analysis of their concentrations in the water supply of the critical group. The results of 1-D transport modeling are used only for the daughter radionuclides. Although transport of the parent radionuclides also is included in the 1-D transport model, the results from the 3-D site-scale SZ flow and transport model are used for the parent radionuclides in the TSPA-SR simulations. The 1-D radionuclide transport model for TSPA differs from the site-scale SZ flow and transport model in that it is implemented directly in the TSPA model. The four simplified decay chains include the following:

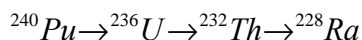
- 1) Actinium series:



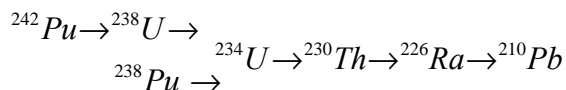
- 2) Neptunium Series:



- 3) Thorium Series:



- 4) Uranium Series:



The 1-D radionuclide transport model is implemented in the TSPA simulator as a series of “pipe” segments, in which the transport of all radionuclides in the decay chains occurs. Except for transverse dispersion, the same radionuclide transport processes that are simulated in the 3-D site-scale SZ flow and transport model (e.g., sorption, matrix diffusion in fractured units, and colloid-facilitated transport) are analyzed in the “pipe” segments. Neglecting the process of transverse dispersion is a conservative approximation, from the perspective of radionuclide dilution. Although strict consistency between the 1-D transport model and the 3-D site-scale SZ model is not possible, average groundwater flow and transport characteristics of the site-scale SZ model are used to define flow and transport properties within the “pipe” segments of the 1-D model. Average specific discharge along different segments of the flowpath is estimated

using the 3-D site-scale SZ flow model. The resulting values of average specific discharge are applied to the individual “pipe” segments in the 1-D transport model.

3.6.3.4 Coupling of Saturated Zone Flow and Transport with Other Components of Total System Performance Assessment Analyses

Coupling of the SZ flow and transport models with the upstream and downstream components to the natural system in the TSPA analyses is accomplished through the mass of radionuclides entering and leaving the SZ system. The mass of radionuclides leaving the UZ transport model at the water table during a time step in the TSPA analysis is transferred to the convolution integral abstraction of the site-scale SZ flow and transport model and to the 1-D SZ transport model. The radionuclide mass leaving the SZ flow and transport models during a time step is converted to a value of radionuclide concentration based on groundwater use in the biosphere component of the TSPA analysis. This process is discussed by CRWMS M&O (2000p, Section 6.2 and 6.3).

3.6.3.4.1 Unsaturated Zone Flow and Transport

The source of radionuclide contamination entering the site-scale SZ flow and transport model is specified as a point within each of four source regions beneath the potential repository. The point source is located at an elevation of 725 m (2,380 ft) in the nominal case, which is approximately 5 m (16 ft) below the water table over most of the area beneath the potential repository. The horizontal location of the point source in each of the four source regions varies stochastically from realization to realization, reflecting uncertainty in the location of leaking waste packages and transport pathways in the UZ. Radionuclide transport simulations with the site-scale SZ flow and transport model are performed using 1,000 particles, which are released at each of the four point source locations at the beginning of the simulation. Each particle represents an equal mass of radionuclide.

The radionuclide mass that reaches the water table from the UZ in the TSPA simulator is assigned to one of the four source regions. This radionuclide mass represents the source term used in the convolution integral method for that source region for a given time step. A point source of radionuclide mass from an entire quadrant of the UZ transport model is physically realistic for the situation in which contamination is coming from a single leaking waste package or in which a high degree of groundwater flow focusing occurs in the UZ flow system. Combining the radionuclide mass from a quadrant of the UZ transport model at later times, when multiple leaking waste packages contribute contamination, may not be physically realistic, but represents a conservative approximation from the perspective of performance of the potential repository.

The timing and hydrologic impacts of climate change are applied with the TSPA simulator in a consistent manner in the SZ and UZ. When the climatic state of the system shifts, the appropriate UZ flow field is applied to radionuclide transport in the UZ, and the lower boundary of the UZ (i.e., the water table) is changed (to higher levels for wetter climatic conditions). Simultaneously, the groundwater flux in the SZ is implicitly scaled to match the prevailing climatic state by scaling the radionuclide mass breakthrough curves for the present climatic state.

Climate change is imposed as an instantaneous change to the new steady-state groundwater flow conditions in the SZ and the UZ.

3.6.3.4.2 Biosphere

The breakthrough curves for the mass fraction of radionuclides delivered to the 20-km (12.5-mi) distance are simulated with the site-scale SZ flow and transport model by obtaining travel times from the FEHM code when particles cross a “fence” of nodes in the model grid. Three fences of nodes (corresponding to distances of 5 km, 20 km, and 30 km [3 mi., 12.5 mi., and 18.6 mi.]) are specified for the breakthrough curves. These fences of grid nodes are located at the prescribed distance from the southern corner of the outline of the potential repository and extend from the upper surface to the lower surface of the site-scale SZ model domain. The SZ groundwater flow pathway from beneath the potential repository extends in a generally southerly direction and all particles are “counted” as they cross the intervening fences of grid nodes. The model setup of the 1-D SZ transport model provides output of radionuclide mass at the exit of each “pipe” segment, and these segments are constructed to end at 5-km, 20-km, and 30-km (3-m, 12.5-m, and 18.6-mi) distances.

The contributions of radionuclide mass flux at the 20-km (12.5-mi) fence from the four source regions in the site-scale SZ flow and transport model are summed to obtain the total radionuclide mass flux for a time step in the TSPA simulator. Summing the values of radionuclide mass flux occurs following the convolution integral calculation. The mass flux of the daughter radionuclides from the 1-D SZ transport model is also included in the calculation at this point.

Radionuclide concentrations in groundwater are used in the TSPA analysis along with the biosphere dose conversion factors to calculate annual dose. The concentrations of radionuclides are calculated by dividing the radionuclide mass delivered to the biosphere per year for that time step by the total groundwater use per year of the hypothetical farming community.

3.6.3.4.3 Implementation with the GoldSim Software Code

Simulation of the entire potential repository and natural system is performed in the TSPA model with the GoldSim software code. The results of the site-scale SZ flow and transport model simulations consist of a “library” of unit radionuclide mass breakthrough curves. These breakthrough curves are contained in a set of files, each one of which includes the radionuclide mass breakthrough curves from all 100 realizations for a particular radionuclide and from a particular source region. The 100 realizations of SZ flow and transport correspond to the 100 realizations with the TSPA simulator. The parameter uncertainty definitions and distributions used to create the 100 SZ model realizations are included in the GoldSim input file for the TSPA simulator, guaranteeing consistency in parameter values with other components of the TSPA for each realization.

At each time step within the GoldSim simulation, the current climate state, and the radionuclide mass flux at the water table from the UZ for each of the radionuclides, at each of the four source-regions, are passed to the convolution integral software code. The convolution integral subroutine calculates the radionuclide mass flux for each of the four source regions at the 20-km (12.5-mi) distance for that time step based on the unit radionuclide breakthrough curves for that

realization (Figure 3-28). The radionuclide mass flux at the 20-km (12.5-mi) distance is then summed for the four source regions in the SZ for each radionuclide at that time step in the GoldSim simulation. The radionuclide mass flux of decay chain daughter products is taken from the 1-D SZ transport model, which is simulated directly in the GoldSim simulation.

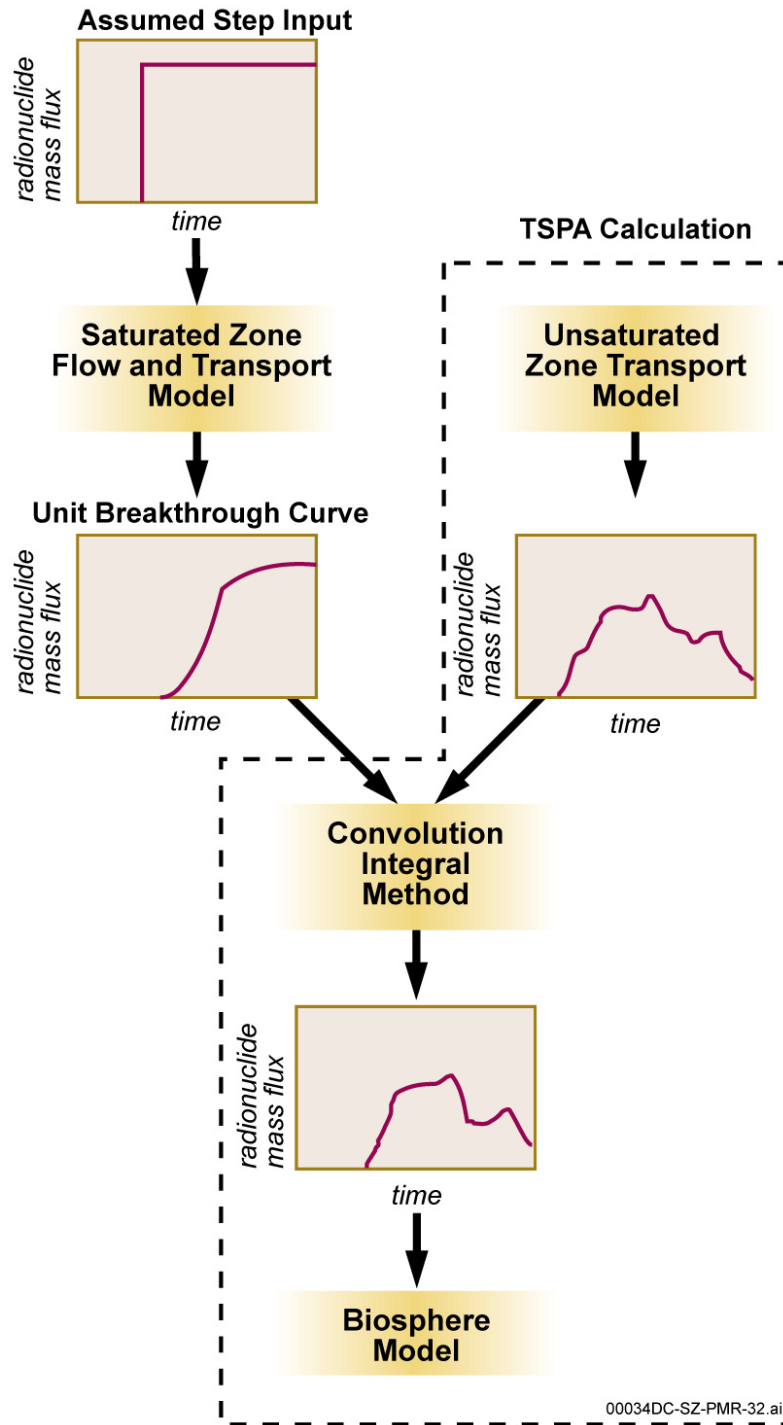


Figure 3-28. The Convolution Integral Method Used in Saturated Zone Flow and Transport Calculations for TSPA-SR

Calculation of radionuclide concentrations is performed with the GoldSim software code by dividing the total radionuclide mass flux by the volumetric groundwater usage of the farming community for each radionuclide. The groundwater usage of the farming community is a stochastic parameter that varies from realization to realization, but is constant through time for a given realization. The calculation of radionuclide concentrations is performed for each time step in the TSPA simulation.

3.7 SATURATED ZONE SITE-SCALE FLOW AND TRANSPORT NOMINAL CASE

For the nominal case of TSPA-SR, analyses of SZ flow and transport incorporate uncertainty in the SZ groundwater flow system and in the parameters relevant to the transport of radionuclides through the system. Uncertainty in groundwater flow is incorporated through the use of six discrete flow fields that consider uncertainty in the magnitude of groundwater flux and uncertainty in horizontal anisotropy in permeability. Multiple realizations of the SZ transport model are constructed using continuous uncertainty distributions for the parameters that define the transport characteristics of the SZ system.

3.7.1 Description of the Nominal Case

The nominal case of SZ flow and transport for the TSPA-SR explicitly incorporates many FEPs of the SZ system and includes others in an implicit fashion. Those FEPs that implicitly are incorporated primarily are captured in the range of uncertainty assigned to parameters varied in the stochastic analyses.

The most important features of the SZ system that explicitly are represented in the simulations are the geometry and variability in properties among hydrogeologic units in the subsurface. Of particular importance is the distinction between units consisting of fractured volcanic rock media and those that consist of porous alluvial media. In addition, numerous hydrologic features corresponding to faults and geologic zones are explicitly incorporated into the site-scale SZ flow and transport model as part of the calibration process (Section 3.3.6.3). The presence of faults and fracture zones that are not explicitly represented in the site-scale SZ flow and transport model and their potential impact on groundwater flow is implicitly included in the nominal case through consideration of horizontal anisotropy in permeability in the fractured volcanic units downgradient of the potential repository. The features of the nominal case are considered permanent, but uncertain, characteristics of the system that are not altered by the potential repository or by future events.

Release of radionuclides from the SZ to the biosphere through groundwater pumping by a hypothetical, future farming community is the event leading to the exposure of the critical group in the nominal case. The presence of the hypothetical farming community is permanent, and the community is located at a distance of 20 km (12.5 mi.) from the potential repository. The discharge of contaminated groundwater explicitly is included in the nominal case analyses to the extent that all radionuclide mass reaching the 20-km (12.5-mi) distance is captured in the groundwater supply of the farming community. Pumping by the hypothetical farming community is implicitly included because actual groundwater withdrawal is not simulated in the site-scale SZ model.

Climate change explicitly is included in the nominal case of SZ flow and transport for TSPA-SR. Increases in SZ groundwater flux for the monsoonal and glacial-transition climate states are included in the analyses. The impact of a rising water table on groundwater flowpaths in the SZ is not explicitly included in the SZ flow and transport model for the nominal case. The assumption that the transport pathways simulated by the TSPA model will not be significantly altered by a rising water table is based on the results of the regional-scale groundwater flow model. This assumption requires justification through sensitivity analysis of the TSPA model.

The release of radionuclides from the UZ to the SZ in the nominal case is by the downward percolation of groundwater containing radionuclides. The radionuclides may be aqueous or attached to colloids. Migration of radionuclides from the UZ to the SZ is assumed to occur by undisturbed, natural movement of recharge at the water table in the nominal case.

Important processes relevant to radionuclide transport in the SZ that are explicitly included in the TSPA-SR analyses are advection in groundwater, dispersion, matrix diffusion in fractured media, sorption of radionuclides, colloid-facilitated transport, and radioactive decay and ingrowth. Advection is the natural movement of groundwater through fractured or porous media in response to gradients in groundwater potential. In the site-scale SZ flow and transport model, dispersion is explicitly simulated as a random-walk process that occurs in the longitudinal and transverse directions; only longitudinal dispersion is simulated in the one-1-D SZ transport model. Diffusion of radionuclides from fractures into the immobile groundwater of the matrix is simulated to occur in fractured volcanic units using an analytical solution for mass transfer in an idealized fracture network. Sorption of radionuclides is simulated to occur in the matrix of volcanic units, but is conservatively disregarded in fractures of the SZ. Colloid-facilitated transport is included in the transport simulations as occurring in two modes: as irreversible attachment of radionuclides to colloids originating from the waste, and as equilibrium attachment of radionuclides to colloids. Radioactive decay is simulated to occur for all radionuclides, and ingrowth is simulated for the daughter radionuclides in four key decay chains in the one-1-D SZ transport model.

The nominal case of site-scale SZ flow and transport for the TSPA-SR includes uncertainty in key model parameters and conceptual models. The probabilistic analysis of uncertainty is implemented through Monte Carlo realizations of the SZ in a manner consistent with the TSPA simulations implemented with the GoldSim software code. A summary of the analysis forming the basis for parameter uncertainty is presented in Section 3.7.2. Alternative models of groundwater flux and horizontal anisotropy are included as uncertainty among six SZ groundwater flow fields. Uncertainty in the location of the contact between volcanic units and the alluvium is incorporated as geometric variability in the alluvium zone. Alternative models of colloid-facilitated transport are considered in the uncertainty analysis by using two coexisting modes of colloid-facilitated transport.

3.7.2 Parameter Uncertainty Distributions

In this section, the stochastic parameters and the constant-value parameters that are used in the site-scale SZ flow and transport model for nominal case TSPA are discussed. All of the parameters used, details of the basis of these parameters, and the associated assumptions are presented by CRWMS M&O (2000o, Section 6).

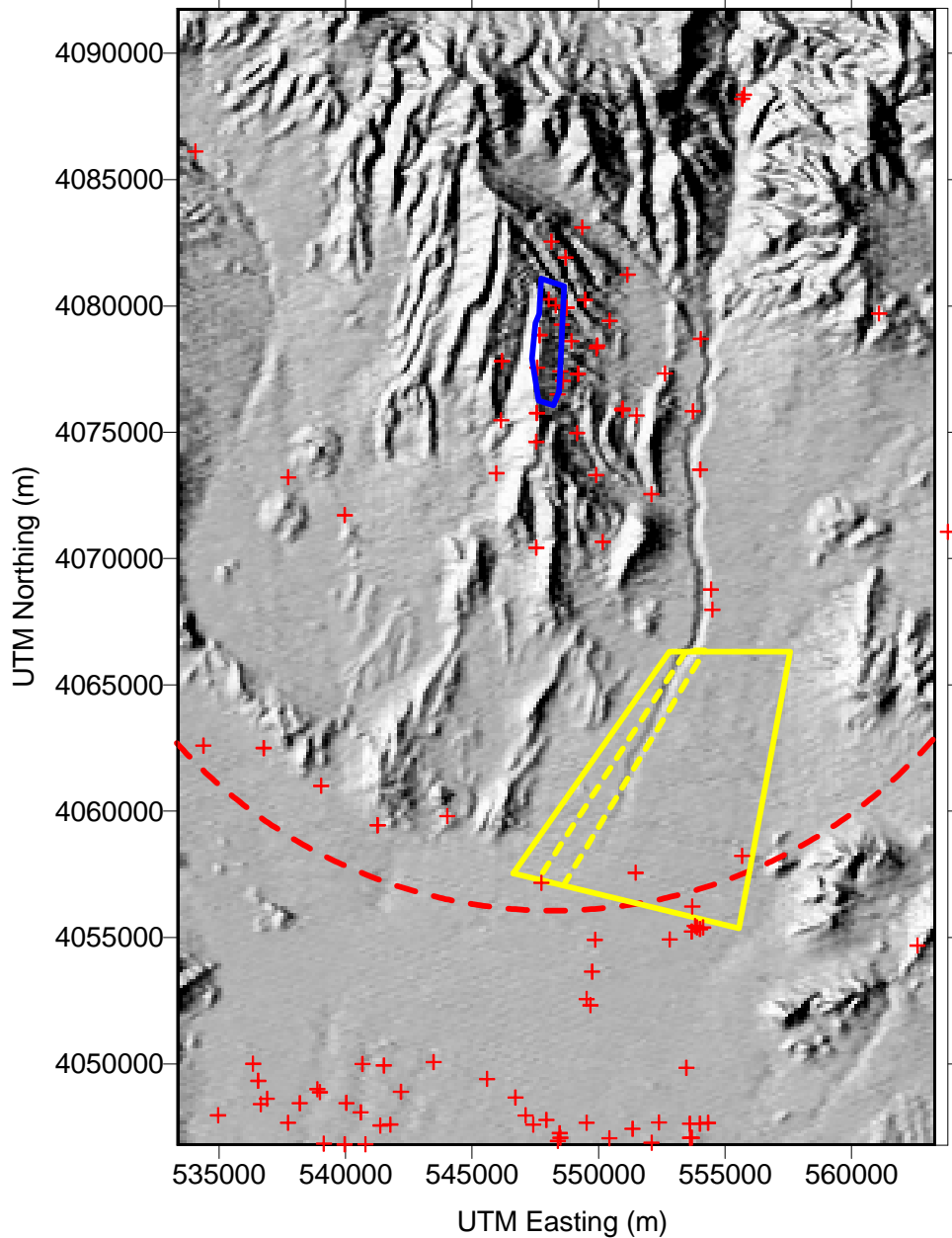
In general, parameters to which the model results are sensitive, due to the importance of the parameter in the model and the uncertainty in the parameter value, are represented stochastically. Conversely, it is determined appropriate that parameters to which the model results are not sensitive, are sufficiently represented by constant values. This is considered appropriate because the results are not significantly altered by variation in those parameters.

Groundwater Specific Discharge (Stochastic)—Considerable uncertainty exists in the groundwater flux in the SZ along the flowpath to the hypothetical point of release to the biosphere. This uncertainty was quantified as a distribution of specific discharge in the volcanic aquifer near Yucca Mountain by the SZ expert elicitation project (CRWMS M&O 1998b). The results of the SZ expert elicitation are used as a quantitative basis for assigning probabilities to three discrete cases of groundwater flux in the SZ (low-, mean-, and high-flux). The calibrated site-scale SZ flow model corresponds to the mean-flux case. The low-flux case is constructed by downwardly scaling the values of permeability and the boundary fluxes in the site-scale SZ flow model by a constant factor of 10 (i.e., the value times 10). The high-flux case is constructed in a similar manner by scaling the values of permeability and boundary fluxes upward by a factor of 10. Proportional scaling of permeability values and boundary fluxes in the site-scale SZ flow model preserves the calibration of the model to head measurements in wells among the three flux cases.

Uncertainty of Alluvium Boundary (Stochastic)—Uncertainty in the geology below the water table exists along the inferred flowpath from the potential repository at distances of approximately 10 km to 20 km (6.2 to 12.5 mi.) down gradient of the potential repository. The location at which groundwater flow moves from fractured volcanic rocks to alluvium is of particular importance from the perspective of assessing the performance of the potential repository. This is because of differences between the fractured volcanic units and the alluvium in terms of groundwater flow (i.e., fracture-dominated flow versus porous-medium flow) and in terms of sorptive properties of the media for some radionuclides.

The uncertainty in the location of the northern boundary of the alluvium is represented in the site-scale SZ flow and transport model as a polygonal region (Figure 3-29) that is assigned radionuclide transport properties representative of the valley-fill aquifer hydrogeologic unit. The alluvial uncertainty region is approximately bounded by wells on the north and south and by surface outcrops of volcanic units on the west. In the site-scale SZ flow and transport simulations for TSPA, the boundaries of the polygonal region are varied stochastically. The northern boundary of the uncertainty zone is varied from its most northerly position (Figure 3-29) to the southern boundary of the uncertainty zone. The western boundary of the uncertainty zone is varied from the western boundary (Figure 3-29) to the eastern-most dashed line.

Future lithologic data from NCEWDP boreholes will provide constraints on the uncertainty in the location of the contact zone between the volcanic tuffs and the alluvium at the water table. Data from these additional boreholes will be evaluated and appropriately incorporated into the HFM and, if necessary, into the assessment of uncertainty in the stochastic analyses for TSPA.



Source: CRWMS M&O (2000c, Figure 2)

NOTE: Alluvial uncertainty zone. The solid outline indicates the largest extent of the alluvial uncertainty zone. The dashed straight lines indicate the most easterly and the median locations of the western boundary of the uncertainty zone. The northern boundary of the uncertainty zone is varied from the most northerly to the most southerly line. The curved dashed line indicates a distance of 20-km (12.5 mi.) from the potential repository. Crosses represent borehole locations.

Figure 3-29. Alluvial Uncertainty Zone

Effective Porosity in the Alluvium (Stochastic) and Volcanic (Constant)—Average linear groundwater velocities are used in the simulation of radionuclide transport in the site-scale SZ model. They are customarily calculated by dividing the volumetric flux rate of water through a model grid cell by the porosity. Average linear velocities are rendered more accurate when dead-end pores are eliminated from consideration (because they do not transmit water), resulting in effective porosity. Effective porosity is less than or equal to total porosity.

Currently there are no site-specific data available for effective porosity in the alluvium. However, data from different sources have applicability and relevance, and some of these sources provide data from areas close to Fortymile Wash. The most useful data comes from a study of hydraulic characteristics of alluvium within the Basin and Range Province (Bedinger et al. 1989). This study appears relevant to the local valley-fill conditions and provides values for effective porosity. Additional information on the effective porosity value of the alluvium is provided by CRWMS M&O (1998b).

Matrix porosity is treated as a constant parameter for 9 of the 19 SZ model hydrogeologic units (matrix porosity varies from one unit to another, but given a particular unit, the porosity is constant for all realizations). Matrix porosity is only one of several parameters involved in the dual-porosity simulations employed for these units. In this formulation, advection does not occur in the matrix. Therefore, the dual-porosity transport simulations are far more sensitive to other parameters, including “flowing interval spacing” and “effective diffusion coefficient,” than they are to matrix porosity.

Flowing Interval Spacing—The flowing-interval parameter is a key parameter in the dual-porosity component of the site-scale SZ flow and transport model. A flowing interval is defined as a fractured zone that transmits flow, as identified through borehole flow-meter surveys. The analysis uses the term “flowing interval spacing” as opposed to “fracture spacing,” which typically is used in the literature. The term fracture spacing was not used because the data used identified a zone (or a flowing interval) that contains fluid-conducting fractures but does not distinguish how many or which fractures comprise the flowing interval. The flowing interval spacing is measured between the midpoints of each flowing interval. This parameter is documented by CRWMS M&O (2000k).

Flowing Interval Porosity—The flowing interval porosity is defined as the volume of pore space in the active flow field relative to the total saturated volume of rock in fractured media. There are no direct measurements of the flowing interval porosity. It is considered appropriate that the fracture system can be represented as a series of parallel plates or intersecting parallel plates for theoretical estimates of flowing interval porosity for tuff deposits in the Yucca Mountain region. If this porosity is equivalent to the flowing interval porosity, it implies that only the fractures associated with flow are measured and that no flow is occurring in the matrix.

There is uncertainty in the flowing interval porosity. Estimates of this parameter value, based on theoretical models, pumping tests, and tracer data, range over four orders of magnitude. The parallel plate model is used to estimate the lower bound of the range, and the upper bound is based on interpretations of pumping tests and tracer data.

Effective Diffusion Coefficients—The effective diffusion coefficient is variable and uncertain. The effective diffusion coefficient is a function of the molecular diffusion and the tortuosity of the material. Variability in the effective diffusion coefficient is caused by differences in molecular diffusion for individual contaminants. The variability in molecular diffusion occurs primarily due to differences in the size (atom, ion, or molecule) and charge of individual contaminants. The effective diffusion coefficients also vary over time and space due to variability (spatial) and changes (temporal) in the temperature of pore fluids, geochemical conditions, and tortuosity. There is additional uncertainty in the effective diffusion coefficient on a field scale due to the limitations of the laboratory measurements such as: limited number of measurements made under limited geochemical conditions, potential effects of fracture coatings on effective diffusion coefficient, and temperature uncertainty and variability along the transport pathway. A brief analysis shows that tortuosity has the greatest impact on the diffusion coefficient. Using the range in tortuosity and molecular diffusion coefficients, a range of effective diffusion coefficients is calculated. Details are provided by CRWMS M&O (2000o).

Bulk Density—Bulk density is treated as a constant parameter for all hydrogeologic units. Constant, in this sense, means that bulk density will vary from one unit to another, but, given a particular unit, the bulk density is constant for all realizations. Bulk density is only one of several parameters involved in the dual-porosity simulations. The dual-porosity transport simulations are more sensitive to flowing interval spacing and effective diffusion coefficient than they are to bulk density. Bulk density is used to calculate the retardation of solutes due to chemical adsorption in the FEHM computer code (Zyvoloski et al. 1997b).

Sorption Coefficients (Stochastic and Constant)—Sorption is the process by which dissolved radionuclides adhere to substrates along a transport path. Sorption occurs because of the electrochemical affinity between the dissolved species and the substrate. Sorption is important because it results in the retardation of radionuclide movement because the radionuclides spend time attached to immobile surfaces.

Sorption is a function of water chemistry and the mineralogy of the rock matrix, both of which vary spatially, and it cannot be defined for all points in space with certainty. Not only are these characteristics of the system variable, but the exact path that a radionuclide takes through the system is uncertain. Uncertainties regarding mineralogy and chemistry implicitly are included in the sorption coefficient uncertainty distributions. Additionally, alternative models for sorption (Section 3.1.4.1) include deviations from the assumption of a linear sorption model, and these deviations also are represented in the uncertainty distributions. The sorption coefficient parameter is highly uncertain, and the probability distributions span several orders of magnitude.

The most recent summary of data on sorption in the alluvium for neptunium, technetium, and iodine is presented by CRWMS M&O (2000r). Sorption coefficients for the volcanic units were determined for neptunium and uranium, and these values were based on sorption coefficients in CRWMS M&O (2000o). For the volcanic units, iodine, technetium, and carbon were classified as constant parameters and given sorption values of 0, indicating no retardation in the volcanic units. The selection of radionuclides included in the analysis is described by CRWMS M&O (2000o).

Longitudinal Dispersivity—Longitudinal dispersion is the mixing of a solute with water that occurs in the direction of the flowpath. This mixing is a function of many factors, including the relative concentrations of the solute, the velocity pattern within the flow field, and properties of the host rock. An important component of dispersion is the dispersivity, a coarse measure of solute (mechanical) spreading properties of the rock. The dispersion process causes spreading of the solute in directions transverse to the flow path as well as in the longitudinal flow direction. Longitudinal dispersivity will be important only at the leading edge of an advancing plume, while transverse dispersivity is the strongest control on plume spreading and possible dilution (CRWMS M&O 1998b, p. LG-12).

The dispersivities (longitudinal, vertical transverse, and horizontal transverse) are used in the advection-dispersion equation governing solute transport and are implemented in the site-scale SZ model as a stochastic parameter. In the site-scale SZ flow and transport model, longitudinal dispersivity is sampled in log-space for 100 realizations, and transverse dispersivities are calculated according to the relationship recommended by the SZ expert elicitation (CRWMS M&O 1998b).

Horizontal Anisotropy—There is uncertainty in the potential for horizontal anisotropy in permeability over the scale of the transport path length. Winterle and La Femina (1999) estimated values for anisotropic transmissivity using data from the pumping tests at the C-well Complex. These estimates are poorly constrained and may not be representative of the anisotropy on the scale of the transport model. The uncertainties include differences in pumping test analysis methods, the fact that only a minimum number of observation wells were used, and uncertainty regarding the validity of assuming a homogenous effective continuum over the scale of the test (Winterle and La Femina 1999, p. 4-29). Given the uncertainty in anisotropy, and to simplify the model, the potential effects of anisotropy are bounded by setting the anisotropy ratio to 1 (isotropic) or 5 (anisotropic), values that are based on the C-wells data.

Source Region Definitions—Variations in SZ transport pathways and radionuclide transport times from various locations beneath the potential repository are considered by defining four radionuclide source regions at the water table. For any particular TSPA realization, a point at the water table is defined randomly within each of the four regions, and this point is used as the source region for simulation of radionuclide transport in the site-scale SZ flow and transport model. A point source of radionuclides in the SZ is appropriate for a single leaking waste package or for highly focused groundwater flow along a fault or fracture in the UZ. Whereas a more diffuse source of radionuclides at the water table may be more realistic for later times when numerous leaking waste packages occur, use of a point source in the SZ is a conservative approach that can be applied for all situations.

Retardation of Radionuclides Irreversibly Sorbed on Colloids—Radionuclides that are irreversibly sorbed onto colloids are conceptualized as embedded in the colloids and are part of the colloidal structure. Thus, these radionuclides are unavailable for dissolution and their transport characteristics are the same as the transport characteristics of the colloids. The most important radionuclides transported by this mechanism are americium and plutonium. The fraction of colloids that are irreversibly sorbed is determined in the engineered barrier system component of TSPA-SR.

Modeling advective and dispersive processes is handled as if colloids were solute. Matrix exclusion in the volcanic units is invoked because of the large size and small diffusivities of the colloids compared to the solute, plus the possibility of similar electrostatic charge of the colloids and the tuff matrix. CRWMS M&O (2000l) derived colloid transport parameters from tracer tests conducted in fractured tuffs at the C-wells Complex. Based on these parameters, the discrete cumulative probability density function for microsphere retardation factors in the fractured tuff is used for colloid filtration in the volcanic units (CRWMS M&O 2000o, Figure 5 and Table 13).

The discrete cumulative probability density function for microsphere retardation factors in the C-wells tracer tests was randomly sampled to obtain retardation factors for PA calculations of colloid transport for the volcanic units. The retardation factor is one of many parameters that are randomly sampled for a large number of simulations that will collectively yield probability distributions for radionuclide transport through the SZ. Because radionuclides are irreversibly sorbed to colloids, colloid-facilitated radionuclide transport in these simulations effectively is the product of colloid transport and the mass loading of radionuclides associated with the colloids.

As with radionuclides that are irreversibly sorbed onto colloids in the volcanic units, filtration in the alluvium is modeled by applying a retardation factor to the transport parameter. CRWMS M&O (2000l) developed the statistical distribution of retardation in the alluvium, and this distribution was used for input into the site-scale SZ model for TSPA-SR (CRWMS M&O 2000o, Figure 6 and Table 14). This distribution is sampled and used in the same manner in PA calculations as for colloid-facilitated transport in fractured tuffs (described in Section 3.2.4.5).

Retardation of Radionuclides Reversibly Sorbed on Colloids—Radionuclides that are reversibly sorbed onto colloids are temporarily attached to the surface of colloids. Thus, these radionuclides are available for dissolution and their transport characteristics are a combination of the transport characteristics of solute and colloids.

For TSPA-SR, radionuclides that are reversibly sorbed onto colloids are modeled using the reversible distribution coefficient, K_c concept (CRWMS M&O 1997, Equation 8-10, p. 8-35). The K_c is a distribution coefficient defined as $K_c = (K_{dcol})(C_{col})$ that represents the equilibrium partitioning of radionuclides between the aqueous and colloidal phases, where K_{dcol} is the sorption coefficient on colloids and C_{col} is the concentration of colloids in the groundwater. The K_c is a function of only radionuclide sorption properties, colloid substrate properties, and colloid concentration; but not any properties of the immobile media through which transport occurs. Thus, the same K_c applies to transport of a radionuclide in the volcanic units and the alluvium.

For TSPA-SR, the K_{dcol} parameter is based on the K_{dcol} for americium onto waste-form colloids (CRWMS M&O 2000f). The C_{col} parameter was taken directly from CRWMS M&O (2000f) and is considered the maximum colloid concentration. The product of K_{dcol} and C_{col} is a simple linear transformation of the K_{dcol} distribution from CRWMS M&O (2000f).

3.7.3 Probabilistic Analyses

A series of radionuclide transport simulations are performed using the site-scale SZ flow and transport model for TSPA. A separate model run is conducted for each realization, for each

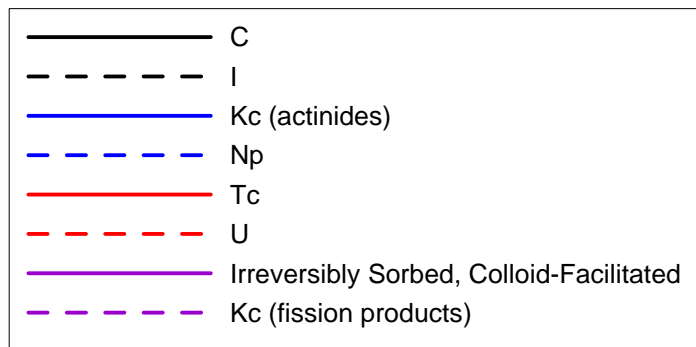
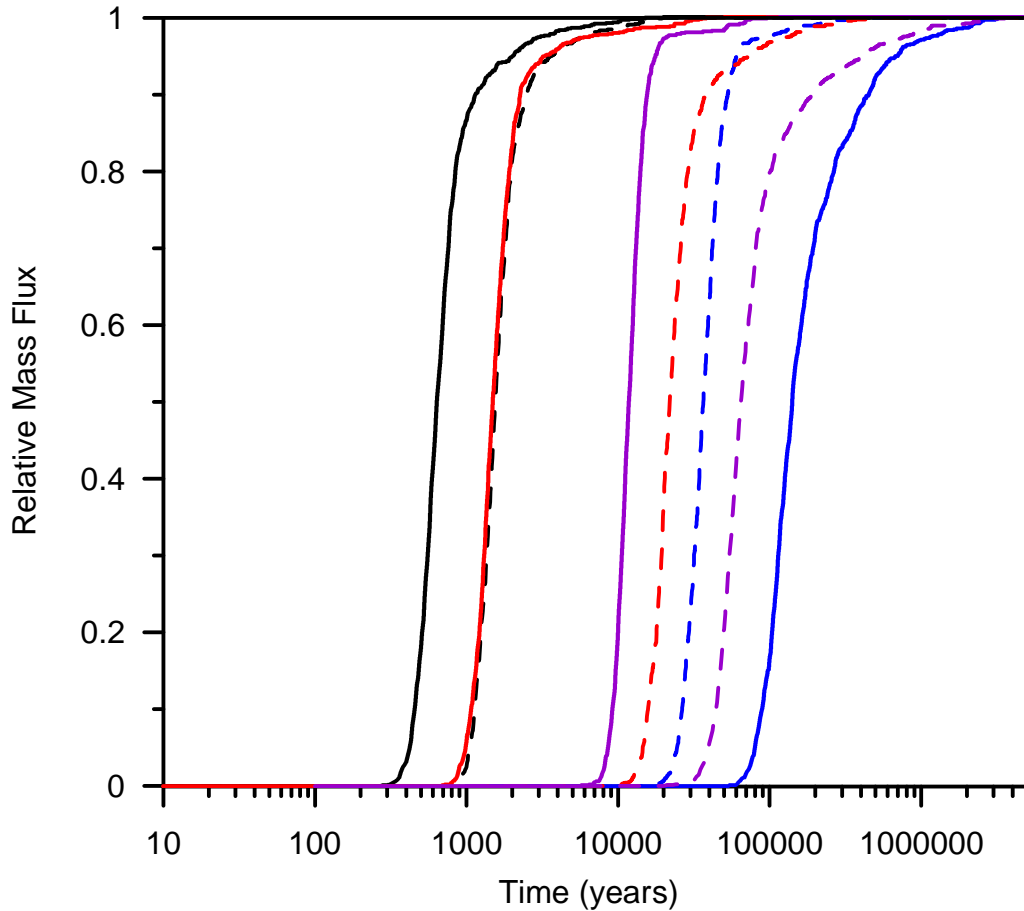
radionuclide (or class of radionuclides), and for each of the four source regions. Parameter vectors for stochastic parameters are generated for all 100 realizations prior to the model runs using the parameter-sampling algorithm in the GoldSim software code. Results of the site-scale SZ flow and transport model runs are archived in files for use by the convolution integral subroutine of the TSPA simulator (see Section 3.6.3.3.1 for a discussion of inputs to the convolution integral method).

The Monte Carlo realizations of the 1-D radionuclide transport model for decay chains are conducted directly in the TSPA simulator with the GoldSim software code. The mass flux for daughter radionuclides to the biosphere is used to calculate the contribution to total radiological dose from each of these daughter radionuclides in a manner similar to that used for radionuclides in the 3-D site-scale SZ flow and transport model.

3.7.4 Results

The results of radionuclide transport simulations using the site-scale SZ flow and transport model consist of the radionuclide mass breakthrough curves for eight species or classes of species (CRWMS M&O 2000p, Section 6.3). Results are obtained for 100 stochastic realizations of the SZ system (the nominal case) and for one additional case utilizing the expected value (i.e., the median) for all stochastic parameters (expected-value case). These results constitute the “library” of SZ flow and transport simulations that are provided to the convolution integral software code in the TSPA-SR simulations. More detailed presentation of the results is given by CRWMS M&O (2000p, Section 6).

Radionuclide mass breakthrough curves for the expected-value realization of the site-scale SZ flow and transport model were generated (Figure 3-30). The distribution of transport times in the SZ (from beneath the potential repository to a distance of 20 km [12.5 mi.]) for the non-sorbing species (e.g., carbon) generally is less than 1,000 yr.. Iodine and technetium are subject to minor sorption in the alluvium and have transport times of 1,000 to 2,000 yr.. For radionuclides that irreversibly attach to colloids (all actinides), the transport times in the SZ are somewhat less than 10,000 yr.. Species that are subject to moderate to high sorption have simulated transport times of greater than 10,000 yr.. These species are categorized into three categories: moderately sorbing species (technetium and iodine in the alluvium, neptunium, and uranium), moderately-strongly sorbing species (cesium, strontium, and palladium), and strongly sorbing species (americium, thorium, and plutonium). The results (Figure 3-30) are for transport from Source Region 1 under the northern portion of the potential repository. Results vary somewhat among source regions, having generally longer transport times from the northern and eastern source regions. The radionuclide mass breakthrough curves shown in Figure 3-30 and subsequent figures do not include radioactive decay, which is implemented in the convolution integral portion of the TSPA analyses.



Source: CRWMS M&O (2000p, Figure 11)

NOTE: Results are shown for 20-km (12.5 mi.) distance from source Region 1.

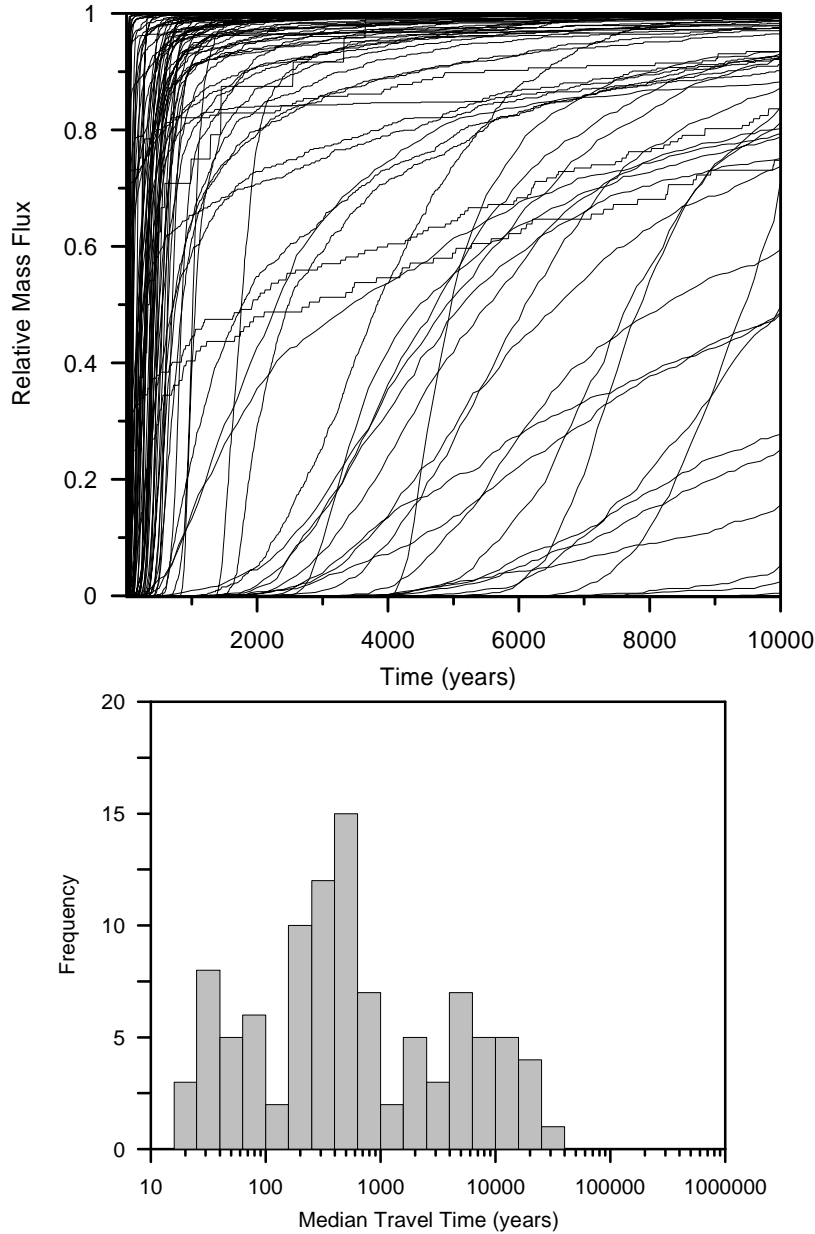
Figure 3-30. Simulated Unit Breakthrough Curves of Radionuclide Mass Flux for the Expected-Value Case

The simulated radionuclide mass breakthrough curves from 100 stochastic realizations for carbon, technetium, neptunium, and the K_c model (Section 3.7.2) of highly sorbing radionuclides are shown in Figures 3-31, 3-32, 3-33, and 3-34, respectively. These results illustrate the variability in radionuclide transport among individual realizations and among species. Results for carbon indicate relatively short transport times of less than 1,000 yr. for most realizations, but significantly longer distributions of transport times for some realizations. Technetium is subjected to slight retardation in alluvium, and the resulting breakthrough curves (Figure 3-32) indicate somewhat longer transport times for the faster breakthrough curves relative to carbon. The results for neptunium (Figure 3-33) indicate that transport times are significantly longer than are those for carbon or technetium. Neptunium is subject to relatively minor sorption in the volcanic units, and to moderate sorption in alluvium. Results for colloid-facilitated transport of strongly sorbing radionuclides (the K_c equilibrium model) show a large degree of retardation relative to the other species modeled (Figure 3-34). For many realizations, the majority of the retardation in radionuclide migration is attributable to the alluvium. This is because of the relatively higher sorption and effective porosity in the alluvium in comparison to that of the fractured tuff.

3.7.5 Interpretations

These SZ flow and transport modeling results can be interpreted, in a general sense, regarding their importance to performance of the potential repository. Detailed and quantitative assessments of the importance of simulated flow and transport behavior in the SZ requires coupling of these results with other components of the TSPA-SR analyses and formal sensitivity analyses. Interpretation of the results presented here is further complicated by the fact that the breakthrough curves presented do not indicate the impact of radioactive decay, which is incorporated in the TSPA simulation by the convolution integral algorithm. Considerable decrease in concentration of radionuclide mass may occur for the radionuclides with half-lives that are short relative to their potential transport times in the SZ (e.g., carbon-14, plutonium-239, plutonium-240, americium-241, and americium-243). The results and interpretations for the 1-D radionuclide transport model for radionuclide daughter products are not presented in this report because these simulations occur within the TSPA simulator.

Radionuclide migration through the SZ affects total system performance in two ways. First, the SZ functions as a mechanism to delay the release of radionuclides to the biosphere. This delay potentially allows radioactive decay to reduce the release of radionuclides to the biosphere. Second, there may be considerable dilution of radionuclides during transport in the SZ. Although the dispersive processes that lead to dilution are incorporated in the site-scale SZ flow and transport model, a simplified approach is mandated by proposed 10 CFR 63 (64 FR 8640). The simplified approach is used to calculate concentrations in the water supply of the hypothetical farming community and negates the need to analyze in situ radionuclide concentrations in the SZ.

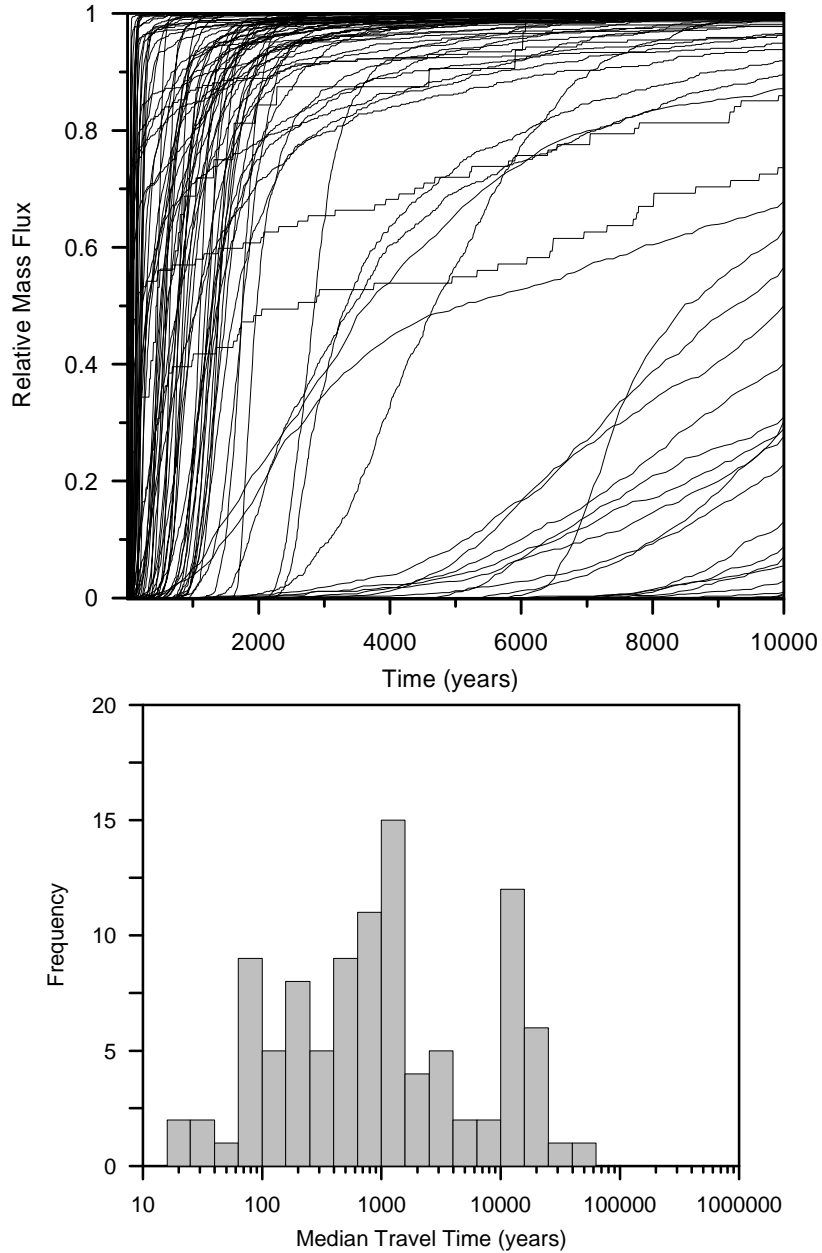


Source: Adapted from CRWMS M&O (2000p, Figure 12)

NOTE: Results are shown for 20-km (12.5 mi.) from the source.

These breakthrough curves are based on a model that is appropriately conservative for TSPA analyses and consequently should not be used to evaluate the expected breakthrough of radionuclides at the compliance boundary.

Figure 3-31. Simulated Unit Breakthrough Curves and Histogram of Median Transport Times of Mass Flux for Carbon

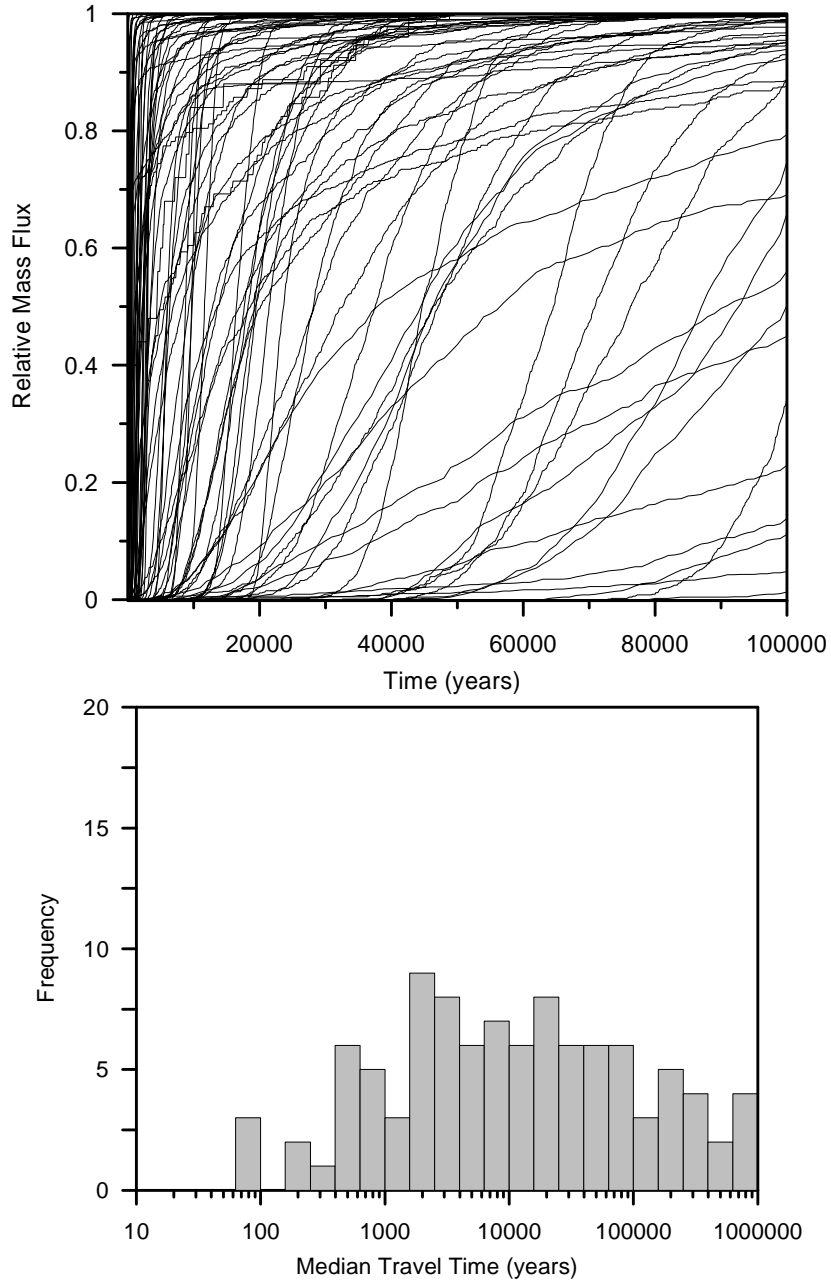


Source: Adapted from CRWMS M&O (2000p, Figure 18)

NOTE: Results are shown for 20-km (12.5 mi.) from the source.

These breakthrough curves are based on a model that is appropriately conservative for TSPA analyses and consequently should not be used to evaluate the expected breakthrough of radionuclides at the compliance boundary.

Figure 3-32. Simulated Unit Breakthrough Curves and Histogram of Median Transport Times of Mass Flux for Technetium

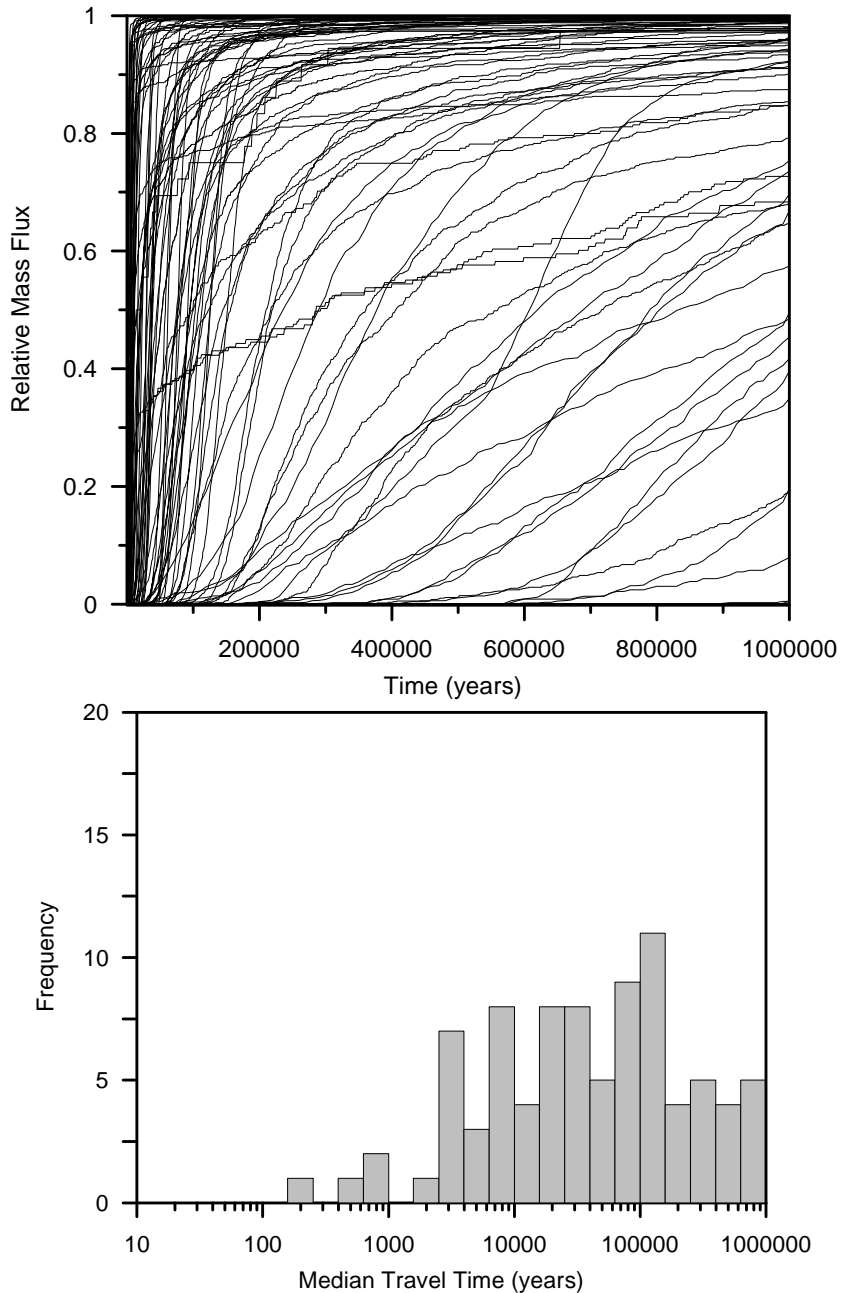


Source: Adapted from CRWMS M&O (2000p, Figure 16)

NOTE: Results are shown for 20-km (12.5 mi.) from the source.

These breakthrough curves are based on a model that is appropriately conservative for TSPA analyses and consequently should not be used to evaluate the expected breakthrough of radionuclides at the compliance boundary.

Figure 3-33. Simulated Unit Breakthrough Curves and Histogram of Median Transport Times of Mass Flux for Neptunium



Source: Adapted from CRWMS M&O (2000p, Figure 14)

NOTE: Results are shown for 20-km (12.5 mi.) from the source.

These breakthrough curves are based on a model that is appropriately conservative for TSPA analyses and consequently should not be used to evaluate the expected breakthrough of radionuclides at the compliance boundary.

Figure 3-34. Simulated Unit Breakthrough Curves of Mass Flux and Histogram of Median Transport Times for the K_c Model of Colloid-Facilitated Transport for Highly Sorbing Radionuclides

Delays in the release of radionuclides due to processes in the SZ potentially are important to performance of the potential repository if transport is long compared to the half-life or if transport is long relative to regulatory time limits. This situation applies to some of the later breakthrough curves for carbon-14 (half-life of 5,730 yr.; Figure 3-31). As a more extreme example, plutonium-240 (half-life of 6,540 yr.) that is subject to SZ transport via the K_c model would experience considerable attenuation due to long travel times for most of the realizations shown in Figure 3-34. However, several of the radionuclides that may be important contributors to doses (i.e., neptunium-237, iodine-129, and technetium-99), would not experience a large amount of decay during transport in the SZ.

Delays in the release of radionuclides from the SZ are highly variable among the radionuclides that were considered. Transport times through the SZ for carbon-14, technetium-99, and iodine-129 primarily are less than 10,000 yr., with many realizations having transport times of less than 1,000 yr.. The sorption of technetium-99 and iodine-129 in the alluvial units results in somewhat longer transport for these radionuclides. Thus, in the context of a 10,000-yr regulatory standard, carbon-14, technetium-99, and iodine-129 are of concern for any early releases from the potential repository and UZ. Transport times for plutonium and americium (which are subject to transport by irreversible attachment to colloids) and uranium are near 10,000 yr. for the expected-value realization (Figure 3-30). Neptunium-237, and other radionuclides that are subject to reversible attachment to colloids, have transport times in the range of 20,000 to 100,000 yr. in the SZ for the expected value realization, indicating that they are of lesser importance in the context of a 10,000-yr regulatory standard.

For particular radionuclides, variability among realizations for SZ transport indicates a high degree of compound uncertainty in the SZ transport processes. Variations in the mean delivery times for different realizations primarily reflect the influences of sorption in the volcanic and alluvium units, the groundwater flux case, matrix diffusion in fractured units, effective porosity in the alluvium units, and fraction of the flowpath in alluvium. The impacts of uncertainty in the SZ transport processes, other than sorption, are visible in the breakthrough curves for carbon-14 (Figure 3-31). Variations among realizations for sorbing radionuclides are even greater (Figure 3-33).

Variations in the shapes of the radionuclide mass breakthrough curves are a function of the matrix diffusion process, dispersion, and to a lesser extent, the variations in the flowpath through the system. Relatively steep breakthrough curves with early first arrival are indicative of limited matrix diffusion due to large flowing interval spacing and small effective diffusion coefficient for the matrix. Breakthrough curves with later arrival and a plateau at relative mass flux near 1.0 indicate a greater degree of matrix diffusion. Realizations in which an intermediate degree of matrix diffusion occurs are characterized by less steep breakthrough curves with longer tails at the upper end of the travel time distribution.

The radionuclide mass breakthrough curves from the stochastic realizations of SZ flow and transport reflect the impacts of uncertainty and conservatism in the stochastic parameters and in the site-scale SZ flow and transport model. As discussed in Section 1, these impacts may take the form of a consistent bias or may be reflected in the “breadth” of the simulated results. Certain modeling assumptions and simplifications, such as neglecting sorption on fracture walls, introduce a conservative bias to the simulation results. The results of this bias shifts the

radionuclide mass breakthrough curves from the stochastic realizations toward shorter travel times relative to the alternative assumptions and more complex modeling approaches. Although it is difficult to quantify the integrated effects of such biases on the radionuclide transport results, it is believed that the overall effect on the stochastic results is not large. Consequently, the median behavior among the 100 stochastic realizations of radionuclide transport constitutes a somewhat conservative, but reasonably realistic representation of SZ system behavior. Conversely, the cumulative effect of stochastic parameters with broad uncertainty distributions results in a few simulations with much shorter radionuclide travel times through the SZ, for which the conservative end of uncertainty distributions have been simultaneously sampled for multiple parameters. Thus the realizations of radionuclide transport in the SZ that represent the worst system performance (i.e., shortest travel times) result from the relatively wide uncertainty in some stochastic parameters and not from systematic conservative bias in the site-scale SZ flow and transport model.

Several stochastic parameters in the site-scale SZ flow and transport model have relatively broad uncertainty distributions and affect the more conservative realizations of radionuclide transport. The most influential of these is the parameter that determines if the low, medium, or high groundwater flux case is used for specific discharge in the SZ. The high groundwater flux case results in significantly shorter travel times. The relatively broad uncertainty in this parameter is primarily a reflection of the fact that multi-well pump test data are available from only one location (the C-wells Complex) along the SZ flowpath. Additional multi-well pump testing is planned at the Alluvial Tracer Complex, which will provide information on hydraulic conductivity (and indirectly on groundwater flux) at another location in the SZ flow system. It is anticipated that these additional data will narrow the uncertainty in specific discharge along the flowpath from the repository. Uncertainty in the transition from groundwater flow in fractured tuff to flow in alluvium also results in some of the shorter radionuclide travel times shown in the results. Lithologic data from additional boreholes being drilled under the NCEWDP will reduce the breadth of the alluvial uncertainty zone that is utilized in the stochastic realizations of SZ flow and transport. Stochastic parameters related to matrix diffusion, such as flowing interval spacing, effective diffusion coefficient, and fracture porosity, also have relatively broad uncertainty distributions that contribute to the more conservative realizations of radionuclide transport. In summary, the stochastic realizations of radionuclide transport that exhibit apparently overly conservative, short travel times are the result of very broad uncertainty distributions for key underlying stochastic parameters. Additional data or reinterpretation of data that narrows the uncertainty distributions for these key parameters may reduce the probability of obtaining these conservative results.

3.8 SUMMARY OF OTHER VIEWS AND ALTERNATIVE MODELS

The main alternative models dealing with the SZ flow and transport system pertain to postulated rises in the water table due to seismic, hydrothermal, or a combination of both processes (Section 3.8.1), and to alternate views of SZ flow in the immediate vicinity of the potential repository (Section 3.8.2).

3.8.1 Disruptive Events and Rises in the Water Table

Field observations at Yucca Mountain have been made of surficial and fault-filling calcite and opaline-silica. The commonly accepted view of the origin of these deposits, which are known as caliche or calcrete and are ubiquitous in the desert Southwest, is that they formed by pedogenic (soil-forming) processes from downward-flowing water. However, an alternative interpretation, the upwelling water model, has been proposed. Based on interpretations of the calcite and opaline-silica mineral deposits, it was proposed that changes in stress in the crust of the earth (caused by earthquakes or recurring hydrothermal activity) had repeatedly forced groundwater up to the land surface such that the water table intermittently and repeatedly rose to, and above, the elevation of the potential repository horizon. This upwelled groundwater, then, is thought to have left the mineral deposits. Discussions of this issue and its history are provided in CRWMS M&O (1998e, Section 3.4.3.4), DOE (1998c, Section 2.2.1.3), and NRC (1999a, Section 4.5.2.13).

The upwelling water model has been evaluated by the following reviewers who are external to the DOE program:

- A five-member peer review panel composed of outside reviewers convened by the YMP (Powers et al. 1991; Archambeau and Price 1991).
- A U.S. Geological Survey (USGS) reviewer at the request of one of the members of the five-member panel (Evernden 1992).
- A 17-member panel established by the National Academy of Science's National Research Council (NAS-NRC) at the request of the DOE (National Research Council 1992).
- U.S. Nuclear Regulatory Commission contractors at the Center for Nuclear Waste Regulatory Analyses (CNWRA) (Leslie 1994).
- An expert elicitation panel convened by the DOE to consider SZ flow and transport and the topic of disruptive events and a rise in the water table (CRWMS M&O 1998b, Section 3.2.9.3). One member of the panel, Tsang, is associated with the Yucca Mountain Project.
- The U.S. Nuclear Waste Technical Review Board (NWTRB) and a panel convened by the NWTRB to review documents submitted to the NWTRB in 1997 in support of the upwelling water model (Cohon 1998a).

Brief discussions of these reviews are provided below. Additionally, scientists associated with the YMP have reviewed reports that support the alternative model. Stuckless et al. (1998) provided comments on a document included in the 1997 submission to the NWTRB, and Hill et al. (1995) and Whelan (1998) provided comments on a recent draft report by Dublyansky (1998).

3.8.1.1 Five-Member Peer Review

A five-member external panel was formed by the DOE to review unpublished reports regarding the upwelling water model. Two panel members (Archambeau and Price) were chosen by the author of the reports, and three members (Powers, Rudnicki, and Smith) were selected by the DOE. Differing opinions developed within the panel, leading to the preparation of minority (Archambeau and Price 1991) and majority (Powers et al. 1991) reports.

3.8.1.1.1 Majority Report

The majority conclusions included (Powers et al. 1991, pp. S-1 to S-3):

- The proposal develops neither an adequate theoretical basis for the mechanisms and consequences, nor a body of evidence that is sufficiently supportive, to require further investigations of the proposed concepts.
- The essential concept (i.e., faults suddenly open, fill with water, close, and force the water to the surface) has not been established, and it is not supported by experience or other evidence.
- The database supporting the stress distribution is very weak.
- Calculations presented in the report are inadequate to support claims about the magnitudes and volumes of fluid movement that could lead to a tectonically-induced rise of the water table.
- There is no convincing evidence to support the claim that the lithostratigraphic framework can be relegated to a role of minor or no importance in influencing rates and patterns of groundwater flow or when interpreting field data.
- Surficial deposits cited as evidence of upwelling fluids are consistent in isotopic and physical character with surficial, pedogenic processes. Isotopically, these deposits are not consistent with known groundwater in the Yucca Mountain area. The majority sees no reason to reject surficial sources of calcite and silica to account for these deposits.
- A major flaw in the reports is that the proposals have not been cast in any testable forms.

The panel majority also had concerns with fundamental elements of the proposed model that purport to explain the linkage between the tectonic and hydrologic systems.

3.8.1.1.2 Minority Report

The minority state that the upwelling water model appears to be a good working model for processes at Yucca Mountain, including water flow and mineral deposition, and the model cannot be rejected as incompatible with current observations or theory (Archambeau and Price 1991).

The views of the minority are outlined below, however, it should be noted that the minority report has an Appendix titled "A Consensus Statement of the Review Panel Evaluation of Key Physical Properties in the Szymanski Model and Recommendation for Additional Investigative Studies" (Archambeau and Price 1991, Appendix 1). Multiple places in the minority report also refer to this "consensus statement." Section IX of the minority report, "Evaluation of the Szymanski CHT Model: September 1990 Consensus Statements of the Entire Panel" contains excerpted statements from the text of Appendix 1, and the claim is made that these statements "represent the shared view of all the members" (Archambeau and Price 1991, p. 121). However, in a letter dated 12/9/1991, the Chairman of the panel wrote: "The appendix in the minority report is not, and should not be taken as, any statement of consensus for the panel about our assessment of the validity of the ideas presented by Szymanski" (Powers 1991). Given this statement by the Chairman, only the Minority Group evaluation from Section X (Archambeau and Price 1991, pp. 125 to 128) is presented and quoted here:

The physical and geologic field evidence relating to observed calcretes and calcite-opal veins at the surface and at depth, such as relationships to faulting and hydrothermal alterations, support the interpretation of deposition by up-welling water from considerable depth. This finding is consistent with the Cyclic Hydro-Tectonic model proposed by Szymanski. The geologic observations are not, in several particulars, consistent with a pedogenic, descending water origin for most of these mineral deposits.

The physical processes and mechanisms incorporated in Szymanski's model for an interactive hydro-tectonic system at Yucca Mountain are meaningful and appear appropriate; and can provide a basis for prediction. The dynamical interactions are, however, highly non-linear and quantitative predictions based on analytical formulations and numerical modeling are very approximate and incomplete, in that only some of the phenomena inherent in the model can presently be incorporated in a computational program. Nevertheless, in principle Szymanski's model can be described in terms of a set of coupled integral-differential equations that analytically express the dynamics of such a system. In this regard, a preliminary computation, designed to simulate a short time history of seismic pumping in a fractured medium following an earthquake, did predict significant water and gas flows that could be indicative of those to be expected at Yucca Mountain. However, no other quantitative aspects of the model, such as long term convection and chemical deposition, could be evaluated. Nevertheless, while only preliminary, the quantitative analysis so far accomplished does support at least one aspect of the Szymanski model; that is the possibility of pressure driven water and gas flows, from upper to mid-crustal depths, following a large earthquake.

Field observations as well as modeling calculations indicate that gas-assisted (CO₂) flows of high energy may occur in some circumstances. In particular, it is concluded that such flows have occurred at Yucca Mountain in the past and that there is a reasonably high probability that they could also occur in the future. This inference is beyond those drawn by Szymanski and specifically incorporated in his model, but nevertheless is compatible with it.

The isotopic and mineralogic characteristics of the calcite-opal vein deposits at the surface and at depth are similar and imply a common origin of deposition. Owing to sealing and near surface erosional infill, pervasive pedogenic descending-water deposition at depth is highly unlikely. Consequently, the numerous veins at depth are almost certainly due to up-welling water from the Precambrian and the Paleozoic limestone formations beneath Yucca Mountain and, by inference based on isotopic similarity, those exposed at the surface should also have this origin as well.

The isotopic characteristics of the calcite-opal veins at the surface at Yucca Mountain, in particular those at Trench 14, appear to be consistent with up-welling water from depth, from 2 to 5 km or deeper, mixed with the shallower water from the tuff formations. If the calcite encrustations on cobbles and soil calcretes used as a pedogenic standard are indeed rain water evaporation deposits, as assumed in the study by Quade and Cerling, then the oxygen-carbon isotopic data for Trench 14 also appears to be consistent with a descending-water "pedogenic" origin. However, if the latter assumption is not true, then a pedogenic model origin is doubtful and deep up-welling water deposition is preferred. If the assumption is true, then both origins can apparently be in agreement with the data and cannot be differentiated on the basis of C-O isotopic data alone.

The isotopic characteristics of the vein calcites at Trench 14 appear consistent with a source of deep up-welling water as inferred by Szymanski through his demonstration of the correlation with the water from current "up-welling source regions" in the area of the Nevada Test Site. The lack of correlation between calcite isotopes at Trench 14 and those from the shallow water currently beneath Yucca Mountain, as inferred by Stuckless et. al., can only enforce the conclusion that young meteoric water from shallow depths was not involved, or was only a minor constituent of the water depositing these vein calcites. This conclusion clearly does not negate the possibility of the source being from up-welling water from great depth.

Stuckless et al. assumed a pedogenic model origin for a number of calcite deposits that they use as a standard. If these are wholly or partly of up-welling origin, then their comparison of these deposits with Trench 14 vein carbonates could force them to a different conclusion; namely that up-welling water from large depths could be responsible for the Trench 14 vein carbonates.

An up-welling, deep source for the water that deposited vein calcites and silica at Yucca Mountain is quite possible based on Szymanski's isotope correlations and is permissible on the basis of the Stuckless et al. study. This possibility is also supported by the inference, by Whelan and Stuckless, of large water table elevation changes at Yucca Mountain in the past; to as much as 500 m above and 300 m below the present level.

Age dates for the deposition of calcretes and calcite-opal veins at Yucca Mountain are somewhat uncertain, so that a highly confident assessment of when the most recent up-welling has occurred, and how frequently it has occurred in the past, is not possible at present. Indirect lines of evidence and inference lead us to believe, however, that the young ages obtained for some veins and calcretes are probably representative of true depositional ages, but we cannot absolutely rule out different, possibly older, ages.

Based on all lines of assessment, the model proposed by Szymanski appears to be a good working model for interactive dynamical processes at Yucca Mountain, including water flow and mineral deposition, and certainly is not one that can be rejected as incompatible with current observations or theory. Indeed, it is the only model that is self consistent and compatible with the field observations.

3.8.1.2 Evernden Review

C.D. Archambeau (a member of the five member panel and co-author of the minority report [Archambeau and Price 1991]) requested to have J.F. Evernden (USGS) evaluate the credibility of the minority report. Evernden evaluated the report based on available data and field excursions, and compared his conclusions to those of the minority report. In his introduction, Evernden (1992, p. 2) stated that he disagreed with almost everything in the minority report. Regarding the Minority Report and the proposed upwelling model, Evernden (1992) concludes:

I find little that I can accept in the interpretations of extant data given in the Minority Report and even less in their proposed model of past or potential future events (Evernden 1992, p. 60).

The minority Report asserts that several lines of evidence refute the idea of a pedogenic source for the Trench 14 calcretes. I have shown that, in every case, they are in error in their interpretations and conclusions. Their errors appear to arise out of an inadequate background in the requisite geologic disciplines (Evernden 1992, p. 60).

Their appeals to such exotic processes as seismic pumping associated with repetitive major earthquakes along the faulted west side of Yucca Mountain and convection of hot groundwater induced by abnormal rates of heat flow under Yucca Mountain and environs are appeals unsupported by data, in fact denied by data (Evernden 1992, p. 60).

Contrary to their assertion, their model is not a model at all, simply a set of unsupported and unsupportable assertions (Evernden 1992, p. 60).

3.8.1.3 National Research Council Evaluation

Detailed discussions of the evidence relating to the issue of groundwater upwelling in the Yucca Mountain area are presented a report by National Research Council (1992). The panel concluded:

The panel's overall conclusion was that none of the evidence cited as proof of ground-water upwelling in and around Yucca Mountain could reasonably be attributed to that process. The preponderance of features ascribed to ascending water clearly: (1) were related to the much older (13-10 million years old [Ma]) volcanic eruptive process that produced the rocks (ash-flow tuffs) in which the features appear, (2) contained contradictions or inconsistencies that made an upwelling ground-water origin geologically impossible or unreasonable, or (3) were classic examples of arid soil characteristics recognized world-wide (National Research Council 1992, p. 3).

3.8.1.4 Saturated Zone Flow and Transport Expert Elicitation Panel

The panel members were asked for their judgments regarding the potential magnitude of water table changes that might accompany disruptive events such as earthquakes, as well as the potential for long-lived or permanent changes in water table (CRWMS M&O 1998b). All of the experts addressing this issue concluded that changes to the water table associated with earthquakes will not be important and will not be long-lived. Freeze and others note that earthquakes can perturb the stress field and can produce short-lived spikes of increased fluid pressure in confined aquifers. Because these events do not cause a large transfer of water, Freeze reasons, they are not likely to lead to large or long-lived changes in water table elevation. Neuman notes that fluctuations from earthquakes tend to be rapid, short lived, and on the order of centimeters to meters; and Tsang concludes that the expected changes will be transitory in the time-frame of the potential repository (CRWMS M&O 1998b, Section 3.2.9.3). It should be noted that Tsang was and is associated with the Yucca Mountain Project.

3.8.1.5 Center for Nuclear Waste Regulatory Analyses Evaluation

The CNWRA completed a systematic analysis of the logic used to conclude that at Yucca Mountain hydrothermal and auxiliary gas-assisted processes pose an important hazard for time spans measured in 10,000 yr. (Leslie 1994). The CNWRA evaluated the validity of the argument, the premises used to support the conclusions of the arguments, and the geological evidence supporting each individual premise. Leslie (1994) identified several flawed premises that were key components to the overall argument presented by Szymanski (1992). Critical evaluation of the site data and the logic used in Szymanski (1992) indicates that there is inadequate documentation to support the assertions (Leslie 1994).

3.8.1.6 Nuclear Waste Technical Review Board Review

The NWTRB and its consultants reviewed recent reports supporting the upwelling water model and reached three conclusions (Cohon 1998a, pp. 2 to 3 of transmittal letter), which are quoted below:

The material reviewed by the Board does not make a credible case for the assertion that there has been ongoing, intermittent hydrothermal activity at Yucca Mountain or that large earthquake-induced changes in the water table are likely at Yucca Mountain. This material does not significantly affect the conclusions of the 1992 NAS report (National Research Council 1992).

There are several areas where additional research could be used to further evaluate the hypotheses of ongoing, intermittent hydrothermal activity and large earthquake-induced changes in the water table at Yucca Mountain. However, because of the lack of any substantive evidence supporting either of these hypotheses, the Board views additional research on these issues, if not already carried out, as generally having a lower priority than more important issues in the evaluation of repository performance.

However, some fluid inclusions found in mineral deposits at Yucca Mountain do provide direct evidence of the past presence of fluids at elevated temperatures (at least 72°C) in the vicinity of the proposed repository. This could be an indicator of some degree of past hydrothermal activity. The critical question is, "At what time in the past were such fluids present?" If fluids at elevated temperatures were present less than 100,000 yr. ago, as some of the reviewed reports claim, this could lend credence to the hypothesis of ongoing hydrothermal activity at Yucca Mountain. On the other hand, if these fluids were present around 10,000,000 yr. ago or earlier, they could be associated with volcanic events related to the original formation of Yucca Mountain and would have no bearing on the hypotheses of ongoing hydrothermal activity. The Board believes that the ages of fluid inclusions should be determined. A joint program between federal and State of Nevada scientists for collecting, dating, and analyzing fluid inclusions would be one way to help eliminate some of the past disagreements associated with sample collection and handling.

In addition to these conclusions, the NWTRB evaluated the quality of the data. Based on these evaluations, the NWTRB noted that (Cohon 1998a, pp. 2 to 3):

Although the data generally appear to be of good quality, often there is poor or insufficient documentation of important details. Examples of this deficiency include the lack of detailed information on the location of the study of Stagecoach Road fault stable isotopes; the lack of clear information on the locations of the fluid-inclusion sample sites in the underground ESF; the lack of adequate description of a proposed hydrothermal eruption breccia; and the lack of a clear and persuasive description of how the critically important ages of fluid inclusions were determined.

Far more serious are the problems associated with the interpretation of the data, which is the critical part of many scientific analyses. Examples include the very tenuous fits of lines to scattered small data sets showing presumed stable-isotope changes with depth and with distance; photographs allegedly demonstrating the hydrothermal origin of zircon that do not show the zircons growing on vein walls or fractures, the sort of evidence that would be required if this interpretation were true; the implication that relatively unimportant differences in chemical analyses of rocks imply large-scale alteration by hydrothermal processes (metasomatism); and the assumption that all fluid inclusions at depth were formed at the same time, permitting the determination of a paleogeothermal gradient although their own very limited data show otherwise.

The NWTRB also evaluated how much credence the data lend to the hypothesis of ongoing, intermittent hydrothermal activity at Yucca Mountain. Based on these evaluations, the NWTRB (Cohon 1998a) noted that:

Little credence is lent by the data to the hypothesis of ongoing, intermittent hydrothermal activity at Yucca Mountain. With the *possible* exception of the fluid inclusions (discussed below), the data presented do not pose a serious challenge either to findings reached in the 1992 NAS report or to the reasoning behind those findings. Above all, the reports can be criticized because of the pervasive presence of unsubstantiated interpretations, examples of which are given above). This is the primary reason for the criticism by the Board's consultants of the quality of the reports they were asked to review. The consultants cited the "... apparent selective use of information ... with non-supporting data being ignored." (insert ellipse); documents that are "... frustrating and confusing to review" and that "...rely heavily on unpublished documents, which are difficult to obtain and which are loosely interpreted, sometimes with a misleading effect. Important dissenting information ... is not mentioned or discussed. In many instances, these documents make conclusions that are so strong as to seem divorced from the preceding data and discussion." (insert ellipse); reports that are "... full of unsubstantiated conclusions, errors of fact and *ex cathedra* statements not supported by any, or dubious, evidence." (insert ellipse); and "... full of non-sequiturs, special pleadings, reliance on dubious conclusions reported in the earlier reports and assertions presented as proofs."

3.8.1.7 Conclusions

The upwelling water model (Szymanski 1992) has been repeatedly reviewed by independent external panels. With the exception of the of the authors of the minority report (Archambeau and Price 1991), who were chosen for the review by the proponent of the upwelling water model, multiple reviewers and review panels have found little or no basis to support it. Evernden (1992, p. 60) noted that the reports in support of the upwelling model include errors in their interpretations and conclusions. Leslie (1994) found that the reports provide inadequate documentation of supporting assertions and that key components of the model are based on flawed premises. The NWTRB states that the reports supporting the upwelling model contain unsubstantiated conclusions; errors of fact and statements supported by, at best, dubious evidence; non-sequiturs; special pleadings; and assertions presented as proofs; and that newer reports rely on dubious conclusions presented in earlier reports (Cohon 1998a, p. 3).

In response to the NWTRB recommendation, a DOE-funded investigation of fluid inclusions has been initiated and is ongoing at the University of Nevada-Las Vegas under the oversight of DOE and the State of Nevada.

3.8.2 Saturated Zone Flow at Yucca Mountain

Lehman and Brown (1996, pp. 24 to 36) use water-table temperature data from the USGS (Sass et al. 1988), together with USGS data on the response of SZ water levels to earthquakes, to develop an alternative conceptual model of the SZ that has the following main features:

- Considerable groundwater flows from west to east across the Solitario Canyon fault.
- Fault and fracture zones act as major flow paths in the SZ.
- A redrawn SZ potentiometric contour map is used as the foundation for the emphasis on fault and fracture flow.
- The hydrologic system may change unpredictably due to local earthquakes that affect fault and fracture permeability.

Using the above features, the model is used to simulate groundwater flows and temperature distributions at the water table. Taking each of the features separately, the positions of the YMP and Lehman and Brown are compared in the following sections.

3.8.2.1 Relationship of the Solitario Canyon Fault Zone to Saturated Zone Flow System

The position of the YMP with respect to the Solitario Canyon fault zone is described by Luckey et al. (1996, p. 25). The Solitario Canyon fault is described as the eastern boundary of a distinct flow domain. In this respect, Lehman and Brown (1996) and Luckey et al. (1996) are in agreement. Luckey et al. (1996, p. 26) and Lehman and Brown (1996) also agree regarding upwelling of warm water along the fault from deeper aquifers. The only important area of disagreement involves groundwater flow across the fault. Lehman and Brown (1996, Figure 17) hypothesize a large groundwater flux across the Solitario Canyon fault, while Luckey et al. (1996, p. 25) indicate that the fault generally acts as a barrier to groundwater flow, although some flow undoubtedly crosses the fault because of the large difference of hydraulic potential (45 m [148 ft]) across it. Luckey et al. (1996, p. 25) further suggest that most of the groundwater west of the fault flows to the south, either along the fault or through an aquifer in Crater Flat.

3.8.2.2 Faults and Fractures as Major Saturated Zone Flow Paths

Lehman and Brown (1996, p. 28) present a model where recharge is focused along fault and fracture zones in the SZ and UZ. This alternative differs from early conceptual models (Montazer and Wilson 1984) in which most recharge was via matrix flow in the UZ.

The conceptual model currently used for UZ and SZ flow and transport modeling (DOE 1998a) proposes that groundwater flow occurs in the UZ almost entirely within well-connected fractures in welded tuff, and that flow occurs only partly in the matrix of the bedded tuffs (i.e., a model that is based on fracture flow data available from the ESF). In this respect the models of Lehman and Brown (1996, p. 28, 30) and DOE (1998a) are in agreement.

3.8.2.3 Revised Potentiometric Surface Map

Lehman and Brown (1996, Figure 16) present a revised potentiometric surface map based on data from Ervin et al. (1994), but which differs from the potentiometric map presented by Ervin et al. (1994, Figure 1) with respect to the 730 m (2,395 ft) contour in the area east of the Solitario Canyon fault (the small hydraulic gradient area). Ervin et al. (1994, Figure 1) show a smooth 730 m (2,395 ft) contour trending generally north to south, more or less parallel to adjacent contours, with a 0.25 m (0.8 ft) interval. Lehman and Brown (1996, Figure 16) indicate a series

of embayments or potentiometric lows in the 730 m (2,395 ft) contour that are coincident with northwest trending shear zones along the eastern flank of the Yucca Mountain.

3.8.2.4 Effects of Earthquakes on Saturated Zone Flow Systems

Lehman and Brown (1996, pp. 26 to 30) present a brief description of the Landers (California), Big Bear (California), and Little Skull Mountain (Nevada) earthquakes of June 28-29, 1992, and discuss water-level changes related to these earthquakes as reported by O'Brien (1993). Some wells near Yucca Mountain showed increases in water levels in response to the earthquakes, while water levels in other wells decreased. Lehman and Brown interpret these responses to possibly indicate that some regions experienced compressive strain, while other areas experienced tensile strain. They also offer an alternative interpretation involving changes in fracture aperture.

3.8.2.5 Simulation of Groundwater Flow and Temperature Distribution at the Water Table

Lehman and Brown (1996, p. 32) present a brief description of a preliminary 2-D numerical model of the SZ flow system at Yucca Mountain. The model consists of 396 elements in a rectangular grid, and the system is divided into 10 domains to which specific values are assigned for porosity, permeability, and element volume (Lehman and Brown 1996, Table 4, Figure 18). Lehman and Brown (1996) used a computer code to model their scenario, calibrated it against water-level measurements via adjustments in permeability values, and obtained good agreement between observed water levels and the model solutions. Lehman and Brown (1996) state that the model poorly predicted temperature patterns in the groundwater. Lehman and Brown conclude that the future use of a 3-D model which includes a representation of vertical heat flow along fractures is warranted.

3.8.2.6 Conclusions

The conceptual model proposed by Lehman and Brown (1996) has much in common with the conceptual models represented by the site-scale SZ flow and transport model. Each of the conceptual models recognize that flow in volcanic rocks occurs primarily in fractures and that structural features have a strong influence on groundwater flow. Lehman and Brown's conceptual model indicates a flow path away from the potential repository that does not pass through valley-fill deposits in the Amargosa Valley. The TSPA-SR model considers such a flow path as being feasible, but considers a path through the fill deposits to be much more likely. This difference is important because transport of radionuclides through the valley-fill deposits will be much slower than transport through fractured volcanic rocks. The conceptual model of Lehman and Brown also holds that future earthquakes might cause adjustments in the hydrologic system including rapid changes in the water table elevation, altered flow patterns, and adjustments in flow velocities. In short, Lehman and Brown (1996) criticize the treatment of the SZ in past TSPA models for not considering a broad enough range of conceptual models, and for not accounting for a sufficient level of complexity in the natural system. This latter concern has been addressed in the current SZ flow and transport model developed for the TSPA-SR by including additional geologic features in the model.

INTENTIONALLY LEFT BLANK

4. RELATIONSHIP TO U.S. NUCLEAR REGULATORY COMMISSION ISSUE RESOLUTION STATUS REPORTS

4.1 SUMMARY OF THE KEY TECHNICAL ISSUES

As part of the review of site characterization activities, the U.S. Nuclear Regulatory Commission (NRC) has undertaken an ongoing review of information on Yucca Mountain site characterization activities to allow early identification and resolution of potential licensing issues. The principal means of achieving this goal is through informal, prelicensing consultation with the U.S. Department of Energy (DOE). By obtaining input and striving for consensus from the technical community, interested parties, and other groups on such issues, this approach reduces the number of, and better defines, issues that may be in dispute during the NRC licensing review.

The NRC has focused prelicensing issue resolution on topics most critical to the postclosure performance of the potential geologic repository. These topics are called Key Technical Issues (KTIs) and each KTI is subdivided into a number of subissues. The KTIs are:

- Activities Related to Development of the Environmental Protection Agency Standard
- Container Lifetime and Source Term
- Evolution of the Near-field Environment
- Igneous Activity
- Radionuclide Transport
- Repository Design and Thermal Mechanical Effects
- Structural Deformation and Seismicity
- Thermal Effects on Flow
- Total System Performance Assessment (TSPA) and Integration
- Unsaturated and Saturated Flow under Isothermal Conditions.

Identifying KTIs, integrating their activities into a risk informed approach, and evaluating their importance for postclosure performance helps ensure that the NRC is focused on technical uncertainties that will have the greatest affect on the assessment of repository safety.

Early feedback among all parties is essential to define what is known, what is not known, and where additional information is likely to make an important difference in the understanding of future repository safety. The Issue Resolution Status Reports (IRSRs) are the primary mechanism used by the NRC to provide feedback to the DOE on the status of the KTI subissues. IRSRs focus on NRC acceptance criteria for issue resolution and the status of issue resolution, including areas of agreement, comments, and questions. Open meetings and technical exchanges between the NRC and the DOE provide additional opportunities to discuss issue resolution, identify areas of agreement and disagreement, and develop plans to resolve disagreements.

KTIs are subdivided into a number of subissues. For most subissues, the NRC staff has identified technical acceptance criteria that the NRC may use to evaluate the adequacy of information related to the KTIs. The NRC also has identified two cross-cutting programmatic criteria that apply to all IRSRs related to the implementation of the Quality Assurance (QA) Program and the expert elicitation. The following sections provide a summary level discussion

of the KTIs by subissue (Section 4.2) and a discussion of the specific NRC acceptance criteria (Section 4.3). Details of the IRSR technical acceptance criteria, and how and where they are addressed in this Process Model Report (PMR), are presented in Appendix B.

4.2 RELATIONSHIP OF THE SATURATED ZONE FLOW AND TRANSPORT PROCESS MODEL REPORT TO THE KEY TECHNICAL ISSUES

The saturated zone (SZ) PMR provides technical analyses that relate to four of the KTIs and their associated IRSRs. These four KTIs and their subissues are presented in Table 4-1. The KTIs and subissues that relate directly to the SZ PMR are discussed in the following sections.

Table 4-1. Issue Resolution Status Report and Key Technical Issues Related to the Saturated Zone Process Model Report

NRC Key Technical Issues	Subissues
Radionuclide Transport	Radionuclide transport through porous rock Radionuclide transport through alluvium ^a Radionuclide transport through fractured rock ^a Nuclear criticality in the far-field ^a
Structural Deformation and Seismicity	Faulting Seismicity Fracturing and structural framework of the geologic setting ^a Tectonic framework of the geologic setting
Total System Performance Assessment (TSPA) and Integration	System description and demonstration of multiple barriers ^a Model abstraction ^a Scenario Analysis ^a Demonstration of overall performance objective
Unsaturated and Saturated Flow Under Isothermal Conditions	Climatic Change Hydrological effects of climate change ^a Present-day shallow groundwater infiltration Deep percolation (present and future) Saturated zone ambient flow conditions and dilution processes ^a Matrix diffusion ^a

NOTES: Programmatic criteria (QA and use of expert elicitations) apply to all subissues.
^aThese subissues directly relate to the SZ PMR.

4.2.1 Radionuclide Transport

The primary objective of the Radionuclide Transport KTI is to evaluate the processes that may affect the transport of radionuclides from the potential repository to the biosphere (NRC 1999b). The key elements of this KTI are retardation of radionuclides in the fractures and matrix of the unsaturated zone (UZ), and retardation in the fractured rock and alluvium of the SZ (NRC 1999b, p. 5). The IRSR focuses on sorption and other chemical processes that affect transport and colloid-facilitated transport. Two mechanisms that can reduce radionuclide concentrations along flow paths (matrix diffusion and dilution) are evaluated separately in the IRSR/KTI for Unsaturated and Saturated Flow under Isothermal Conditions (Section 4.2.4). Resolution of the KTI for radionuclide transport requires adequate characterization of the physical and chemical processes that affect radionuclide transport (NRC 1999b, p. 3).

Three of the subissues for this KTI relate to the SZ PMR, as described in the following subsections. The UZ PMR (CRWMS M&O 2000b) also provides information relevant to radionuclide transport.

4.2.1.1 Radionuclide Transport Through Alluvium

This subissue focuses on consideration of the flow paths through the alluvium, the alluvial materials encountered by radionuclides transported from the site through fractured rock into the alluvium, and the processes affecting transport (NRC 1999b, p. 3).

Few data are available for this subissue and considerable information will be provided from the Nye County Early Warning Drilling Program (NRC 1999b, pp. 93 to 94). NRC indicates resolution of this issue will await the collection of data from the Nye County drilling program.

Fluid flow in the alluvium is likely to be well represented using a porous continuum conceptual model. Data to quantify the alluvial portion of the flow path are sparse, and hydrologic parameters used in numerical models should be considered to be bounding (Section 3.2.4.1.2).

Transport of sorbing solutes in porous media not controlled by fractures is a subject that has been well studied. Sorption coefficients for alluvium from the Nye County Drilling Program have been measured for a few key radionuclides; for the remaining radionuclides, sorption coefficients have been estimated based on the corresponding values measured for crushed tuff.

The conceptual model for colloid-facilitated transport in the alluvium is essentially the same as in fractured tuffs in that colloid transport is assumed to occur only in advective water (no diffusion into stagnant water or into grains) and colloid attachment and detachment onto alluvial surfaces are described by first-order rate expressions (Section 3.2.4.5.3). Because no site-specific data for colloid transport in the alluvium are available, filtration theory and literature data are used to obtain distributions or bounds for attachment and detachment rate constants.

4.2.1.2 Radionuclide Transport Through Fractured Rock

This subissue evaluates radionuclide transport in fractured rock where there is a potential for preferential pathways for transport and limited radionuclide-rock interactions (NRC 1999b, p. 3). The transport characteristics of the Yucca Mountain site must be adequately estimated and radionuclide transport through fractured rocks must be appropriately considered in assessments of performance of the potential repository.

The site-scale SZ flow and transport model is a three-dimensional, site-scale numerical model that simulates groundwater flow and radionuclide transport from the water table beneath the potential repository to the accessible environment using an equivalent continuum formulation and implicit fault and fracture representation to capture flow through fracture and matrix.

Numerous hydrologic features corresponding to faults and geologic zones are explicitly incorporated into the site-scale SZ flow and transport model as part of the model building process (Section 3.2.1). The presence of faults and fracture zones that are not explicitly represented in the site-scale SZ flow and transport model, and their potential impact on groundwater flow, is implicitly included through consideration of horizontal anisotropy in

permeability in the fractured volcanic units along the SZ flow path from Yucca Mountain. These features are considered to be permanent, but uncertain, characteristics of the system that are not altered by the potential repository or by future events.

Important processes relevant to radionuclide transport in the SZ that are explicitly included in the TSPA-SR analyses are advection in groundwater, dispersion, matrix diffusion in fractured media, sorption of radionuclides, colloid-facilitated transport, and radioactive decay and ingrowth. Advection is the natural movement of groundwater through fractured or porous media in response to gradients in groundwater potential. Dispersion is explicitly simulated as a random-walk process in the site-scale SZ flow and transport model that occurs in the longitudinal and transverse directions. Only longitudinal dispersion is simulated in the one-dimensional SZ transport model. Diffusion of radionuclides from fractures into the immobile groundwater of the matrix is simulated to occur in the fractured volcanic units of the SZ system using an analytical solution for mass transfer in an idealized fracture network. Sorption of radionuclides is simulated to occur in the rock matrix of volcanic units, but is conservatively disregarded in fractures of the SZ. Colloid-facilitated transport is included in the transport simulations as occurring in two modes: as irreversible attachment of radionuclides to colloids originating from the waste, and as equilibrium attachment of radionuclides to colloids. Radioactive decay is simulated to occur for all radionuclides, and ingrowth is simulated for the daughter radionuclides in four key decay chains in the one-dimensional SZ transport model.

4.2.1.3 Nuclear Criticality in the Far Field

This subissue focuses on mechanisms and conditions that could concentrate fissile material into a critical configuration in the geologic environment removed from the thermally perturbed area.

The DOE plans to evaluate criticality using the method in the criticality analysis methodology topical report (YMP 1998) and its supporting documents. Features, events, and processes (FEPs) screening considers criticality events in the far field to be low probability. Preliminary analyses show no significant effect on calculated performance in the first 10,000 yr. even if waste packages are breached.

4.2.2 Structural Deformation and Seismicity

The objective of this KTI is to evaluate the tectonic FEPs that may affect performance of the potential repository (NRC 1999c). Two of the acceptance criteria for one of the subissues for this KTI relate to the SZ PMR. The Disruptive Events PMR (CRWMS M&O 2000d) provides information relevant to the remaining subissues.

4.2.2.1 Fracturing and Structural Framework of the Geologic Setting

The NRC will evaluate alternative modeling approaches for distribution and properties of fractures that are consistent with current data and geologic understanding. They will review representations of fracture data and properties in the SZ flow and transport models and their abstractions to evaluate the degree to which data on fracture variability are honored, the justification for excluding data, and the degree to which fracture data are adequately integrated into the SZ flow and transport models (NRC 1999c, p. 51).

The NRC indicates that the assumptions in the TSPA-Viability Assessment (VA) (DOE 1998b) of homogeneous and isotropic material properties lack a technical basis and are not conservative. The NRC was concerned that these assumptions do not capture anisotropy due to fault and fracture orientations that could influence groundwater flow paths (NRC 1999c, p. 119).

Numerous hydrologic features corresponding to faults and geologic zones are explicitly incorporated into the site-scale SZ flow and transport model (Section 3.2.2.5). The presence of faults and fracture zones that are not explicitly represented in the site-scale SZ flow and transport model and their potential impact on groundwater flow is implicitly included in the nominal case through consideration of horizontal anisotropy in permeability in the fractured volcanic units downgradient of the potential repository. Given the uncertainty in anisotropy, and to simplify the model, the potential effects of anisotropy are bounded in the model. Anisotropy and incorporation of the effects of anisotropy in the model are discussed in Sections 3.5.1 and 3.7.2, respectively.

4.2.3 Total System Performance Assessment and Integration

The objective of this KTI is to describe an acceptable methodology for conducting assessments of the performance of the potential repository, and using these assessments to demonstrate compliance with the overall performance objective and requirements for multiple barriers (NRC 2000).

Three of the subissues for this KTI relate to the SZ PMR, as described in the following subsections.

4.2.3.1 System Description and Demonstration of Multiple Barriers

The system description and demonstration of multiple barriers subissue focuses on the demonstration of multiple barriers and includes: identification of design features of the engineered barrier system and natural features of the geologic setting that are considered barriers important to waste isolation; descriptions of the capability of barriers to isolate waste; and identification of degradation, deterioration, or alteration processes of engineered barriers that would adversely affect the performance of natural barriers. In addition, it addresses NRC expectations of the contents of the TSPA and the supporting documents. Specifically, it focuses on those aspects of the TSPA that will allow for an independent analysis of the results (NRC 2000, p. 4).

4.2.3.2 Model Abstraction

The model abstraction subissue focuses on the information and technical needs related to the development of abstracted models for TSPA. Specifically, the following aspects of model abstraction are addressed under this subissue: data used in development of conceptual approaches or process-level models that are the basis for abstraction in a TSPA, resulting abstracted models used to perform the TSPA, and overall performance of the repository system as estimated in a TSPA. In particular, this subissue addresses the need to incorporate numerous FEPs into the PA and the integration of those factors to ensure a comprehensive analysis of the total system (NRC 2000, p. 4). For the site-scale SZ flow and transport model, this KTI focuses on two elements of the abstraction process: groundwater flow paths (NRC 2000, p. 98) and

radionuclides transport in the SZ (NRC 2000, p. 106). The acceptance criteria for each subissue address five general principles of the TSPA model for the Yucca Mountain site (NRC 2000, p. 32):

- Data and model justification
- Data uncertainty and verification
- Model uncertainty
- Model verification
- Integration.

These two elements of the abstraction process relate to the subissues discussed in Section 4.2.4 (Unsaturated and Saturated Flow and Transport under Isothermal Conditions) and Section 4.2.1 (Radionuclide Transport). For each of these elements, this PMR addresses the five general NRC principles that are listed in Section 4.2.3. The PMR summarizes: 1) data available to support the conceptual basis of the process models and abstractions, 2) the basis for bounding assumptions and representations of uncertainties and parameter variabilities, 3) model uncertainty and alternative conceptual models, 4) abstractions based on, and consistent with, the underlying process models, and 5) incorporation of design features, physical phenomena, couplings, and use of consistent assumptions throughout the abstraction process. To address consistency in the assumptions, the analysis model reports (AMRs) that document assumptions have been subjected to interdisciplinary review to help ensure that assumptions are applied consistently to the extent practicable. In addition, the PMRs have been reviewed by a single team whose main objective was to identify inconsistencies among the PMRs. These measures provide confidence that consistent assumptions are used in the abstraction process, as appropriate.

4.2.3.3 Scenario Analysis

The scenario analysis subissue considers the process of identifying possible processes and events that could affect repository performance, assigning probabilities to categories of events and processes, and the exclusion of processes and events from PA (NRC 2000, p. 4). The scenario analysis process is a key factor in ensuring the completeness of the TSPA.

A systematic method was applied to identify and screen FEPs for SZ flow and transport phenomena. One hundred and fifteen FEPs have been identified and grouped into two broad categories of primary and secondary FEPs. The primary FEPs capture the issues associated with the secondary FEPs. The FEPs are further divided into “included” and “excluded” FEPs.

Included FEPs are those directly represented in TSPA models and process models that support the TSPA. Analyses have focused on the identification and screening of FEPs; this work partially addresses this subissue (Section 1.3).

4.2.4 Unsaturated and Saturated Flow under Isothermal Conditions

The main objective of this KTI is to evaluate all aspects of the ambient hydrological regime at Yucca Mountain that may adversely affect the performance of a potential repository (NRC 1999a). Another objective is to assess the adequacy of the characterization of key

hydrological processes and features at the site and in the region that may adversely affect performance.

Three of the subissues for this KTI relate to the SZ PMR, as described in the following subsections. The UZ PMR (CRWMS M&O 2000b) provides additional information on this subissue.

4.2.4.1 Hydrological Effects of Climate Change

The NRC considers all acceptance criteria for this subissue (NRC 1999a, pp. 172 to 174) closed with the exception of the programmatic criterion on adequacy of the QA program. This PMR includes revisions to the evaluation of climate effects since the VA (DOE 1998a). The effect of climate change is calculated with the site-scale SZ flow and transport model using the modern, monsoon, and glacial transition climate states (Section 3.2.6).

4.2.4.2 Saturated Zone Ambient Flow Conditions and Dilution Processes

The NRC considers that characterization of the ambient flow conditions and dilution processes in the SZ at Yucca Mountain is important for the performance of the potential repository. Ambient flow conditions can be affected by subsurface geology; areal recharge patterns; inter-basin, inter-aquifer mixing, and transfer of groundwaters; and long-term climate cycles. Reliable estimates of groundwater flowpaths, flux, and aquifer hydrologic and transport properties are needed to estimate radionuclide concentrations and delivery at receptor locations, should a release occur (NRC 1999a, p. 182).

The SZ PMR presents a model that has been revised from the TSPA-VA and that includes new data (Section 3.7.2). Uncertainty in travel distances through aquifers of differing properties is stochastically bounded in the model by varying the amount of alluvium along the flow path. A dual porosity approach is incorporated explicitly into the transport methodology for volcanic units to simulate matrix diffusion. Potential effects of horizontal anisotropy are bounded by setting the anisotropy ratio stochastically to either 1 (isotropic) or 5 (based on the C-wells data) by making permeability values for the volcanic units 5 times greater in the north-south direction than in the east-west direction. Uncertainty in groundwater flux is incorporated by considering three discrete cases of low, mean, and high flux by scaling the values of permeability and the boundary fluxes of the mean-flux case downward or upward by a constant factor of 10. Proportional scaling preserves the calibration of the model to head measurements among the three cases. Potentiometric levels in the carbonate aquifer at UE-25p#1 are about 21 m (69 ft) higher than levels in the overlying rocks. This indicates a potential for upward flow and suggests that water will not flow from the tuffs into the carbonates.

4.2.4.3 Matrix Diffusion

If the DOE takes credit for matrix diffusion in the SZ, then the NRC will expect rock matrix and solute diffusion parameters to be based on a SZ transport model that reasonably matches the results of the field tracer-tests that are conducted over different distance scales and flow rates with multiple tracers of different diffusive properties, and is consistent with laboratory data (NRC 1999a, p. 192).

Diffusion of radionuclides from fractures into the immobile groundwater of the matrix occurs in the fractured volcanic units of the SZ and slows the rate of travel of radionuclides. The conceptual models for transport in the volcanic tuffs and the alluvium are different in that matrix diffusion occurs only in the volcanic tuffs, and sorption in the volcanic tuffs occurs only after radionuclides diffuse into the matrix. Diffusion of radionuclides from fractures into the immobile groundwater of the matrix is simulated to occur in the fractured volcanic units of the SZ system using an analytical solution for mass transfer in an idealized fracture network.

The C-wells reactive tracer test (Section 3.1.3.2) demonstrated that models that incorporate matrix diffusion provide more reasonable fits to the tracer-experiment data than do models that use a single continuum. The matrix sorption coefficient that fit the data for the lithium tracer in the C-wells reactive tracer experiment was similar to values determined in laboratory sorption tests. This provides confidence that the matrix-diffusion model is appropriate. The fact that the early lithium response had the same timing as that of the nonsorbing tracers, but with a lower normalized peak concentration, is consistent with matrix diffusion coupled with sorption in the matrix (Figure 3-9).

4.3 U.S. NUCLEAR REGULATORY COMMISSION ACCEPTANCE CRITERIA

Specific technical acceptance criteria for each of the subissues that relate to this PMR are summarized in Table 4-1. Details of the approach to addressing the criteria, and the sections of the PMR where these approaches and details are discussed, are provided in Appendix B.

The SZ PMR also addresses NRC programmatic criteria for QA and the use of expert elicitation. These programmatic criteria apply to all subissues and are not repeated under each subissue in Table 4-1.

The acceptance criteria for QA address the implementation of an adequate QA program by the DOE. The SZ PMR was developed in accordance with project procedures for documenting data, analyses, models, computer codes, and preparing and reviewing technical reports (Section 1.4). The programmatic criterion for expert elicitation specifies that expert elicitation should be conducted in accordance with NUREG-1563 (Kotra et al. 1996) or other acceptable approaches.

The statements for the programmatic criterion relating to expert elicitations vary among IRSRs, but the overall requirements are similar in all the IRSRs: expert elicitations are to be conducted and documented using the guidance in the Branch Technical Position on Expert Elicitation (Kotra et al. 1996) or other acceptable approaches.

A SZ flow and transport expert elicitation (CRWMS M&O 1998b) was sponsored by the DOE to characterize the knowledge and uncertainties associated with certain key issues related to the SZ system in the Yucca Mountain area and the downgradient region. The procedures and approaches for eliciting expert judgments were developed through conducting many studies and have been formalized in guidance documents prepared by the DOE, NRC, and a study sponsored by the NRC, the DOE, and the Electrical Power Research Institute (CRWMS M&O 1998b, p. 2-2). The process followed in the expert elicitation was consistent with these guidance documents and studies. The NRC (1999a, p. 190) indicates that the expert elicitation on SZ flow and transport (CRWMS M&O 1998b) was conducted and documented in an acceptable way.

Even though the NRC indicates that the expert elicitation was conducted and documented in an acceptable way, NRC 1999a (Attachment D) cautions that the NRC is not bound by the conclusions of an elicitation based solely on adherence to guidance provided by the staff.

INTENTIONALLY LEFT BLANK

5. SUMMARY AND CONCLUSIONS

This document summarizes the development of the site-scale saturated-zone (SZ) flow and transport model, the results of which will be used in calculations presented in the Total System Performance Assessment (TSPA)-Site Recommendation (SR) report. The site-scale SZ flow and transport model was developed in several stages. First, the hydrogeology of a region around Yucca Mountain was characterized. Many aspects of this characterization were synthesized while conceptualizing and numerically simulating a regional-scale groundwater flow system (referred to as the Death Valley regional groundwater flow system). Second, a detailed conceptual model of flow and transport processes was developed for a smaller region (i.e., the site-scale region) that is appropriate for TSPA-SR calculations. Third, a numerical model of groundwater flow and radionuclide transport was developed (i.e., the site-scale SZ flow and transport model). Finally, results of the numerical model (i.e., those that describe the transport of radionuclides and the associated uncertainty in the SZ) were abstracted for use in the TSPA-SR calculations.

The organization of this section follows that of Chapter 3 of this document. Sections 5.1 and 5.2 refer to characterization of site-scale SZ flow and transport (Section 3.1) and the conceptual model of site-scale SZ flow and transport (Section 3.2), respectively. Material presented in Sections 3.3 and 3.4 regarding the mathematical model and numerical approach are summarized in Section 5.3. Section 5.4 summarizes the SZ model abstraction for TSPA discussed in Sections 3.6 and 3.7. Conclusions are presented in Section 5.5.

5.1 SATURATED ZONE FLOW AND TRANSPORT CHARACTERIZATION

A large amount of information about the regional-scale hydrogeology is known from activities of the Yucca Mountain Site Characterization Project (YMP), as well as from numerous additional hydrogeologic studies that have been conducted in the vicinity of the Nevada Test Site (NTS). Specifically, sufficient information is available to describe the stratigraphy, structure, and hydraulic properties of rocks in this region, recharge and discharge regions, and groundwater flow paths.

The climate in the Yucca Mountain area is arid and the SZ generally is far below the land surface. Natural recharge to the SZ is from precipitation that infiltrates at the land surface and percolates through the unsaturated zone. Recharge occurs primarily in mountainous areas where relatively larger amounts of snow and rainfall occur. Areas of recharge include Yucca Mountain and other regions of higher elevation to the north and northeast, and the Spring Mountains 50 km (31 mi.) southeast of Yucca Mountain. Estimates of recharge rates at the regional scale are based on empirical relationships. Confidence in these estimates comes from numerical models which ensure that, at a regional scale, recharge to and discharge from the SZ are equal. Natural discharge from the Death Valley flow system is from evapotranspiration and springs at low elevations, mainly in Death Valley and Ash Meadows. Groundwater flows from regions of recharge to regions of discharge. Flow paths in the SZ are well characterized at the regional scale because a large number of measurements of water levels in boreholes are available. Taken together, information about recharge and discharge and measured water levels provide a sound understanding of groundwater flow paths in the SZ in the Death Valley regional groundwater flow system.

In the area near Yucca Mountain, water level measurements, hydraulic testing in wells, and geochemical analyses provide more detailed information on groundwater flow in the SZ. Water level measurements indicate considerable differences in the magnitude of the hydraulic gradient to the north (apparent large hydraulic gradient), west (moderate hydraulic gradient), and southeast (low hydraulic gradient) of Yucca Mountain. The hydraulic gradient results in the flow of groundwater away from the potential repository to the southeast and south. A vertical, upward hydraulic gradient from the underlying carbonate aquifer and the deeper volcanic units is observed at one location immediately downgradient of Yucca Mountain. Hydraulic testing in wells provides estimates of the variability in permeability for tuffs and information on the distribution of groundwater flow in fractured volcanic units. Data on groundwater chemistry indicate significant spatial variability in geochemical and isotopic composition that results from differences in flow paths, recharge locations, and groundwater age.

Due to the long period of time over which the performance of the potential Yucca Mountain repository must be evaluated, the possible impact of a future wetter climate must be considered. Modeling studies suggest that greater and more widespread recharge would result in a higher water table and steeper hydraulic gradients. Field mapping of the occurrence of zeolites and paleospring deposits has confirmed that a higher water table existed during past wetter climates and provides confidence in numerical simulations of the possible impacts of climate change. The general locations of areas of recharge and discharge depend mainly on the topography of the land surface. Consequently, wetter climates in the future are expected to result in faster groundwater flow rates along essentially present-day flow paths.

As groundwater in the Death Valley system moves from recharge to discharge areas, flow rates and paths depend largely on the hydraulic properties of the rocks and materials along the flow paths. Geologic studies have resulted in a sufficient understanding to identify the important rock types and their spatial distribution. The rock types that play the largest role in regional hydrogeology are Paleozoic carbonates, Quaternary-Tertiary volcanic rocks, and Quaternary-Tertiary sediments and volcanic tuffs that fill structural depressions (referred to as valley-fill material in portions of this report). The valley fill primarily is alluvium. Relatively shallow flow occurs in the volcanic rocks and valley fill. Deeper flow occurs in the regionally extensive carbonate aquifer. Along the inferred shallow flow path in the SZ from Yucca Mountain, groundwater flow occurs in volcanic rocks near the potential repository site and in younger valley-fill deposits at greater distances.

The permeability of the volcanic rocks in the vicinity of Yucca Mountain typically is increased by the presence of fractures. An extensive suite of field observations, interpretations of borehole logs, hydrologic tests in boreholes, lab-scale tests, and field tracer tests (C-wells Complex) confirm that fractures enhance groundwater flow in the volcanic rocks. However, flow in the alluvium occurs through the primary porosity of these sediments.

Tracer testing between wells in fractured volcanic units and laboratory measurements have provided information on the processes controlling the transport of potential radionuclide contamination, including matrix diffusion, sorption, dispersion, and colloid-facilitated transport. Field-scale tests and laboratory experiments have demonstrated the occurrence of solutes diffusing from fractures into the immobile groundwater in the rock matrix. Data on the sorption of radionuclides onto volcanic rocks and alluvium have been obtained in laboratory experiments.

Tracer testing using an analog sorbing species has demonstrated reasonable agreement with laboratory-scale measurements of sorption for the same species. Values of longitudinal dispersivity, derived from tracer tests in fractured tuffs, generally agree with measurements made at other sites. Field-scale tests and laboratory experiments provide information on the transport of colloids in fractured media from the site.

5.2 CONCEPTUAL MODEL OF SITE SCALE FLOW AND TRANSPORT

The site-scale conceptual model is a synthesis of what is known about flow and transport processes at the scale required for TSPA-SR calculations. This knowledge builds on, and is consistent with, knowledge that has accumulated at the regional scale, but is more detailed because a higher density of data is available for the site-scale level.

Information from geologic maps and cross sections, borehole data, fault-trace maps, and geophysical data were used to construct a three-dimensional (3-D) interpretation (hydrogeologic framework model) of the hydrostratigraphy and geologic structure within the domain of the site-scale model. Rock stratigraphic units within the framework model are grouped into 18 hydrogeologic units that are classified as having relatively large permeability (aquifers), or relatively small permeability (confining units). The framework model specifies the position and geometry of these hydrogeologic units. In addition, the framework model identifies major faults that affect groundwater flow.

The source of most of the groundwater flow through the site-scale model is lateral flow across the western, northern, and eastern boundaries. A small portion (approximately 5 percent) of the total flux through the site-scale model is from recharge of precipitation falling within the model domain and surface runoff infiltrating along Fortymile Wash. Outflow from the site-scale region mainly is by groundwater flow across its southern boundary. A small amount of water is removed by pumping wells located in the Amargosa Valley near the southern boundary of the model domain.

As groundwater moves away from the area beneath the potential repository, it first flows through a series of welded and nonwelded volcanic tuffs. These flow paths pass into alluvium after traveling approximately 15 km (9 mi.). The distance to the contact between the tuffs and the alluvium is uncertain.

The conceptual model of radionuclide transport in the SZ includes the processes of advection, dispersion, matrix diffusion in fractured volcanic units, sorption, and colloid-facilitated transport. Advection is the process by which groundwater flow moves contaminants along the flow path in the SZ. The process of dispersion spreads solute in the longitudinal and transverse directions due to small-scale variations in groundwater flow velocity. Matrix diffusion is the process by which solute moves between the relatively rapidly moving groundwater in fractures to the immobile groundwater in the low-permeability rock matrix by the process of molecular diffusion. As noted above, groundwater flow in tuffs primarily is in fractures, and flow in the alluvium is in the primary porosity. The extent to which flow occurs in fracture porosity, primary porosity, or both, plays an important role in the transport and retardation of radionuclides. Sorption is the process in which solute may be attached to the surface of solid grains in the aquifer. The conceptual model of the sorption process includes potential sorption of radionuclides onto the

rock matrix in fractured volcanic units and onto the granular medium of the alluvium. Sorption onto the walls of fractures in the volcanic units is conservatively neglected in the current conceptual model, requiring matrix diffusion to allow access of radionuclides to the sorptive capacity of the matrix in fractured units. Colloid-facilitated transport of radionuclides is conceptualized to occur by two possible modes. Radionuclides may be irreversibly attached to some colloids that form during degradation of the waste. The colloids with irreversibly attached radionuclides are subject to filtration and resuspension as they move through the fractured volcanic units and alluvium. The second mode of colloid-facilitated transport is a conceptual model in which radionuclides are reversibly attached to colloids in the SZ flow system. In this mode, equilibrium exists among the radionuclide concentration on colloids, the aqueous-phase concentration of the radionuclide, and the concentration of the radionuclide sorbed on the mineral grains of the aquifer.

5.3 MATHEMATICAL MODEL AND NUMERICAL APPROACH

The mathematical basis of the site-scale SZ flow and transport model, and the associated numerical approaches, are designed to assist in quantifying the uncertainty in the permeability of rocks in the geologic framework model and to accurately represent the flow and transport processes included in the site-scale conceptual model. A description of the methodology used to simulate transport processes is given in Section 3.3.4. An inverse approach was used to estimate the distribution of rock permeability that resulted in calculated values of hydraulic head that best matched measured values, and calculated rates of lateral flow across model boundaries that are compatible with results of the regional-scale model.

Calculations of groundwater flow (specific-discharge field) assume the flow field does not change with time and that flow occurs in a continuous porous media. The approach of not explicitly representing fractures in the volcanic rocks is valid at the scale required for TSPA-SR (tens of kilometers) but is not accurate at length scales shorter than the dimensions of model grid blocks (tens to hundreds of meters). The transport processes considered include advection and dispersion of solutes and colloids by moving groundwater, diffusion of solutes, and equilibrium sorption of radionuclides on mineral surfaces, and reversible and irreversible sorption of radionuclides onto colloid particles. A particle tracking approach is used to simulate advection and dispersion of solutes to minimize numerical dispersion. A semi-analytic method is used to calculate the retardation of radionuclide transport due to diffusion into the matrix of the fractured tuffs.

Confidence in the results of the mathematical model was obtained by comparing calculated to observed hydraulic heads, estimated to measured permeabilities, and lateral flow rates calculated by the site-scale SZ flow and transport model to those calculated by the regional-scale model. In addition, it was confirmed that the flowpaths leaving the region of the potential repository are consistent with those inferred from gradients of measured head and those inferred independently from water chemistry data.

5.4 SUMMARY OF SATURATED ZONE MODEL ABSTRACTION FOR TOTAL SYSTEM PERFORMANCE ASSESSMENT-SITE RECOMMENDATION

The objective of the analysis implemented using the site-scale SZ flow and transport model is to simulate unit breakthrough curves for radionuclide mass at the interface between the SZ and the biosphere. These breakthrough curves contain information on the radionuclide transport through the SZ that is used in the TSPA calculations to determine the mass fraction of radionuclides delivered to the biosphere.

The starting point for the analysis of the site-scale SZ flow and transport is the calibrated site-scale SZ groundwater flow model. Input files for the site-scale SZ flow model are modified to include relevant radionuclide transport parameters and to produce the output needed for breakthrough curves of radionuclide mass. The simulation of radionuclide decay chains and radioactive ingrowth in the SZ is performed using the simplified one-dimensional (1-D) radionuclide transport model and are conducted directly in the TSPA simulator.

Uncertainties are explicitly incorporated into the SZ TSPA site-scale flow and transport abstractions through key parameters and conceptual models. The probabilistic analysis of uncertainty is implemented through Monte Carlo realizations of the site-scale SZ flow and transport system, in a manner consistent with the TSPA simulations implemented with the GoldSim software code. Alternative models of groundwater flux and horizontal anisotropy are included as uncertainty among six SZ groundwater flow fields. Uncertainty in the location of the contact between volcanic units and the alluvium is incorporated as geometric variability in the alluvium zone in the site-scale SZ flow and transport model. Alternative models of colloid-facilitated transport of radionuclides are considered in the uncertainty analysis through the use of two coexisting modes of colloid-facilitated transport. The nominal case of SZ flow and transport for the TSPA-SR explicitly incorporates many features, events, and processes of the SZ system and implicitly includes others.

Abstraction methods for conducting TSPA simulations include the convolution integral method, alternative climate states, dilution of radionuclides in the water supply of the critical group, and radionuclide decay chains. The convolution integral method is used in TSPA-SR analyses to calculate the radionuclide mass flux at the interface of the SZ and the biosphere, based on the transient radionuclide mass flux at the water table beneath the potential repository and the appropriate unit breakthrough curve simulated by the site-scale SZ flow and transport model. This computationally efficient method combines information about the unit response of the SZ system with the radionuclide source history from the UZ to calculate transient system behavior. The effects of climate change on radionuclide transport in the SZ are incorporated in the TSPA-SR analyses by scaling the radionuclide mass breakthrough curves to reflect the greater groundwater specific discharge under wetter climatic conditions. The hypothetical release of radionuclides from groundwater to the biosphere occurs by the pumping of groundwater to supply water for a future farming community in the nominal case for TSPA-SR. Radionuclide concentrations in the water supply of the hypothetical farming community are calculated by assuming that all of the radionuclide mass is captured by the pumping wells and that this mass is uniformly distributed in the total volume of groundwater used by the community. The 1-D radionuclide transport model for TSPA-SR is used for simulating radioactive decay and radionuclide ingrowth in the SZ for four decay chains. The 1-D radionuclide transport model,

while based on results of the 3-D site-scale SZ flow and transport model, represents a simplification or abstraction of the site-scale SZ flow and transport model.

5.5 CONCLUSIONS

Site characterization activities in the SZ at Yucca Mountain have provided a basic understanding of the SZ system in terms of groundwater flow and potential radionuclide transport. This understanding includes the general flow pathway from beneath Yucca Mountain to areas of potential groundwater discharge to the biosphere by future pumping. Subsurface data also provide information on the geologic media present in the SZ, water levels, and the groundwater flow characteristics in fractured volcanic rocks. Field-scale and laboratory-scale studies of transport characteristics in the SZ establish an understanding of the processes relevant to the potential migration of radionuclides. Regional-scale studies of the groundwater flow system in the SZ constitute an important framework of understanding into which the Yucca Mountain site-scale SZ system is placed.

Taken in total, these data provide an appropriate and adequate basis for the conceptual model and numerical modeling of the site-scale SZ flow and transport system. The site-characterization information, along with inferences based on that information, support a conceptual model in which groundwater flow is controlled by the spatial distribution of geologic units and structural features. Site-specific data, together with regional-scale studies, suggest that a large fraction of groundwater flowing in the SZ enters the Yucca Mountain site area as lateral flow from the north with a small fraction contributed by recharge near Yucca Mountain. The conceptual model of radionuclide transport in fractured rocks includes the processes of advection, dispersion, matrix diffusion, sorption, and colloid-facilitated transport, as supported by site data. These components of the conceptual model are implemented numerically in the site-scale SZ flow and transport model, which represents the processes relevant to radionuclide migration from a potential repository at Yucca Mountain to the biosphere.

The site-scale SZ flow and transport model forms the basis for analyses of performance of the potential repository in the TSPA-SR. The site-scale SZ flow and transport model constitutes a reasonable and adequate representation of the SZ system for the purposes of TSPA, particularly when considered in the context of the uncertainty of key model parameters incorporated in the Monte Carlo analyses performed for TSPA-SR. Abstraction methods used to incorporate SZ modeling results into the TSPA simulations are appropriate numerical simplifications that retain information embodied in the results of the underlying site-scale SZ model.

Radionuclide migration through the SZ could affect total system performance in two ways. First, the SZ functions as a mechanism to delay the release of radionuclides to the biosphere. This delay potentially allows radioactive decay to reduce the release of radionuclides to the biosphere. Second, the radionuclide concentrations may be diluted during the transport in the SZ. Although the dispersive processes that lead to dilution are incorporated in the site-scale SZ flow and transport modeling, the simplified approach used to calculate concentrations in the water supply of the critical group negates the need to analyze in situ radionuclide concentrations in the SZ. These two factors are of primary importance to performance of the potential repository. The transport time of contaminants in the SZ allows for considerable radioactive decay of some radionuclides and may delay the release of some radionuclides beyond the limits of regulatory

concern. The calculated dose in TSPA analyses is directly proportional to the concentration of radionuclides in the groundwater supply of the receptors of interest.

The site-scale SZ flow and transport model, as used in TSPA-SR analyses, contains aspects that are potentially conservative from the perspective of assessing performance of the potential repository. The defensibility of assumptions, modeling approach, and parameter values was given high priority in the model development, analysis process, and TSPA abstractions. Consequently, the models and results may be more conservative than the best estimate of expected behavior of the site-scale SZ flow and transport system. The resulting potential conservatism in simulations of radionuclide transport with the site-scale SZ model is embedded in the underlying conceptual model, the numerical implementation of the model, or in the uncertainty distributions for parameters used in the TSPA analyses.

INTENTIONALLY LEFT BLANK

6. REFERENCES

6.1 DOCUMENTS CITED

Ahola, M. and Sagar, B. 1992. *Regional Groundwater Modeling of the Saturated Zone in the Vicinity of Yucca Mountain, Nevada, Iterative Performance Assessment – Phase 2*. NUREG/CR-5890. Washington, D.C.: U.S. Nuclear Regulatory Commission. TIC: 232662.

Archambeau, C.B. and Price, N.J. 1991. *An Assessment of J.S. Szymanski's Conceptual Hydro-Tectonic Model and Its Relevance to Hydrologic and Geologic Processes at the Proposed Yucca Mountain Nuclear Waste Repository, Minority Report of the Special DOE Review Panel*. Washington, D.C.: U.S. Department Of Energy. ACC: NNA.19911210.0057.

Arnold, B.W. and Kuzio, S.P. 1998. "SZ Transport Sensitivity to Radionuclide-Source Size." Memorandum from B.W. Arnold (SNL) and S.P. Kuzio (SNL) to Distribution, September 16, 1998. ACC: MOL.19990517.0228.

Barnard, R.W. and Dockery, H.A., eds. 1991. "Nominal Configuration" *Hydrogeologic Parameters and Computational Results*. Volume 1 of *Technical Summary of the Performance Assessment Computational Exercises for 1990 (PACE-90)*. SAND90-2726. Albuquerque, New Mexico: Sandia National Laboratories. ACC: NNA.19910523.0001.

Barnard, R.W.; Wilson, M.L.; Dockery, H.A.; Gauthier, J.H.; Kaplan, P.G.; Eaton, R.R.; Bingham, F.W.; and Robey, T.H. 1992. *TSPA 1991: An Initial Total-System Performance Assessment for Yucca Mountain*. SAND91-2795. Albuquerque, New Mexico: Sandia National Laboratories. ACC: NNA.19920630.0033.

Barnett, D.B.; Bergeron, M.P.; Cole, C.R.; Freshley, M.D.; and Wurstner, S.K 1997. *Tritium Monitoring in Groundwater and Evaluation of Model Predictions for the Hanford Site 200 Area Effluent Treatment Facility*. PNNL-11665. Richland, Washington: Pacific Northwest National Laboratory. TIC: 246769.

Barr, G.E. and Miller, W.B. 1987. *Simple Models of the Saturated Zone at Yucca Mountain*. SAND87-0112. Albuquerque, New Mexico: Sandia National Laboratories. ACC: NNA.19870811.0058.

Beasley, T.M.; Dixon, P.R.; and Mann, L.J. 1998. "99Tc, 236U, and 237Np in the Snake River Plain Aquifer at the Idaho National Engineering and Environmental Laboratory, Idaho Falls, Idaho." *Environmental Science & Technology*, 32, (24), 3875-3881. Easton, Pennsylvania: American Chemical Society. TIC: 243863.

Bedinger, M.S.; Langer, W.H.; and Reed, J.E. 1989. "Hydraulic Properties of Rocks in the Basin and Range Province." *Studies of Geology and Hydrology in the Basin and Range Province, Southwestern United States, for Isolation of High-Level Radioactive Waste—Basis of Characterization and Evaluation*. Professional Paper 1370-A. A16-A18. Denver, Colorado: U.S. Geological Survey. ACC: NNA.19910524.0125.

Blomqvist, R.; Suksi, J.; Ruskeeniemi, T.; Ahonen, L.; Niini, H.; Vuorinen, U.; and Jakobsson, K. 1995. *The Palmottu Natural Analogue Project, Summary Report 1992—1994, The Behaviour of Natural Radionuclides in and Around Uranium Deposits; Nr. 8.* Report YST-88. Espoo, Finland: Geological Survey of Finland. TIC: 247142.

Brookins, D.G. 1978. “Retention of Transuranic and Actinide Elements and Bismuth at the Oklo Natural Reactor, Gabon: Application of Eh-pH Diagrams.” *Chemical Geology*, 23, 309-323. Amsterdam, The Netherlands: Elsevier Scientific Publishing Company. TIC: 247321.

Buddemeier, R.W. and Hunt, J.R. 1988. “Transport of Colloidal Contaminants in Groundwater: Radionuclide Migration at the Nevada Test Site.” *Applied Geochemistry*, 3, 535-548. Oxford, England: Pergamon Press. TIC: 224116.

Budnitz, B.; Ewing, R.C.; Moeller, D.W.; Payer, J.; Whipple, C.; and Witherspoon, P.A. 1999. *Peer Review of the Total System Performance Assessment-Viability Assessment Final Report.* Las Vegas, Nevada: Total System Performance Assessment Peer Review Panel. ACC: MOL.19990317.0328.

Carrigan, C.R.; King, G.C.P.; Barr, G.E.; and Bixler, N.E. 1991. *Water-Table Excursions Induced by Seismic and Volcanic Events at Yucca Mountain.* SAND 91-00105. Albuquerque, New Mexico: Sandia National Laboratories. ACC: MOL.19980506.0294.

Chapman, N.A.; McKinley, I.G.; Shea, M.E.; and Smellie, J.A.T. 1991. *The Poços de Caldas Project: Summary and Implications for Radioactive Waste Management.* SKB Technical Report 90-24. Stockholm, Sweden: Swedish Nuclear Fuel and Management Company. TIC: 205593.

Claassen, H.C. 1983. *Sources and Mechanisms of Recharge for Ground Water in the West-Central Amargosa Desert, Nevada--A Geochemical Interpretation.* Open-File Report 83-542. Denver, Colorado: U.S. Geological Survey. ACC: NNA.19870406.0176.

Cohen, A.J.B.; Oldenburg, C.M.; Simmons, A.M.; Mishra, A.K.; and Hinds, J. 1997. *S4Z: Sub-Site Scale Saturated Zone Model for Yucca Mountain.* Milestone SP25UM4. Berkeley, California: Lawrence Berkeley National Laboratory. ACC: MOL.19971204.0732.

Cohon, J.L. 1998a. Nuclear Waste Technical Review Board Review of Reports by Jerry Syzmanski and Harry Swainston. Letter from J.L. Cohon (NWTRB) to L.H. Barrett (DOE/OCRWM), July 24, 1998, with attachment. ACC: MOL.19980814.0396.

Cohon, J.L. 1998b. Board’s Comments on the January Meeting and Reflects Ongoing Effort to Provide Feedback to the Office of Civilian Radioactive Waste Management (OCRWM) after Board Meetings. Letter from J.L. Cohon (NWTRB) to L.H. Barrett (DOE/OCRWM), April 7, 1998. ACC: HQO.19980716.0038.

Cohon, J.L. 1999a. Comments on the January 1999 NWTRB Meeting Letter from J.L. Cohon (NWTRB) to L.H. Barrett (OCRWM/DOE), March 3, 1999. ACC: HQO.19990812.0006.

Cohon, J.L. 1999b. Comments on the Scientific Program, June 1999 Nuclear Waste Technical Review Board Meeting. Letter from J.L. Cohon (NWTRB) to L.H. Barrett (OCRWM), August 3, 1999. ACC: MOL.20000317.0405.

Cowan, G.A. 1976. "A Natural Fission Reactor." *Scientific American*, 235, (1), 36-47. New York, New York: Scientific American. TIC: 233076.

Craig, R.W. 1997. "Review of Reports Relating to Hydrothermal Activity and Modeling of Potential Water Table Rise at Yucca Mountain, Nevada by TRAC-NA on Behalf of the Nevada Nuclear Waste Project Office." Memorandum from R.W. Craig (USGS) to S.J. Brocoum (DOE), October 8, 1997, with attachments. ACC: MOL.19980224.0078.

Cramer, J. 1995. "Cigar Lake: A Natural Example of Long-Term Isolation of Uranium." *Radwaste Magazine*, 2, (3), 36-40. La Grange Park, Illinois: American Nuclear Society. TIC: 247698.

Cramer, J.J. 1986. "Sandstone-Hosted Uranium Deposits in Northern Saskatchewan as Natural Analogs to Nuclear Fuel Waste Disposal Vaults." *Chemical Geology*, 55, 269-279. Amsterdam, The Netherlands: Elsevier Science Publishers B.V. TIC: 246760.

Cramer, J.J. and Sargent, F.P. 1994. "The Cigar Lake Analog Study: An International R&D Project." *High Level Radioactive Waste Management, Proceedings of the Fifth Annual International Conference, Las Vegas, Nevada, May 22-26, 1994*. 4, 2237-2242. La Grange Park, Illinois: American Nuclear Society. TIC: 210984.

Cramer, J.J. and Smellie, J.A.T. 1994. *Final Report of the AECL/SKB Cigar Lake Analog Study*. AECL-10851. Pinawa, Manitoba, Canada: Atomic Energy of Canada Limited. TIC: 212783.

CRWMS M&O 1994. *Total System Performance Assessment - 1993: An Evaluation of the Potential Yucca Mountain Repository*. B00000000-01717-2200-00099 REV 01. Las Vegas, Nevada: CRWMS M&O. ACC: NNA.19940406.0158.

CRWMS M&O 1995. *Total System Performance Assessment - 1995: An Evaluation of the Potential Yucca Mountain Repository*. B00000000-01717-2200-00136 REV 01. Las Vegas, Nevada: CRWMS M&O. ACC: MOL.19960724.0188.

CRWMS M&O 1997. *The Site-Scale Unsaturated Zone Transport Model of Yucca Mountain*. Milestone SP25BM3, Rev. 1. Las Vegas, Nevada: CRWMS M&O. ACC: MOL.19980224.0314.

CRWMS M&O 1998a. "Hydrologic System." Book 2 - Section 5 of *Yucca Mountain Site Description*. B00000000-01717-5700-00019 REV 00. Las Vegas, Nevada: CRWMS M&O. ACC: MOL.19980729.0051.

CRWMS M&O 1998b. *Saturated Zone Flow and Transport Expert Elicitation Project*. Deliverable Number SL5X4AM3. Las Vegas, Nevada: CRWMS M&O. ACC: MOL.19980825.0008.

CRWMS M&O 1998c. "Geology." Book 1 - Section 3 of *Yucca Mountain Site Description*. B00000000-01717-5700-00019 REV 00. Las Vegas, Nevada: CRWMS M&O. ACC: MOL.19980729.0049.

CRWMS M&O 1998d. *Yucca Mountain Site Description*. B00000000-01717-5700-00019 REV 00. Las Vegas, Nevada: CRWMS M&O. ACC: MOL.19981202.0492.

CRWMS M&O 1998e. "Saturated Zone Flow and Transport." Chapter 8 of *Total System Performance Assessment-Viability Assessment (TSPA-VA) Analyses Technical Basis Document*. B00000000-01717-4301-00008 REV 01. Las Vegas, Nevada: CRWMS M&O. ACC: MOL.19981008.0008.

CRWMS M&O 1999a. *Recharge and Lateral Groundwater Flow Boundary Conditions for the Saturated Zone Site-Scale Flow and Transport Model*. ANL-NBS-MD-000010 REV 00. Las Vegas, Nevada: CRWMS M&O. ACC: MOL.19991118.0188.

CRWMS M&O 1999b. *YMP FEP Database Rev. 00C*. Las Vegas, Nevada: CRWMS M&O. ACC: MOL.19991214.0518; MOL.19991214.0519.

CRWMS M&O 1999c. *Work Package Planning Summary for Saturated Zone Flow and Transport PMR, 8191213SU1, Revision 00*. WPP-NBS-MD-000009. Las Vegas, Nevada: CRWMS M&O. ACC: MOL.19991008.0221.

CRWMS M&O 1999d. *M&O Site Investigations*. Activity Evaluation, January 23, 1999. Las Vegas, Nevada: CRWMS M&O. ACC: MOL.19990317.0330.

CRWMS M&O 1999e. *M&O Site Investigations -- (Q)*. Activity Evaluation, September 28, 1999. Las Vegas, Nevada: CRWMS M&O. ACC: MOL.19990928.0224.

CRWMS M&O 1999f. *Work Package Planning Summary for Saturated Zone Flow and Transport PMR, 1401213SM1, Revision 00*. WPP-NBS-MD-000012. Las Vegas, Nevada: CRWMS M&O. ACC: MOL.19991008.0217.

CRWMS M&O 1999g. *Work Package Planning Summary for Saturated Zone Flow and Transport PMR Product Checking, 1401213SM2, Revision 00*. WPP-NBS-MD-000011. Las Vegas, Nevada: CRWMS M&O. ACC: MOL.19991008.0224.

CRWMS M&O 1999h. *Work Package Planning Summary for Saturated Zone Flow and Transport PMR Product Checking, 819113SU2 Revision 00*. WPP-NBS-MD-000010. Las Vegas, Nevada: CRWMS M&O. ACC: MOL.19991008.0222.

CRWMS M&O 2000a. *Repository Safety Strategy: Plan to Prepare the Postclosure Safety Case to Support Yucca Mountain Site Recommendation and Licensing Considerations*. TDR-WIS-RL-000001 REV 03. Las Vegas, Nevada: CRWMS M&O. ACC: MOL.20000119.0189.

CRWMS M&O 2000b. *Unsaturated Zone Flow and Transport Model Process Model Report*. TDR-NBS-HS-000002 REV 00. Las Vegas, Nevada: CRWMS M&O. ACC: MOL.20000320.0400.

CRWMS M&O 2000c. *Biosphere Process Model Report*. TDR-MGR-MD-000002 REV 00. Las Vegas, Nevada: CRWMS M&O. ACC: MOL.20000323.0634.

CRWMS M&O 2000d. *Disruptive Events Process Model Report*. TDR-NBS-MD-000002 REV 00. Las Vegas, Nevada: CRWMS M&O. ACC: MOL.20000504.0295.

CRWMS M&O 2000e. *Integrated Site Model Process Model Report*. TDR-NBS-GS-000002 REV 00 ICN 01. Las Vegas, Nevada: CRWMS M&O. ACC: MOL.20000121.0116.

CRWMS M&O 2000f. *Waste Form Degradation Process Model Report*. TDR-WIS-MD-000001 REV 00. Las Vegas, Nevada: CRWMS M&O. ACC: MOL.20000403.0495.

CRWMS M&O 2000g. *Engineered Barrier System Degradation, Flow, and Transport Process Model Report*. TDR-EBS-MD-000006 REV 00. Las Vegas, Nevada: CRWMS M&O. ACC: MOL.20000324.0558.

CRWMS M&O 2000h. *Colloid-Associated Radionuclide Concentration Limits: ANL*. ANL-EBS-MD-000020 REV 00. Las Vegas, Nevada: CRWMS M&O. ACC: MOL.20000329.1187.

CRWMS M&O 2000i. *Modeling Sub Gridlock Scale Dispersion in Three-Dimensional Heterogeneous Fractured Media*. ANL-NBS-HS-000022 REV 00. Las Vegas, Nevada: CRWMS M&O. ACC: MOL.20000622.0363.

CRWMS M&O 2000j. *Saturated Zone Transport Methodology and Transport Component Integration*. MDL-NBS-HS-000010 REV 00. Las Vegas, Nevada: CRWMS M&O. Submit to RPC URN-0402

CRWMS M&O 2000k. *Probability Distribution for Flowing Interval Spacing*. ANL-NBS-MD-000003 REV 00. Las Vegas, Nevada: CRWMS M&O. ACC: MOL.20000602.0052.

CRWMS M&O 2000l. *Saturated Zone Colloid-Facilitated Transport*. ANL-NBS-HS-000031 REV 00. Las Vegas, Nevada: CRWMS M&O. ACC: MOL.20000609.0266.

CRWMS M&O 2000m. *Geochemical and Isotopic Constraints on Ground-Water Flow Directions, Mixing, and Recharge at Yucca Mountain, Nevada*. ANL-NBS-HS-000021 REV 00. Las Vegas, Nevada: CRWMS M&O. Submit to RPC URN-0060

CRWMS M&O 2000n. *Calibration of the Site-Scale Saturated Zone Flow Model*. MDL-NBS-HS-000011 REV 00. Las Vegas, Nevada: CRWMS M&O. Submit to RPC URN-0191

CRWMS M&O 2000o. *Uncertainty Distribution for Stochastic Parameters*. ANL-NBS-MD-000011 REV 00. Las Vegas, Nevada: CRWMS M&O. ACC: MOL.20000526.0328.

CRWMS M&O 2000p. *Input and Results of the Base Case Saturated Zone Flow and Transport Model for TSPA*. ANL-NBS-HS-000030 REV 00. Las Vegas, Nevada: CRWMS M&O. ACC: MOL.20000526.0330.

CRWMS M&O 2000q. *Features, Events, and Processes in SZ Flow and Transport*. ANL-NBS-MD-000002 REV 00. Las Vegas, Nevada: CRWMS M&O. ACC: MOL.20000526.0338.

CRWMS M&O 2000r. *Unsaturated Zone and Saturated Zone Transport Properties*. ANL-NBS-HS-000019 REV 00. Las Vegas, Nevada: CRWMS M&O. Submit to RPC URN-0038

CRWMS M&O 2000s. *Waste Package Degradation Process Model Report*. TDR-WIS-MD-000002 REV 00. Las Vegas, Nevada: CRWMS M&O. ACC: MOL.20000328.0322.

CRWMS M&O 2000t. *Near Field Environment Process Model Report*. TDR-NBS-MD-000001 REV 00. Las Vegas, Nevada: CRWMS M&O. ACC: MOL.20000421.0034.

CRWMS M&O 2000u. *Saturated Zone Flow and Transport Process Model Report*. Development Plan TDP-NBS-HS-000086 REV 00. Las Vegas, Nevada: CRWMS M&O. ACC: MOL.20000424.0675.

CRWMS M&O 2000v. *Performance Confirmation Plan*. TDR-PCS-SE-000001 REV 01. Las Vegas, Nevada: CRWMS M&O. ACC: MOL.20000302.0312.

CRWMS M&O 2000w. *Yucca Mountain Site Description*. TDR-CRW-GS-000001 REV 01. Las Vegas, Nevada: CRWMS M&O. ACC: MOL.20000717.0292.

Curtis, D.; Benjamin, T.; Gancarz, A.; Loss, R.; Rosman, K.; DeLaeter, J.; Delmore, J.E.; and Maeck, W.J. 1989. "Fission Product Retention in the Oklo Natural Fission Reactors." *Applied Geochemistry*, 4, 49-62. New York, New York: Pergamon Press. TIC: 237970.

Curtis, D.; Fabryka-Martin, J.; Dixon, P.; and Cramer, J. 1999. "Nature's Uncommon Elements: Plutonium and Technetium." *Geochimica et Cosmochimica Acta*, 63, (2), 275-285. New York, New York: Pergamon. TIC: 246120.

Curtis, D.B. 1986. "Geochemical Controls on 99TC Transport and Retention." *Chemical Geology*, 55, 227-231. Amsterdam, The Netherlands: Elsevier. TIC: 246745.

Curtis, D.B.; Benjamin, T.; and Gancarz, A.J. 1981. "The Oklo Reactors: Natural Analogs to Nuclear Waste Repositories." Volume 1 of *The Technology of High-Level Nuclear Waste Disposal*. Hofmann, P.L. and Breslin, J.J., eds. DOE/TIC 4621. 255-283. Washington, D.C.: U.S. Department of Energy. TIC: 246763.

Czarnecki, J.B. 1984. *Simulated Effects of Increased Recharge on the Ground-Water Flow System of Yucca Mountain and Vicinity, Nevada-California*. Water-Resources Investigations Report 84-4344. Denver, Colorado: U.S. Geological Survey. ACC: HQS.19880517.1750.

Czarnecki, J.B. 1990. *Geohydrology and Evapotranspiration at Franklin Lake Playa, Inyo County, California*. Open-File Report 90-356. Denver, Colorado: U.S. Geological Survey. ACC: NNA.19901015.0195.

Czarnecki, J.B.; Faunt, C.C.; Gable, C.W.; and Zyvoloski, G.A. 1997. *Hydrogeology and Preliminary Three-Dimensional Finite-Element Ground-Water Flow Model of the Site Saturated Zone, Yucca Mountain, Nevada*. Milestone SP23NM3. Denver, Colorado: U.S. Geological Survey. ACC: MOL.19990812.0180.

Czarnecki, J.B. and Waddell, R.K. 1984. *Finite-Element Simulation of Ground-Water Flow in the Vicinity of Yucca Mountain, Nevada-California*. Water-Resources Investigations Report 84-4349. Denver, Colorado: U.S. Geological Survey. ACC: NNA.19870407.0173.

D'Agnese, F.A.; Faunt, C.C.; Turner, A.K.; and Hill, M.C. 1997. *Hydrogeologic Evaluation and Numerical Simulation of the Death Valley Regional Ground-Water Flow System, Nevada and California*. Water-Resources Investigations Report 96-4300. Denver, Colorado: U.S. Geological Survey. ACC: MOL.19980306.0253.

D'Agnese, F.A.; O'Brien, G.M.; Faunt, C.C.; and San Juan, C.A. 1999. *Simulated Effects of Climate Change on the Death Valley Regional Ground-Water Flow System, Nevada and California*. Water-Resources Investigations Report 98-4041. Denver, Colorado: U.S. Geological Survey. TIC: 243555.

DOE (U.S. Department of Energy) 1988. *Site Characterization Plan Yucca Mountain Site, Nevada Research and Development Area, Nevada*. DOE/RW-0199. Nine volumes. Washington, D.C.: U.S. Department of Energy, Office of Civilian Radioactive Waste Management. ACC: HQO.19881201.0002.

DOE (U.S. Department of Energy) 1995. *Applications of Natural Analogue Studies to Yucca Mountain as a Potential High Level Radioactive Waste Repository*. DOE/YMSCO-002. Washington, D.C.: U.S. Department of Energy, Office of Civilian Radioactive Waste Management. ACC: MOL.19980928.0280.

DOE (U.S. Department of Energy) 1998a. *Viability Assessment of a Repository at Yucca Mountain*. DOE/RW-0508. Washington, D.C.: U.S. Department of Energy, Office of Civilian Radioactive Waste Management. ACC: MOL.19981007.0027; MOL.19981007.0028; MOL.19981007.0029; MOL.19981007.0030; MOL.19981007.0031; MOL.19981007.0032.

DOE (U.S. Department of Energy) 1998b. *Total System Performance Assessment*. Volume 3 of *Viability Assessment of a Repository at Yucca Mountain*. DOE/RW-0508. Washington, D.C.: U.S. Department of Energy, Office of Civilian Radioactive Waste Management. ACC: MOL.19981007.0030.

DOE (U.S. Department of Energy) 1998c. *Introduction and Site Characteristics*. Volume 1 of *Viability Assessment of a Repository at Yucca Mountain*. DOE/RW-0508. Washington, D.C.: U.S. Department of Energy, Office of Civilian Radioactive Waste Management. ACC: MOL.19981007.0028.

DOE (U.S. Department of Energy) 2000. *Quality Assurance Requirements and Description*. DOE/RW-0333P, Rev. 10. Washington, D.C.: U.S. Department of Energy, Office of Civilian Radioactive Waste Management. ACC: MOL.20000427.0422.

Dublyansky, Y.V. 1998. *Fluid Inclusion Studies of Samples from the Exploratory Study Facility, Yucca Mountain, Nevada*. Takoma Park, Maryland: Institute for Energy and Environmental Research. ACC: HQO.19990201.0012.

Dudley, W.W., Jr. and Larson, J.D. 1976. *Effect of Irrigation Pumping on Desert Pupfish Habitats in Ash Meadows, Nye County, Nevada*. Professional Paper 927. Washington, D.C.: U.S. Geological Survey. TIC: 219489.

Erickson, J.R. and Waddell, R.K. 1985. *Identification and Characterization of Hydrologic Properties of Fractured Tuff Using Hydraulic and Tracer Tests--Test Well USW H-4, Yucca Mountain, Nye County, Nevada*. Water-Resources Investigations Report 85-4066. Denver, Colorado: U.S. Geological Survey. ACC: NNA.19890713.0211.

Ervin, E.M.; Luckey, R.R.; and Burkhardt, D.J. 1994. *Revised Potentiometric-Surface Map, Yucca Mountain and Vicinity, Nevada*. Water-Resources Investigations Report 93-4000. Denver, Colorado: U.S. Geological Survey. ACC: NNA.19930212.0018.

Evernden, J.F. 1992. *Safety of Proposed Yucca Mountain Nuclear Repository as Regards Geological and Geophysical Factors: Evaluation of Minority Report by Archambeau and Price*. Open-File Report 92-516. Denver, Colorado: U.S. Geological Survey. TIC: 235252.

Faunt, C.C. 1997. *Effect of Faulting on Ground-Water Movement in the Death Valley Region, Nevada and California*. Water-Resources Investigations Report 95-4132. Denver, Colorado: U.S. Geological Survey. ACC: MOL.19980429.0119.

Fayek, M.; Janeczek, J.; and Ewing R.C. 1997. "Mineral Chemistry and Oxygen Isotopic Analyses of Uraninite, Pitchblende and Uranium Alteration Minerals from the Cigar Lake Deposit, Saskatchewan, Canada." *Applied Geochemistry*, 12, 549–565. Oxford, United Kingdom: Elsevier Science. TIC: 235776.

Ferrill, D.A.; Winterle, J.; Wittmeyer, G.; Sims, D.; Colton, S.; Armstrong, A.; and Morris, A.P. 1999. "Stressed Rock Strains Groundwater at Yucca Mountain, Nevada." *GSA Today*, 9, (5), 1-8. Boulder, Colorado: Geological Society of America. TIC: 246229.

Flint, A.L.; Hevesi, J.A.; and Flint, L.E. 1996. *Conceptual and Numerical Model of Infiltration for the Yucca Mountain Area, Nevada*. Milestone 3GUI623M. Denver, Colorado: U.S. Geological Survey. ACC: MOL.19970409.0087.

Forester, R.M.; Bradbury, J.P.; Carter, C.; Elvidge, A.B.; Hemphill, M.L.; Lundstrom, S.C.; Mahan, S.A.; Marshall, B.D.; Neymark, L.A.; Paces, J.B.; Sharpe, S.E.; Whelan, J.F.; and Wigand, P.E. 1996. *Synthesis of Quaternary Response of the Yucca Mountain Unsaturated and Saturated Zone Hydrology to Climate Change*. Milestone 3GCA102M. Las Vegas, Nevada: U.S. Geological Survey. ACC: MOL.19970211.0026.

Freeze, R.A. and Cherry, J.A. 1979. *Groundwater*. Englewood Cliffs, New Jersey: Prentice-Hall. TIC: 217571.

Fridrich, C.J.; Dudley, W.W., Jr.; and Stuckless, J.S. 1994. "Hydrogeologic Analysis of the Saturated-Zone Ground-Water System, Under Yucca Mountain, Nevada." *Journal of Hydrology*, 154, 133-168. Amsterdam, The Netherlands: Elsevier Science B.V. TIC: 224606.

Gauthier-Lafaye F.; Weber F.; and Ohmoto, H. 1989. "Natural Fission Reactors of Oklo." *Economic Geology*, 84, (8), 2286-2295. El Paso, Texas: Economic Geology Publishing Company. TIC: 246605.

Geldon, A.L. 1996. *Results and Interpretation of Preliminary Aquifer Tests in Boreholes UE-25c #1, UE-25c #2, and UE-25c #3, Yucca Mountain, Nye County, Nevada*. Water-Resources Investigations Report 94-4177. Denver, Colorado: U.S. Geological Survey. ACC: MOL.19980724.0389.

Geldon, A.L.; Umari, A.M.A.; Earle, J.D.; Fahy, M.F.; Gemmell, J.M.; and Darnell, J. 1998. *Analysis of a Multiple-Well Interference Test in Miocene Tuffaceous Rocks at the C-Hole Complex, May-June 1995, Yucca Mountain, Nye County, Nevada*. Water-Resources Investigations Report 97-4166. Denver, Colorado: U.S. Geological Survey. TIC: 236724.

Geldon, A.L.; Umari, A.M.A.; Fahy, M.F.; Earle, J.D.; Gemmell, J.M.; and Darnell, J. 1997. *Results of Hydraulic and Conservative Tracer Tests in Miocene Tuffaceous Rocks at the C-Hole Complex, 1995 to 1997, Yucca Mountain, Nye County, Nevada*. Milestone SP23PM3. Denver, Colorado: U.S. Geological Survey. ACC: MOL.19980122.0412.

Gelhar, L.W. 1998. *Report on U.S. Nuclear Waste Technical Review Board, Winter Meeting, 20-21, January 1998, Amargosa Valley, Nevada*. Arlington, Virginia: U.S. Nuclear Waste Technical Review Board. ACC: MOL.19981026.0334.

Golian, C. and Lever, D.A. 1992. "Radionuclide Transport." Volume 14 of *Alligator Rivers Analogue Project*. DOE/HMIP/RR/92/084. Menai, New South Wales, Australia: Australian Nuclear Science and Technology Organisation. TIC: 235988.

Grasso, D.N. 1996. *Hydrology of Modern and Late Holocene Lakes, Death Valley, California*. Water-Resources Investigations Report 95-4237. Denver, Colorado: U.S. Geological Survey. ACC: MOL.19970204.0218.

Haws, S.J. 1990. *The Distribution of Vertical Groundwater Flow in the Saturated Zone of the Yucca Mountain Area: A Cross-Sectional Finite Element Model*. Master's thesis. Las Vegas, Nevada: University of Nevada, Las Vegas. TIC: 237284.

Hill, C.A.; Dublyansky, Y.V.; Harmon, R.S.; and Schluter, C.M. 1995. "Overview of Calcite/Opal Deposits at or Near the Proposed High-Level Nuclear Waste Site, Yucca Mountain, Nevada, USA: Pedogenic, Hypogene, or Both?." *Environmental Geology*, 26, 69-88. New York, New York: Springer-Verlag. TIC: 222318.

Hoffman, D.C. and Daniels, W.R. 1981. "Assessment of the Potential for Radionuclide Migration from a Nuclear Explosion Cavity." *Groundwater Contamination Symposium*. LA-UR-81-3181. Los Alamos, New Mexico: Los Alamos Scientific Laboratory. TIC: 204725.

Hoffman, D.C.; Stone, R.; and Dudley, W.W., Jr. 1977. *Radioactivity in the Underground Environment of the Cambrian Nuclear Explosion at the Nevada Test Site*. LA-6877-MS. Los Alamos, New Mexico: Los Alamos National Laboratory. ACC: HQS.19880517.1989.

Holliger, P. 1993. "Geochemical and Isotopic Characterization of the Reaction Zones (Uranium, Transuranium, Lead and Fission Products)." *Oklo Working Group Meeting, Proceedings of the 2nd Joint CEC-CEA Progress Meeting Held in Brussels on 6-7 April 1992*. von Maravic, H., ed. EUR 14877 EN. 25-35. Luxembourg, Luxembourg: Commission of the European Communities. On Order Library Tracking Number-247912

Isobe, H.; Murakami, T.; and Ewing, R.C. 1992. "Alteration of Uranium Minerals in the Koongarra Deposit, Australia: Unweathered Zone." *Journal of Nuclear Materials*, 190, 174-187. Amsterdam, The Netherlands: Elsevier Science Publishers. TIC: 246371.

Ivanovich, M.; Duerden, P.; Payne, T.; Nightingale, T.; Longworth, G.; Wilkins, M.A.; Edghill, R.B.; Cockayne, D.J.; and Davey, B.G. 1987. "Natural Analogue Study of the Distribution of Uranium Series Radionuclides Between the Colloid and Solute Phases in the Hydrogeological System of the Koongarra Uranium Deposit N.T., Australia." *Natural Analogues in Radioactive Waste Disposal*. Come, B. and Chapman, N.A., eds. EUR-11037-EN. 300-313. Norwell, Massachusetts: Graham & Trotman. TIC: 247594.

Jaakkola, T.; Suksi, J.; Suutarinen, R.; Niini, H.; Ruskeeniemi, T.; Söderholm, B.; Vesterinen, M.; Blomqvist, R.; Halonen, S.; and Lindberg, A. 1989. *The Behaviour of Radionuclides in and Around Uranium Deposits. II: Results of Investigations at the Palmottu Analogue Study Site, SW Finland*. YST-64. Espoo, Finland: Geological Survey of Finland. TIC: 247721.

Janeczek, J. and Ewing, R.C. 1992. "Dissolution and Alteration of Uraninite Under Reducing Conditions." *Journal of Nuclear Materials*, 190, 157-173. Amsterdam, The Netherlands: Elsevier Science. TIC: 247465.

Karasaki, K. and Galloway, D. 1990. *Method Development and Strategy for the Characterization of Complexly Faulted and Fractured Rhyolitic Tuffs, Yucca Mountain, Nevada, USA*. LBL-30146. Berkeley, California: Lawrence Berkeley National Laboratory. TIC: 211538.

Karasaki, K.; Landsfeld, M.; and Grossenbacher, K. 1990. "Building of a Conceptual Model at the UE25-C Hole Complex." *High Level Radioactive Waste Management, Proceedings of the International Topical Meeting, Las Vegas, Nevada, April 8-12, 1990*. 2, 811-817. La Grange Park, Illinois: American Nuclear Society. TIC: 242396.

Kersting, A.B.; Efurud, D.W.; Finnegan, D.L.; Rokop, D.J.; Smith, D.K.; and Thompson, J.L. 1999. "Migration of Plutonium in Ground Water at the Nevada Test Site." *Nature*, 397, 56-59. London, England: Macmillan Publishers. TIC: 243597.

Kilroy, K.C. 1991. *Ground-Water Conditions in Amargosa Desert, Nevada-California, 1952-87*. Water-Resources Investigations Report 89-4101. Carson City, Nevada: U.S. Geological Survey. TIC: 209975.

Kotra, J.P.; Lee, M.P.; Eisenberg, N.A.; and DeWispelare, A.R. 1996. *Branch Technical Position on the Use of Expert Elicitation in the High-Level Radioactive Waste Program*. NUREG-1563. Washington, D.C.: U.S. Nuclear Regulatory Commission. TIC: 226832.

Kuzio, S. 1999. "Saturated Zone Flow/Transport and Biosphere Workshop Summary Document" Memorandum from S. Kuzio (SNL) to Distribution, May 25, 1999, with enclosure. ACC: MOL.19991217.0096.

La Camera, R.J. and Locke, G.L. 1997. *Selected Ground-Water Data for Yucca Mountain Region, Southern Nevada and Eastern California, Through December 1996*. Open File Report 97-821. Carson City, Nevada: U.S. Geological Survey. TIC: 236683.

Lehman, L. and Brown, T. 1998. The State of Nevada's Technical Issues and Concerns Expressed in a Letter on December 4, 1998. Letter from K. Guinn (State of Nevada) and B. Miller (State of Nevada), December 4, 1998, with attachments "The Yucca Mountain Site Is Not Suitable for Development as a Repository", and "Appendix A: Report on the Significance of Ground Water Travel Time." ACC: HQO.19990811.0010; HQO.19990811.0011.

Lehman, L.L. and Brown, T.P. 1996. *Summary of State of Nevada - Funded Studies of the Saturated Zone at Yucca Mountain, Nevada, Performed by L. Lehman & Associates, Inc.* Burnsville, Minnesota: L. Lehman and Associates. TIC: 231894.

Leslie, B.W. 1994. *An Annotated Analysis of Logic in the 1992 Report, "The Origin and History of Alteration and Carbonatization of the Yucca Mountain Ignimbrites," by J.S. Szymanski*. San Antonio, Texas: Center for Nuclear Waste Regulatory Analyses. TIC: 247428.

Lichtner, P.C. 1996. "Continuum Formulation of Multicomponent-Multiphase Reactive Transport." *Reactive Transport in Porous Media*. Lichtner, P.C.; Steefel, C.I.; and Oelkers, E.H., eds. Reviews in Mineralogy Volume 34. Washington, D.C.: Mineralogical Society of America. TIC: 236866.

Luckey, R.R.; Tucci, P.; Faunt, C.C.; Ervin, E.M.; Steinkampf, W.C.; D'Agnese, F.A.; and Patterson, G.L. 1996. *Status of Understanding of the Saturated-Zone Ground-Water Flow System at Yucca Mountain, Nevada, as of 1995*. Water-Resources Investigations Report 96-4077. Denver, Colorado: U.S. Geological Survey. ACC: MOL.19970513.0209.

Maloszewski, P. and Zuber, A. 1985. "On the Theory of Tracer Experiments in Fissured Rocks with a Porous Matrix." *Journal of Hydrology*, 79, 333-358. Amsterdam, The Netherlands: Elsevier Science Publishers B.V. TIC: 222390.

Maxey, G.B. and Eakin, T.E. 1950. *Ground Water in White River Valley, White Pine, Nye, and Lincoln Counties, Nevada*. Water Resources Bulletin No. 8. Carson City, Nevada: State of Nevada, Office of the State Engineer. TIC: 216819.

Miekeley, N.; Coutinho de Jesus, H.; Porto da Silveira, C.L.; and Degueldre, C. 1991. *Chemical and Physical Characterisation of Suspended Particles and Colloids in Waters from the Osamu Utsumi Mine and Morro do Ferro Analogue Study Sites, Poços de Caldas, Brazil*. SKB Technical Report 90-18. Stockholm, Sweden: Swedish Nuclear Fuel and Waste Management Company. TIC: 206355.

Miekeley, N.; Jesus, H.C.; Porto da Silveira, C.L.; and Kuechler, I.L. 1989. "Colloid Investigations in the Poços de Caldas Natural Analogue Project." *Scientific Basis for Nuclear Waste Management XII, Symposium Held October 10-13, 1988, Berlin, Germany*. Lutze, W. and Ewing, R.C., eds. 127, 831-842. Pittsburgh, Pennsylvania: Materials Research Society. TIC: 203660.

Montazer, P. and Wilson, W.E. 1984. *Conceptual Hydrologic Model of Flow in the Unsaturated Zone, Yucca Mountain, Nevada*. Water-Resources Investigations Report 84-4345. Lakewood, Colorado: U.S. Geological Survey. ACC: NNA.19890327.0051.

National Research Council 1992. *Ground Water at Yucca Mountain: How High Can It Rise?, Final Report of the Panel on Coupled Hydrologic/Tectonic/Hydrothermal Systems at Yucca Mountain*. Washington, D.C.: National Academy Press. TIC: 204931.

National Research Council 1995. *Technical Bases for Yucca Mountain Standards*. Washington, D.C.: National Academy Press. TIC: 217588.

Nordstrom, D.K.; Smellie, J.A.T.; and Wolf, M. 1990. *Chemical and Isotopic Composition of Groundwaters and Their Seasonal Variability at the Osamu Utsumi Mine and Morro do Ferro Analogue Study Sites, Poços de Caldas, Brazil*. SKB Technical Report 90-15. Stockholm, Sweden: Swedish Nuclear Fuel and Waste Management Company. TIC: 206353.

NRC (U.S. Nuclear Regulatory Commission) 1998. "Proposed Rule 10 CFR Part 63, Disposal of High-Level Radioactive Wastes in a Proposed Geologic Repository at Yucca Mountain, Nevada. SECY-98-225." Washington, D.C.: U.S. Nuclear Regulatory Commission. Accessed 10/20/98. TIC: 240520. <http://www.nrc.gov/NRC/COMMISSION/SECYS/1998-225scy.html>

NRC (U.S. Nuclear Regulatory Commission) 1999a. *Issue Resolution Status Report Key Technical Issue: Unsaturated and Saturated Flow Under Isothermal Conditions*. Rev. 2. Washington, D.C.: U.S. Nuclear Regulatory Commission. ACC: MOL.19990810.0641.

NRC (U.S. Nuclear Regulatory Commission) 1999b. *Issue Resolution Status Report Key Technical Issue: Radionuclide Transport*. Rev. 1. Washington, D.C.: U.S. Nuclear Regulatory Commission. ACC: MOL.19991214.0621.

NRC (U.S. Nuclear Regulatory Commission) 1999c. *Issue Resolution Status Report Key Technical Issue: Structural Deformation and Seismicity*. Rev. 2. Washington, D.C.: U.S. Nuclear Regulatory Commission. ACC: MOL.19991214.0623.

NRC (U.S. Nuclear Regulatory Commission) 1999d. Minutes, 113th Advisory Committee on Nuclear Waste, October 13, 1999. ACC: MOL.20000421.0222.

NRC (U.S. Nuclear Regulatory Commission) 2000. *Issue Resolution Status Report Key Technical Issue: Total System Performance Assessment and Integration*. Rev. 2. Washington, D.C.: U.S. Nuclear Regulatory Commission. TIC: 247614.

NWTRB (Nuclear Waste Technical Review Board) 1998a. *Winter Board Meeting, January 20, 1998*. Arlington, Virginia: Nuclear Waste Technical Review Board. ACC: MOL.20000421.0223.

NWTRB (Nuclear Waste Technical Review Board) 1998b. *Panel on Performance Assessment TSPA-VA, April 23, 1998*. Arlington, Virginia: Nuclear Waste Technical Review Board. ACC: MOL.20000424.0695.

NWTRB (Nuclear Waste Technical Review Board) 1998c. *Summer Board Meeting, June 24, 1998*. Arlington, Virginia: Nuclear Waste Technical Review Board. ACC: MOL.20000421.0224.

NWTRB (Nuclear Waste Technical Review Board) 1998d. *Report to the U.S. Congress and the U.S. Secretary of Energy, November, 1998*. Arlington, Virginia: U.S. Nuclear Waste Technical Review Board. ACC: MOV.19981201.0015.

NWTRB (Nuclear Waste Technical Review Board) 1999a. *Moving Beyond the Yucca Mountain Viability Assessment*. Arlington, Virginia: U.S. Nuclear Waste Technical Review Board. TIC: 243860.

NWTRB (Nuclear Waste Technical Review Board) 1999b. *Report to the U.S. Congress and the Secretary of Energy, January to December 1998*. Arlington, Virginia: U.S. Nuclear Waste Technical Review Board. ACC: HQO.19990706.0007.

NWTRB (Nuclear Waste Technical Review Board) 1999c. *Summer Meeting, Repository Design and the Scientific Program, June 30, 1999*. Arlington, Virginia: Nuclear Waste Technical Review Board. ACC: MOL.20000421.0234.

Nye County Nuclear Waste Repository Project Office 1999. "NC-Washburn - 1X Site Summary." Pahrump, Nevada: Nye County Nuclear Waste Repository Project Office. Accessed 4/22/00. TIC: 247621. http://www.nyecounty.com/Washburn_main.htm

Nye County Nuclear Waste Repository Project Office 2000. "Early Warning Drilling Program." Pahrump, Nevada: Nye County. Accessed 04/24/2000. TIC: 247627. <http://www.nyecounty.com/ewdpmain.htm>.

O'Brien, G.M. 1993. *Earthquake-Induced Water-Level Fluctuations at Yucca Mountain, Nevada, June 1992*. Open-File Report 93-73. Denver, Colorado: U.S. Geological Survey. ACC: NNA.19930326.0022.

O'Brien, G.M. 1997. *Analysis of Aquifer Tests Conducted in Boreholes USW WT-10, UE-25 WT#12, and USW SD-7, 1995-96, Yucca Mountain, Nevada*. Water-Resources Investigations Report 96-4293. Denver, Colorado: U.S. Geological Survey. ACC: MOL.19980219.0822.

O'Brien, G.M. 1998. *Analysis of Aquifer Tests Conducted in Borehole USW G-2, 1996, Yucca Mountain, Nevada*. Water-Resources Investigations Report 98-4063. Denver, Colorado: U.S. Geological Survey. ACC: MOL.19980904.0095.

Oberlander, P.L. 1979. *Development of a Quasi Three-Dimensional Groundwater Model for a Portion of the Nevada Test Site*. NVO-1253-14. Las Vegas, Nevada: U.S. Department of Energy. TIC: 217362.

Ohnuki, T.; Murakami, T.; Sekine, K.; Yanase, N.; Isobe, H.; and Kobayashi, Y. 1990. "Migration Behaviour of Uranium Series Nuclides in Altered Quartz-Chlorite Schist." *Scientific Basis for Nuclear Waste Management XIII, Symposium held November 27-30, 1989, Boston, Massachusetts*. Oversby, V.M. and Brown, P.W., eds. 176, 607-614. Pittsburgh, Pennsylvania: Materials Research Society. TIC: 203658.

Paces, J.B.; Forester, R.M.; Whelan, J.F.; Mahan, S.A.; Bradbury, J.P.; Quade, J.; Neymark, L.A.; and Kwak, L.M. 1996. *Synthesis of Ground-Water Discharge Deposits Near Yucca Mountain*. Milestone 3GQH671M. Las Vegas, Nevada: U.S. Geological Survey. ACC: MOL.19970205.0007.

Paperiello, C.J. 1999. "U.S. Nuclear Regulatory Commission Staff Review of the U.S. Department of Energy Viability Assessment for a High-Level Radioactive Waste Repository at Yucca Mountain, Nevada." Letter from C.J. Paperiello (NRC) to L.H. Barrett (DOE), June 2, 1999, with enclosures, "U.S. Nuclear Regulatory Commission's Staff Evaluation of U.S. Department of Energy's Viability Assessment" and Letter from B.J. Garrick (NRC Advisory Committee on Nuclear Waste) to S.A. Jackson (NRC), dated April 8, 1999. ACC: HQO.19990811.0007; HQO.19990811.0008.

Payne, T.E.; Edis, R.; and Seo, T. 1992. "Radionuclide Transport by Groundwater Colloids at the Koongarra Uranium Deposit." *Scientific Basis for Nuclear Waste Management XV, Symposium Held November 4-7, 1991, Strasbourg, France*. Sombret, C.G., ed. 257, 481-488. Pittsburgh, Pennsylvania: Materials Research Society. TIC: 204618.

Peters, R.R.; Klavetter, E.A.; Hall, I.J.; Blair, S.C.; Heller, P.R.; and Gee, G.W. 1984. *Fracture and Matrix Hydrologic Characteristics of Tuffaceous Materials from Yucca Mountain, Nye County, Nevada*. SAND84-1471. Albuquerque, New Mexico: Sandia National Laboratories. ACC: NNA.19900810.0674.

- Plume, R.W. and La Camera, R.J. 1996. *Hydrogeology of Rocks Penetrated by Test Well JF-3, Jackass Flats, Nye County, Nevada*. Water-Resources Investigations Report 95-4245. Carson City, Nevada: U.S. Geological Survey. ACC: MOL.19970626.0500.
- Powers, D.W. 1991. Transmittal Indicating Confusion About An Appendix to the Review Panel Minority Report by Charles Archambeau and Neville Price. Letter from D.W. Powers to C. Gertz (Project Manager, YMP), December 9, 1991. ACC: MOL.19980408.0471.
- Powers, D.W.; Rudnicki, J.W.; and Smith, L. 1991. *External Review Panel Majority Report: A Review of "Conceptual Considerations of the Yucca Mountain Groundwater System with Special Emphasis on the Adequacy of this System to Accommodate a High-Level Nuclear Waste Repository" dated July 26, 1989 by Jerry S. Szymanski*. Washington, D.C.: U.S. Department of Energy. ACC: NNA.19911210.0056.
- Prudic, D.E.; Harrill, J.R.; and Burbey, T.J. 1993. *Conceptual Evaluation of Regional Groundwater Flow in the Carbonate-Rock Province of the Great Basin, Nevada, Utah, and Adjacent States*. Open-File Report 93-170. Carson City, Nevada: U.S. Geological Survey. ACC: MOL.19950105.0016.
- Reimus, P.W.; Adams, A.; Haga, M.J.; Humphrey, A.; Callahan, T.; Anghel, I.; and Counce, D. 1999. *Results and Interpretation of Hydraulic and Tracer Testing in the Prow Pass Tuff at the C-Holes*. Milestone SP32E7M4. Los Alamos, New Mexico: Los Alamos National Laboratory. TIC: 246377.
- Rice, W.A. 1984. *Preliminary Two-Dimensional Regional Hydrologic Model of the Nevada Test Site and Vicinity*. SAND83-7466. Albuquerque, New Mexico: Sandia National Laboratories. ACC: NNA.19900810.0286.
- Robinson, B.A. 1994. "A Strategy for Validating a Conceptual Model for Radionuclide Migration in the Saturated Zone Beneath Yucca Mountain." *Radioactive Waste Management and Environmental Restoration*, 19, (1-3), 73-96. Yverdon, Switzerland: Harwood Academic Publishers. TIC: 222513.
- Rousseau, J.P.; Kwicklis, E.M.; and Gillies, D.C., eds. 1996. *Hydrogeology of the Unsaturated Zone, North Ramp Area of the Exploratory Studies Facility, Yucca Mountain, Nevada*. Milestone 3GUP431M. Denver, Colorado: U.S. Geological Survey. ACC: MOL.19980220.0164.
- Sass, J.H.; Lachenbruch, A.H.; Dudley, W.W., Jr.; Priest, S.S.; and Munroe, R.J. 1988. *Temperature, Thermal Conductivity, and Heat Flow Near Yucca Mountain, Nevada: Some Tectonic and Hydrologic Implications*. Open-File Report 87-649. Denver, Colorado: U.S. Geological Survey. ACC: MOL.19971027.0303.
- Savard, C.S. 1998. *Estimated Ground-Water Recharge from Streamflow in Fortymile Wash Near Yucca Mountain, Nevada*. Water-Resources Investigations Report 97-4273. Denver, Colorado: U.S. Geological Survey. TIC: 236848.

Sinnock, S.; Lin, Y.T.; and Brannen, J.P. 1984. *Preliminary Bounds on the Expected Postclosure Performance of the Yucca Mountain Repository Site, Southern Nevada*. SAND84-1492. Albuquerque, New Mexico: Sandia National Laboratories. ACC: NNA.19870519.0076.

Sinnock, S.; Lin, Y.T.; and Tierney, M.S. 1986. *Preliminary Estimates of Groundwater Travel Time and Radionuclide Transport at the Yucca Mountain Repository Site*. Sinnock, S., ed. SAND85-2701. Albuquerque, New Mexico: Sandia National Laboratories. ACC: NNA.19891129.0550.

Sinton, P.O. 1987. *Three-Dimensional, Steady-State, Finite-Difference Model of the Ground-Water Flow System in the Death Valley Ground-Water Basin, Nevada-California*. Master's thesis. Golden, Colorado: Colorado School of Mines. TIC: 236959.

Smellie, J.A.T.; Chapman, N.A.; McKinley, I.G.; Penna Franca, E.; and Shea, M. 1989. "Testing Safety Assessment Models Using Natural Analogues in High Natural Series Groundwaters. The Second Year of the Poços de Caldas Project." *Scientific Basis for Nuclear Waste Management XII, Symposium Held October 10-13, 1988, Berlin, Germany*. Lutze, W and Ewing, R.C., eds. 127, 863-870. Pittsburgh, Pennsylvania: Materials Research Society. TIC: 241379.

Snelling, A.A. 1980. "Uraninite and Its Alteration Products, Koongarra Uranium Deposit." *Proceedings of International Uranium Symposium on the Pine Creek Geosyncline, 1980*. Ferguson, J. and Goleby, A.B., eds. 487-498. Vienna, Austria: International Atomic Energy Agency. TIC: 236806.

Stock, J.M.; Healy, J.H.; and Hickman, S.H. 1984. *Report on Televiwer Log and Stress Measurements in Core Hole USW G-2, Nevada Test Site October-November, 1982*. Open-File Report 84-172. Menlo Park, California: U.S. Geological Survey. ACC: NNA.19870406.0157.

Streeter, V.L. and Wylie, E.B. 1979. *Fluid Mechanics*. 7th Edition. New York, New York: McGraw-Hill. TIC: 4819.

Stuckless, J.S.; Marshall, B.D.; Vaniman, D.T.; Dudley, W.W.; Peterman, Z.E.; Paces, J.B.; Whelan, J.F.; Taylor, E.M.; Forester, R.M.; and O'Leary, D.W. 1998. "Comments on 'Overview of Calcite/Opal Deposits at or Near the Proposed High-Level Nuclear Waste Site, Yucca Mountain, Nevada, USA: Pedogenic, Hypogene, or Both' by C.A. Hill, Y.V. Dublansky, R.S. Harmon, and C.M. Schluter." *Environmental Geology*, 34, (1), 70-78. New York, New York: Springer-Verlag. TIC: 238097.

Sudicky, E.A. and Frind, E.O. 1981. "Carbon 14 Dating of Groundwater in Confined Aquifers: Implications of Aquitard Diffusion." *Water Resources Research*, 17, (4), 1060-1064. Washington, D.C.: American Geophysical Union. TIC: 247712.

Sunder, S.; Taylor, P.; and Cramer, J.J. 1988. "XPS and XRD Studies of Uranium Rich Minerals from Cigar Lake, Saskatchewan." *Scientific Basis for Nuclear Waste Management XI, Symposium held November 30-December 3, 1987, Boston, Massachusetts*. Apted, M.J. and Westerman, R.E., eds. 112, 465-472. Pittsburgh, Pennsylvania: Materials Research Society. TIC: 203662.

Szabo, B.J.; Kolesar, P.T.; Riggs, A.C.; Winograd, I.J.; and Ludwig, K.R 1994. "Paleoclimatic Inferences from a 120,000-Yr Calcite Record of Water Table Fluctuation in Browns Room of Devils Hole, Nevada." *Quaternary Research*, 41, 59-69. New York, New York: Academic Press. TIC: 234642.

Szymanski, J.S. 1989. *Conceptual Considerations of the Yucca Mountain Groundwater System with Special Emphasis on the Adequacy of This System to Accommodate a High-Level Nuclear Waste Repository*. Two volumes. Las Vegas, Nevada: U.S. Department of Energy. ACC: NNA.19890831.0152.

Szymanski, J.S. 1992. *The Origin and History of Alteration and Carbonatization of the Yucca Mountain Ignimbrites*. Two volumes. Las Vegas, Nevada: Department of Energy. TIC: 207762.

Thompson, J.L., ed. 1986. *Laboratory and Field Studies Related to the Radionuclide Migration October 1, 1984-September 30, 1985*. LA-10644-PR. Los Alamos, New Mexico: Los Alamos National Laboratory. TIC: 246828.

Triay, I.; Degueldre, C.; Wistrom, A.; Cotter, C.; and Lemons, W. 1996. *Progress Report on Colloid-Facilitated Transport at Yucca Mountain*. LA-12959-MS. Los Alamos, New Mexico: Los Alamos National Laboratory. TIC: 225473.

Triay, I.R.; Meijer, A.; Conca, J.L.; Kung, K.S.; Rundberg, R.S.; Strietelmeier, B.A.; Tait, C.D.; Clark, D.L.; Neu, M.P.; and Hobart, D.E. 1997. *Summary and Synthesis Report on Radionuclide Retardation for the Yucca Mountain Site Characterization Project*. LA-13262-MS. Los Alamos, New Mexico: Los Alamos National Laboratory. ACC: MOL.19971210.0177.

Tucci, P. and Burkhardt, D.J. 1995. *Potentiometric-Surface Map, 1993, Yucca Mountain and Vicinity, Nevada*. Water-Resources Investigations Report 95-4149. Denver, Colorado: U.S. Geological Survey. ACC: MOL.19960924.0517.

USGS (U.S. Geological Survey) 2000a. *Hydrogeologic Framework Model for the Saturated-Zone Site-Scale Flow and Transport Model*. ANL-NBS-HS-000033 REV 00. Denver, Colorado: U.S. Geological Survey. ACC: MOL.20000802.0010.

USGS (U.S. Geological Survey) 2000b. *Water-Level Data Analysis for the Saturated Zone Site-Scale Flow and Transport Model*. ANL-NBS-HS-000034 REV 00. Denver, Colorado: U.S. Geological Survey. Submit to RPC URN-0281

USGS (U.S. Geological Survey) 2000c. *Future Climate Analysis*. ANL-NBS-GS-000008 REV 00. Denver, Colorado: U.S. Geological Survey. ACC: MOL.20000629.0907.

Valkiainen, M. 1989. "Finnish Natural Analogue Research." *Nuclear Science and Technology, CEC Natural Analogue Working Group, Third Meeting, Snowbird, Near Salt Lake City, USA, June 15 to 17, 1988*. Côme, B. and Chapman, N.A., eds. 110-118. Luxembourg, Luxembourg: Commission of the European Communities. TIC: 7639.

Vilks, P.; Cramer, J.J.; Shewchuk, T.A.; and Larocque, J.P.A. 1988. "Colloid and Particulate Matter Studies in the Cigar Lake Natural Analog Program." *Radiochimica Acta*, 44/45, (2), 305-310. Munich, Germany: R. Oldenbourg Verlag. TIC: 247532.

Waber, N. 1991. *Mineralogy, Petrology and Geochemistry of the Poços de Caldas Analogue Study Sites, Minas Gerais, Brazil II: Morro do Ferro*. SKB Technical Report 90-12. Stockholm, Sweden: Swedish Nuclear Fuel and Waste Management Company. TIC: 206350.

Waddell, R.K. 1982. *Two-Dimensional, Steady-State Model of Ground-Water Flow, Nevada Test Site and Vicinity, Nevada-California*. Water-Resources Investigations Report 82-4085. Denver, Colorado: U.S. Geological Survey. ACC: NNA.19870518.0055.

Waddell, R.K.; Robison, J.H.; and Blankennagel, R.K. 1984. *Hydrology of Yucca Mountain and Vicinity, Nevada-California--Investigative Results through Mid-1983*. Water-Resources Investigations Report 84-4267. Denver, Colorado: U.S. Geological Survey. ACC: NNA.19870406.0343.

Walker, G.E. and Eakin, T.E. 1963. *Geology and Ground Water of Amargosa Desert, Nevada-California*. Ground-Water Resources – Reconnaissance Series Report 14. Carson City, Nevada: State of Nevada, Department of Conservation and Natural Resources. TIC: 208665.

West, J.M.; McKinley, I.G.; and Vialta, A. 1989. "The Influence of Microbial Activity on the Movement of Uranium at OSAMU UTSUMI Mine, Poços de Caldas, Brazil." *Scientific Basis for Nuclear Waste Management XII, Symposium held October 10-13, 1988, Berlin, Germany*. Lutze, W. and Ewing, R.C., eds. 127, 771-777. Pittsburgh, Pennsylvania: Materials Research Society. TIC: 236107.

Whelan, J. 1998. "Review of Yuri Dublyansky's Reports Entitled 'Fluid Inclusion Studies of Samples from the Exploratory Studies Facility, Yucca Mountain, Nevada' and an Attachment Entitled 'Fluid Inclusions in Calcite Samples from the ESF, Nevada Test Site, Nevada.'" Memorandum from J. Whelan (USGS) to D. Williams (DOE), November 9, 1998, with enclosure. ACC: MOL.19981209.0014.

Wilson, M.L.; Gauthier, J.H.; Barnard, R.W.; Barr, G.E.; Dockery, H.A.; Dunn, E.; Eaton, R.R.; Guerin, D.C.; Lu, N.; Martinez, M.J.; Nilson, R.; Rautman, C.A.; Robey, T.H.; Ross, B.; Ryder, E.E.; Schenker, A.R.; Shannon, S.A.; Skinner, L.H.; Halsey, W.G.; Gansemer, J.D.; Lewis, L.C.; Lamont, A.D.; Triay, I.R.; Meijer, A.; and Morris, D.E. 1994. *Total-System Performance Assessment for Yucca Mountain – SNL Second Iteration (TSPA-1993)*. SAND93-2675. Executive Summary and two volumes. Albuquerque, New Mexico: Sandia National Laboratories. ACC: NNA.19940112.0123.

Winograd, I.J. and Thordarson, W. 1975. *Hydrogeologic and Hydrochemical Framework, South-Central Great Basin, Nevada-California, with Special Reference to the Nevada Test Site*. Professional Paper 712-C. Washington, D.C.: U.S. Geological Survey. TIC: 206787.

Winterle, J.R. and La Femina, P.C. 1999. *Review and Analysis of Hydraulic and Tracer Testing at the C-Holes Complex Near Yucca Mountain, Nevada*. San Antonio, Texas: Center for Nuclear Waste Regulatory Analyses. TIC: 246623.

Yang, I.C.; Rattray, G.W.; and Yu, P. 1996. *Interpretation of Chemical and Isotopic Data from Boreholes in the Unsaturated Zone at Yucca Mountain, Nevada*. Water-Resources Investigations Report 96-4058. Denver, Colorado: U.S. Geological Survey. ACC: MOL.19980528.0216.

YMP (Yucca Mountain Site Characterization Project) 1998. *Disposal Criticality Analysis Methodology Topical Report*. YMP/TR-004Q, Rev. 0. Las Vegas, Nevada: Yucca Mountain Site Characterization Office. ACC: MOL.19990210.0236.

YMP (Yucca Mountain Site Characterization Project) 1999. *Repository Safety Strategy: U.S. Department of Energy's Strategy to Protect Public Health and Safety After Closure of a Yucca Mountain Repository*. YMP/96-01, Rev. 03. Las Vegas, Nevada: Yucca Mountain Site Characterization Office. ACC: MOL.19990406.0237.

Zyvoloski, G.A.; Robinson, B.A.; Dash, Z.V.; and Trease, L.L. 1997a. *User's Manual for the FEHM Application – A Finite-Element Heat- and Mass-Transfer Code*. LA-13306-M. Los Alamos, New Mexico: Los Alamos National Laboratory. TIC: 235999.

Zyvoloski, G.A.; Robinson, B.A.; Dash, Z.V.; and Trease, L.L. 1997b. *Summary of Models and Methods for the FEHM Application - A Finite Element Heat- and Mass-Transfer Code*. LA-13307-MS. Los Alamos, New Mexico: Los Alamos National Laboratory. TIC: 235587.

6.2 CODES, STANDARDS, REGULATIONS, AND PROCEDURES

50 FR 38066. Protection of Environment: Environmental Standards for the Management and Disposal of Spent Nuclear Fuel, High-Level and Transuranic Radioactive Wastes; Final Rule. Readily available.

64 FR 8640. Disposal of High-Level Radioactive Wastes in a Proposed Geologic Repository at Yucca Mountain, Nevada. Proposed rule 10 CFR 63. Readily available.

64 FR 46976. Environmental Radiation Protection Standards for Yucca Mountain, Nevada; Proposed rule 40 CFR 197. Readily available.

AP-2.13Q, Rev. 0, ICN 3. *Technical Product Development Planning*. Washington, D.C.: U.S. Department of Energy, Office of Civilian Radioactive Waste Management. ACC: MOL.20000504.0305.

AP-2.14Q, Rev. 0, ICN 0. *Review of Technical Products*. Washington, D.C.: U.S. Department of Energy, Office of Civilian Radioactive Waste Management. ACC: MOL.19990701.0616.

AP-2.15Q, REV 0, ICN 1. *Work Package Planning Summaries*. Washington, D.C.: U.S. Department of Energy, Office of Civilian Radioactive Waste Management. ACC: MOL.19990930.0101.

AP-2.21Q, Rev. 0, ICN 0. *Quality Determinations and Planning for Scientific, Engineering, and Regulatory Compliance Activities*. Washington, D.C.: U.S. Department of Energy, Office of Civilian Radioactive Waste Management. ACC: MOL.20000802.0003.

AP-3.10Q, Rev. 1, ICN 0. *Analyses and Models*. Washington, D.C.: U.S. Department of Energy, Office of Civilian Radioactive Waste Management. ACC: MOL.19990702.0314.

AP-3.11Q, Rev. 0, ICN 0. *Technical Reports*. Washington, D.C.: U.S. Department of Energy, Office of Civilian Radioactive Waste Management. ACC: MOL.19990701.0620.

AP-3.15Q, Rev. 1, ICN 1. *Managing Technical Product Inputs*. Washington, D.C.: U.S. Department of Energy, Office of Civilian Radioactive Waste Management. ACC: MOL.20000218.0069.

AP-SI.1Q, Rev. 2, ICN 4. *Software Management*. Washington, D.C.: U.S. Department of Energy, Office of Civilian Radioactive Waste Management. ACC: MOL.20000223.0508.

AP-SIII.2Q, Rev. 0, ICN 2. *Qualification of Unqualified Data and the Documentation of Rationale for Accepted Data*. Washington, D.C.: U.S. Department of Energy, Office of Civilian Radioactive Waste Management. ACC: MOL.19991214.0625.

Nuclear Waste Policy Act of 1982. 42 U.S.C. 10101 et seq. Readily available

QAP-2-0, Rev. 5. *Conduct of Activities*. Las Vegas, Nevada: CRWMS M&O. ACC: MOL.19980826.0209.

6.3 SOURCE DATA, LISTED BY DATA TRACKING NUMBER

MO0002COV00088.001. Coverage: BORES Q2. Submittal date: 02/24/2000.

APPENDIX A

ISSUES FOR SATURATED ZONE FLOW AND TRANSPORT

APPENDIX A

ISSUES FOR SATURATED ZONE FLOW AND TRANSPORT

Table A-1. Issues for Saturated Zone Flow and Transport

Issue	Source	PMR Approach
<p>The saturated-zone (SZ) needs additional characterization:</p> <ul style="list-style-type: none"> • Between the repository and the accessible environment 20 to 30 km (12.5 to 18.6 mi.) away. • Information about long-range colloid transport, • The Nye County Early Warning Drilling Program (NCEWDP) should provide valuable information on the part of the SZ downgradient of Yucca Mountain. However, the wells may not provide sufficient data, and additional testing may be needed at other sites closer to Yucca Mountain. 	<p>Paperiello 1999; NWTRB 1999a; NWTRB 1999b; Budnitz et al. 1999</p>	<ul style="list-style-type: none"> • NCEWDP was started, in part, to characterize areas between the potential repository and areas 30 km (18.6 mi.) down gradient. The program is continuing. Hydrologic data discussed in Section 3.1.2. • Laboratory colloid experiments discussed in Section 3.1.4.3; C-wells hydraulic testing with microspheres discussed in Section 3.1.3.2. • Next phases of NCEWDP testing are ongoing and are closer to Yucca Mountain.
<p>Evaluate, integrate, and incorporate alternate models (such as those developed by State of Nevada hydrologists) into coherent SZ model.</p>	<p>Cohon 1998b; Cohon 1999b</p>	<p>Alternative conceptual models, including the models presented by State of Nevada hydrologists, are evaluated. Discussion in Section 3.8.</p>
<p>Borehole WT-24 drilling was stopped too soon to evaluate the large hydraulic gradient.</p> <p>Much work was planned to characterize the large hydraulic gradient, but was not done. People will ask why.</p>	<p>Cohon 1999a; NWTRB 1998a</p>	<p>Borehole WT-24 provides sufficient information to determine that the large hydraulic gradient is due in part to perching. The large hydraulic gradient is discussed in Sections 3.2.2.3 and 3.2.5.1.</p>
<p>Warm water in some NCEWDP wells needs investigation.</p>	<p>Cohon 1999a; NRC 1999c</p>	<p>Warm water is not anomalous compared to other wells in region (e.g., Sass et al. 1988). NCEWDP and U.S. Department of Energy (DOE) investigations are ongoing.</p>
<p>Characterizing effects of molecular diffusion, hydrodynamic dispersion, and sorption on dilution in the SZ will be difficult and may be impractical because it could take many years for the tracers to travel from Yucca Mountain to the monitoring wells. Some data may be obtained from long term tracer test at proposed second SZ well complex.</p>	<p>Cohon 1998b</p>	<p>Tracer tests have been done using multiple tracers to identify effects. Characterization discussed in Section 3.1; hydraulic well tests in Section 3.1.2.2; tracer tests in Section 3.1.3.2; laboratory data in Section 3.1.4.</p> <p>Transport and transport processes discussed in Sections 3.2.4, 3.3.2, 3.3.4, 3.5.2, and 3.6.3.</p>

Table A-1. Issues for Saturated Zone Flow and Transport (Continued)

Issue	Source	PMR Approach
SZ modeling needs more model integration and reality checking using data from the site.	Cohon 1998b	Model validation now includes comparisons of: permeability data to calibrated permeability values, fluxes from regional models with fluxes from calibrated model, measured upward gradient with predicted upward gradient, hydrochemical data with calculated particle pathways, and natural analogs. These activities and process model uncertainties are discussed in Section 3.4.
Current estimates of SZ dilution eventually may prove to be conservative, but supporting a larger dilution factor will be difficult unless new data are obtained.	NWTRB 1999b	More data have been obtained from multi-well, multi-tracer tests, and work continues to collect more data. Characterization discussed in Section 3.1; hydraulic well tests in 3.1.2.2; tracer tests in 3.1.3.2; laboratory data in 3.1.4. Transport and transport processes discussed in Sections 3.2.4, 3.3.2, 3.3.4, 3.5.2, and 3.6.3.
Presentation reported "Gamma spike" in geophysical logs in borehole NCEWDP-3D in conjunction with high uranium content.	NWTRB 1999c; NRC 1999d [Nye County Presentation]	NCEWDP investigations and DOE work are ongoing.
Presentation indicated that driller's log for old Washburn Well (approximately north of Town of Amargosa Valley) predicted about 91 m (300 ft) to water; however, it went to 248 m (815 ft) and did not hit water. NCEWDP to investigate this anomaly.	NWTRB 1998c [Nye County Presentation]	NCEWDP could not reenter original Washburn hole (caved too much and liability concerns). NC-Washburn-1X was sited about 400 m (0.25 mi.) from the original Washburn Well site, drilled to a depth of 200 m (658 ft), and the static water level in the well after completion was 107.8 m (353.8 ft) below land surface. (Hole elevation: 823.5 m [2701.7 ft] above mean sea level determined by Global Positioning System). Water table altitude about 716 m (2,350 ft) at NC-Washburn-1X is consistent with regional trends (Nye County Nuclear Waste Repository Project Office 1999). No water table anomaly noted in new hole. Possible anomaly does not appear to have regional significance. No further Nye County investigations indicated at this location.
Concerns expressed regarding transparency of stream tubes model of SZ flow and transport model.	NWTRB 1998b	New three-dimensional (3-D) finite element site model developed; evolution of model discussed in Section 2; improvements to old model discussed in Section 2.4.6.

Table A-1. Issues for Saturated Zone Flow and Transport (Continued)

Issue	Source	PMR Approach
<p>Transport in the SZ adopted a streamtube-based approach. This is less desirable than a more detailed treatment of dispersion but it is appropriate given the limitations in the data concerning the SZ.</p>	<p>Budnitz et al. 1999</p>	<p>New 3-D finite element site model developed; evolution of model discussed in Section 2; improvements to old model discussed in Section 2.4.6. Transport and transport processes discussed in Sections 3.2.4, 3.3.2, 3.3.4, 3.5.2, and 3.6.3.</p>
<p>Current SZ flow and transport at Yucca Mountain has three main weaknesses</p> <ol style="list-style-type: none"> 1. Lack of data for some important parameters 2. Incomplete nature of site characterization 3. Continuing questions regarding the adequacy of the numerical models. 	<p>Budnitz et al. 1999</p>	<p>More data have been, and continue to be, gathered. Parameters have been bounded or treated stochastically where appropriate.</p> <p>This is discussed in CRWMS M&O (2000o) and Section 3.5. Saturated zone flow and transport model revised from the Total System Performance Assessment for the Viability Assessment (TSPA-VA) model. Characterization discussed in Section 3.1; hydraulic well tests in Section 3.1.2.2; tracer tests in Section 3.1.3.2; laboratory data in Section 3.1.4. Transport and transport processes discussed in Sections 3.2.4, 3.3.2, 3.3.4, 3.5.2, and 3.6.3.</p> <p>Mathematical and numerical modeling approach discussed in Section 3.3; validation and calibration activities discussed in Section 3.4.</p>
<p>Lack of site data results in:</p> <ul style="list-style-type: none"> • An apparent difficulty in estimating vertical flow in the SZ • Establishing location of the lower boundary • Lack of account for anisotropy and heterogeneity. 	<p>Budnitz et al. 1999</p>	<p>More data have been, and continue to be, gathered. Saturated zone flow and transport model revised from TSPA-VA model. Anisotropy and heterogeneity explicitly considered in model. SZ flow system discussed in Section 3.1.1; conceptual model and hydrologic framework discussed in Section 3.2.1; vertical gradient discussed in Section 3.2.2.1; relationship of SZ PMR to Integrated Site Model (ISM) PMR (CRWMS M&O 2000e) discussed in Section 1.5.1; heterogeneity discussed in Section 3.2.2.4; anisotropy included in model, discussed in Sections 3.2.5.3 and 3.5.1.</p>
<p>Evaluating the effects of retardation on radionuclide transport is an inherent problem with two aspects:</p> <ol style="list-style-type: none"> 1. The division of flow between the matrix and fractures in the SZ zone 2. The magnitude of the sorption values to be used. 	<p>Budnitz et al. 1999</p>	<p>Multi-well, multi-tracer tracer tests have been done and provide more confidence in representativeness of sorption values. Laboratory data on sorption, matrix diffusion, and colloid transport discussed in Section 3.1.4; hydraulic well tests discussed in Section 3.1.2.2, tracer tests discussed in Section 3.1.3.2.</p>

Table A-1. Issues for Saturated Zone Flow and Transport (Continued)

Issue	Source	PMR Approach
<p>Sorption values cannot be used without knowing how representative they are of field conditions.</p>	<p>Budnitz et al. 1999; CRWMS M&O 1998b</p>	<p>Multi-well, multi-tracer tracer tests have been done and provide more confidence in representativeness of sorption values. Laboratory data on sorption, matrix diffusion, and colloid transport discussed in Section 3.1.4; hydraulic well tests discussed in Section 3.1.2.2, tracer tests discussed in Section 3.1.3.2.</p>
<p>Estimating the permeability field currently is based on the calibration of pressure heads. Data are lacking over a substantial region of the SZ. It is acknowledged that pressure data inversion does not guarantee uniqueness in parameter estimates. Thus, potential fast paths in the SZ (such as permeability channels) may be underestimated.</p>	<p>Budnitz et al. 1999</p>	<p>Model validation now includes comparisons of: permeability data to calibrated permeability values, fluxes from regional models with fluxes from calibrated model, measured upward gradient with predicted upward gradient, hydrochemical data with calculated particle pathways, and natural analogs. These activities and process model uncertainties are discussed in Section 3.4.</p>
<p>Three vertical layers are used to represent the large-scale hydrology and a typical grid has a linear size of the order of 1,500 m (4,920 ft) in regional model. Intra-grid heterogeneity is seriously misrepresented. This also applies to the site-scale model, with a grid resolution of 200 m (655 ft). As permeability spans 7 orders of magnitude, this limited resolution raises the issue of the relevance of numerical predictions regarding the postulated flow fields.</p>	<p>Budnitz et al. 1999</p>	<p>A more detailed regional-scale model (D'Agnese et al. 1997) was used than the one used in TSPA-VA. Comparison of regional- and site-scale models discussed in Section 3.4.2. New 3-D finite element site model developed; evolution of model discussed in Section 2; improvements to old model discussed in Section 2.4.6. Transport and transport processes discussed in Sections 3.2.4, 3.3.2, 3.3.4, 3.5.2, and 3.6.3.</p>
<p>Streamtubes are assumed not to vary with time, regardless of the changes in climate. This assumption is not consistent with the change in the ratio of the water flux through the unsaturated zone (UZ) and the SZ.</p>	<p>Budnitz et al. 1999</p>	<p>New 3-D finite element site model developed; evolution of model discussed in Section 2; climate change in conceptual model discussed in Section 3.2.6; alternative climate states in the abstraction of radionuclide transport discussed in Section 3.6.3.3.2.</p>
<p>Recharge on top of the projected flow path would alter the streamlines resulting in a substantial layer of clean water above the contaminated water that could be 100 to 150 m (325 to 500 ft) thick. This would call into doubt the basic biosphere model, in which a farm family is assumed to pump contaminated water from the plume.</p>	<p>Budnitz et al. 1999; Gelhar 1998</p>	<p>Saturated zone flow and transport flow path model revised. Assumptions regarding biosphere model and pumping are governed by regulation. Relationship to Biosphere PMR (CRWMS M&O 2000c) discussed in Section 1.5.3.</p>

Table A-1. Issues for Saturated Zone Flow and Transport (Continued)

Issue	Source	PMR Approach
<p>A numerical approach to the modeling of dispersion and dilution based on a streamtube formalism, well-resolved near the plume and with a correct representation of dispersion and retardation, is feasible (provided that a good description of the heterogeneity from field data is available). Development of such an approach would permit sensitivity studies to be conducted of the effects of various factors, including geostatistics, and would circumvent the necessity to rely solely on estimates from the expert Panel and/or empirical corrections.</p>	<p>Budnitz et al. 1999</p>	<p>New 3-D finite element site model developed; evolution of model discussed in Section 2; improvements to old model discussed in Section 2.4.6; Transport and transport processes discussed in Sections 3.2.4, 3.3.2, 3.3.4, 3.5.2, and 3.6.3. Model validation now includes comparisons of: permeability data to calibrated permeability values, fluxes from regional models with fluxes from calibrated model, measured upward gradient with predicted upward gradient, hydrochemical data with calculated particle pathways, and natural analogs. These activities and process model uncertainties are discussed in Section 3.4.</p>
<p>In the TSPA-VA model, flow is assumed to occur only through the fractures. The problem with this representation is that the degree of fracture-matrix interaction is fixed a priori, rather than being a time-dependent process as it is in reality. Given that retardation is associated with the matrix, this assumption will affect the transport predictions.</p>	<p>Budnitz et al. 1999</p>	<p>New 3-D finite element site model developed; evolution of model discussed in Section 2; improvements to old model discussed in Section 2.4.6. Transport and transport processes discussed in Sections 3.2.4, 3.3.2, 3.3.4, 3.5.2, and 3.6.3. Model validation now includes comparisons of: permeability data to calibrated permeability values, fluxes from regional models with fluxes from calibrated model, measured upward gradient with predicted upward gradient, hydrochemical data with calculated particle pathways, and natural analogs. These activities and process model uncertainties are discussed in Section 3.4.</p>
<p>Averaging the source concentrations over six areas at the interface between the UZ and the SZ. Introduces an artificial spreading which will lead to non-conservative estimates, particularly at early times (e.g., within the first 10,000 yr.) when leakage of radionuclides from waste packages is associated with isolated failures. [Note: refers to streamtube model].</p>	<p>Budnitz et al. 1999</p>	<p>New 3-D finite element site model developed; evolution of model discussed in Section 2; improvements to old model discussed in Section 2.4.6. Transport and transport processes discussed in Sections 3.2.4, 3.3.2, 3.3.4, 3.5.2, and 3.6.3. Coupling of SZ flow and transport with UZ discussed in Section 3.6.3.4.1.</p>
<p>The project conducted a sensitivity analysis (Arnold and Kuzio 1998) of the effect of the source size on the dilution factor at the 20-km (12.5-mi) point. The TSPA-VA underestimates the dose rates, for the base case parameter values, by a factor of 3. A correction was not introduced in the TSPA-VA, however. The Panel recommends that the current TSPA-VA treatment be modified to correct the existing deficiency.</p>	<p>Budnitz et al. 1999</p>	<p>New 3-D finite element site model developed; evolution of model discussed in Section 2; improvements to old model discussed in Section 2.4.6. Transport and transport processes discussed in Sections 3.2.4, 3.3.2, 3.3.4, 3.5.2, and 3.6.3.</p>

Table A-1. Issues for Saturated Zone Flow and Transport (Continued)

Issue	Source	PMR Approach
<p>One critical aspect of the TSPA-VA is the degree to which an appropriate conceptual model and approach were applied to the behavior of the radionuclides in the UZ and SZ environments that involve complex coupled processes or data-intensive analyses of a large heterogeneous site. The difficulty stems from the heterogeneity of the site and the large distances over which the transport of radionuclides is to be assessed. It is not feasible to know the structure of the flow paths in sufficient depth to model these phenomena in detail.</p>	<p>Budnitz et al. 1999</p>	<p>Conceptual model and mathematical model have been revised since TSPA-VA to account for heterogeneity more explicitly. Conceptual model of SZ flow and transport discussed in Section 3.2, heterogeneity addressed in Section 3.2.2.4. Model validation now includes comparisons of: permeability data to calibrated permeability values, fluxes from regional models with fluxes from calibrated model, measured upward gradient with predicted upward gradient, hydrochemical data with calculated particle pathways, and natural analogs. These activities and process model uncertainties are discussed in Section 3.4.</p>
<p>The merits of the two different approaches taken for modeling transport in the UZ and the SZ, namely the use of particle-tracking vs. the use of an overall dilution factor, need to be compared. It is the Panel's position that a uniform approach should be adopted for both cases.</p>	<p>Budnitz et al. 1999</p>	<p>Particle tracking method adopted in SZ modeling; discussed in Section 3.3.4.</p>
<p>The four performance factors most affected by climate change appear to be:</p> <ol style="list-style-type: none"> 1. The fraction of waste packages that experience liquid drips 2. The transport time for water through the UZ 3. Subsequent transport time in SZ 4. Dilution in the SZ. 	<p>Budnitz et al. 1999</p>	<ol style="list-style-type: none"> 1. Discussed in Waste Package PMR (CRWMS M&O 2000s). 2. Discussed in UZ PMR (CRWMS M&O 2000b). 3. Transport and transport processes discussed in Sections 3.2.4, 3.3.2, 3.3.4, 3.5.2, and 3.6.3. 4. Transport and transport processes discussed in Sections 3.2.4, 3.3.4, 3.5.2, and 3.6.3.
<p>The large hydraulic gradient is a manifestation of the local flow system controlled by interactions between topography, geology, and recharge. It is not a cause for alarm.</p> <p>The large hydraulic gradient is not considered a crucial issue.</p>	<p>CRWMS M&O 1998b</p> <p>[summaries, Freeze and Gelhar]</p>	<p>The large hydraulic gradient is discussed in Sections 3.2.2.3 and 3.2.5.1.</p>
<p>The horizontal flux vector in the uppermost part of the SZ beneath Yucca Mountain is needed for the TSPA both for current conditions and for climate change or repository heating scenarios.</p>	<p>CRWMS M&O 1998b</p> <p>[summaries, Freeze]</p>	<p>Groundwater flow discussed in Section 3.2.2; conceptual model of changes in SZ flow system due to climate change discussed in Section 3.2.6.</p>
<p>There will also be mixing in the wellbore of water-supply wells in the Amargosa Desert. If future groundwater exploitation were to increase substantially, and if such pumping rates were spatially and temporally erratic, then there might also be considerable mixing in the capture zones of those wells due to the pumping transients.</p>	<p>CRWMS M&O 1998b</p> <p>[summaries, Freeze]</p>	<p>Dilution in water supply discussed in Section 3.6.3.3.4.</p>

Table A-1. Issues for Saturated Zone Flow and Transport (Continued)

Issue	Source	PMR Approach
<p>Recommendations For Reducing Uncertainty:</p> <p>1. Careful construction of flow nets in the vicinity of the large hydraulic gradient, using all available head data in a 3-D context, would aid in settling the large hydraulic gradient controversy. Uncertainties with respect to the large hydraulic gradient could be further laid to rest by two or three well-placed boreholes. However, ordinary drilling protocols will not suffice. It is difficult to determine whether low-permeability rocks are fully saturated (or just nearly so), and special protocols would be needed to obtain the necessary downhole information on saturation.</p>	<p>CRWMS M&O 1998b</p> <p>[summaries, Freeze]</p>	<p>Borehole WT-24 drilled to investigate the large hydraulic gradient and indicates that some perching was involved in previous mapping of the large hydraulic gradient. The large hydraulic gradient is discussed in Sections 3.2.2.3 and 3.2.5.1.</p>
<p>2. Fault zone hydraulic uncertainties properties measured in the UZ probably can be meaningfully projected into the SZ. Hydraulic tests in the vicinity of a known fault might also clarify fault properties, as might further simulation and calibration of the new site-scale model.</p>	<p>CRWMS M&O 1998b</p> <p>[summaries, Freeze]</p>	<p>New site-scale model developed. Role of faults discussed in Section 3.2.3.4.</p>
<p>3. Further well-controlled field tracer tests may help clarify the nature of dispersion, matrix diffusion, and sorption in the fractured volcanic rocks. Laboratory K_d values should be confirmed in situ.</p>	<p>CRWMS M&O 1998b</p> <p>[summaries, Freeze]</p>	<p>Multi-well, multi-tracer tracer tests have been done to clarify the nature of dispersion, matrix diffusion, and sorption. Tracer tests discussed in Section 3.1.3.2; laboratory data discussed in Section 3.1.4.</p>
<p>4. Underground testing is still needed to clarify thermohydrologic processes associated with repository heating. Continued thermohydrologic modeling should be carried out to identify more fully the possible impacts on the SZ.</p>	<p>CRWMS M&O 1998b</p> <p>[summaries, Freeze]</p>	<p>Underground testing ongoing, discussed in Near Field Environment PMR (CRWMS M&O 2000t).</p>
<p>Perhaps a variety of models should be considered, ranging from a homogeneous continuum model to a highly channelized model, and the importance of their differences evaluated. In the flow system downgradient from the repository, it is difficult to see hydraulic evidence for channelization. Experience elsewhere has shown that large-scale lateral persistence of geologic features may not imply lateral persistence of hydraulics properties.</p>	<p>CRWMS M&O 1998b</p> <p>[summaries, Gelhar]</p>	<p>New 3-D finite element site model developed; evolution of model discussed in Section 2; improvements to old model discussed in Section 2.4.6. Model validation now includes comparisons of: permeability data to calibrated permeability values, fluxes from regional models with fluxes from calibrated model, measured upward gradient with predicted upward gradient, hydrochemical data with calculated particle pathways, and natural analogs. These activities and process model uncertainties are discussed in Section 3.4. Assumptions, uses, and limitations of the site-scale SZ flow and transport model discussed in Section 3.5. Other views and alternative conceptual models discussed in Section 3.8.</p>

Table A-1. Issues for Saturated Zone Flow and Transport (Continued)

Issue	Source	PMR Approach
<p>Large-scale (kilometer-scale) tracer tests are needed to examine the large-scale interconnected nature of the flow system.</p>	<p>CRWMS M&O 1998b [summaries, Gelhar]</p>	<p>No kilometer-scale tracer tests have been done, however multi-well, multi-tracer tracer tests have been done at the C-wells. These data have been integrated with the hydrologic framework model. Tracer tests discussed in Section 3.1.3.2. Integration of the hydrologic framework model with the conceptual model discussed in Section 3.2.</p>
<p>In evaluating recharge and discharge in the regional model, there are considerable uncertainties that will be difficult to reduce. In addition to the amounts of recharge and discharge, we don't know the internal distribution of permeability throughout the regional system. To evaluate whether the regional system is steady state, I would look at the response times and transmissivities. The regional model is most important as a tool for evaluating the effect of climate change on the flow system.</p>	<p>CRWMS M&O 1998b [summaries, Gelhar]</p>	<p>Regional flow system discussed in Section 3.1.1.1; boundary conditions of site-scale model discussed in Section 3.2.3; response of conceptual model to climate change discussed in Section 3.2.6.</p>
<p>The plume from the repository is not likely to move down deep into the aquifer system. There may be some tendency for the plume's movement to have a stronger downward component in the confining units in the volcanics, but in general the plume will stay shallow. At distances of 20 to 30 km (12.5 to 18.6 mi.), the plume likely will be depressed somewhat below the water table because of the recharge occurring along the path of the plume. A continuum model for the alluvium probably is sufficient.</p>	<p>CRWMS M&O 1998b [summaries, Gelhar]</p>	<p>As currently modeled, plume stays shallow. Particle tracking method for new SZ model discussed in Section 3.3.4.</p>
<p>The large hydraulic gradient and the evidence for perching beneath Yucca Mountain confirm the presence of low-permeability zones. During climate change, the potential for increased perched water beneath the repository is a greater concern than the potential for a change in the large hydraulic gradient.</p>	<p>CRWMS M&O 1998b [summaries, Gelhar]</p>	<p>The large hydraulic gradient is discussed in Sections 3.2.2.3 and 3.2.5.1. Climate change discussed in Section 3.2.6.</p>

Table A-1. Issues for Saturated Zone Flow and Transport (Continued)

Issue	Source	PMR Approach
<p>Some of the sources of uncertainty and limitations to the site-scale model include the following:</p> <ul style="list-style-type: none"> • The representation of the geology in the model may not be adequate. • The spatial distribution of units occurring at the water table shows major inconsistencies with Fridrich et al. (1994, Figure 5). • The scheme used for assigning head boundary conditions is not defensible. • Using the PEST code for only one parameter at a time will not provide meaningful estimates of uncertainties. • No site-specific hydraulic conductivity data. • The estimated hydraulic conductivity values of 0.1 m/day (0.3 ft/day) for basin fill and 0.026 m/day (0.09 ft/day) for the middle volcanic aquifer seem low in comparison with the site data and with experience with similar formations. 	<p>CRWMS M&O 1998b</p> <p>[summaries, Gelhar]</p>	<p>Uncertainty of new model discussed in several Sections:</p> <ul style="list-style-type: none"> • Hydrogeologic framework discussed in 3.2.1; new representation based on ISM PMR (CRWMS M&O 2000e) has been developed, and relationship of SZ PMR to ISM PMR discussed in Section 1.5.1. • Hydrogeologic framework model discussed in Sections 3.2.1 and 3.3.5.2. • Boundary conditions discussed in Section 3.2.3. • Parameter uncertainty discussed in Section 3.7.2. • Hydrologic data summarized in Section 3.1.2; hydraulic well tests in Section 3.1.2.2. • Validation of new model by various methods discussed in Section 3.4.
<p>This effect of concentration variability around the mean represents an additional source of uncertainty that is not accounted for in the classical advection-dispersion models being used to simulate contaminant transport for Yucca Mountain. The degree of dilution ultimately is controlled by local dispersion and molecular diffusion, but is strongly influenced by the fine-scale variations in the flow field. Very small-scale variations in flow create large concentration gradients and large surface areas over which local dispersion can act to more effectively decrease concentration differences.</p>	<p>CRWMS M&O 1998b</p> <p>[summaries, Gelhar]</p>	<p>New model developed that includes diffusion and dispersion due to heterogeneities. Mathematical model of radionuclide transport discussed in Section 3.3.2. Particle tracking method for new SZ model discussed in Section 3.3.4.</p>
<p>During wetter climates there will be more fluctuations in hydraulic gradients, which will likely lead to greater dispersion. I would expect increases of factors of 2 to 3 times in transverse dispersivity during wetter periods and no change in longitudinal dispersivity.</p>	<p>CRWMS M&O 1998b</p> <p>[summaries, Gelhar]</p>	<p>Response of model to climate change discussed in Sections 3.2.6 and 3.6.3.3.2.</p>
<p>Recommendations For Reducing Uncertainty:</p> <ol style="list-style-type: none"> 1. Large-Scale Hydraulic and Tracer Tests: Probably the most important activity that would contribute to significant reduction of uncertainty would be additional large-scale, multi-hole hydraulic and tracer testing. These tests should be conducted in the area south-south-east of the site (south of the C-wells) to gain information along the flowpaths from the repository. 	<p>CRWMS M&O 1998b</p> <p>[summaries, Gelhar]</p>	<p>No kilometer-scale tracer tests have been done, however multi-well, multi-tracer tracer tests have been done at the C-wells. Testing in another well complex not accomplished to date, but is planned. Alluvial Tracer Complex is currently being drilled and will be tested during fiscal year 2000; second complex in tuffs planned for fiscal year 2001.</p>

Table A-1. Issues for Saturated Zone Flow and Transport (Continued)

Issue	Source	PMR Approach
<p>2. Re-evaluation of Single-Borehole Tests: The existing single-borehole data should be re-analyzed using the latest techniques, possibly including 3-D numerical simulation with discrete fracture effects, to see whether a quantitative explanation can be found for the apparent bias in the original interpretations. If an appropriate correction can be devised, the single-borehole data would be very useful in defining the spatial distribution of hydraulic properties at the site.</p>	<p>CRWMS M&O 1998b [summaries, Gelhar]</p>	<p>Task has not been done. Multi-well testing at C-wells provides hydraulic data capable of providing bounding parameters.</p>
<p>3. Improvements of the Site-Scale Model: The grid used in the model should be refined to adequately represent the known hydrogeologic units and to resolve the expected plume structure (with small transverse dispersivities). The model grid should also be designed to simulate the C-wells aquifer test and any future multi-well hydraulic testing at the site; the flux imposed by these tests would be the primary basis for calibrating the site-scale model.</p>	<p>CRWMS M&O 1998b [summaries, Gelhar]</p>	<p>New 3-D finite element site model developed; evolution of model discussed in Section 2; improvements to old model discussed in Section 2.4.6; grid discussed in Section 3.3.5.1; hydrogeologic framework model discussed in Section 3.3.5.2; relationship of SZ PMR to ISM PMR (CRWMS M&O 2000e) discussed in 1.5.1; transport and transport processes discussed in Sections 3.2.4, 3.3.2, 3.3.4, 3.5.2, and 3.6.3. Calibration discussed in Sections 3.3.6 and 3.3.7. Model validation now includes comparisons of: permeability data to calibrated permeability values, fluxes from regional models with fluxes from calibrated model, measured upward gradient with predicted upward gradient, hydrochemical data with calculated particle pathways, and natural analogs. These activities and process model uncertainties are discussed in Section 3.4.</p>
<p>4. Field Measurements of Ambient Matrix Diffusion Effects: Sampling and water analyses similar to those reported by Rousseau et al. (1996, p. 187) for the perched water at UZ-14 should be done. If similar differences in water chemistry between fracture and matrix are seen at several locations, this would call into question the effectiveness of matrix diffusion under natural flow conditions. Diffusion cell lab tests on natural fracture surfaces also are suggested.</p>	<p>CRWMS M&O 1998b [summaries, Gelhar]</p>	<p>Suggested tests not done on perched zones. Laboratory matrix diffusion experiments discussed in Section 3.1.4.2. Multi-well tracer tests at C-wells with multiple tracers provides evidence for effectiveness of matrix diffusion. Tracer tests discussed in Section 3.1.3.</p>
<p>5. Improved Interpretation and Documentation of the C-Wells Multi-Tracer Test: Many important details of experimental and interpretative methodology ... must be provided. For example, explicit experimental evidence is needed to demonstrate that the two nonsorbing tracers behave ideally for the geochemical conditions corresponding to the field. The interpretative analyses implicitly neglect any effects of transverse mixing, but this process likely will come into play with a model that contains multiple paths having different advective transport rates</p>	<p>CRWMS M&O 1998b [summaries, Gelhar]</p>	<p>Referenced document not published, to date.</p>

Table A-1. Issues for Saturated Zone Flow and Transport (Continued)

Issue	Source	PMR Approach
<p>6. Improvements to the Report on the Los Alamos National Laboratory Sorption/Diffusion Testing: Although the draft report (Triay et al. 1997) contains many specifics about experimental equipment and procedures, it lacks crucial details about the overall experimental design and the justification in terms of field applicability. From the material presented, the reader is unable to determine where samples were collected, particularly in relation to the in situ hydrologic characteristics of the SZ.</p>	<p>CRWMS M&O 1998b [summaries, Gelhar]</p>	<p>Comment was not incorporated into subject document as the document was published prior to final SZ Expert Elicitation report (CRWMS M&O 1998b).</p>
<p>Groundwater levels downgradient vary so slowly that any error in their measurement translates into a large error in the estimation of hydraulic gradients. Groundwater elevation data in this area are sufficiently ambiguous to allow some hydrogeologists to contour them by means of smooth curves unaffected by faults, while allowing others to contour them to delineate embayments around faults. The available data are insufficient to compute ambient fluxes underneath Yucca Mountain with any reasonable degree of certainty. It is important to base calculations of groundwater flux in the Yucca Mountain area not only on site hydraulic data, but also on regional recharge and discharge data in a manner that renders all such calculations fully compatible and consistent with each other.</p>	<p>CRWMS M&O 1998b [summaries, Neuman]</p>	<p>Water level data discussed in Section 3.1.2.1. Model validation now includes comparisons of: permeability data to calibrated permeability values, fluxes from regional models with fluxes from calibrated model, measured upward gradient with predicted upward gradient, and hydrochemical data with calculated particle pathways, as well as natural analogs. These activities and process model uncertainties are discussed in Section 3.4. Alternative models of SZ discussed in Section 3.8.</p>
<p>Bomb-pulse isotopes at depth within the UZ attest to the occurrence of intermittent fast flow through both welded and nonwelded volcanic units. Major springs associated with the Paleozoic carbonate aquifer constitute evidence for highly localized flow in parts of the Death Valley basin. It is safe to assume that focused flow is ubiquitous throughout both the UZ and SZ in the basin on many scales. I therefore propose that corresponding narrow channels of elevated permeability be included in high-resolution conditional simulations of flow and transport in and around the Yucca Mountain area. The low potential for dilution associated with such potentially fast-flow channels should (in my view) be weighted against the probability (which could be high for detectable features such as major faults) that they may be intercepted by water supply wells.</p>	<p>CRWMS M&O 1998b [summaries, Neuman]</p>	<p>Anisotropy included in the model, discussed in Sections 3.2.5.3 and 3.5.1. Heterogeneity and hydrologic features of the Hydrologic framework discussed in Section 3.2.2.4 and 3.2.2.5. Role of faults as internal boundaries discussed in Section 3.2.3.4.</p>

Table A-1. Issues for Saturated Zone Flow and Transport (Continued)

Issue	Source	PMR Approach
<p>Site-scale and regional flow models developed for the SZ to date are consistent neither with each other nor with site measurements of rock hydraulic properties. The models differ in their hydrogeologic and gridding structures; in their prescribed or computed parameters; in conditions computed or prescribed along their interfaces; and in conditions computed or prescribed along their overlapping upper surfaces. The regional model consists of three layers that represent not hydrogeologic units but perceived (not clear how established) shallow, intermediate, and deep flow systems. The permeabilities ascribed to hydrologic units in both models, including calibrated values, are orders of magnitude lower than values determined in field tests, most notably pumping tests conducted in the C-wells.</p> <p>Because the site-scale and regional flow models incorporate at most a few discrete faults explicitly within their respective grids, it would have been logical for them to incorporate the effect of all other faults implicitly by rendering all hydrogeologic units anisotropic in the horizontal and vertical directions, yet this was not done.</p> <p>The site-scale model was calibrated in a manner that fails to guarantee unique or meaningful results; calibration of the regional model has led to reliability estimates that seem to be unduly optimistic and hence of questionable validity. This is especially true when considering that uncertainty of the input data into these models has not been fully and convincingly quantified. Additionally, the models are too crude to provide reliable qualitative insight into, or quantitative information about, 3-D flow at the site or within the basin.</p> <p>In their present form, the site-scale and regional flow models are of very limited value.</p>	<p>CRWMS M&O 1998b</p> <p>[summaries, Neuman]</p>	<p>A more detailed regional-scale model, developed by D'Agnesse et al. (1997), was used than the one used in TSPA-VA. Comparison of regional- and site-scale models is discussed in Section 3.4.2. New 3-D finite element site flow and transport model developed; evolution of model discussed in Section 2; improvements to old model discussed in Section 2.4.6. Relationship of SZ PMR to ISM PMR (CRWMS M&O 2000e) discussed in Section 1.5.1. Transport and transport processes discussed in Sections 3.2.4, 3.3.2, 3.3.4, 3.5.2, and 3.6.3. Model validation now includes comparisons of: permeability data to calibrated permeability values, fluxes from regional models with fluxes from calibrated model, measured upward gradient with predicted upward gradient, hydrochemical data with calculated particle pathways, and natural analogs. These activities and process model uncertainties are discussed in Section 3.4. Heterogeneity and hydrologic features of the hydrogeologic framework discussed in Section 3.2.2.4 and 3.2.2.5. Role of faults as internal boundaries discussed in Section 3.2.2.</p>
<p>The only mechanisms by which dilution can take place in the absence of groundwater withdrawal for sampling or use are molecular diffusion, advective dispersion caused by space-time meandering of pathlines and variations in velocity along as well as among stream tubes, and turbulent eddies that are unlikely to occur in the vicinity of Yucca Mountain. Otherwise, dilution can occur when water is drawn into samplers or wells from multiple horizons and/or directions, and when waters in samplers or wells mix by diffusion and turbulence caused by shaking, stirring, or rapid flow. Density effects due to space-time variations in solution chemistry, temperature, and pressure may either enhance or prevent mixing (as in buoyant or gravity segregation of fluids having different densities). Another factor that may contribute to mixing is instability of fluid interfaces and resultant fingering; this does not appear to play a role in the SZ of Yucca Mountain.</p>	<p>CRWMS M&O 1998b</p> <p>[summaries, Neuman]</p>	<p>Dilution in water supply discussed in Section 3.6.3.3.4.</p>

Table A-1. Issues for Saturated Zone Flow and Transport (Continued)

Issue	Source	PMR Approach
<p>The “stirred tank” model, in which contaminated waters from the UZ mix rapidly with pristine waters in the SZ down to some specified “mixing depth” does not appear credible.</p> <p>Buoyancy of warmer waters from the repository area, and small vertical dispersivity will probably keep the incoming plume of radionuclides at shallow depth except where it is intercepted by major vertical fractures or faults within which there is significant downward flow.</p> <p>The scientific basis for the notion that waters from neighboring subbasins mix naturally along a flow path is also questionable; only where flow paths from the two subbasins converge will their waters mix by dispersion under natural conditions.</p>	<p>CRWMS M&O 1998b</p> <p>[summaries, Neuman]</p>	<p>Site-scale SZ flow and transport model does not incorporate “stirred tank.” Previous modeling discussed in Sections 2.3 and 2.4; conceptual model transport processes discussed in Section 3.2.4; mathematical modeling of transport discussed in Section 3.3.2; particle tracking for radionuclide transport discussed in Section 3.3.4.</p>
<p>Mixing by dispersion may occur, but it is important to recognize that dispersion cannot be interpreted as dilution except in special cases.</p> <p>On the laboratory scale, dispersion coefficients compensate for our inability to resolve the intricacies of advective transport and diffusion in the pore space, about which we have no direct information. On the field scale, dispersion coefficients compensate additionally for our inability to resolve the intricacies of advective transport and local-scale dispersion in a heterogeneous porous or fractured rock, about which we have only partial information.</p> <p>Clearly, lack of resolution does not necessarily imply mixing and dilution; only if we sample on a scale comparable to that of unresolved heterogeneities should we expect dispersion to imply mixing and dilution. Hence, confusing dispersion with mixing and dilution is inappropriate except in special circumstances.</p>	<p>CRWMS M&O 1998b</p> <p>[summaries, Neuman]</p>	<p>Site-scale SZ flow and transport model is being used. Previous modeling discussed in Sections 2.3 and 2.4; conceptual model transport processes discussed in Section 3.2.4; mathematical modeling of transport discussed in Section 3.3.2, particle tracking for radionuclide transport discussed in Section 3.3.4.</p>
<p>Recommendations For Reducing Uncertainty:</p> <ol style="list-style-type: none"> Investigate the hydrogeology of the Timber Mountain area between Pahute Mesa and Yucca Mountain, which may hold the key to a reliable estimation of fluxes under and downstream of a repository at the site. 	<p>CRWMS M&O 1998b</p> <p>[summaries, Neuman]</p>	<p>Borehole USW WT-24 drilled north of the site. New regional model developed and integrated with site model. Model validation now includes comparisons of: permeability data to calibrated permeability values, fluxes from regional models with fluxes from calibrated model, measured upward gradient with predicted upward gradient, hydrochemical data with calculated particle pathways, and natural analogs. These activities and process model uncertainties are discussed in Section 3.4.</p>

Table A-1. Issues for Saturated Zone Flow and Transport (Continued)

Issue	Source	PMR Approach
<p>2. Conduct field tests to help determine hydraulic properties of faults and fault zones in Yucca Mountain area. Likewise, utilize available information about the pneumatic properties of faults in the unsaturated Topopah Spring unit when analyzing flow and transport in the saturated part of this unit.</p>	<p>CRWMS M&O 1998b [summaries, Neuman]</p>	<p>Characterization discussed in Section 3.1. Hydraulic well tests discussed in Section 3.1.2; tracer tests discussed in Section 3.1.3.</p>
<p>3. Base calculations of groundwater flux in the Yucca Mountain area not only on site hydraulic data, but also on regional recharge and discharge data in a manner that renders all such calculations fully compatible and consistent with each other.</p>	<p>CRWMS M&O 1998b [summaries, Neuman]</p>	<p>New regional-scale model developed and integrated with site model. Infiltration and recharge discussed in Section 3.1.2.3. Model validation now includes comparisons of: permeability data to calibrated permeability values, fluxes from regional models with fluxes from calibrated model, measured upward gradient with predicted upward gradient, hydrochemical data with calculated particle pathways, and natural analogs. These activities and process model uncertainties are discussed in Section 3.4. Fluxes from regional-scale model compared with fluxes from calibrated model discussed in Section 3.4.2. Use of boundary flux in model calibration discussed in Section 3.3.6.2.2.</p>
<p>4. Where faults are not incorporated explicitly into flow models, account for them implicitly by rendering all hydrogeologic units anisotropic in horizontal and vertical directions parallel to dominant fault planes.</p>	<p>CRWMS M&O 1998b [summaries, Neuman]</p>	<p>Heterogeneity and hydrologic features of the hydrogeologic framework discussed in Sections 3.2.2.4 and 3.2.2.5. Role of faults as internal boundaries discussed in Section 3.2.3.4.</p>
<p>5. Plan and conduct several additional tests similar to the C-wells, using existing boreholes, to better characterize the hydraulic properties of hydrogeologic units at the site; identify the hydraulic influence and properties of faults in the test area; and provide data against which it may be possible to calibrate a comprehensive, high-resolution groundwater flow model.</p>	<p>CRWMS M&O 1998b [summaries, Neuman]</p>	<p>Alluvial Tracer Complex is currently being drilled and will be tested in Fiscal Year 2000. Additional test complex in tuffs scheduled for Fiscal Year 2001. Model validation now includes comparisons of: permeability data to calibrated permeability values, fluxes from regional models with fluxes from calibrated model, measured upward gradient with predicted upward gradient, hydrochemical data with calculated particle pathways, and natural analogs. These activities and process model uncertainties are discussed in Section 3.4.</p>

Table A-1. Issues for Saturated Zone Flow and Transport (Continued)

Issue	Source	PMR Approach
<p>6. Develop a comprehensive, high-resolution groundwater flow model and render it compatible with all relevant site and basin-wide hydrologic and hydrogeologic data. Make the horizontal and vertical spatial resolutions of this model much greater than those of present site and regional flow models, especially in and downstream of the Yucca Mountain area, and coordinate its development with that of a similar-scale model recently constructed for environmental management of the Nevada Test Site.</p>	<p>CRWMS M&O 1998b [summaries, Neuman]</p>	<p>Site-scale SZ flow and transport 3-D finite element model developed; evolution of model discussed in Section 2; improvements to TSPA-VA model discussed in Section 2.4.6. Model validation now includes comparisons of: permeability data to calibrated permeability values, fluxes from regional model with fluxes from calibrated model, measured upward gradient with predicted upward gradient, hydrochemical data with calculated particle pathways, and natural analogs. These activities and process model uncertainties are discussed in Section 3.4.</p>
<p>7. Quantify the uncertainty of all input data into the above model and include reliable prior information, especially that concerning hydraulic parameters from large-scale pumping tests, formally in its calibration. A model that encompasses the entire basin has better-defined boundary inflows and outflows than does a site model that has artificial boundaries, and is therefore better suited for calculation and calibration of water balance.</p>	<p>CRWMS M&O 1998b [summaries, Neuman]</p>	<p>Model validation now includes comparisons of: permeability data to calibrated permeability values, fluxes from regional model with fluxes from calibrated model, measured upward gradient with predicted upward gradient, hydrochemical data with calculated particle pathways, and natural analogs. These activities and process model uncertainties are discussed in Section 3.4.</p>
<p>8. To further improve the prospects of constructing and calibrating a meaningful regional flow model, strengthen the isotope hydrology program of the Yucca Mountain Project to obtain more extensive and reliable information about groundwater ages and directions of flow throughout the basin.</p>	<p>CRWMS M&O 1998b [summaries, Neuman]</p>	<p>Geochemistry Analysis and Model Report (CRWMS M&O 2000m) discusses hydrochemistry in detail and provides evaluation of groundwater ages and confirmation of flow paths; Section 3.1.3.1 discusses spatial patterns of groundwater chemistry. Model validation now includes comparisons of: permeability data to calibrated permeability values, fluxes from regional model with fluxes from calibrated model, measured upward gradient with predicted upward gradient, hydrochemical data with calculated particle pathways, and natural analogs. These activities and process model uncertainties are discussed in Section 3.4.</p>
<p>9. Drill an additional borehole strategically into the large hydraulic gradient area, then log and sample it thoroughly enough to confirm or deny that the large hydraulic gradient is an artifact of perched conditions, as some propose.</p>	<p>CRWMS M&O 1998b [summaries, Neuman]</p>	<p>Borehole WT-24 drilled in large hydraulic gradient area and indicates that the large hydraulic gradient is, in part, due to perching. The large hydraulic gradient is discussed in Sections 3.2.2.3 and 3.2.5.1.</p>

Table A-1. Issues for Saturated Zone Flow and Transport (Continued)

Issue	Source	PMR Approach
<p>10. To investigate mixing and dilution, conduct high-resolution, statistically based conditional flow and transport simulations in the manner described within the text. Even a small number of conditional Monte Carlo simulations, conducted in this manner, may be more telling with regard to dilution and mixing than would deterministic or stochastic simulations that do not achieve a comparable degree of resolution. They may also provide meaningful, if not fully accurate, insight into the uncertainty associated with such simulations.</p>	<p>CRWMS M&O 1998b [summaries, Neuman]</p>	<p>Calibration discussed in Sections 3.3.6 and 3.3.7. Validation activities discussed in Section 3.4.</p>
<p>11. Include narrow channels of elevated permeability in high-resolution conditional simulations to allow for focused flow and transport.</p>	<p>CRWMS M&O 1998b [summaries, Neuman]</p>	<p>Horizontal anisotropy included in model, discussed in Sections 3.2.5.3 and 3.5.1. Heterogeneity and hydrologic features included in model, discussed in Sections 3.2.2.4 and 3.2.2.5. Role of faults as internal boundaries discussed in Section 3.2.3.4.</p>
<p>12. Conduct large-scale, long-term tracer experiments in and around the C-holes to obtain meaningful parameters (kinematic porosities, dispersivities, slow/fast path transfer coefficients, and retardation factors) for transport simulations.</p>	<p>CRWMS M&O 1998b [summaries, Neuman]</p>	<p>No kilometer-scale tracer tests have been done, however multi-well, multi-tracer tracer tests have been done at the C-wells. Multi-well, multi-tracer tests conducted, tracer tests discussed in Section 3.1.3.2.</p>
<p>A comparison of average $\delta^{18}\text{O}$, δD, Na, Ca, Cl, and SO_4 concentrations in groundwaters under Yucca Mountain, with their concentrations in the presumed groundwater flow direction in wells J-13 and J-12 along Fortymile Wash, suggests that groundwater under Yucca Mountain contributes a negligible fraction of flow to the groundwaters in Fortymile Wash. The data also tentatively suggest that significant surface runoff (snowmelt runoff?) infiltrates to groundwater east of Yucca Mountain in Fortymile Wash. Such infiltration could significantly dilute radionuclide concentrations introduced from a Yucca Mountain repository. Groundwater from beneath Yucca Mountain can be thought of as being titrated into the relatively large Fortymile Wash groundwater system.</p>	<p>CRWMS M&O 1998b [summaries, Langmuir]</p>	<p>CRWMS M&O (2000m) discusses hydrochemistry; Section 3.1.3.1 discusses spatial patterns of groundwater chemistry. Model validation now includes comparisons of: permeability data to calibrated permeability values, fluxes from regional models with fluxes from calibrated model, measured upward gradient with predicted upward gradient, hydrochemical data with calculated particle pathways, and natural analogs. These activities and process model uncertainties are discussed in Section 3.4.</p>
<p>A key issue for radionuclide transport is whether or not, and to what degree, flowpaths from the repository enter the carbonate aquifer at distances of 5 to 30 km (3.1 to 18.6 mi.). The regional hydrologic model suggests that groundwater flow paths enter the carbonate aquifer about 10 km (6.2 mi.) south of the site and, farther south, come back up into the alluvial aquifer. If flow in the carbonates occurs, important Np(V) adsorption by calcite could be expected.</p>	<p>CRWMS M&O 1998b [summaries, Langmuir]</p>	<p>No indication of flow in carbonates to date. Characterization discussed in Section 3.1; geologic setting of regional flow system discussed in Section 3.1.1.1.1; geologic setting of site flow system discussed in Section 3.1.1.2.1; relationship of SZ PMR to ISM PMR (CRWMS M&O 2000e) discussed in Section 1.5.1; hydrogeologic framework discussed in Sections 3.2.1 and 3.3.5.2.</p>

Table A-1. Issues for Saturated Zone Flow and Transport (Continued)

Issue	Source	PMR Approach
<p>The DOE approach to defining amounts of radionuclides that could be released from the buried waste and transported to the accessible environment through the UZ and SZ is in general highly conservative. The possible benefits of sorption, solubility, and redox reactions on reducing the maximum possible concentrations of radionuclides in groundwater have not been sufficiently emphasized. An analysis of transport processes and parameters that considers only sorption reactions as the geochemical control on maximum radionuclide concentrations is inadequate. Sorption only delays the peak release of long-lived radionuclides such as neptunium-237 to the environment. Solubility, if applicable, can greatly reduce or eliminate releases.</p>	<p>CRWMS M&O 1998b [summaries, Langmuir]</p>	<p>Solute transport processes in conceptual model discussed in Section 3.2.4; in mathematical model in Section 3.3.2; particle tracking discussed in Section 3.3.4; assumptions, uses, and limitations of radionuclide transport processes discussed in Section 3.5.2; abstraction of transport for TSPA discussed in Section 3.6.3.3.</p>
<p>Some of the assumptions in TSPA-95 (CRWMS M&O 1995) that may be unnecessarily conservative are:</p> <ol style="list-style-type: none"> 1. The assumed solubility of U(VI) in Yucca Mountain groundwater probably is about 10^2 too high. 2. The assumed solubility of neptunium(V) in Yucca Mountain groundwater probably is at least about 10^1 too high. 3. Reduction of neptunium(V) to neptunium(IV) by Iron(II)-containing minerals in the matrix of the volcanic rocks seems likely during groundwater flow. Reduction could lower the solubility of neptunium by about 10^3 times 4. Adsorption of Np(V) by trace or minor minerals in the tuff, which are relatively ubiquitous and include Mn oxides, Iron(II)-containing silicates, and calcite, could reduce neptunium concentrations in the rock matrix by orders of magnitude. 	<p>CRWMS M&O 1998b [summaries, Langmuir]</p>	<p>Assumptions, uses, and limitations of radionuclide transport processes discussed in Section 3.5.2; abstraction of transport for TSPA discussed in Section 3.6.3.3.</p>
<p>The potential effect of the thermal pulse on the SZ beneath the site will be a function of whether the flow occurs in the fractures or in the matrix (which includes tight fractures). If there is fracture flow only, then effects will occur at greater distances from the repository. If there is significant matrix flow, I would expect the increased temperatures to cause silica in the volcanic rocks to dissolve, to move to cooler locations, and then to precipitate and possibly clog the system. If calcite is saturated in the water, because of its retrograde solubility, it will precipitate and may clog the matrix and fine fractures adjacent to the hot waste. The clogging may lead to additional residence time for radionuclides in the matrix. Refluxing of condensed water may cause similar effects to occur at the water table beneath the site.</p>	<p>CRWMS M&O 1998b [summaries, Langmuir]</p>	<p>UZ PMR (CRWMS M&O 2000b). Relationship of SZ to UZ discussed in Section 1.5.2; coupling of SZ with UZ discussed in Section 3.6.3.4.1.</p>

Table A-1. Issues for Saturated Zone Flow and Transport (Continued)

Issue	Source	PMR Approach
<p>The likely fate of colloids will be the following:</p> <ul style="list-style-type: none"> • Many will be filtered out by crushed tuff backfill or tuff invert under unsaturated conditions. • Degradation colloids (such as Pu oxides) and radiocolloids will be undersaturated with respect to the groundwater as soon as they move away from the waste. They will therefore tend to dissolve in the groundwater and, once in solution, tend to be adsorbed by rock surfaces in fractures and especially in the matrix. • Actinides on the surfaces of geocolloids will tend to desorb with groundwater flow. They will be reabsorbed by surrounding rock surfaces that have the same surface bond strengths toward the actinides but have unoccupied surface sites and orders of magnitude more reactive surface area. The colloidal microspheres tracer test in the C-wells showed that the peak arrival preceded the conservative tracers (20 hrs versus 30 hrs). About 85% of the microspheres were lost. This suggests that colloids can move in the SZ, but radionuclides/colloidal particles must travel first through the UZ, and losses are expected in the SZ. 	<p>CRWMS M&O 1998b</p> <p>[summaries, Langmuir]</p>	<ul style="list-style-type: none"> • This is discussed in the Engineered Barrier System PMR (CRWMS M&O 2000g) and UZ PMR (CRWMS M&O 2000b). • This is discussed in the Engineered Barrier System PMR (CRWMS M&O 2000g) and UZ PMR (CRWMS M&O 2000b). • Tracer tests discussed in Section 3.1.3.2. Colloid lab experiments discussed in Section 3.1.4.3; modeling of colloid-facilitated transport discussed in Sections 3.2.4.5 and 3.3.2.4.
<p>The key radionuclide of concern in colloidal transport is Pu. Pu transport has been documented in a shallow aquifer in Mortland Canyon, Los Alamos National Laboratory. Pu movement was at the surface in alluvial sediments and was washed downward on sediments to the shallow groundwater table. This scenario is not analogous to possible Pu migration in the SZ beneath Yucca Mountain. In a second study, Pu from underground nuclear tests at the Nevada Test Site moved in the groundwater several kilometers from an underground test. The Pu was probably within melted tuff particles that were transported by explosive injection. This is obviously not an analogue for Yucca Mountain. Bomb pulse chlorine-36-aged water found deep in the UZ under Yucca Mountain indicates the existence of fast paths that may extend to the SZ. It is possible that colloidal radionuclides could take the same pathways.</p>	<p>CRWMS M&O 1998b</p> <p>[summaries, Langmuir]</p>	<p>Colloid-facilitated transport is now explicitly modeled. Tracer tests discussed in Section 3.1.3.2. Colloid laboratory experiments discussed in Section 3.1.4.3; modeling of colloid-facilitated transport discussed in Sections 3.2.4.5 and 3.3.2.4.</p>
<p>Recommendations For Reducing Uncertainty:</p> <ol style="list-style-type: none"> 1. C-wells tests should be run for longer times to evaluate the relative importance of matrix vs. fracture flow in the Tertiary volcanic rocks. 	<p>CRWMS M&O 1998b</p> <p>[summaries, Langmuir]</p>	<p>Multi-well, multi-tracer testing at C-wells has been done. Hydraulic well testing discussed in Section 3.1.2.2, tracer tests discussed in Section 3.1.3.2.</p>

Table A-1. Issues for Saturated Zone Flow and Transport (Continued)

Issue	Source	PMR Approach
<p>2. Available groundwater chemistry and isotopic data for the whole Yucca Mountain-Fortymile Wash flow system to its discharge area in the Amargosa Desert should be mapped in detail. The southern end of this system was last examined by Claassen (1983). This task might lead to conclusions regarding amounts of possible mixing of volcanic, carbonate, and alluvial groundwaters in southern Fortymile Wash.</p>	<p>CRWMS M&O 1998b [summaries, Langmuir]</p>	<p>Maps have been done. CRWMS M&O (2000m) and Section 3.1.3 discuss hydrochemical data and provide detailed maps. Section 3.1.1.1.3 discusses the hydrochemistry of regional system. Section 3.1.1.2.3 discusses the hydrochemistry of site system. Section 3.4.4 discusses comparison of hydrochemical data with calculated flow pathways.</p>
<p>3. Delta carbon-14 groundwater data from the literature should be corrected using the NETPATH code approach presented to us by Kwicklis in a SZ Expert Elicitation Workshop (CRWMS M&O 1998b). This would provide an internally consistent delta carbon-14 data set for the general area, including the complete Yucca Mountain groundwater flow system. Such data might be useful for computing groundwater travel times and matrix versus fracture flow.</p>	<p>CRWMS M&O 1998b [summaries, Langmuir]</p>	<p>CRWMS M&O (2000m, Table 8) document results of the NETPATH code corrections to groundwater carbon-14 ages; Section 3.1.3 discuss hydrochemical data; Section 3.1.1.1.3 discusses the hydrochemistry of regional system; Section 3.1.1.2.3 discusses the hydrochemistry of site system. Section 3.4.2 discusses calibration of model to hydrochemical observations.</p>
<p>4. Interpreting and modeling the groundwater geochemical data in the vicinity of Yucca Mountain in the context of the geology and groundwater hydrology should be emphasized. Groundwater chemistry should be related to sampling depths, water levels and transmissivity, fracture zones, specific formations and their mineralogy, and rock matrix versus fracture flow properties. Such an analysis could help explain much of the water chemistry information, which in turn should help us resolve ambiguous interpretations of the groundwater hydrology.</p>	<p>CRWMS M&O 1998b [summaries, Langmuir]</p>	<p>Extensive interpretation of groundwater geochemical data done and documented in CRWMS M&O (2000m). Section 3.1.3 discuss hydrochemical data. Section 3.1.1.1.3 discusses the hydrochemistry of regional system. Section 3.1.1.2.3 discusses the hydrochemistry of site system. Section 3.4.4 discusses comparison of hydrochemical data with calculated flow pathways.</p>
<p>5. Geochemical and hydrologic data and models should be used to evaluate the relative contributions of infiltrating surface runoff and groundwater from under Yucca Mountain to the volume of groundwater flow in Fortymile Wash east and southeast of Yucca Mountain. Runoff infiltration in Fortymile Wash may be the chief diluent for radionuclides released from the repository.</p>	<p>CRWMS M&O 1998b [summaries, Langmuir]</p>	<p>Section 3.1.3 discusses hydrochemical data; Section 3.1.1.1.3 discusses the hydrochemistry of regional system; Section 3.1.1.2.3 discusses the hydrochemistry of site system; Section 3.4.4 discusses comparison of hydrochemical data with calculated flow pathways.</p>

Table A-1. Issues for Saturated Zone Flow and Transport (Continued)

Issue	Source	PMR Approach
<p>6. Pump tests of shallow wells in the Tertiary volcanics under Yucca Mountain probably will sample fracture flow which is likely to be oxidizing with an Eh above 300 mv. The only way to determine if matrix flow will lead to Eh values low enough to cause reduction of Np(V) to insoluble Np(IV) is theoretically, or preferably experimentally, in the laboratory. My predictions of percentile of CDF values for Np(V) adsorption were based on theory. Lab experiments could be performed in closed vessels using rock fragments or an ultracentrifuge and rock cores to speed up flow, with measurements being made of dissolved oxygen levels and Eh as a function of time.</p>	<p>CRWMS M&O 1998b [summaries, Langmuir]</p>	<p>Oxidation potential discussed in 3.1.3.3. Laboratory sorption discussed in Section 3.1.4.1.</p>
<p>7. The prediction that maximum uranium concentrations in Yucca Mountain groundwater are limited by the solubility of uranophane is based on computer modeling. Experiments should be performed on the solubility of uranophane in simulated groundwater in the presence of volcanic tuff materials to confirm model calculations.</p>	<p>CRWMS M&O 1998b [summaries, Langmuir]</p>	<p>Tests not done to date. UZ model provides input to SZ model on concentrations of radionuclides.</p>
<p>It is possible to analyze the tracer breakthrough curves to obtain information and parameters associated with the small-scale heterogeneities that control flow channeling. A more direct way is to obtain permeability values from packed-off intervals in the many boreholes at the site. This can also be done by flow-meter testing without packers. In this case, a conventional spinner flow meter may not be accurate enough. One may need to use a heat-pulse flow meter or the fluid logging method. C-hole data already indicate that strong variations in permeability occur at Yucca Mountain. Flows into C#1, C#2, and C#3 are dominated by three, three, and four specific vertical intervals, respectively, with one interval in each case carrying more than 50 percent of the flow into the well. This is consistent with the current knowledge that roughly 10 to 20 percent of the fractures contribute to flow, with only 1 to 10 percent contributing significantly.</p>	<p>CRWMS M&O 1998b [summaries, Tsang]</p>	<p>Multi-well, multi-tracer tests done at C-wells. Characterization discussed in Section 3.1; hydraulic well tests in Section 3.1.2.2; tracer tests in Section 3.1.3.2; laboratory data in Section 3.1.4.</p> <p>Model validation now includes comparisons of: permeability data to calibrated permeability values, fluxes from regional models with fluxes from calibrated model, measured upward gradient with predicted upward gradient, hydrochemical data with calculated particle pathways, and natural analogs. These activities and process model uncertainties are discussed in Section 3.4.</p>

Table A-1. Issues for Saturated Zone Flow and Transport (Continued)

Issue	Source	PMR Approach
<p>We need to know the source term at the unsaturated-saturated zone interface, where channelized flow from the unsaturated region enters the saturated region, and where flow is expected to be channeled. The source term must be studied carefully and its characteristics evaluated.</p> <p>Two potentially important issues need to be considered:</p> <ol style="list-style-type: none"> 1. Under steady flow conditions in the UZ, flow is expected to be channeled along relatively small pores (corresponding perhaps to smaller local permeabilities), because the large pores will be occupied by air, while the main flow in the SZ will be channeled along higher-permeability regions. The switch-over from lower-permeability areas to higher-permeability areas of the heterogeneous field needs to be evaluated in terms of possible dilution process. 2. The water table cuts through a number of hydrogeologic units, whose permeabilities differ by several orders of magnitude. The particular units in which leakage from the potential repository reaches the SZ may each provide different source term characteristics. These two issues are in addition to the usual concern of solute transport through the capillary fringe and effects of changes in the water table. 	<p>CRWMS M&O 1998b</p> <p>[summaries, Tsang]</p>	<p>UZ model (CRWMS M&O 2000b) provides input to SZ model on concentrations of radionuclides. Coupling of SZ flow and transport with UZ flow and transport discussed in Section 3.6.3.4.1.</p>
<p>Beyond the source region at the water table, flow will follow hydrogeologic units, probably primarily the Bullfrog unit. Here, flow will be according to stream lines, and dilution will be minor. As it encounters offsets due to faults cutting through the hydrogeologic unit, it will digress, bifurcate, or spread out depending on the fault permeability and local conditions. It is not clear whether there will be significant dilution at such locations, but careful analysis can, and should, be made to answer this question. Solutes along the stream lines are subjected to local dispersion or molecular diffusion and can spread to neighboring stream lines. The dilution resulting from this process would be much smaller than that commonly assumed for dispersion.</p>	<p>CRWMS M&O 1998b</p> <p>[summaries, Tsang]</p>	<p>Site-scale SZ flow and transport model developed. Roles of faults discussed in Section 3.2.3.4.</p> <p>Heterogeneity discussed in Section 3.2.2.4.</p> <p>Particle tracking method for radionuclide transport discussed in Section 3.3.4.</p>
<p>After a tortuous journey, flow arrives at the users' area and is collected from a so-called capture zone. If a fault or special feature occurs near this area, it may provide a focusing effect near the location where the regulatory criteria are to be applied. Such features must be included in the model.</p>	<p>CRWMS M&O 1998b</p> <p>[summaries, Tsang]</p>	<p>Dilution in water supply discussed in Section 3.6.3.3.4.</p> <p>Relationship to Biosphere PMR (CRWMS M&O 2000c) discussed in Section 1.5.3.</p> <p>Coupling with biosphere model discussed in Section 3.6.3.4.2.</p>

Table A-1. Issues for Saturated Zone Flow and Transport (Continued)

Issue	Source	PMR Approach
<p>The "mixing depth" concept is not realistic. Rather, we need to consider the three stages of tracer transport to address this issue. First, one must consider the source term to the SZ. It is likely that there will be channeled flow in the UZ, and that these channeled flow paths will then enter the SZ. Thus the source term is not a smeared-out plume, but a number of localized, higher-concentration "point sources." Second, once the solutes enter the SZ, they will again follow certain stream tubes, or flow channels, with only minor dispersion within each stream tube. The degree of such channelization depends on the degree of heterogeneity (standard deviation of the hydraulic conductivity values), and the spacing of these channels depends on the spatial correlation structure of heterogeneities in permeability. Then, thirdly, the different flow paths will come to the observational "fence" area and to an extraction well, where they will be captured and pumped for various uses. At this point, a dosage limit is to be imposed.</p>	<p>CRWMS M&O 1998b [summaries, Tsang]</p>	<p>UZ model (CRWMS M&O 2000b) provides input to SZ model on concentrations of radionuclides. Relationship of SZ to UZ discussed in Section 1.5.2. Coupling of UZ flow and transport model with SZ flow and transport discussed in Section 3.6.3.4.1.</p>
<p>Large dilution of the solute concentration between the source zone at the unsaturated-saturated zone interface and the capture zone of the users' wells is not expected. Molecular diffusion will occur within the flow channels, but there will likely be only a small longitudinal dispersion. Dilution is expected to be only about a factor of 2 to 10 over even kilometers of distance. This is because longitudinal dispersion occurs from Taylor dispersion, which has a characteristic length that is on the order of the width of the channel.</p>	<p>CRWMS M&O 1998b [summaries, Tsang]</p>	<p>Site-scale SZ flow and transport model developed that addresses dispersion better. Conceptual model diffusion, sorption, and dispersion discussed in Sections 3.2.4.2, 3.2.4.3, and 3.2.4.4; mathematical model diffusion, sorption, and dispersion discussed in Sections 3.3.2.2, 3.3.2.3, and 3.3.2.4; transport processes assumptions, uses, and limitations discussed in Section 3.5.2.</p>
<p>There are two places where significant dilution may occur. The first is at the interface between the unsaturated and the saturated zones, especially if the interface (i.e., the water table) fluctuates. If flow channels go from a low-permeability area in the UZ to a high-permeability area in the SZ, spreading may also occur. Unfortunately, this has not been carefully studied. Research is underway; we hope to have some results and know their implications in the near future. The other dilution step is at the production well. The production well creates what is called a capture zone, inside of which all the stream lines are captured and mixed in the production wells.</p>	<p>CRWMS M&O 1998b [summaries, Tsang]</p>	<p>Coupling of UZ flow and transport model with SZ flow and transport discussed in Section 3.6.3.4.1. Dilution in water supply discussed in Section 3.6.3.3.4.</p>

Table A-1. Issues for Saturated Zone Flow and Transport (Continued)

Issue	Source	PMR Approach
<p>A "dilution factor" can be assessed by using a "bundle-of-particle-lines" model. Consider the source term at the SZ-UZ interface to be represented by a number of localized "point sources" that correspond to channeled flow in the UZ. Then, from each point source, particles are traced along stream lines through the hydrogeologic units, allowing for flow around fault-related offsets and across or around faults. Along the way one can account for molecular diffusion and local dispersion by allowing particles to jump to neighboring stream lines. These particle lines are traced to the capture zone of the users' wells, where these lines and flow lines without contamination are collected. Thus, dilution can be calculated.</p>	<p>CRWMS M&O 1998b [summaries, Tsang]</p>	<p>Site-scale SZ flow and transport model developed. Coupling of UZ flow and transport model with SZ flow and transport discussed in Section 3.6.3.4.1. Particle tracking method for radionuclide transport discussed in Section 3.3.4. Dilution in water supply discussed in Section 3.6.3.3.4.</p>
<p>If the data are carefully considered, it should be possible to use the laboratory K_d derived for Yucca Mountain rocks. A migration experiment done at the Grimsel site found good agreement between laboratory and field measurements of K_d and demonstrated that matrix diffusion exists in the field by examining the tails of the breakthrough curves. To obtain consistency, the flow model must be conceptualized correctly based on a careful analysis of field hydraulic data. Under such a "strong" prerequisite, results from column experiments probably are consistent and useful for estimating field data. It is somewhat troubling that there is a ten-fold discrepancy between the C-wells data and laboratory data. It is likely that the flow field was not properly modeled</p>	<p>CRWMS M&O 1998b [summaries, Tsang]</p>	<p>Multi-well, multi-tracer tests done at C-wells. Laboratory data on sorption, matrix diffusion, and colloid transport discussed in Section 3.1.4; hydraulic well tests discussed in Section 3.1.2.2; tracer tests discussed in Section 3.1.3.2. Model validation now includes comparisons of: permeability data to calibrated permeability values, fluxes from regional model with fluxes from calibrated model, measured upward gradient with predicted upward gradient, hydrochemical data with calculated particle pathways, and natural analogs. These activities and process model uncertainties are discussed in Section 3.4.</p>
<p>K_d use is open to some questions. It would be useful to consider real chemistry and perform chemical modeling, accounting for detailed chemical reactions to assess the range and limit of this approach.</p>	<p>CRWMS M&O 1998b [summaries, Tsang]</p>	<p>Laboratory data on sorption, matrix diffusion, and colloid transport discussed in Section 3.1.4; hydraulic well tests discussed in Section 3.1.2.2; tracer tests discussed in Section 3.1.3.2.</p>

Table A-1. Issues for Saturated Zone Flow and Transport (Continued)

Issue	Source	PMR Approach
<p>Recommendations For Reducing Uncertainty:</p> <p>1. Perform long-term interference tests with pumping in a C-well (or another well) and monitoring as many observation wells as possible over a wide area. These tests will help determine the horizontal distribution of hydraulic conductivity and the hydraulic parameters associated with major faults. Analysis using a multi-parameter fit of a numerical model will be needed. Associated with this effort, a long-term tracer test should also be performed. Careful design studies with numerical model are needed.</p>	<p>CRWMS M&O 1998b</p> <p>[summaries, Tsang]</p>	<p>Multi-well, multi-tracer tests done at C-wells.</p> <p>Characterization discussed in Section 3.1; hydraulic well tests in Section 3.1.2.2; tracer tests in Section 3.1.3.2; laboratory data in Section 3.1.4.</p> <p>Model validation now includes comparisons of: permeability data to calibrated permeability values, fluxes from regional model with fluxes from calibrated model, measured upward gradient with predicted upward gradient, hydrochemical data with calculated particle pathways, and natural analogs. These activities and process model uncertainties are discussed in Section 3.4.</p> <p>Uses of the SZ model in site characterization activities discussed in Section 3.5.3.</p>
<p>2. Re-drill borehole G-2 and emplace packers to study relative changes in packed intervals to reduce the uncertainty concerning the causes for the large hydraulic gradient.</p>	<p>CRWMS M&O 1998b</p> <p>[summaries, Tsang]</p>	<p>The large hydraulic gradient is discussed in Sections 3.2.2.3 and 3.2.5.1.</p> <p>Borehole WT-24 drilled to investigate the large hydraulic gradient indicates that the large hydraulic gradient is partially due to perching.</p>
<p>3. Use temperature log data in a calibration of a 3-D site- or subsite-scale model, especially to address the question of upward flow into the volcanic aquifer.</p>	<p>CRWMS M&O 1998b</p> <p>[summaries, Tsang]</p>	<p>Temperature-log data not used in calibration as most temperature data were not collected in a manner that would allow their use for this purpose (i.e., cased boreholes or temperature measured without allowing hole to equilibrate).</p> <p>Model validation now includes comparisons of: permeability data to calibrated permeability values, fluxes from regional model with fluxes from calibrated model, measured upward gradient with predicted upward gradient, hydrochemical data with calculated particle pathways, and natural analogs. These activities and process model uncertainties are discussed in Section 3.4.</p>

Table A-1. Issues for Saturated Zone Flow and Transport (Continued)

Issue	Source	PMR Approach
<p>4. Recalibrate site-scale model, allowing for a more careful and definite coupling with the regional model. For example, the fluxes into and out of the site-scale area in the regional model must be consistent with the imposed boundary conditions on the site-scale model, so that total fluxes at the boundaries are conserved. This eventually would yield more convincing results from the site model.</p>	<p>CRWMS M&O 1998b [summaries, Tsang]</p>	<p>New site and regional models developed; groundwater flux relationship between models discussed in Section 3.4.2.</p> <p>Model validation now includes comparisons of: permeability data to calibrated permeability values, fluxes from regional model with fluxes from calibrated model, measured upward gradient with predicted upward gradient, hydrochemical data with calculated particle pathways, and natural analogs. These activities and process model uncertainties are discussed in Section 3.4.</p>

INTENTIONALLY LEFT BLANK

APPENDIX B

**U.S. NUCLEAR REGULATORY COMMISSION ISSUE RESOLUTION
STATUS REPORTS AND KEY TECHNICAL ISSUES**

APPENDIX B

U.S. NUCLEAR REGULATORY COMMISSION ISSUE RESOLUTION STATUS REPORTS AND KEY TECHNICAL ISSUES

Table B-1. Issue Resolution Status Report Technical Acceptance Criteria

Key Technical Issue: Radionuclide Transport	
Subissue 2 Radionuclide Transport Through Alluvium	PMR Approach
1a. For the estimation of radionuclide transport through alluvium, the Department of Energy (DOE) has determined, through performance assessment (PA) calculations, whether radionuclide attenuation processes such as sorption, precipitation, radioactive decay, and colloidal filtration are important to performance.	PA calculations indicate these processes are important. Laboratory data on sorption, matrix diffusion and colloids discussed in Section 3.1.4; conceptual models of solute transport, Section 3.2.4; mathematical models of radionuclide transport, Section 3.3.1; sorption and matrix diffusion sub-model, Section 3.3.4.2; assumptions and limitations associated with radionuclide transport processes, Section 3.5.2; abstraction of radionuclide transport in Total System PA, Section 3.6.3.
1b. For the estimation of radionuclide transport through alluvium, DOE has (i) assumed the sorption coefficient is zero and radionuclides travel at the rate of groundwater flow, if it has been found that radionuclide attenuation is unimportant to performance and it can be demonstrated that this assumption is conservative, in which case Criteria 2 and 3 do not have to be met or (ii) demonstrated that Criterion 2 or 3 has been met, if radionuclide attenuation in alluvium is important to performance or if an assumption that the sorption coefficient is zero in alluvium is not conservative.	For radionuclides with essentially no sorption potential (e.g., carbon, chlorine, iodine), the sorption coefficient (K_d) is assumed to be zero in alluvium. Laboratory data on sorption, matrix diffusion, and colloids discussed in Section 3.1.4; tracer tests, Section 3.1.3.2; conceptual models of solute transport, Section 3.2.4; mathematical models of radionuclide transport, Section 3.3.1; sorption and matrix diffusion sub-model, Section 3.3.4.2; assumptions and limitations associated with radionuclide transport processes, Section 3.5.2; abstraction of radionuclide transport in Total System Performance Assessment (TSPA), Section 3.6.3.3.
2a. For the valid application of the K_d approach, using equation (1) $R_f = 1 + \rho_b K_d/n$, DOE has demonstrated that the flow path acts as a single continuum porous medium. If the flow cannot be shown to be a single continuum porous medium, then the acceptance criteria for radionuclide transport in fractured rock apply.	Fluid flow in the alluvium is likely to be well represented using a porous continuum conceptual model. Data to quantify the alluvial portion of the flow path are sparse, and hydrologic parameters used in numerical models should be considered to be bounding (Section 3.2.4.1.2).
2b. For the valid application of the K_d approach, using equation (1) $R_f = 1 + \rho_b K_d/n$, DOE has demonstrated that appropriate values for the parameters, K_d , n or τ , and ρ_b have been adequately considered (e.g., experimentally determined or measured).	Transport of sorbing solutes in porous media is a subject that has been well studied. Sorption coefficients onto alluvium from the Nye County Early Warning Drilling Program (NCEWDP) wells have been measured for a few key radionuclides; for the remaining radionuclides, sorption coefficients have been estimated based on the corresponding values measured for crushed tuff. Recent evaluations for the sorption of neptunium, technetium, and iodine have been accomplished for alluvium. Laboratory data on sorption, matrix diffusion, and colloids are discussed in Section 3.1.4. In the alluvium, n is modeled stochastically and r_b is modeled as a constant.

Table B-1. Issue Resolution Status Report (IRSR) Technical Acceptance Criteria (Continued)

<p align="center">Subissue 2 Radionuclide Transport Through Alluvium (Continued)</p>	<p align="center">PMR Approach</p>
<p>2c. For the valid application of the K_d approach, using equation (1) $R_f = 1 + \rho_b K_d/n$, DOE has demonstrated that the following assumptions (i.e., linear isotherm, fast reversible sorption reaction, and constant bulk chemistry) are valid.</p>	<p>Sorption is incorporated into the site-scale saturated-zone (SZ) flow and transport model using a linear isotherm model (Sections 3.2.4.3 and 3.3.2.3). Laboratory data on sorption, matrix diffusion, and colloids are discussed in Section 3.1.4; tracer tests, Section 3.1.3.2; conceptual models of solute transport, Section 3.2.4.</p>
<p>3a. For the valid application of process models such as surface complexation, ion exchange, precipitation/dissolution, and processes involving colloidal material, DOE has demonstrated that the flow path acts as a single continuum porous medium (see USFIC IRSR [NRC 1999a], deep percolation on subissue describing methods of estimating matrix properties as parameters).</p>	<p>Fluid flow in the alluvium is likely to be well represented using a porous continuum conceptual model. Data to quantify the alluvial portion of the flow path are sparse, and hydrologic parameters used in numerical models should be considered to be bounding (Section 3.2.4.1.2). Conceptual model of SZ flow and transport discussed in Section 3.2, heterogeneity in Section 3.2.2.4. Model validation now includes comparisons of: permeability data to calibrated permeability values, fluxes from regional model with fluxes from calibrated model, measured upward gradient with predicted upward gradient, and hydrochemical data with calculated particle pathways; as well as natural analogs. These activities and process model uncertainties are discussed in Section 3.4. (Note: criterion refers to deep percolation in USFIC IRSR (NRC 1999a), which is an unsaturated zone [UZ] subissue.)</p>
<p>3b. For the valid application of process models such as surface complexation, ion exchange, precipitation/dissolution, and processes involving colloidal material, DOE has demonstrated that appropriate values are used in process models.</p>	<p>Characterization discussed in Section 3.1; laboratory data, Section 3.1.4; hydraulic well tests, Section 3.1.2.2; tracer tests, Section 3.1.3.2. Model validation now includes comparisons of: permeability data to calibrated permeability values, fluxes from regional model with fluxes from calibrated model, measured upward gradient with predicted upward gradient, hydrochemical data with calculated particle pathways, and natural analogs. These activities and process model uncertainties are discussed in Section 3.4.</p>
<p>3c. For the valid application of process models such as surface complexation, ion exchange, precipitation/dissolution, and processes involving colloidal material, DOE has demonstrated that the three implicit assumptions (as in 2c) are valid, if process models are intended to yield a constant K_d for use in equation (1); otherwise determined transport in a dynamic reactive transport system model (e.g., PHREEQC, MULTIFLO, HYDROGEOCHEM, etc.)</p>	<p>Laboratory data on sorption, matrix diffusion, and colloids discussed in Section 3.1.4; tracer tests, Section, 3.1.3.2; conceptual models of solute transport, Section 3.2.4. Model validation now includes comparisons of: permeability data to calibrated permeability values, fluxes from regional model with fluxes from calibrated model, measured upward gradient with predicted upward gradient, hydrochemical data with calculated particle pathways, and natural analogs. These activities and process model uncertainties are discussed in Section 3.4.</p>

Table B-1. Issue Resolution Status Report (IRSR) Technical Acceptance Criteria (Continued)

KTI: Radionuclide Transport	
Subissue 3 Radionuclide Transport Through Fractured Rock	PMR Approach
1a. For the estimation of radionuclide transport through fractured rock, DOE has determined, through PA calculations, whether radionuclide attenuation processes such as sorption, precipitation, radioactive decay, and colloidal filtration are important to performance.	PA calculations have determined that such processes are important. Abstraction of radionuclide transport in TSPA is discussed in Section 3.6.3.3; laboratory data on sorption, matrix diffusion, and colloids, Section 3.1.4; conceptual models of solute transport, Section 3.2.4; mathematical models of radionuclide transport, Section 3.3.1; sorption and matrix diffusion sub-model, Section 3.3.4.2; assumptions and limitations associated with radionuclide transport, Section 3.5.2; heterogeneity, Section 3.2.2.4.
1b. For the estimation of radionuclide transport through fractured rock, DOE has assumed K_d (or K_A) is zero and radionuclides travel at the rate of groundwater flow through fractures, if it has been found that radionuclide attenuation in fractures is unimportant to performance and it can be demonstrated that this assumption is conservative. In this case, Acceptance Criterion 2 does not have to be met.	For radionuclides with essentially no sorption potential (e.g., carbon, chlorine), the sorption coefficient (K_d) is assumed to be zero. Laboratory data on sorption, matrix diffusion, and colloids discussed in Section 3.1.4; tracer tests, Section, 3.1.3.2; heterogeneity, Section 3.2.2.4; conceptual models of solute transport, Section 3.2.4; mathematical models of radionuclide transport, Section 3.3.1; sorption and matrix diffusion sub-model, Section 3.3.4.2; assumptions and limitations associated with radionuclide transport processes, Section 3.5.2; abstraction of radionuclide transport in TSPA, Section 3.6.3.3.
1c. For the estimation of radionuclide transport through fractured rock, DOE has justified the length of the flowpath to which these fracture transport conditions apply.	Chloride data (Figure 3-3), as well as other chemical and isotopic data (CRWMS M&O 2000m and Section 3.1.1.2.3) and the potentiometric surface map (Figure 3-5), have been used to constrain flowpaths. Particle tracking methodology is discussed in Section 3.3.4; validation in Section 3.4; assumptions, uses, and limitations of flow model, Section 3.5.
2a. If credit is to be taken for radionuclide attenuation in fractured rock, DOE has demonstrated the capability to predict breakthrough curves of reactive, nonreactive, and colloidal tracers in field tests.	Model of fracture flow and matrix diffusion consistent with data. Sorbing tracer (lithium) breakthrough consistent with combined matrix diffusion/sorption model. Microspheres break through slightly earlier than solutes, but are attenuated. Tracer tests discussed in Section 3.1.3.2. Calibration to pump tests in C-wells discussed in Section 3.4.3.
2b. If credit is to be taken for radionuclide attenuation in fractured rock, DOE has demonstrated nonradioactive tracers used in field tests are appropriate homologues for radioelements.	Model of fracture flow and matrix diffusion consistent with data. Sorbing tracer (lithium) breakthrough consistent with combined matrix diffusion/sorption model. Microspheres break through slightly earlier than solutes, but are attenuated Tracer tests discussed in Section 3.1.3.2. Calibration to pump tests in C-wells discussed in Section 3.4.3.
2c. If credit is to be taken for radionuclide attenuation in fractured rock, DOE has justified the length of the flowpath to which these fracture transport conditions apply.	Chloride data (Figure 3-3), as well as other chemical and isotopic data (CRWMS M&O 2000m and Section 3.1.1.2.3) and the potentiometric surface map (Figure 3-5), have been used to constrain flowpaths. Particle tracking methodology discussed in Section 3.3.4; validation, Section 3.4; Assumptions, uses, and limitations of flow model, Section 3.5.

Table B-1. Issue Resolution Status Report (IRSR) Technical Acceptance Criteria (Continued)

<p align="center">Subissue 4 Nuclear Criticality in the Far Field</p>	<p align="center">PMR Approach</p>
<p>1. DOE has determined the probabilities of scenarios that lead to the accumulation of a critical mass of fissile material into a critical configuration within 10,000 years in the far-field using appropriate site characteristics.</p>	<p>The DOE plans to evaluate criticality using the method in the criticality analysis methodology topical report (YMP 1998) and its supporting documents. Features, events, and processes (FEPs) screening considers criticality event in far field to be low probability. Preliminary analyses show no significant effect on calculated performance in first 10,000 yr., even if waste packages are breached. FEPs are discussed in Section 1.3.</p>
<p>2. For those scenarios that have probabilities greater than 10^{-7}, the DOE has determined their effects on performance.</p>	<p>The DOE plans to evaluate criticality using the method in the criticality analysis methodology topical report (YMP 1998) and its supporting documents. FEPs screening considers criticality event in far field to be low probability. Preliminary analyses show no significant effect on calculated performance in first 10,000 yr., even if waste packages are breached. FEPs are discussed in Sections 1.3.</p>
<p align="center">Key Technical Issue: Structural Deformation and Seismicity</p>	
<p align="center">Subissue 3 Fracturing and Structural Framework of the Geologic Setting</p>	<p align="center">PMR Approach</p>
<p>Criterion 3—Alternative modeling approaches for fracture distribution and properties of fractures consistent with available data and current geologic understanding are investigated, and results and limitations are appropriately considered in process, TSPA, or both models of ambient and perturbed repository conditions. (Review method [p. 51 in IRSR] indicates that staff will examine the fracture data and properties that DOE has abstracted into its process level models and SZ groundwater flow models to ensure adequate integration.)</p>	<p>Heterogeneity and hydrologic features of the hydrogeologic framework are discussed in Sections 3.2.2.4 and 3.2.2.5. Role of faults as internal boundaries is discussed in Section 3.2.3.4. Numerous hydrologic features corresponding to faults and geologic zones are explicitly incorporated into the site-scale SZ flow and transport model as part of the calibration process (Section 3.2.2.5). The presence of faults and fracture zones that are not explicitly represented in the site-scale model, and their potential impact on groundwater flow, is implicitly included in the nominal case through consideration of horizontal anisotropy in permeability in the fractured volcanic units downgradient of the repository. Given the uncertainty in anisotropy, and to simplify the model, the potential effects of anisotropy are bounded in the model. Anisotropy and incorporation of effects in the model are discussed in Sections 3.5.1 and 3.7.2. Horizontal anisotropy discussed in Section 3.2.5.3.</p>
<p>Criterion 5—Integration results of abstractions of fracture data are consistent with physical and geological phenomena and coupled processes. (Review method [p. 52 in IRSR] indicates that staff will examine input of fracture models to SZ flow modules to ensure adequate integration.)</p>	<p>Heterogeneity and hydrologic features of the hydrogeologic framework are discussed in Sections 3.2.2.4 and 3.2.2.5; role of faults as internal boundaries, Section 3.2.3.4</p>

Table B-1. Issue Resolution Status Report (IRSR) Technical Acceptance Criteria (Continued)

Key Technical Issue: Total System Performance Assessment and Integration	
System Description and Demonstration of Multiple Barriers	PMR Approach
Element 1 - Transparency and Traceability of the Analysis	
T1. Documents and reports are complete, clear, and consistent.	The SZ PMR was carefully structured to be complete, clear, and consistent. Reviews of the draft document included checks for completeness, clarity, and consistency.
T2. Information is amply cross referenced.	The SZ PMR contains ample references to data sources, codes, assumptions, and conclusions.
Element 2 - Features, Events, and Processes Identification and Screening	
T1. The screening process by which FEPs were included or excluded from the TSPA is fully described.	Excluded and included FEPs, including the rationale for these decisions, are summarized in Section 1.3.
T2. Relationships between relevant FEPs are fully described.	Relationship between primary and secondary FEPs described in Section 1.3. Additional documentation including the TSPA disposition of FEPs, IRSR issues relevant to specific FEPs, and analysis and discussion on specific FEPs are provided in the SZ FEPs AMR (CRWMS M&O 2000g).
Element 3 - Abstraction Methodology	
T1. The levels and method(s) of abstraction are described starting from assumptions defining the scope of the assessment down to assumptions concerning specific processes and the validity of given data.	For each submodel in the SZ PMR, descriptions are provided of process models and, if the models are abstracted, descriptions of the abstractions of the models. The description includes a summary of data and assumptions used to construct models. The AMRs describing the models and the abstracted models provide additional details regarding data and assumptions.
T2. A mapping (e.g., a road map diagram, a traceability matrix, a cross-reference matrix) is provided to show what conceptual features (e.g., patterns of volcanic events) and processes are represented in the abstracted models, and by what algorithms.	The SZ PMR and supporting AMRs provide descriptions of the basis for the decisions and assumptions that were made during the abstraction process.
T3. An explicit discussion of uncertainty is provided to identify which issues and factors are of most concern or are key sources of disagreement among experts.	The SZ PMR provides a discussion of uncertainties and limitations for the major process models included in the report. The AMRs describing the abstracted models provide additional details regarding uncertainties and limitations.
Element 4 - Data Use and Validity	
T1. The pedigree of data from laboratory tests, natural analogs, and the site is clearly identified.	The quality assurance status of the data and software used in the component models is summarized in Section 1.4.
T2. Input parameter development and basis for their selection is described.	Input parameter development and the basis for using the parameters are discussed in the SZ PMR. The AMRs describing the models provide additional details regarding input parameter development and the basis for input selection.

Table B-1. Issue Resolution Status Report (IRSR) Technical Acceptance Criteria (Continued)

System Description and Demonstration of Multiple Barriers (Continued)	PMR Approach
T3. A thorough description of the method used to identify performance confirmation program parameters	The Performance Confirmation Plan (CRWMS M&O 2000v) specifically addresses the methodology for identifying and selecting parameters that are important to performance based upon TSPA sensitivity analyses and the repository safety strategy. Methods used to collect information for each parameter will be described by the performance confirmation plan or relevant supporting documents to support the license application. Performance confirmation test selection and rationale is described in the plan based upon the importance of the parameter being measured, and the ability of the test to distinguish construction, emplacement, or time dependent changes in the parameter important to performance.
Element 5 - Assessment Results	
T1. PA results (i.e., the peak expected annual dose within the compliance period) can be traced back to applicable analyses that identify the FEPs, assumptions, input parameters, and models in the PA.	Features, processes, conceptual models, and their implementation into the TSPA are summarized in the TSPA-SR. This discussion will be based in part on information provided by the SZ PMR.
T2. The PA results include a presentation of intermediate results that provide insight into the assessment (e.g., results of intermediate calculations of the behavior of individual barriers).	TSPA-SR provides performance analysis results for the total system and will include intermediate results for the components of the system.
Element 6 - Code Design and Data Flow	
T1. The flow of information (input and output) between the various modules is clearly described.	A description of information flow between component models including couplings between information and data, conceptual and process-level models, and abstracted models are provided in the TSPA-SR.
T2. Supporting documentation (e.g., user's manuals, design documents) clearly describes code structure and relationships between modules.	The TSPA code and supporting documentation (i.e., the user's guide) are described or referenced in the TSPA-SR.
Subissue 3 Model Abstraction	PMR Approach
Element 8 – Flow Paths in the Saturated Zone	
T1. Sufficient hydrogeologic data (field, laboratory, and/or natural analog data) are available to adequately define relevant parameters and conceptual models necessary for developing the flow paths in the SZ abstraction in TSPA. Where adequate data do not exist, other information sources such as expert elicitation have been appropriately incorporated into TSPA.	Characterization and site data discussed in Section 3.1; conceptual models, Section 3.2; abstraction of radionuclide transport, Section 3.6.3.3; synthesis of SZ model and model abstractions, Section 3.6.
T2. Parameter values, assumed ranges, probability distributions, and/or bounding assumptions used in the flow paths in the SZ abstraction, such as the effect of climate change on the SZ fluxes and water table level and well pumping practices, are technically defensible and reasonably account for uncertainties and variability.	Synthesis of SZ model and model abstractions discussed in Section 3.6; parameter uncertainty distributions, Section 3.7.2; probabilistic analyses, Section 3.7.3.
T3. Alternative modeling approaches consistent with available data and current scientific understanding are investigated, and results and limitations appropriately factored into the flow paths in the SZ.	Synthesis of SZ model and model abstractions discussed in Section 3.6; assumptions, uses, and limitations of model, Section 3.5.

Table B-1. Issue Resolution Status Report (IRSR) Technical Acceptance Criteria (Continued)

<p align="center">Subissue 3 Model Abstraction (Continued)</p>	<p align="center">PMR Approach</p>
<p>T4. Flow paths in the SZ abstraction output are verified through comparison to output of detailed process models, and/or empirical observations (laboratory tests or natural analogs, or both).</p>	<p>Synthesis of SZ model and model abstractions discussed in Section 3.6; validation, Section 3.4.</p>
<p>T5. Important site (geologic and hydraulic) features, physical phenomena and couplings, and consistent and appropriate assumptions are incorporated into the flow paths in the SZ abstraction.</p>	<p>Synthesis of SZ model and model abstractions discussed in Section 3.6; assumptions, uses, and limitations of model, Section 3.5.</p>
<p>Element 9 - Radionuclide Transport in the Saturated Zone</p>	
<p>T1. Sufficient data (field, laboratory, and/or natural analog data) are available to adequately define relevant parameters and conceptual models necessary for developing the radionuclide transport in the saturated zone abstraction in TSPA. Where adequate data do not exist, other information sources such as expert elicitation have been appropriately incorporated into TSPA.</p>	<p>SZ characterization and data discussed in Section 3.1; laboratory data, Section 3.1.4.; Synthesis of SZ model and model abstractions, Section 3.6.</p>
<p>T2. Parameter values, assumed ranges, probability distributions, and/or bounding assumptions used in the radionuclide transport in the saturated zone abstraction, such as sorption on fracture surfaces and K_d for matrix, are technically defensible and reasonably account for uncertainties and variability.</p>	<p>SZ characterization and data discussed in Section 3.1; laboratory data, Section 3.1.4. parameter uncertainty distributions, Section 3.7.2; probabilistic analyses, Section 3.7.3; synthesis of SZ model and model abstractions, Section 3.6.</p>
<p>T3. Alternative modeling approaches consistent with available data and current scientific understanding are investigated, and results and limitations appropriately factored into radionuclide transport in the saturated zone abstraction.</p>	<p>Assumptions, uses, and limitations of model, Section 3.5; synthesis of SZ model and model abstractions, Section 3.6.</p>
<p>T4. Radionuclide transport in the saturated zone abstraction output is verified through comparison to output of detailed process models, and/or empirical observations (laboratory tests or natural analogs, or both).</p>	<p>Validation is discussed in Section 3.4; synthesis of SZ model and model abstractions, Section 3.6.</p>
<p>T5. Important site (geologic and hydrologic) features, physical phenomena and couplings, and consistent and appropriate assumptions are incorporated into the radionuclide transport in the saturated zone abstraction.</p>	<p>Assumptions, uses, and limitations of model, Section 3.5; synthesis of SZ model and model abstractions, Section 3.6.</p>
<p>Element 12 - Dilution of radionuclides Due to Well Pumping</p>	
<p>T1. Sufficient data (field, laboratory, and/or natural analog data) are available to adequately define relevant parameters and conceptual models necessary for developing the dilution of radionuclides due to well-pumping abstraction in the TSPA. Where adequate data do not exist, other information sources such as expert elicitation have been appropriately incorporated into TSPA.</p>	<p>No credit for dilution specifically due to well pumping is taken in TSPA. A detailed analysis of the groundwater use by the hypothetical farming community is presented in CRWMS M&O (2000c). Concentration in water supply in abstraction of radionuclide transport discussed in Section 3.6.3; synthesis of SZ model and model abstractions, Section 3.6.</p>

Table B-1. Issue Resolution Status Report (IRSR) Technical Acceptance Criteria (Continued)

<p align="center">Subissue 3 Model Abstraction (Continued)</p>	<p align="center">PMR Approach</p>
<p>T2. Parameter values, assumed ranges, probability distributions, and/or bounding assumptions used in the dilution of radionuclides in groundwater due to well pumping abstraction, such as the pumping well characteristics and water usage by the receptor groups, are technically defensible and account for uncertainties and variability.</p>	<p>No credit for dilution specifically due to well pumping is taken in TSPA. A detailed analysis of the groundwater use by the hypothetical farming community is presented in CRWMS M&O (2000c). Concentration in water supply in abstraction of radionuclide transport discussed in Section 3.6.3; parameter uncertainty distributions, Section 3.7.2; probabilistic analyses, Section 3.7.3; synthesis of SZ model and model abstractions, Section 3.6.</p>
<p>T3. Alternative modeling approaches consistent with available data and current scientific understanding are investigated, and results and limitations appropriately factored into the dilution of radionuclides in groundwater due to well pumping abstraction.</p>	<p>No credit for dilution specifically due to well pumping is taken in TSPA. A detailed analysis of the groundwater use by the hypothetical farming community is presented in CRWMS M&O (2000c). Concentration in water supply in abstraction of radionuclide transport discussed in Section 3.6.3; assumptions, uses, and limitations of model, Section 3.5; synthesis of SZ model and model abstractions, Section 3.6.</p>
<p>T4. Dilution of radionuclides in groundwater due to well pumping abstraction output is verified through comparison to outputs of detailed process models or empirical observations (laboratory tests).</p>	<p>No credit for dilution specifically due to well pumping is taken in TSPA. A detailed analysis of the groundwater use by the hypothetical farming community is presented in CRWMS M&O (2000c). Concentration in water supply in abstraction of radionuclide transport discussed in Section 3.6.3; validation, Section 3.4; synthesis of SZ model and model abstractions, Section 3.6.</p>
<p>T5. PA analyses incorporate important hydrogeologic features, physical phenomena and couplings, and consistent and appropriate assumptions are incorporated into the dilution of radionuclides due to well pumping abstraction.</p>	<p>No credit for dilution specifically due to well pumping is taken in TSPA. A detailed analysis of the groundwater use by the hypothetical farming community is presented in CRWMS M&O (2000c). Concentration in water supply in abstraction of radionuclide transport discussed in Section 3.6.3; assumptions, uses, and limitations of model, Section 3.5; synthesis of SZ model and model abstractions, Section 3.6.</p>
<p align="center">Scenario Analysis</p>	<p align="center">PMR Approach</p>
<p>Element 1 - Identification of initial FEPs</p>	
<p>T1. DOE has identified a comprehensive list of processes and events that: (1) are present or might occur in the Yucca Mountain region and (2) include those processes and events that have the potential to influence repository performance.</p>	<p>Relevant FEPs for SZ flow and transport are discussed in Section 1.3. Included FEPs are directly represented in the process models and abstractions that support TSPA, and discussed in sections of the PMR corresponding to the specific models.</p>
<p>Element 2 - Classification of Processes and Events</p>	
<p>T1. DOE has provided adequate documentation identifying how its initial list of processes and events has been grouped into categories.</p>	<p>Identification and categories of relevant FEPs for SZ flow and transport are discussed in Section 1.3.</p>
<p>T2. Categorization of processes and events is compatible with the use of categories during the screening of processes and events.</p>	<p>Categories of relevant FEPs for SZ flow and transport and their use are discussed in Section 1.3.</p>
<p>Element 3 - Screening of processes and events</p>	
<p>T1. Categories of processes and events that are not credible for the Yucca Mountain repository because of waste characteristics, repository design, or site characteristics are identified and sufficient justification is provided for DOE's conclusions.</p>	<p>Excluded FEPs and the rationale for exclusion are discussed in Section 1.3. The exclusion of FEPs from TSPA is based on arguments of low probability or low consequence.</p>

Table B-1. Issue Resolution Status Report (IRSR) Technical Acceptance Criteria (Continued)

Scenario Analysis (Continued)	PMR Approach
T2. The probability assigned to each category of processes and events not screened based on criterion T1 or T2 is consistent with site information, well documented, and appropriately considers uncertainty.	Rationale for excluding FEPs is discussed in Section 1.3.
T3. DOE has demonstrated that processes and events screened from the PA on the basis of their probability of occurrence, have a probability of less than one chance in 10,000 of occurring over 10,000 years.	Rationale for excluding FEPs is discussed in Section 1.3.
T4. DOE has demonstrated that categories of processes and events omitted from the PA on the basis that their omission would not significantly change the calculated expected annual dose, do not significantly change the calculated expected annual dose.	Excluded FEPs and the rationale for their exclusion are discussed in Section 1.3.
Element 4 - Formation of scenarios	
T1. DOE has provided adequate documentation identifying (1) whether processes and events have been addressed through consequence model abstraction or scenario analysis and (2) how the remaining categories of processes and events have been combined into scenario classes.	Information on FEPs that are directly or indirectly included in the analysis of UZ flow and transport are discussed in Section 1.3.
T2. The set of scenario classes is mutually exclusive and complete.	Information on FEPs that are directly or indirectly included in the analysis of UZ flow and transport are discussed in Section 1.3.
Element 5 - Screening of scenario classes	
T1. Scenario classes that are not credible for the Yucca Mountain repository because of waste characteristics, repository design, or site characteristics--individually or in combination--are identified and sufficient justification is provided for DOE's conclusions.	FEPs screening database has been assembled, SZ FEPs AMR has been written (CRWMS M&O 2000q); FEPs discussed in Section 1.3.
T2. The probability assigned to each scenario class is consistent with site information and well documented and appropriately considers uncertainty.	FEPs screening database has been assembled, SZ FEPs AMR has been written (CRWMS M&O 2000q); FEPs discussed in Section 1.3.
T3. Scenario classes that combine categories of processes and events may be screened from the PA on the basis of their probability of occurrence, provided (1) the probability used for screening the scenario class is defined from combinations of initiating processes and events and (2) DOE has demonstrated that they have a probability of less than one chance in 10,000 of occurring over 10,000 years.	FEPs screening database has been assembled, SZ FEPs AMR has been written (CRWMS M&O 2000q); FEPs discussed in Section 1.3.
T4. Scenario classes may be omitted from the PA on the basis that their omission would not significantly change the calculated expected annual dose, provided DOE has demonstrated that excluded categories of processes and events would not significantly change the calculated expected annual dose.	FEPs screening database has been assembled, SZ FEPs AMR has been written (CRWMS M&O 2000q); FEPs discussed in Section 1.3.

Table B-1. Issue Resolution Status Report (IRSR) Technical Acceptance Criteria (Continued)

Key Technical Issue: Unsaturated and Saturated Flow Under Isothermal Conditions	
Subissue 2 Hydrologic Effects of Climate Change	PMR Approach
<p>Criterion 1—If bounding analyses are used to predict climate-induced effects (e.g., water table rise), the analyses are based on a reasonably complete search of paleoclimate data pertinent to water table rise and other effects (e.g., changes in precipitation and geochemistry), including, at a minimum, information contained in Paces et al. (1996), Szabo et al. (1994), and Forester et al. (1996).</p>	<p>A comprehensive literature search of the paleoclimate data has been completed and documented in the <i>Yucca Mountain Site Description</i> (CRWMS M&O 1998d). This description references Paces et al. (1996) in Section 5 (Hydrologic System). Szabo et al. (1994) and Forester et al. (1996) are referenced in Section 4 (Climatology and Meteorology).</p> <p>Response of conceptual model to climate change discussed in Section 3.2.6; alternative climate states abstraction of radionuclide transport, Section 3.6.3.3.2.</p>
<p>Criterion 2—Regional and sub-regional models for the SZ that are used to predict climate-induced consequences are calibrated with the paleohydrology data and are consistent with evidence that the water-table rise during the late Pleistocene was up to 120 m (394 ft).</p>	<p>Climate change, response of conceptual model to climate change discussed in Section 3.2.6; alternative climate states abstraction of radionuclide transport, Section 3.6.3.3.2. (NOTE: Newest USFIC IRSR [NRC 1999a] provides evidence that water table rise in Pleistocene was not up to 120 m [394 ft].)</p>
<p>Criterion 3—DOE has incorporated future climate changes and associated effects in its PAs. For example, available information does not support an assumption that present-day climate will persist unchanged for 10,000 yr. or more.</p>	<p>Alternative climate states abstraction of radionuclide transport discussed in Section 3.6.3.3.</p> <p>Effects of Climate Change on SZ Flux: Incorporated in TSPA by increases in flux by a factor of about 3.9 for glacial-transition state and about 2.7 for monsoonal, the increases are modeled as an instantaneous change (Section 3.6.3.3.2). By assuming an instantaneous shift to the increased flux, the simulations tend to overestimate radionuclide transport velocities.</p> <p>Effects of Climate Change on Water Table Rise: Flow paths assumed to be similar to those at present; water table rise beneath the repository would place presently unsaturated, less permeable volcanic units at or just below the water table; disregarding rises in groundwater, which would be redirected into lower-permeability units generally is conservative with regard to radionuclide transport.</p>
Subissue 5 Saturated Zone Ambient Flow Conditions and Dilution Processes	PMR Approach
<p>Criterion 1—DOE has considered conceptual flow and data uncertainties. Uncertainties due to sparse data or low confidence in the data interpretations have been considered by analyzing reasonable conceptual flow models supported by site data or by demonstrating through sensitivity studies that the uncertainties have little impact on repository performance.</p>	<p>Model validation now includes comparisons of: permeability data to calibrated permeability values, fluxes from regional model with fluxes from calibrated model, measured upward gradient with predicted upward gradient, hydrochemical data with calculated particle pathways, and natural analogs. These activities and process model uncertainties are discussed in Section 3.4; assumptions, uses, and limitations, Section 3.5; SZ base case, uncertainty, parameter uncertainty distribution, and probabilistic analysis discussed in Section 3.7.</p>

Table B-1. Issue Resolution Status Report (IRSR) Technical Acceptance Criteria (Continued)

<p align="center">Subissue 5 Saturated Zone Ambient Flow Conditions and Dilution Processes (Continued)</p>	<p align="center">PMR Approach</p>
<p>Criterion 2—DOE has reasonably delineated possible flow paths from beneath the repository to potential receptor locations based on data that is sufficient to elucidate (i) the relative travel distances through aquifers of differing hydrologic and geochemical properties; (ii) in fractured-rock aquifers, the portions of flow through rock matrix and fractures; (iii) flow directions with respect to the hydraulic gradient, considering the potential effects of horizontal anisotropy; (iv) approximate volume fluxes and pore velocities; and (v) vertical hydraulic gradients, including the potential for flow between the Paleozoic carbonate aquifer and the volcanic tuff aquifer. A sufficient number of wells and exploratory holes should be drilled, and an adequate number of tests conducted, to reasonably bound the hydraulic and transport properties of the units downgradient from the proposed repository.</p>	<p>Uncertainty in travel distances through aquifers of differing properties stochastically bounded in model by varying amount of alluvium along the flow path. Dual porosity approach is incorporated explicitly into the transport methodology for volcanic units to simulate matrix diffusion. Potential effects of horizontal anisotropy are bounded by setting the anisotropy ratio stochastically to either 1 (isotropic) or 5 (based on the C-wells data) by making permeability values for the volcanic units 5 times greater in the north-south direction than in the east-west direction. Uncertainty in groundwater flux is incorporated by considering three discrete cases of low-, mean-, and high-flux by scaling the values of permeability and the boundary fluxes of the mean-flux case downward or upward by a constant factor of 10. Proportional scaling preserves the calibration of the model to head measurements among the three cases. Potentiometric levels in the carbonate aquifer at well UE-25p#1 are about 21 m (69 ft) higher than levels in the overlying rocks. This indicates a potential for upward flow and suggests that water will not flow from the tuffs into the carbonates. Regional-scale flow system discussed in Section 3.1.1.1; site-scale flow system, Section 3.1.1.2; conceptual model of hydrogeologic framework, Section 3.2.1. Uncertainty discussed in CRWMS M&O (2000o). SZ base case, uncertainty, parameter uncertainty distribution, and probabilistic analysis discussed in Section 3.7. Horizontal anisotropy discussed in Section 3.2.5.3.</p>
<p>Criterion 3—DOE has provided an hydrologic assessment to describe likely causes of the "moderate hydraulic gradient" and the "large hydraulic gradients."</p>	<p>Relationship of moderate and large hydraulic gradients to hydrogeologic framework discussed in Section 3.2.2.3; large hydraulic gradient alternative models, Section 3.2.5.1.</p>
<p>Criterion 4—DOE has provided maps of approximate potentiometric contours of the regional uppermost aquifer for an area that, at a minimum, includes wells J-11 on the east, VH-1, VH-2, and the GEXA Well on the west, UE-29a#2 to the north, and domestic and irrigation wells south of Amargosa Valley (aka Lathrop Wells). Maps of regional and site-scale recharge and discharge should be provided, along with site-scale hydrostratigraphic cross sections constructed along the paths to the accessible environment, and site-scale flow-net analysis of the SZ.</p>	<p>New maps of approximate potentiometric contours (Figure 3-5) based on new data provided. Regional-scale flow system discussed in Section 3.1.1.1; hydrologic data, Section 3.1.2; water level data, Section 3.1.2.1; recharge, Section 3.2.3.2; discharge, Section 3.2.3.3.</p>

Table B-1. Issue Resolution Status Report (IRSR) Technical Acceptance Criteria (Continued)

<p align="center">Subissue 5 Saturated Zone Ambient Flow Conditions and Dilution Processes (Continued)</p>	<p align="center">PMR Approach</p>
<p>Criterion 5—DOE estimates of key hydrologic parameters are described in the form of either probability distributions or deterministic bounding values that are reasonably consistent with site data. These parameters should include transmissivity, hydraulic gradient, effective flow porosity, effective immobile porosity, and effective aquifer thickness.</p>	<p>Estimates of key hydrologic parameters are described in the form of either probability distributions or deterministic bounding values that are reasonably consistent with site data. The descriptions are as follows: matrix porosity description is deterministic bounding; hydraulic gradient description is deterministic bounding; flow porosity description is probabilistic. Transmissivity and effective aquifer thickness are not pertinent parameters. However, for permeability related to transmissivity and thickness, description is probabilistic.</p> <p>Uncertainty discussed in CRWMS M&O (2000o). Section 3.7 discusses SZ base case, uncertainty, parameter uncertainty distribution, and probabilistic analysis. Model validation now includes comparisons of: permeability data to calibrated permeability values, fluxes from regional model with fluxes from calibrated model, measured upward gradient with predicted upward gradient, hydrochemical data with calculated particle pathways, and natural analogs. These activities and process model uncertainties are discussed in Section 3.4.</p>
<p>Criterion 6—DOE has used mathematical groundwater model(s) that incorporate site-specific climatic and subsurface information. The models were reasonably calibrated and reasonably represent the physical system. Fitted aquifer parameters compare reasonably well with observed site data. Implicitly- or explicitly-simulated fracturing and faulting are consistent with the data in the 3D geologic model. Abstractions are based on initial and boundary conditions consistent with site-scale modeling and the regional models of the Death Valley groundwater flow system. Abstractions of the groundwater models for use in PA simulations should use appropriate spatial- and temporal-averaging techniques.</p>	<p>The 3-D site-scale SZ flow and transport numerical model simulates groundwater flow and radionuclide transport from the water table beneath the potential repository to the accessible environment using an equivalent continuum formulation and implicit fault and fracture representation to capture flow through fracture and matrix.</p> <p>The site-scale SZ flow and transport model is generated based on data from the hydrogeologic framework, integrated site, rock properties, and mineralogy models. It is calibrated and tested against relevant data that include water level, permeability, temperature, and ambient hydrochemistry data. The conceptual model of the SZ model is also validated using natural analogues.</p> <p>Model validation includes comparisons of: permeability data to calibrated permeability values, fluxes from regional model with fluxes from calibrated model, measured upward gradient with predicted upward gradient, hydrochemical data with calculated particle pathways, and natural analogs. These activities and process model uncertainties are discussed in Section 3.4.</p>
<p>Criterion 7—If credit for wellbore dilution is taken, a demonstration has been provided that reasonable assumptions have been made about well design, aquifer characteristics, plume geometry, withdrawal rates, and capture zone analysis for the receptor location.</p>	<p>Dilution in water supply is discussed in Section 3.6.3.3.4.</p>
<p>Criterion 8—If credit is taken for dilution due to either dispersion, groundwater mixing below the repository footprint, or mixing of the Yucca Mountain water with water from the north in Fortymile Wash, reasonable assumptions have been made about spatial and temporal variations of aquifer properties and groundwater volumetric fluxes.</p>	<p>Assumptions, uses, and limitations of site-scale flow and transport model are in Section 3.5.</p>

Table B-1. Issue Resolution Status Report (IRSR) Technical Acceptance Criteria (Continued)

<p align="center">Subissue 5 Saturated Zone Ambient Flow Conditions and Dilution Processes (Continued)</p>	<p align="center">PMR Approach</p>
<p>Criterion 9—DOE has incorporated key conclusions regarding potential geothermal and seismic effects on the ambient SZ flow system (e.g., National Research Council 1992; NWTRB 1998d; Craig 1997).</p>	<p>Other views, alternative conceptual models, and incorporation of key conclusions are discussed in Section 3.8.</p>
<p align="center">Subissue 6 Matrix Diffusion</p>	<p align="center">PMR Approach</p>
<p>Criterion 2—If credit for matrix diffusion in the SZ is taken, rock matrix and solute diffusion parameters must be (i) based on an SZ transport model that reasonably matches the results of the field tracer tests that are conducted over different distance scales and flow rates with multiple tracers of different diffusive properties and (ii) consistent with laboratory data.</p>	<p>The C-wells reactive tracer test (Section 3.1.3.2) demonstrated that models that incorporate matrix diffusion provide more reasonable fits to the tracer-experiment data than those that assume a single continuum. The matrix sorption coefficient that fit the data for the lithium tracer in the C-wells reactive tracer experiment agreed well with the value determined in laboratory sorption tests. This provides confidence that the matrix-diffusion model is appropriate. The fact that the early lithium response had the same timing as that of the nonsorbing tracers, but with a lower normalized peak concentration, is consistent with matrix diffusion coupled with sorption in the matrix (see Figure 3-9). Matrix diffusion laboratory tests are discussed in Section 3.1.4.2; tracer tests, Section 3.1.3.2; matrix diffusion in conceptual model, Section 3.2.4.2; matrix diffusion in mathematical model, Section 3.3.2.2; matrix diffusion sub-model in particle tracking methodology, Section 3.3.4.2; validation, Section 3.4.</p>

INTENTIONALLY LEFT BLANK